N° d'ordre : 3178

THESE

Présentée à

L'UNIVERSITE BORDEAUX 1

ECOLE DOCTORALE

« Sciences du vivant, géosciences et sciences de l'environnement »

par **BOGDAN MURESAN PASLARU**

pour obtenir le grade de

DOCTEUR

Spécialité : Biogéochimie de l'environnement

Géochimie du mercure dans le continuum de la retenue de Petit-Saut et de l'estuaire du Sinnamary, Guyane française

Soutenue le 15 juin 2006

Devant la commission d'examen formée de :

M. Amyot	Professeur, Université de Montréal, rapporteur
G. Blanc	Professeur, Université Bordeaux 1, examinateur
A. Boudou	Professeur, Université Bordeaux 1, co-directeur de thèse
L. Charlet	Professeur, Université J. Fourier, invité
P. Ciffroy	Ingénieur-chercheur, EDF, invité
D. Cossa	Chercheur Ifremer, directeur de thèse
D. Jézéquel	Maître de Conférence, Université D. Diderot, rapporteur
F.M.M. Morel	Professeur, Université de Princeton, examinateur

RESUME

La retenue de Petit-Saut et, à l'aval, l'estuaire du Sinnamary sont deux centres d'altération du cycle naturel du mercure. Les processus sont, entre autres, (i) la photoréduction, (ii) la sorption / désorption en surface des particules, (iii) l'activité méthylante des bactéries, (iv) la dissolution / précipitation des oxyhydroxydes et des sulfures de fer.

Les sources de mercure vers la retenue sont variées. Elles regroupent, en premier lieu, les affluents (partiellement orpaillés), l'atmosphère, les sols et la végétation ennoyés. Dans la colonne d'eau, les formes divalentes du mercure subissent un train complet de transformations couplant changements de phase et de spéciation. Nos résultats illustrent ces processus et démontrent que la retenue constitue un site privilégié de recyclage vers l'atmosphère et de méthylation. A l'interface air / eau, les exports en mercure de la retenue excèdent de 50 % le dépôt atmosphérique. La production endogène de monométhylmercure (MMHg) a lieu dans des sites particuliers : la chemocline et l'interface benthique. Elle atteint pour l'ensemble de la retenue 8,1 moles a^{-1} soit un taux de méthylation de 0,06 % j^{-1}. On estime que la retenue exporte vers l'estuaire du Sinnamary 13,5 moles a^{-1} de MMHg alors qu'elle n'importe que 5,4 moles a^{-1}.

L'estuaire dynamique du Sinnamary constitue le véritable réacteur chimique du système fonctionnant en liaison avec celui de la retenue. Le mercure y décrit un cycle rapide aux processus de partition, de recyclage et de méthylation marqués. Ces processus résultent de l'oxygénation incomplète et durable des masses d'eau anoxiques exportées par la retenue de Petit-Saut. L'expression de gradients rédox prononcés conjuguée à un intense recyclage de la matière organique y favorise la production de formes méthylables de mercure ainsi que l'activité des bactéries sulfatoréductrices (agents de la méthylation). C'est pourquoi, l'estuaire dynamique du Sinnamary exporte 60 % plus de MMHg qu'il n'importe : 27 contre 17 moles a^{-1}. Plus en aval, dans l'estuaire salin, nous avons mis en évidence : (i) un comportement non conservatif du mercure dissous, (ii) un appauvrissement du mercure des particules suite au mélange avec le panache de l'Amazone et (iii) une dilution des concentrations par les masses d'eau océaniques.

ABSTRACT

The mercury cycle was explored in the Petit-Saut reservoir / Sinnamary Estuary continuum in French Guiana. Main processes involve (i) photo-induced reduction, (ii) adsorption and desorption at the particle surfaces, (iii) methylating bacterial activity, (iv) precipitation and dissolution of iron oxyhydroxides and sulfides.

Sources of mercury to the Petit-Saut reservoir consist of the partly impacted river-tributaries, the atmospheric deposition and the flooded soils or vegetation. Once into the reservoir, divalent mercury undergoes a large spectrum of transformations including speciation and phase changes. We, here, probe these processes and demonstrate that the Petit-Saut reservoir behaves as a privileged site for atmospheric recycling and *in situ* methylation. At the air / water interface, the mercury evasion exceeds by 50 % the direct atmospheric deposition. The *in situ* monomethylmercury (MMHg) production mostly occurs at the water-column chemocline and near the benthic interface. It reaches, for the whole reservoir, 8.1 moles yr^{-1} which corresponds to a 0.06 % d^{-1} methylation rate. We calculated that the 2003/04 period MMHg outputs from the reservoir to the Sinnamary Estuary averaged 13.5 moles yr^{-1} while the inputs were 5.4 moles yr^{-1}.

The dynamic Sinnamary Estuary is the genuine geochemical reactor of the continuum. There, the divalent mercury undergoes rapid yet profound partitioning among phases, recycling to the atmosphere and methylation processes. Those mostly originate from the long-scale oxygen paucity of the dam discharged waters. The expression of marked redox gradients and the intense organic matter turnover enhance the production of methylable inorganic mercurial species and tend to favor the sulfate reducing bacteria (methylating agents) activity. As a result, the dynamic Sinnamary Estuary exports 60 % more MMHg than it does import: 27 versus 17 moles yr^{-1}. Further at large, in the saline estuary, we determined: (i) a non conservative behavior of dissolved (< 0.2 µm) mercury, (ii) a lowering of the mercury level of particles during mixing with the Amazon plume and (iii) a gradual dilution of the estuarine mercury concentrations by oceanic waters.

REMERCIEMENTS

– Maître quelle est l'essence du dosage du mercure ?

– Pratiquer les techniques ultra-propres, éviter la contamination pour obtenir des données fiables.

– Mais tous les chatons le savent !

– Oui, mais même un vieux matou n'arrive pas toujours à le mettre en pratique…

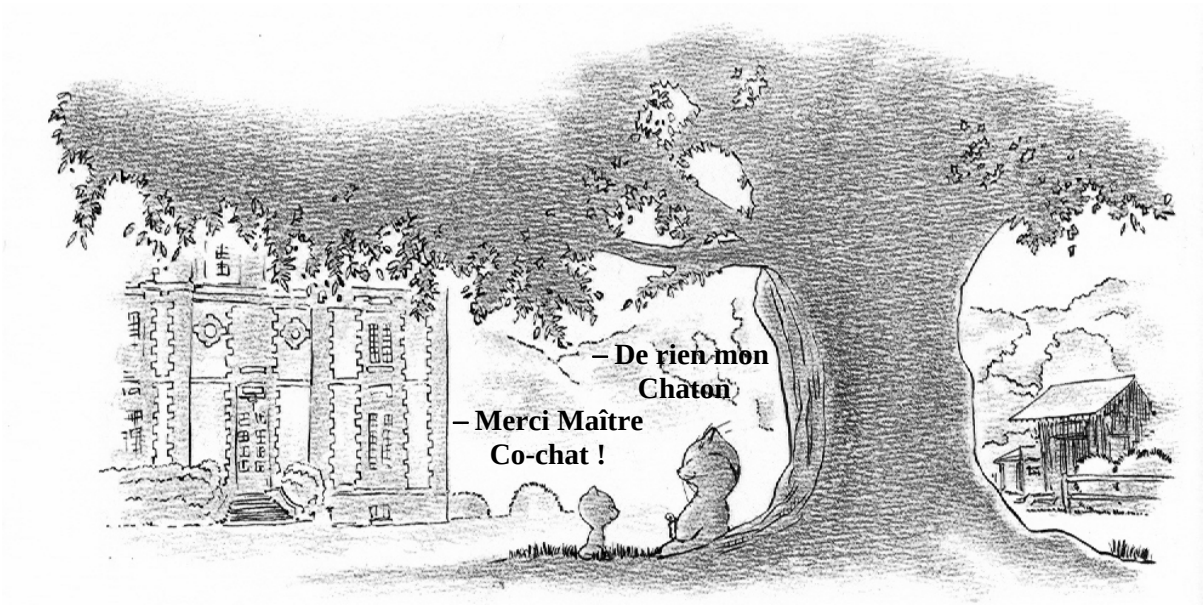

Et aussi :
Gilgamesh, Bouddha, Aristophane, Lao-Tseu, Eratosthène, Jésus, Néron, Mahomet, Dôgen, Dante, Averroès, Shakespeare, Molière, Descartes, Galileo Galilei, Isaac Newton, Emmanuel Kant, Joseph Fourier, Suzuki Harunobu, Alexandre Dumas (père), Les frères Grimm, G.W.F. Hegel, Karl Marx, Lewis Carroll, Emile Zola, Friedrich Nietzsche, Mihai Eminescu, Maupassant, Henri Poincaré, Marie Curie, Jules Romain, Max Planck, Sigmund Freud, Mohandas Karamchand Gandhi, Franz Kafka, Erwin Schrodinger, Sergueï Eisenstein, Jacques Prévert, Werner Heisenberg, James Lovelock, Les Marx Brothers, René Magritte, Pavel Alekseïevitch Tcherenkov, Jean-Paul Sartre, Akira Kurozawa, Che Guevara, M.G.J. Colucci (alias Coluche), Alain Saliot, Kofi Annan, Takeshi Kitano, Wong Kar-Wai, Alain Boudou, Didier Jézéquel, Yannick Dominique, Benoit Burban, Bernard Averty, Edouard Metzger, Sandrine Richard, Cécile Reynouard, Véronique Horeau, André Tessier, Charles Gobeil, Joel Radford Knoery, Régine Maury-Brachet, Caroline Simonucci, l'A.S.S.E.D.I.C. de Nantes, l'I.F.R.E.M.E.R., l'E.D.F., le C.N.R.S., Google, Mozilla Firefox, Paint, MS Office (en particulier Word, Excel et PowerPoint) et ceux de ma 6-T : Yann Koffi, Sebastien Djema, Vincent Vieira, Abdoulaye et Ousmane Bathily, Didier Lebastard, Stéphane et Patrick Vorachack, Igor Artieda, Yann Kolb…, ma Femme, mon Fils, ma Famille.

REMERCIEMENTS AU JURY DE THESE

Il faut remercier l'arbre à karité sous lequel on a ramassé de bons fruits pendant la bonne saison

Ahmadou Kourouma

Suite à la soutenance de thèse, je souhaite remercier la commission d'examen formée de :

M. Amyot	Professeur, Univ. de Montréal, rapporteur
G. Blanc	Professeur, Univ. Bordeaux 1, examinateur
A. Boudou	Professeur, Univ. Bordeaux 1, co-directeur
L. Charlet	Professeur, Univ. de Grenoble, invité
P. Ciffroy	Ingénieur-chercheur, EDF, invité
D. Cossa	Chercheur Ifremer, directeur de thèse
D. Jézéquel	Maître de conférence, Univ. Paris VII, rapporteur
F. Morel	Professeur, Univ. de Princeton, examinateur

Merci pour l'agréable partage des connaissances, pour vos critiques et l'amitié exprimée.

SIGLES DES ORGANISMES

BRGM	Bureau de Recherche Géologique & Minière
CFBR	Comité Français des Barrages et Réservoirs
CIA	Central Intelligence Agency
CNRS	Centre National de la Recherche Scientifique
DIREN	Direction Régionale de l'Environnement
DRIRE	Direction Régionale de l'Industrie, de la Recherche et de l'Environnement
DSDS	Direction de la Santé et du Développement Social
EDF	Electricité De France
HYDRECO	Laboratoire de recherche en environnement (Site du barrage de Petit-Saut)
IFREMER	Institut Français de Recherche pour l'Exploitation de la Mer
INRS-ETE	Institut National de la Recherche Scientifique Centre Eau, Terre & Environnement
InVS	Institut de Veille Sanitaire
IRD	Institut de Recherche pour le Développement
MMSD	Mining Minerals, Sustainable Development
OMS	Organisation Mondiale de la Santé
ONF	Office National des Forêts
UNEP	United Nations Environmental Program
UNIDO	United Nations Industrial Development Organization

SIGLES DES PRINCIPALES ESPECES DE MERCURE

Hg	Le mercure est un élément chimique de symbole Hg et de numéro atomique 80. Sous les conditions normales de température et de pression, c'est le seul métal à l'état liquide. La toxicité du mercure dépend de son degré d'oxydation.
Hg^0	Le mercure zéro-valent (élémentaire) est le seul élément en dehors des gaz rares à exister sous forme de vapeur monoatomique. Les vapeurs de mercure sont nocives.
Hg^{2+} - $[Hg_2]^{2+}$	L'ion libre de Hg présente, de par son aptitude à se combiner, des niveaux naturels extrêmement faibles ($< 10^{-20}$ moles L^{-1}). Il possède deux degrés d'oxydation : Hg^{2+} - l'ion mercurique et $[Hg_2]^{2+}$ - l'ion mercureux.
HgT	Le mercure total est la somme des espèces de Hg présentes dans la fraction non filtrée (HgT_{UNF}), dissoute (HgT_D) ou particulaire (HgT_P).
HgR	Le mercure réactif comprend essentiellement les espèces minérales (hormis sulfures et séléniures) et organiques labiles au pH de la réduction par le chlorure stanneux, c'est-à-dire autour de 1.
HgS^0	Complexe soufré du Hg dont l'existence demeure théorique mais dont on pense qu'il joue un rôle clef dans les processus de méthylation.
HgS_x	Complexes polysoufrés du Hg formés en présence de soufre élémentaire.
HgT_{UNM}	Le mercure non méthylé est calculé comme la différence entre la concentration de HgT et celle de monométhylmercure
MMHg	Le monométhylmercure regroupe l'ensemble des espèces complexées à la fois par un ligand de méthyle et un ligand minéral (i.e. CH_3-Hg-X). Il constitue la forme la plus toxique du Hg car la plus bioaccumulable.
DMHg	Mercure comportant deux groupements méthyle : $Hg(CH_3)_2$. Le diméthylmercure est un composé volatil et instable. Suivant les environnements, il

	représente une part variable du Hg atmosphérique (entre 0 et 5 %).
DGM	Le mercure gazeux dissous est la somme des espèces volatiles de Hg présentes dans l'eau. Il regroupe principalement le Hg^0 et le DMHg.
TGM	Le mercure total gazeux est la somme des espèces de Hg présentes à l'état de gaz dans l'atmosphère. Plus de 95 % du Hg de l'air est sous forme de Hg gazeux
GEM	Mercure élémentaire présent dans l'atmosphère sous forme de gazeuse (Hg^0). Il compose la plus grande partie du TGM (près de 98 %).
RGM	Le mercure réactif gazeux (probablement $HgCl_2$) rassemble moins de 1 % du GEM. Le RGM est susceptible de s'adsorber sur les aérosols ou se dissoudre dans les gouttelettes de pluie, et donc de se déposer à la surface du sol et les plans d'eau.

SOMMAIRE

1. INTRODUCTION GENERALE

1.1. Présentation du thème de recherche

Le 28 février 2005, la Charte de l'Environnement (copie en annexes) est adoptée par le Parlement français et promulguée le 1er mars 2005 par le Président de la République. L'article premier stipule que « chacun a le droit de vivre dans un environnement équilibré et respectueux de la santé ». Or, ces dernières années ont vu les services de l'Etat (DIREN, InVS, ONF, etc.) et certains acteurs politiques prendre conscience du désordre régnant dans les méthodes d'exploitation de l'or en Guyane Française et des conséquences de l'exposition au mercure pour la santé et l'environnement. Il était temps! Sur l'ensemble de la Guyane on compte 2 compagnies internationales, 26 PME, 60 artisans et 600 à 800 chantiers illégaux d'orpaillage. On (sous)estime ainsi que l'orpaillage illégal emploie près de 10 000 personnes souvent dans des conditions sanitaires déplorables et participe chaque année au rejet direct de 5 à 10 tonnes de mercure dans l'environnement. Les orpailleurs professionnels guyanais admettent un rapport de 1,3 grammes de mercure additionné pour 1 gramme d'or produit. Cependant, les importations de mercure et la production déclarée d'or ne correspondent guère (respectivement 8,4 et 3,2 tonnes en 2003)! Ce mercure d'origine anthropique, d'une part a réalisé des stocks historiques énormes (300 tonnes selon le BRGM) et d'autre part se partage le terrain avec un mercure naturellement important (10 fois plus concentré qu'en Europe selon Charlet et Boudou, 2002), partiellement libéré par l'activité d'extraction minière. C'est pourquoi, l'abandon du mercure légal dont l'interdiction est prévue en 2006, ne réglera ni la question de l'orpaillage illégal ni celle de la remobilisation du mercure naturel.

Les premiers signes d'une « problématique contemporaine du mercure guyanais » apparaissent dès 1994 avec l'étude de l'imprégnation des populations des villages amérindiens du Haut Maroni (InSV). Celle-ci met en évidence de fortes concentrations dans les cheveux (supérieures à 10 $\mu g\ g^{-1}$ en moyenne) qui seront reliées à une consommation importante de certaines espèces de poissons piscivores. Plus récemment (2001), une étude menée par le CNRS dans le cadre de la phase I du programme « Mercure en Guyane » a estimé la contamination des poissons dans la retenue de

Petit-Saut et à l'aval (dans le fleuve Sinnamary) au double de ce qu'elle est dans le Haut Maroni. Ces teneurs reflèteraient les modifications brutales et profondes de la qualité de l'eau et des écosystèmes aquatiques lors de la mise en eau du barrage hydroélectrique. De plus, le lac néoformé est en partie alimenté en eau par deux rivières (i.e. Courcibo et Leblond) drainant la région minière de St.-Elie. En 2001, les études ont montré que si les eaux de surface (les 5 premiers mètres) de la retenue de Petit-Saut étaient oxygénées, les eaux plus profondes (les trente derniers mètres) ne l'étaient pas. Cette partie de la colonne d'eau, non oxygénée, riche en matière organique ainsi qu'en composés réduits issus de la dégradation des sols et de la végétation immergée est propice à la production d'espèces hautement toxiques du mercure. La conclusion de cette étude met en avant « l'existence d'un réel problème sanitaire si des pêches conduisent à la consommation régulière d'espèces carnivores par les populations ».

1.2. Objectifs et méthodologie des travaux

C'est dans ce contexte préoccupant qu'a été initiée en 2003 la phase II du programme « Mercure en Guyane ». Les recherches qui y ont été et continuent d'y être menées visent à renforcer les connaissances acquises au cours de la phase I ainsi qu'à aborder des thématiques nouvelles et complémentaires. L'axe II de la phase II du programme (incluant le présent travail) a pour vocation d'étudier le cycle biogéochimique du mercure depuis les sources d'émission jusqu'aux voies de transfert vers les populations humaines. Il a pour cadre géographique le continuum formé par la retenue de Petit-Saut et l'Estuaire du Sinnamary. Il regroupe deux équipes de chercheurs (IFREMER et CNRS) rendant possible une approche biogéochimique des études d'écotoxicologie. Le présent travail consiste par conséquent à fournir cette base de données biogéochimiques. Pour cela, il s'est attaché à analyser l'impact de la retenue sur le cycle du mercure dans les compartiments sols, eau et atmosphère du continuum. Il a permis d'identifier, de décrire et de quantifier les sites privilégiés de transformation, les cinétiques des processus et les flux de mercure aux interfaces. Les principales étapes de l'investigation *in situ* étant :

- Le suivi saisonnier de 3 ans (2003-2005) de la spéciation du mercure et des paramètres physico-chimiques dans la colonne d'eau du réservoir et l'Estuaire du Sinnamary

(missions Matoutou 1 à 5)

- Le déploiement de l'analyseur de mercure atmosphérique Tekran 2537A et de l'unité de spéciation Tekran 1130.
- La mise en place du suivi hebdomadaire du mercure contenu dans la pluie (2003-2004).
- Le suivi hebdomadaire de 2 ans (2003-2004) des exports de mercure en contrebas du barrage de Petit-Saut.
- L'exploration des zones en amont de la retenue, aussi bien au niveau des affluents orpaillées (rivières Leblond et Courcibo en avril 2005) qu'apparemment préservés (rivière Sinnamary en novembre 2004)

Dans ce document, nous avons le plus souvent possible essayé de lier nos données aux nombreuses observations recueillies par les différents spécialistes amenés à travailler sur le site ou sur la thématique du mercure. Parallèlement, plusieurs voies nouvelles de recherche on été ouvertes et empruntées avec un succès encore incertain. Les résultats de nos études sont effectivement amenés à être largement discutés et à devenir quelques éléments de réponse à des questions encore plus nombreuses.

Ce travail est le fruit d'une démarche pluridisciplinaire conjuguant des approches physiques, chimiques, biologiques et de modélisation. Nous avons essayé de donner une vision, la plus juste possible à défaut d'être complète, de la biogéochimie de ce métal si unique qu'est le mercure dans une retenue tropicale et son environnement immédiat.

2. PROBLEMATIQUE DU MERCURE EN MILIEU TROPICAL

2.1. Pourquoi le mercure est-il une préoccupation environnementale?

Le mercure (Hg), notamment l'une de ses formes appelée monométhylmercure (MMHg), est préoccupant pour la santé humaine et l'environnement parce qu'il est toxique et s'accumule le long des chaînes trophiques. Le nombre croissant d'études concernant l'exposition des populations humaines au Hg *via* la consommation de poissons (de 10 à 93 études a^{-1} entre 1985 et 2005 ; Elsevier publications) est révélateur de ces préoccupations sanitaires. Parmi elles, les études menées en Amazonie attestent de la corrélation entre les niveaux d'imprégnation des populations par le monométhylmercure et leur régime alimentaire (Lebel *et al*., 1998 ; Grandjean, 1999 ; Dolbec *et al*., 2000) : les personnes à risque sont de fortes consommatrices de poissons. Cette substance est par ailleurs préoccupante pour l'environnement car ses effets toxiques, caractérisés par des lésions au niveau des centres nerveux (tremblements, dysfonctionnements de la rapidité des mouvements fins, déficits d'organisation visuospatiale), peuvent perturber le cycle de vie des écosystèmes naturels. Par exemple, sur la côte Est du Canada, la teneur sanguine en mercure des plongeons huards est deux fois plus élevée que dans toute autre région d'Amérique du Nord. Ces populations d'oiseaux, exposés au Hg *via* les poissons dont ils se nourrissent, ont des difficultés à se reproduire (Environnement Canada). Le présent document donne un aperçu de la question du mercure dans les milieux aquatiques perturbés par l'activité humaine. Il aborde, en particulier, les mécanismes fondamentaux qui contrôlent les flux et transformations du mercure aux interfaces air/eau/sédiments.

Amalgame : Le Hg forme des alliages avec presque tous les métaux hormis le fer, le nickel et le cobalt. L'alliage est par ailleurs difficile avec le cuivre, le platine sans oublier l'antimoine. L'alliage formé est également appelé amalgame. Cette propriété du mercure présente de nombreux usages.

2.2. Qu'est qui se passe?

Introduction au mercure

Les alchimistes l'appelaient « vif-argent » (*hydrargyrum* d'où son sigle chimique Hg) et le représentaient grâce au symbole de la planète Mercure, d'où son nom actuel.

L'histoire du Hg est inextricablement lié à celle de l'or (Au). Dès 2 700 avant notre ère le Hg était utilisé pour **amalgamer**

l'or, l'argent ou d'autres métaux. Aujourd'hui encore de nombreux chercheurs d'or l'utilisent pour récupérer l'or présent sous forme de paillettes. L'amalgame obtenu est chauffé vers 400-500 °C, ce qui conduit à l'évaporation du mercure et à l'apparition d'une pépite en métal précieux. Ce procédé très artisanal concerne près de 20 % de la production mondiale d'or (2300 tonnes en 2005 ; UNIDO). Il pose de graves problèmes de pollution, notamment des rivières en Amazonie, au Ghana ainsi qu'en Birmanie entre autres. Citons quelques chiffres, selon l'UNIDO (2005), l'**orpaillage** artisanal est pratiqué par ~ 13 millions de personnes (dont 4 millions de femmes et 6 millions d'enfants). Entre 80 et 100 millions de personnes en dépendent et se trouvent indirectement exposés à la toxicité du Hg. La hausse du prix de l'or (de 9 à 16 € g^{-1} entre 1985 et 2005) conditionne l'essor de l'orpaillage « sauvage » et par conséquent celle de l'utilisation du Hg dans plus de 30 pays d'Asie, Afrique et Amérique Latine. On estime que chaque gramme d'or récupéré a nécessité l'emploi de 1 à 2 g de Hg dont 50-60 % sont émis vers l'atmosphère lors du chauffage de l'amalgame tandis que 40-50 % sont rejetés dans les cours d'eau lors de l'amalgamation.

Orpaillage : A l'aide d'une pompe, l'eau puisée est restituée dans des lances à haute pression. Les jets désagrègent les sols entraînant une boue liquide vers une fosse. La boue est transférée vers une table inclinée recouverte de plans de moquette où l'or reste piégée. Enfin, les dernières boues reçoivent du Hg, qui s'amalgame aux fines paillettes d'or.

On estime les émissions globales de mercure à ~ 4 500 tonnes a^{-1} (Mason *et al*., 1994). Les humains introduisent dans le cycle global du mercure une quantité excédentaire de cet élément (~ 2 600 tonnes a^{-1}) qui, sans cela, resterait enfouie dans le sol, et en grande partie inactive dans les processus environnementaux (schéma en annexes). Les activités humaines comme l'exploitation minière ont pour effet de libérer plus de mercure des roches et des minéraux que les processus naturels d'altération. A l'état naturel, le mercure se dégage lentement des roches et des minéraux à mesure que la végétation et les intempéries les altèrent et/ou les érodent. Parmi les sources naturelles citons entre autres : les volcans, les sources hydrothermales, les incendies de forêt, le dégazage à l'interface air/eau et les émissions biogéniques (Nriagu, 1989 ; Mason *et al*., 1994). L'activité humaine n'a apporté que peu de changement au stock de Hg des sols (~ 300 10^9 tonnes dans les sédiments). Elle a principalement changé sa répartition, ses formes chimiques (ou spéciations) et ses concentrations par l'expression de nouveaux modes de dispersion (fumées, altération accrue des sols, rejets urbains, agricoles et industriels etc.). Par exemple, les niveaux en Hg atmosphérique sont deux fois plus élevés dans l'hémisphère Nord du globe que dans l'hémisphère Sud (UNEP, 2002). Les changements relatifs à l'activité humaine, depuis plus de 100 ans, soulèvent de nombreuses interrogations liées à l'augmentation des concentrations en Hg du vivant. Celle-ci a dors

et déjà été mesurée dans les sédiments de plusieurs lacs éloignés des sources ponctuelles et dans l'Arctique (Evans, 1986 ; Johnson, 1987; Rasmussen *et al*., 1998b).

2.3. Le mercure du bassin de l'Amazone

Les orpailleurs ou les sols ?

Si, à l'échelle globale, les parts des émissions naturelles et anthropiques de mercure sont relativement comparables, il est difficile de différencier à l'échelle locale la quantité (ainsi que l'impact environnemental) de Hg provenant de chacune des deux sources. La situation de l'Amérique de Sud l'illustre pleinement : l'utilisation mondiale de mercure aux fins de l'extraction de l'or s'établirait à au moins 500 tonnes a^{-1} (Lacerda 1997a, b, MMSD, 2002) dont près de la moitié le long du bassin de l'Amazone. Certaines régions du bassin de l'Amazone (particulièrement les zones alluvionnaires e.g., Rio Madeira) sont fortement contaminées par le mercure à cause de l'extraction de l'or à petite échelle. Le Hg y est présent non seulement dans les résidus miniers au niveau des sites d'exploitation et comptoirs commerciaux, mais aussi dans les sols, les végétaux, les sédiments et les cours d'eau. Par ailleurs, des niveaux critiques d'imprégnation par le Hg (> 10 µg g^{-1} de cheveux, **valeur limite** selon l'OMS) ont également été mesurés chez plusieurs populations amérindiennes éloignées de l'influence directe de tout site d'orpaillage (Carmouze *et al*., 2001). Des travaux récents (Roulet *et al*., 1999, 2001) ont, en effet, montré que les apports de Hg attribuables aux activités d'orpaillage et à la déforestation des 30 dernières années représenteraient moins de 3 % des concentrations cumulées dans les sols superficiels. Les sols tropicaux ont naturellement accumulé, durant plusieurs millions d'années, de grandes quantités de mercure *via* les retombées atmosphériques des émissions océaniques (Guédron *et al*., 2006) et volcaniques. Ils constituent de véritables réservoirs à Hg (de 10 à 30 mg m^{-2} dans les 20 premiers cm du sol) qu'ils stockent d'autant plus qu'ils sont riches en matière organique et en oxydes de fer.

Limite d'exposition : le cas du MMHg. Suivant les normes, on compte 4 valeurs distinctes de la dose journalière tolérable provisoire de MMHg. Pour un adulte de près de 70 kg elle représente :

Can : 0,2 µg kg^{-1} j^{-1}

USA : 0,3 µg kg^{-1} j^{-1}

OMS : 0,4 µg kg^{-1} j^{-1}

UE : 0,5 µg kg^{-1} j^{-1}

L'action locale de l'homme (comme les activités minières, la déforestation, l'agriculture, la construction de barrages et réseaux routiers) perturbe indirectement mais sensiblement les cycles naturels des métaux traces et parmi eux celui du mercure. Elle a pour effet de libérer plus de mercure des roches et des minéraux que les processus naturels d'altération atmosphérique. Celui-ci passe dès lors d'un milieu naturel à l'autre (vivant et

inanimé), est transporté sur de grandes distances et subit toute une chaîne de réactions chimiques. Dans les milieux aquatiques, le Hg peut être transformé chimiquement en monométhylmercure, la forme toxique que l'on retrouve dans les cheveux des Amérindiens. Le MMHg est très peu abondant au sein des biotopes aquatiques (colonne d'eau et sédiments) : il y représente le plus souvent moins de 1% du Hg. La production de MMHg dépend de nombreux facteurs qu'on ne comprend pas encore entièrement : la quantité de mercure inorganique, le type de bactéries, le pH, la quantité de matière organique ou la température. Cependant, même à partir des teneurs très faibles, voire négligeables, dans l'eau et les sédiments, le MMHg est capable d'atteindre des concentrations spectaculaires dans le tissu musculaire des espèces situées au sommet des réseaux alimentaires. A titre d'exemple, 1 mg de MMHg à partir de 10 millions de litres d'eau se concentre dans 1 kg de poisson.

2.4. Exemple d'impact sanitaire

Cas des Amazoniens du Tapajos

Chez la plupart des Amazoniens, les problèmes de santé liés au mercure sont légers (Lebel *et al*., 1996). Les concentrations de Hg mesurées dans les cheveux révèlent que 97 % des individus sondés ont un taux inférieur à 50 µg g^{-1}, seuil reconnu par l'OMS comme potentiellement dangereux pour la santé. La moyenne se situe aux alentours de 13 µg g^{-1} pour une valeur référence de 10 µg g^{-1} (voir encadré « MMHg et cheveux »). Cependant, malgré ces taux modérés, certaines populations de la rivière Tapajos semblent développer des problèmes neuromoteurs et visuels (Mergler, 2006). Il a également été mis en évidence une baisse de l'indice mitotique (nombre de cellules se divisant) chez des lymphocytes, soit une baise de leur capacité de se reproduire (Amorim *et al*., 2000). Les recherches effectuées ont permis de montrer que si les populations Amazoniennes ingèrent du Hg en quantité relativement modérée, elles le font de façon chronique. En effet, les populations bordant la rivière Tapajos sont de grandes consommatrices de poissons le plus souvent carnivores. Trônant au sommet de la chaîne alimentaire, elles ingurgitent le Hg accumulé au fil des maillons, de la bactérie au poisson en passant par le zooplancton. Suivant ces études, il est très probable que la durée d'exposition au mercure soit un facteur important dans les processus d'intoxication : l'exposition des Amazoniens est relativement faible, mais elle dure depuis plusieurs dizaines d'années !

2.5. Chronique d'une contamination annoncée

Construction de barrages en milieu tropical

Barrage : On estime que ~ 16 % de la production mondiale d'électricité provient de l'hydroélectricité. En Amérique du Sud, elle représente 25 % de la production totale d'énergie. Elle est de 30 % au Brésil, au Pérou, en Suède, en Islande et atteint jusqu'à 69 % en Norvège. L'hydroélectricité en France est la 2nde source d'électricité (13 %).

L'eau est un enjeu. Son utilisation à des fins énergétiques est d'autant plus manifeste que les besoins ne cessent d'augmenter au détriment des ressources disponibles. Une simple constatation : sur notre planète bleue moins de 2,5 % de l'eau est douce, moins de 33% de l'eau douce est fluide, moins de 1,7 % de l'eau fluide s'écoule dans les rivières ou les fleuves. Et l'Homme s'obstine à bloquer le cours de la fraction restante. Alors que la moitié des fleuves et des rivières subissent la régulation de **barrages**, leur construction ne cesse de s'accélérer à un rythme et une échelle sans précédents. Ainsi, un barrage est construit toutes les heures (World Commission on Dams, 2000) et leur nombre dépasse 45 000 (dont 22 000 en Chine, 6 400 aux Etats-Unis d'Amérique et à peine plus de 4 000 en Inde). La construction de barrages a pour vocation de permettre l'irrigation de diverses cultures, l'utilisation domestique ou industrielle de l'eau, la production d'hydroélectricité ainsi que la maîtrise des crues. Toutefois, plus un projet est ambitieux, plus ses conséquences sont lourdes et durables (jusqu'à plusieurs dizaines d'années). En noyant des vallées entières, la construction de barrages peut provoquer à la fois (i) des bouleversements humains en forçant des populations entières à se déplacer (barrage des Trois Gorges en Chine) et (ii) avoir un impact écologique en perturbant fondamentalement l'écosystème local (par exemple en empêchant la migration d'espèces aquatiques entre l'amont et l'aval d'un barrage). En modifiant le cours, les débits ou la qualité des eaux rejetées, les barrages conditionnent par ailleurs l'accès ainsi que le droit d'une partie des populations riveraines à l'eau (e.g., barrage Atatürk sur l'Euphrate en Turquie). Ils constituent un outil politique, économique et environnemental incontournable du 21ème siècle, aussi bien à l'échelle régionale, nationale qu'internationale.

Les réservoirs d'eau créés par les barrages et l'inondation des zones avoisinantes sont particulièrement préoccupants parce qu'ils instaurent des conditions favorables à la formation de monométhylmercure. En submergeant d'immenses surfaces, les barrages contribuent à une brusque dégradation de la matière organique (MO) contenue dans les sols ou la végétation. Celle-ci libère du Hg qui dans certaines conditions se transforme en MMHg susceptible de s'accumuler le long des chaînes alimentaires (World Commission on Dams, 2000). Selon Hydro-Québec, dans plusieurs réservoirs du Canada (e.g., complexe hydroélectrique La Grande,

barrage et la baie James), les concentrations en Hg des poissons sont supérieures à celles jugées sans danger pour la consommation par les humains ou par les animaux ichtyophages comme les loutres ou les huards. Près de ces barrages, les femmes enceintes et les enfants doivent s'en tenir à une consommation limitée de poissons (moins de 200 grammes par semaine d'une espèce contenant 1 µg g^{-1} de Hg). Ce constat n'est pas limité aux hautes latitudes, il s'applique surtout aux régions tropicales (e.g., barrage de Tucurui au Brésil, de Guri au Venezuela, d'Assouan en Egypte, de Mae-peum en Thaïlande). Une présence accrue de mercure, des conditions favorables de méthylation (températures stables et élevées, forte dégradation de la MO, intense activité bactérienne) et des changements notables de la chaîne alimentaire, expliqueraient les fortes teneurs en MMHg rencontrées dans les poissons des réservoirs tropicaux et en aval de ceux-ci. Ainsi, dans les lacs de barrage du Brésil, les organismes aquatiques sont en règle générale plus fortement imprégnés en MMHg que dans les milieux non perturbés situés en amont (Porvari, 1995). Par ailleurs, il est fréquent que des communautés humaines s'installent sur les rives des réservoirs néoformés construisant des villages et ouvrant des voies d'accès vers l'intérieur des terres. En procédant au déboisement, elles accroissent la lixiviation et l'érosion des sols et, par conséquent, l'exportation de Hg vers le milieu aquatique (Roulet *et al*., 1999). Finalement, la mise en eau de réservoirs amazoniens génère un risque de développement de maladies tropicales comme le paludisme, la fièvre jaune et la dengue. L'affaiblissement de l'état de santé des populations riveraines les rend dès alors plus sensibles à l'intoxication par le Hg *via* la consommation de poissons contaminés.

3. LE MERCURE EN GUYANE

3.1. Stigmates du mercure anthropique

Exposition manifeste de certaines populations amérindiennes

L'exploitation de l'or en Guyane s'est déroulée en deux cycles. Le premier cycle de l'or (1857-1950) correspond à la pénétration de l'intérieur guyanais avec la découverte de gisements sédimentaires détritiques ou alluvionnaires (appelés placers). Mais dès le premier quart du 20ème siècle, on assiste à une diminution de la quantité d'or dans ces placers. L'épuisement de la ressource aurifère et les difficultés d'approvisionnement liées aux deux guerres mondiales provoquèrent le déclin de l'extraction de l'or. Au bilan, 200 à 300 tonnes de mercure auraient ainsi été rejetées dans l'environnement guyanais lors du premier cycle de l'or. Après la seconde guerre mondiale, l'État français s'intéressa à la géologie de la Guyane. Un investissement des pouvoirs publics visant à améliorer cette connaissance permit le repérage de 18 sites miniers au début des années 1990. C'est pendant cette période que débute véritablement le deuxième cycle de l'or guyanais : des sociétés minières internationales investissent dans la prospection de l'or et, parallèlement, des exploitations artisanales se développent le plus souvent illégalement (Delannon, 2000).

La production totale d'or en Guyane Française varie suivant les sources : elle représente 3 tonnes a^{-1} pour la DRIRE, 6 tonnes a^{-1} d'après les déclarations aux services des douanes, 10 tonnes a^{-1} selon des sources non officielles tenant compte des exploitations illégales (Charlet et Boudou, 2002). C'est donc en gros entre 5 et 10 tonnes de mercure qui sont rejetées dans l'air, les sols et les rivières de Guyane chaque année. Ce chiffre peut raisonnablement se comparer avec les 200 tonnes a^{-1} rejetées à l'échelle du bassin de l'Amazone, un territoire 80 fois plus étendu. Les activités minières sont anciennes en Guyane ; toutefois les études réalisées à ce jour sur les sols guyanais montrent des teneurs uniformes et importantes en Hg sur toute leur profondeur (Guédron *et al.*, 2006). Sur les deux premiers mètres de profondeur, les sols ferrallitiques du craton guyanais cumulent entre 0,1 et 1 g m^{-2} de Hg. Il en résulte que la mobilisation, naturelle et/ou anthropique, d'une très faible fraction puisse s'avérer suffisante pour contaminer les réseaux trophiques aquatiques. Dès qu'il y a un déboisement, pour exploiter la forêt, valoriser une terre, creuser une route, extraire de l'or, etc.,

le Hg contenu dans les particules devient accessible. Les pluies denses opèrent un lessivage qui conduit le mercure dans les rivières ou dans les eaux stagnantes, dans lesquelles il rencontre des conditions optimales pour se transformer en monométhylmercure.

MMHg et cheveux : Le MMHg compose plus de 70 % du Hg des cheveux. La plus faible teneur pouvant engendrer un risque de neurotoxicité pour le fœtus fut évaluée par l'OMS à 50 µg g^{-1}. Appliquant une marge de sécurité, le seuil d'innocuité du MMHg dans les cheveux fut fixé à 5 µg g^{-1}. Il a été proposé une valeur de référence qui est de 10 µg g^{-1}.

Si l'exposition directe au mercure métallique (Hg^0) concerne essentiellement les orpailleurs, c'est principalement *via* sa forme monométhylée, contenue dans les poissons, qu'a lieu l'exposition des populations amérindiennes. En 1994, une étude est menée sur l'imprégnation par le monométhylmercure des **cheveux** de 500 personnes réparties sur l'ensemble de la Guyane (Cordier *et al*., 1994, 1997). Elle conclut à un niveau d'imprégnation moyen de 3,9 µg g^{-1} chez les hommes, de 2,4 µg g^{-1} chez les femmes et de 2,5 µg g^{-1} chez les enfants et met en évidence une forte imprégnation des populations Wayana des villages amérindiens du Haut Maroni. Une étude complémentaire (Fréry *et al*., 1999, 2001) souligne que l'exposition excessive au Hg est significativement liée à une forte consommation de poissons du fait de certaines espèces piscivores présentant des teneurs élevées en mercure. Sur 242 poissons analysés, ~ 15 % contenaient un taux de mercure supérieur à la norme de 0,5 mg kg^{-1} poids frais (le taux le plus élevé se situant à 1,62 mg kg^{-1}). En se fondant sur les habitudes de consommation de poisson des Wayana, on a déterminé que les adultes consommaient de 40 à 60 µg de mercure total par jour ; les nourrissons environ 3 µg j^{-1} ; les enfants âgés de 1 à 3 ans 7 µg j^{-1} ; ceux âgés de 3 à 6 ans environ 15 µg j^{-1} ; et enfin, ceux âgés de 10 à 15 ans en consommaient de 28 à 40 µg j^{-1} (la valeur limite hebdomadaire recommandée par l'OMS étant de 200 µg Hg organique). Plus de la moitié de la population présente un taux de mercure dans les cheveux supérieur à la dose recommandée par l'OMS (10 µg g^{-1} de cheveu), la moyenne se situant à 11,4 µg g^{-1}.

3.2. Phase I du programme « Mercure en Guyane »

Contexte politique et objectifs scientifiques

La première étude (menée par le Réseau National de Santé Publique / Institut de Veille Sanitaire) en 1994, ayant montré des niveaux élevés chez les communautés amérindiennes (Wayana et Emérillon) du Haut-Maroni, une deuxième étude était lancée en 1996 par le RNSP/InVS. Celle-ci déboucha sur la création d'une commission Mercure Solidarité Guyane ainsi que sur la prise de conscience à l'échelle nationale du problème lié au Hg en Guyane. En mars 2000, le Premier Ministre, Lionel Jospin, a demandé un

rapport sur l'orpaillage clandestin et l'utilisation du mercure à Madame Christiane Taubira, députée de Guyane. Ce rapport publié sous le nom de « L'or en Guyane Eclats et Artifices » proposait 28 recommandations précises permettant une évolution de la situation dans un sens positif. Toutefois, la population guyanaise attend toujours la mise en place effective des mesures préconisées : le groupe de travail chargé de suivre le dossier ne s'est réuni qu'une fois (proposition de résolution N° 1503). Au cours de l'unique réunion, le comité de suivi interministériel a demandé que les études épidémiologiques d'imprégnation déjà menées auprès des Amérindiens du Haut Maroni soient étendues à l'ensemble des populations des fleuves Maroni et Oyapock ainsi qu'à celles de Sinnamary soumises aux phénomènes de pollution mercurielle en aval du barrage de Petit-Saut (résultats en annexes). Par ailleurs, l'interdiction par arrêté préfectoral (8 juin 2004) de l'utilisation du mercure à partir de 2006 a été formulée. Elle ne résout cependant qu'une partie du problème. La majorité du mercure guyanais est d'origine naturelle tandis qu'une grande partie de la fraction anthropique est importée illégalement depuis le Brésil ou le Surinam (1 kg de Hg coûte l'équivalent d'1 g d'Au). Ainsi, on estime la production réelle d'or (i.e. quantité de Hg utilisée pour l'orpaillage) de 2 à 3 fois supérieure à la production déclarée (i.e. quantité de Hg importée légalement).

Sur ces constats, l'action publique décide, dès 1997, de s'intéresser plus avant aux conditions d'existence et du devenir du mercure, utilisé par l'orpaillage traditionnel, dans les écosystèmes guyanais. Citons ainsi Madame Christiane Taubira, députée de Guyane : « le développement de programmes de recherches sur la contamination par le mercure en Guyane revêt une importance primordiale » (Delannon, 2000). Ils doivent en effet fournir les éléments nécessaires aux prises de décisions adaptés, à la fois du point de vue de l'environnement (politiques de gestion et d'aménagement du territoire) et de santé publique (estimation des risques et définition des politiques sanitaires). Le programme scientifique pluriannuel « Mercure en Guyane » conduit dans le cadre du programme « Environnement, Vie et Société » du CNRS est mis sur pied par un groupe de chimistes, biologistes et hydrogéologues rattachés aux Universités de Grenoble, Bordeaux, Toulouse, Pau et Pays de l'Adour, à l'IRD et l'IFREMER. Financé dans le cadre des 11ème Contrat de plan et Docup Guyane, l'ambition de cette vaste étude était de mettre en lumière les processus biogéochimiques complexes qui permettent au mercure de traverser les écosystèmes et d'atteindre, par l'intermédiaire de la

chaîne alimentaire, les consommateurs terminaux. Il s'agissait également de documenter une situation guyanaise qui n'avait jusqu'à lors fait l'objet d'aucune étude importante, celles existantes décrivant le système amazonien sur la base de résultats obtenus essentiellement au Brésil.

Les principaux résultats de la phase I du programme « Mercure en Guyane » permettent aujourd'hui, grâce en partie au modèle étudié autour du barrage du Petit-Saut, de connaître les conditions de transfert du mercure de sa forme métallique (Hg°, métal liquide utilisé pour la réaction d'amalgamation par les orpailleurs) à sa forme organique toxique, le méthylmercure. Les processus en jeu, de la remobilisation au niveau des sols à la transformation sous l'effet de bactéries qui vivent dans les biotopes aquatiques peu oxygénés, ainsi que les phénomènes de bio-amplification le long des chaînes alimentaires, sont à présent parfaitement décrits ; les facteurs de risques liés à la contamination de l'environnement guyanais par le mercure sont identifiés (Rapports CNRS I & II, 2001).

3.3. Barrage de Petit-Saut, Guyane Française

Réacteur chimique du mercure

Entre 1976 et 1983 les besoins en énergie de la Guyane ont triplé, passant de 59 à 164 GWh. Compte tenu de l'accroissement démographique (~ 2,9 % en 2000), du développement de projets tels que Télédiffusion de France ou du Centre Spatial Guyanais (CSG), la consommation d'électricité a continué d'augmenter à raison de 10 % a^{-1}. En 2002, elle représentait près de 460 GWh (CIA World Factbook, 2005). C'est pour faire face à la demande et pour limiter l'importance des combustibles fossiles qu'en 1989 la décision de construction du barrage de Petit-Saut fut prise. Edifié par Electricité de France (EDF), le barrage de Petit-Saut est situé à la confluence du moyen Sinnamary et d'un cours d'eau mineur, la crique Cœur Maroni, dans le resserrement naturel favorable à une telle installation (coordonnées GPS, 5°03,45'N - 53°02,46'O). Sa construction s'achèvera en 1994 après quatre ans de travaux sans guère provoquer de mobilisations écologiques, à l'exception notable d'une campagne de banderoles le jour de la mise en eau. Avec une puissance de 116 MWh, la centrale hydroélectrique de Petit-Saut a fourni en 1999 près de la moitié (~ 47 %) de l'énergie électrique guyanaise.

La mise en eau du barrage a conduit à la création d'un lac

artificiel de 60 km de long par 60 km de large. Il s'agit de la plus grande retenue d'eau et surface immergée sur le territoire français (données CFBR, 2005). Avec une profondeur maximale de 35 m en son centre, la retenue recouvre près de 350 km^2 de forêt primaire pour un volume de 3,5 milliards de m^3 (Huynh *et al*., 1997). Le temps de résidence moyen des masses d'eau y est estimé entre 5 et 6 mois (Sissakian, 1997). Le réservoir est alimenté en permanence par le fleuve Sinnamary (débit moyen de 190 $m^3 s^{-1}$) et suivant les saisons *via* les cours d'eau (localement appelées « Criques ») Courcibo, Leblond et Tigre. Il est intéressant de noter que les criques Leblond et Courcibo drainent la zone minière de St.-Elie où l'or demeure exploité artisanalement. Deux mois après la mise en eau, la dégradation de la matière organique (MO) des sols et de la végétation immergée (certains troncs laissés sur pied mesurent près de 30 m de haut) a abouti à la stratification de la colonne d'eau (Richard *et al*., 1997). Le réservoir stratifié, quasi **méromictique**, est composé d'un épilimnion oxygéné depuis la surface jusqu'à 7 m de profondeur. Plus en profondeur, selon Horeau *et al*. (1998), l'hypolimnion anoxique est enrichi par un flux constant de produits de dégradation de la MO inondée (N ammoniacal, phosphates, acides humiques, etc.) et de matériaux relargués par le substrat géologique (fer, manganèse, silice et… mercure). En aval du barrage, le fleuve Sinnamary se prolonge sur 70 km et sous couvert forestier tropical jusqu'à l'océan Atlantique. Si l'on définit l'extension de l'estuaire par l'intrusion de la marée dynamique, une grande partie de ce fleuve est en fait son estuaire. Sur la base de la marée saline, il ne commence toutefois que dans les parages du village de Sinnamary. A la sortie des turbines, une cascade artificielle provoque l'oxygénation des eaux en grande partie issue de l'hypolimnion de la retenue. Toutefois, des produits réducteurs résiduels (e.g., sulfures, fer dissous, méthane) entraînent une consommation graduelle de l'oxygène apporté. La distribution de l'oxygène dissous vers l'aval adopte un profil en sac du pied du barrage à l'embouchure de l'estuaire.

Méromicticité : Un lac est méromictique si une certaine tranche d'eau qui le compose reste en dehors du brassage de la colonne d'eau lors des périodes de circulation.

En 2001 (phase I du programme « Mercure en Guyane »), sept ans après la mise en eau, seuls les 5 premiers mètres de la colonne d'eau étaient oxygénés. Tout le reste semble donc un milieu favorable tant à la réduction qu'à la méthylation du Hg (Charlet et Boudou, 2002 ; Amouroux *et al*., 1999). Les dosages de méthylmercure à diverses profondeurs dans le lac, et juste à l'aval du barrage, indiquent des concentrations moyennes de 0,50 ng L^{-1}, soit plus de dix fois celles mesurées en amont et dans les autres sites (Coquery *et al*., 2003). Ainsi, la retenue de Petit-Saut se

comporte comme un véritable réacteur biogéochimique capable de générer de fortes quantités de méthylmercure qui sont exportées vers l'aval, *via* les eaux profondes de la retenue qui alimentent les turbines du barrage. Les concentrations mesurées chez neuf espèces de poissons communes aux différentes stations (Courcibo, Leblond, retenue, aval du barrage) prouvent à nouveau le rôle clé du méthylmercure dans l'eau. Les poissons capturés juste en aval du barrage en accumulent nettement plus que ceux pris en amont et dans les autres sites, jusqu'à dix fois plus pour l'espèce *Curimata cyprinoides* (Boudou *et al*., 2005).

3.4. Phase II du programme « Mercure en Guyane »

Questions ayant guidé notre recherche

La seconde phase du programme « Mercure en Guyane » débute en 2003 impliquant des partenaires variés aussi bien en métropole que sur le territoire de la Guyane. En accord avec le Rectorat, l'inventaire, à l'échelle de l'ensemble de la Guyane, de la présence de Hg dans les hydrosystèmes a bénéficié de l'aide des scolaires sollicités pour l'échantillonnage de poissons (Aymaras), utilisés en tant que bioindicateurs de la contamination des cours d'eau par le méthylmercure. Le suivi de l'évolution de la zone du barrage de Petit-Saut et du Sinnamary, jusqu'à l'estuaire, a été mené en partenariat avec EDF et le laboratoire de biologie et de chimie HYDRECO. Une collaboration avec un site d'orpaillage va permettre d'étudier les processus géochimiques en jeu sur un chantier minier dans le but d'en améliorer les pratiques d'exploitation. D'autres collaborations avec des instituts de recherche (BRGM, Institut Pasteur) et des services de l'Etat (DRIRE, DIREN, DSDS, etc.), sont également en œuvre pour cette continuité d'étude de la problématique « mercure » en Guyane. De manière schématique, la phase II du programme repose sur l'approche pluridisciplinaire du cycle du mercure en milieu tropical suivant 4 axes principaux :

- L'axe I constitue un inventaire à l'échelle de l'ensemble de la Guyane des niveaux de contamination des cours d'eau par le mercure (échantillonnage de sédiments et de poissons).
- L'axe II (qui inclut le présent travail et la thèse de Y. Dominique) est consacré à l'étude des flux et processus biogéochimiques et écotoxicologiques au niveau du continuum retenue de Petit-Saut / Estuaire du Sinnamary.

- L’axe III se propose d’étudier le devenir des rejets mercuriels au niveau d’un site d’orpaillage à partir (i) de l’érosion naturelle, (ii) anthropique et (iii) de l’amalgamation sans recyclage du Hg^0.
- L’axe IV constitue un couplage des études à l’interface « Environnement / Santé », notamment pour définir les conditions d’exposition des populations guyanaises.

L’axe II de la phase II du programme « Mercure en Guyane » regroupe un large spectre d’analyses des principaux processus biogéochimiques et écotoxicologiques relatifs au cycle du Hg au niveau du continuum retenue de Petit-Saut / Estuaire du Sinnamary. L’aspect biogéochimique que constitue le contenu de cette thèse a été étudié pendant trois ans (de 2003 à 2005). Les 5 campagnes de prélèvement (désignées Matoutou-1 à 5), les suivis temporels (apports atmosphériques et exports de la retenue) ainsi que les expériences de terrain et en laboratoire, ont permis l’obtention de multiples données regroupées dans les 4 articles ci-après. Ceux-ci ont pour vocation d’apporter les réponses aux questions suivantes :

- Quelles sont les concentrations et variations du mercure atmosphérique au niveau de la retenue ?
- Quelle est l’importance de la réduction du mercure dans les eaux de la retenue ? Quelle est celle des retombées atmosphériques et du recyclage air / eau ?
- Quelle est la part des sources anthropiques de mercure vis-à-vis de celles naturelles ?
- Quelle est la production endogène de MMHg ? Se stabilise-t-elle ? Où sont les sites principaux de la méthylation ?
- Quelles sont les formes de mercure servant de substrat à la méthylation ?
- Quels sont les flux et les processus de transformation de mercure aux principales interfaces de la colonne d’eau ?
- Quels sont les exports annuels de Hg et MMHg de la retenue vers l’aval ?
- Quels sont les niveaux de contamination de l’Estuaire du Sinnamary ? Quelle y est l’importance des réactions de méthylation / déméthylation ?

- Quel comportement adopte le mercure à l'interface eau douce / salée ?

L'article 1 porte sur l'étude des processus d'échange de Hg entre l'air et l'eau et sur la spéciation du Hg à cette interface. Les données présentées proviennent surtout de différents exercices de suivis des concentrations d'espèces de Hg dans l'air, la pluie et les eaux de surface. L'article 2 met l'accent sur les sources, et la production de MMHg. Les flux entrants et sortants de la retenue, ainsi que la variation saisonnière des espèces dans la colonne d'eau y sont présentés. L'article 3 a pour objectif de comprendre les transformations de partitionnement, de spéciation et d'oxydo-réduction que subit le Hg et le MMHg lors de leur transition vers l'océan, via l'estuaire du Sinnamary. L'article 4 présente une étude de la complexation du Hg et du MMHg dans le continuum, et propose que le complexe $HgSO_4$ joue un rôle important lors de la méthylation. Ce dernier est préférentiellement formé dans les zones de fort gradient rédox.

Cette étude veut concourir à une meilleure connaissance du cycle du mercure et de sa dynamique spatio-temporelle dans les écosystèmes tropicaux permettant de comprendre comment ce métal toxique se propage jusqu'aux poissons et à l'Homme tout en étant à peine détectable dans l'eau. Elle permettra aussi d'analyser l'impact des grands aménagements (tels que les sites miniers ou hydroélectriques) sur la dynamique du Hg et ses conséquences en matière de Santé Publique.

Article I

Spéciation et flux de mercure à l'interface air / eau d'un lac artificiel en milieu tropical, Guyane Française

RESUME

Afin d'évaluer les échanges entre l'atmosphère et la retenue de Petit-Saut (Guyane Française), la distribution et la spéciation du mercure (Hg) ont été étudiées pendant plus d'un an (2003-2004) dans l'air, la pluie et les eaux de surface. Dans l'air, le mercure total gazeux (TGM) est composé à 98 % de mercure élémentaire gazeux (GEM) et représente 12 ± 2 pmol m^{-3}. Le mercure réactif gazeux (RGM) compose moins de 1 % du GEM et représente 4 ± 3 fmol m^{-3}. Le GEM suit un cycle jour-nuit aux concentrations fortes (plus de 15 pmol m^{-3}) le matin et plus faibles (moins de 5 pmol m^{-3}) le soir ; RGM et GEM s'opposent. Dans la pluie, la somme des espèces mercurielles non filtrées (HgT_{UNF}) vaut 16 ± 12 pmol L^{-1}. Le suivi des précipitations témoigne de fortes concentrations de HgT_{UNF} en saisons sèches (jusqu'à 57,5 pmol L^{-1}) et de plus faibles en saisons humides (jusqu'à 2,7 pmol L^{-1}). Les formes réactives (HgR_{UNF}), gazeuses dissoutes (DGM) et monométhylées ($MMHg_{UNF}$) du mercure non filtré composent respectivement 20, 5 et 5 % du HgT_{UNF}. Les concentrations de ces formes de Hg corrèlent positivement entre elles mais inversement avec le pH de la pluie. Dans les eaux de surface, la somme des espèces mercurielles dissoutes (HgT_D) vaut 3,4 ± 1,2 pmol L^{-1} dont ~ 10 % sont composés de DGM. Le DGM présente de fortes concentrations en saison sèche (480 ± 270 fmol L^{-1}) et de plus faibles au cours des saisons humides (230 ± 130 fmol L^{-1}). Le suivi jour-nuit des concentrations témoigne de processus photochimiques de production

(environ 60 fmol L^{-1} h^{-1}) et de cycles biologiques d'oxydation / réduction à l'échelle de quelques minutes (d'amplitude > 100 fmol L^{-1}). Finalement, à l'aide de modèles conceptuels couplant réactions, transports et bilan de masse à l'interface air / eau, nous avons calculé les flux de Hg entre la retenue de Petit-Saut et l'atmosphère avoisinante. La quantité de Hg déposée à la surface des eaux représente 14 moles a^{-1} tandis que l'évasion du Hg vers l'atmosphère atteint 23 moles a^{-1}. Comparativement, ~ 75 % du dépôt atmosphérique total empruntent la voie constituée par la pluie.

Statut : en cours de soumission à « Science of The Total Environment »

Mercury speciation and exchanges at the air-water interface of a tropical artificial reservoir, French Guiana

B. Muresan*, D. Cossa*[1] , S. Richard** B. Burban**

**Institut français de recherche pour l'exploitation durable de la mer (IFREMER), BP 21105, F.44311 Nantes cedex 3, France (EU)*

***HYDRECO, Laboratoire de Petit-Saut, BP 823, F.97388 Kourou, French Guiana (EU)*

ABSTRACT

The distribution and speciation of mercury (Hg) in air, rain, and surface waters from the artificial tropical lake of Petit-Saut in French Guiana were investigated during the 2003/04 period in order to probe its role as a source. In the air, total gaseous mercury (TGM) at the dam station averaged 12 ± 2 pmol m^{-3} of which 98% was gaseous elemental mercury (GEM). Reactive gaseous mercury (RGM) represented less than 1 % of the GEM with a mean concentration of 4 ± 3 fmol m^{-3}. GEM distribution depicts a day-night cycling with high concentrations (up to 15 pmol m^{-3}) at dawn and low concentrations (down to 5 pmol m^{-3}) at nightfall; RGM and GEM varied conversely. In the rain, the sum of all Hg species in the unfiltered (HgT_{UNF}) averaged 16 ± 12 pmol L^{-1}. Temporal distribution of HgT_{UNF} exhibited a pattern of high concentrations during the late dry seasons (up to 57.5 pmol L^{-1}) and low concentrations (down to 2.7 pmol L^{-1}) in the course of the wet seasons. Unfiltered reactive (HgR_{UNF}), dissolved gaseous (DGM) and monomethyl ($MMHg_{UNF}$) mercury orderly composed 20, 5 and 5 % of HgT_{UNF}. All measured Hg species were positively interrelated and displayed negative relationships with the rain pH. In surface waters, dissolved total mercury

[1] Corresponding author (Tel.: 33 2 40 37 41 76; Email: dcossa@ifremer.fr)

(HgT_D) averaged 3.4 ± 1.2 pmol L^{-1} of which ~ 10 % were composed by DGM. The former showed a trend of high concentrations during the dry season (480 ± 270 fmol L^{-1}) and lower (230 ± 130 fmol L^{-1}) in the course of the wet seasons. On a shorter timescale, diel variations included diurnal photo-induced DGM production (of about 60 fmol L^{-1} h^{-1}) coupled to minute to hour biologically mediated oxidation / reduction cycles (of > 100 fmol L^{-1} amplitude). Finally, using reaction-transport conceptual models and a mass balance calculation with well constrained AWI concentrations, we determinated the reservoir Hg exchanges with the immediate atmosphere. The calculated fluxes showed that atmospheric Hg inputs to the Petit-Saut reservoir represented 14 moles yr^{-1} whereas DGM evasion reached 23 moles yr^{-1}. Apportionment among forms of mercury deposition indicated that ~ 75 % of the total Hg invasive flux follow the rainfall pathway.

Keywords: Atmosphere; Artificial reservoir; Mercury; Speciation; Fluxes

1. INTRODUCTION

Divalent inorganic mercury (Hg^{II}) in natural surface waters follows two main alternative pathways. It can either be methylated and transferred to the aquatic food webs or, alternatively, be reduced to elemental mercury (Hg^0) and then evolved into the air. Thus, the rate of reduction is of fundamental importance, since this reaction would contribute restricting the quantity of Hg^{II} available for bioaccumulation and auxiliary toxicity in predator animals and human consumers. Because of its high residence time (~ 1 year), mercury is dispersed in the troposphere as gaseous elemental mercury (GEM) (Fitzgerald *et al*., 1991). However, in the last few years, accumulating evidence has shown that GEM is quickly oxidized as "reactive gaseous mercury" (RGM, presumably composed of $HgCl_2$) in the atmosphere, leading to a rapid and intense re-deposition on water surfaces (Lindberg and Stratton, 1998). More deposition may also mean more re-emission because the ambient background concentration of GEM appears quite stable. Thus, for understanding the processes and quantifying the net exchange, mercury speciation in the atmosphere, as well as speciation in deposition, must be documented. A significant number of studies have provided such data in boreal, temperate and marine environments (e.g., Schroeder *et al.*, 1998; Hedgecock and Pirrone, 2001, Mason and Sheu, 2001 Laurier *et al.*, 2003), while few are available for tropical ecosystems.

In tropical areas, the high temperatures may favor evasion and the high rainfall deposition. The high density of the vegetation favors recycling with high evasion and scavenging through the foliage (Lindberg and Zhang, 2000). In the Amazon basin, in addition to environmental conditions, anthropogenic damage (the burning of forest, gold mining and erosion) may make mercury recycling through air and water even more active. Based on data for the initial burning of primary forest and annual deforestation rates, Roulet *et al*. (1998 and 2000) estimated that forest burning releases 6 to 9 tons of Hg yr^{-1}. According to Pfeiffer *et al*.

(1989) roughly half of the mercury emitted from gold mining activities (~ 200 tons of Hg yr^{-1}) would be released into the atmosphere and the other half into the rivers. Hence, gold mining activities appear as the source of about 60% of the mercury present in the Amazonian atmosphere (Artaxo *et al*., 2000). By increasing the ambient air levels of Hg, anthropogenic activity results both in the increase of direct human exposure and the increase of mercury flux entering terrestrial and aquatic ecosystems, leading to elevated concentrations of monomethylmercury in freshwater fish and marine biota. For Mangal (2001), the intense convection in the Amazon, together with the long residence times for atmospheric mercury, make regional atmospheric GEM transport quite efficient. This contributes to the indirect Hg impregnation of the Amerindian populations who are not apparently involved in gold mining or any other environmental by damaging activities. Such a contingency might have a great impact on levels of atmospheric mercury in tropical regions.

Even if located outside the Amazon catchment area, the French Guiana territory presents several characteristics of an Amazonian environment: climate, soils, vegetation, gold mining, etc.. Soils have been shown to be mercury rich (Roulet *et al*., 1998) and gold mining began in the second part of the 19^{th} century. According to the DRIRE (French Agency for Regional Industry, Research and Environment), the official gold production between 1857 and 2002 has been estimated at about 200 tons corresponding to 200-300 tons of mercury disseminated into the Guianan environment. Starting a few years ago, the amount of mercury released into the atmosphere was tended to decrease: it is partially recuperated through distillation and re-used (up to three times). This was long overdue since recent research has demonstrated that the Guianan gold mining activities are (at least indirectly) responsible for the local exposure of Amerindians (Cordier *et al*., 1994; Fréry *et al*., 1999, 2001). The main source of Hg consisted of the daily consumption of heavily contaminated fishes: ~ 15 % of piscivorous fishes exceeded 0.5 µg g^{-1} Hg, fresh weight. On the Sinnamary basin, gold mining

has been active since 1866 at the site of Adieu-Vat and in the St Elie region. According to Petot (1993), local gold production since the end of the last century (probably underestimated) would have been around 27 tons. The corresponding amount of mercury rejected into the immediate environment would be approximately 23 tons. According to Richard *et al*. (2002), the recent survey of the Sinnamary River has permitted the detection of elevated concentrations of Hg in some fish species, especially piscivorous (up to 1.94 µg g^{-1}, fresh weight). In the 1990s, the Sinnamary River was harnessed by the construction of the Petit-Saut hydroelectric dam and the filling of its artificial reservoir started in 1994 (Fig. 1). The development of such a neotropical body of water has brought about considerable changes in water quality and the natural Hg cycling of the ancient basin of the Sinnamary River.

The Petit-Saut hydroelectric reservoir is located in the tropical forest of French Guiana on the Sinnamary River (Fig. 1). The Sinnamary is 250 km long and has its source in the center of French Guiana at an altitude of 125 m. Its catchment area spans over 7000 km² of crystalline formation overgrown by uninhabited primary forest. The Courcibo and the Tigre tributaries run into it. The Petit-Saut hydroelectric dam was built between 1989 and 1994, some 70 km e upstream of the Sinnamary outlet to the Atlantic. The impounding of the Sinnamary and its tributaries started in Jan. 1994 and was completed in July 1995. As a result, the he reservoir lake (5°04’ North, 53°03’ West) stretched over 60 km length and 60 km in width. At that time, the maximum water depth reached 35 m. This depth corresponded to the immersion of approximately 350 km² of uncleared primary forest and the creation of about 105 km² of small islands (Huynh *et al.,* 1997). During the 2003-2004 period, water depth maxima averaged 32 m. The filling of the Petit-Saut hydroelectric dam generated major modifications in the water chemistry of the Sinnamary River. Initially, the waters were warm, acidic, only slightly conductive, oxygenated, nutrient poor and relatively homogeneous (Horeau *et al.*, 1998). As the forest and fluvial ecosystem became a lacustrine environment

thermal stratification occurred and the waters of the reservoir were subjected to the rapid development of an oxygenated epilimnion and an anoxic hypolimnion (Richard, 1996).

In June 1998, TGM concentrations were investigated in the vicinity of the reservoir for a 24 hour period by Amouroux *et al.* (1999); the authors found a tendency for diurnal variation and an average of Hg^0 concentrations of 14 ± 7 pmol m^{-3} (n = 19). Inspired by this study, the present work focuses on the impact of the Petit-Saut reservoir on the local atmospheric cycling of Hg. It is based on data collected during a one year monitoring (Apr. 2003 - Apr. 2004) in the atmosphere of the Petit-Saut reservoir for total (TGM = GEM + RGM) and reactive (RGM) gaseous mercury. Specifically, atmosphere sampling for TGM took place from April 2003 to April 2004 whereas RGM measurements were made from January to April 2004. Further monitoring for TGM and RGM corresponded to a shorter period between November 2004 and January 2005. Mercury speciation in unfiltered precipitations was measured weekly between April 2003 and January 2005. Samples were collected about 200 m in front of the Petit-Saut dam and consisted of total (HgT_{UNF}), reactive (HgR_{UNF}), dissolved gaseous (DGM) and monomethyl ($MMHg_{UNF}$) unfiltered mercury measurements. Finally, DGM analyses and monitoring were also made seasonally in the surface waters of the reservoir. Here, we used the measured concentration and speciation of Hg in air, rain and water samples in combination with interfacial transportation models to: (i) examine the atmospheric cycling of Hg in the tropical region of the Sinnamary basin (ii) describe Hg transformations in the surface waters of the neoformed Petit-Saut reservoir (iii) establish a mass balance calculation for Hg exchanges between the reservoir and the surrounding atmosphere. In a general way, the current study aims to demonstrate the role of the Petit-Saut reservoir as a source of elemental Hg for the atmosphere.

2. MATERIAL AND METHODS

2.1. Sample collection

2.1.1. Air sampling

In the immediate vicinity of the Petit-Saut dam, temporal distribution and speciation of atmospheric Hg were studied for nearly one year (2003-2004). TGM measurements were obtained by using an automated Tekran Model 2537A mercury vapor analyzer. Both gaseous elemental (GEM) and reactive gaseous (RGM) mercury were simultaneously measured. RGM was specifically sampled using the Tekran Model 1130 Speciation Unit in connection to the 2737A Model. Durations of 5 and 180 minutes were adopted as sampling time resolution for TGM and RGM respectively. Excepting the months of September and October 2003, TGM (thereafter GEM) was uninterruptedly measured from April 2003 to April 2004. The temporal distribution of RGM was fully recorded from January 2004 to April 2004. Additional samplings for TGM were made on April ,1st 2005 a few meters downstream of the outflow of the turbines in the vicinity of an artificial aeration system set up in order to maintain the downstream concentrations of O_2 compatible with aquatic life. Since the turbines are fed with water from the anoxic part of the reservoir, TGM measurements locally accounted for the partial degassing of discharged hypolimnetic waters during the aeration process.

2.1.2. Rain sampling

Wet deposition was collected at the HYDRECO field laboratory station about 200 m downstream from the dam (Fig. 1). Compiled data account for approximately 20 months of regular sampling from Apr. 2003 to Dec. 2004. Samples for rainfall amount, conductivity, pH and occasionally total organic carbon (TOC) determinations were collected by means of a polyethylene bag. For mercury, the collection system consisted of a 14 cm diameter Teflon (PTFE) funnel attached to a 500 mL acid-clean Teflon (FEP) bottle. A 16 cm long flute of

Teflon (PTFE) gently drove the rainfall water directly from the base of the funnel to the bottom of the bottle. Samples for mercury were collected on a weekly basis using ultra-clean sampling techniques. The high precipitation (up to 150 mm hr^{-1}) rate allowed rapid collection of the necessary rain amount for analyses and thus limited the mercury photo-reduction and adsorption processes to the duration of the rain event (in the range of 5 to 10 minutes). Bottles were double bagged then frozen at –20 °C in dark conditions. Precipitation waters were analyzed for HgT_{UNF}, HgR_{UNF}, DGM and $MMHg_{UNF}$ (see below for definitions).

2.1.3. Surface water sampling

Surface water samples were collected just below the air-water interface by immersing an acid clean Teflon bottle (FEP) by gloved hand (Fig. 1). Analyses of dissolved gaseous mercury (DGM) were performed within 2 hours of collection. The sum of all the mercury species (HgT_{UNF}) along with the dissolved (HgT_D) and reactive (HgR_{UNF} is the easily reducible fraction obtained by pH 1 direct reduction with $SnCl_2$) fractions were processed the same day. In addition, aliquots were kept to determine monomethylmercury (MMHg) in the unfiltered ($MMHg_{UNF}$), dissolved ($MMHg_D$) and the particulate ($MMHg_P$) phases. Water samples were filtered using hydrophilic Teflon membranes (0.45 µm pore size, 45 mm diameter, LCR®, Millipore), then acidified with 0.5 % (v/v) HCl (Suprapur®, Merck). For each sample, the filtered amount of water was gravimetrically determined. Used filters (particulate samples) and corresponding filtered solutions were ultimately double bagged and stored at –20 °C in dark conditions until analysis.

2.2. Sample analysis

2.2.1. Ancillary variables

In the epilimnion, measurements for temperature, pH, dissolved oxygen, conductivity and redox were determined *in situ* by means of an YSI multiparameter probe sonde 600XLM.

Additional analyses for organic matter (OM) content, pH and conductivity in atmospheric wet deposition were carried out at the HYDRECO field laboratory. Total organic and inorganic carbon in the global and the dissolved fractions were analyzed by IR spectroscopy after oxidative or acidic digestion of the samples.

2.2.2. Atmospheric gaseous mercury

Automated mercury speciation analyzer systems were concurrently used during the field measurement study. The analyzer systems included a Tekran Model 2537A, which was used together with a Model 1130 Speciation Unit to simultaneously monitor GEM and RGM in air. This instrumentation and its implementation are described in detail by Poissant *et al*. (2005). The analytical train of the Tekran 2537A instrument is based on the amalgamation of mercury onto gold cartridges followed by a thermodesorption and analysis by cold vapor atomic fluorescence spectrophotometry providing analysis of GEM in the air at sub-pmol m^{-3} levels. The dual cartridge design allows alternate sampling and desorption, resulting in continuous measurement of mercury in the air stream. The systems allowed a fully automated operation with both components being concurrently measured. The analytical precision was estimated to be better than 2%. During sampling, RGM in the atmosphere was captured in the Model 1130 KCl-coated quartz annular denuder module. The denuders collect oxidized RGM compounds with a diffusion coefficient >0.1 cm^2 s^{-1} that readily adheres to a KCl coating at 50 °C. GEM passed through RGM speciation unit and was continuously analyzed by the Model 2537A. The RGM component was then desorbed during the analysis phase. The 1130 speciation unit was configured to collect 3 hour samples at a 10 L min^{-1} flow rate. During the 3 hours sampling period, the 2537A analyzer continuously quantified 5-min GEM samples. After the 3 hour sampling period, the 1130 Speciation Unit was flushed with Hg-free air then RGM was thermodesorbed and analyzed. The annular denuder was heated to 500 °C for 15 min. Thus, collected RGM was thermally decomposed into an Hg-free air stream and

subsequently analyzed as GEM, respectively. The denuders were biweekly reconditioned using the Tekran protocol (Tekran, 2001). Finally, the internal temperature of the whole apparatus was set to 50 °C in order to prevent any moisture related amalgamation artifacts.

In 2005, some air measurements were made in the vicinity of the aerators located at the tailrace of the turbine where the TGM concentrations were high. We used a portable a mercury analyzer RA-915+ (LUMEX) allowing us to get TGM data in a continuous mode with a detection limit of 10 pmol m^{-3}. The RA-915+ mercury analyzer employs the atomic absorption spectrometry technique, which is implemented using the direct Zeeman Effect.

2.2.3. Mercury speciation in water

All mercury species in water samples were detected by cold vapor atomic fluorescence spectrometry (AFS), a 2500 model detector from Tekran or a Merlin instrument from PSA. Dissolved gaseous mercury (DGM, mainly Hg^0) analyses were processed onto 100 mL of unfiltered aliquots of sampled water. Samples for DGM were sparged for 20 min with Hg-free argon at 200 mL min^{-1} within 2 hours after collection. The divalent "total" (HgT) and "reactive" (HgR) mercury were determined in compliance with Bloom and Fitzgerald (1988), by the formation of volatile elemental Hg and its preconcentration on a gold column before its AFS measurement. HgR is an easily reducible fraction, which is obtained within 4 hours of sampling by direct reduction with $SnCl_2$. The HgR is thought to consist mostly of inorganic mercury compounds (except for sulfide or selenide) and labile organic complexes (Lamborg, 2003). HgT is obtained with a similar method applied to a sub-sample oxidized with acidic BrCl for 30 minutes. The detection limits, defined as 3.3 times the standard deviation on the blanks, depend of the water volume of the sample analyzed and were usually 0.05 pmol L^{-1} for the HgT and HgR, and 0.025 pmol L^{-1} for DGM. The reproducibilities (the coefficient of variation in percentage of five replicate samples) were lower than 10 %. The accuracy for HgT determinations was regularly checked, using the reference material (ORMS-3) from the

National Council of Canada as certified reference material (CRM). Monomethylmercury (MMHg) was determined in the unfiltered ($MMHg_{UNF}$) and dissolved ($MMHg_D$) phases using the method initially proposed by Bloom (1989) and modified by Liang *et al*. (1994) and Leermarkers *et al*. (2001). The water samples were stored with 0.5 % (v/v) HCl, which is a reliable method for a 3 week storage period (Parker and Bloom, 2005). MMHg in acidified water was extracted by CH_2Cl_2 and then transferred into 40 mL of Milli-Q water by evaporating the organic solvent. The aqueous solutions were analyzed for MMHg by gas chromatography after ethylation and adsorption / desorption on a Tenax® column. For particulate MMHg (i.e. $MMHg_P$), a 3 hour acidic dissolution (HNO_3 65 %) of the filtered SPM took place before the procedure described previously. Detection limits were 0.01 pmol L^{-1} and 0.005 pmol g^{-1} for respectively a 100 mL water and 200 mg solid sample. Precision surpassed 10 % for all analyses. Using the available reference material (IAEA-405), the accuracy of the method was estimated to be more than 10 % with 91 ± 8 % recovery. The detailed procedure is given by Cossa *et al*. (2002 and 2003).

3. TROPOSPHERIC AND SURFACE WATER CHARACTERISTICS

The convergence of the streams of trade winds generated by the Azores and the St. Helena anticyclones results in the formation of the low intertropical convergence zone (ICZ). The ICZ is animated by an oscillatory movement reflecting the apparent seasonal changes in the inclination of the Earth. This feature determines a seasonal pattern of four uneven periods, consisting of the short wet season (from the middle of November to the middle of February), the short summer of March, the long wet season (from April until July) and the long dry season (from the middle of August to middle of November). The precipitations vary from 1700 mm yr^{-1} in the Northwest to 3800 mm yr^{-1} in the region of Régina-Cacao, i.e., eastward of the Sinnamary basin. The annual recorded rainfall is 3000 mm on average on the shore line

from Kourou to Cayenne and reaches 2500 mm on the regions inland. Rains are generally plentiful, of short duration and often occur at night. The average intensity of the precipitation is approximately 30-40 mm hr^{-1}, their duration is of the order of 5 to 10 minutes. Crests can exceed 150 mm hr^{-1} but the duration of such showers is approximately one minute (Meteo-France, weather reports).

Atmospheric gaseous compounds and/or aerosols display both anthropogenic and natural sources. Anthropogenic sources are all located along the shoreline and regroup guianese industry (power facilities, the European Space Center etc.), the car induced rejections and the biomass burning. Natural sources mainly consist of the Atlantic Ocean, the ferralitic soils and the overlying vegetation. Despite the fact that sources may change with time, it is possible to monitor their proper signature (Richard, 2001). In wet seasons, oceanic air masses spread over French Guiana: this source is apparent through sodium, sulfate and magnesium loaded aerosols (up to 50, 8 and 5 nmol m^{-3}, respectively). According to Holy (1976), the average evaporation of water is estimated to be about 1600 mm yr^{-1}. Hence, the local importance of the oceanic source would (at least partially) originate from the long exposure to the sun which usually exceeds 2000 h yr^{-1} and can reach up to 7 kWh m^{-2} d^{-1}. In dry seasons, the intensification of slash-and-burn agriculture induces higher potassium, nitrates and oxalic acid levels (up to 10, 5 and 0.9 nmol m^{-3}, respectively). According to Richard (2001), in 1999, the acidity of rainfall significantly correlated with its measured organic acid content. To illustrate, between the wet and the dry season of 1999, pH increased from 5.2 to 4.9 concurrently to a doubling in oxalic and acetic acid concentrations. As a result the anthropic activity may define an important source of volatile organic acids to the local atmosphere including rain and aerosols.

Average temperature in surface waters (at 0.5 m depth) from the Petit-Saut reservoir for the 2003/04 period was 29.7 ± 0.6 °C (roughly equivalent to that in the atmosphere, 27.3 ±

0.5 °C). Unlike temperature, pH (6.2 ± 0.2 *vs* 4.6 ± 0.4 units) and conductivity (21.4 ± 0.4 *vs* 14 ± 8 µS cm^{-1}) exhibited higher values in the first centimeters of the water-column than in rain. This observation presumably resulted from the slightly buffered milieu of the Petit-Saut reservoir due to the alteration of the Fe and Al hydrous oxides from soils and clay minerals such as kaolinite. The rain lower but more variable (from 7.3 to 38.0 µS cm^{-1}) conductivity also suggests that its ionic content and/or sources undergo significant changes during the duration for the whole year. In surface waters, high conductivity (i.e. lowest pH: 4.4 units) depicted the dry seasons whereas low conductivity (i.e. highest pH: 5.0 units) the wet seasons. Regarding the redox (Eh), maxima were measured in the dry season (340 ± 20 mV) and minima in the wet seasons (290 ± 20 mV). According to Dumestre *et al*. (1999), the dry season is a period of high primary production and development of phytoplanktonic and phototrophic bacterial communities. This hypothesis was supported by the positive correlations between redox and the percentage of O_2 saturation in the surface waters (r^2 = 0.77; $Eh_{mV} = 3\ [O_2]_{\%} + 50$) along with the particulate organic carbon (POC) concentrations (r^2 = 0.59; $Eh_{mV} = 150\ [POC]_{mmol\ L\text{-}1} + 300$). Since total organic carbon in rain average 0.10 ± 0.06 and 0.39 ± 0.03 mmol L^{-1} in surface waters, rainfalls contribute to the dilution with OM of the first centimeters of the reservoir water column. The low rain pH (below 5) may additionally support the mobilization of metallic species, such as Al, Fe or Mn, from the partial dissolution of aerosols, poorly crystallized clay minerals and/or AWI suspended particulate matters.

4. RESULTS

4.1. Mercury in air

During the 2003-2004 period, TGM at the HYDRECO laboratory station averaged 12 ± 2 pmol m^{-3}. This was similar to the mean North Atlantic level of 11.5 pmol m^{-3} measured by Slerm and Langer (1992). The GEM composed more than 98 % of TGM. Maxima of GEM concentrations were usually measured in wet seasons (14.5 pmol m^{-3}) and minima in the dry season (9.8 pmol m^{-3}). Typically, GEM displayed a significant ($p \leq 0.05$) increase with the percentage of rainfall excess ($r^2 = 0.45$; n = 11 and $[GEM]_{pmol\ m\text{-}3} = 0.03\ \%Rain_{exce} + 12.3$). Regarding its diurnal distribution, GEM depicted a regular nycthemeral cycle with high concentrations (up 15 pmol m^{-3}) measured at dawn and low concentrations (down to 5 pmol m^{-3}) at nightfall (Fig. 2). RGM represented less than 1 % of GEM with a mean concentration of 4 ± 3 fmol m^{-3}. Measured concentrations varied from the apparatus limit detection (close to 0.05 fmol m^{-3}) up to 180 fmol m^{-3}. These were in the same range as RGM data from temperate climate location: e.g., from the St. Anicet region on the St. Lawrence River in Quebec, Canada (Poissant *et al.*, 2005). It is worthwhile to note that RGM and GEM varied in mirror (Fig. 2). The minimum of GEM, usually observed during the late day period, corresponded to a maximum of RGM in the atmosphere. Finally, particulate MMHg was measured during the short dry (April 2003) and the long wet (June 2004) seasons. Sampled filters (a 0.2 µm Teflon filter from the Tekran 2537A unit) accounted respectively for 21 and 9 days of particulate $MMHg_P$ accumulation. Compared to the collected amount of particles, atmospheric $MMHg_P$ concentrations were 310 and 10 pmol g^{-1} with respect to the short dry and long wet seasons. If the sampled air volume is considered, $MMHg_P$ concentrations for the same periods of the year were 0.75 and 0.07 fmol m^{-3}.

The TGM measured downstream from the dam at the tailrace of the turbine ranged from below the detection limit of the LUMEX detector (~ 10 pmol m^{-3}) to 115 pmol m^{-3}. The

average concentration was 47 ± 21 pmol m^{-3} for 78 discrete values measured between 06:30 and 10:00 in the morning. Highest concentration occurred with the H_2S odors. Reaching the artificial aeration system, a vertical profile (from the AWI to 2 m height) of TGM was additionally determined in order to examine the Hg volatilization from dam discharged waters (Fig. 3). Maxima of concentrations were measured at the AWI (380 ± 330 pmol m^{-3}) and showed a marked variability (from 95 to 1060 pmol m^{-3}). Higher up, TGM levels underwent a pronounced decrease within the first centimeters: from 380 ± 330 to 120 ± 20 then 33 ± 2 pmol m^{-3} orderly at AWI, 0.5 and 1 m height. Concerning lateral variations, TGM concentrations were measured on the same day in the vicinity of the aerators, on the reservoir and near the HYDRECO laboratory (Fig. 3). As for the vertical distribution, lateral TGM concentrations rapidly diminished with increasing distance from the artificial cascade constituting the aeration system. To illustrate, at 1 m height, TGM rose from 23 ± 11 to 13 ± 4 then <10 pmol m^{-3} at 10, 50 and 200 m distance from the aeration system. The low concentrations (<10 pmol m^{-3}) indicated that, at these locations and time of year, the plume gas evolved from the aerators was mostly diluted in the atmosphere.

4.2. Mercury in rain

HgT_{UNF} concentrations in the wet season the deposition collected between Apr. 2003 and Dec. 2004 near the HYDRECO laboratory (84 rain events) averaged 16 ± 12 pmol L^{-1} (Table 1). This is within the range of concentrations (17.8 ± 2.9 pmol L^{-1}) of the South and equatorial Atlantic environments measured by Lamborg *et al*. (1999). Temporal distribution of HgT_{UNF} exhibited a pattern of high concentrations during the late dry season (up to 57.5 pmol L^{-1} in Nov. 2004) and low concentrations in the course of the wet season (down to 2.7 pmol L^{-1} in Mar. 2004). Besides HgT_{UNF}, the speciation of mercury was investigated through HgR_{UNF}, DGM and $MMHg_{UNF}$ analyses (Fig. 4). Reactive mercury composed approximately 20 % of HgT_{UNF}. With concentrations varying from 0.1 to 20.8 pmol L^{-1}, its temporal

distribution revealed a positive correlation with that of HgT_{UNF} (r^2 = 0.54). The temperature dependence of the Henry coefficient (H = 466 atm mol^{-1} at 28 °C) resulted in low DGM concentrations of rain (0.8 ± 0.9 pmol L^{-1}). As a matter of fact, DGM composed 25 % of HgR_{UNF} and close to 5 % of HgT_{UNF}. The DGM displayed an analogous temporal distribution to HgR_{UNF} (r^2 = 73) and therefore HgT (r^2 = 0.42). Regarding $MMHg_{UNF}$, concentrations varied widely from 0.05 to 10.2 pmol L^{-1} with a mean value around 0.8 pmol L^{-1}. These were in the high range of values found in the literature (0.2-0.8 pmol L^{-1}; Bloom and Watras, 1989; Mason *et al.*, 1997; Lawson and Mason, 2001; Hall *et al.*, 2005). Despite the pronounced variability, $MMHg_{UNF}$ showed significant positive correlations with HgT_{UNF} (r^2 = 0.39), HgR_{UNF} (r^2 = 0.52) and DGM (r^2 = 0.59). An additional relationship was found when considering pH (r^2 = 0.52); the $MMHg_{UNF}$ concentration in rainfalls appeared to increase with their measured acidity.

4.3. Mercury in surface waters

Mercury speciation and distribution in the Petit-Saut epilimnion has already been described in a companion paper (Muresan *et al.*, submitted). Here we only present the Hg concentrations in the uppermost 0.5 m of the Petit-Saut reservoir water-column. Particular care was accorded to the distribution of the volatile species directly involved in the air / water exchanges.

In the vicinity of the AWI, the sum of all Hg species averaged 4.5 ± 1.8 pmol L^{-1} of which ~ 75 % (3.4 ± 1.2 pmol L^{-1}) was dissolved. The particulate phase (composed be SPM) represented 1.1 ± 0.9 pmol L^{-1} (i.e. 7 ± 6 mg L^{-1} of SPM at 230 ± 190 pmol g^{-1} of HgT_P). Concerning temporal variability, maxima of HgT_{UNF} (up to 5.5 pmol L^{-1}) were measured during the high runoff period of the short wet season. In effect, the short wet season grouped higher HgT_D (3.8 ± 1.1 pmol L^{-1}) and SPM (12 ± 2 mg L^{-1}) coupled to moderate HgT_P concentrations (150 ± 80 pmol g^{-1}). Conversely the dry seasons displayed among the lowest

HgT_D, SPM and HgT_P values: 2.7 ± 0.8 pmol L^{-1}, 6 ± 4 mg L^{-1} and 80 ± 30 pmol g^{-1} respectively. The comparative study between sampling stations also showed that stations from the ancient Sinnamary riverbed had highest HgT concentrations: orderly 5.2 ± 1.7, 3.8 ± 1.0 and 1.4 ± 0.9 (i.e. 270 ± 230 pmol g^{-1}) pmol L^{-1} for HgT_{UNF}, HgT_D and HgT_P. The observed spatial variability apparently followed that of SPM which nearly doubled between the remote flooded forest and the Sinnamary riverbed stations (from 5 to 8 mg L^{-1}). Monomethylmercury at the AWI occupied ~ 15 % (0.6 ± 0.3 pmol L^{-1}) of the HgT_{UNF} and respectively reached 0.3 ± 0.1 and 0.3 ± 0.2 (i.e. 130 ± 80 pmol g^{-1}) pmol L^{-1} in the dissolved and particulate phases. Unlike HgT, maxima of $MMHg_{UNF}$ concentrations occurred during the high productivity period of the dry season (up to 0.9 ± 0.2 pmol L^{-1}). $MMHg_{UNF}$ variations then positively correlated with $MMHg_P$ (r^2 = 0.84; $[MMHg_{UNF}]_{pmol\ L\text{-}1}$ = 0.8 $[MMHg_P]_{pmol\ L\text{-}1}$ + 0.3) but opposed to $MMHg_D$ (r^2 = 0.55; $[MMHg_{UNF}]_{pmol\ L\text{-}1}$ = -3.7 $[MMHg_D]_{pmol\ L\text{-}1}$ + 1.7). The surface water loading with authigenic OM was supported by paired distributions of $MMHg_P$ and particulate organic carbon (r^2 = 0.46; $[MMHg_P]_{pmol\ L\text{-}1}$ = 5 $[POC]_{mmol\ L\text{-}1}$ + 0.7). Finally, it should be noted that, as for HgT species, lateral distribution of $MMHg_{UNF}$ exhibited their highest concentrations at the AWI of the ancient Sinnamary riverbed stations (up to 3.8 pmol L^{-1}). Those stations display a reduced a tree cover and undergo occasional yet brutal freshwater inputs from upstream of the dam.

Since volatile dimethylmercury (H_3C-Hg-CH_3) dissociates to MMHg in acidic waters, dissolved gaseous Hg (noted DGM) is mostly present as elemental mercury (Hg^0). According to Amouroux *et al*. (1999), about 99 % of DGM is composed of Hg^0. Considering our data (the 2003/04 period), DGM in surface waters averaged 350 ± 200 fmol L^{-1} (n = 70) which represents roughly twice the 1999 measured concentrations (close to 190 fmol L^{-1}). DGM at the AWI composed ~ 10 ± 7 % of HgT_D and reached up to 25 % during the dry season at the ancient Sinnamary riverbed stations (Table 1). In the dry season, the high light exposure

(occasionally above 1 kWh m^{-2}) coupled to the reduced cloud / vegetation cover show that the ancient Sinnamary riverbed is a privileged site for DGM production. As a matter of fact, DGM rose from 230 ± 130 to 480 ± 270 fmol L^{-1} between wet and dry seasons and from 100 ± 20 to 480 ± 150 fmol L^{-1} between the remote flooded forest and the ancient Sinnamary riverbed. Furthermore, we have additionally investigated (i) DGM in surface waters during a day long period (ii) DGM production either in the presence of light or in dark conditions and (iii) the role of HgR_{UNF} as a source for DGM (Fig. 5).

(i) DGM concentrations at the AWI were monitored *in situ* with a 2 hour time lapse (Fig. 5). Concentrations exhibited a steady increase of 60 fmol L^{-1} h^{-1} that started early in the morning and lasted until late afternoon (640 fmol L^{-1}). As dark conditions prevailed, DGM concentrations at the AWI declined (35 fmol L^{-1} h^{-1}) and reached their lowest values prior to sunrise (70 fmol L^{-1}). This pattern, observed during the dry season, was extensively altered by changes in atmospheric conditions. In effect, the cloudy weather and the homogenized epilimnion that depicted the short wet (Feb. 2004) season ensured low DGM concentrations and poor diurnal variability (180 ± 45 fmol L^{-1}).

(ii) DGM concentrations were measured on 50-100 mL of surface water samples taken from two simultaneously collected 2 L stock solutions. One was exposed to the direct sunlight whereas the other was kept in dark conditions (Fig. 5). To reproduce the surface water movements, both stock solutions were gently agitated (50 RPM). The temperature was stable during the incubation experiments (around 29°C). Light exposed samples displayed ~ 3 times higher DGM concentrations than unexposed ones (670 ± 100 *vs* 220 ± 150 fmol L^{-1}). Despite the marked shift in concentrations, dark and light exposed water samples exhibited analogous DGM distributions: sequential phases of DGM production and consumption. Interestingly, the overall production / consumption kinetic appeared fairly equilibrated in both cases. For

instance, average DGM production and consumption were calculated about 430 and 410 fmol L^{-1} h^{-1}.

(iii) HgR_{UNF} and DGM concentrations were sequentially determined on 50-100 mL of surface waters taken from a 5 L stock solution (Fig. 5). The experiment was performed in dark conditions under gentle agitation (50 RPM). Initially (within the first 4 hours of the experiment), DGM composed about one third of the HgR_{UNF} (respectively 400 ± 40 *vs* 1200 ± 30 fmol L^{-1}). Both species displayed comparable evolutions characterized by low amplitude sinusoidal variations following an initial decrease of concentrations ($r^2 = 0.54$; $[DGM]_{fmol\ L\text{-}1} = 0.35\ [HgR_{UNF}]_{fmol\ L\text{-}1} + 15$). About 260 minutes after the beginning of the experiment we decided to agitate (300 RPM for 20 seconds) the remaining AWI stock solution in order to simulate the stormy weather of such tropical regions. As a result HgR_{UNF} and DGM underwent rapid concentration changes: DGM increased from 350 to 600 fmol L^{-1} while HgR_{UNF} locally decreased from 1350 to 1050 fmol L^{-1}. Actually, following the brutal agitation, HgR_{UNF} and DGM adopted inversed evolutions ($r^2 = 0.45$; $[DGM]_{fmol\ L\text{-}1} = -2.4\ [HgR_{UNF}]_{fmol\ L\text{-}1} + 1450$). The overall increase of DGM concentrations roughly corresponded to the HgR_{UNF} decrease (both around 280 fmol L^{-1}).

5. DISCUSSION

5.1. Mercury in the atmosphere

Regarding the Petit-Saut region, the proximity with Atlantic Ocean supposes three distinct sources of atmospheric Hg: (i) the marine aerosols enriched in Na^+, Mg^{2+} and SO_4^{2-}, (ii) the transatlantic terrigenous source due to the transport on a large scale of African aerosols partially enriched in Ca^{2+} and SO_4^{2-} and (iii) the biogenic source resulting from the local vegetation. According to Meteo-France (2005), and excepting casual events (storms, Saharan

dust, etc.), the marine source dominated in the course of 2003-2004. As a result, average TGM concentration at the dam station (12 ± 2 pmol m^{-3}) was comparable to the mean North Atlantic level of 11.5 pmol m^{-3} (Slerm and Langer, 1992). The temporal monitoring of atmospheric Hg exhibited a positive correlation between GEM and pH of rainfalls ($r^2 = 0.62$). This relationship (Fig. 6) suggested that lowering pH in atmospheric waters might contribute scavenging GEM from the atmosphere. Since pH also appeared positively correlated to the amount of rainfall ($r^2 = 0.42$), the maximum GEM removal would take place in the course of the dry seasons. Indeed, this period exhibited the highest HgT_{UNF} concentrations in rain (up to 57.5 pmol L^{-1} in Nov. 2004). More striking was the daytime reverse correlation between GEM and RGM: the minimum of GEM, usually observed during the late day period, corresponded to a maximum of RGM into the atmosphere (Fig. 2). According to various authors (Iverfeldt and Lindqvist, 1986; Mason *et al*., 2001; Poissant *et al*., 2005), the brutal increase in the RGM concentrations would be the result of the photochemically induced oxidation of atmospheric Hg^0. Although the majority of atmospheric mercury was present in elemental form, reactive mercury has much higher wet and dry deposition rates than elemental mercury does. It might thus contribute to the deposition of mercury towards the reservoir.

As exposed in the previous section, the highest concentrations of HgT_{UNF} in rain were measured in the late dry season (Table 1). A possible explanation for those elevated values would be the episodic intensification of slash and burn cultures that release mercury from vegetation or that adsorbed on the surface of the soil. According to Richard (2001), the decline of the marine ionic signature in aerosols (Cl^-, Na^+ and Mg^{2+}), observed during the dry season, was concomitant to an increase of the fire ionic signature (i.e. K^+ and NO_3^- species). Another reason accounting for the HgT_{UNF} temporal pattern could be the pH of the rainfalls. We actually observed that pH in rain presented lower values in the dry season (4.4 units) than in the wet season (5.0 units). Consequently, HgT_{UNF} and pH were negatively correlated (r^2 =

0.29, $p \leq 0.05$; Fig. 6). Since the bottle induced adsorption during the rain collection barely accounted for the broad HgT_{UNF} variability (close to 60 pmol L^{-1}), atmospheric geochemical mechanisms ought to be considered. Lowering the rain pH through the increase of organic (oxalic and/or acetic) acid concentrations (Richard, 2001), would contribute to the oxidation of GEM and ultimately promotes Hg transfer towards the rain droplets. This was supported by literature data (Pleijel and Munthe, 1995) stating that the increase of fog droplets pH lead to lowered concentrations of dissolved Hg^{II} due to an enhanced production of volatile Hg^0. Conversely, the low concentrations observed in the course of the wet season indicate the existence of a dilution process that had already been described for the Maryland (USA) seashore by Lawson and Mason (2001). Accordingly, elevated rainfalls would simultaneously contribute to the partial removal of the Hg-aerosol bounded fraction and to the dilution of Hg^0 in rain. As the local atmosphere progressively became depleted of mercury, Hg concentrations in rain would drop even more.

Regarding Hg speciation in rain, the percentage of reactive mercury (~ 20 % of HgT_{UNF}) was relatively elevated in comparison with data from temperate latitudes or in the absence of direct oceanic influence (Mason *et al.*, 1997). However, the percentage of HgR_{UNF} in rain at Petit-Saut was low in comparison with central oceanic regions. To illustrate, the percentage of HgR_{UNF} in rainfalls collected above the South and Equatorial Atlantic Ocean averaged about 72 % of HgT (Lamborg *et al.*, 1999). Hence, the HgR_{UNF} / HgT_{UNF} ratios confirm that the air masses around the Petit-Saut reservoir are typical of those of continental areas with a very strong marine influence. As HgT_{UNF}, $MMHg_{UNF}$ concentrations in rain revealed a negative correlation with pH ($r^2 = 0.52$); the local concentrations of $MMHg_{UNF}$ significantly increased with acidity. This behavior suggests that detected monomethylmercury is either the result of the photochemical degradation of ambient dimethylmercury (H_3C-Hg-CH_3) evolved from suboxic wet zones or the result of the abiotic methylation within the rain

droplets. Supposing a constant dimethylmercury degradation and since the maxima of $MMHg_{UNF}$ concentrations (up to 10 pmol L^{-1}) corresponded to the annual slash and burn period, we hypothesized that MMHg production occurred mostly in the rain droplets. Such mechanisms (including the presence of organic acids) were investigated by Gårdfeldt *et al*. (2003a).

5.2. Mercury exchanges at the Air-Water interface

Rainfall distribution exhibited a broad variability with the seasons (from nothing up to 300 mm per week). As a result, the annual precipitation rate for the 2003/04 period averaged 3000 mm. Multiplying this value by the measured Hg concentrations in rain, we were able to calculate the annual wet deposition of this metal to the Petit-Saut reservoir (Table 2). Thus, the HgT_{UNF}, HgR_{UNF}, DGM and $MMHg_{UNF}$ wet depositions averaged 46 ± 35, 9 ± 11, 2 ± 3 and 3 ± 5 nmol m^{-2} yr^{-1} respectively. Transposed to the 2003/04 flooded area (close to 230 km^2), the associated annual amounts of deposited HgT_{UNF}, HgR_{UNF}, DGM and $MMHg_{UNF}$ were 11, 2 0.5 and 0.7 moles (i.e. 2200, 400, 100 and 140 grams). Since the amount of rainfall tends to dilute the ambient mercury concentrations, the Hg wet deposition fluxes emerged relatively balanced during the whole year. However, the dry seasons corresponded rather to reduced rainfalls of high Hg concentrations (30 ± 20 mm $week^{-1}$ of 20 ± 14 pmol L^{-1} HgT_{UNF}) whereas the wet seasons accumulated high rainfalls with low Hg contents (70 ± 50 mm $week^{-1}$ of 10 ± 6 pmol L^{-1} HgT_{UNF}). With the notable exception of $MMHg_{UNF}$, reported values corresponded to the low range of data found in the literature (Mason *et al*., 1997, 1999). Besides, the total atmospheric deposition has previously been estimated using Pb^{210} and HgT data in air, rain and atmosphere ("Mercure en Guyane" program, 2001). According to these authors, the total atmospheric deposition of Hg within the reservoir area reaches a minimum of 60 nmol m^{-2} yr^{-1}. Analogous estimates were reported by Lacerda *et al*. (1999) for the whole Amazonian basin (40-60 nmol m^{-2} yr^{-1}). Ultimately, an additional rough estimation of Hg total

atmospheric deposition was provided using Pb^{210} datation of HgT_P sedimentary profiles (Barriel *et al*., 2001). The obtained results were on the same order of magnitude (150-200 nmol m^{-2} yr^{-1}) as the atmospheric Pb^{210} and HgT provided data. With 46 nmol m^{-2} yr^{-1}, wet atmospheric deposition corresponded to approximately 75 % of total atmospheric deposition of Hg (60 nmol m^{-2} yr^{-1}). This result showed that rainfalls represented an efficient pathway for atmospheric mercury to reach the reservoir

As previously shown by Peretyazhko *et al*. (2005b), DGM profiles from the water column of the reservoir displayed three distinct maxima: (i) one to the air-water interface (AWI) due to photochemical reduction of dissolved Hg species, (ii) one below oxycline and (iii) one close to the SWI originating from iron and/or bacterial reduction of mercury. Both DGM and GEM at the AWI showed a broad variability with sunlight incidence that drove photochemical and photosynthetic processes (Fig. 2 and 5). Despite the fact that the maximum production rate was observed during the day period, all water samples were found supersaturated with DGM relative to the atmosphere. As the surface waters represented a potential source of elemental mercury to the atmosphere, the lake-air transfer of Hg^0 can be estimated by the following relation:

$$\text{Flux} = K\,(C_a\,H^{-1} - C_w)$$

Briefly, K (3.4 cm h^{-1}), the mass transfer coefficient of Hg^0 can be correlated with the mass transfer of CO_2 across the air-water interface through (Wanninkhof et al., 1985; Hornbuckle et al., 1994)

$$K = (0.45\,U_{10}^{1.64})\,[Sc_w(Hg^0) / Sc_w(CO_2)]^{-0.5}$$

where U_{10} is the wind speed (3 m s^{-1}) at 10 m, $Sc_w(CO_2)$ and $Sc_w(Hg^0)$ are the Schmidt numbers for Hg^0 and CO_2 in water (560 and 315 at 28°C). The Henry coefficient (H = 466 atm mol^{-1} at 28 °C) is calculated using the temperature-corrected dependency

$$\text{Log } H = -1078/T + 6.25 \text{ ; } T \text{ (°K)}$$

C_a is the air concentration of GEM (12 pmol m^{-3}) and C_w the water concentration of DGM (350 fmol L^{-1}). The evasional Hg^0 flow on a daily basis averaged 400 ± 240 and 130 ± 100 pmol m^{-2} d^{-1} for the dry and wet seasons respectively. On an annual basis, mean AWI degassing approached 90 ± 50 nmol m^{-2} yr^{-1} (Table 2). This efflux is in the same range of values as available data on several temperate lakes from Wisconsin (Vandal *et al*., 1991), Ontario (Amyot *et al*., 1997b) or Michigan (Mason and Sullivan, 1997). Relative to annual atmospheric deposition, the Hg^0 efflux from the Petit-Saut reservoir was as large as the wet mean deposition of HgT_{UNF} (46 ± 35 nmol m^{-2} yr^{-1}). Yet, this ratio displayed a broad seasonal variability as wet deposition prevailed during wet seasons (150 *vs* 130 pmol m^{-2} d^{-1}) while effluxes dominated during dry seasons (400 *vs* 100 pmol m^{-2} d^{-1}).

Interestingly, the diel variations of aquatic DGM anticorrelated with atmospheric GEM but were analogous with RGM pattern (see Section 4.1. and 4.3.). RGM is thought to be produced through photolytic degradation of GEM (*via* potential reactions with O_3, H_2O_2, $OH^{\cdot}$, Br, Cl, etc.) and also constitutes a privileged sink for gaseous atmospheric Hg towards rain and/or aerosols (e.g., Lu and Schroeder, 1998; Hedgecock *et al*., 2003; Poissant *et al*., 2005). Thus RGM production and its wet and/or particulate depositions may determine the Hg atmospheric lifetime. In the present case, the local mean deposition of reactive Hg could be determined from RGM concentrations through the formulation proposed by Laurier (pers com.):

$$\text{Flux} = k_A \text{ (RGM)}$$

k_A is the air-side mass transfer coefficient (~ 1.6 cm s^{-1}) calculated using the air-side diffusion coefficient (D_A = 0.28 cm^2 s^{-1}) and the wind speed 10 m above the water surface (U_{10} = 3 m s^{-1})

$$k_A = D_A^{0.5} [(0.98 \pm 0.1) U_{10} + (1.26 \pm 0.3)]$$

where ± is the 95% confidence interval. The mean RGM deposition was 2.0 ± 1.5 nmol m^{-2} yr^{-1}, which respectively represented 4 and 13 % of the wet and dry deposition of HgT (Table 2). These values shall however be regarded as indicative ranges since RGM undergoes rapid seasonal and diel variations. To illustrate, during the same day, calculated RGM deposition varied from > 100 pmol m^{-2} h^{-1} to below the apparatus detection limit (determinated to 2 pmol m^{-2} h^{-1}). However, recorded patterns of DGM, GEM and RGM concentrations (Fig. 2 and 5) still suggests that atmospheric Hg is preferentially oxidized during the day period (maximum of RGM) contributing to the observed decrease of GEM (around 8 pmol m^{-3}) and the increase of DGM (350 pmol m^{-3}). Considering that the GEM decrease in a 10 m height air-column (zone of direct deposition) is RGM-transferred to the first meter of the reservoir epilimnion, the diel atmospheric deposition would represent close to 20 % of the AWI measured DGM increase. In these particular conditions, the calculated deposition flux shall average 6 ± 4 pmol m^{-2} h^{-1} which is compatible with formerly given deposition ranges but exceeds the average annual RGM value. This result underlines the fact that either (i) RGM production and subsequent deposition occurs in the close vicinity (less than 1 m distance) of the AWI and/or (ii) that RGM production takes place in short periods of time (less than a few hours) of intense solar exposure.

5.3. AWI mercury transformations and budget

Redox conditions and biologically mediated reactions at the AWI play a major role in controlling the availability of Hg species towards reduction / oxidation processes (Beucher *et al.*, 2002; Lanzillotta *et al.*, 2004; Peretyazhko *et al.*, 2005a). These transformations significantly affect the local cycling of mercury: once inside the epilimnion of the reservoir, mercury can either be eliminated towards the atmosphere after photochemical reduction (Xiao *et al.*, 1995; Amyot *et al.*, 1997b), transferred to the hypolimnion after adsorption on SPM, or

undergo further transformations such as methylation and (co)precipitation (e.g., with Fe species). In order to probe the Hg transformations at the AWI, let us consider the *in situ* and incubation experiments presented in Section 4.3. (Fig. 5). From the *in situ* experiment (i) we conclude that light exposure significantly enhances the overall DGM levels (Amyot *et al*., 2001). According to Beucher *et al*. (2002), the AWI maxima DGM concentrations (10 % of the HgT_D) reflect the photochemical production of Hg^0 in the presence of a reductive agent such as organic matter and especially iron-carboxylated ionic complexants. Experiment (ii) made on surface water sample incubations showed that direct light exposure barely accounts for the observed minute to hour scale variations (production / consumption). Since the recorded pattern (on the range of the 0.1 pmol L^{-1}) was similar in light and dark conditions, the role of biologically catalyzed oxidation / reduction mechanisms is conceivable. Rapid Hg oxidation / reduction mechanisms have already been reported in the literature by Siciliano *et al*. (2002), Lanzillotta *et al*. (2004) or Garcia *et al*. (2005). Accordingly, observed variability may reflect the response of (epi)neuston to the photochemical or endogenical production of oxidant species (O_3, H_2O_2, $OH^{\cdot}$, etc.). Finally, experiment (iii) suggests that, in the surface waters of the reservoir and in dark conditions, HgR_{UNF} constitutes a potential source for DGM (Fig. 7). Initially, DGM and HgR_{UNF} appear to behave like two connected compartments of an open system: external sources / sinks dominating endogenic redox transformations. After vigorous agitation, DGM and HgR_{UNF} behave rather like two compartments of a closed system: reducible Hg circulates in a dominant way between both considered species. The observed pattern (changing in DGM *vs* HgR_{UNF} correlation with agitation) may result from the relaxation mechanism initiated during brutal DGM degassing and the subsequent biologically induced return to equilibrium.

As shown in Section 5.2. (and in Fig. 8), the 2003/04 annual Petit-Saut reservoir wet depositions averaged respectively 11, 2, 0.5 and 0.7 moles (i.e. 2200, 400, 100 and 140

grams) for HgT_{UNF}, HgR_{UNF}, DGM and $MMHg_{UNF}$. With 46 ± 35 nmol m^{-2} yr^{-1}, the HgT_{UNF} wet atmospheric deposition occupied nearly to 75 % of the total (~ 60 nmol m^{-2} yr^{-1}). This was about twice as low as that measured by Da Silva *et al.* (2005) for the inland Negro River basin (close to 115 nmol m^{-2} yr^{-1}). This observation, coupled to comparable fluxes for the South and equatorial Atlantic (18-36 nmol m^{-2} yr^{-1}; Lamborg *et al.*, 1999), support the dominant oceanic contribution of rainfall HgT_{UNF} in the vicinity of the reservoir (Table 3). Despite small values (2.0 ± 1.5 nmol m^{-2} yr^{-1}), RGM production also seemed to play an important role in overall Hg deposition due to cycles of oxidation, deposition, reduction and re-emission. As a matter of fact, the daytime deposition fluxes of RGM occasionally peaked over 100 pmol m^{-2} h^{-1}. Considering the emissions, Hg^0 volatilization at the AWI was estimated to 90 ± 50 nmol m^{-2} yr^{-1}. This is higher than the average value for the Negro River flooded area (around 20 nmol m^{-2} yr^{-1}; Da Silva *et al.*, 2005), but comparable to the published data for Atlantic Ocean (around 110 nmol m^{-2} yr^{-1}; Mason *et al.*, 2001; Gardfeldt *et al.*, 2003b) evasional DGM fluxes (Table 3). This result, presumably due to the sparse vegetation cover proper to permanently flooded areas, underscores the role of tropical reservoirs as local but significant sources of atmospheric Hg. Grouping all available data, the 2003/04 Petit-Saut reservoir AWI depositions and emissions of mercury averaged 60 and 90 nmol m^{-2} yr^{-1} respectively (i.e. 2800 and 4200 g yr^{-1}). The reservoir / atmosphere mass balance is thrown all the more out of equilibrium when considering the waters expelled from the dam: DGM exportations then reach 4600 g yr^{-1} to which one may add the subsequent Sinnamary Estuary degassing. Indeed, from the tailrace monitoring data (Muresan *et al.*, submitted), average DGM concentrations in dam discharged waters and the annual exported amount were on the order of 0.3 ± 0.2 pmol L^{-1} and 2 ± 1 moles (i.e. 400 ± 200 grams).

6. CONCLUDING REMARKS

The present study reinforces the hypothesis that artificial reservoirs in tropical regions constitute important sources for atmospheric Hg. The application of transport-reaction models to monitored AWI mercury distributions from the Petit-Saut reservoir made it possible to determine the periods of production and consumption of DGM GEM and RGM, probe the reactions that regulate AWI Hg exchanges, identify the atmospheric sources, and evaluate Hg fluxes across the air-water interface and downstream from the dam. They revealed (Fig. 8) that atmospheric Hg inputs to the reservoir represented 14 moles yr^{-1} (60 nmol m^{-2} yr^{-1}) of which 75 and 3 % corresponded to wet and RGM-mediated deposition (~ 46 and 2 nmol m^{-2} yr^{-1}). The associated DGM evasion represented 23 moles yr^{-1} of which 90 and 10 % corresponded to AWI degassing (90 nmol m^{-2} yr^{-1}) and the dam discharged amount (180 m^3 s^{-1} at 0.3 ± 0.2 pmol L^{-1}). In comparison, 76 moles yr^{-1} HgT_{UNF} came from tributaries (Muresan *et al.*, submitted). DGM, GEM and RGM displayed marked patterns of nycthemeral cycles including oxidation, deposition, reduction and re-emission processes. These features followed the general pattern of diurnal solar radiation variations: the DGM and RGM levels were found to increase with solar radiation (660 and 0.05 fmol Wh^{-1} m^{-1}) whereas GEM concentrations declined (- 9 fmol Wh^{-1} m^{-1}). Yet, in surface waters, short period (minute to hour time scale) transformations ought also to be carefully considered. Biologically catalyzed reduction / oxidation mechanisms also seemed to play a significant role in controlling reducible Hg speciation and therefore Hg^0 volatilization. The study of such aphotic mechanisms should be useful to constrain the estimated values required in rapid and/or dark condition evasion models.

Air and rain Hg levels, as determinate from the Petit-Saut monitoring enabled us to successfully differentiate between oceanic, terrigenic and anthropic sources. With the notable exception the $MMHg_{UNF}$ (affected by the slash and burn human activity), the HgT_{UNF} of rain

mostly originated from the adjacent Atlantic ocean (orderly 16 ± 12 and 17.8 ± 2.9 pmol L^{-1}). The average GEM concentrations at the dam station were also comparable to the mean North Atlantic level (12 ± 2 and 11.5 pmol m^{-3}). However, GEM in air and HgT_{UNF} in rain experienced reversed distributions with the seasons.

*Acknowledgments***:** We would like to thank C. Reynouard and V. Horeau for their help in getting the air and rain samples. We also acknowledge F. Schaedlich from Tekran Inc. for his technical assistance. This work was supported by the French National Scientific Research Center (CNRS/PEVS, "Mercury in French Guiana" research program), the European Union Feder funds and the French Ministry for the Environment (MEDD). This work also received the financial support of Electricité de France (EDF) through a scholarship grant to one of us (BM) (#F01381/0). Thanks are due to W. Delor who edited the transcript.

REFERENCES

AMOUROUX D., WASSERMAN J.C., TESSIER E. and DONARD O.F.X. (1999) Elemental mercury in the atmosphere of a tropical Amazonian Forest (French Guiana). *Environmental Science and Technology* **33**, 3044-3048.

AMYOT M., AUCLAIR J.C. and POISSANT L. (2001) *In situ* high temporal resolution analysis of elemental mercury in natural waters. *Analytica Chimica Acta* **447**, 153-159.

AMYOT, M., MIERLE, G., LEAN, D. and MCQUEEN, D.J. (1997b) Effect of solar radiation on the formation of dissolved gaseous mercury in temperate lakes. *Geochimica et Cosmochimica Acta* **61**, 975-987.

ARTAXO P., CALIXTO DE CAMPOS R., FERNANDES E., MARTINS J., XIAO Z., LINDQUIST O., FERNANDEZ-JIMENEZ M. and MAENHAUT W. (2000) Large scale mercury and trace element measurements in the Amazon basin. *Atmospheric Environment* **34**, 4085-4096.

BARRIEL L.A., YI Y., LEAITCH W.R., LOHMANN U., KASIBHATLA P., ROELOFS G.J., WILSON J., MCGOVERN F., BENKOVITZ C., MÉLIÈRES M.A., LAW K., PROSPERO J., KRITZ M., BERGMANN D., BRIDGEMAN C., CHIN M., CHRISTENSEN J., EASTER R., FEICHTER J., LAND C., JEUKEN A., KJELLSTRÖM E., KOCH D. and RASCH P. (2001) A comparison of large scale atmospheric sulphate aerosols models (COSAM) overview and highlights. *Tellus* **53B**.

BEUCHER C., WONG W.C.P., RICHARD C., MAILHOT G., BOLTE M. and COSSA D. (2002). Dissolved gaseous mercury formation under UV irradiation of unamended tropical waters from French Guyana. *Science of the Total Environment* **290**, 131-138.

BLOOM N.S. and WATRAS C.J. (1998) Observations of methylmercury in precipitation. *The Science of The Total Environment* **87-88**, 199-207.

BLOOM N.S. (1989) Determination of picogram levels of methylmercury by aqueous phase ethylation followed by cryogenic gas chromatography with cold vapour atomic fluorescence detection. *Canadian Journal of Fisheries and Aquatic sciences* **46**, 1131-1140.

BLOOM N.S. and FITZGERALD W.F. (1988) Determination of volatile mercury species at picogram level by low temperature gas chromatography with cold-vapour atomic fluorescence detection. *Analytica Chimica Acta* **28**, 151-161.

CORDIER S. and GRASMICK C. (1994) Etude de l'imprégnation par le mercure dans la population guyanaise. *Rapport Réseau National de Santé Publique / Direction Générale de la Santé*, 28 pp.

COSSA D., AVERTY B., BRETAUDEAU J. and SENARD A.S. (2003) Spéciation du mercure dissous dans les eaux marines. *Méthodes d'analyse en milieu marin. Editions Ifremer*, **ISBN 2-84433-125-4**, 27 pp.

COSSA D., COQUERY M., NAKHLE K. and CLAISSE D. (2002) Dosage du mercure total et du monomethylmercure dans les organismes et les sédiments marins. *Méthodes d'analyse en milieu marin, Editions Ifremer*, **ISBN 2-84433-105-X**, 27pp.

DA SILVA G.S., JARDIM W.F. and FADINI P.S. (2005) Elemental gaseous mercury flux at the water/air interface over the Negro River basin, Amazon, Brazil. *Science of The Total Environment*, **In Press**

DA SILVA G.S. (2004) A dinâmica biogeoquímica do mercúrio na bacia do Negro River (AM) e fluxos na interface água/atmosfera. *Doctoral Thesis*, Chemistry Institute-State University of Campinas.

DUMESTRE J.F., VAQUER A., GOSSE P., RICHARD S. and LABROUE L. (1999) Bacterial ecology of a young equatorial hydroelectric reservoir (Petit-Saut, French Guyana). *Hydrobiologia* **400**, 75-83.

FADINI P.S. and JARDIM W.F. (2000a) Is the Negro River Basin (Amazon) impacted by naturally occurring mercury? *Sci Total Environ* **275**, 71-82.

FITZGERALD W.F., MASON R.P. and VANDAL G.M. (1991) Atmospheric cycling and air-water exchange of mercury over mid-continental lacustrine regions. *Water, Air, and Soil Pollution* **56**, 745-768.

FOSTIER H., FORTI M.C., GUIMARÃES J.R.D., MELFI A.J., BOULET R., ESPIRITO SANTO C.M. and KRUG F.J. (2000) Mercury fluxes in a natural forested Amazonian catchment (Serra do Navio, Amapá State, Brazil). *The Science of The Total Environment* **260**, 201-211.

FRÉRY N., MAURY-BRACHET R., MAILLOT E., DEHEEGER M., DE MERONA B. and BOUDOU A. (2001). Goldmining activities and mercury contamination of native Amerindian communities in French Guiana: key role of fish in dietary uptake. *Environ. Health. Perspect.* **109**, 449-456.

FRÉRY N., MAILLOT E., DEHEEGER M., BOUDOU A. and MAURY-BRACHET R. (1999). Exposition au mercure de la population amérindienne wayana de Guyane: enquête alimentaire. *Paris, Institut de veille sanitaire*.

GARCIA E., POULAIN A.J., AMYOT M. and ARIYA P.A. (2005) Diel variations in photoinduced oxidation of Hg^0 in freshwater. *Chemosphere* **59**, 977-981.

GÅRDFELDT K., MUNTHE J., STROMBERG D. and LINDQVIST O. (2003a) A kinetic study on the abiotic methylation of divalent mercury in the aqueous phase. *The Science of The Total Environment* **304**, 127-136.

GÅRDFELDT K., SOMMAR J., FERRARA R., CECCARINI C., LANZILLOTTA E., MUNTHE J., WÄNGBERG I., LINDQVIST O., PIRRONE N., SPROVIERI F., *et al*. (2003b) Evasion of mercury from coastal and open waters of the Atlantic Ocean and the Mediterranean Sea. *Atmospheric Environment* **37**, 73-84

HALL B.D., MANOLOPOULOS H., HURLEY J.P., SCHAUER J.J., ST. LOUIS V.L., KENSKI D., GRAYDON J., BABIARZ C.L., CLECKNER L.B. and KEELER G.J. (2005) Methyl and total mercury in precipitation in the Great Lakes region. *Atmospheric Environment* **39**, 7557-7569.

HEDGECOCK I.M., PIRRONE N., SPROVIERI F. and PESANTI E. (2003) Reactive gaseous mercury in the marine boubdary layer. Modelling and Experimental evidence of its formation in the Mediterranean region. *Atmos. Environ*. **37**, 21-39.

HEDGECOCK I.M. and PIRRONE N. (2001) Mercury and photochemistry in the marine boundary layer-modelling studies suggest the *in situ* production of reactive gas phase mercury. *Atmospheric Environment* **35**, 3055-3062.

HOLY M. (1976) An overview. In Arid land irrigation in developing countries, edited by E.B. Worthington, *Pergamon Press*, New York: 343-350.

HOREAU V., CERDAN P., CHAMPEAU A. and RICHARD S. (1998) Importance of aquatic invertebrates in the diet of rapids-dwelling fish in the Sinnamary River, French Guiana. *J. Trop. Ecol*. **14**, 851-864.

HORNBUCKLE K.C., JEREMIASON J.D., SWEET C.W. and EISENREICH S.J. (1994) Seasonal variations in air-water exchange of polychlorinated biphenyls in Lake superior. *Environ. Sc. Tech*. **28**, 1491-1501.

HUYNH F., CHARRON C., BETOULLE J.L., PANECHOU K., GARDEL A., PROST M.T. and LOUBRY D. (1997) Suivi de l'évolution géomorphologique et botanique de l'estuaire du Sinnamary par télédétection. *Final report* **ORSTOM-EDF**, 64pp.

IVERFELDT A. and LINDQVIST O. (1986) Atmospheric oxidation of elemental mercury by ozone in the aqueous phase. *Atmospheric Environment* **20**, 1567-1573.

LACERDA L.D., RIBEIRTO M.G., CORDEIRO R.C., SOFEDDINE A. and TURCQ B. (1999). Atmospheric mercury deposition over Brazil during the past 30,000 years. *Ciência e Cultura* **51**, 363-371.

LAMBORG C.H. (2003) Mercury Speciation and Reactivity in the Coastal and Estuarine Waters of Long Island Sound. Ph D Dissertation, University of Connecticut (USA).

LAMBORG C.H., ROLFHUS K.R., FITZGERALD W.F. and KIM G. (1999) The atmospheric cycling and air-sea exchange of mercury species in the South and equatorial Atlantic Ocean. *Deep Sea Research* **46**, 957-977.

LANZILLOTTA E., CECCARINI C., FERRARA R., DINI F., FRONTINI F.P. and BANCHETTI R. (2004) Importance of the biogenic organic matter in photo-formation of dissolved gaseous mercury in a culture of the marine diatom Chaetoceros sp. *The Science of The Total Environment* **318**, 211-221.

LAURIER F.F.J.G., MASON R.P. and WHALIN L. (2003) Reactive gaseous mercury formation in the North Pacific Ocean's marine boundary layer: A potential role of halogen chemistry. *J. Geophys. Res*. (D17) 4529, d.

LAWSON N.M. and MASON R.P. (2001) Concentration of Mercury, Methylmercury, Cadmium, Lead, Arsenic, and Selenium in the Rain and Stream Water of Two Contrasting Watersheds in Western Maryland. *Water Research* **35**, 4039-4052.

LEERMARKERS M., GALETTI S., DE GALAN S., BRION N. and BAEYENS W. (2001) Mercury in the Souther North Sea and Sheldt Estuary. *Marine Chemistry* **75**, 229-248.

LIANG L., HORVAT M. and BLOOM N.S. (1994). An improved speciation method for mercury by GC/CVAFS after aqueous phase ethylation and room temperature precollection. *Talanta* **41**, 371-379.

LINDBERG S.E. and ZHANG H. (2000). Air/water exchange of mercury in the Everglades II: Measuring and modeling evasion of mercury from Surface Waters. *Sci. Total Environ.* **259**, 135-143.

LINDBERG S.E. and STRATTON W.J. (1998) Atmospheric mercury speciation: Concentrations and behavior of reactive gaseous mercury in ambient air. *Envir. Sci. & Technol*. **32**, 49-57.

LU J.Y. and SCHROEDER W.H. (1998) Comparison of conventional filtration and a denuder-based methodology for sampling of particulate-phase mercury in ambient air. *Talanta* **49**, 15-24.

MANGAL M.J. (2001) Assessing mercury contamination in the Amazon Basin. http://www.mangal.dk/mercury.pdf

MASON R.P., LAWSON N.M. and SHEU G.R. (2001) Mercury in the Atlantic Ocean: factors controlling air–sea exchange of mercury and its distribution in the upper waters. Deep Sea Research Part II : *Topical Studies in Oceanography* **48**, 2829-2853.

MASON R.P. and SHEU G.R. (2001) An examination of the methods for the measurements of reactive gaseous mercury in the atmosphere. *Environ. Sci. Technol.* **35**, 1209-1216.

MASON R.P., LAWSON N.M, LAWRENCE A.L., JOY J.L., LEE J.G. and SHEU G.R. (1999) Mercury in the Chesapeake Bay. *Marine Chemistry* **65**, 77-96.

MASON R.P., LAWSON N.M. and SULLIVAN K.A. (1997) The concentration, speciation and sources of mercury in Chesapeake Bay precipitation. *Atmospheric Environment* **31**, 3541-3550.

MASON R.P. and SULLIVAN K.A. (1997) Mercury in Lake Michigan. *Environ. Sci. Technol.* **31**, 942-947.

MASON R.P., FITZGERALD W.F. and MOREL F.M.M. (1994a) The biogeochemical cycling of elemental mercury: anthropogenic influences. *Geochimica Cosmochimica Acta* **58**, 3191-3198.

Mercure en Guyane project (2001) CHARLET L., BOUDOU A., GRIMALDI M. and COSSA D. *Region de Saint Elie et retenue de Petit-Saut*. **Final report part 1**, 70pp.

Meteo-France: French institute for weather forecast and meteorological research. 2005 database on wind direction and rain events. http://www.meteofrance.com.

MURESAN B., COSSA D., RICHARD S. and DOMINQUE Y. Mercury Cycling in a Tropical Artificial Reservoir: Monomethylmercury Production and Sources. Submitted to *Applied Geochemistry* (Feb. 2006).

PARKER J.L. and BLOOM N.S. (2005) Preservation and storage techniques for low-level aqueous mercury speciation. *Sci Total Environ*. **337**, 253-63.

PERETYAZHKO T., VAN CAPELLEN P., MEILE C., COQUERY M., MUSSO M., REGNIER P. and CHARLET L. (2005a) Biogeochemistry of major redox elements and mercury in a tropical reservoir lake (Petit Saut, French Guiana). *Aquat. Geochem*. **11**, 33-35.

PERETYAZHKO T., CHARLET L., MURESAN B., KAZIMIROV V. and COSSA D. (2005b) Formation of dissolved gaseous mercury in a tropical lake (Petit-Saut reservoir, French Guiana). *Science of The Total Environment*, **In Press**.

PETOT J. (1993) Histoire de l'or en Guyane. L'Harmattan, Paris, 256 pp.

PFEIFFER W.C., LACERDA L.D., MALM O., SOUZA C.M., SILVEIRA E.G. and BASTOS W.R. (1989) Mercury Concentrations in Inland Waters of Goldmining Areas in Rondonia, Brazil. *The Science of the Total Environment* **87-88**, 233-240.

PLEIJEL K. and MUNTHE J. (1995) Modeling the atmospheric mercury cycle-chemistry in fog droplets. *Atmos Environ* **29**, 1441-1457.

POISSANT L., PILOTE M., BEAUVAIS C., CONSTANT P. and ZHANG H.H. (2005) A year of continuous measurements of three atmospheric mercury species (GEM, RGM and Hgp) in southern Québec, Canada. *Atmospheric Environment* **39**, 1275-1287.

RICHARD S., ARNOUX A., CERDAN P., REYNOUARD C., HOREAU V. and VIGOUROUX R. (2002) Influence of the setting up of a man-made lake on mercury levels in the flesh of fish in a neotropical habitat: the Sinnamary river (French Guiana). *Rev. Ecol*. **8**, 59-76.

RICHARD S. (2001) Monitoring of the IDAF (IGAC / DEBITS / AFRIQUE) network stations of Petit-Saut in French Guiana: the sources of emissions. *IDAF/SEARCH workshop* Toulouse 3-5 Dec.

RICHARD S. (1996) La mise en eau du barrage de Petit-Saut. Hydrochimie 1 – du fleuve Sinnamary avant la mise en eau, 2 – de le retenue pendant la mise en eau, 3 – du fleuve en aval. *Doctoral Thesis*, Aix – Marseille University I, 278 pp.

ROULET M., LUCOTTE M., CANUEL R., FARELLA N., COURCELLES M., GUIMARAES J., MERGLER D. and AMORIM M. (2000) Increase in mercury contamination recorded in lacustrine sediments following deforestation in central Amazon. *Chemical Geology* **165**, 243-266.

ROULET M., LUCOTTE M., CANUEL R., FARELLA N., COURCELLES M., GUIMARAES J.R.D., MERGLER D. and AMORIM M. (1998) The geochemistry of mercury in central Amazonian soils developed on the Alter-do-Chao formation of the lower Tapajos River Valley, Para state, Brazil. *Science of the Total Environment* **223**, 1-24.

SCHROEDER W.H., ANLAUF K.G., BARRIE L.A., LU J.Y., STEFFEN A., SCHNEEBERGER D.R. and BERG T. (1998) Artic springtime depletion of mercury. *Nature* **394**, 331-333.

SICILIANO S.D., O'DRISCOLL N.J. and LEAN D.R.S. (2002) Microbial reduction and oxidation of mercury in freshwater lakes. *Environ Sci Technol* **36**, 3064-3068.

SLERM F. and LANGER E. (1992) Increase in global atmospheric concentrations of mercury inferred from measurements over the Atlantic Ocean. *Nature* **355**, 434-436.

TEKRAN Inc. (2001) Model 1130 mercury speciation unit maintenance manual. Tekran.com.

VANDAL G.M., MASON R.P. and FITZGERALD F. (1991) Cycling of volatile mercury in temperate lakes. *Water, Air and Soil Pollution* **56**, 791-803.

VEIGA M.M., HINTON J. and LILLY C. (1999) Mercury in the Amazon: A Comprehensive Review with Special Emphasis on Bioaccumulation and Bioindicators. *NIMD (National Institute for Minamata Disease)* **Forum'99**, 19-39.

WANNINKHOF R., LEDWELL R. and BROECKER W.S. (1985) Gas exchange – wind speed relationship measured with sulfur hexafluoride on a lake. *Science* **227**, 1224-1226.

XIAO Z.F., STROMBERG D. and LINDQVIST O. (1995) Influence of humic substances on photolysis of divalent mercury in aqueous solution. *Water, Air and Soil Pollution* **80**, 789-798.

TABLE CAPTIONS

SEASON	GEM / air (pmol m^{-3})	HgT_{UNF} / rain (pmol L^{-1})	DGM / AVM water (fmol L^{-1})
Dry seasons	10.9 ± 0.9	20 ± 14	480 ± 270
Wet seasons	12.8 ± 1.1	10 ± 6	230 ± 130
Annual	12.0 ± 1.4	16 ± 12	350 ± 200

Tab. 1. Seasonal and annual means (± standard deviations) of gaseous elemental (GEM), the sum of all species (HgT_{UNF}) and dissolved gaseous (DGM) mercury. Measurements for GEM ($n > 10^5$) in air, HgT_{UNF} (n = 84) in rain and DGM (n = 70) in surface waters corresponds to the Matoutou 1-5 (2003/04) sampling campaigns.

Hg EXCHANGES	FLUXES (nmol m^{-2} yr^{-1})	AMOUNTS (moles yr^{-1})
Total Hg deposition	40 - 200 (~ 60 on average)	9 - 46 (~ 14 on average)
Wet deposition	46 ± 35	11 ± 8
RGM deposition	2.0 ± 1.5	0.5 ± 0.3
DGM dam exportations		2 ± 1
AWI degassing	90 ± 50	21 ± 11

Tab. 2. Mercury fluxes (and corresponding amounts) at the AWI of Petit-Saut reservoir, and downstream dam DGM exportations.

DOMAIN	RAINFALLS (Hg fluxes in nmol m^{-2} yr^{-1})	AWI EFFLUX	REFERENCE
Atlantic Ocean	18-36		Lamborg et al., 1999
/	39		Mason et al., 1994a
/		118	Gårdfeldt et al., 2003b
/		110	Mason et al., 2001
Amazon Basin	115		Da Silva et al., 2005
/	102		Fadini and Jardim, 2000a
/	91		Fostier et al., 2000
/		60	Veiga et al., 1999
/		20	Da Silva, 2004
Petit-Saut	46 ± 35	90 ± 50	this work

Tab. 3. Comparison of reported values of wet Hg deposition and AWI evasion fluxes from Atlantic Ocean and Amazon Basin with measured values in Petit-Saut area.

FIGURE CAPTIONS

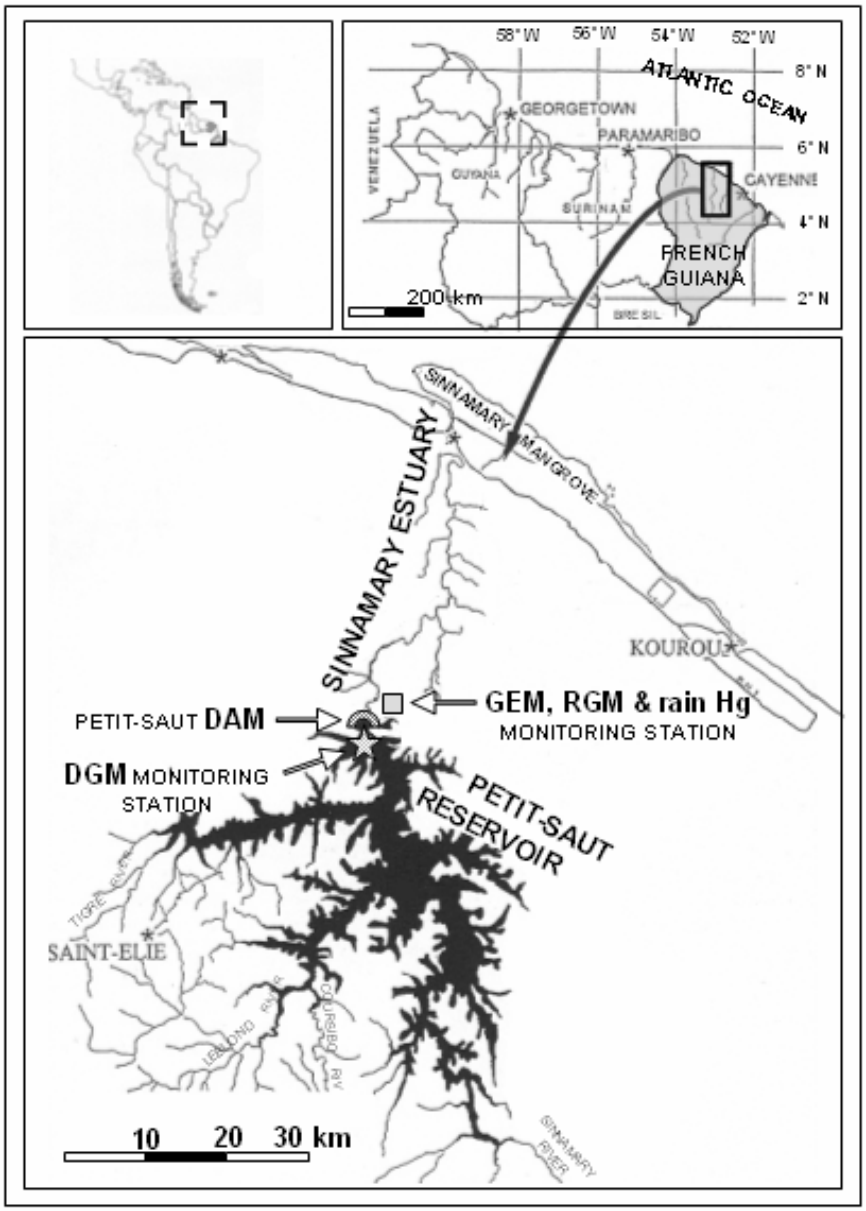

Fig. 1. Location map of the Petit-Saut reservoir / Sinnamary Estuary continuum. Detailed map of the areas where (and dates when) water sampling occurred, including associated geochemical descriptions, is given in Muresan *et al*. (submitted).

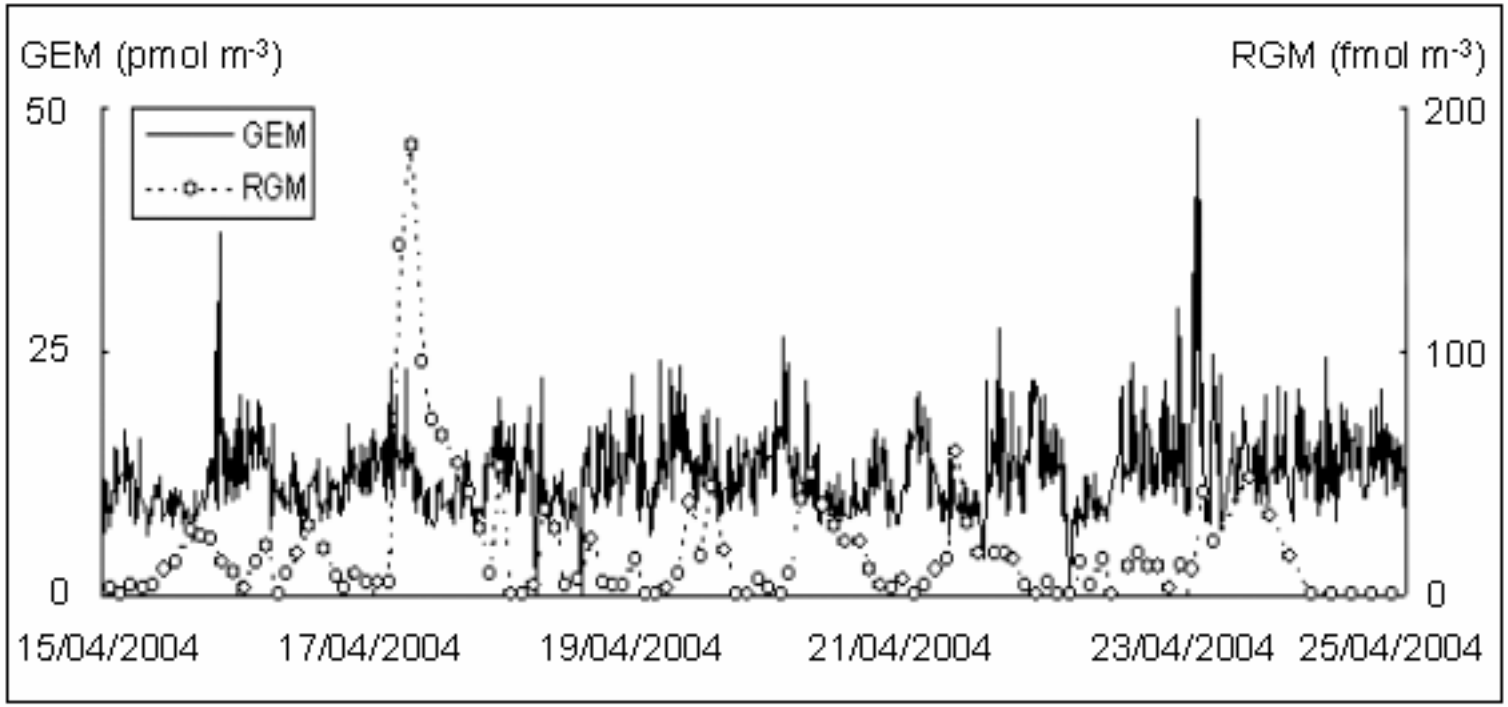

Fig. 2. Monitoring of gaseous elemental (GEM) and reactive gaseous (RGM) mercury concentrations in air. Samples for GEM and RGM were collected on a 5 and 180 min basis at the HYDRECO field laboratory using a Tekran Model 1130 Speciation Unit connected to a Model 2737A vapour analyzer.

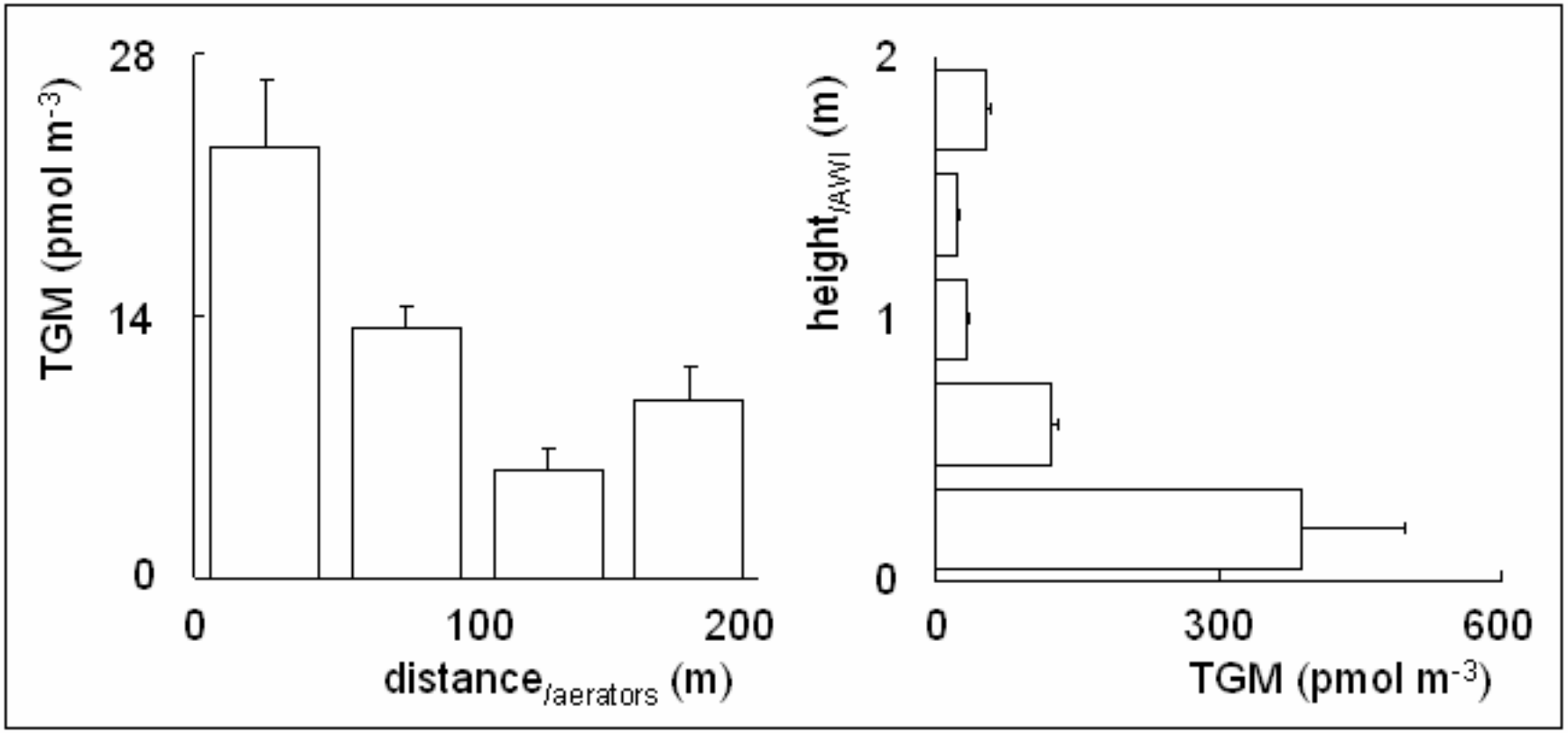

Fig. 3. Transept and height distribution of total gaseous mercury (TGM) in the air-column of the aerators. Error bars represent the mean errors for each sampling. Samples were collected by means of a portable a mercury analyzer RA-915+ (LUMEX) allowing continuous measurements with a detection limit of 10 pmol m^{-3}.

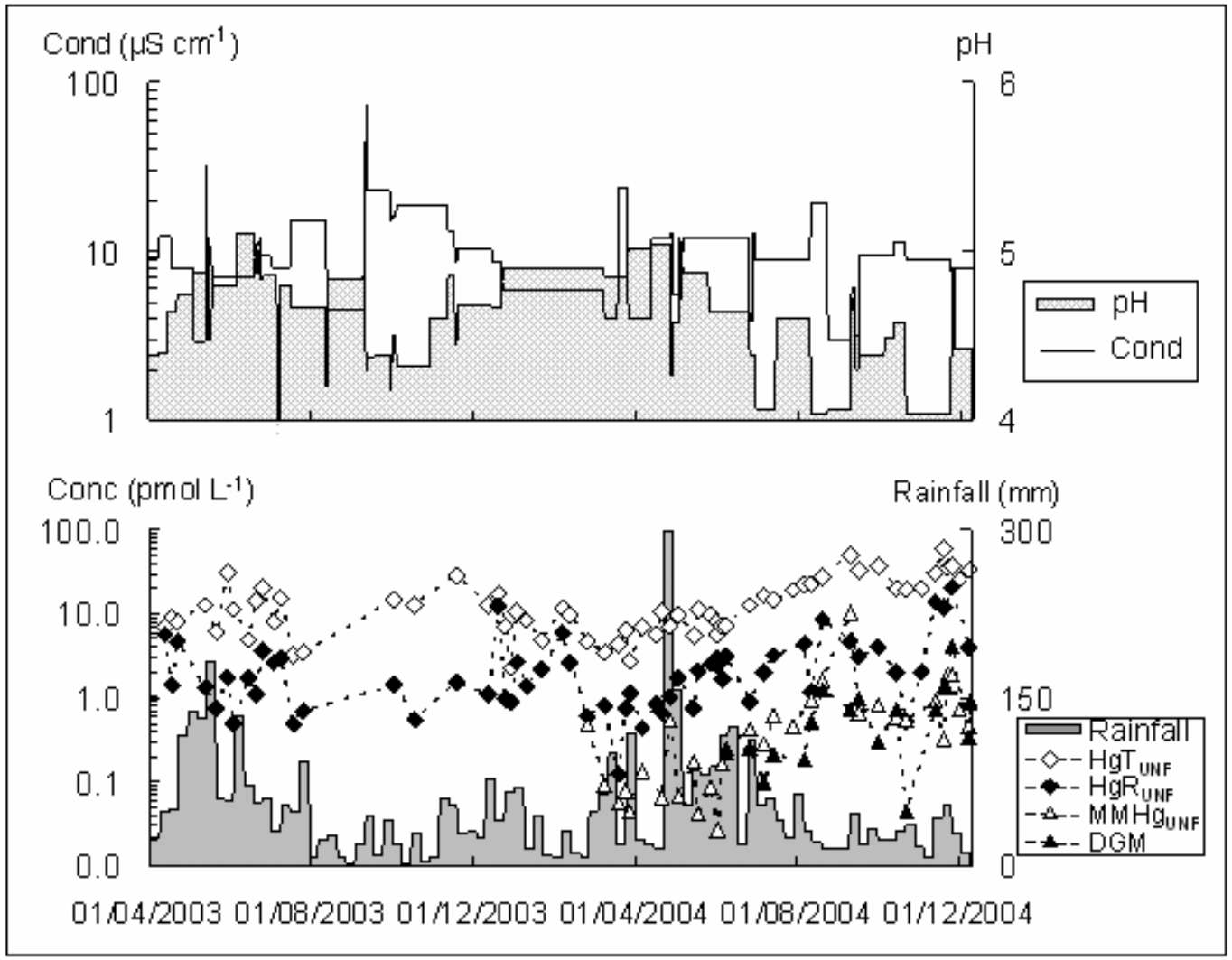

Fig. 4. Monitoring of total (HgT_{UNF}), reactive (HgR_{UNF}), monomethyl ($MMHg_{UNF}$) and dissolved gaseous (DGM) mercury concentrations in rain. Deposited amount and when achievable pH and conductivity were determined on a weekly basis at the HYDRECO field laboratory.

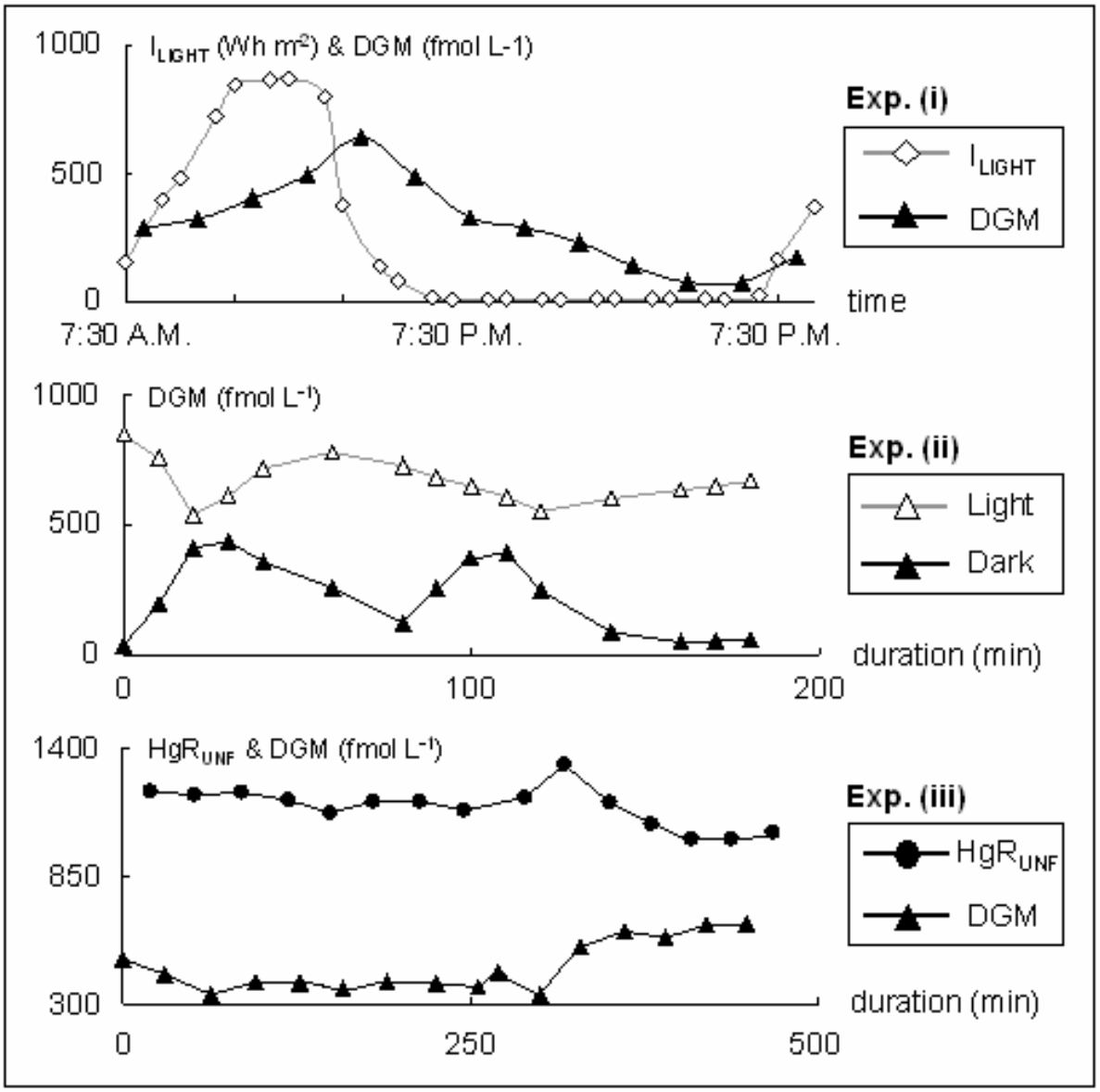

Fig. 5. Exp (i): Diel variations in the intensity of light exposure and dissolved elemental mercury (DGM) concentrations in the Petit-Saut reservoir surface waters. Exp (ii): DGM variations in surface water samples incubated in the dark or under the full spectrum of solar radiation. Exp (iii): DGM and HgR_{UNF} variations in surface water samples incubated in dark conditions.

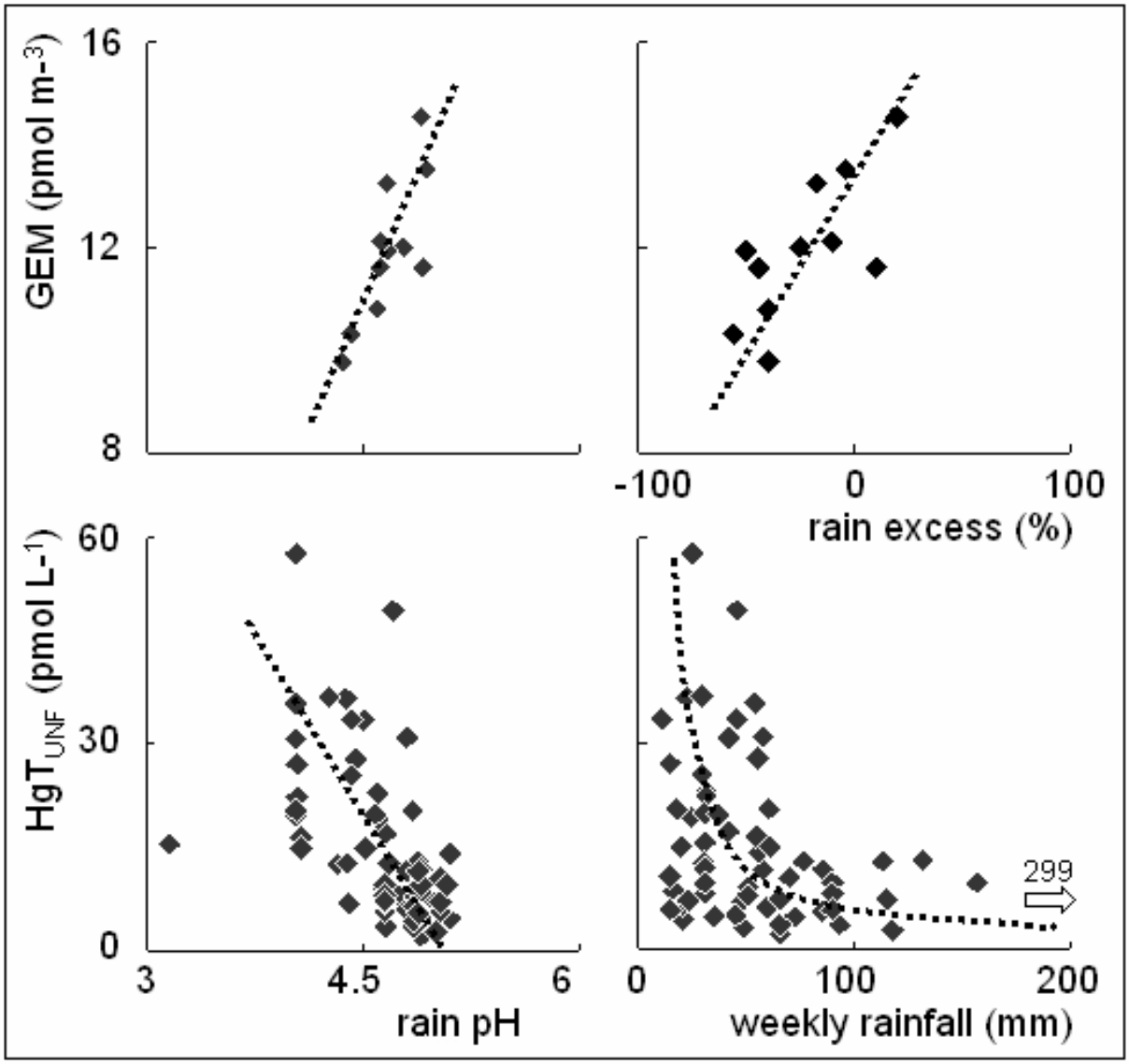

Fig. 6. Upper graphs: monthly GEM concentrations as a function of rain pH and percentage of rain excess. Lower graphs: weekly rain HgT_{UNF} concentrations in relation to rain pH and deposited amounts.

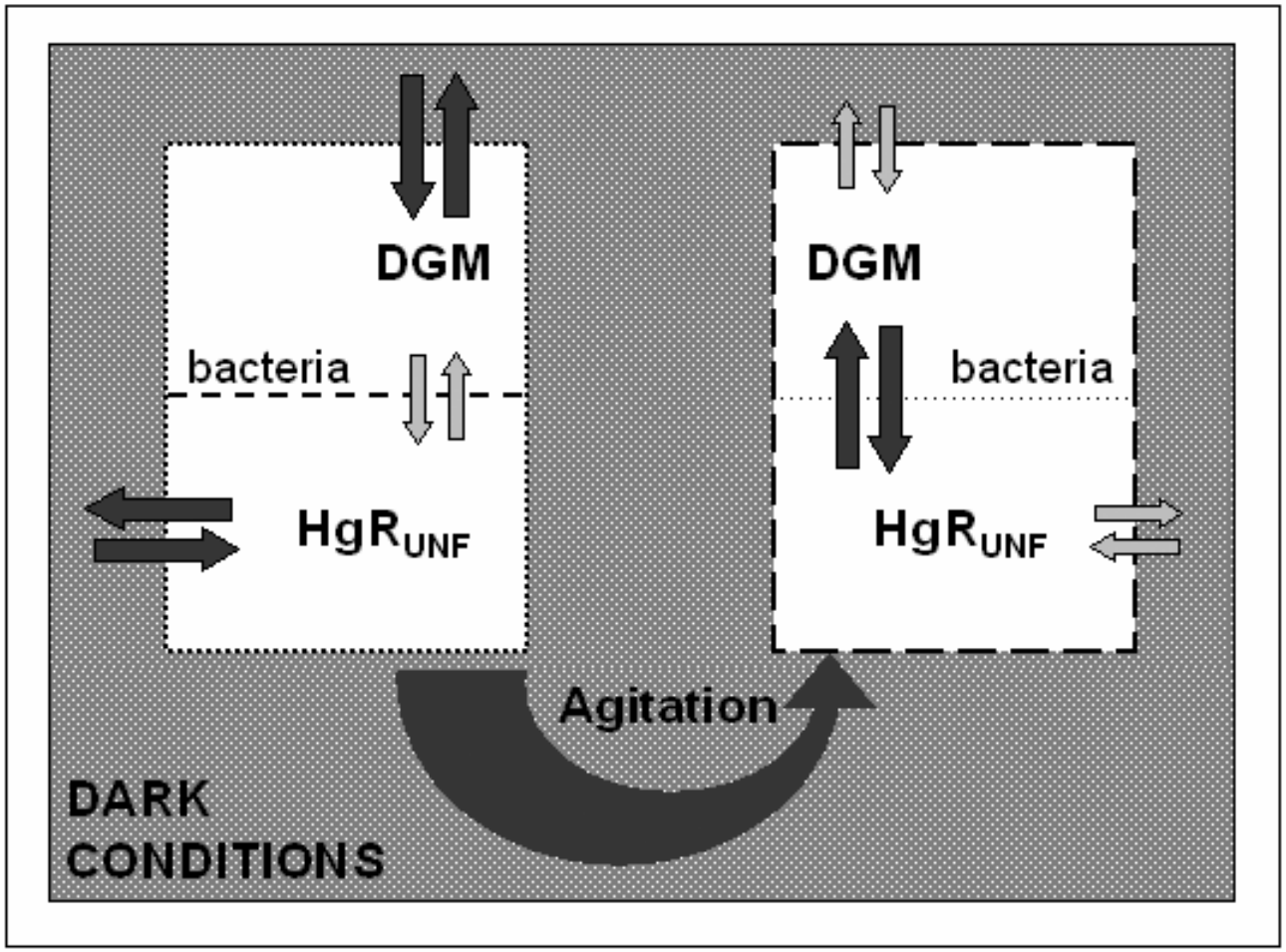

Fig. 7. A schematic diagram of the simple box model for DGM and HgR_{UNF} concentrations prior to and after vigorous agitation of the incubated surface waters. Prior to agitation: external sources / sinks dominated upon endogenic redox transformations. After agitation: reducible Hg circulates in a dominant way between both considered species.

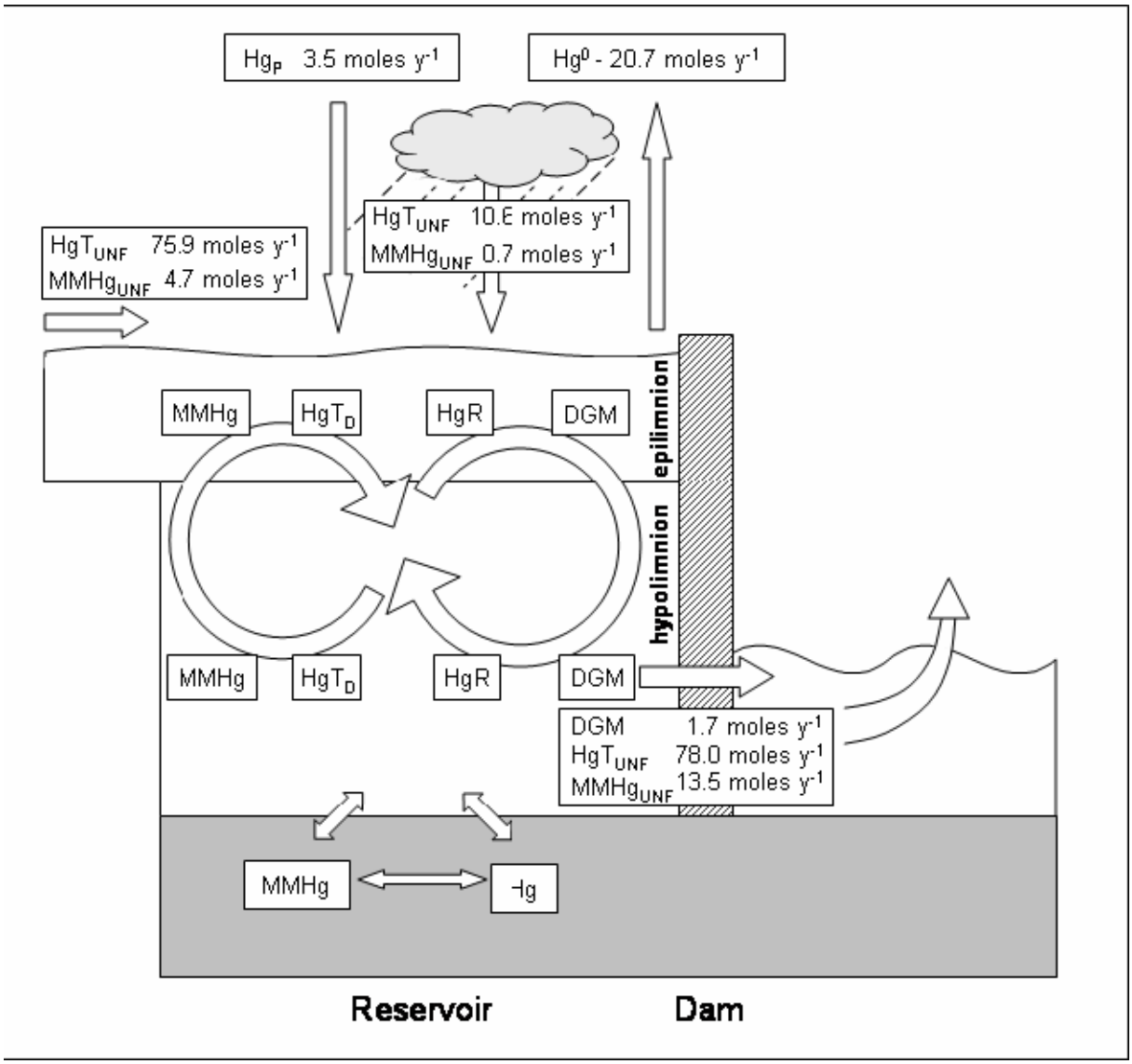

Fig. 8. Mercury budget for the AWI of Petit-Saut reservoir and downstream dam DGM exportations. The whole HgT_{UNF} and $MMHg_{UNF}$ reservoir budget is given in Muresan *et al*. (under submission).

Article II

Cycle du mercure dans un lac artificiel tropical : Sources et production de monométhylmercure

RESUME

La distribution et la spéciation du mercure (Hg) ont été analysées à l'échelle saisonnière dans la colonne d'eau partiellement anoxique du réservoir tropical de Petit-Saut (Guyane Française) afin d'étudier ses transformations. Parallèlement, un suivi des flux entrants (*via* les dépôts humides et les affluents) et sortants (évasion atmosphérique, rejets en contrebas du barrage) de Hg au niveau de la retenue a été initié afin d'étudier son recyclage. Dans les eaux oxygénées de l'épilimnion, les concentrations totales de mercure (HgT) étaient de 5 ± 3 pmol L^{-1} dans les échantillons non filtrés (HgT_{UNF}) et 4 ± 2 pmol L^{-1} dans ceux dissous (HgT_D). En moyenne, le monométhylmercure (MMHg) représentait 18% du mercure total non filtré ($MMHg_{UNF}$) alors qu'il rassemblait 8 et 40 % du mercure dissous ($MMHg_D$) et particulaire ($MMHg_P$). La corrélation observée entre $MMHg_P$ et chlorophylle*a* suggère que l'activité planctonique pourrait, de manière directe ou détournée, contrôler les processus de méthylation dans la partie oxygénée du réservoir. Dans les eaux anoxiques de l'hypolimnion, les concentrations respectives de HgT_{UNF} et HgT_D étaient de 13 ± 6 et 8 ± 4 pmol L^{-1}. Celles de $MMHg_P$ et $MMHg_D$ (2 et 3 fois supérieures aux valeurs de l'epilimnion) étaient de 170 ± 90 pmol g^{-1} et 0,9 ± 0,5 pmol L^{-1}. La distribution bimodale du $MMHg_D$, maxima de concentration sous l'oxycline et à l'interface eau / sédiments, suggère l'existence de sites privilégiés dans la colonne d'eau pour la production et/ou la mobilisation du $MMHg_D$. Le

dépôt atmosphérique humide représentait 11 moles a^{-1} de HgT_{UNF} (dont 0,7 moles a^{-1} de $MMHg_{UNF}$), tandis que 76 moles a^{-1} de HgT_{UNF} (dont 4,7 moles a^{-1} de $MMHg_{UNF}$) provenaient des apports par les affluents. Simultanément, environ 78 moles de HgT_{UNF} (~ 17 % en tant que $MMHg_{UNF}$) sont exportées chaque année en aval du barrage. Selon un bilan de masse, la production locale de $MMHg_{UNF}$ (i.e. $MMHg_D$) atteint 8,1 (7,3) moles a^{-1} soit un taux de méthylation de 0,06 (0,08) % j^{-1}. Cette valeur met en évidence le rôle de réacteur chimique joué par la retenue de Petit-Saut : altération de la spéciation du mercure au profit des composés méthylés.

Statut : soumis à « Applied Geochemistry »

Mercury cycling in a tropical artificial reservoir: monomethyl-mercury production and sources

B. Muresan*, D. Cossa*[1], S. Richard**, Y. Dominique***

**Institut français de recherche pour l'exploitation durable de la mer (IFREMER), BP 21105, F.44311 Nantes cedex 3, France (EU)*

***Laboratoire de recherche en environnement barrage de Petit-Saut (HYDRECO), BP 823, F.97388 Kourou, French Guiana (EU)*

****Laboratoire d'écophysiologie et écotoxicologie des systèmes aquatiques (LEESA), UMR CNRS 5805, F.33120 Arcachon, France (EU)*

ABSTRACT

The distribution and speciation of mercury (Hg) in the water-column of an artificial partially anoxic tropical lake (Petit-Saut reservoir, French Guiana), and inputs (wet deposition, tributaries) and output (atmospheric evasion and turbine outlets) were investigated on a seasonal basis in order to appraise the cycling and transformations of this metal. In the oxygenated epilimnion, the total mercury (HgT) concentrations averaged 5 ± 3 pmol L^{-1} in the unfiltered (HgT_{UNF}) and 4 ± 2 pmol L^{-1} in the dissolved (HgT_D) samples. On average, monomethylmercury (MMHg) constituted 18% of the total mercury in the unfiltered samples ($MMHg_{UNF}$). It orderly composed 8 and 40 % of the dissolved phase ($MMHg_D$) and suspended particulate matter ($MMHg_P$) mercury. Covariant elevated concentrations of $MMHg_P$ and chlorophyll*a* suggest that surface planktonic activity may drive the mercury methylation process within the oxic part of the reservoir. In the anoxic hypolimnion, HgT_{UNF} and HgT_D averaged 13 ± 6 and 8 ± 4 pmol L^{-1}. The hypolimnetic $MMHg_P$ and $MMHg_D$

concentrations were two and three times the corresponding values of the epilimnion, 170 ± 90 pmol g^{-1} and 0.9 ± 0.5 pmol L^{-1} respectively. The generally observed bimodal distributions of $MMHg_D$ concentrations, with maxima below the oxycline and near the benthic interface, suggest these two main sites for water-column $MMHg_D$ production and mobilization. Regarding mercury cycling, direct wet atmospheric deposition accounted for 11 moles yr^{-1} HgT_{UNF} (0.7 moles yr^{-1} as $MMHg_{UNF}$) while 76 moles yr^{-1} HgT_{UNF} (4.7 moles yr^{-1} as $MMHg_{UNF}$) came from tributaries. Simultaneously, around 78 moles of HgT_{UNF} (~17 % as $MMHg_{UNF}$) are annually exported downstream the dam. A mass balance calculation revealed that the endogenic production of $MMHg_{UNF}$ (i.e. $MMHg_D$) attained 8.1 (7.3) moles yr^{-1}, corresponding to a methylation rate of 0.06 (0.08) % L^{-1} d^{-1}. As a result, the Petit-Saut reservoir is a man-made huge reactor that has extensively altered mercury speciation in favor of methylated species.

Keywords: Mercury; Artificial reservoir; Tropical environment

[1] Corresponding author (Tel.: 33 2 40 37 41 76; Email: dcossa@ifremer.fr)

1. INTRODUCTION

The toxicological concerns regarding mercury (Hg) has given rise extensive studies regarding its distribution and speciation in freshwater environments. Special attention has been paid to monomethylmercury (MMHg) because of its toxicity (Zahir *et al*., 2005) and huge bioaccumulative capacity in aquatic food webs (e.g., up to 10^7 according to Boudou *et al.*, 2005). If bacterial methylation of inorganic divalent mercury (Hg^{II}) in low oxygen environments is reasonably recognized as being the main source of MMHg before its incorporation into food webs (e.g., Devereux *et al*., 1996; Benoit *et al*., 1999; King *et al*., 2001), identifying the various environments where alkylation processes occur is still a task in progress. There has been much research on mercury speciation in temperate and cold regions where several meromictic and oligomictic lakes were shown to assist the build up of MMHg in their anoxic deep-water layers (e.g., Korthals and Winfrey, 1987; Cossa *et al*., 1994; Morrison and Watras, 1999). Redox (Eh) margins, containing sulfate-reducing bacteria (SRB), have also been recognized as privileged domains for microbial Hg methylation [e.g., Jensen and Jernelov, 1969; Gilmour *et al*., 1992; King *et al*., 1999; Mason and Lawrence, 1999; Benoit *et al*., 2003]. Similar situations fostering MMHg formation have been found in artificial lakes and a number of authors have even pointed out that filling hydroelectric reservoirs may result in increasing the mercury concentrations of fishes (e.g., Surma Aho *et al.*, 1986; Verdon *et al.*, 1991; Tremblay, 1996; Schetagne and Verdon, 1999).

To date, the methylating potential of equatorial or tropical lakes has been poorly explored and only a few studies on mercury speciation have focused on such areas (e.g., Guimares *et al*., 2000 a and b; Roulet *et al*., 2000 and 2001). However, tropical watersheds, such as the Amazon region, present a background of high mercury concentrations coupled to the active cycling of this metal. Their ferralitic soils are naturally enriched with mercury (e.g., Roulet and Grimaldi, 2001; Roulet *et al.*, 2001). In addition, anthropogenic activities linked to

gold mining are responsible for improved Hg mobilization and/or direct rejections into the aquatic systems. The resulting elevated concentrations of inorganic Hg combined to favorable methylating conditions (active SRB due to high temperature, high OM and low oxygen), support the hypothesis of high MMHg levels in the vicinity of redox boundaries constitutive of tropical waterbodies (e.g., oxycline or sediment / water interface). These features have been recently evidenced in the Petit-Saut artificial lake in French Guiana (Coquery *et al*., 2003), where the flooding of more than 350 km² of uncleared primary forest created an anoxic water-column of more than 20 m depth. Furthermore, Durrieu *et al*. (2005) and Boudou *et al*. (2005) have described the mercury bioamplification in fishes found in this system.

Here, we present the gained data on Hg transfers and transformations in this artificial tropical reservoir (Fig. 1). The aim of this study was to identify the Hg and MMHg sources to the system and to quantify the probable formation of MMHg within the lake. Sources include the river tributaries (some draining active and former gold mining sites), the atmospheric deposition, the release from flooded soils / vegetation and the *in situ* production. For this purpose, we determined the Hg speciation in the water-column during both the dry and wet seasons. Concurrently, mercurial inputs and outputs of the system were described by a monitoring approach. Ultimately, the distributions of main physical parameters (temperature, pH, conductivity and turbulent diffusion) and major chemical species (oxygen, iron, sulfides, and OM) were used to try to build up a comprehensive pattern of the mercury cycle in the system.

2. MATERIAL AND METHODS

2.1. Sample collection

2.1.1. Rain sampling -- Wet deposition was collected for Hg analyses at the HYDRECO field laboratory station, 200 m away from the dam (Fig. 1). Compiled data account for approximately 20 months of regular sampling from April 2003 to December 2004. Additional samples for rainfall amount, conductivity, pH and occasionally total organic carbon (TOC) determinations were collected in a polyethylene bag. Regarding mercury, ultra-clean procedures were used in order to maintain the integrity of the samples. The collection system consisted of a 14 cm diameter Teflon (PTFE) funnel attached to a 500 mL acid-clean Teflon (FEP) bottle. A Teflon net (76 µm pore size, Savillex) was added at the funnel bottom to prevent large particles collection. A 16 cm long flute of Teflon (PTFE) gently poured the rainfall water directly from the base of the funnel to the bottom of the bottle. Samples for mercury were collected on a weekly basis using ultra-clean sampling techniques. Bottles were double bagged then frozen at –20 °C in dark conditions until analysis. Wet deposition waters were analyzed for HgT_{UNF}, HgR_{UNF}, DGM and $MMHg_{UNF}$ (see below for definitions).

2.1.2. Water-column sampling -- Samples from the reservoir were collected during three sampling campaigns of approximately two months that took place in March-April 2003 (the short dry season), January-February 2004 (the short wet season) and May-June 2004 (the long wet season). These were designated as Matoutou 1, 2 and 3 respectively. For each campaign, the water-column was sampled at the same three stations: the flooded forest (FF), the center of the reservoir (CR) and 200 m upstream of the dam (UD). Sampling stations were chosen in order to suitably describe the temporal and spatial variability of the biogeochemical and physical processes that affect mercury speciation (Fig. 1). The flooded forest sampling station characterizes a creek that does not exceed 17 m in depth (4°55.67'N - 52°59.96'W). Except for the riverbed, proper macrophyte (trees, shrubs) immerged vegetation covered more than 90 % of the surface of the reservoir before flooding. The second sampling station (CR) characterizes the main waterbody of the Petit-Saut lake (4°56.382'N - 53°02.610'W). It was

located at the vertical point of the pre-flood riverbed. Nowadays, the water-column usually exceeds 20 m in depth and displays a sharp and permanent stratification. Lastly, the dam sampling station provided mercury distribution and speciation in some of the most altered masses of water from the reservoir (5°03.77'N - 53°02.45'W). These 3 stations enabled to describe the mercury distribution and transformations in the water-column of the reservoir prior to dam exportation.

The ultra clean sampling techniques and analytical methods applied for water analyses are those described and discussed in detail by Bloom (1989) and Cossa *et al*. (2002 and 2003). In short, water-column samples were collected using a peristaltic pump and acid-cleaned polypropylene tubing. Polyethylene gloves were used for handling operations. Samples were collected in acid-clean Teflon (PFA) bottles. The bottles were rinsed three times prior to filling, then filled, double-bagged, and transported in coolers back to the field laboratory. Analyses of dissolved gaseous mercury (DGM) were performed within 2 hours of collection. The sum of all mercury species (HgT_{UNF}) along with the dissolved (HgT_D) and reactive (HgR is the easily reducible fraction obtained by pH 1 direct reduction with $SnCl_2$, i.e. a proxy of the labile Hg^{II}) fractions were processed the same day. In addition, aliquots were kept to measure monomethylmercury (MMHg) in the unfiltered ($MMHg_{UNF}$), dissolved ($MMHg_D$) and the particulate ($MMHg_P$) phases. Water samples were filtered using hydrophilic Teflon membranes (0.45 µm pore size, 45 mm diameter, LCR®, Millipore), then acidified with 0.5 % (v/v) HCl (Suprapur®, Merck). For each sample, the filtered amount of water was gravimetrically determined. Used filters (particulate samples) and corresponding filtered solutions were ultimately double bagged and stored at –20 °C in dark conditions until analysis.

2.1.3. Tributaries and tailrace sampling -- Since March 2003, mercury exportations downstream of the dam had been monitored on a weekly basis. Samples were collected a few

meters downstream the outflow of the turbines along the left bank of the channel that conveys exported water. As turbines are fed with water from the hypolimnion, samples from Station CS (Channel Station) accounted for the exported water flow from the anoxic part of the reservoir (Fig. 1). The CS site precedes an aeration system set up in order to maintain the downstream concentrations of dissolved oxygen compatible with aquatic life. Regarding water inputs to the artificial lake, upstream tributaries (Sinnamary, Courcibo and Leblond streams) were sampled in December 2004 and March 2005. In a general way, the water samples were collected with gloved hands directly in acid washed 1 liter Teflon (FEP) bottles. These were stored in a cooler without direct light exposure and carried back to the field laboratory for analysis within 6 hours of collection.

2.1.4. Sediments sampling -- Within the dam water-body, the decomposition of submerged vegetation follows a slow degradation kinetics. Ten years after the impounding completion, dead tree trunks still emerging from water provide little access to the sediments of the reservoir. As a result, sediments can only be found close to the ancient Sinnamary riverbed (Fig.1). The Sinnamary River being the main fresh water input into the system. Hence, two cores of sediments (noted #1 and #2) were collected for solid phase Hg analysis. Core #1 originated from the Saut Dalles station (SD), 11 km ahead of the reservoir entrance, while core #2 was collected further down the Takari Tanté fall (200 m inside the reservoir itself). Sediment cores were sampled by hand using acid-cleaned Plexiglas tubes (6.5 cm i.d.) then transported in coolers back to the field laboratory. The same day, horizontal sectioning was performed at a centimetric resolution using a polypropylene knife. Sediment slices were immediately placed into 50 mL acid-cleaned polycarbonate tubes, sealed, frozen at –20 °C in dark conditions then freeze-dried for total mercury (HgT_P) analyses.

2.2. Sample analyses

2.2.1. Ancillary parameters – Water-column measurements for temperature, pH, dissolved oxygen, conductivity and redox were recorded *in situ* with a YSI 600XLM multiparameter probe sonde. Additional analyses for major chemical species were carried out in the laboratory. Briefly, the concentrations of total sulfides (ΣH_2S) and dissolved (<0.45 µm) iron (FeT_D) were colorimetrically measured by means of specific photometric test kits (Spectroquant®, Merck). Chlorophyll*a* (Chl*a*) was spectrophotometrically determined in 90% acetone, in accordance with Ameel *et al.* (1998). For ΣH_2S determination, 4 ml of water poured from the collection tubing were added to 6 ml of a $ZnCl_2$ trapping solution. Samples were transported to the field laboratory and methylene blue method was then applied within 2 hours of collection. Concerning FeT_D, around 2 L of water were individually collected while making sure t that the headspace of the bottle was minimized. After returning to the HYDRECO laboratory, samples were filtered in a nitrogeneous atmosphere. Then 10 mL of a sample diluted ten times were colorimetrically analyzed. The colored reaction consists in synthesizing an iron red-violet complex, given that reduced Fe^{II} encounter a triazine derivative in a thioglycolate-buffered medium. Samples for Chl*a* were collected on 0.7 µm (Whatman, GF/C) glass filters from 200 ml of water. Worn filters (Chl*a* samples) were stored at –20 °C in dark conditions until spectrophotometric determination was applied. This method consists in measuring the standard absorbances at 750 nm and 664 nm of a 4 mL 90% acetone extract before and after acidification (100 µL of 0.12N HCl).

2.2.2. Mercury speciation -- All mercury species in water samples were detected by cold vapor atomic fluorescence spectrometry (AFS). Unfiltered and dissolved Hg were determined according to Bloom and Fitzgerald (1988), by the formation of volatile elemental Hg (released by $SnCl_2$ reduction, after 30 minutes of acidic BrCl oxidation) and its preconcentration on a gold column. The detailed procedure is provided by Cossa *et al*. (2003). Reactive mercury, the easily reducible fraction, was obtained within 4 hours of sampling by

direct reduction with $SnCl_2$. Dissolved gaseous mercury (DGM) analyses were processed onto 250 mL of unfiltered aliquots of sampled water. Samples for DGM were sparged for 40 min with Hg-free argon at 200 mL min^{-1} within 2 hours of collection. The suspended particulate matter (SPM) collected on a preweighed LCR® filter was reweighed in order to estimate the SPM load and digested with concentrated HCl/HNO_3 (1/9, v/v) in Teflon (PFA) reactors (80 °C; 4 hours) to determine HgT_P concentrations. An automatic atomic absorption spectrometer (AMA-254®, Altec) was also used for HgT_P determinations in the solid phase of the sediments. This technique comprises a calcination of the freeze-dried samples under an oxygen gas stream in order to produce elemental mercury vapor and its subsequent amalgamation on a gold trap; mercury vapor subsequently being measured by AAS (Cossa *et al*., 2002). The detection limits, defined as 3.3 times the standard deviation of the blanks, amounted to 0.05 pmol L^{-1} and 0.025 nmol·g^{-1} for the HgT_D and HgT_P respectively. The corresponding reproducibilities (the coefficient of variation in percentage of five replicate samples) were lower than 10 %. The accuracy for Hg determinations in solids was regularly checked using the reference material (MESS-3) from the National Council of Canada as certified reference material (CRM). In parallel with HgT_P, loss on ignition (LOI) was determined as a proxy for organic matter content by measuring the weight loss on lyophilized sediment after 24 hours at 450°C. Monomethylmercury was determined using the method initially proposed by Bloom (1989) and modified by Liang *et al*. (1994) and Leermarkers *et al*. (2001). $MMHg_{UNF}$ and $MMHg_D$ in acidified water were extracted by CH_2Cl_2 and then transferred into 40 mL of Milli-Q water by evaporating the organic solvent. The aqueous solutions were analyzed for MMHg by gas chromatography after ethylation and adsorption / desorption on a Tenax® column. For $MMHg_P$, a 3 hour acidic dissolution (HNO_3 65 %) of the filtered SPM took place before the procedure described previously. Detection limits were 0.01 pmol L^{-1} and 0.005 pmol·g^{-1} for respectively a 100 mL water and 200 mg solid sample.

Precision surpassed 10 % for all analyses. Using the available reference material (IAEA-405), the accuracy of the method was estimated to be more than 10 % with 91 ± 8 % recovery. The detailed procedure is given by Cossa *et al*. (2002).

2.3. Modeling the turbulent diffusion

The applied turbulent diffusion model is according to Peretyazhko *et al*. (2005). $MMHg_D$ and HgT_D turbulent fluxes are formulated at the sediment-water interface (SWI) and water-column chemocline (WCC) as the product of a vertical turbulent diffusion coefficient K_z ($m^2\ s^{-1}$), and the concentration gradient:

$$\Im = -K_z\ (\partial C/\partial z)$$

Eddy diffusivities are estimated on wind speed data and temperature profiles. In the well-mixed surface layer, turbulence is assumed to be wind driven and K_z is estimated by:

$$K_z = \gamma_{mix}\left(\frac{\rho_{air}\ C_{10}}{\rho}\right)^{3/2} \frac{\varpi_{10}^{3}}{N^2\ k\ z} \qquad\qquad N = \left(-\frac{g}{\rho}\ \frac{\partial \rho}{\partial z}\right)^{1/2}$$

where γ_{mix} is the non-dimensional mixing efficiency (a value of 0.15 was assumed), ϖ_{10} is the wind speed at 10 m altitude (of 3 m s^{-1}, HYDRECO data), C_{10} is the wind-stress coefficient (approximately 10^{-3} for ϖ_{10} < 7 m s^{-1}), k = 0.4 is the Karman constant, z is the depth (m), ρ and ρ_{air} are the densities of water and air, respectively. The temperature is used as a conservative tracer in order to determine the mixing profile form below the well-mixed surface layer:

$$K_z\ (\partial T/\partial z) = K_{z0}\ (\partial T/\partial z)_{z0}$$

where T is the temperature, $(\partial T/\partial z)$ is the temperature gradient and z_0 is the depth of the lower boundary of the well-mixed epilimnion (4 to 10 m).

3. THE PETIT-SAUT RESERVOIR: ENVIRONMENTAL SETTINGS

3.1. Local geography

The Petit-Saut hydroelectric dam (http://www.cg.ensmp.fr/Guyane/Compte_rendus/petit_saut-hydreco.htm) was built in the tropical forest of French Guiana on the Sinnamary River basin (Fig. 1). The Sinnamary is a 250 km long river which spring is located in the center of French Guiana at an altitude of 125 m. Its catchment area spans over 7000 km² of crystalline rock formation overgrown by uninhabited primary forest (Richard, 1996). The Leblond, Courcibo and Tigre creeks are its main tributaries. The construction of the Petit-Saut hydroelectric dam took place between 1989 and 1994, *circa* 70 km ahead of the Sinnamary River confluence with the Atlantic Ocean (5°04' N; 53°03' W). The flooding started in January 1994 and ended in July 1995 with a resulting artificial lake stretching over 60 km length and a maximum 60 km width. At that time, the maximum water depth was 35 m. This depth corresponded to the submersion of approximately 350 km² of primary forest and the creation of about 105 km² of small islands (Huynh *et al*., 1997). During the 2003-2004 period, corresponding to our three major sampling campaigns, the maximum water depth (near Station CR) was 32 m and the flooded area covered 230 km². Total water volume and mean water depth were therefore estimated to 3 10^9 m^3 and 13 m respectively. The annual mean discharge was measured downstream of the dam at ~ 180 m^3 s^{-1} which accounted for a residence time of the impounded water of approximately 6 months.

3.2. Reservoir stratification

The filling of the Petit-Saut hydroelectric reservoir sparked major modifications in the water chemistry of the former Sinnamary River. Initially, the waters were warm, acidic, only slightly conductive, oxygenated, nutrient poor and relatively homogenous (Horeau *et al*., 1998). As the forest and fluvial ecosystems became a lacustrine environment thermal

stratification occurred (Fig. 2). The waters of the reservoir rapidly stratified as an oxygenated epilimnion and an anoxic hypolimnion (Richard, 1996). The degradation of immerged OM combined to the mixing regime of water masses and the light limitation govern the vertical distribution of aquatic substances within the stratified water-body. Reduced substances such as methane and hydrogen sulfide are distributed along a marked vertical concentration gradient in the vicinity of the oxycline (Dumestre *et al.*, 1999). In comparison with the epilimnion, the hypolimnion exhibited elevated concentrations of reduced elements. The main processes responsible for water enrichment were OM degradation (ammonium, phosphates, humic acids, etc.) and mobilization from the geological substratum (iron, manganese, silica, etc.).

3.3. Water-column characteristics

At a preliminary stage of the project, the water-column was sampled in order to characterize the physical chemistry of major chemical species. Figures 2A to 2C show the water-column profiles of main physical characteristics and major chemical compounds at A: Flooded Forest (FF), B: Roche Génipa (CR) and C: upstream dam (UD) stations. Each graph displays the distribution of a same parameter with regard to Matoutou 1, 2 and 3 campaigns.

3.3.1. Temperature -- The temperature of the reservoir ranged between 25 and 30 °C. Depending on the season and site, the thermocline was located between 5 and 10 m in depth. No marked gradient ever developed as mean temperatures of the epilimnic and hypolimnetic waters varied only from 28.6 to 30.0 °C and 25.8 to 27.0°C respectively.

3.3.2. Conductivity – Water-column conductivity varied from 19.6 µS cm^{-1} (CR, June 2004) to 67.3 µS cm^{-1} (UF, February 2004). Measured data displayed a strong time dependency with high values listed during the short dry season and lower ones by the end of the long wet season. Vertical profiles of conductivity usually increased with depth displaying a sharp gradient close to the oxycline that increased the stability of the water-column. By way

of example, conductivity at the Station UD during the short dry season (February 2004) increased from 22 µS cm^{-1} in the epilimnion to 68 µS cm^{-1} at the sediment water interface (SWI). However, it is worthwhile noticing that during the wet season conductivity may occasionally drop in the vicinity of the SWI (CR, February 2004).

3.3.3. pH -- The pH in the Petit-Saut reservoir was slightly acidic in the epilimnion (6.1 ± 0.3 units) and acidic in the hypolimnion (5.6 ± 0.5 units). As a matter of fact, pH was widely conditioned by the geological composition of soils. Ferralitic and acidic minerals are widespread in the Amazon region. These consist mainly in Fe and Al hydrous oxides and clay minerals such as kaolinite. As a result of their alteration, leach waters contain low pH values and pronounced organic content. In addition, elevated precipitation rates (close to 3000 mm yr^{-1}) of acid rains (4.6 ± 0.4 pH units in 2003/04) tend to accentuate the alteration phenomena in the region of the reservoir maintaining the pH below neutrality.

3.3.4. Oxygen -- The vertical distributions of dissolved oxygen (O_2) showed a correlation with thermal stratification. O_2 concentrations were usually close to saturation with values approaching 0.2 mmol L^{-1} towards the surface. In fact, O_2 concentrations correlated positively with temperature (r^2 =70) in the upper oxygenated layer then started to drop below 0.01 mmol L^{-1} in the transition zone located from 4 to 9 m in depth. Because of the flux of reduced OM from submerged vegetation / soils declines since the beginning of the filling, the oxycline rose from a depth of 1m in January 1994 to a maximum of 10 m depth in June 2004. Except for occasional advection processes and/or the in-depth injection of epilimnic water, usually observed during the long wet season, anoxic conditions prevailed further down the hypolimnion.

3.3.5. Iron – The degradation of the ferralitic soils (including soil flooding, erosion, deforestation and cultivation) is the main source of iron in the Petit-Saut reservoir. FeT_D concentrations in the hypolimnion averaged 30 ± 20 µmol L^{-1} and attained up to 68 µmol L^{-}

[1]during the short dry season (April 2003). In comparison with the hypolimnion, FeT_D concentrations in the epilimnion were generally low (< 1 µmol L^{-1}). FeT_D concentrations displayed a broad seasonal variability. On the one hand, the dry season corresponded to a phase of accumulation for reduced chemical compounds in the water-column (i.e. low Eh values, high conductivity and marked O_2 gradient). On the other hand, the wet season defined a period of occasional dilution of the hypolimnion by surface waters. This pattern is confirmed by FeT_D measurements. Averaging data from the hypolimnion of all stations, the maximum value of 38 ± 11 µmol L^{-1} was recorded during the short dry season (April 2003). The short (February 2004) and long (June 2004) wet seasons displayed concentrations of 27 ± 17 µmol L^{-1} and 14 ± 16 µmol L^{-1} respectively.

3.3.6. Sulfides -- The vertical distribution of ΣH_2S displayed a diminution from the SWI (up to 4.9 µmol L^{-1}) to the surface (< 0.1 µmol L^{-1}) with a marked gradient under the oxycline. Heavily laden with iron (laterite), the soil reacts with hydrogen sulfides causing the appearance of iron sulfides complexes, suggested by the correlation between ΣH_2S and FeT_D (r^2 = 0.73). In addition, ΣH_2S and FeT_D exhibited analog temporal trends: at Station CR, hypolimnetic concentrations of sulfides decreased from 3.6 ± 0.8 µmol L^{-1} to 1.2 ± 1.1 then 0.2 ± 0.1 µmol L^{-1} starting with short dry season then short wet and finally long wet seasons. According to Dumestre *et al*. (1999), the sulfur gradient was always superimposed on a sharp peak of bacterial abundance. This bacterial assemblage, mainly composed of green sulfide-oxidizing bacterium of *Chlorobium* species, showed cyclic growth with a maximum development during the dry season and a minimum of abundance during the wet season. Albeit minor, sulfate-reducing bacteria (SRB) were preferentially found just below the oxic-anoxic interface (Dumestre *et al*., 2001). A small but active fraction of the green sulfur bacteria were closely associated with the sulfate-reducing population. Thus, a loop between sulfide producing and sulfide consuming bacteria was established in the reservoir.

4. RESULTS AND DISCUSSION

4.1. The water-column

As expected from the physico-chemical characteristics, the vertical profiles of mercury species in the water-column demonstrated a considerable discontinuity between the epi and hypolimnion. Apart from DGM and $HgR_{UNF,}$ The highest concentrations of all the Hg species were generally located in the hypolimnion of the reservoir (Table 1, Fig. 3A to 3C). Such a pattern was particularly marked for $MMHg_D$ which exhibited a factor 3 of enrichment between the surface layer and the deep compartment. Reported results were consistent with earlier observations made by Coquery *et al*. (2003) in the course of the first methylmercury survey measurements in the reservoir. In addition, the operationally defined HgR_{UNF} was more than 50% of DGM, which implies that labile divalent mercury species were at very low concentrations. The corollary is that most of the Hg^{II} seemed strongly bound to organic carbon and/or sulfur.

4.1.1. The epilimnion –Epilimnetic HgT was predominantly (74 ± 4 % of HgT_{UNF}) present as dissolved (< 0.45 µm). To the opposite, the particulate phase prevailed for MMHg (60 ± 20 % of as $MMHg_P$). There was a noticeable temporal variability of mercury within the epilimnion (Fig. 3). Observed variations were related to the suspended particulate matter (SPM) load, water discharges and resulting variations in the stability of the water-column stratification. The maximum of HgT_{UNF} (6.0 ± 1.4 pmol L^{-1}) corresponded to the short wet season which generally depicts a period of intense soil erosion (SPM of water averaged 14 ± 3 mg L^{-1}). In comparison, the short dry and long wet seasons, HgT_{UNF} (and SPM) respectively averaged 3.9 ± 0.8 pmol L^{-1} (10 ± 3 mg L^{-1}) and 3.7 ± 0.7 pmol L^{-1} (2 ± 2 mg L^{-1}). The Hg content of the particle (HgT_P) followed a mirror image of that of SPM: as SPM increased in

the epilimnion (up to 35 mg L^{-1}), one could observe the gradual decrease in HgT_P (to below 50 pmol g^{-1}). The dilution of the epilimnetic autochthonous SPM load by eroded particles from the tributaries banks and beds (with lower Hg content, Peretyazhko, 2002) may coincide with a decrease in the overall HgT_P concentrations during the high runoff periods. HgT_P actually declined from 290 ± 60 to 120 ± 110 pmol g^{-1} between the short dry to short wet season, then leveled up to 700 ± 200 pmol g^{-1} during the long wet season. Since HgT_D behaved in the opposite way with HgT_P, a marked narrowing of the Hg partition coefficient ($Kd_{Hg} = HgT_P / HgT_D$) was noticeable with an elevation in the SPM concentration ($\log Kd_{Hg} = -0.07$ (SPM) + 5.3; $r^2 = 0.38$). Such a relationship suggested that a significant fraction of eroded particles are composed by readily labile colloids which contribute to the so-called "dissolved" phase (Schuster, 1991; Lee and Iverfeldt, 1991; Hurley *et al*., 1995).

Regarding methylated species, inverse patterns were observed between SPM and dissolved or particulate monomethylmercury concentrations. The maxima of $MMHg_D$ (0.4 ± 0.2 pmol L^{-1}) and $MMHg_P$ (180 ± 70 pmol g^{-1}) occurred in the short dry season (Fig. 3A to 3C). The dry season is a period of high primary production and development of the phototrophic bacterial community (Dumestre *et al*., 1999). We then observed a positive significant ($p \leq 0.05$) relationship between the chlorophyll*a* and $MMHg_P$ concentrations in the water ($r^2 = 0.44$; $[MMHg_P]_{pmol\ L\text{-}1} = 5\ 10^{-3}\ [Chl\textit{a}]_{\mu g\ L\text{-}1} + 5\ 10^{-2}$). Low towards the surface waters, the Chl*a* (from 16 to 32 µg L^{-1}) and $MMHg_P$ (from 0.12 to 0.20 pmol L^{-1}) increased with depth. Highest concentrations were measured between 3 and 5 m below AWI. This suggests that plankton related activities might drive mercury methylation in the oxic epilimnion. In the wet season, the decrease in water-column stratification and subsequent mixing between hypolimnetic and epilimnetic bacterial guilds should limit the phototrophic driven methylation mechanisms. This phenomenon may be accentuated by the common diminution in light exposure (as cloudiness cover increases) and water residence time within

the reservoir (from 9 to 4 month). This interpretation is consistent with the lowest $MMHg_D$ (0.2 ± 0.1 pmol L^{-1}) and $MMHg_P$ (35 ± 15 pmol g^{-1}) levels determined during the short wet season.

The spatial variability of Hg was considered by comparing average concentrations in the epilimnion at the three stations (Table 2). While the ancient Sinnamary riverbed stations (CR and UD) displayed relatively homogenous mercury concentrations (3.7 ± 1.3 and 3.9 ± 1.8 pmol L^{-1} respectively), the flooded forest station (FF) showed lower HgT_D concentrations (2.7 ± 1.5 pmol L^{-1}). Apart from the extreme runoff episodes, the rapid sedimentation of the inflowing particles ensured a reduced lateral variability of the SPM concentrations (from 6 ± 4 to 11 ± 6 mg L^{-1} on average). As a result, a moderate lateral variability was also observed for HgT_P (overall average of 200 ± 150 pmol g^{-1}). Regarding methylated species, Station FF displayed lower $MMHg_{UNF}$ concentrations than other both other sites: 0.5 ± 0.3 *versus* 1.1 ± 0.4 and 1.0 ± 0.3 pmol L^{-1}. Such a difference primarily originated from a lesser contribution of the particulate phase (40 ± 20 *versus* 70 ± 20 % of the $MMHg_{UNF}$). Whereas a relative homogeneity was observed for $MMHg_D$ (all stations around 0.3 pmol L^{-1}), the $MMHg_P$ concentrations increased from 50 ± 30 to 100 ± 80 pmol g^{-1} between FF and the former riverbed stations (CR and UD). With respect to DGM, the former riverbed stations most exposed to solar irradiation displayed the highest concentrations: 0.5 ± 0.2 and 0.4 ± 0.1 pmol L^{-1} for CR and UD respectively. At Station FF, where a dense tree cover was present, DGM averaged 0.16 ± 0.08 pmol L^{-1}.

4.1.2. The hypolimnion -- The hypolimnetic HgT_{UNF}, $MMHg_{UNF}$, HgT_D and $MMHg_D$ average concentrations were twice as high as in the epilimnion (Table 1, Fig. 3A to 3C). The highest HgT_{UNF} (17 ± 5 pmol L^{-1}) and HgT_D (10 ± 4 pmol L^{-1}) concentrations were measured during the intense runoff episode that occurred during the short wet season. In addition, these results tally with previous observations by Peretyazhko *et al*. (2005). During this period,

relatively high SPM (12 ± 5 mg L^{-1}) and HgT_P (600 ± 350 pmol g^{-1}) concentrations provided the highest HgT levels in the particulate phase (8 ± 3 pmol L^{-1}). On the contrary, the short dry season contained the lowest mercury concentrations (3 ± 2 pmol L^{-1}) in the particulate phase due to a low HgT content in the SPM (250 ± 200 pmol g^{-1}).

With a mean concentrations of 0.9 ± 0.5 pmol L^{-1} (Table 1), the $MMHg_D$ to HgT_D contribution stood at16 ± 6 %. While no significant trend was observed at Station FF (0.5 ± 0.1 pmol L^{-1}), $MMHg_D$ levels in the vicinity of the ancient Sinnamary riverbed (CR and UD) showed a substantial increase during the long wet season (Fig. 4). By way of example, $MMHg_D$ concentrations at Station CR reached, for a 26 m deep hypolimnetic water-column, 1.8 ± 1.0 pmol L^{-1} during the June 2004 campaign. It is useful to observe (Fig. 3A to 3C) that vertical profiles of both $MMHg_D$ and $MMHg_P$ concentrations usually accounted for a bimodal distribution (with two distinct maxima): one close to the water-column chemocline (WCC) and the other to the sediment water interface (SWI). $MMHg_D$ concentrations at the WCC and the SWI respectively attained 2.8 pmol L^{-1} (CR, June 2004) and 5.9 pmol L^{-1} (CR, April 2003) corresponding to a $MMHg_D$ / HgT_D ratio close to unit. Such high $MMHg_D$ concentrations highlighted the role of the water-column chemocline and sediment water interface as potential sites for mercury methylation and/or methylmercury remobilization. From the acquired profiles (Fig. 2 and 3) and using the turbulent diffusion model (section material and methods) it was possible to assess the global amount of $MMHg_D$ that originated from WCC and SWI to roughly 7 moles yr^{-1}. In contrast to $MMHg_D$, $MMHg_P$ showed a trend of high concentrations in the short dry season (200 ± 150 pmol g^{-1} i.e. 2.5 ± 1.0 pmol L^{-1}) and low concentrations in the long wet season (150 ± 100 pmol g^{-1} i.e. 0.3 ± 0.1 pmol L^{-1}). As a result, the corresponding mean percentages of mercury as methylated species amounted to 80 ± 20 % and 4 ± 9 %. Despite this wide seasonal variability, the vertical distribution $MMHg_P$ exhibited a constant relationship with organic matter degradation. During the dry season, a

period of intense OM mineralization (Dumestre *et al*., 1999-2001; Horeau 1999), a positive correlation was observed between $MMHg_P$ and particulate inorganic carbon ($r^2 = 0.59$).

In short, the vertical distributions of mercurial species were globally characterized by high levels in the hypolimnion. Relatively wide variations were observed with seasons and sampling location. Accordingly, a contrast between the ancient Sinnamary riverbed (Stations CR and UD) and the flooded forest (Station FF) was also observed (Table 2). In addition, monomethylmercury concentrations both in the dissolved and particulate phases were enriched in the hypolimnion and peaked at the WCC and SWI, which respectively represent suboxic and anoxic zones where OM is actively recycled.

4.1.3. Epi-hypolimnion exchanges -- As already noticed by various authors, the vertical stratification of the reservoir was seasonally affected due to intense rainfalls and peaked riverine inputs (e.g., Peretyazhko, 2002). Observed differences between wet and dry seasons, were mainly due to the strong precipitation inflow between warm epilimnic waters and colder hypolimnetic waters in water mixing at the oxycline (Fig. 3A to 3C). As a result, the turbulent diffusion flux of hypolimnetic HgT_D that entered the epilimnion increased from the dry to the wet season. During the dry season (April 2003), the mean flux of HgT_D was oriented towards the hypolimnion (200 ± 100 pmol $m^{-2} \cdot d^{-1}$). Later, in the short wet season (February 2004), the HgT_D flux depicted a broad turn round towards the epilimnion (330 ± 100 pmol $m^{-2} \cdot d^{-1}$). In the course of the long wet season (June 2004), as the mixing regime weakened the water-column stratification, the flux of HgT_D remained directed towards the epilimnion with a mean value of 250 ± 50 pmol $m^{-2} \cdot d^{-1}$. Annual fluxes of HgT_D and $MMHg_D$ from the hypolimnion to the epilimnion were estimated to be 45 and 25 nmol $m^{-2} \cdot y^{-1}$. A comparative study between the oxycline and the SWI revealed that the equivalent of 40 and 70 % of the apparent annual sediment efflux of HgT_D and $MMHg_D$ were respectively transported to the epilimnion. The maxima of $MMHg_D$ concentrations (up to 0.5 pmol L^{-1})

were generally recorded in the dry season at 3 m in depth. This depth usually corresponded to a layer of high chlorophyll abundance (up to 20 µg L^{-1}) which accounted for more than 80 % of total pigments (Dumestre *et al*., 2001; De Junet, 2004).

4.2. The sediments

Little is still known about the sedimentary processes in the Petit-Saut reservoir. Thus, we consider the main allochthonous and autochthonous sources of sedimentary particles. The first group is from riverine sources and consists of detrital material and eroded soils carried in during flood events and among sediments within the mouths of the creeks inflowing the reservoir (De Junet, 2004). Autochthonous sources are of planktonic origin. We accessed the mercury and methylmercury content of these materials by collecting deposited sediments at Station SD (mouth of the Sinnamary River), using particles from surficial sediments from Stations CR, UD and FF, and sediment from traps moored at Station CR. Table 3 and Fig. 5 describe the obtained results. In the former riverbed (CR and UD sites), the mean HgT_P concentrations of the superficial sediment and particles from the moored traps were respectively 1100 ± 100 and 1800 ± 200 pmol g^{-1}. Mean concentrations were lower (200 to 900 pmol g^{-1}) near the shorelines (Station FF). Considering the sedimenting methylated fraction of HgT_P, deposited sediments exhibited higher $MMHg_P$ levels than particles from the moored traps (10 ± 1 *vs* 5 ± 3 % of HgT_P). This suggests a net SWI mercury methylation and its export from the sediment.

4.2.1. Particulate mercury flux to the sediments -- Sediment traps were deployed over a period of 6 weeks in November-December 2003 (dry season) at Station CR (De Junet, 2004). According to these authors, particulate vertical transport in the water-column originated from endemic plankton and it is mainly composed of chlorophyceae (> 90 %),

chlorobiaceae (< 10 %) and a lesser fraction of biofilm coupled to terrestrial OM. The sedimentary fluxes were estimated using the following relation:

$$\text{Flux} = \frac{\Delta m}{S \bullet \Delta t}$$

with Δm mass of accumulated material, S section of the collection cone (0.13 m^2) and Δt sampling period. The deposition fluxes were thus estimated to be 160, 90 and 165 mg m^{-2} d^{-1} at 7, 20 and 30 (near bottom) m depth respectively, suggesting particle dissolution between the epilimnion layer and 20 m, and particulate formation or resuspension near the bottom. Because of the likely resuspension events recorded in the fluxes, it is probable that the real HgT_P and $MMHg_P$ deposition fluxes correspond to an intermediate situation between those estimates at a depth of 20 and 30 m. Thus, from the deposition fluxes and mercury content of particles, it is possible calculate the November-December 2003 particulate HgT deposition to be 59-297 pmol m^{-2} d^{-1}. Assuming a constant annual flux, annual deposition should then vary between 22-105 nmol m^{-2} yr^{-1}. Applied to the entire surface of the reservoir (close to 2.3 10^8 m^2), *circa* 5-24 moles yr^{-1} HgT_P would reach the SWI; up to 10 % (5 ± 3 % on average) as monomethylmercury. However, since we can expect seasonal variability both in the particle flux and the HgT_P concentrations; these figures should be regarded as an order of magnitude estimate.

4.2.2. Effluxes of dissolved mercury out of the sediment -- According to Peretyazhko *et al*. (2005), the main flux of dissolved Hg to the hypolimnion originated from both degradation of flooded vegetation and partial dissolution of ferralitic soils. In fact, the flooding of this type of soils leads to a reductive dissolution of Fe oxyhydroxides and a migration of the released mercury into the aquatic ecosystem (Roulet *et al*., 1998b). As a result of the permanent sedimentary Hg efflux, observed profiles of HgT_D and $MMHg_D$ usually displayed higher concentrations to the SWI (Fig. 3A to 3C). Turbulent fluxes of HgT_D and $MMHg_D$ at the

SWI, formulated as the product of the vertical turbulent diffusion coefficient and the mean concentration gradient within the first meter above the sediments, were estimated to be 120-650 and 50-400 pmol m^{-2} d^{-1}, respectively. The corresponding annual effluxes were 100 ± 90 and 32 ± 20 nmol m^{-2} yr^{-1}, respectively. Comparing the SWI transportations, the annual sedimentary efflux and the particulate deposition of HgT_P were in the same order of magnitude (100 ± 90 *vs* 60 ± 50 nmol m^{-2} yr^{-1}). Nevertheless, the methylated percentage was substantially higher in the dissolved fraction outgoing from the sediments (about 30 %) than in the particulate fraction incoming to the SWI (around 5 %). Such a discrepancy suggests (i) that sediments are a major source of $MMHg_D$ to the water-column coupled to (ii) a substantial mobility of methylated species at the SWI that could limit its sedimentary accumulation. These estimates are however based on momentum situations, and a subduction of surface waters could have led to the dilution of HgT_D and $MMHg_D$ near bottom concentrations and thus increase the respective concentration gradients. Because of the relative isolation from the former riverbed, relevant effluxes of HgT_D and $MMHg_D$ were determined at Station FF. These were 190, 100 and 200 pmol m^{-2} d^{-1} for HgT_D in the short dry, short wet and long wet seasons respectively. For the same periods $MMHg_D$ effluxes were 50, 30 and 60 pmol m^{-2} d^{-1}. With an average of 60 ± 20 and 16 ± 5 nmol m^{-2} yr^{-1} respectively, the annual effluxes of HgT_D and $MMHg_D$ at Station FF were 50 % less than mean “apparent” effluxes calculated at Stations CR and UD. Seasonal variations of HgT_D and $MMHg_D$ effluxes covaried with those of FeT_D (3, 0.2 and 8 mmol m^{-2} d^{-1} in that order). This suggests that the reductive dissolution of iron contributed to mobilizing dissolved mercury species at the SWI. On the other hand, the positive relationship between the HgT content of particles (respectively 140, 550 and 2100 pmol g^{-1}) and ΣH_2S effluxes (orderly 0.05, 0.09 and 0.14 mmol m^{-2} d^{-1}) suggests that mobilized HgT_D is rapidly recycled onto the particulate phase through precipitation as cinnabar or iron sulfide trapping processes. Since $MMHg_D$ effluxes exhibited a similar

development to methylmercury in surficial sediments (respectively 130, 60 and 70 pmol g^{-1}), we hypothesized that a notable fraction of mobilized $MMHg_D$ may be composed of colloids. On the other hand, in contrast to HgT_D, divergences between $MMHg_P$ and ΣH_2S effluxes make it possible to surmise that $MMHg_D$ colloids are more composed of degraded OM than purely sulfide ligands.

4.3. Hg exchanges at boundaries

4.3.1. Inputs by rain -- In the vicinity of the reservoir, Hg concentrations in rain were representative of unimpacted North Atlantic environments (Lamborg *et al.*, 1999). Indeed, HgT_{UNF} concentrations averaged 16 ± 12 pmol L^{-1} (Table 2). The temporal distribution of HgT_{UNF} (Fig. 6) exhibited a pattern of high concentrations during the late dry season (up to 57.5 pmol L^{-1} in November 2004) and low concentrations in the course of the wet season (down to 2.7 pmol L^{-1} in March 2004). Besides HgT_{UNF}, the speciation of mercury was investigated through HgR_{UNF}, DGM and $MMHg_{UNF}$ analyses. Approximately 20 % of the HgT_{UNF} was composed by HgR_{UNF} (a proxy of labile Hg^{II} fraction). With concentrations varying from 0.1 to 20.8 pmol L^{-1}, its temporal distribution revealed a positive correlation with HgT_{UNF} ($r^2 = 0.54$; $p \leq 0.05$). The temperature dependence of the Henry coefficient (H = 466 atm mol^{-1} at 28 °C) ensured low DGM concentrations in rain (0.8 ± 0.9 pmol L^{-1}). As a matter of fact, DGM composed about 25% of HgR_{UNF} and close to 5 % of HgT_{UNF}. Yet, DGM still displayed a temporal distribution analogous to HgR_{UNF} ($r^2 = 0.73$; $p \leq 0.05$) and therefore to HgT_{UNF} ($r^2 = 0.42$; $p \leq 0.05$). Regarding $MMHg_{UNF}$, concentrations varied widely from 0.05 to 10.2 pmol L^{-1} with a mean value of 0.80 pmol L^{-1}.

When coupling the 3 m of annual precipitation rate of the 2003-2004 period to the Hg concentrations in rain, one can estimate the annual wet deposition at the reservoir surface.

Thus, HgT_{UNF}, HgR_{UNF}, DGM and $MMHg_{UNF}$ bulk wet deposition averaged respectively 46 ± 35, 9 ± 11, 2 ± 3 and 3 ± 5 nmol m^{-2} yr^{-1}. With the notable exception of $MMHg_{UNF}$, wet deposition corresponded to the low range of data found in the literature (e.g., Mason *et al*., 1997, 1999). On the other hand, Pb^{210} and Hg analysis in air, rain and atmosphere (http://lgge.ujf-grenoble.fr/publiscience/rapports/activite-2001.pdf) provided access to the total atmospheric deposition of Hg within the reservoir area. This was estimated to be 60 nmol m^{-2} yr^{-1}. Computed value was consistent with those reported by Lacerda *et al*. (1999) for the whole Amazonian basin (40-60 nmol m^{-2} yr^{-1}). An additional rough estimation of Hg total atmospheric deposition was provided using Pb^{210} datation of HgT_P sedimentary profiles (Barriel *et al*., 2001). The obtained result was in the same order of magnitude (150-200 nmol m^{-2} yr^{-1}). With 46 nmol m^{-2} yr^{-1}, wet atmospheric deposition corresponded to approximately 75 % of total atmospheric deposition of Hg (60 nmol m^{-2} yr^{-1}). This result underlined that rainfall was an efficient pathway for atmospheric mercury to reach the reservoir (11 moles yr^{-1}).

4.3.2. Inputs from tributaries -- In December 2004 and March 2005, main water inputs to the reservoir (the Sinnamary River and the Courcibo, Leblond creeks) were sampled and analyzed for HgT_D and $MMHg_D$ (Table 4). These data constituted the first mercury measurements for the upstream of the Sinnamary River (Saut-Dalles station). Except for the high HgT_D levels recorded during the 1999 dry season into the Leblond creek (Fig. 7), the recently measured HgT_D and $MMHg_D$ concentrations were comparable to previous surveys (Coquery *et al*., 2003). Based on measured concentration ranges and mean water discharge (190 m^3 s^{-1} for the 2003/04 period), we estimated the range within the annual Hg inputs to the reservoir should be: 45-105 and 1-4 moles for HgT_D and $MMHg_D$ respectively. At the mouth of the river tributaries, the part of HgT_{UNF} and $MMHg_{UNF}$ associated with the particulate phase stood at 41 and 25 % respectively. However, most of particles and the associated

mercury settle near the entrances of the reservoir. This was testified for the Sinnamary River by the parallel decreases in total mercury concentrations in the unfiltered samples and their SPM content (HgT_{UNF} = 13 ± 2 pmol L^{-1} at Saut Dalles *vs* 6 ± 3 pmol L^{-1} in surface water at CR).

4.3.3. Tailrace exportations -- Mercury concentrations and speciation were monitored at the output of the dam (Station CS) on a weekly basis from March 2003 to December 2004 (Fig. 8). The HgT_{UNF} concentrations at Station CS varied between 3.8 (June 2003) and 27.9 (July 2004) pmol L^{-1}. The average concentration of HgT_{UNF} was 13 ± 5 pmol L^{-1}. According to measurements performed on the filtrated samples, about 60 % (8 ± 2 pmol L^{-1}) of the mercury outflowing the reservoir was composed of HgT_D. In comparison, similar concentrations were measured into the hypolimnion of the reservoir between 8 and 15 m depth. In spite of the relative uniformity of HgT_{UNF} concentrations, seasonal pattern was apparent through semi-annual cycles. For instance, we observed a tendency towards elevated concentrations at the beginning and in the middle of the dry season (March to April then August to November). In contrast, the wet seasons displayed the lowest measured values (May to July then December to February). This pattern was in agreement with the general hypothesis that reduced species concentrated inside the hypolimnion during the dry season and were diluted in the course of the wet season. The relative homogeneity of HgT_{UNF} and HgT_D concentrations between the upstream (9-16 pmol L^{-1} of the river tributaries) and downstream (13 ± 5 pmol L^{-1}) of the reservoir would account for the reduced amplitude of these cycles (about 10 pmol L^{-1}).

The dam Hg exportation fluxes have been calculated (Table 5) using the weekly water discharges and weekly mercury concentrations. These significantly followed mercury concentrations in the tailrace water (r^2 = 0.40; $p \leq 0.05$). Such a relationship suggests that hypolimnetic processes may extensively affect Hg levels downstream of the dam. For total

mercury, the estimations are similar whatever the annual period being considered (March 2003 to March 2004 or October 2003 to September 2004). Yet, as for concentrations, exportation fluxes exhibited a significant variability with seasons (Fig. 8). Except for the intense runoff episodes (peaks of exportation), HgT_{UNF} outputs were 25 % higher during the dry seasons than in the course of the wet seasons (6.4 *vs* 4.7 moles $month^{-1}$). Two distinct mechanisms can be cited: (i) transport [the 4-5 month interval between the wet seasons maximal water inputs and the dry seasons elevated HgT_{UNF} discharges equals the residence time of water into the system] and (ii) *in situ* production or mobilization [the dry season depict the overall hypolimnetic water loading with reduced compounds (Section 3.3.5.)]. With regards to the methylated species, $MMHg_{UNF}$ levels in the dam-expelled waters exhibited a maximum of concentrations (8.4 pmol L^{-1}) and of exportation fluxes (0.15 moles d^{-1}) during the late wet season (Fig. 8). This period characterizes the confluence of elevated amounts of water leaving the reservoir (around 200 m^3 s^{-1}) and relatively high $MMHg_{UNF}$ levels in its hypolimnion (close to 4 pmol L^{-1}). Except for isolated Station FF, HgT_D and $MMHg_D$ presented similar developments in the hypolimnion of the reservoir and discharged waters (Fig. 4). However, long term processes (exceeding the annual scale) or episodic events (such as extreme particle discharge or water-column destabilization) may also account for these variations.

4.4. Mercury transformation in the water-column

A preliminary budget can be built up for methylmercury in the Petit-Saut reservoir using the measurements in the main water sources. The most striking conclusion concerning the 2003-2004 period was that dam exportations of $MMHg_{UNF}$ averaged 13.5 moles yr^{-1} although a maximum of 5.4 moles yr^{-1} reached the Petit-Saut artificial lake *via* rain and upstream tributaries. Despite the uncertainty surrounding these figures, there is a strong

suggestion that a large quantity of MMHg was produced in the reservoir itself. Referring to the 76 moles yr^{-1} of HgT_{UNF} passing through the artificial lake, the endogenic production of $MMHg_{UNF}$ attained 0.06 % L^{-1} d^{-1}. What is the nature of the mechanisms and which are the particular sites involved in mercury transformations within such environment?

The Regional Bureau for Industry, Research and Environment (DRIRE), estimated that 200 to 300 tons of mercury have been disseminated into the environment in French Guiana since 1850 (Richard *et al*., 2002). The local discharge of elemental Hg to the Petit-Saut reservoir originates principally from the upstream gold-mining area of Saint Elie. The respective amount of rejected Hg since the last century was (under)estimated to be approximately 23 tons (Petot, 1993). However, in the course of our study and except for the intense runoff events (mainly in wet seasons), the signature of the upstream Hg contamination rapidly diminished with distance from the gold-mining area (Fig. 7). This phenomenon was presumably related to a broad dilution of impacted waters while entering the artificial lake and/or to the rapid sedimentation of particulate fraction of HgT (90 % of the HgT_{UNF}) in the upstream area of the reservoir. To evaluate the role of the geological background, a rough comparison was made between “natural” (atmosphere, apparently unimpacted tributaries, flooded soils or vegetation) and anthropically affected (Leblond and Courcibo creeks) Hg sources to the system. In 10 years of flooding, Hg inputs to the Petit-Saut reservoir were (under)estimated to be *circa* 8000 moles (i.e. 1.6 tons Hg). The dominant fraction corresponds to the originally flooded vegetation and soils (60 and 20 % respectively). Unimpacted atmospheric, riverine and sedimentary source approaches 15 % of Hg inputs. Ultimately, local discharge from the upstream gold-mining area of Saint Elie was estimated to be less than 5 % of the total. Thus, it appears that most of the mercury introduced into the Petit-Saut reservoir is from natural sources including leaching and erosion of the drainage basin and atmospheric deposition.

Once inside the epilimnion of the reservoir, mercury can either be eliminated towards the atmosphere after photochemical reduction (Xiao *et al*., 1995; Amyot *et al*., 1997b), transferred to the hypolimnion after adsorption on SPM, or undergo further transformations such as methylation and (co)precipitation (e.g., with Fe species). In all likelihood, the AWI pronounced DGM concentrations (10 % of the HgT_D) reflect the photochemical production of Hg^0 in the presence of a reductive agent such as organic matter and especially iron-carboxylated ionic complexants (Beucher *et al*., 2002). Consequently, gas exchanges play a dominant role in the cycle of Hg in the upper waters of the reservoir. As described in a companion paper (Muresan *et al*., to be submitted), the partial evasion of mercury at the AWI (90 ± 50 nmol m^{-2} yr^{-1}) was twice as high as the mean wet deposition of HgT_{UNF} (46 ± 35 nmol m^{-2} yr^{-1}). Regarding methylated species, elevated $MMHg_D$ concentrations measured a few meters below the AWI (up to 0.5 pmol L^{-1}) suggested the existence of aerobic Hg methylation pathways (Fig. 3A to 3C). Further in depth, as reaching the oxic / anoxic margin, potential transfer of methylated Hg from the hypolimnion additionally contributed to enhance the epilimnetic $MMHg_D$ levels. As a comparison, similar levels of impregnation (close to 0.4 pmol L^{-1}) were measured during the maximum stratification period in the epilimnion of the Caballo reservoir (New Mexico) by Canavan *et al*. (2000). The accumulation of MMHg in the epilimnion of the Petit-Saut reservoir was obvious when measuring $MMHg_P$. $MMHg_P$ in SPM increased from 2.3 ± 0.3 to 40 ± 30 % of the HgT_P (i.e. 25 ± 15 to 80 ± 70 pmol g^{-1}) between the upstream of the Sinnamary River and the epilimnion of the reservoir.

As shown by Roulet *et al*. (1998a) and Peretyazhko *et al*. (2005), the erosion of fine particles from the pedological horizon prompts an increase in Hg discharges into the aquatic environment. The concentration and speciation of Hg bound to particles that reached the hypolimnion of the reservoir actually displayed a high seasonal variability. In the dry season, strong stratification between epi/hypolimnion as well as intense degradation of the OM would

have contributed to the accumulating MMHg (150 ± 70 pmol g^{-1}) on an endogenic, strongly mineralized and Hg-impoverished particulate substratum (150 ± 50 pmol g^{-1}). Conversely, in the wet season, the weak stratification between epi/hypolimnion, as well as the increasing of particulate discharges to the reservoir (the wash out of Hg-enriched particles, 4300 ± 2000 pmol g^{-1}), would have contributed to reduce the recycling of OM and consequently the methylated fraction in SPM (55 ± 25 pmol g^{-1}). Furthermore, the relative acidity of hypolimnetic waters (~ 5.6 pH units) combined with the intense microbial reduction of iron oxhydroxydes that prevail beyond a depth of 6 m (Peretyazhko *et al*., 2005) support the idea of the progressive mobilization (desorption) of Hg from sedimenting particles. This assumption is borne out by the gradual decrease in the Hg partition coefficient with SPM ($\log Kd_{Hg} = -0.06\ SPM_{mgL\text{-}1} + 5.5$; $r^2 = 0.42$ and $p \leq 0.05$).

The high $MMHg_D$ concentrations measured in the hypolimnion of the reservoir (0.9 ± 0.5 pmol L^{-1}) are consistent with the presence of low pH and Eh, which according to Compeau and Bartha (1985) and Gilmour and Henry (1991), not only help to increase methylation rates but also to decrease demethylation rates. Furthermore, the overall mean $MMHg_D$ concentrations displayed a high variability among sampling stations during the wet season (Fig. 3). The highest concentrations in the reservoir corresponded to the stations close to the former Sinnamary riverbed (1.5 ± 0.8 pmol L^{-1}). According to Dumestre *et al*. (1997), the in-depth injection of oxygenated water helps to stimulate the SRB activity through the formation of sulfates in a suboxic milieu. When plotted against ΣH_2S, the dissolved methylated fraction ($MMHg_D$ / HgT_D; a proxy of *in situ* methylation) exhibited a maximum of around 0.3 µmol L^{-1} (Fig. 9). The bulging shape of the dissolved methylated fraction *vs* ΣH_2S relation suggested that an optimum sulfide concentration favors mercury methylation. This observation is consistent with the hypothesis of neutral Hg-S complexes controlling the bioavailability of inorganic mercury for SRB methylation (Benoit *et al*., 2001 and 2003). It

was thus presumed that the elevated concentrations of $MMHg_D$, measured at Stations CR and UD during the long wet season, originated from both *in situ* methylation due to SRB activity and MMHg mobilization due to Fe oxyhydroxides dissolution and/or partial resuspension of the sediments.

4.5. Mercury speciation and mobilization at the SWI

HgT_D speciation at the SWI (Eh close to 100 mV) is potentially dominated by sulfide and bisulfide complexes such as $HgS_{(aq)}$, $Hg(SH)_2$, HgS_2H^- and HgS_2^{2-} (Morel *et al.*, 1998). At the SWI pH (close to 5.6) and ΣH_2S concentration (up to 4.9 µmol L^{-1}), the principal forms of Hg and MMHg are thus supposed to be $HgS_{(aq)}$ and CH_3HgS^- (the respective complexation constants at T = 298 °K and I = 0 are LogK_c = 43.8 and 21). In fact, applying the MINEQL® complexation model to our data:

$$HgS_{(s)} \Leftrightarrow HgS_{(aq)} \quad K_f = 10^{-8.9}$$

$$Hg^{2+} + OH^- + HS^- \Leftrightarrow HgS_{(aq)} + H_2O \quad K_c = 10^{43.8}$$

$$MMHg^+ + OH^- + HS^- \Leftrightarrow MMHgS^- + H_2O \quad K_c = 10^{21}$$

it was possible to calculate the equilibrium concentration of $HgS_{(aq)}$ complex to nearly 5.5 pmol L^{-1}. This accounted for more that 95 % of the dissolved unmethylated HgT fraction at the SWI (around 5.6 pmol L^{-1}). On the other hand, following a similar approach for $MMHg_D$, barely one-fifth the of this compound is calculated to be complexed as CH_3HgS^- (about 0.2 pmol L^{-1} i.e. 17 % of the $MMHg_D$). The broad discrepancy between modeled CH_3HgS^- and measured $MMHg_D$ concentrations suggests both formation of polysulfidic complexes and additional competition with other authigenic ligands. The high affinity of the mercuric ion for OM (6.3 ± 1.3 mg L^{-1} of dissolved organic C) and iron (30 ± 20 µmol L^{-1} of FeT_D) might

dramatically affect the speciation of monomethylmercury. The MMHg free ions would rather be bound to humic acids or inorganic particles, such as iron oxyhydroxides, than being complexed like CH_3HgS^- (Reddy and Aiken, 2001).

According to Roulet *et al*. (1999), the anthropogenic contribution from gold-mining sources accounts for 3 % of the overall content of Hg in Amazonian soils. Hence, Hg would have been principally accumulated through natural pedologic processes. Ferralitic soils are widespread in the area of the Petit-Saut reservoir. The inundation of such soil, usually leads to the rapid establishment of reducing conditions through the entire soil profile and results in a net loss of 25-40 % of the initial Fe oxyhydroxides (Vizier, 1978; Gunnison *et al*., 1985). As oxygen deficiency favors the reductive dissolution of Fe oxyhydroxides, it subsequently may strongly enhance the mobilization of mercury at the SWI. Apart from those, the anoxic condition that usually prevailed at the SWI supports the absence of an oxic barrier limiting the release of Hg from sediments.

A permanent diffusion of complexed Hg towards the water-column was therefore likely. For instance, the annual turbulent efflux of FeT_D at the SWI of the FF station averaged 1.3 ± 1.0 mol m^{-2} yr^{-1}. Such a high value accounted for substantial remobilization of Fe in the reservoir. According to Roulet and Lucotte (1995), Fe oxihydroxides are fairly abundant in ferralitic soils even after ten years of inundation (300-500 µmol g^{-1} which correspond to 20 $t(Fe_{Ox})$ ha^{-1}). The reductive dissolution mechanisms thus allowed nearly 20 % of the initially Fe-bounded Hg (estimated to 7 g(Hg) ha^{-1}) to escape from the ferralitic soil matrix. With *circa* 1.2 g(Hg) ha^{-1} (i.e. 60 ± 20 nmol m^{-2} yr^{-1}), the cumulated effluxes of HgT_D at Station FF confirmed this trend.

Apart from iron, depth distribution of HgT_P and LOI in core #1 and #2 suggested that mercury was also affected by OM content (Fig. 5). The acidic conditions that prevailed in the hypolimnion (5.6 ± 0.5 pH units) as well as the elevated organic content of sediments (close

to 20 %) supported the hypothesis of a potential leaching of free humic substances at the SWI. As a matter of fact, in Core #2, the simultaneous increase with depth of HgT_P (200-1100 pmol g^{-1}) and LOI (6-27 %) suggests a concomitant mobilization of humic substances and mercury due to upward migration. This pattern was not observed in Core #1 neither for HgT_P nor LOI. The differentiation between both profiles probably resulted from the change in sedimentation rate between the upstream of the Sinnamary River (Core #1) and the Petit-Saut artificial lake (Core #2). If we admit that average HgT_P concentration in Core #1 was representative of local impregnation by HgT (730 ± 70 pmol g^{-1}), the remobilization of OM permitted about 30 % of complexed Hg to escape the flooded soils. It is worthwhile noticing that the given estimation is only representative of an order of magnitude given that sharp differences in both OM content and water chemistry may occur within the reservoir.

The warm temperatures, anaerobic conditions and elevated organic content measured at the SWI defined suitable conditions for production and/or mobilization of MMHg. Despite $MMHg_P$ concentrations being low in ferralitic soils (around 1 % of HgT_P; Roulet and Lucotte, 1995), high levels of $MMHg_D$ were measured in the deepest part of the water-column (Fig. 9). In fact, rapid recycling of endogenous and/or deposited OM may still act as a potential source of MMHg in the vicinity of the SWI ten years after the impounding completion. Compared to the average concentration of the hypolimnion (0.9 ± 0.5 pmol L^{-1}), mean concentration of $MMHg_D$ at the SWI was significantly higher (1.4 ± 0.5 pmol L^{-1}). Applying the turbulent diffusion model to Station FF data, the corresponding annual efflux of $MMHg_D$ at the SWI was estimated to be 16 ± 5 nmol m^{-2} yr^{-1}. This value roughly represented 30 % of the HgT_D exported by inundated soils. On the other hand, it was possible to observe that the gradual enrichment of epibenthic waters with $MMHg_D$ occurred with the decease of $MMHg_P$ in SPM. This trend was confirmed by lower values of MMHg partition coefficient ($logKd_{MMHg}$; 4.9 ± 0.2 *vs* 5.6 ± 0.5) and $MMHg_P$ concentrations (130 ± 40 *vs* 300 ± 100 pmol g^{-1}) at the SWI than

a few meters above. It is thus likely that reductive dissolution and/or partial desorption of Hg enriched SPM may additionally have participated to the leveling up of epibenthic $MMHg_D$ concentrations. For instance, elevated $logKd_{MMHg}$ values were determined within the low conductivity layer that usually developed in the wet season due to the in-depth injection of surface water.

5. SUMMARY AND CONCLUSIONS

Sources of mercury to the Petit-Saut reservoir consist of the atmospheric deposition, the river tributaries and the flooded soils. Atmospheric deposition accounted for *circa* 14 moles yr^{-1} HgT of which approximately 75 % (11 moles yr^{-1}) originated from rainfall. Atmospheric deposition represented around 18 % of the minimum HgT_{UNF} input *via* river tributaries (close to 76 moles yr^{-1}). Remnant degradation of flooded vegetation and partial dissolution of ferralitic soils seemingly release 14 moles yr^{-1} HgT_D into the hypolimnetic waters. The exports of mercury from the Petit-Saut reservoir include the atmospheric volatilization, the dam water discharges; the sink is *via* particles sedimentation. Atmospheric volatilization at the air-water interface represented *circa* 21 moles yr^{-1} of Hg^0 (in a parent paper, Muresan *et al*, to be submitted), which is twice the HgT_{UNF} rainfall deposition. The outflow of HgT_{UNF} through the Petit-Saut dam (close to 78 moles yr^{-1}) seemed balanced with the upstream riverine inputs. At the SWI the particulate bounded Hg deposition (14.6 moles yr^{-1}) was roughly equilibrated with the calculate effluxes (13.8 moles yr^{-1}). This suggested that the reservoir did not significantly affect the overall HgT_{UNF} concentrations in the whole Sinnamary system (Fig. 10).

Sources of monomethylmercury at the Petit-Saut reservoir correspond to those of HgT with an extra contribution of the water-column chemocline. As for HgT_{UNF}, $MMHg_{UNF}$ was

primarily imported by local tributaries (close to 4.7 moles yr^{-1}). Comparatively, the atmospheric $MMHg_{UNF}$ deposition was monitored in rainfall to *circa* 0.7 moles yr^{-1} (i.e. around 7 % of HgT_{UNF}). Despite uncertainties, our results strongly suggest that a large quantity of MMHg was produced in the reservoir itself. Sharp concentration gradients and high methylated percentages, proxies for net methylation, depicted the WCC and SWI. The cumulative net endogenous production of $MMHg_D$ for those particular sites reached 7.3 moles yr^{-1}. Identified sinks of monomethylmercury in the Petit-Saut reservoir are the particle sedimentation and the dam water discharges. These respectively accounted for 0.7 (as $MMHg_P$) and 13.5 (as $MMHg_{UNF}$) moles yr^{-1}. The poor contribution of the particulate pump seemingly originated from the reductive conditions that prevailed at the SWI: dissolution and/or partial desorption of the MMHg enriched particles. Unlike HgT, which sinks locally equilibrated with sources, broad discrepancies were observed in the MMHg balance. As a result, most of the endogenically generated MMHg (the dominant source for the system) was exported from the reservoir, downstream of the dam.

During the 2003-2004 period, whereas a maximum of 5.4 moles yr^{-1} $MMHg_{UNF}$ reached the Petit-Saut reservoir *via* rainfall and river tributaries, dam exportations averaged 13.5 moles yr^{-1}. Referring to the 76 moles yr^{-1} of HgT_{UNF} passing through the artificial lake, the *in situ* net production of $MMHg_{UNF}$ averaged 0.06 % L^{-1} d^{-1}. Following a similar approach, the *in situ* net production of $MMHg_D$ attained 0.08 % L^{-1} d^{-1}. Hence, the Petit-Saut reservoir can be considered as a reactor that deeply altered mercury speciation in favor of the methylated species. With balanced contributions, the main sites for water-column $MMHg_D$ production and/or mobilization appears to be the WWC (3.6 ± 1.8 moles yr^{-1}) and the SWI (3.7 ± 1.2 moles yr^{-1}). This bimodal distribution of $MMHg_D$ sources reflects many geochemical processes: (i) a mobilization of MMHg associated with the particles from the water-column occurring during their degradation, (ii) a net methylation mechanism and/or

(iii) a permanent efflux of $MMHg_D$ at the SWI. However, the observed relationship between $MMHg_D$ and sulfides lends support to the hypothesis of neutral Hg-S complexes controlling (at least partially) the bioavailability of inorganic mercury for SRB methylation (Benoit *et al*., 2001 and 2003).

Aknowledgments: Thanks are due to J. Knoery for his helpful comments on an early version of the manuscript. We also thank B. Burban, C. Reynouard, P. Cerdan, V. Horeau, R. Aboïkoni, L. Guillemet and R. Vigouroux for their participation and facilitation to sampling and analyses. This work has been financially supported by CNRS (Conseil National de la Recherche Scientifique) and EDF (Electricité de France) grant N° F01381/0.

REFERENCES

AMEEL J., RUZYCKI E. and AXLER R.P. (1998) Analytical chemistry and quality assurance procedures for natural water samples. 6th edition. *Central Analytical Laboratory*, **NRRI Tech. Rep**. NRRI/TR98/03.

AMYOT M., MIERLE G., LEAN D. and MCQUEEN D.J. (1997b). Effect of solar radiation on the formation of dissolved gaseous mercury in temperate lakes. *Geochimica et Cosmochimica Acta* **61**, 975-987.

BARRIEL L.A., YI Y., LEAITCH W.R., LOHMANN U., KASIBHATLA P., ROELOFS G.J., WILSON J., MCGOVERN F., BENKOVITZ C., MÉLIÈRES M.A., LAW K., PROSPERO J., KRITZ M., BERGMANN D., BRIDGEMAN C., CHIN M., CHRISTENSEN J., EASTER R., FEICHTER J., LAND C., JEUKEN A., KJELLSTRÖM E., KOCH D. and RASCH P. (2001) A comparison of large scale atmospheric sulphate aerosols models (COSAM) overview and highlights. *Tellus* **53B**.

BENOIT J.M., GILMOUR C.C., HEYES A., MASON R.P. and MILLER C.L. (2003) Geochemical and biological controls over mercury production and degradation in aquatic systems. *Biogeochemistry of Environmentally Important Trace Elements* **835**, 262-297.

BENOIT J.M., MASON R.P., GILMOUR C.C. and AIKEN G.R. (2001) Constants for mercury binding by dissolved organic matter isolates from the Florida Everglades. *Geochimica et Cosmochimica Acta* **65**, 4445-445.

BENOIT J.M., GILMOUR C.C., MASON R.P. and HEYES A. (1999) Sulfide Controls on Mercury Speciation and Bioavailability to Methylating Bacteria in Sediment Pore Waters. *Environmental Science & Technology* **33**, 951-957.

BEUCHER C., WONG W.C.P., RICHARD C., MAILHOT G., BOLTE M. and COSSA D. (2002) Dissolved gaseous mercury formation under UV irradiation of unamended tropical waters from French Guiana. *Science of the Total Environment* **290**, 131-138.

BLOOM N.S. (1989) Determination of picogram levels of methylmercury by aqueous phase ethylation followed by cryogenic gas chromatography with cold vapour atomic fluorescence detection. *Canadian Journal of Fisheries and Aquatic Sciences* **46**, 1131-1140.

BLOOM N.S. and FITZGERALD W.F. (1988) Determination of volatile mercury species at picogram level by low temperature gas chromatography with cold-vapour atomic fluorescence detection. *Analytica Chimica Acta* **28**, 151-161.

BOUDOU A., MAURY-BRACHET R., COQUERY M., DURRIEUX G. and COSSA D. (2005) Synergic effect of goldmining and damming on mercury contamination in fish. *Environmental Science & Technology* **39**, 2448-2454.

CANAVAN M., CALDWELL C. A. and BLOOM N. S. (2000) Discharge of methylmercury-enriched hypolimnetic water from a stratified reservoir. *The Science of The Total Environment* **260**, 159-170.

COMPEAU G. and BARTHA R. (1985) Sulfate reducing bacteria: principal methylators of Hg in anoxic estuarine sediments. *Applied Environmental Microbiology* **50**, 498-502.

COQUERY M., COSSA D., AZEMARD S., PERETYAZHKO T. and CHARLET L. (2003) Methylmercury formation in the anoxic waters of the Petit-Saut reservoir (French Guiana) and its spreading in the adjacent Sinnamary River. *Journal de Physique IV* **107**, 327-331.

COSSA D., AVERTY B., BRETAUDEAU J. and SENARD A.S. (2003) Spéciation du mercure dissous dans les eaux marines. *Méthodes d'analyse en milieu marin, Editions Ifremer*, **ISBN 2-84433-125-4**, 27 pp.

COSSA D., COQUERY M., NAKHLE K. and CLAISSE D. (2002) Dosage du mercure total et du monomethylmercure dans les organismes et les sédiments marins. *Méthodes d'analyse en milieu marin, Editions Ifremer*, **ISBN 2-84433-105-X**, 27pp.

COSSA D., MASON R.P. and FITZGERALD W.F. (1994) Chemical Speciation of Mercury in a Meromictic Lake. *Mercury Pollution Integration and Synthesis* **Lewis Publishers**, 57-67.

DE JUNET A. (2004) Etude qualitative de la matière organique particulaire dans le réservoir de Petit-Saut (Guyane Française): Composition Isotopique ($\delta^{13}C$), élémentaire (C/N) et pigmentaire. *Master Report* **Talence**, 41 pp.

DEVEREUX R., WINFREY M.R., WINFREY J. and STAH D.A. (1996) Depth profile of sulfate-reducing bacterial ribosomal RNA and mercury methylation in an estuarine sediment FEMS. *Microbiology Ecology* **20**, 23-31.

DUMESTRE J.F., EMILIO C.O., RAMON M. and PEDROS-ALIO C. (2001) Changes in bacterial assemblages in a equatorial river induced by water eutrophication of Petit-Saut dam reservoir (French Guiana). *Aquat. Microb. Ecol.* **26**, 209-221.

DUMESTRE JF., VAQUER A., GOSSE P., RICHARD S. and LABROUE L. (1999) Bacterial ecology of a young equatorial hydroelectric reservoir (Petit-Saut, French Guiana). *Hydrobiologia* **400**, 75-83.

DUMESTRE J.F., LABROUE L., GALY-LACAUX C., REYNOUARD C. and RICHARD S. (1997) Biomasses et activités bactériennes dans la retenue et à l'aval du barrage de Petit-Saut (Guyane): influence sur les émissions du méthane et la consommation d'oxygène. *Hydroécologie Appliquée* **9**, 139-167.

DURRIEU G., MAURY-BRACHET R. and BOUDOU A. (2005) Gold-mining and mercury contamination of the piscivorous fish *Hoplias aimara* in French Guiana (Amazon basin). *Ecotoxicology and Environmental Safety* **60**, 315-323.

GILMOUR C.C., HENRY E.A. and MITCHELL R. (1992) Sulfate Stimulation of Mercury Methylation in Freshwater Sediments. *Environmental Science & Tech*nology **26**, 2281-2287.

GILMOUR C.C. and HENRY E.A. (1991) Mercury methylation in aquatic systems affected by acid deposition. *Environmental Pollution* **71**, 131-169.

GUIMARAES J.R.D., ROULET M., LUCOTTE M. and MERGLER D. (2000a) Mercury methylation along a lake-forest transect in the Tapajós river floodplain, Brazilian Amazon: seasonal and vertical variations. *The Science of the Total Environment* **261**, 91-98.

GUIMARAES J.R.D., MEILI M., HYLANDER L.D., SILVA E., ROULET M., MAURO J.B.N. and LEMOS R.A. (2000b) Mercury net methylation in five tropical flood plain regions of Brazil: high in the root zone of floating macrophyte mats but low in surface sediments and flooded soils. *The Science of the Total Environment* **261**, 99-107.

GUNNISON D., ENGLER R.M. and PATRICK W.H. (1985) Microbial processes in reservoirs. *Dr W. Junk Publishers* **Dordrecht**, 39pp.

HOREAU V., RICHARD S., CERDAN P., ABOIBONI R., GUILLEMET L., REYNOUARD C., VALERE J. and ZOUITEN C. (1999) Variabilités temporelles de la qualité physico-chimique et biologique des eaux liées au barrage hydroélectrique de Petit-Saut (Guyane française). *4th International Congress on Limnology and Oceanography*, Bordeaux.

HOREAU V., CERDAN P., CHAMPEAU A. and RICHARD S. (1998) Importance of aquatic invertebrates in the diet of rapids-dwelling fish in the Sinnamary River, French Guiana. *J. Trop. Ecol.* **14**, 851-864.

HURLEY J.P., BENOIT J.M., BABIARZ C.L., SHAFER M.M., ANDREN A.W., SULLIVAN J.R., HAMMOND R. and WEBB D.A. (1995) Influences of watershed characteristics on mercury levels in Wisconsin rivers. *Environmental Science & Technology* **29**, 1867-1875.

HUYNH F., CHARRON C., BETOULLE J.L., PANECHOU K., GARDEL A., PROST M.T. and LOUBRY D. (1997) Suivi de l'évolution géomorphologique et botanique de l'estuaire du Sinnamary par télédétection. *Final report ORSTOM-EDF*, 64pp.

HYDRECO: Laboratory for biological and chemical monitoring and analysis on the Petit-Saut reservoir. http://hydreco.mediasfrance.org/hydreco/

JENSEN S. and JERNELÖV A. (1969) Biological Methylation of Mercury in Aquatic Organisms. *Nature* **223**, 753-754.

KING J.K., KOSTKA J.E., FRISCHER M.E., SAUNDERS F.M. and JAHNKE R.A. (2001) A quantitative relationship that demonstrates mercury methylation rates in marine sediments are based on the community composition and activity of sulfate-reducing bacteria. *Environmental Science & Technology* **35**, 2491-2496.

KING J.K., SAUNDERS F.M., LEE R.F. and JAHNKE R.A. (1999) Coupling mercury methylation rates to sulfate reduction rates in marine sediments. *Environmental Toxicology and Chemistry* **18**, 1362-1369.

KORTHALS E.T. and WINFREY M.R. (1987) Seasonal and Spatial Variations in Mercury Methylation and Demethylation in an Oligotrophic Lake. *Environmental Microbiology* **53**, 2397-2404.

LACERDA L.D., RIBEIRTO M.G., CORDEIRO R.C., SOFEDDINE A. and TURCQ B. (1999) Atmospheric mercury deposition over Brazil during the past 30,000 years. *Ciência e Cultura* **51**, 363-371.

LAMBORG C.H., ROLFHUS K.R., FITZGERALD W.F. and KIM G. (1999) The atmospheric cycling and air-sea exchange of mercury species in the South and equatorial Atlantic Ocean. *Deep Sea Research* **46**, 957-977.

LEE Y.-H. and IVERFELDT. A. (1991) Measurement of methylmercury and mercury in runoff, lake and rain waters. *Water Air Soil Pollution* **56**, 309-321.

LEERMARKERS M., GALETTI S., DE GALAN S., BRION N. and BAEYENS W. (2001) Mercury in the Souther North Sea and Sheldt Estuary. *Marine Chemistry* **75**, 229-248.

LIANG L., HORVAT M. and BLOOM N.S. (1994) An improved speciation method for mercury by GC/CVAFS after aqueous phase ethylation and room temperature precollection. *Talanta* **41**, 371-379.

MASON R.P. and LAWRENCE A.L. (1999) Concentration, distribution, and bioavailability of mercury and methylmercury in sediments of Baltimore harbor and Chesapeake Bay, Maryland, USA. *Environmental Toxicology and Chemistry* **18**, 2438-2447.

MASON R.P., LAWSON N.M, LAWRENCE A.L., JOY J.L., LEE J.G. and SHEU G.R. (1999) Mercury in the Chesapeake Bay. *Marine Chemistry* **65**, 77-96.

MASON R.P., LAWSON N.M. and SULLIVAN K.A. (1997) The concentration, speciation and sources of mercury in Chesapeake Bay precipitation. *Atmospheric Environment* **31**, 3541-3550.

MERCURE EN GUYANE (2001) CHARLET L., BOUDOU A., GRIMALDI M. and COSSA D. Region de Saint Elie et retenue de Petit-Saut. *Final report part 1*, 70pp.

MOREL F.M.M., KRAEPIEL A.M.L. and AMYOT M. (1998) The chemical cycle and bioacculumation of mercury. *Annu. Rev. Ecol. Syst.* **29**, 543-566.

MORRISON K.A. and WATRAS C.J. (1999) Mercury and methyl mercury in freshwater seston: direct determination at picogram per litre levels by dual filtration. *Can. J. Fish. Aquat. Sci.* **56**, 760-766.

MURESAN B., COSSA D., RICHARD S. and BURBANT B. Mercury speciation and exchanges at the air-water interface of a tropical artificial reservoir, French Guiana. To be submitted.

PERETYAZHKO T., VAN CAPELLEN P., MEILE C., COQUERY M., MUSSO M., REGNIER P. and CHARLET L. (2005) Biogeochemistry of major redox elements and mercury in a tropical reservoir lake (Petit-Saut, French Guiana). *Aquatic Geochemistry* **11**, 33-35.

PERETYAZHKO T. (2002) Formation de Hg^0 dans les milieux aquatiques tropicaux (Lacs et sols). *Doctoral Thesis*, **Univ Grenoble**, 161 pp.

PETOT J. (1993) Histoire de l'or en Guyane. L'Harmattan, Paris, 256 pp.

REDDY M.M. and AIKEN G.R. (2001) Fulvic acid-sulfide ion competition for mercury ion binding in the Florida Everglades. *Water, Air, and Soil Pollution* **132**, 89-104.

RICHARD S., ARNOUX A., CERDAN P., REYNOUARD C., HOREAU V. and VIGOUROUX R. (2002) Influence of the setting up of a man-made lake on mercury levels in the flesh of fish in a neotropical habitat: the Sinnamary River (French Guiana). *Rev. Ecol*. **8**, 59-76.

RICHARD S. (1996) La mise en eau du barrage de Petit-Saut. Hydrochimie 1 – du fleuve Sinnamary avant la mise en eau, 2 – de le retenue pendant la mise en eau, 3 – du fleuve en aval. *Doctoral Thesis*, **Aix – Marseille Univ I**, 278 pp.

ROULET M. and GRIMALDI C. (2001) Le mercure dans les sols d'Amazonie. Origine et comportement du mercure dans les couvertures ferrallitiques du bassin amazonien et des Guyanes. *Editions de l'IRD*, collection Expertise collégiale, 121-166.

ROULET M., GUIMARAES J.R.D. and LUCOTTE M. (2001) Methylmercury production and accumulation in sediments and soils of an Amazonian floodplain. Effect of seasonal inundation. *Water, Air and Soil Pollution* **128**, 41-60.

ROULET M., LUCOTTE M. and GUIMARAES J.R.D. (2000) Methylmercury in the water, seston and epiphyton of an Amazonian river and its floodplain, Tapajos river, Brazil. *Sci. Total. Environ.* **261**, 43-59.

ROULET M., LUCOTTE M., FARELLA N., SERIQUE G., COELHO H., SOUSSA PASSOS C.J., DE JESSUS DA SILVA E., SCAVONE DE ANDRADE P., MERGLER D. and GUIMARAES J.R.D. (1999) Effects of recent human colonization on the presence of mercury in amazonian ecosystem. *Water, Air and Soil Pollution* **112**, 297-313.

ROULET M., LUCOTTE M., CANUEL R., RHEAULT I., TRAN S., *et al*. (1998a) Distribution and partition of total mercury in waters of the Tapajós River Basin, Brazilian Amazon. The *Science of The Total Environment* **213**, 203-211.

ROULET M., LUCOTTE M., CANUEL R., FARELLA N., COURCELLES M., GUIMARAES J.R.D., MERGLER D. and AMORIM M. (1998b) The geochemistry of mercury in central Amazonian soils developed on the Alter-do-Chao formation of the lower Tapajos River Valley, Para state, Brazil. *Science of the Total Environment* **223**, 1-24.

ROULET M. and LUCOTTE M. (1995) Geochemistry of mercury in pristine and flooded ferralitic soils of a tropical rain forest in French Guiana, South America. *Water, Air and Soil Pollution* **80**, 1079-1088.

SCHETAGNE R. and VERDON R. (1999) Post-impoundment evolution of fish mercury levels at the La Grande complex, Québec, Canada (from 1978 to 1996). *Environmental Science Series*, **Springer**, 235-258.

SCHUSTER E. (1991) The behavior of mercury in the soil with special emphasis on complexation and adsorption processes-A review of literature. *Water Air Soil Pollution* **56**, 667-680.

SURMA-AHO K., REKOLAINEN J.P.S. and VERTA M. (1986) Organic and inorganic mercury in the food chain of some lakes and reservoirs in Finland. *Chemosphere* **15**, 353-372.

TREMBLAY A. (1996) Methymercury in a benthic food web of two hydroelectric reservoirs and a natural lake of Northern Québec (Canada). *Water, Air and Soil Pollution* **91**, 3-4.

VERDON R., BROUARD D., DEMERS C., LALUMIÈRE R., LAPERLE M. and SCHETAGNE R. (1991) Mercury evolution (1978–1988) in fishes of the La Grande Hydroelectric Complex, Québec, Canada. *Water, Air and Soil Pollution* **56**, 405–417.

VIZIER J.F. (1978) Étude de la dynamique du fer des sols évoluant sous l'effet d'un excès d'eau. *Cah. ORSTOM, Pedol* **16**, 23-41.

XIAO Z.F., STROMBERG D. and LINDQVIST O. (1995) Influence of humic substances on photolysis of divalent mercury in aqueous solution. *Water, Air and Soil Pollution* **80**, 789-798.

ZAHIR F., RIZWI S.J., HAQ K.S. and KHAN R.H. (2005) Low dose mercury toxicity and human health. *Environmental Toxicology and Pharmacology* **20**, 351-360.

TABLE CAPTIONS

Layer	HgT_{UNF} (pmol L^{-1})	$MMHg_{UNF*}$ (pmol L^{-1})	HgT_D (pmol L^{-1})	$MMHg_D$ (pmol L^{-1})	HgT_P (pmol g^{-1})	$MMHg_P$ (pmol g^{-1})	DGM (pmol L^{-1})	HgR_{UNF} (pmol L^{-1})
Epilimnion	5 ± 3 (n = 35) (2.0 – 15.3)	0.9 ± 0.6 (n = 35) (0.17 - 3.84)	4 ± 2 (n = 35) (1.0 - 8.8)	0.3 ± 0.2 (n = 35) (0.03 – 1.13)	200 ± 150 (n = 31) (15 - 810)	80 ± 70 (n = 34) (7 - 350)	0.3 ± 0.2 (n = 35) (0.08 - 0.76)	0.5 ± 0.3 (n = 14) (<0 0.1 - 1.08)
Hypolimnion	13 ± 6 (n = 43) (4 – 25)	2.2 ± 1.0 (n = 43) (0.35 - 8.36)	8 ± 4 (n = 43) (1.0 - 19.4)	0.9 ± 0.5 (n = 43) (0.06 - 5.88)	1300 ± 950 (n =37) (40 - 5290)	170 ± 90 (n = 43) (15 - 840)	0.2 ± 0.2 (n = 43) (0.07 - 0.74)	0.4 ± 0.3 (n = 14) (<0.01 - 0.9)

Tab. 1. Summary statistics on mercury species concentrations in the water-column of the Petit-Saut reservoir; mean ± standard deviation, (n) number of determination, range in brackets. Subscript D and P refer to dissolved and particulate phases respectively; subscript UNF corresponds to unfiltered samples; (*) calculated from $MMHg_D$, $MMHg_P$ and SPM.

Nature / origin of the samples		HgT_{UNF} (pmol L^{-1})	HgT_D (pmol L^{-1})	HgT_P (pmol g^{-1})	$MMHg_D$ (pmol L^{-1})	$MMHg_P$ (pmol g^{-1})	DGM (pmol L^{-1})
Rain		16 ± 12 (n = 62) (2.3 - 57.7)			0.8 ± 1.4 as MMHg (n = 34) (0.05 - 10.2)		0.82 ± 0.93 (n = 17) (0.05 - 3.96)
Sinnamary river (Saut-Dalles; SD)		13 ± 2 (n = 4) (10.8 - 15.6)	8 ± 1 (n = 4) (6.1 - 8.8)	1100 ± 400 (n = 4) (860 - 1800)	0.5 ± 0.2 (n = 4) (0.35 - 0.53)	25 ± 15 (n = 4) (17 - 44)	0.38 ± 0.15 (n = 4) (0.24 - 0.57)
Flooded forest (FF)	Epilimnion	5 ± 4 (n = 10) (2.0 - 15.3)	3 ± 2 (n = 10) (1.2 - 6.8)	200 ± 150 (n = 8) (100 - 470)	0.3 ± 0.2 (n = 10) (0.10 - 0.64)	50 ± 30 (n = 9) (13 - 130)	0.17 ± 0.12 (n = 9) (0.08 - 0.44)
	Hypolimnion	8 ± 5 (n = 11) (4.0 - 19.0)	5 ± 4 (n = 11) (1.0 - 12.4)	1300 ± 750 (n = 11) (65 - 2300)	0.5 ± 0.1 (n = 11) (0.06 - 0.94)	230 ± 200 (n = 11) (58 - 840)	0.15 ± 0.15 (n = 11) (0.07 - 0.66)
Center reservoir (CR)	Epilimnion	5 ± 1 (n = 12) (3.8 - 7.7)	4 ± 1 (n = 12) (1.4 - 5.6)	230 ± 200 (n = 12) (40 - 810)	0.3 ± 0.3 (n = 12) (0.03 - 1.07)	100 ± 100 (n = 12) (7 - 350)	0.45 ± 0.18 (n = 12) (0.18 - 0.76)
	Hypolimnion	14 ± 5 (n = 22) (8.0 - 25.0)	7 ± 3 (n = 22) (3.9 - 16.3)	1500 ± 1100 (n = 22) (40 - 5290)	1.4 ± 0.4 (n = 22) (0.13 - 5.88)	140 ± 90 (n = 22) (15 - 410)	0.28 ± 0.13 (n = 22) (0.09 - 0.51)
Upstream dam (UD)	Epilimnion	5 ± 2 (n = 13) (2.7 - 8.9)	4 ± 2 (n = 13) (1.0 - 8.8)	130 ± 100 (n = 11) (34 - 440)	0.3 ± 0.2 (n = 13) (0.04 - 1.13)	100 ± 75 (n = 13) (27 - 290)	0.32 ± 0.12 (n = 13) (0.22 - 0.57)
	Hypolimnion	14 ± 6 (n = 10) (7.7 - 21.9)	9 ± 6 (n = 10) (3.0 - 19.4)	1300 ± 1100 (n = 10) (86 - 4210)	0.8 ± 0.5 (n = 10) (0.22 - 2.54)	140 ± 60 (n = 10) (66 - 340)	0.43 ± 0.28 (n = 10) (0.07 - 0.74)
Tailrace (CS)		13 ± 5 (n = 88) (3.7 - 27.9)	8 ± 2 (n = 27) (0.5 - 10.7)	800 ± 700 (n = 27) (32 - 3310)	0.5 ± 0.4 (n = 27) (0.11 - 2.94)	150 ± 100 (n = 27) (27 - 320)	0.30 ± 0.20 (n = 50) (0.06 -0.95)

Tab. 2. Summary of the average concentrations of total (HgT, HgT_D, HgT_P), monomethyl ($MMHg_D$ and $MMHg_P$) and dissolved gaseous (DGM) mercury in various compartments constitutive of the Petit-Saut reservoir. Given values regroup the whole data from Matoutou 1 (03-04/2003), 2 (01-02/04) and 3 (05-06/2004) campaigns.

Nature of the sample	Station	HgT_P (pmol g^{-1})	$MMHg_P$ (pmol g^{-1})
Sediment from trap (7 m)	CR	950 ± 60 (n = 3)	26 ± 7 (n = 2)
Sediment from trap (20 m)	CR	650 ± 80 (n = 3)	70 ± 12 (n = 2)
Sediment from trap (30 m)	CR	1800 ± 130 (n = 3)	32 ± 10 (n = 2)
Surficial sediment	FF	550	60
Surficial sediment	CR	1100	90
Surficial sediment	UD	1000	100

Tab. 3. Mercury concentrations in surficial sediments and particles from sediment traps from the Petit-Saut reservoir.

Sampling sites	Mean HgT_D concentrations (pmol L^{-1})	Mean $MMHg_D$ concentrations (pmol L^{-1})
Sinnamary (Saut-Dalles)	9 ± 3 (n = 6)	0.3 ± 0.1 (n = 5)
Courcibo	16 ± 3 (n = 2)	0.34 ± 0.07 (n = 2)
Leblond	14 ± 4 (n = 4)	0.34 ± 0.07 (n = 4)

Tab. 4. Dissolved total (HgT_D) and monomethyl ($MMHg_D$) mercury from December 2004 and March 2005 sampling campaigns of main tributaries of the Petit-Saut reservoir. According to Coquery *et al.* (2003), during the 1999 wet and dry seasons, the HgT_D mean concentrations orderly were (i) 15 ± 2 and 41 ± 6 pmol L^{-1} in Leblond and (ii) 12 ± 2 and 8 ± 1 pmol L^{-1} in Courcibo creeks. The respective $MMHg_D$ concentrations were (i) 0.20 ± 0.04 and 0.31 ± 0.05 pmol L^{-1} in Leblond and (ii) 0.13 ± 0.03 and 0.16 ± 0.04 pmol L^{-1} in Courcibo creeks.

Compounds	Dry season (mol d^{-1}) (15/07/03 - 15/12/03)	Wet season (mol d^{-1}) (01/04/03 - 15/07/03)	Annual (mol yr^{-1}) (18/03/03 - 17/03/04)	Annual (mol yr^{-1}) (1/10/03 - 30/09/04)
DGM	$4.0\ 10^{-3}$	$3.3\ 10^{-3}$	1.3	2.0
HgR_{UNF}	0.03	0.02	9.5	16
$MMHg_{UNF}$	0.03	0.06	6.5	13.5
HgT_{UNF}	0.21	0.16	61.5	79

Tab. 5. Mercury exportation from the reservoir for various periods. The calculated fluxes are the cumulative weekly fluxes (concentration x water discharge) for the reference period.

FIGURE CAPTIONS

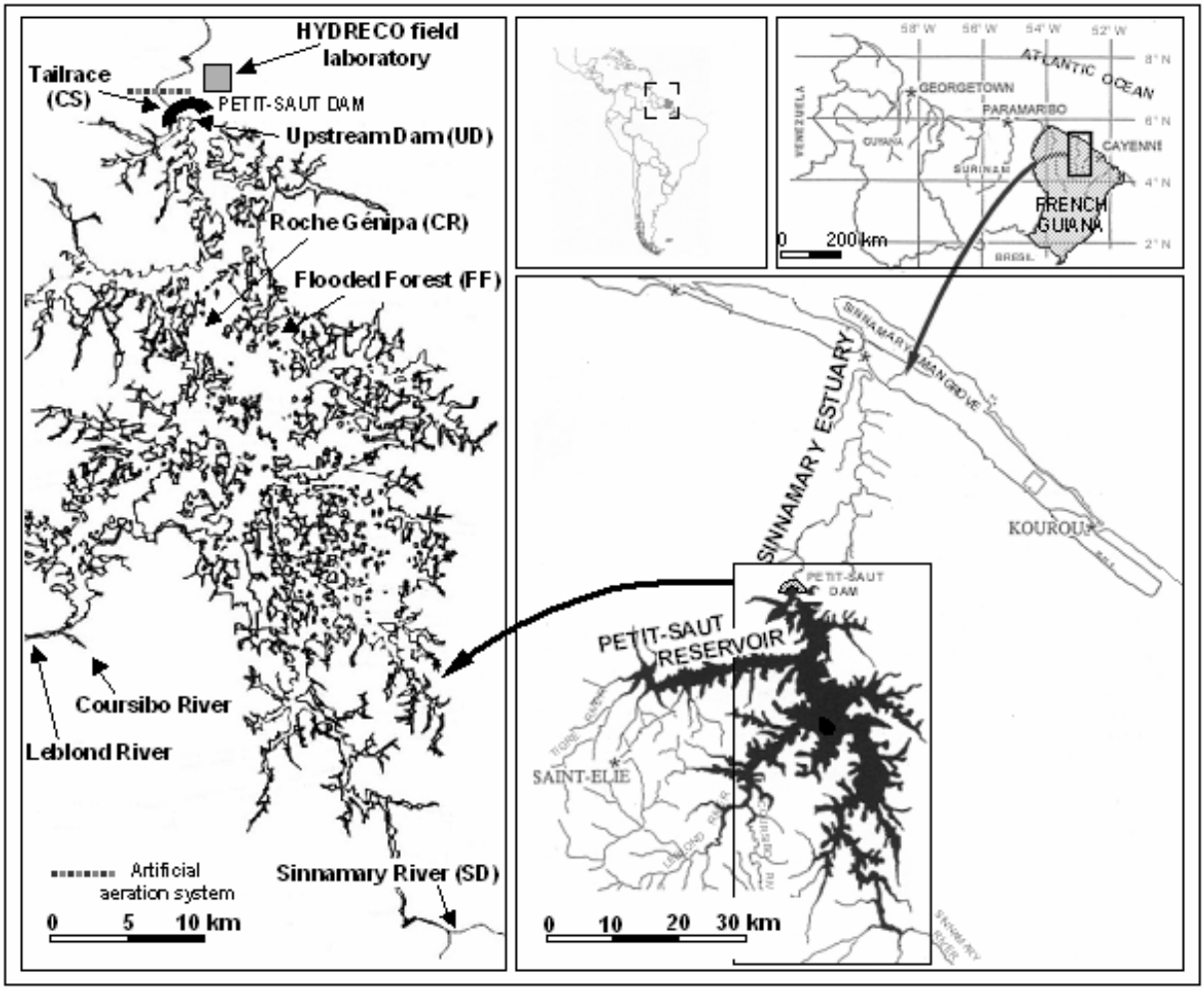

Fig. 1. Study area. The flooded forest (FF), Roche Génipa (CR), upstream dam (UD) and tailrace (CS) stations were systematically investigated during Matoutou 1 (March-April 2003), 2 (January-February 2004) and 3 (May-June 2004) campaigns. The Sinnamary, Leblond and Courcibo streams were studied during Matoutou 4 (November-December/2004) and 5 (March-April/2005).

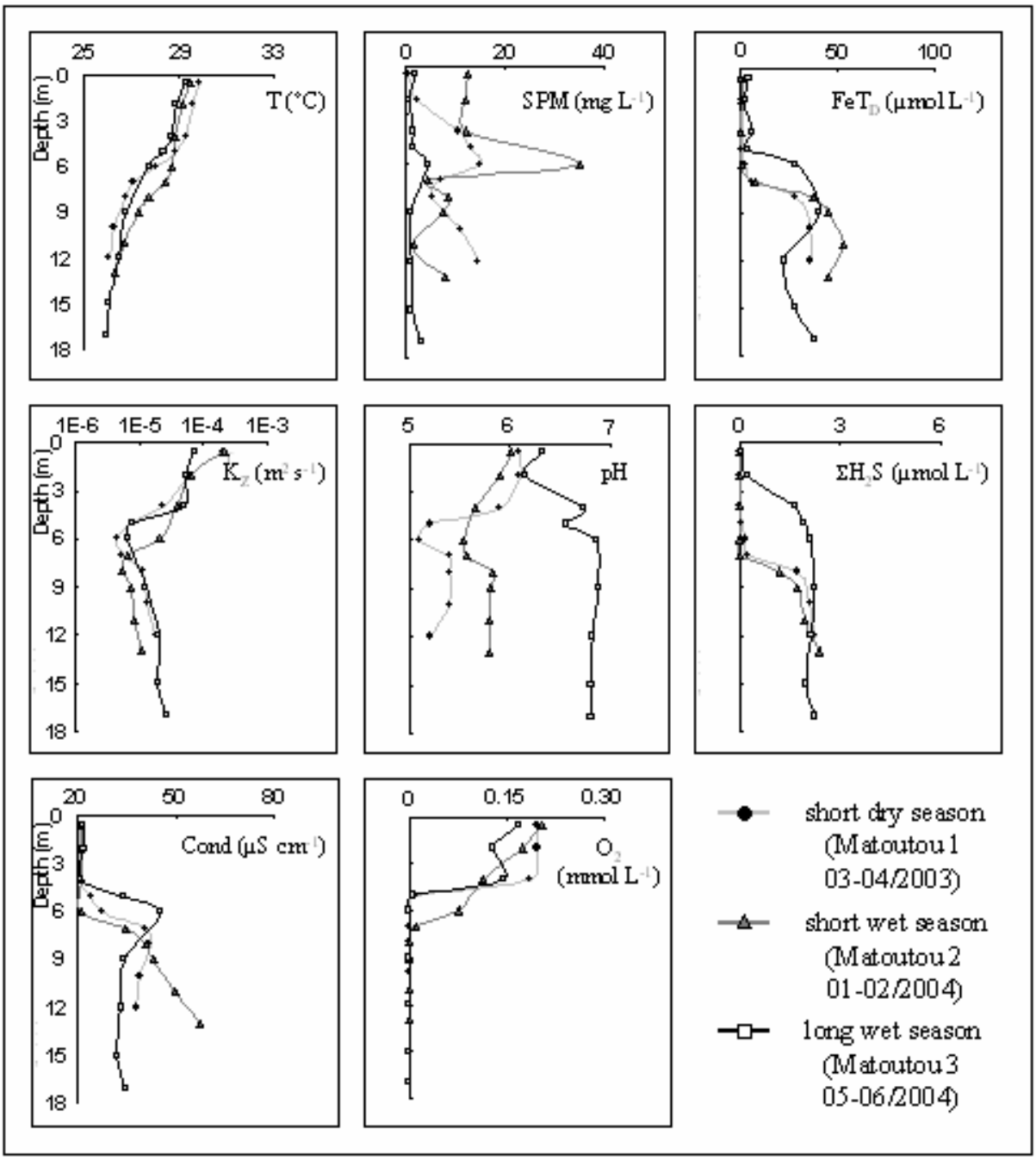

Fig. 2.A. Water-column profiles of principal physical characteristics and major chemical compounds at Flooded Forest (FF) station. Each graph displays the distribution of a same parameter with regard to Matoutou 1, 2 and 3 campaigns.

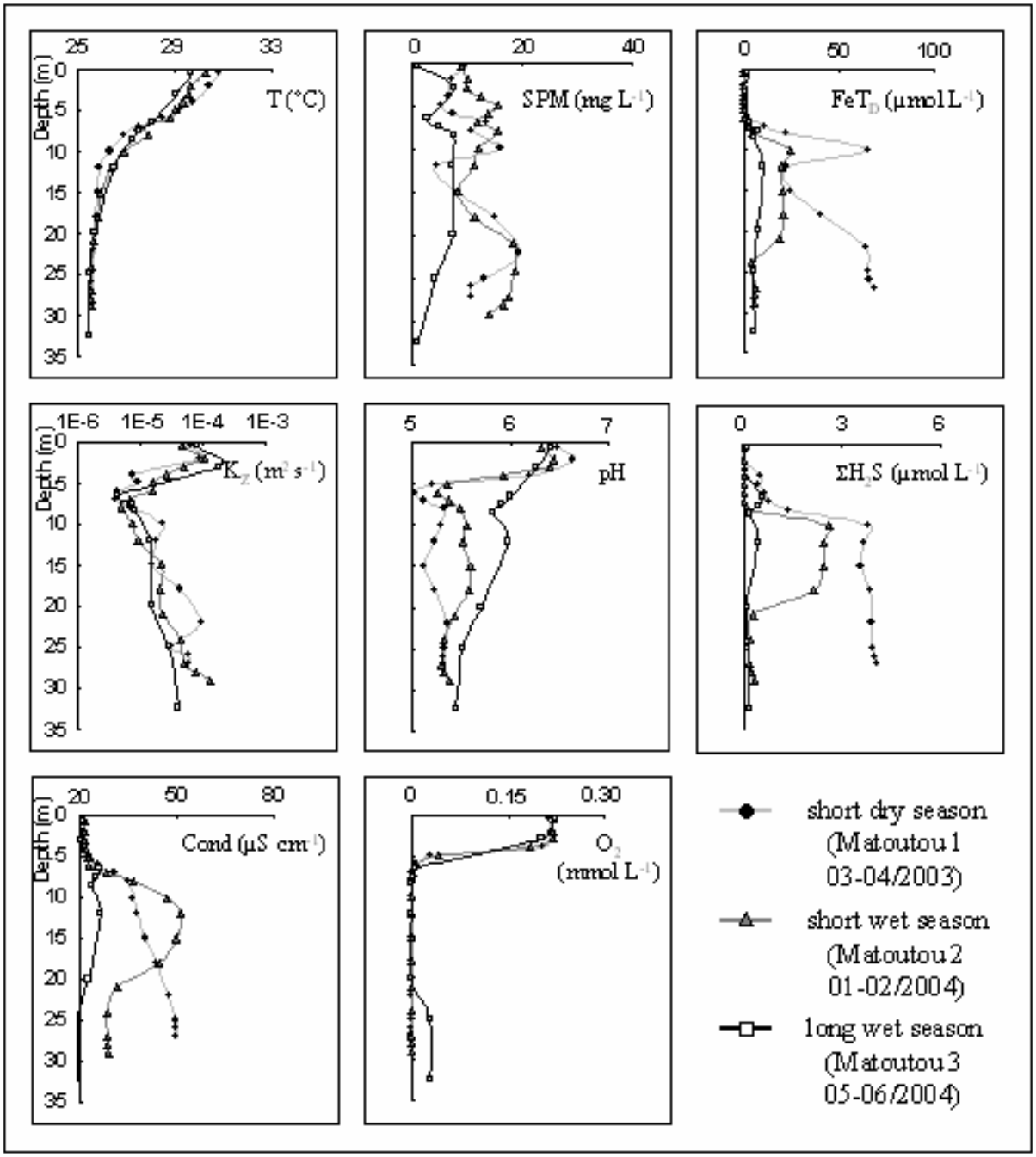

Fig. 2.B. Water-column profiles of principal physical characteristics and major chemical compounds at Roche Génipa (CR) station. Each graph displays the distribution of a same parameter with regard to Matoutou 1, 2 and 3 campaigns.

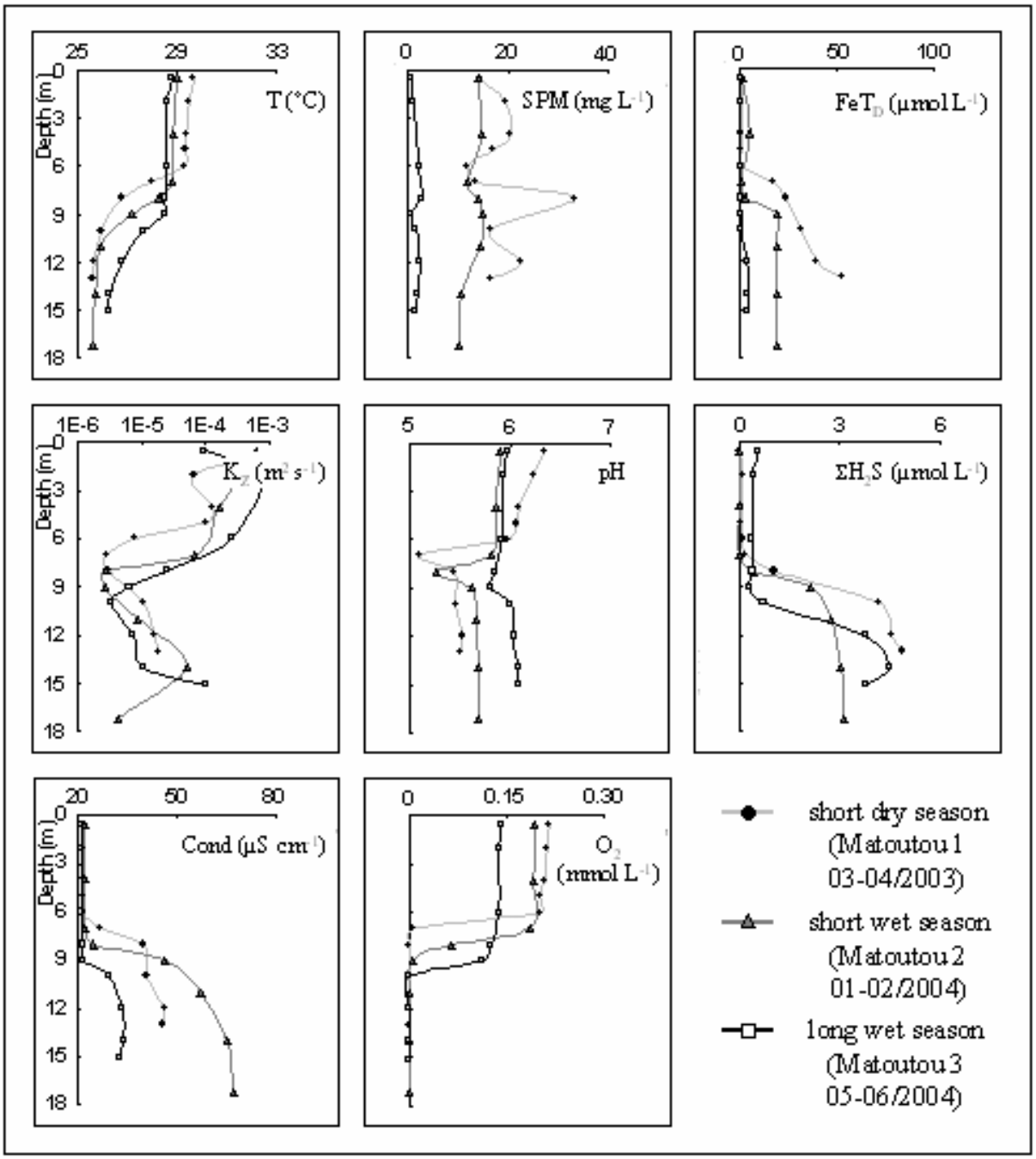

Fig. 2.C. Water-column profiles of principal physical characteristics and major chemical compounds at Upstream Dam (UD) station. Each graph displays the distribution of a same parameter with regard to Matoutou 1, 2 and 3 campaigns.

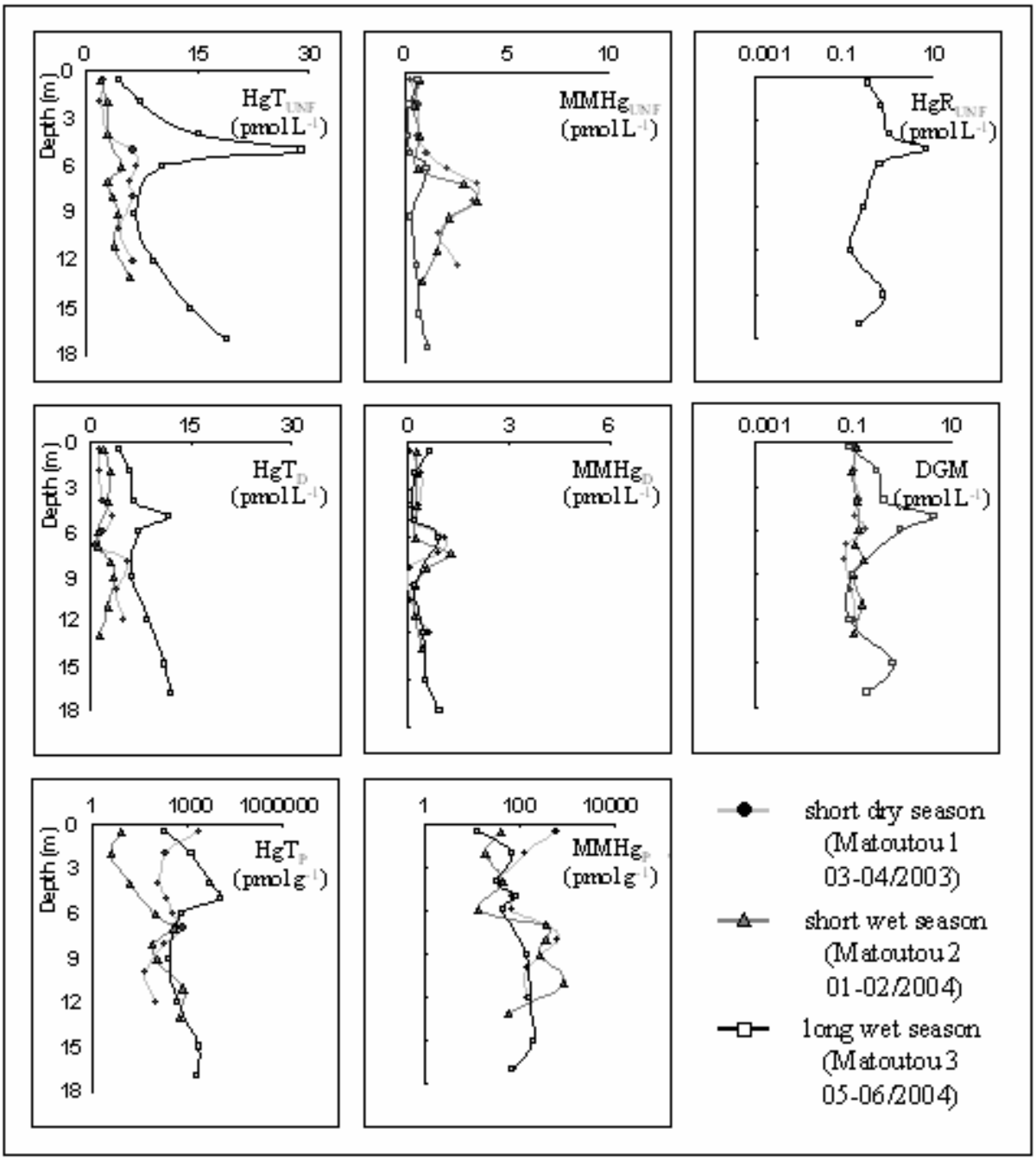

Fig. 3.A. Water-column profiles of main Hg species at Flooded Forest (FF) station. Each graph displays the distribution of same specie with regard to Matoutou 1, 2 and 3 campaigns.

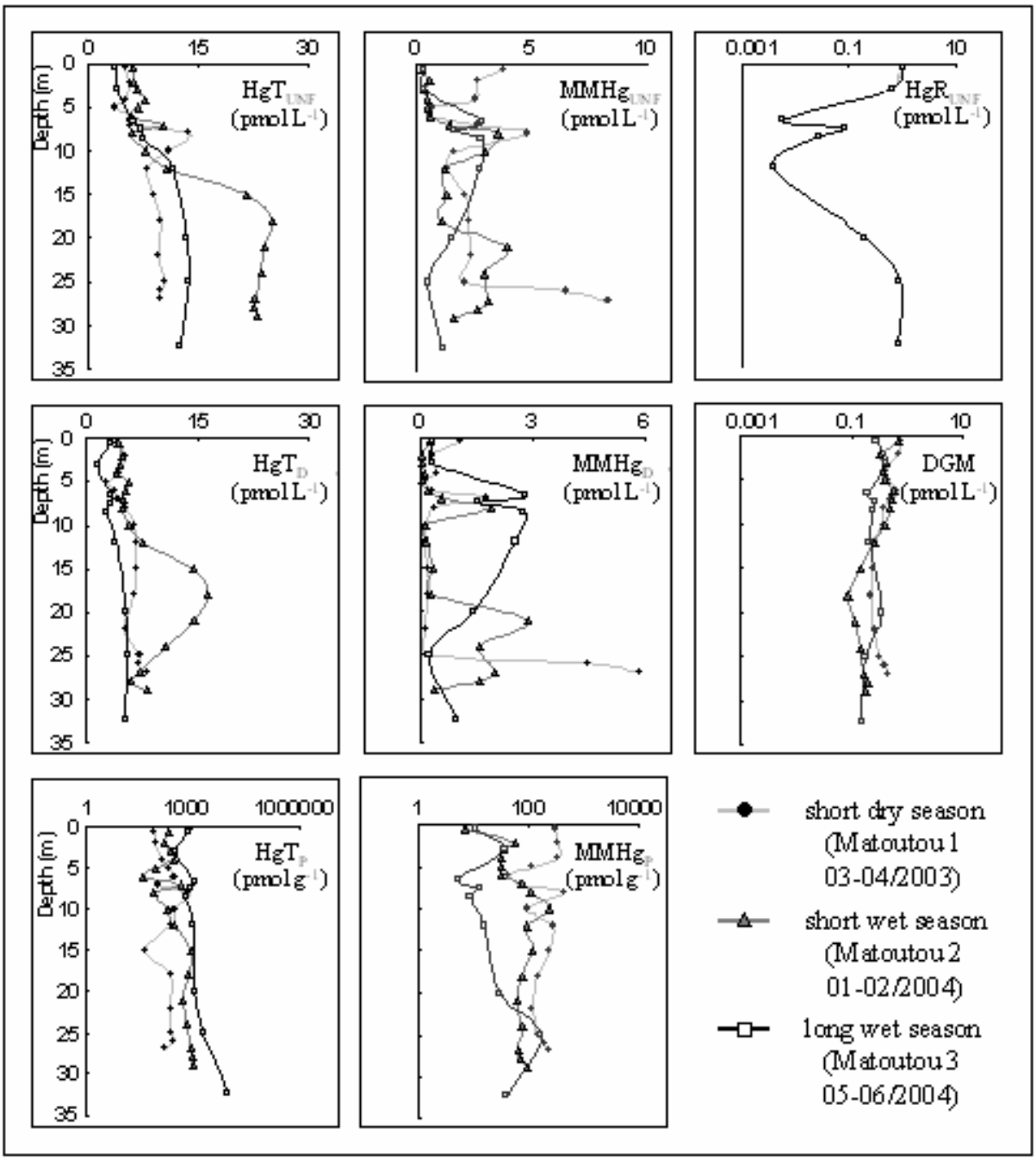

Fig. 3.B. Water-column profiles of main Hg species at Roche Génipa (CR) station. Each graph displays the distribution of same specie with regard to Matoutou 1, 2 and 3 campaigns.

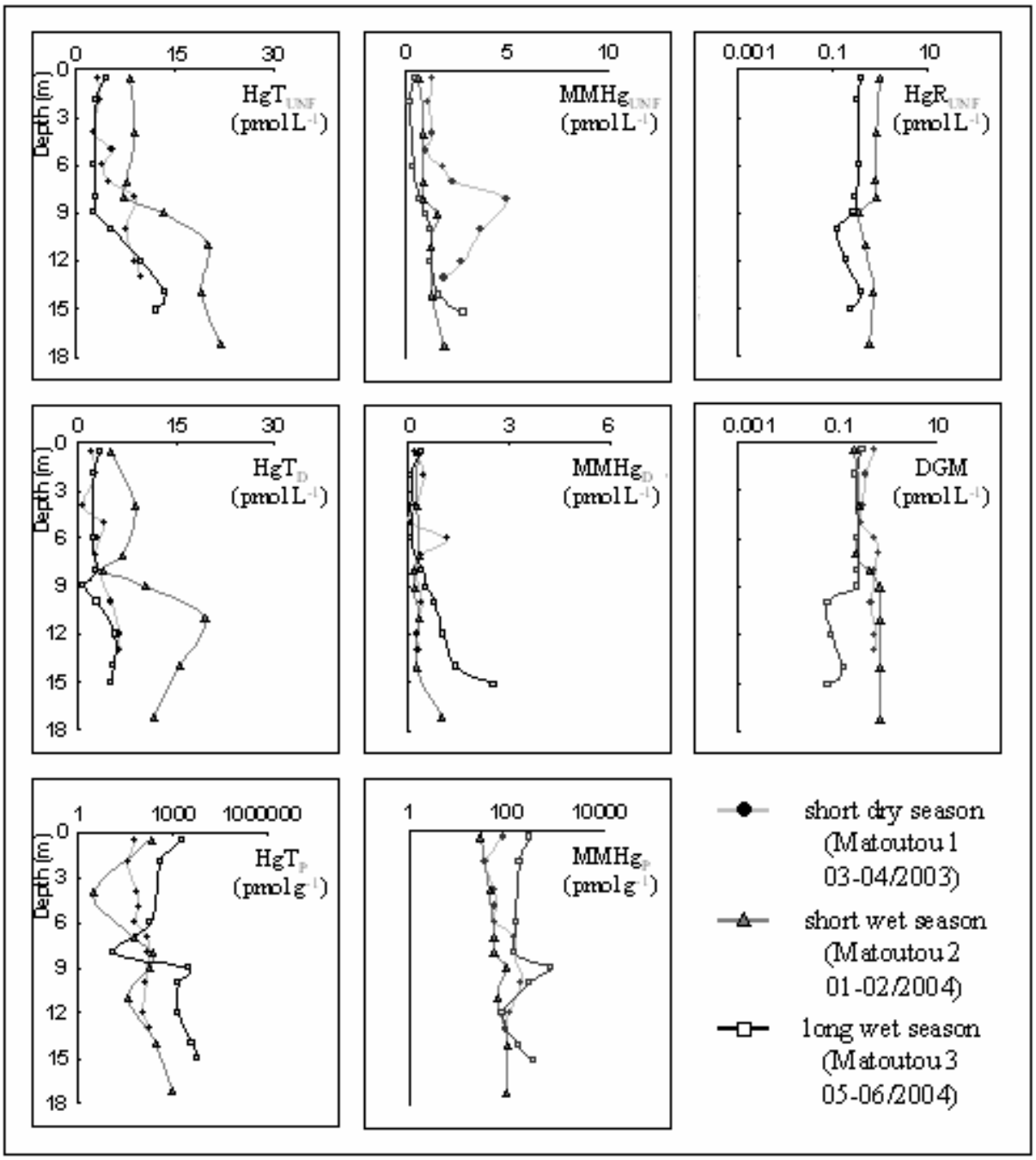

Fig. 3.C. Water-column profiles of main Hg species at Upstream Dam (UD) station. Each graph displays the distribution of same specie with regard to Matoutou 1, 2 and 3 campaigns.

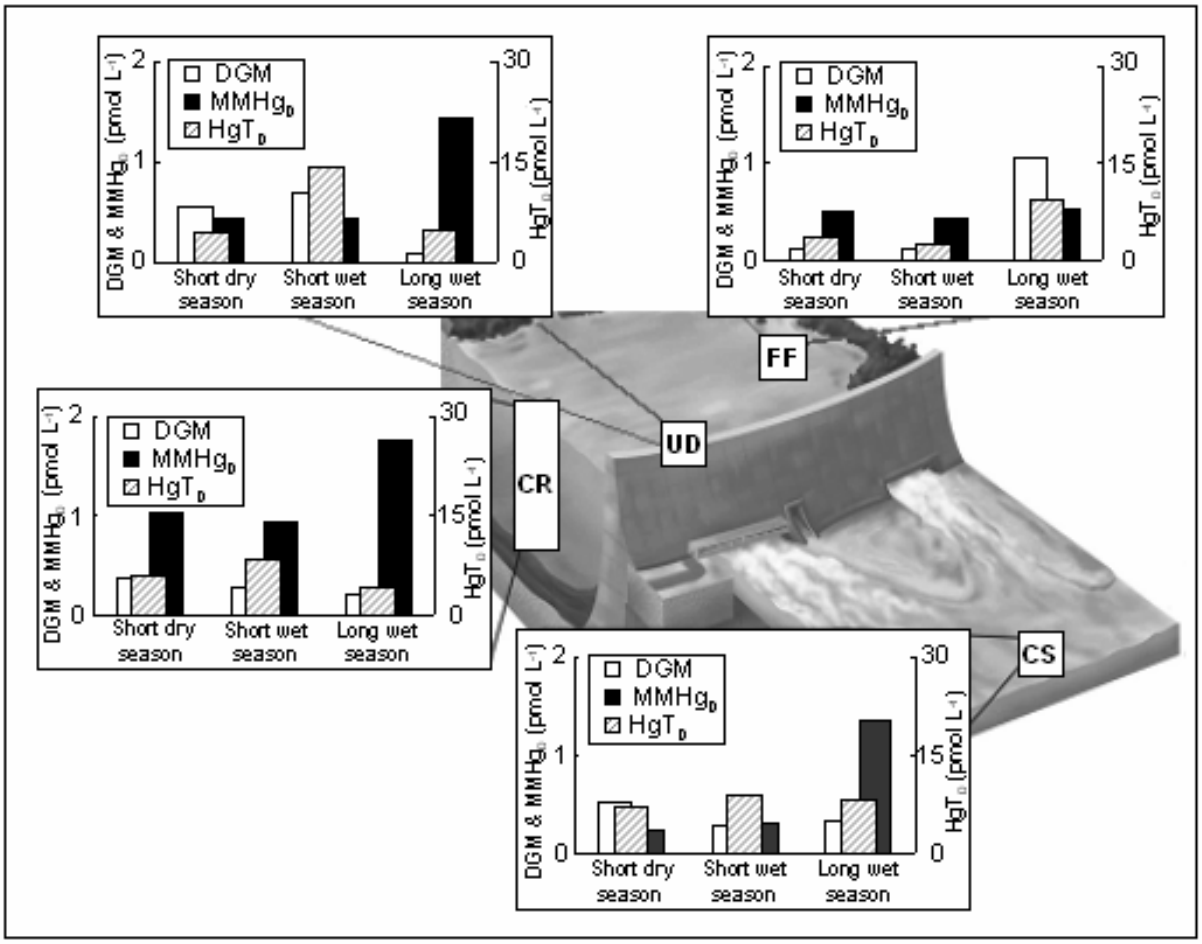

Fig. 4. Average concentrations of main dissolved species of mercury (HgT_D, $MMHg_D$ and DGM) within the hypolimnion of reservoir and dam discharged waters. To illustrate the seasonal variability, average concentrations were reported for every sampled station with distinction between Matoutou 1 (short dry season), 2 (short wet season) and 3 (long wet season) campaigns.

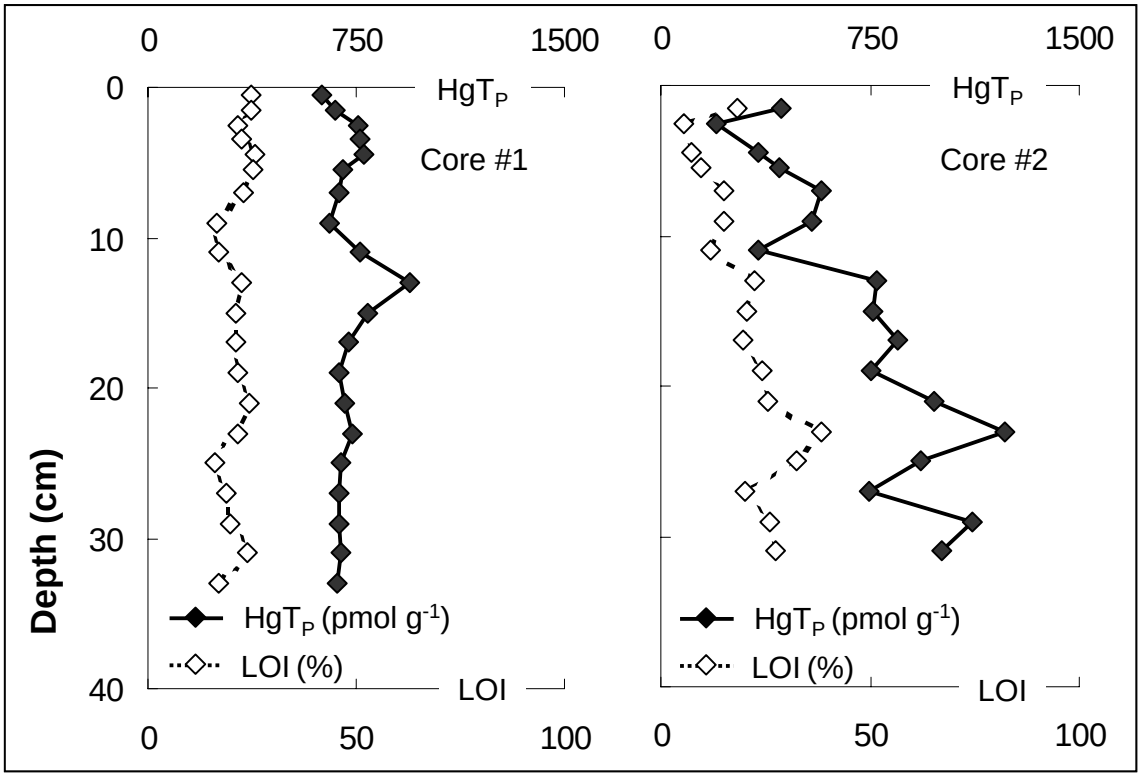

Fig. 5. Profiles of total particulate mercury (HgT_P ; filled diamonds) and percentage of loss to ignition (LOI; open diamonds) in sediments. Both cores were collected in the riverbed of the Sinnamary River: core #1 originated from the Saut Dalles (SD) station (11 km ahead of the reservoir entrance) while core #2 was collected further down the Takari Tanté fall (200 m inside the reservoir itself).

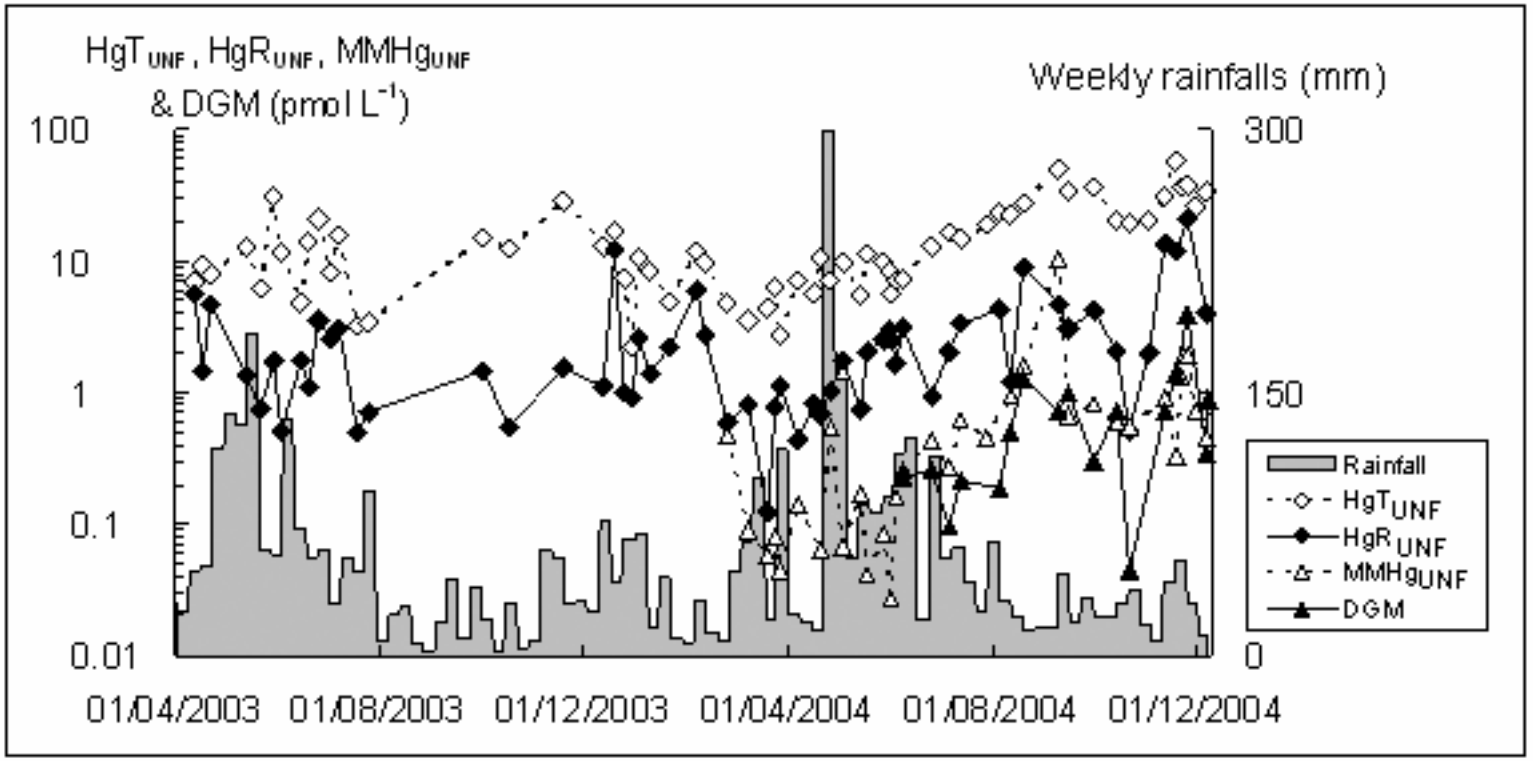

Fig. 6. Monitoring of total (HgT_{UNF}), reactive (HgR_{UNF}), monomethyl ($MMHg_{UNF}$) and dissolved gaseous (DGM) mercury concentrations in rain. Wet deposition was collected on a weekly basis at the HYDRECO field laboratory station *circa* 200 m downstream of the dam. Shaded motif account for the cumulated quantity of rain fallen every week.

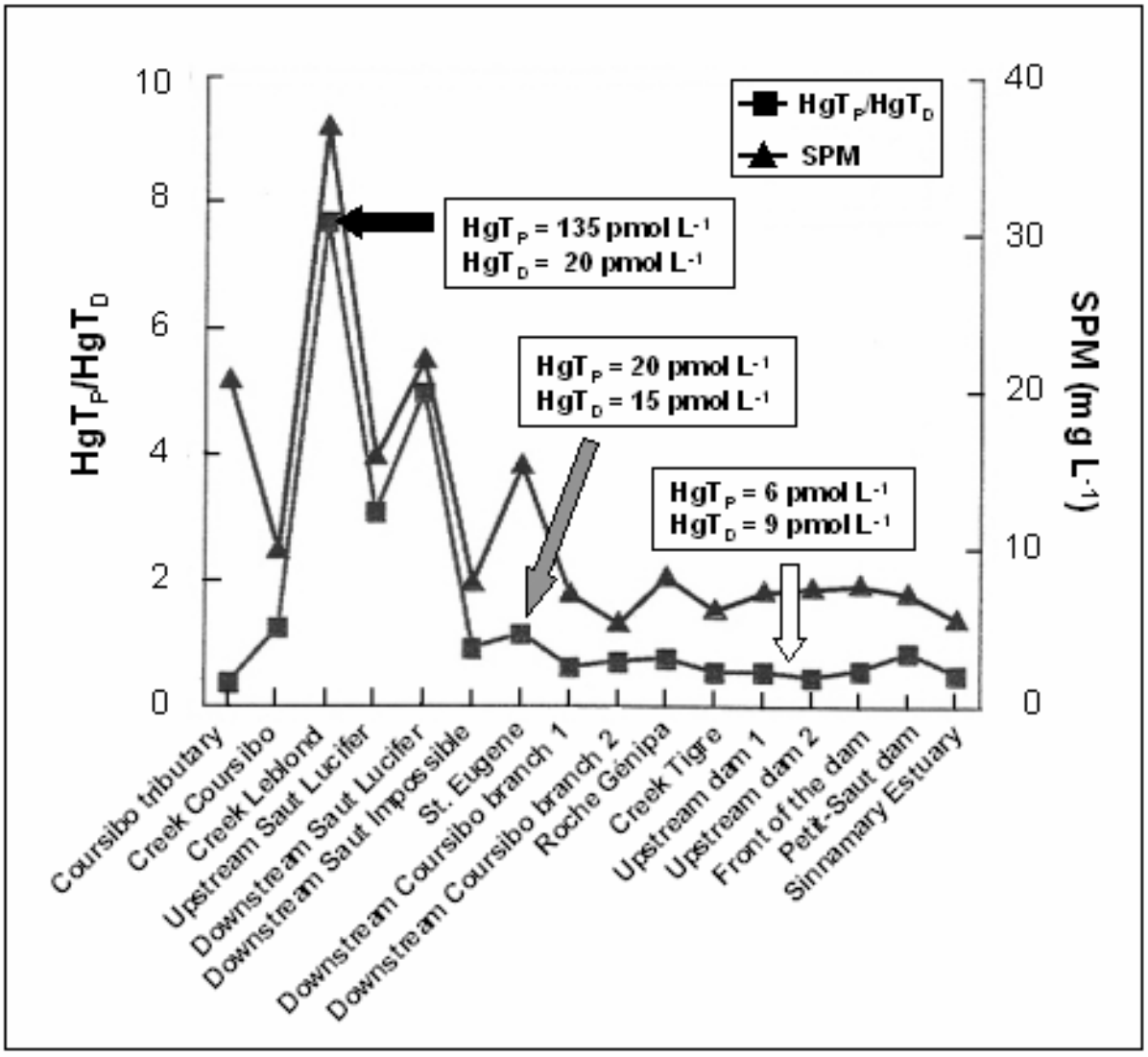

Fig. 7. Evolution of particulate to dissolved fraction of total mercury (HgT_P / HgT_D) between the upstream Courcibo and Leblond tributaries (gold-mining area of Saint Elie) and the Sinnamary Estuary (December 1999).

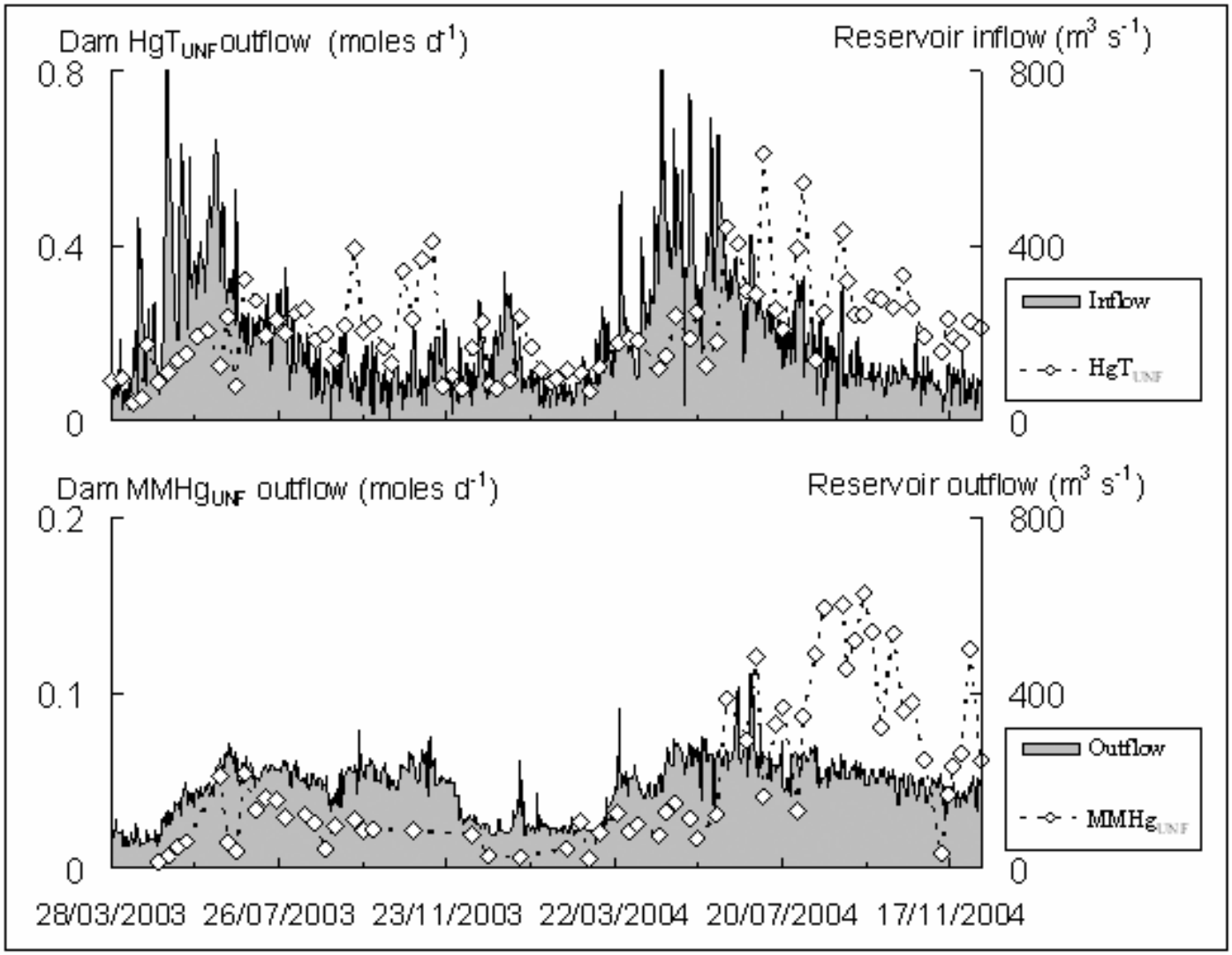

Fig. 8. Monitoring of unfiltered total (HgT_{UNF}) and monomethyl ($MMHg_{UNF}$) mercury exportation fluxes (moles d^{-1}) downstream of the dam (CS station). Water in/outputs to/from the reservoir were recorded daily(HYDRECO data). Samples for Hg analyses were collected on a weekly basis.

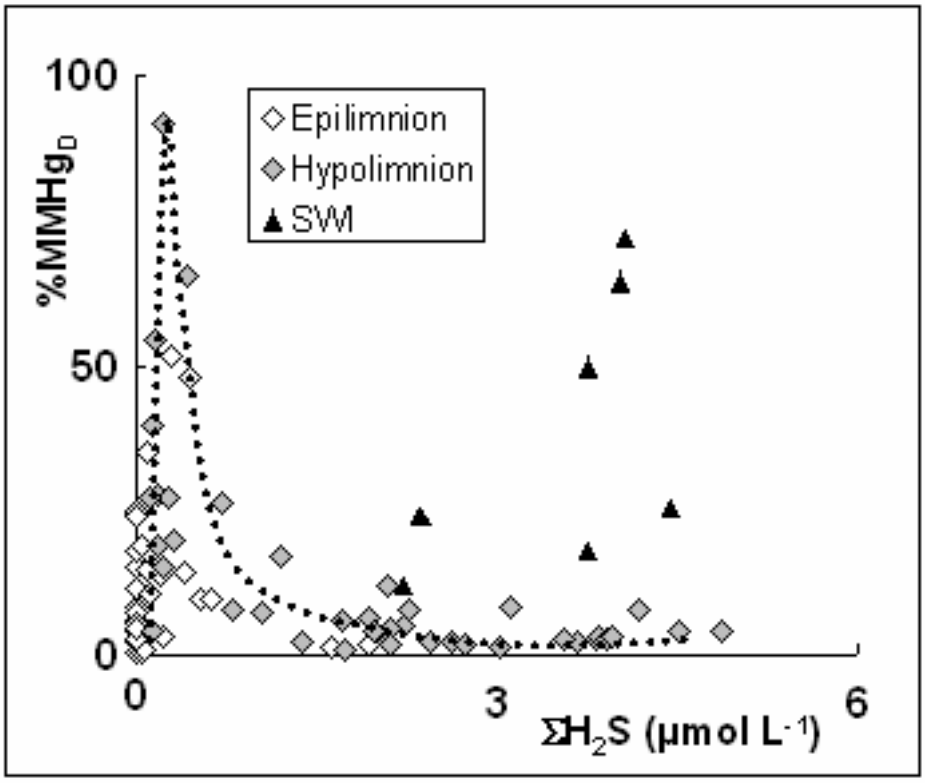

Fig. 9. Relationship between dissolved methylated percentage (%MMHg$_D$) and total sulfides (ΣH_2S) in the water-column of the reservoir. Differentiation was made between samples that were collected into the epilimnion (open diamonds), the hypolimnion (filled diamonds) and at the SWI (bold triangles).

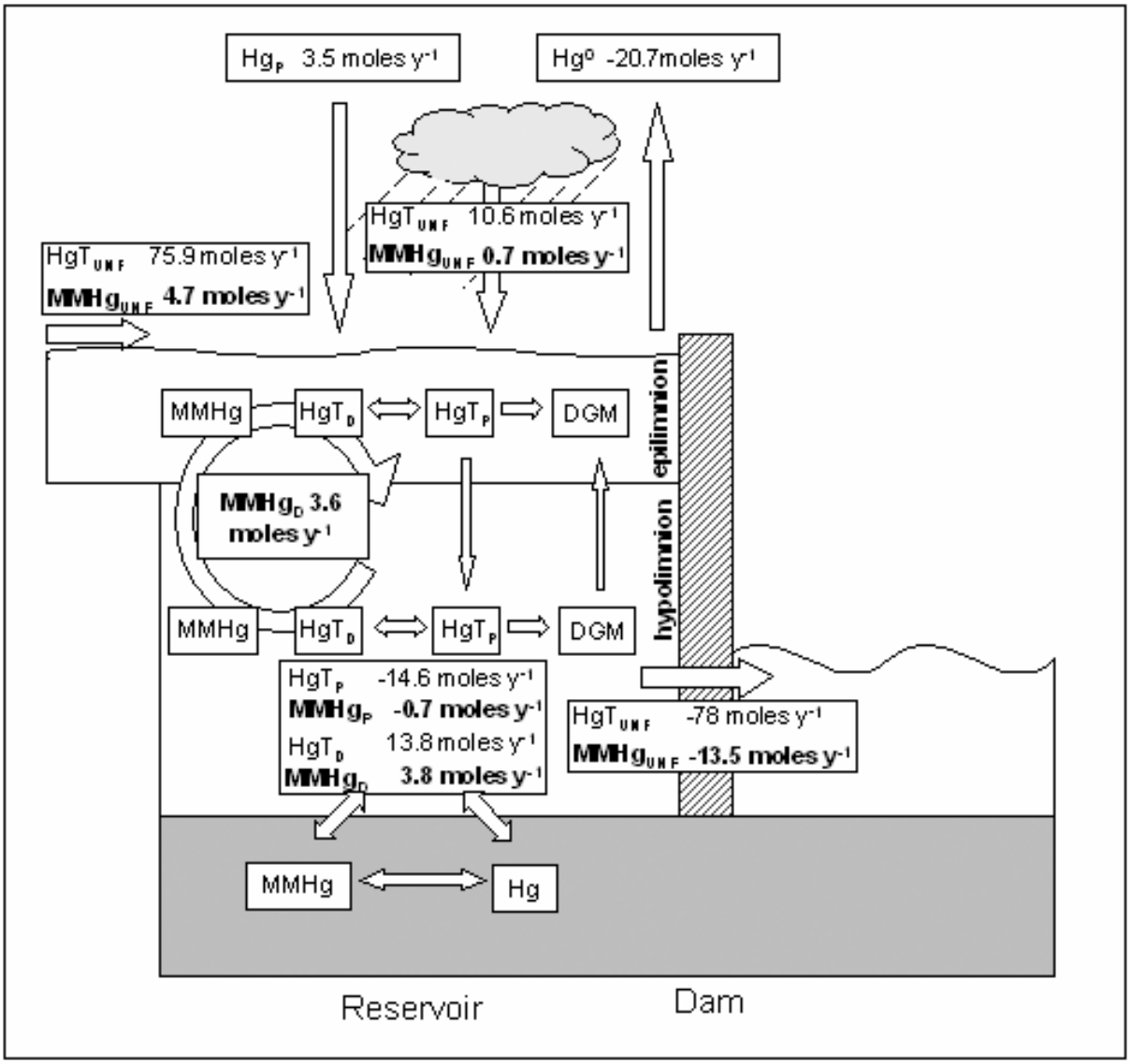

Fig. 10. HgT_{UNF} and $MMHg_{UNF}$ budget for the Petit-Saut reservoir. Flux calculations corresponded to the Matoutou 1 to 3 campaigns. Thus, the mass balance estimation only provides indicative data on a particular state of the reservoir on a seasonal time scale.

Article III

Transformations du mercure dans un estuaire tropical dégradé par l'action humaine

RESUME

La distribution, partition et spéciation du mercure (Hg) ont été investiguées le long du gradient rédox de l'estuaire du Sinnamary en Guyane Française. Il s'agit d'un système dégradé par l'activité humaine où les eaux sulfuriques du fleuve Sinnamary transitent jusqu'à l'océan Atlantique, s'y mêlant au panache de l'Amazone.

L'oxygénation brutale et incomplète des masses d'eau y contribue au développement de gradients de concentration chez de multiples espèces chimiques (fer, sulfures, etc.) ainsi qu'a un recyclage intense de la matière organique (MO). La présence µ-molaire de sulfures dans un milieu riche en MO dépeint l'HES (Haut Estuaire du Sinnamary : région soumise à l'onde de la marée mais qui précède l'intrusion saline) comme un site potentiel de méthylation du Hg. Les concentrations de mercure total (HgT) dans les échantillons d'eau non filtrés (HgT_{UNF}), dissous (HgT_D) et particulaires (HgT_P) de l'HES étaient de 11 ± 3, 6 ± 2 et 5 ± 3 (i.e. 600 ± 200 pmol g^{-1}) pmol L^{-1}. Le monométhylmercure (MMHg) dans les échantillons non filtrés ($MMHg_{UNF}$), dissous ($MMHg_D$) et particulaires ($MMHg_P$) valait 3,8 ± 0,6, 2,0 ± 0,9 et 1,8 ± 1,2 (i.e. 220 ± 130 pmol g^{-1}) pmol L^{-1}. L'oxygénation et la sulfuration des eaux semblent déterminer en grande partie les niveaux de MMHg. Parallèlement, divers processus impliquant la chimie du fer, les réactions pH et/ou rédox dépendantes conditionnent sa partition. L'estuaire salin (noté BES pour Bas Estuaire du Sinnamary) définit un domaine

actif de transformations du Hg incluant des changements de phase et de forme. Atteignant le BES, le flux particulaire du HES rencontre l'immense réservoir de matières en suspension (180 ± 40 pmol g^{-1} de HgT_P) formant le panache de l'Amazone (jusqu'à 1330 mg L^{-1}). Dans cette même région, le $MMHg_D$ adopte un profil non conservatif (de 0,72 à 0,03 pmol L^{-1}) lorsqu'il est mis en relation avec la salinité (jusqu'à 24 ‰). Cette observation suggère l'existence d'un mécanisme d'enlèvement du $MMHg_D$ de la colonne d'eau. Hormis les processus endogéniques de déméthylation, ce comportement est explicable par un modèle de complexation : au niveau du gradient de salinité, le Hg complexé par la MO est partiellement mobilisé puis pris en charge par des ligands minéraux.

Dans l'ensemble, l'estuaire du Sinnamary se comporte comme un réacteur chimique regroupant (parmi d'autres) des processus de partition et de méthylation. La source anoxique de l'amont ainsi que l'intense méthylation *in situ* concourent à maintenir les concentrations de MMHg à un niveau élevé aussi bien dans le dissous que les particules. A titre d'exemple, l'HES exporte 60 % plus de $MMHg_{UNF}$ qu'il n'en importe : 5,5 contre 3,5 kg a^{-1}.

Statut : soumis à « Estuaries »

Mercury transformations in man-perturbed tropical estuary

B. Muresan*, D. Cossa*[1], M. Coquery**, S. Richard***

**Institut français de recherche pour l'exploitation durable de la mer (IFREMER), BP 21105, F.44311 Nantes cedex 3, France (EU)*

***Centre national du machinisme agricole, du génie rural et des eaux et forêts (CEMAGREF), BP 220, F.69336 Lyon cedex 9, France (EU)*

****Laboratoire de recherche en environnement barrage de Petit-Saut (HYDRECO), BP 823, F.97388 Kourou, French Guiana (EU)*

ABSTRACT

The distribution, partition and speciation of mercury (Hg) were studied along the redox gradient of an anthropically perturbed tropical estuary, the Sinnamary Estuary in French Guiana. This system is a partially mixed estuary characterized by an anoxic freshwater end-member, while the marine end-member consists of the Amazon Plume.

The set up of an artificial oxygenation system in the anoxic freshwater end-member generates sharp gradients of major chemical species (iron, sulfides, etc.) coupled to intense organic matter (OM) turnover. The coexistence of oxygenated waters and dissolved sulfides in an organic rich environment depicts the USE (Upper Sinnamary Estuary: part of Sinnamary Estuary under the tidal influence but upstream the salt intrusion) as a potential site for Hg methylation. The concentrations of all mercurial species (HgT) in the unfiltered samples (HgT_{UNF}), in the dissolved (HgT_D) and particulate (HgT_P) phases of the USE average 11 ± 3, 6 ± 2 and 5 ± 3 (i.e. 600 ± 200 pmol g^{-1}) pmol L^{-1} respectively. Average concentrations of

[1] Corresponding author (Tel.: 33 2 40 37 41 76; Email: dcossa@ifremer.fr)

monomethylmercury (MMHg) in the unfiltered ($MMHg_{UNF}$), dissolved ($MMHg_D$) and particulate ($MMHg_P$) phases were 3.8 ± 0.6, 2.0 ± 0.9 and 1.8 ± 1.2 (i.e. 220 ± 130 pmol g^{-1}) pmol L^{-1} respectively. Water oxygenation and sulfides concentrations emerged to play a critical role in controlling MMHg levels. Besides, iron cycling, acid-base mechanisms, and redox-dependent processes were involved in the MMHg partitioning between phases. The saline estuary (noted LES: Lower Sinnamary Estuary) depicted a transitional environment of rapid and sequential changes in Hg speciation and distribution. Entering the LES, the USE particles encountered a considerable amount of lower Hg content particles (180 ± 40 pmol g^{-1}) derived from the Amazonian plume (up to 1330 mg L^{-1}). Concomitantly, in the dissolved phase, the relationship between $MMHg_D$ concentrations (from 0.72 to 0.03 pmol L^{-1}) and salinity (up to 24 ‰) showed a departure from the dilution line. Such a pattern suggests a removal of $MMHg_D$. Along with $MMHg_D$ demethylation, this behavior was explained by a complexation model: exchangeable Hg from the riverine Hg^{II}-organic complexes is mobilized in forming mineral complexes with the increasing of salinity.

In general, the Sinnamary Estuary constitutes a biogeochemical reactor that gathers partitioning and methylation processes. The permanent MMHg inputs from the anoxic freshwater end-member combined to the intense endogenous Hg methylation ensures high MMHg levels in both dissolved and particulate phases. To illustrate, the USE exports 60 % more $MMHg_{UNF}$ than it does import: 5.5 *versus* 3.5 kg y^{-1}.

Keywords: Estuary; Reservoir; Mercury; Redox; Speciation; Partitioning

1. INTRODUCTION

Estuaries define transitional environments of active biogeochemical transformations. The strong chemical and physical gradients characterizing these continent-ocean interfaces affect the local cycle of numerous metals (e.g., Fe, Mn, Al, Ni, Cd, Hg, Pb, etc.; Mantoura *et al*., 1978; Boughriet *et al*., 1992; Mota *et al*., 2005). Reciprocally, the speciation and partition of these metals reflect ongoing biogeochemical processes (Weijden *et al*., 1977; Shibu *et al*., 1990; Rodas *et al*., 2005). Among those, mercury (Hg) physico-chemical transformations (partition between dissolved, particulate and gaseous phases along with speciation changes) are particularly important. Indeed, its multiple valence states and chemical associations (with methyl, thiol or sulfide groups) are widely achievable in natural conditions (Baeyens and Leemarkers, 1998; Cossa *et al*., 1996; Coquery *et al*., 1997). Besides, Hg cycle also involve biologically mediated processes such as reduction/oxidation or methylation/demethylation (e.g., Choi *et al*., 1994; Siciliano 2002). As a result, Hg represents a remarkable tracer that can be followed along estuaries, providing significant information on the pattern of biogeochemical events, processes or distribution among physical phases or chemical substrata. Last but not the least, Hg toxicity represents a serious threat to the health of people and wildlife in many environments that are not obviously polluted (RTECS; Zahir *et al*., 2005). Mercury circulates between air, water, sediments, soils and biota in various forms. In aquatic environment, monomethylmercury (MMHg) is the form of greatest concern since it has the capacity to collect in organisms (bioaccumulate) and to concentrate up food chains (biomagnify). It is now generally accepted that maxima of monomethylmercury concentrations generally match to redox transition zones containing sulfate-reducing bacteria (SRB) which are thought to be the key methylator agents (e.g., Jensen and Jernelov, 1969; Gilmour *et al*., 1992; King *et al*., 1999; Benoit *et al*., 2003; Bisinoti and Jardim, 2005). Exploration of redox dependant and biologically driven mechanisms is of great significance

for predicting the distribution and speciation of Hg inputs to the main adjacent reservoirs, namely the coastal sediments, the Ocean and the atmosphere, including their living organisms.

In temperate and cold regions, the potential methylation of inorganic Hg to MMHg has given rise to numerous studies dealing with mercurial speciation and partition (e.g. Furutani and Rudd, 1980; Compeau and Bartha, 1985; Korthals and Winfrey, 1987; Ramlal *et al*., 1993; Branfireun *et al*., 1999; Rodriguez *et al*., 2004; Nguyen *et al*., 2005) In contrast, mercury behavior in equatorial or tropical estuaries is very poorly known (Guimaraes *et al*., 2000a and b; Roulet *et al*., 2000 and 2001; Sergio *et al*., 2005). Despite the increasing set up of hydroelectric reservoirs, the paucity of data is all the more flagrant when considering tropical estuaries that undergo hypolimnetic discharges from a stratified man-made lake. There yet exists a multitude of evidences that filling tropical reservoirs results in increasing mercury concentrations of fishes from the downstream discharged waters (Aula *et al.*, 1992; Porvari, 1995; Mol *et al*., 2001; Richard *et al.*, 2002). Firstly, stratified reservoirs exhibit a great potential for increased MMHg production in the hypolimnion of their water column and/or in the anoxic zone of their sediments (Parks *et al*., 1989; Bloom and Effler, 1990; Watras *et al*., 1994; Jacobs *et al*., 1995). A notable fraction of the hypolimnetic MMHg may subsequently be exported in the downstream of the reservoir where it could bioaccumulate in the aquatic food web (Muresan *et al*., under submission). Secondly, discharged waters generally contain high levels of organic matters (OM) and hydrogen sulfides (ΣH_2S) produced during the process of anaerobic decomposition. Build up of favorable methylating conditions (intense microbial activity coupled to reduced water oxygenation) in the downstream of the reservoir supports the formation of endogenous MMHg. Thirdly, the progressive degradation of water quality drastically affects the food chain edifice. The MMHg organism bioaccumulation and trophic chain biomagnification tend to increase markedly in omnivorous

and carnivorous fishes (Verdon *et al*., 1991; Brouard *et al*., 1994; Schetagne *et al*., 1997, 1999a).

In short, cycling Hg allowed us to enlighten the peculiar processes occurring in a unique anthropically affected tropical estuary (i.e. magnitude and dynamics of redox gradients in governing the Hg speciation, partitioning and mobility). Beyond particular considerations, and in order to appraise the methylation potential of tropical water bodies, we have also tested the general hypothesis stating that sulfides control the mercury speciation and bioavailability to SRB (Benoit *et al*., 1999 and 2003). To reach this goal we addressed the following questions (i) What is the role of estuaries that undergo hypolimnetic discharges in the biogeochemical cycle of mercury? (ii) Is there a redistribution of the species between the dissolved and particulate phase? (iii) What are the roles of OM and iron in the process? (iv) What is the importance of the *in situ* methylation with respect to exogen sources of MMHg? and (v) Which parameters and/or processes govern the importance of MMHg in the aquatic environment? We address these questions with, the Sinnamary Estuary (French Guiana, Fig. 1), an example of estuary that undergo permanent hypolimnetic discharges from the hydroelectric reservoir of Petit-Saut. The Sinnamary Estuary exhibits high levels of partially degraded OM and an important fraction of residual reducing agents (as Fe^{II} and ΣH_2S) that contribute to the gradual consumption of dissolved oxygen. Indeed, despite artificial aeration of the reservoir outflowing waters, large communities of anaerobic bacteria were identified in the downstream estuary. Finally, a 10 years survey of Hg levels in fish samples has revealed high concentrations of mercury especially in carnivorous fishes (up to 9.7 nmol/g, fresh weight).

2. THE SINNAMARY ESTUARY

The Sinnamary Estuary spans over 70 km from the dam of the artificial reservoir of Petit-Saut to the Atlantic Ocean. Its marine end-member consists of the Amazon plume while its freshwater extremity is mainly composed by the hypolimnetic water outflowing from the reservoir and, seaward, the water contributions of a few small tributaries. The main characteristic of this system is the high content of reduced species in the freshwater inflow due to the anoxicity of the reservoir. The tidal amplitude ranges from a few centimeters near the dam to a maximum close to 3 m at the mouth of the estuary during spring tide (Amouroux, 2003). However, the salt intrusion never exceeds a few km beyond the village of Sinnamary (Fig. 1). We choose to call the tidal estuary Upper Sinnamary Estuary (USE), and the saline estuary the Lower Sinnamary Estuary (LES). The Sinnamary Estuary is a macrotidal estuary with the resulting development of a High Turbidity Zone (HTZ) mostly at the entrance of the Sinnamary mangrove (Fig. 1). Its position, near at the entrance of the LES, varies accordingly with the hydrodynamic conditions governed by the freshwater discharge and the tidal magnitude. At the marine end-member the LES is diluted in the Amazon plume which spread North-West along the South American coast from the mouth of the Amazon. Here the LES designation will include the HTZ of the Sinnamary Estuary and the part of the Amazon plume, which locally leaches the coast.

The Sinnamary River is 250 km long and springs up in the center of French Guiana at an altitude of 125 m (Fig. 1). Its catchment area spans over 7000 km² of crystalline formation overgrown by uninhabited primary forest. Between 1989 and 1994, the construction of the hydroelectric dam of Petit-Saut took place. The resulting reservoir (5°04’ North, 53°03’ West) stretched over 60 km length and 60 km width and with a 35 m maximum depth, flooding approximately 350 km² of uncleared primary forest (Huynh *et al*., 1997). The annual mean freshwater input to the reservoir is estimated to 190 m^3 s^{-1}. This corresponds to a residence

time of the impounded water close to 6 month. Downstream the dam, the USE is *circa* 50 m width and its course displays an overall slope of 0.03 m per km. The associated residence time of the discharged water varies, accordingly to the turbining regime, between 24 and 48 hours (HYDRECO data). Some minor creeks run into the USE and contribute to the global water discharge to the ocean.

The filling of Petit-Saut reservoir generated major modifications in the water chemistry of the Sinnamary River. Initially, the waters were warm, acidic, only slightly conductive, oxygenated, nutrient poor and relatively homogenous (Horeau *et al*., 1998). In the reservoir, the water body underwent rapid establishment of an oxygenated epilimnion and an anoxic hypolimnion (Richard, 1996). By comparison with the epilimnion, the hypolimnion exhibited elevated concentrations of reduced elements. The main processes involved in water enrichment were OM degradation (ammonium, phosphates, humic acids, etc.) and mobilization from the geological substratum (iron, manganese, silica, etc.). As a result of the reservoir stratification, the Sinnamary Estuary started to convey mineralized waters coupled to elevated amounts of OM and reduced species. In order to maintain the dissolved oxygen concentrations compatible with aquatic life, an aeration system was set up in the outflow of the turbines. This system triggered the build up of marked concentration gradients for several reduced compounds such as dissolved iron and methane. Nonetheless, a strong oxygen consumption remained apparent within the estuary (up to 0.1 mmol L^{-1} of biological oxygen demand according to Richard *et al*., 1997).

3. MATERIAL AND METHODS

3.1. Sample collection

Samples from the Sinnamary Estuary were all but collected during five main campaigns that orderly took place in March-April 2003, January-February 2004, May-June 2004, November-December 2004 and February-March 2005. The sequence between *in situ* campaigns, designated respectively as Matoutou 1, 2, 3, 4 and 5, reflects the major seasons of the guianese climate (Tab. 1). Those are the short wet season (from November to February), the short dry season (from February to April), the long wet season (April to July) and the long dry season (from July to November). During Matoutou 1 to 5 campaigns, from 200 m below the dam (5°04.01'N - 53°03.26'W) to the downstream saline gradient (5°26.03'N - 52°59.62'W), the USE was invariably sampled at the same eight stations: Pas., Ker., Cha., Ven., Bra., Com., Deg. and Sin. (Fig. 1). These were chosen in order to account for the temporal and spatial variability of the main chemical characteristics of the USE (see below).

The determination of mercury speciation in the principal freshwater sources of the Sinnamary Estuary has been carried out. For this purpose, water samples were collected on a weekly basis between March 2003 and December 2004 a few meters downstream the outflow of the Petit-Saut reservoir. The so called "tailrace" (channel that conveys turbined waters prior to artificial oxygenation) represents the principal freshwater source to the Sinnamary Estuary (close to 180 m^3 s^{-1}). Related station for water sampling (noted Tail., 5°03.89'N - 53°02.85'W) reflects the average conditions of the hypolimnetic dam discharges. Apart from the Petit-Saut end-member, USE tributaries of apparently unimpacted freshwaters, were sampled during Matoutou 2, 3, 4 and 5 sampling campaigns (Tab. 1). Locally named "creeks", four major tributaries were investigated (i.e. Creek Gregoire, Creek Chapeau, Creek Venus and Creek Saulnier). The 2003/04 water flow was weekly measured at the Com. station

(40 km downstream the dam). Recorded values provided an integrated estimation of the USE to LES water exportations (close to 230 m^3 s^{-1}). Hence, we estimated the freshwater contribution of local creeks to *circa* 1 / 5 of the total USE flow. Yet, small tropical rivers in French Guiana exhibit extreme short term variability in discharge throughout the November-February and April-July rainy seasons (Ponton and Vauchel, 1998). The given flow ratio must thus be carefully considered.

Regarding the saline estuary, the HTZ entrance (from 5°22.74'N - 52°57.63'W to 5°26.03'N - 52°59.62'W) and the subsequent Amazon plume (from 5°26.03'N - 52°59.62'W to 5°30.94'N - 53°07.92'W) were considered separately. The HTZ entrance, part of the LES characterized by a salinity < 5 ‰ was sampled at 4 occasions (Matoutou 2, 3, 4 and 5). It this region, the behavior of major chemical and Hg compounds appeared substantially driven by non conservative processes. Further at large, were mixing mechanisms prevailed, the local Amazon plume was widely scrutinized during December 1999 cruise (Tab. 1). Finally, to compare with a remote station from the direct LES influence, marine samples were collected during Matoutou 2 and 5 campaigns near the "îles du Salut". Those islands are located *circa* 15 km North, offshore from the city of Kourou (5°16.60'N - 52°35.11'W). Despite the distance with the continent, the corresponding station (noted IS) remained under the influence of the suspended particulate matters (SPM) forming the Amazon plume.

The ultra clean sampling techniques applied for water collection and storage are those presented and discussed in detail by Gill and Fitzgerald (1985), Bloom (1989), Quémerais and Cossa (1997), and Cossa *et al*. (2002 and 2003). In short, subsurface water samples [20 cm below the air-water interface (AWI)] were collected in acid-cleaned Teflon (FEP) bottles held by hand worn polyethylene gloves. The bottles were rinsed three times, filled, tightly capped and double-bagged, then transported in coolers back to the dam adjacent field laboratory (named HYDRECO). Filtrations and analyses of dissolved gaseous mercury (DGM) on

unfiltered samples were performed within 2 hours after collection. Reactive mercury (HgR is an easily reducible fraction obtained by direct reduction with $SnCl_2$ at pH 1) and the sum of all mercurial species or "total" mercury (HgT) analyses were processed during the same day. The HgR was determined on unfiltered (HgR_{UNF}) samples and casually in the dissolved (HgR_D) phase. HgT determinations were performed on both unfiltered and filtered samples. Related fractions were respectively noted HgT_{UNF} and HgT_D. Aliquots were kept to determine monomethylmercury (MMHg) in the unfiltered ($MMHg_{UNF}$) dissolved ($MMHg_D$) and the particulate ($MMHg_P$) phases. The water samples were filtered on LCR and/or Sterivex 0.45 µm membranes; the LCR membranes are Teflon made while Sterivex membrane consists of hydrophilic PVDF. No significant differences in HgT_D or $MMHg_D$ concentrations were observed between the two materials, upon the condition of discarding the first 20 mL of filtrate. For each sample, filtered amount of water was carefully determined then acidified with 1 % (v/v) Suprapur® HCl. Worn filters (particulate samples) and corresponding filtered solutions were ultimately double bagged and stored at –20 °C in dark conditions until HgT_P, $MMHg_P$ and $MMHg_D$ analyses were performed.

2.2. Sample analysis

2.2.1. Physical and chemical variables

The water pH, dissolved oxygen, conductivity and redox were recorded *in situ* with a YSI multiparameter probe sonde 600XLM. Additional analyses for major chemical species were carried out in laboratory. Briefly, total organic carbon in the global and the dissolved fraction were analyzed by IR spectroscopy after conditional filtration followed by oxidative or acidic digestion of the samples. The concentrations of total sulfides (ΣH_2S) and dissolved (<0.45 µm) iron (FeT_D) were colorimetricaly measured by means of specific photometric test kits (MERCK, Spectroquant). For ΣH_2S determinations, 4 ml of water pouring from the

collection tubing were added to 6 ml of a $ZnCl_2$ trapping solution. Samples were transported to HYDRECO then methylene blue method was applied within 2 hours after collection. Concerning FeT_D, around 2 L of water were individually collected paying great attention to minimize the oxygenated headspace of the bottle. After returning to HYDRECO, samples were filtered under nitrogen atmosphere then 10 mL of a one to ten diluted solution were colorimetricaly analyzed. Colored reaction consists in synthesizing an iron red-violet complex as reduced Fe^{II} encounters a triazine derivative in a thioglycolate-buffered medium.

2.2.2. Mercurial speciation in solid and dissolved phases

All mercury species in water samples were detected by cold vapor atomic fluorescence spectrometry (AFS). Total and dissolved Hg were determined in compliance with Bloom and Fitzgerald (1988), by the formation of volatile elemental Hg (released by $SnCl_2$ reduction, after 30 minutes of acidic BrCl oxidation, and its preconcentration on a gold column). DGM analyses were processed onto 100 mL of unfiltered aliquots of sampled water. Samples for DGM were sparged for 20 min with Hg-free argon at 200 mL min^{-1} within 2 hours after collection. Reactive mercury, an easily reducible fraction, was obtained within 4 hours of sampling by direct reduction with $SnCl_2$. The suspended particulate matters (SPM) collected on a preweighed LCR® filter were freeze-dried and weighed to estimate the SPM load. Sampled material was digested with concentrated HCl/HNO_3 (1/9, v/v) in Teflon (PFA) reactors (80 °C; 4 hours). The standard procedure for water was subsequently applied to 100 µL of obtained SPM solution to determine HgT_P concentrations. An automatic atomic absorption spectrometer (AAS: AMA-254®, Altec Ltd.) was used for HgT_P determinations in sediments. This technique consists of a calcination of the freeze-dried samples under an oxygen gas stream in order to produce elemental mercury vapor and its subsequent amalgamation on a gold trap; mercury vapor then being measured by AAS (Cossa *et al*., 2002). The detection limits, defined as 3.3 times the standard deviation of the blanks, were

0.05 pmol L^{-1} and 0.025 nmol·g^{-1} for the dissolved and particulate mercury analyses respectively. The corresponding reproducibilities (the coefficient of variation in percentage of five replicate samples) were lower than 10 %. The accuracy for HgT_P determinations in solids was regularly checked using the reference material (MESS-3) from the National Council of Canada as certified reference material (CRM). Monomethylmercury was determined using the method initially proposed by Bloom (1989) and modified by Liang *et al*. (1994). $MMHg_{UNF}$ or $MMHg_D$ in acidified water were extracted by CH_2Cl_2 and then transferred into 40 mL of Milli-Q water by evaporating the organic solvent. The aqueous solution was analyzed for MMHgCl by chromatography after ethylation and adsorption/desorption on a Tenax® column. For $MMHg_P$, a 3 hours acidic dissolution (HNO_3 65 %) of the freeze-dried samples of sediment or filtered SPM took place before the procedure described previously. Detection limits were 0.01 pmol L^{-1} and 0.005 nmol·g^{-1} for respectively a 100 mL water and 200 mg solid sample. Precision was less than 10 % for all analyses. Using the available reference material (IAEA-405), the accuracy of the method was estimated to be less than 10 % with an average recovery of 91 ± 8 %. This technique was adapted from Leermakers *et al*. (2001) and the detailed procedure is given by Cossa *et al*. (2002 and 2003).

2.3. Modeling the mercurial scavenging

The scavenging of dissolved Hg (Q_a, kg) was formulated, for in the Sinnamary Estuary, as the product of the average trapping coefficient of Hg (k, no units) and the local consumption of scavenging agent (Q_s, kg):

$$Q_a = k\, Q_s$$

The chemical equilibrium between dissolved Hg, ligands and suspended matters is usually based on the surface complexation theory (Stumm *et al*., 1980; Westall, 1987; Dzombak and Morel, 1990). In this approach, the high affinity of Hg for sulfides, oxyhydroxides, and OM ensures that equilibrium between the dissolved and the solid phase is quickly achieved (Morel

et al., 1998). As a result, dissolved Hg levels are essentially driven by the available quantity of sorbent:

$$\Delta[A] = - k\ \Delta[S] \quad ; \quad k = \frac{[SA]}{K_{ads}\ [S]^2}$$

Where [S] is the particulate fraction of the sorbent (µmol L^{-1}), [A] is the concentration of dissolved Hg (pmol L^{-1}) and [SA] is the concentration of the Hg-sorbent bounded complexes (pmol L^{-1}). Calling [D] the dissolved fractions of the sorbent (µmol L^{-1}) and considering that the global amount of sorbent remains relatively unchanged between the dam and the HTZ:

$$k = - \frac{\Delta[A]}{\Delta[S]} \approx \frac{\Delta[A]}{\Delta[D]}$$

One could thus approach the trapping coefficient (k) by measuring the concentrations of dissolved Hg along with that of dissolved scavenging agent (i.e. OM, iron, sulfides etc.).

4. RESULTS AND DISCUSSION

This chapter introduces the obtained results and their respective discussions within five selfmeaning sections. Their common aim is to call attention upon the intense methylation and active partitioning of Hg in water bodies that undergo hypolimnetic discharges. General considerations on the biogeochemistry of the Sinnamary Estuary are presented in Section 4.1.. Section 4.2. details the speciation, fluxes and transformations of Hg at the dam end-member within first minutes of brutal water oxygenation. Thence, Section 4.3. individually monitors the behavior of HgT, DGM and MMHg within the USE domain. Saline estuaries usually play a large role in mercury recycling and transfer to the adjacent coastal waters (Gagnon *et al*., 1996; Cossa and Gobeil, 2000; Laurier *et al*., 2002). Consequently, the fate of Hg in the LES

is covered in Section 4.4. with a distinction between the HTZ entrance, the Amazon plume and the IS station. In a clarity attempt, and in order to appreciate the spatial variability of methylation in the Sinnamary continuum, a global vision should be ultimately given. This is the topic of Section 4.5..

4.1. Chemical characterization of the Sinnamary Estuary

The estuarine waters were sampled in order to characterize the distribution of major chemical species (oxygen, carbon, iron, sulfides) and physical parameters (pH, conductivity and redox). Figure 2 shows the lateral profiles obtained during Matoutou 1 (March-April 2003), 2 (January-February 2004), 3 (May-June 2004) 4 (November-December 2004) and 5 (February-March 2005) campaigns at the same nine stations respectively.

4.1.1. pH

The pH in the USE was plainly acidic (5.7 ± 0.3 units) and became slightly acidic in the LES (6.3 ± 0.3 units). While pH neutrality was achieved within the vicinity of maximum turbidity, highest pH (8.1± 0.2 units) corresponded to the offshore IS (îles du Salut) station. Within the USE, the pH was mostly controlled by the discharged hypolimnetic waters (5.7 ± 0.2 units). In addition, the intense alteration of the ferralitic soil as well as the elevated precipitation rates (close to 3 m y^{-1}) of acid rains (4.6 ± 0.4 pH units in 2003/04) tended to maintain the pH below neutrality. Temporal variation displayed a trend of lower values in the course of the dry seasons (5.4 ± 0.1 units) while highest values were measured during the long wet season (6.1 ± 0.1 units). Since pH in the USE and at the center of the reservoir exhibited similar seasonal evolutions ($r^2 = 0.73$), acidity in the downstream of the dam mostly reflected the average condition of the artificial lake.

4.1.2. Dissolved oxygen

Lowest O_2 concentrations were measured at the Tail. station (0.07 ± 0.04 mmol L^{-1}). This pattern reflects the hypolimnetic origin of dam discharged waters. Despite the artificial aeration as well as the partial degassing of reducing volatile species, dissolved oxygen in the USE regularly exhibited critically low levels (< 0.1 mmol L^{-1}). In general, one has to reach the HTZ (*circa* 70 km downstream the dam) in order to measure O_2 concentrations above 0.2 mmol L^{-1} (HYDRECO data). According to our campaigns, lowest concentrations corresponded to the high runoff periods, which depicted both short (February 2004) and long (June 2004) wet seasons (around 0.13 ± 0.02 mmol L^{-1}). Comparatively, dry seasons exhibited the best water oxygenation (up to 0.18 mmol L^{-1}). This pattern suggested that the fate of dissolved oxygen in the Sinnamary Estuary is extensively governed by the load of reducing agents (Fe^{II}, CH_4, ΣH_2S etc.) and OM that flows through the aeration system. Indeed, the longitudinal distribution of dissolved oxygen showed a pattern of gradual consumption as minimum of concentration was usually located between Com. and Sin. stations (*circa* 40 km downstream the Petit-Saut dam).

4.1.3. Conductivity

Conductivity at the Pas. station (*circa* 200 m bellow the dam) ranged from 25 to 40 µS cm^{-1} according the seasons (Fig. 2). Similar values were obtained between 8 and 15 m depth in the water column of the reservoir. The elevated loads in dissolved metallic species (mainly Fe^{II}) and organic acids of discharged waters contributed to maintain high conductivity levels in the USE. Indeed, between the Petit-Saut dam and the Sin. station (70 km downstream), conductivity lessened by less that 7 µS cm^{-1} (from 34 ± 4 to 27 ± 2 µS cm^{-1}). Dilution of waters coupled to oxidative processes (precipitation of Fe^{II}) would be the principal factors responsible for this diminution. Finally, as a signature of the salinity gradient, conductivity leveled up to 150 µS cm^{-1} once entering the LES. Considering the USE seasonal variability,

an inverted evolution was observed between conductivity and dissolved oxygen. The maximum of conductivity (31 ± 3 µS cm^{-1}) of the short wet season coincided with the minimum of oxygenation (0.12 ± 0.03 mmol L^{-1}). On the other hand, in dry seasons, low conductivity values corresponded to elevated O_2 concentrations (24 ± 1 µS cm^{-1} and 0.18 ± 0.02 mmol L^{-1} in this order). Thus, the temporal distribution of conductivity in the Sinnamary Estuary depends on both the seasonal variability of hypolimnetic discharges and the lateral contribution of downstream tributaries.

4.1.4. Redox

Grouping all available data on the Sinnamary Estuary, redox (Eh) values spanned between 150 and 400 mV and averaged 290 mV. In mirror with conductivity, the lateral distribution of Eh increased with distance from the dam. As Eh reflects the local concentration in reducing elements, one could assist to the progressive oxidation of water masses along their course to the Atlantic Ocean. Eh in the Sinnamary Estuary showed a marked seasonal variability: maximum in the short dry season (210 to 390 mV), redox declined during the short wet season (220 to 350 mV) to reach its lowest values in the long wet season (150 to 320 mV). The long dry season ultimately accounted for a partial recovery of initial redox condition in the estuarine milieu (170 to 370 mV). Besides, in dry seasons, Eh displayed a continuous increase as USE waters were exposed to the atmosphere. On the contrary, in wet seasons, Eh gradient was negligible within first meters downstream the dam then markedly leveled up till has reached a well defined maximum. This pattern would result from the combination of the turbining regime (between 50 and 450 m^3 s^{-1} depending the season) that controlled the amount of reducing species and the efficiency of water oxygenation *via* the artificial aeration system and/or the downstream tributaries (estimated to 350 ± 30 mV).

4.1.5. Carbon

According to Guerin (2004), exported carbon from the reservoir (volatilization from the water column plus dam discharges) represents 6 to 7 times the imported amount *via* the upstream tributaries (250 10^9 *vs* 40 10^9 g(C) y^{-1}). The annual loss of carbon corresponds to 3 % of the originally flooded biomass of approximately 10 million tons (Galy-Lacaux *et al*., 1999). From De Junet (2004), carbon exportations downstream dam the attained in 2003 *circa* 80 10^9 g(C) y^{-1} and were dominated by volatile compounds (50 10^9 g(C) y^{-1} mostly as CO_2 and CH_4). Those values were in agreement with Matoutou campaigns data: total organic carbon (TOC) in the USE averaged 0.47 ± 0.02 mmol L^{-1} of which 90 % (0.41 ± 0.04 mmol L^{-1}) was the dissolved fraction (DOC). In comparison, the particulate fraction (POC) averaged only 0.06 ± 0.03 (i.e. 9 ± 5 mmol g^{-1}) mmol L^{-1}. Yet, with distance from the dam, we observed a gradual increase of POC (from < d.l. to 0.08 mmol L^{-1}) to the detriment of DOC (from 0.48 to 0.37 mmol L^{-1}). Such a pattern pointed out an intense overall OM recycling. According to De Junet (2004), the presence of bactériochlorophyll-d in the Sinnamary Estuary reveals a transfer of autochtonous OM from the water column of the reservoir that is progressively degraded downstream. Indeed, suboxic conditions and low light penetrability (< 1 m) tend to limit the development of primary production and enhance the gradual mineralization of discharged planktonic biomass (Vaquer *et al*., 1997). Hence, an inverted relationship was reported with seasons between the average conductivity and POC concentrations in the USE (r^2 = 0.68; $[POC]_{mmol\ L\text{-}1} = -7\ 10^{-4}\ [Cond]_{\mu S\ L\text{-}1} + 0.08$). Corollarly, a parallel behavior was reported with O_2 (r^2 = 0.85; $[POC]_{mmol\ L\text{-}1} = 0.12[O_2]_{mmol\ L\text{-}1} + 0.04$). The maximum of OM mineralization (minimum of POC) would thus mainly be located within the first kilometers downstream the dam and shall develop during the wet periods of the year. Quantitatively, the mineralization of autochthonous particulate OM in the Sinnamary Estuary represented 30 % of its gaseous CO_2 and CH_4 emissions (De Junet, 2004).

4.1.6. Iron

From the HYDRECO 1994 to 2003 chemical monitoring, *circa* 7000 tons of FeT_D are annually discharged downstream the dam. Excepting for Matoutou 2 (short wet season), profiles of FeT_D in the Sinnamary Estuary were comparable to those of conductivity: (i) a global trend of decreasing concentrations with distance from the dam, and (ii) initial stability of concentrations during the wet seasons while dry seasons usually depicted steady and spatially expanded gradients. Mean FeT_D concentration estimated from the Matoutou 1 to 5 campaigns was 8 ± 6 µmol L^{-1}. Maxima were usually measured at the tailrace (dam end-member) and the HTZ (orderly 17 ± 6 and 16 ± 4 µmol L^{-1}). Lowest FeT_D concentrations (below 0.5 µmol L^{-1}) corresponded to Creek Gregoire and IS station. In the USE, the FeT_D distribution was extensively driven by the redox ($r^2 = 0.62$; $[FeT_D]_{\mu mol\ L\text{-}1} = -0.08\ Eh_{mV} + 30$). Simultaneous removal of both iron and oxygen from the dissolved phase suggested a partial oxidation of FeT_D (presumably Fe^{2+}) to Fe oxyhydroxides. The Fe^{II} / Fe^{III} oxidation was also apparent through a bulge shape relationship between both species (HYDRECO data). Maximum of Fe^{III} concentrations (around 50 µmol L^{-1}) were located in the vicinity of the Ker. station *circa* 20 km downstream the dam (15 ± 8 µmol L^{-1} of Fe^{II}). Seasonal variability of FeT_D in the Sinnamary Estuary essentially depended on the origin of the dam expelled waters (Richard, 1996). Dry seasons generally corresponded to phases of accumulation for reduced chemical compounds into the hypolimnion of the reservoir. Yet, low conductivity and FeT_D concentrations also pointed out a notable contribution of epilimnetic waters to dam exportations (28 µS cm^{-1} and 12 µmol L^{-1} in this order). An opposite evolution occurred in the course of the wet seasons. Casual dilution of the hypolimnion by surface waters accompanied a dominance of hypolimnetic waters into the dam exportations. This typically ensured relatively high conductivity and FeT_D levels at the Tail. station (40 µS cm^{-1} and 18 µmol L^{-1} in this order).

4.1.7. Sulfides

The concentrations of ΣH_2S in the Sinnamary Estuary ranged from < 0.1 to 2 µmol L^{-1} and averaged 0.7 ± 0.5 µmol L^{-1}. As a signature of the partial degassing and/or *in situ* sulfides oxidation processes, concentration profiles of ΣH_2S exhibited a gradual diminution within the first kilometers downstream the dam. This diminution, however, tended to fade out revealing localized maxima of concentrations (Com. and Sin. stations). As identified ΣH_2S maxima superimposed to low O_2 stations, those may rather reflect the ongoing biochemical processes than a local water quality alteration (Richard *et al.*, 1997). Actually, potential formation of sulfates through *in situ* sulfide oxidation coupled to locally reducing (< 200 mV) and suboxic (< 0.1 mmol L^{-1} O_2) conditions would contribute to sustain the USE endogenous activity of SRB. According to Dumestre *et al.* (2001), the extinction of phototrophic green bacteria (decrease of the beta-chlorophyll-d signature) tends to favor the expansion of minor bacterial guilds (such as SRB). This observation was confirmed in the USE by water and biofilms incubation experiments that developed substantial SRB concentrations (Jorand pers. com.). Seasonal variability of ΣH_2S concentrations depicted a contrasted behavior with other species. Improved efficiency of the aeration system (> 1.5 mmol L^{-1} O_2) and epilimnetic contribution to dam exportations (< 25 µS cm^{-1} of conductivity) resulted in the USE low (0.2 ± 0.2 µmol L^{-1}) and intermediary (0.4 ± 0.2 µmol L^{-1}) ΣH_2S levels of the short and long dry seasons. On the other hand, the elevated concentrations recorded during the short wet seasons (1.0 ± 0.3 µmol L^{-1} on average) corresponded to a phase of high OM content and intense turn over into the Sinnamary Estuary ($r^2 = 0.59$; $[\Sigma H_2S]_{\mu mol\ L\text{-}1} = -14\ [DOC]_{mmol\ L\text{-}1} - 4.8$).

4.2. Mercury at the tailrace of the dam

General results on monitoring Hg exportations in the downstream of the Petit-Saut reservoir are given in details elsewhere (Muresan *et al.*, under submission). Gained

conclusions are yet briefly reminded. This section focuses on Hg partition and speciation changes during the brutal air exposure of the dam discharged hypolimnetic waters.

4.2.1. Inputs to the Estuary: the role of the dam

HgT_{UNF} concentrations at the Tail. station varied between 3.8 pmol L^{-1} (June 2003) and 27.9 pmol L^{-1} (July 2004). Average HgT_{UNF} concentration was 13 ± 5 pmol L^{-1} of which about 60 % (8 ± 2 pmol L^{-1}) were HgT_D (Tab. 2). In comparison, similar concentrations were measured into the hypolimnion of the reservoir between 8 and 15 m depth (Muresan *et al*., under submission). Seasonal variability of HgT_{UNF} in the outflowing waters was apparent through semi-annual cycles (Fig. 3). We observed a trend towards elevated HgT_{UNF} concentrations (up to 28 pmol L^{-1}) in the beginning and middle of dry seasons (March to April then August to November). In contrast, wet seasons (May to July then December to February) displayed the lowest values (down to 4 pmol L^{-1}). This pattern was in agreement with the general assumption that reduced species concentrated into the hypolimnion of the reservoir during the dry season and were diluted in the course of the wet season (Muresan *et al*., under submission, Tab. 3). The mean flow of water leaving the reservoir was provided on a daily basis by HYDRECO. It averaged 180 ± 70 m^3 s^{-1} for the 2003/04 period. From the tailrace monitoring data, average HgT_{UNF}, HgT_D, $MMHg_{UNF}$ and DGM concentrations in discharged waters were estimated to 13 ± 5, 8 ± 2, 2.5 ± 1.5 and 0.3 ± 0.2 pmol L^{-1} respectively. As a result, relative exportations of Hg reached 16 ± 5, 9 ± 2, 3 ± 2 and 0.4 ± 0.2 $kg \cdot y^{-1}$ respectively.

4.2.2. Water oxygenation and in situ *Hg speciation*

The role of the artificial oxygenation of waters (100 m downstream the dam) was evaluated by determining Hg speciation on both sides of the aeration system. While HgT_{UNF} and HgT_D were similar (Fig. 5; Tail. *vs* Pas. stations), DGM concentrations dropped by

approximately 40 %. These measurements suggest a notable "evasion" of volatile mercury. Actually, during the Matoutou-5 campaign (March 2005), the total atmospheric gaseous mercury within 10 m above the aeration system peaked from the “background” levels (around 10 pmol m^3) up to 60 pmol m^3 (Muresan *et al.*, to be submitted). More unusual was the behavior of $MMHg_D$ which show a tendency toward significant concentrations increase in the seaward (Fig. 5). In order to confirm such a pattern, an exclusive sampling campaign took place in March 2005. Table 3 gathers the obtained $MMHg_D$ determinations performed on the same sampling day. The observed increase is statistically significant averaging 50%. Two complementary processes might account for this observation: (i) an intense biological reduction of sulfates initiated by the sudden oxygenation of the hypolimnetic waters and (ii) an oxidative dissolution of MMHg loaded AVS (acid volatile sulfides). Considering the first mechanism, notable amount of organic substratum (0.44 ± 0.07 mmol L^{-1} of TOC) combined to elevated Hg levels (13 ± 5 pmol L^{-1} of HgT_{UNF}) and sulfidic conditions (1.2 ± 0.8 µmol L^{-1} of ΣH_2S) depict the tailrace as a privileged zone for Hg methylation. Besides, according to Dumestre *et al*. (2001), sulfide-producing and sulfide-consuming bacteria are closely associated within the tailrace of the reservoir. Such a loop represents a small but extremely active proportion of the microbial assemblage. Considering the second mechanism, dam expelled waters mainly originated from AVS and $MMHg_P$ enriched layer of the hypolimnion (between 8 and 15 m). Partial dissolution of the discharged particulate fraction would therefore provide high $MMHg_D$ levels into the Sinnamary Estuary. The rapid enrichment of the dissolved fraction was all the more flagrant when considering the log partition coefficient [$\log K_d$(MMHg); $K_d = MMHg_P/MMHg_D$], which stepped from 5.4 ± 0.2 to 4.7 ± 0.3 in less than 300 m.

4.2.3. Water oxygenation and in vitro *Hg partition*

Laboratory experiments (December 2004) with tailrace water samples were designed in order to evaluate the dynamics of dissolved Hg and MMHg under brutal oxygenation. To reach this goal, we measured at different periods of time the concentrations of FeT_{UNF} and FeT_D then HgT_{UNF}, HgT_D, HgR_D and $MMHg_D$ in two separate samples (Fig. 4). Both samples, of (i) unfiltered and (ii) filtered to 0.45 µm (under nitrogen atmosphere) tailrace water, were exposed to the atmosphere in dark conditions and under moderate agitation (100 rpm). During the "unfiltered experiment", concentrations of all dissolved species (FeT_D, HgT_D, HgR_D, $MMHg_D$) tended to decrease with time. The maximum concentration decrease took place within one hour of oxygen exposition and reached 7 µmol L^{-1} h^{-1} for FeT_D, 4.1, 0.2 and 1.6 pmol L^{-1} h^{-1} for HgT_D, HgR_D and $MMHg_D$ respectively. After 6 hours of oxygen exposure, *circa* 30 % of the initial FeT_D and HgT_D amount were scavenged from the dissolved fraction. For the same period, about 10 % of the initial HgR_D and $MMHg_D$ amount were scavenged. Excepting an isolated value (25 hours), total fractions of FeT_{UNF} and HgT_{UNF} remained steady to 38 ± 1 µmol L^{-1} and 16 ± 2 pmol L^{-1}. In the "filtered experiment", except $MMHg_D$, concentrations of dissolved species (FeT_D, HgT_D, HgR_D) showed a gradual decreasing trend. Comparing to the previous experiment, maximum decrease of dissolved Hg species occurred later: between 1 and 3 hours of water oxygenation. Corresponding kinetics were determinated to 6 µmol L^{-1} h^{-1} for FeT_D, 2.4, 0.2 and 1.1 pmol L^{-1} h^{-1} for HgT_D, HgR_D and $MMHg_D$ respectively. Despite a lower instantaneous value, integrated scavenging reached, after 3 hours of oxygen exposition, *circa* 50 % of the initial FeT_D and HgT_D amount and close to 20 % of that of HgR_D. More noticeable was the behavior of $MMHg_D$. Within first hour of oxygenation $MMHg_D$ concentration displayed a increase of 25 % (from 6.0 to 7.5 pmol L^{-1}) followed by a gradual decrease then stabilization (around 4.3 pmol L^{-1}). As a result, in three hours, only 10 % of the initial amount of $MMHg_D$ was scavenged. Finally, as for unfiltered

water, FeT_{UNF} and HgT_{UNF} were stable during the course of whole experiment (33 ± 3 µmol L^{-1} and 14 ± 1 pmol L^{-1}).

From the unfiltered water experiment, we concluded that endogenous formation of $MMHg_D$ and HgR_D would barely counterbalance the removal mechanism and/or that colloidal Hg (divalent Hg bounded to thiols, AVS, humic acids, etc.) may become readily available for scavenging processes on newly formed Fe oxyhydroxides particles. Considering the filtered water experiment, Fe and Hg monitoring pointed out an activation of the removal kinetic with the lessening of dissolved species concentrations. The newly formed Fe oxyhydroxides particles would thus contribute to catalyze the scavenging of dissolved Hg. Finally, brutal increase of $MMHg_D$ concentrations suggested partial mobilization of complexed MMHg. We hypothesized that the mobile MMHg fraction originated principally from the intense AVS dissolution due to rapid water oxygenation.

4.3. Mercury in the Upper Sinnamary Estuary (USE)

Summary statistics of Hg speciation and partitioning in the USE are given in table 2 and the geographical distributions shown on figure 5. The aim of this section is to describes, one after another, the HgT, DGM and MMHg geochemical transformations and transfers between phases due to the variable chemistry of the USE.

4.3.1. Inputs to the Estuary: the role of tributaries

Local tributaries to the Sinnamary Estuary displayed HgT_{UNF} concentrations varying from 5.0 to 19.5 pmol L^{-1} and averaging 13 ± 5 pmol L^{-1}. Except the high runoff episodes, dissolved (< 0.45 µm) mercury appeared to dominate the HgT_{UNF} partitioning (7 ± 2 pmol L^{-1} on average). Maximum of HgT_{UNF} concentrations (17 ± 4 pmol L^{-1}) were measured during the wet seasons (January-February and May-June 2004). At that time, *circa* 80 % of the HgT_{UNF}

(14 ± 5 pmol L^{-1} i.e., 800 ± 600 pmol g^{-1}) were composed by HgT_P. Despite HgT concentrations in tributaries and dam tailrace were fairly homogenous, a marked shift was apparent when considering the methylated species (Tab. 3). As a matter of fact, for Matoutou 1 to 5 campaigns, average $MMHg_D$ concentrations stepped from 0.8 ± 0.5 to 1.6 ± 0.7 pmol L^{-1} between those two regions. Besides, from the 2003-2004 flow monitoring at the Tail. and Com. stations, the USE water inputs *via* local tributaries were calculated to 50 ± 30 m^3 s^{-1}. Using the average Hg concentrations from the main creeks, we could roughly estimate the annual amounts of Hg transported by tributaries to the Sinnamary Estuary. Those orderly were 4 ± 3, 2 ± 1, 0.5 ± 0.2 and 0.03 ± 0.02 kg·y^{-1} for HgT_{UNF}, HgT_D, $MMHg_{UNF}$ and DGM. Such values respectively corresponded to 25, 20, 15 and 8 % of the associated Hg dam exportations.

4.3.2. Total mercury transport and distribution

HgT_{UNF} and HgT_D varied between 5.9-16.9 and 2.2-10.5 pmol L^{-1} respectively and averaged 11 ± 3 and 6 ± 2 pmol L^{-1} in that order (Fig. 5). Their longitudinal distribution mainly resulted from the local geochemical (redox, pH, OM, etc.) and geophysical (tidal wave, dilution *via* tributaries etc.) conditions. To illustrate, HgT presented a global pattern of diminution with proximity to the ocean both in unfiltered and dissolved phases. Indeed, between the Tail. (dam end-member) and Sin. (saline end-member) stations, HgT_D stepped from 9 ± 2 to 5 ± 2 (i.e. 80 to 60 % of HgT_{UNF}) pmol L^{-1}. Local increases of the particulate contribution generally collocated with tributaries junctions and were clearly identifiable by sight in the course of the wet seasons (Creek Kerenrock, Creek Venus and Creek Saulnier). As a matter of fact, regarding seasonal variability, concentrations of HgT_D were highest in long dry season (9 ± 1 pmol L^{-1}) declined in short wet and dry (orderly 5 ± 2 and 7 ± 1 pmol L^{-1}) seasons and reached lowest values in long wet season (3 ± 1 pmol L^{-1}). An inverted tendency was observed for the particulate bounded Hg. In conclusion, HgT_D concentrations

measured in dry seasons (8 ± 1 pmol L^{-1}) mainly reflect the average hypolimnion of the reservoir (about 8 ± 2 pmol L^{-1}, Section 4.2.1.). On the other hand, the wet season diminution (to 4 ± 2 pmol L^{-1}) would, at least partially, have resulted from the dilution of dam outflow by downstream tributaries (5 ± 2 pmol L^{-1}) or lateral runoff waters.

Apart from geophysical phenomena, ongoing geochemical process greatly affected Hg speciation and partition. High percentages of dissolved humic mercury (close to 50 % of the HgT_D, the Hg_{DH} was calculated as $Hg_{DH} = HgT_D – HgR_D – MMHg_D$) suggested that a notable proportion of HgT_D in the USE was colloidal. Depending on the geochemical background, colloids consist mainly of clay, oxyhydroxides, humic ligands etc. (Beckett and Le, 1990). Related to the particulate phase, colloids might easily have been transferred into water samples during filtration. Indeed, colloids depict a transitional domain (from 10^{-3} to 1 µm) between which was considered dissolved (<0.45 µm) and particulate (>0.45 µm). In the USE, intense degradation of OM suggested that organic ligands (such as thiols) played a major role in complexation of HgT_D (Fig. 6). This hypothesis was supported by a positive correlation between HgT_D and DOC ($r^2 = 0.78$) and a negative one with POC ($r^2 = 0.62$). Besides, the existence of ΣH_2S at micromolar level (0.7 ± 0.5 µmol L^{-1}) pointed out an additional participation of sulfidic ligands. The “U” shape of the HgT_D *vs* ΣH_2S relationship indicates that for an intermediate sulfide concentration the HgT_D is minimal; this suggested an optimum ΣH_2S concentration for HgT_D scavenging (around 1 µmol L^{-1}). Lower ΣH_2S levels (< 1 µmol L^{-1}) would induce a predominance of AVS oxidative dissolution processes and thus enhance Hg transfer to the dissolved phase. Conversely, more elevated ΣH_2S levels (> 1 µmol L^{-1}) would enhance Hg mobilization through thermodynamic equilibrium with cinnabar ($HgS_{(s)}$): possible formation of $HgS_{(aq)}$ colloids (Morel *et al*., 1998).

Average concentrations of HgT_{UNF} and HgT_D in the USE were respectively 15 and 30 % lower than average concentrations at the Tail. station (Tab. 2). As shown previously in

Section 4.2.3., broad diminution of HgT_D concentrations may have resulted from a dissolved phase removal mechanism (adsorption and/or (co)precipitation). Indeed, the significantly positive correlation between FeT_D and ΣH_2S ($r^2 = 0.82$) suggests a dynamic equilibrium between dissolved species and iron sulfides (monosulfide/AVS and/or pyrite). Their elevated specific surface (several $m^2\ g^{-1}$) coupled to the high affinity of Hg for sulfide ligands depicted AVS as potential trapping agents. Furthermore, the parallel evolution of ΣH_2S and HgT_P concentrations ($r^2 = 0.32$) enforced the hypothesis of a turn-over between HgT_D scavenging due to AVS formation and Hg mobilization due to AVS dissolution. Beyond AVS, the main pathway for HgT_D scavenging was related to Fe oxyhydroxides. Most abundant metal in solution, FeT_D stepped from 18 ± 5 to 4 ± 2 µmol L^{-1} between Tail. and Sin. stations. 30 % of the observed decrease originated from the artificial aeration of waters *circa* 100 m downstream the dam (Fig.2). Thus, applying the model described in Section 2.3. to HgT_D *vs* FeT_D relationship ($r^2 = 0.69$), we estimated that nearly 400 nmol of HgT_D are scavenged per mol of FeT_D consumed (Fig. 6). As *circa* 7000 tons of FeT_D were annually dam exported, oxidation of Fe^{II} to Fe oxyhydroxides would virtually remove 10 kg y^{-1} of Hg from the dissolved phase. This limit value is lower than annual dam exportations of HgT_{UNF} (16 kg y^{-1}) but exceeded those of HgT_D (9 kg y^{-1}).

4.3.3. Mercury degassing from water: production and consumption

One could expect the progressive degassing of DGM in the USE. Actually, between the Petit-Saut dam and Sin. station (70 km downstream), DGM stepped from 0.37 ± 0.10 to 0.14 ± 0.10 pmol L^{-1}. This corresponded to an average diminution of above 60 % (Fig. 5). In a first step, let us consider the apparent amount of DGM transferred to the atmosphere. This was determined by multiplying the annual amount of discharged water (about $6\ 10^9\ m^3$) and the entire decrease of DGM concentrations (close to 0.2 pmol L^{-1}). The calculation supposed that the whole DGM decrease issued only from degassing processes and that endogenous

DGM production was negligible. Thus, the USE virtually transferred 0.2 kg y^{-1} of elemental Hg to the atmosphere which represented less than 2 % of the dam exported amount of HgT_{UNF} (16 kg y^{-1}). About 50 % (i.e. 0.1 kg y^{-1}) of the transferable DGM degassed when passing through the artificial aeration system. As a comparison, the evasional Hg^0 flow for the whole Petit-Saut reservoir and "Saut Lucifer" station (a portion of successive waterfalls located in the upstream of the reservoir) attained 4 and 0.3 kg y^{-1} (phase I of the "Mercure en Guyane" project, 2001).

In a second step, geochemical and geophysical mechanisms ought to be taken into account. DGM production is governed by the availability of Hg species towards reduction processes (e.g., Allard and Arsenie, 1991; Vandal *et al*., 1991; Xiao *et al*., 1995). However, downstream the dam, reduced penetrability of light (< 1 m, Richard pers. com.) tends to limit the effect of mercury photoreduction to the benefits of abiotic processes: Hg^0 production by Fe^{II} to $Fe(OH)_3$ oxidation and/or in presence of hematite particles (Peretyazhko, 2002). In the hypolimnion of the Petit-Saut reservoir, production of DGM up to 2 pmol L^{-1} h^{-1} within 5 mg L^{-1} hematite solution has already been demonstrated (Peretyazhko *et al*., 2005). Within the USE, between Tail. and Ven. stations (Fig. 2 and 5), DGM production by Fe^{II} to $Fe(OH)_3$ oxidation was noticeable by the analogous evolution of DGM and FeT_D concentrations (r^2 = 0.73). Following a similar approach to the model described in Section 2.3., we estimated that *circa* 15 nmol of DGM are in equilibrium with every mol of FeT_D (Fig. 6). As roughly 7000 tons of FeT_D were annually discharged downstream the dam, *circa* 0.3 kg y^{-1} of DGM were abiotically formed. As a result, Fe driven production of DGM within the first 30 km of the USE was almost equivalent to dam exportations (0.4 ± 0.2 kg·y^{-1}, Section 4.2.1). Finally, considering the degassed amount of 0.2 kg y^{-1}, approximately 70 % of the abiotically formed DGM appeared to be degassed.

Along with endogenous formation of DGM, oxidation processes should be equally considered. There now exists a multitude of evidences that OM plays a key role in the photochemical reduction of ionic mercury to elemental mercury (Alberts *et al*., 1974; Allard and Arsenie, 1991; Nriagu, 1994) and its subsequent reoxidation to ionic mercury. (Amyot *et al*., 1997; Ravichadran, 2004; O'Driscoll *et al*., 2005). In a general way, in presence of oxygen, the OM catalyzed Hg^0 reoxidation can be formulated as:

$$2CH_2O + Hg^0 + 2.5O_2 \rightarrow Hg(OH)_2 + 2CO_2 + H_2O$$

The inverse relationship between DGM and POC ($r^2 = 78$) supported this observation (Fig.6). Applying the model described in Section 2.3. to DGM *vs* POC relationship, we estimated that nearly 5 nmol of DGM were consumed per mol of POC in solution. Reported to the $4\ 10^9$ g y^{-1} POC discharged in the downstream of the reservoir, the amount of oxidized DGM in the USE was estimated to 0.3 kg y^{-1}. DGM oxidation due endogenous mineralization of OM, thus amazingly compensate the Fe driven formation of endogenous DGM (both around 0.3 kg y^{-1}). Yet, spatial distribution of both mechanisms appeared to vary along the course of water to the Atlantic Ocean. Within the first 30 km downstream the Petit-Saut dam, where Fe driven formation of endogenous DGM prevailed, approximately 40 % of the abiotically formed DGM appeared to be oxidized. Consequently, the apparent flux of DGM to the atmosphere resulted from both dam exportations and a net balance between *in situ* reduction and oxidation processes.

In dark conditions, DGM production in the epilimnion of reservoir was low in filtered water samples whereas significant reduction occurred in unfiltered waters (Beucher *et al*., 2002). Due to the low redox (290 mV) and elevated conductivity (34 µS cm^{-1}) the role played by particles was more problematic within the USE. For instance, in the USE, DGM concentrations and log partition coefficient of HgT [$\log K_d$(HgT); $K_d = HgT_P/HgT_D$] tended to

vary in an opposite way (r^2 = 0.45). In other words, the increase of DGM concentrations accompanied those of HgT_D (r^2 = 0.63) to the detriment of HgT_P (r^2 = 0.23). As most of the logK_d(HgT) variability originated from HgT_D contribution ($[DGM]_{pmol\ L\text{-}1}$ = 0.015 $[HgT_D]_{pmol\ L\text{-}1}$), the dissolved phase (< 0.45 µm) might thus contain the ultimate substratum for endogenous production of DGM. Investigating the HgT_D speciation, we observed a marked inverse relationship between DGM and $MMHg_D$ (r^2 = 0.45; $[DGM]_{pmol\ l\text{-}1}$ = -0.1 $[MMHg_D]_{pmol\ L\text{-}1}$ + 0.35) or $MMHg_D/HgT_D$ (%) {r^2 = 0.61; $[DGM]_{pmol\ L\text{-}1}$ = 1.1 $[MMHg_D/HgT_D\ (\%)]^{-0.6}$}. Such observations suggested either (i) a bacterial resistance to mercury through potential demethylation by the *mer* operon or (ii) that $MMHg_D$ production limits Hg availability with respect to reduction (Fig. 7). More unusual was the absence of significant correlation with HgR_{UNF} (commonly considered as a precursor of DGM). The reduced penetrability of light combined to high OM concentrations (0.47 mmol L^{-1} of TOC) and a substantial pool of reduced ligands (0.7 µmol L^{-1} of ΣH_2S) may explain the lack of relationship. Hence, in this particular environment, the dissolved humic mercury (Hg_{DH}, calculated as $Hg_{DH} = HgT_D - HgR_D - MMHg_D$) may define the active fraction involved in the DGM formation process.

4.3.4. The methylmercury redox cycle: roles of O_2, ΣH_2S, pH and Fe.

The concentration of $MMHg_{UNF}$ in the USE averaged 3.7 ± 1.0 pmol L^{-1} with 2.0 ± 0.9 pmol L^{-1} as dissolved and 1.8 ± 1.2 (i.e. 220 ± 130 pmol g^{-1}) pmol L^{-1} as particulate (Tab. 2). Similar concentrations of $MMHg_{UNF}$ (2.5 ± 1.4 pmol L^{-1}) and $MMHg_D$ (0.6 ± 0.4 pmol L^{-1}) were measured by Canavan *et al*. (2000) downstream of the Elephant Butte reservoir, New Mexico (USA). However, unlike the Elephant Butte artificial lake, permanent stratification of the Petit-Saut reservoir contributes to maintain the USE elevated MMHg concentrations for the entire year duration. In the dissolved phase, the methylated percentage [$MMHg_D/HgT_D$ (%)] of the USE averaged 40 ± 20 % and occasionally peaked at more than 90 % in wet seasons. In the particulate phase, the methylated percentage [$MMHg_P/HgT_P$ (%)] averaged 40

± 20 % and reached up to 97 % in dry seasons (Fig. 5). Regarding logK_d(MMHg), calculated values, averaging 5.0 ± 0.4, were in the upper range of data available from the literature (e.g., Cai *et al*., 1999; Choe *et al*., 2001). Similar log partition coefficients were determinated within the Trinity River (USA) comparing colloidal (1 kDa-0.45 µm) and truly dissolved (< 1 kDa) fractions (Choe *et al*., 2001). In the USE, $MMHg_D$ and POC displayed a significant positive relationship with seasons (r^2 = 0.61; $[MMHg_D]_{pmol\ L\text{-}1}$ = 180 $[POC]_{mmol\ L\text{-}1}$ − 8.8). Parallel increase was also reported with organic content of particles (r^2 = 0.44; $[MMHg_D]_{pmol\ L\text{-}1}$ = 0.12 $[POC]_{mmol\ g\text{-}1}$ − 0.8, Fig. 6). Such correlations suggested that a wide proportion of the $MMHg_D$ present in the Sinnamary Estuary was composed by organic colloids.

Figure 5 illustrates the longitudinal profiles of $MMHg_D$ concentrations along the USE. Significant variations were observed with seasons (from 1.1 ± 0.5 to 3.2 ± 1.1 pmol L^{-1}). Concentrations (4.47 pmol L^{-1}) and longitudinal variability (2.76 pmol L^{-1}) were maximal in the course of the long dry season. Recorded profiles accounted for the parameters potentially affecting the local mobility of monomethylmercury and/or methylation pathways. Firstly, one has to consider the local influence of creek-tributaries. With 1.3 ± 0.6 pmol L^{-1} $MMHg_{UNF}$ of which 0.8 ± 0.5 and 0.4 ± 0.3 (i.e. 80 ± 60 pmol g^{-1}) pmol L^{-1} were respectively $MMHg_D$ and $MMHg_P$, creeks globally contributed to the dilution of the USE. This phenomenon was visible during the wet seasons in the vicinity of Creek Kerenrock, Creek Venus and Creek Saulnier (Fig. 5). Secondly, since the elevated $MMHg_{UNF}$ concentrations corresponded to the dam expelled waters, the USE partitioning and/or methylating mechanisms should be, at least partially, related to the discharged volume of reduced elements (e.g., FeT_D, ΣH_2S, altered OM, CH_4 etc.). From the 2003/04 water monitoring at the Tail. station, a remarkable inverse relationship was observed between $MMHg_{UNF}$ and the redox (r^2 = 0.56; $[MMHg_{UNF}]_{pmol\ L\text{-}1}$ = -0.03 Eh_{mV} + 8.3, Fig. 3). Besides, according to Section 4.1.4., lowest Eh values correspond to highest dam outflows. Hence, reductive conditions not only promote the endogenous Hg

methylation but also accompany the increase of $MMHg_{UNF}$ dam exportations. Corollarly, in wet seasons, we assist to the confluence of two opposite processes: (i) elevated $MMHg_{UNF}$ exportations *via* the dam tailrace (up to 0.15 mol d^{-1}) and (ii) localized dilution of concentrations by creeks inflows (above 80 m^3 s^{-1}).

Among the whole set of data, the USE distribution of $MMHgB_D$ was mostly influenced by dissolved oxygen and sulfides (Fig. 7). Substantial ΣH_2S concentrations (0.7 ± 0.5 µmol L^{-1}) and relative balance between O_2 and $MMHg_D$ levels ($r^2 = 0.47$; $[MMHg_D]_{pmol\ L\text{-}1} = 15\ [O_2]_{mmol\ L\text{-}1}$) support the *in situ* Hg methylation hypothesis. Accordingly, sulfates production (i.e. ΣH_2S oxidation) due to the brutal aeration of hypolimnetic waters enhances the SRB methylating activity. In consequences, the role played by oxygen in the USE Hg methylation is dual. On the one hand, water oxygenation tends to favor the ΣH_2S oxidation to SO_4 (SRB substratum). To illustrate, between Tail. and Ven. stations, SO_4 increased from 6 to 16 µmol L^{-1} varying in mirror with ΣH_2S ($r^2 = 0.55$; $[SO_4]_{\mu mol\ L\text{-}1} = -3\ [\Sigma H_2S]_{\mu mol\ L\text{-}1} + 14$). On the other hand, an excess of oxygenation tends to inhibit the SRB activity to the benefits of oxygen metabolizing bacteria (e.g., Fe^{II}, ΣH_2S CH_4, oxidizers; Dumestre *et al*., 2001). For instance, percentages of dissolved oxygen [O_2 (%) up to saturation] and those of monomethylmercury [$MMHg_D/HgT_D$ (%) defines a proxy of the local production of $MMHg_D$] displayed an inverse evolution [$r^2 = 0.37$; $MMHg_D/HgT_D$ (%) = -1.2 O_2 (%) + 100]. Low oxygen levels thus depicted sites of moderate $MMHg_D$ concentrations but intense endogenous Hg methylation (such as Deg. station).

The hypothesis of an *in situ* methylation primarily emerged from: (i) the brutal increasing of $MMHg_{UNF}$ and $MMHg_D$ concentrations between Tail. and Pas. stations (Fig. 5) and (ii) the parallel study of ΣH_2S concentrations and $MMHg_D/HgT_D$ (%) in the USE. The bulge shape of the $MMHg_D/HgT_D$ (%) *vs* ΣH_2S relationship suggested an optimum sulfide concentration for mercury methylation (Fig. 7). Sites of low and intermediate ΣH_2S

concentrations (< 1 µmol L^{-1}) exhibited analogous variations of both parameters {r^2 = 0.70; $MMHg_D/HgT_D$ (%) = 100 $[\Sigma H_2S]_{\mu mol\ L^{-1}}$ + 10}. This is consistent with the hypothesis of neutral Hg-S complexes controlling the bioavailability of inorganic mercury towards SRB (Benoit *et al*., 2001, 2003). On the contrary, more sulfidic environments (> 1 µmol L^{-1}) exhibited inverse variations between $MMHg_D/HgT_D$ (%) and ΣH_2S concentrations {r^2 = 0.76; $MMHg_D/HgT_D$ (%) = -50 $[\Sigma H_2S]_{\mu mol\ L^{-1}}$ + 120}. This would account for a lessening in Hg bioavailability due to formation of ionic Hg-S complexes [$HgS(SH)^-$, HgS_2^{2-} etc.] and/or precipitation of inorganic Hg as cinnabar. In conclusion, balance between water oxygenation which controls SRB activity through production of sulfates and ΣH_2S level that governs Hg bioavailability played a large role in the local production of MMHg.

Besides oxygen and sulfides, various physical parameters, such as temperature and pH, modulated the endogenous mechanisms of Hg methylation and demethylation. Lowering pH contributed to decrease the partition coefficient of HgT [r^2 = 0.33; $\log K_d(HgT)$ = 0.5 pH + 2.0] and increase that of MMHg [r^2 = 0.46; $\log K_d(MMHg)$ = -0.9 pH + 10.0]. In other words, water acidification would firstly result in HgT_P mobilization towards the dissolved phase. Secondly, according to Benoit *et al*. (2003) formulation:

$$RSHg^+ + H_2O + HS^- = HgS^0 + RSH + H^+$$

increasing $[H^+]$ leads to decreasing $[HS^-]$, and as a result, HgS^0 (the hypothetical substratum of methylation) will decrease relative to $RSHg^+$ *i.e.*, methylation rate and $MMHg_D$ should at length decrease. This theoretical consideration was confirmed by the positive correlation between pH and $MMHg_D/HgT_D$ (%) [r^2 = 0.42; $MMHg_D/HgT_D$ (%) = 60 pH – 300]. Slightly acidic waters, as in the USE, should thus contribute to maintain $MMHg_D$ at a relatively high level. The effect of temperature was mainly apparent at a seasonal time scale. Increasing of water temperature induced an overall elevation of $MMHg_D$ concentrations (r^2 = 0.54; $[MMHg_D]_{pmol\ L^{-1}}$ = 1.5 $T_{°C}$ – 40). Direct link between the water temperature and the Hg

methylating kinetic was not yet established. As evoked in Section 4.1.7., the average water temperature, dam outflows and ΣH_2S concentration were markedly associated within the USE. Improved efficiency of the aeration system (> 1.5 mmol L^{-1} of O_2) due to the reduced flow of water leaving the dam (around 80 m^3 s^{-1}) accompanied the USE low (0.2 ± 0.2 µmol L^{-1}) and intermediary (0.4 ± 0.2 µmol L^{-1}) ΣH_2S levels measured in short and long dry seasons respectively. Hence, the resulting enhancement of Hg bioavailability towards SRB (moderate ΣH_2S levels and endogenous production of sulfate) would actually be the true actor of the observed $MMHg_D$ increase.

As shown previously, MMHg appeared to be strongly complexed by OM, Fe oxyhydroxides or AVS. According to Benoit *et al*. (2003), the complexation of MMHg to OM or inorganic sulfide phases are comparable since both involve interactions with thiols or other reduced S species. Besides, the same authors proposed that a lowering of pH would favor association of methylmercury with solid phase:

$$RS\text{-}H + CH_3Hg(OH) = RS\text{-}HgCH_3 + H_2O$$

This hypothesis was verified with our data: diminution of pH contributed to a notable increase of $MMHg_P$ whether expressed as water concentration (r^2 = 0.61) or particle content (r^2 = 0.31). Furthermore, parallel precipitation of humic and/or fulvic acids may accentuate metals and especially MMHg removal from the dissolved phase (Cossa *et al*., 1988; Stordal *et al*., 1996; Coquery *et al*., 1997). Considering methylated percentages, an inverse relationship (r^2 = 0.60) was observed between methylated fractions in the particulate [$MMHg_P/HgT_P$ (%)] and in the dissolved phases [$MMHg_D/HgT_D$ (%)] (Fig. 7). From the previous relationship and the one to one average contributions of dissolved and particulate phases to $MMHg_{UNF}$, we concluded to the marked mobility of methylated species along the USE. Acid-base mechanisms and ΣH_2S levels appeared to have the most significant impact on MMHg partitioning. Maximum of $MMHg_P/HgT_P$ (%) usually corresponded to most acidic and

oxidized waters (such as Ker. or Ven. stations) while slightly acidic and sulfidic environments displayed highest $MMHg_D/HgT_D$ (%) levels (like Pas. or Deg. stations). Overall, changes in MMHg binding resulted in nearly 5 % of $MMHg_P/HgT_P$ (%) elevation per 0.1 pH unit of water acidification.

Scavenging of $MMHg_D$ and $MMHg_P$ mobilization constituted dynamic processes that simultaneously occur along the Sinnamary Estuary. To illustrate, we should consider the relation between $MMHg_D$ and Fe (Fig. 6). Below 10 µmol L^{-1}, longitudinal distributions of FeT_D and $MMHg_D$ covaried positively ($r^2 = 0.65$; $[MMHg_D]_{pmol\ L^{-1}} = 0.24\ [FeT_D]_{\mu mol\ L^{-1}} + 0.73$). Conversely, above that limit, concentrations of both species varied in mirror ($r^2 = 0.54$; $[MMHg_D]_{pmol\ L^{-1}} = -0.12\ [FeT_D]_{\mu mol\ L^{-1}} + 4.2$). In addition, as for ΣH_2S, an inverse pattern was observed when plotting the FeT_D *vs* $MMHg_P$ relationship. Thus, $MMHg_P$ mobilization (probably due to AVS dissolution) dominated in the vicinity of the Petit-Saut dam while $MMHg_D$ scavenging (possible precipitation of Fe oxyhydroxides) prevailed further along the way to the Atlantic Ocean. Applying the model described in Section 2.3. to the $MMHg_D$ and $MMHg_P$ *vs* FeT_D relationships, we can easily estimate that (i) about 130 nmol of $MMHg_P$ are mobilized per mol of FeT_D discharged and (ii) nearly 250 nmol of $MMHg_D$ are scavenged per mol of FeT_D consumed. Reported to the 7000 tons of FeT_D annually exported by the reservoir, *circa* 3.0 kg y^{-1} of $MMHg_P$ were transferred to the dissolved phase while close to 4.9 kg y^{-1} were subsequently recycled as Fe oxyhydroxides. If we admit that the excess of scavenging (close to 1.9 kg) originated mainly from *in situ* methylation processes, it results that at least 30-50 % of the downstream $MMHg_{UNF}$ amount (around 5.5 kg) was endogenically produced.

4.4. Mercury in the Lower Sinnamary Estuary (LES)

The current section describes the fate of Hg in the LES. A distinction is done between the high turbidity zone (HTZ) entrance (S < 5 ‰), the Amazon plume (5 < S < 21 ‰) and the

IS station (S > 21 ‰). This sequence orderly corresponds to the reactive, mixing and dilution regions of the saline Sinnamary Estuary.

4.4.1. The reactive region of the HTZ

Entering the HTZ (up to 5 ‰ of salinity), HgT_{UNF} concentrations rapidly stepped from 10 ± 3 to 19 ± 3 pmol L^{-1} (Fig. 8 and 9). Observed increase, especially in particulate phase (from 5 ± 3 to 12 ± 2 pmol L^{-1}), accompanied that of SPM (from 9 ± 3 to 70 ± 30 mg L^{-1}). Most remarkable was the opposite behavior between the HgT_P concentration of water (pmol L^{-1}) and that of particles (pmol g^{-1}). As water concentration increased, the Hg content of particles tended to decline (from 760 ± 90 to 350 ± 200 pmol g^{-1}). The impoverishment of the average Hg content of particles was also apparent *via* higher $\log K_d$(HgT) values in the USE than in the first kilometers of the LES (respectively 5.0 ± 0.3 and 4.6 ± 0.2). Actually, it has been shown that the Amazon River constitutes a huge source of relatively uncontaminated particles (Roulet *et al*., 1998a, b; Bourgoin *et al.*, 2003) which plume spreads North-West over 2000 to 3000 km of South American continent coasts (Steven and Brooks, 1972). The local distribution of HgT_P thus illustrates both changes in physicochemical conditions and mixing between the USE and Amazon plume waters (Fig. 8 and 9). If we admit that the local Hg content of particles forming the Amazon plume is fairly recorded by coastal sediments, its HgT_P concentrations would average 250 ± 50 pmol g^{-1} (Marchand *et al*., 2005). Comparing to autochthonous HgT_P (350 ± 200 pmol g^{-1}) and using mass balance calculation, we estimated that the amount of SPM reaching the HTZ through the USE was 5 to 7 times lower than *via* the Amazon plume (50 10^9 *vs* 300 10^9 g y^{-1}).

Regarding DGM, the HTZ entrance had among lowest measured concentrations (0.08 ± 0.06 pmol L^{-1} i.e. 20 % the Tail. station levels) (Fig. 9). As discussed previously, low DGM levels primarily reflect a progressive degassing along the Sinnamary Estuary. Yet, in order to explain such a decrease, *in situ* oxidation and subsequent scavenging of Hg^0 ought to be

equally considered. Indeed, the weak penetrability of light (15 cm of Secchi) depicted the HTZ entrance as an unfavorable milieu for photochemical and biological production of DGM. Furthermore, notable FeT_D and ΣH_2S concentrations (16 ± 4 and 0.2 ± 0.3 µmol L^{-1} in this order) suggested a rapid turnover of redox sensitive elements. The surface production of organic free radicals through the photolysis of Fe^{III}–organic acid (DOC) complexes, might thus have favored the iron driven oxidation processes (Zhang and Lindberg, 2001):

$$Fe^{III}\text{-}\{DOC\} + h\nu \rightarrow Fe^{II} + \{DOC\}^*$$

$$\{DOC\}^* + Hg^0 \rightarrow Hg^{II}\text{-}\{DOC\}$$

These authors hypothesized that in the dark oxidation reaction organic free radicals ({DOC}*) cause the formation of hydrogen peroxide from oxygen, which in turn forms hydroxyl free radical ($OH^{\bullet}$) capable of oxidizing Hg^0 to Hg^{II}. The existence of a Hg^0 oxidation mechanism relative to the Fe^{III} / Fe^{II} reduction process was enforced by the local inverse distributions of DGM and FeT_D ($r^2 = 0.35$). Applying the model described in Section 2.3., we estimated to 10 nmol the amount of DGM oxidized per mol of FeT_D produced. Since FeT_D concentrations increased by 8 µmol L^{-1} between Sin. station and HTZ entrance (Fig. 2), DGM oxidation was calculated to 0.08 ± 0.07 pmol L^{-1}. Hence, a substantial fraction of the DGM reaching the HTZ (close to 0.2 ± 0.1 kg y^{-1}) might undergo local oxidation processes and subsequent complexation with SPM and/or OM (Stordal *et al*., 1996; Laurier *et al*., 2002).

$MMHg_{UNF}$ concentrations at the HTZ entrance averaged 4 ± 2 pmol L^{-1} of which *circa* 80 % were $MMHg_P$ (Tab. 2). As for HgT_P, $MMHg_P$ concentrations were mostly driven by the SPM load. Reaching the HTZ (from 9 ± 3 up to 70 ± 30 mg L^{-1} of SPM), the particulate fraction of $MMHg_{UNF}$ increased (from 1.7 ± 1.0 to 3 ± 2 pmol L^{-1}) while the $MMHg_P$ concentrations decreased (from 180 ± 100 to 70 ± 40 pmol g^{-1}). From the USE (50 10^9 g y^{-1}) *vs* LES (300 10^9 g y^{-1}) SPM transportation to the HTZ entrance, the $MMHg_P$ content of

particles forming the Amazon plume was calculated to about 30 pmol g^{-1}. Using mass balance calculations, the amounts of HgT_P and $MMHg_P$ attaining the HTZ entrance through the LES (10 and 2 kg y^{-1} respectively) were comparable to those *via* the USE (7 and 2 kg y^{-1} respectively). Besides, beyond purely transportation phenomena, biogeochemical mechanisms such as (i) poral water diffusion, (ii) partitioning or (iii) endogenous Hg methylation were investigated.

(i) This source seems negligible. We studied mercury speciation in the interstitial waters of the LES during Matoutou 3 campaign (May-June 2004) using the Rhizon sampling technique (Seeberg *et al.*, 2005). Applying Fick's first law of diffusion between poral uppermost (*i.e.*, 20 mm) and overlaying waters, diffusive fluxes of HgT_D and $MMHg_D$ were estimated to 34 and 3.4 pmol m^2 d^{-1}. Those were calculated with an estimated porosity of 0.9 and respective diffusion coefficients of 2 10^{-6} and 2 10^{-5} cm^2 s^{-1} (as Hg and MMHg complexed by OM). Reported to the surface of sediments (close to 7.5 10^5 m^2) and water residence period (around 3 hours), poral water diffusion represented less than 0.3 ‰ of the HgT_D and $MMHg_D$ flowing through the HTZ entrance.

(ii) Dilution of the Sinnamary waters by seawaters (from 30 to 150 µS cm^{-1} of conductivity) led to the sharp decrease of $MMHg_D$ concentrations (from 2.0 ± 0.8 to 0.7 ± 0.4 pmol L^{-1}) (Fig. 8 and 9). Yet, trapping on particulate phase may contribute as well to the observed $MMHg_D$ diminution. Beyond 10 µmol L^{-1}, FeT_D was shown to covary positively with $MMHg_P$ and negatively with $MMHg_D$ (Fig. 6). This trend was confirmed by an overall positive correlation between $\log K_d$(MMHg) and FeT_D {r^2 = 0.80; $\log K_d$(MMHg) = 0.04 $[FeT_D]_{\mu mol\ L^{-1}}$ + 4.4}. Consequently, the high FeT_D concentrations of the HTZ entrance (16 ± 4 µmol L^{-1}) tended to favor the progressive enrichment of the particulate phase with respect to the dissolved. The maximum of $MMHg_P$ (close to 10 pmol g^{-1}), observed in the surface

sediments during Matoutou 3 (May-June 2004), would ultimately reflect the depositional flux of the MMHg enriched particles.

(iii) As mixing and/or scavenging processes extensively dominated local distribution of $MMHg_D$, the role played by the HTZ entrance in endogenous methylation of Hg remains problematic. Yet, moderate O_2 concentrations (0.12 ± 0.02 mmol L^{-1}) in presence of ΣH_2S (0.2 ± 0.3 µmol L^{-1}) depicted the Sinnamary HTZ entrance as a privileged site for Hg methylation. For instance, from the $MMHg_D/HgT_D$ (%) to ΣH_2S relationships one could indirectly calculate the maximum amount of locally produced $MMHg_D$ to 1.2 kg y^{-1}. This value is in the same order of magnitude than global estimated MMHg production of USE (1.9 kg y^{-1}).

4.4.2. The Amazon plume mixing domain

In December 1999, the main body of the HTZ corresponded to the particulate plume of the Amazon (Fig. 9). The marine source of particles was apparent through a linear relationship between salinity (spanning from 0 to 20.7 ‰) and SPM concentrations (from 26 to 1326 mg L^{-1}). The pronounced increase of the SPM load contributed to enhance that of HgT_{UNF} concentrations, which stepped from 15 to 230 pmol L^{-1}. The observed HgT_{UNF} *vs* salinity relationship ($r^2 = 0.99$; $[HgT_{UNF}]_{pmol\ L^{-1}} = 11.7\ S_{‰} - 10.7$) mainly originated from the combination of a rapid increase of the particulate contribution (from 57 to 99 % of HgT_{UNF}) and a progressive decline of their HgT_P content (from 250 to 180 pmol g^{-1}). Recorded distributions suggested that direct mixing processes dominated upon sedimentation (i.e. resuspension) and/or redistribution of the originally particle bound mercury. To enforce this hypothesis, maximum of HgT_{UNF} corresponded to *circum* marine pH and conductivity (respectively 7.7 units and 48 mS cm^{-1}). Beyond this maximum (around 21 ‰ of salinity), the Amazon plume contribution in the local cycle of Hg tend to fade out. Indeed, as a signature of the progressive dilution with pristine oceanic waters, pH and salinity reached 8.1 and 24 ‰

circa 10 km offshore. Concurrently, the HgT_{UNF} concentrations stepped down from 230 to 31 pmol L^{-1} (from 99 to 92 % as HgT_P).

Dissolved Hg species in the Amazon plume exhibited broad variations with salinity. HgT_D averaged 4 ± 2 pmol L^{-1} of which 0.6 ± 0.4 and 0.3 ± 0.3 pmol L^{-1} were HgR_D and $MMHg_D$ respectively. While mixing processes primarily drove the distributions of the particulate phase, concentrations profiles of HgR_D and $MMHg_D$ significantly diverged from the saline dilution line: $r^2 = 0.82$; $[HgR_D]_{pmol\ L^{-1}} = 0.13 \exp[0.08\ S_{‰}]$ and $r^2 = 0.97$; $[MMHg_D]_{pmol\ L^{-1}} = 1.9\ S_{‰}^{-1.35}$ (Fig. 9). Since seasonal variability of USE for HgR_D and $MMHg_D$ (0.4-0.6 and 1.5-3.7 pmol L^{-1} orderly) was too small to generate the minimum HTZ concentrations, the apparent non-conservative behavior within the Amazon plume may either be due to removal or demethylation mechanisms. Removal processes have already been observed in various estuaries where riverine dissolved Hg concentrations contrast with those of the marine end-member. (Cossa *et al*., 1988; Guentzel *et al*., 1996; Laurier *et al*., 2002). Mechanisms usually used to explain those observations are related to partial adsorption of Hg onto particles, flocculation of organic colloids and scavenging on newly formed iron oxyhydroxides (e.g., Boyle *et al*., 1977; Honeyman and Santschi 1989; Wen *et al*., 1999). Regarding HgR_D, the Amazon plume behaved as a sink. High percentages of dissolved humic mercury (from 42 to 92 % of the HgT_D, the Hg_{DH} was calculated as $Hg_{DH} = HgT_D - HgR_D - MMHg_D$) support local complexation of marine HgR_D with organic ligands (such as thiols). Besides, according to Turner *et al*. (2001), the salting of Hg^{II}-organic contributes to enhance the mercury distribution coefficient. Thus, the most likely mechanism for the HgR removal is the formation of Hg^{II}-organic colloidal material and its subsequent flocculation due to the high suspended load environment. Considering the $MMHg_D$ non-conservative behavior, two distinct mechanisms are of interest. Firstly, looking at $MMHg_D$ as any conventional Hg^{II}-organic complex, an inverted process to that of HgR_D should be considered. Increasing water

salinity favors the potential complexation of Hg with inorganic ligands (such as Cl^-) to the detriment of Hg^{II}-organic complexes (Rolfhus and Fitzgerald, 2001; Lamborg *et al*., 2004). This assumption is locally supported by the rapid lessening of OM and Hg_{DH} percentages with distance to the estuarine mouth ($r^2 = 0.96$; $\%Hg_{DH} = 100 - 4.9 \exp[0.1\ S_{‰}]$). Secondly, apart from speciation changes, gradual exposure to light (due to SPM dilution) and establishment of a strict water oxygenation (up to 2.8 mmol L^{-1}) would substantially limit the net methylation rates (Mason and Fitzgerald, 1991; Sellers *et al*., 1996). Such pattern was visible through a marked decrease of the $MMHg_D/HgT_D$ (%) from 5 to less than 1 % between 10 and 20 ‰ of salinity.

4.4.3. The "îles du Salut" dilution area

Total mercury in surface waters from the offshore IS station (15 km remote from continental coast) averaged 3.0 ± 0.8 pmol L^{-1} (Tab. 2). HgT_{UNF} was mainly present as dissolved (2.0 ± 0.5 pmol L^{-1}) while particulate phase concentration was 1.0 ± 0.5 pmol L^{-1} (i.e. 170 ± 100 pmol g^{-1}). The reactive fraction [HgR_{UNF}/HgT_{UNF} (%)] accounted approximately for 50 % of HgT_{UNF} (i.e. 1.5 ± 0.6 pmol L^{-1}). Despite comparative HgR_{UNF} levels were determined by Mason *et al*. (1999b) for the South and equatorial Atlantic, DGM was substantially lower in the studied case (1.2 ± 0.8 *vs* 0.2 ± 0.1 pmol L^{-1}). Such a discrepancy presumably originates from the remnant complexation of mercury with local OM (0.31 ± 0.07 mmol L^{-1} of DOC) and/or iron driven oxidation mechanisms of Hg^0. Actually, in spite of the relative distance to the continent, water masses generally remained under the influence of the Amazon plume (SPM reached up to 40 mg L^{-1}). The local pool of ligands would contribute to maintain Hg under oxidized speciation and thus limit photochemical or biological reduction processes (Coquery *et al*., 1997). Once leaving the turbid area, progressive enhancement of primary production would ultimately account for the elevated

DGM concentrations usually observed in the marine extremity most of estuaries (Baeyens and Leermakers, 1998).

Methylmercury concentrations in seawater averaged 0.4 ± 0.2 pmol L^{-1}. Dissolved and particulate fractions respectively accounted for 0.09 ± 0.05 and 0.27 ± 0.15 (i.e. 12 ± 7 pmol g^{-1}) pmol L^{-1} (Fig. 9). Methylated percentages [$MMHg_{D-P}/HgT_{D-P}$ (%)] were 4 ± 2 and 7 ± 5 %, respectively. With distance from the continent, one could observe the progressive dilution of the Amazon plume by marine waters (from 21 to 24 ‰ of salinity) and supposedly the gradual deposition of particulate maters. As a matter of fact, the diminution of $MMHg_{UNF}$ levels (from 30 to 0.4 pmoL L^{-1}) accompanied that of SPM concentrations (from above 1 g L^{-1} to 20 mg L^{-1}) and redox elevation (from 330 to 400 mV). Besides, as a signature of the "particle concentration effect" hypothesis stating that colloidal mass and not preferential partitioning drives MMHg log partition coefficient, the logK_d(MMHg) stepped from 5.5 ± 0.2 to 4.3 ± 0.3 between the HTZ and marine milieu. Finally, notable $MMHg_D/HgT_D$ (%) values (> 5% of HgT_D) combined to reduce DGM percentages (< 10 % of HgT_D) suggested that methylated Hg production may casually occur in coastal regions of high OM content (> 0.1 mmol L^{-1} of DOC).

4.5. Global view of Hg cycle in the Sinnamary system

Common features to Hg geochemistry in the Sinnamary River, the Petit-Saut reservoir, the USE and LES are hereafter discussed. Figure 9 shows the average (Matoutou 1 to 5) Hg distributions along a longitudinal transect starting from the water inputs to the reservoir down to the offshore IS station.

4.5.1. Redox cycle of iron and sulfides in the Sinnamary watershed

Scavenging, transfers or Hg methylation are extensively affected by redox conditions (Compeau and Bartha, 1984; Mason *et al.*, 2001; DeLaune *et al.*, 2004). A cautious study of

major redox components is thus of critical interest in Hg cycling. Hence, average (Matoutou 1 to 5) sulfides, dissolved total iron and redox values were determinated along the Sinnamary watershed. Briefly, FeT_D and ΣH_2S were low (orderly 2.7 ± 0.8 and 0.2 ± 0.2 µmol L^{-1}) in the Sinnamary River (main water input to the Petit-Saut reservoir). Water samples of maximum concentrations originated from in the hypolimnion of the reservoir (33 ± 12 and 3.1 ± 0.5 µmol L^{-1} respectively, Fig. 5). As exposed in see sections 4.1.6. and 4.1.7., once reached the Sinnamary Estuary, FeT_D and ΣH_2S concentrations exhibited a global decrease with distance from the dam. In a general way, a positive correlation was observed between FeT_D and ΣH_2S (r^2 = 0.56; $[\Sigma H_2S]_{\mu mol\ L^{-1}}$= 0.07 $[FeT_D]_{\mu mol\ L^{-1}}$ + 0.22) while a common diminution was apparent with redox (r^2 = 0.79; $[FeT_D]_{\mu mol\ L^{-1}}$= -0.09 Eh_{mV} + 37 and r^2 = 0.70; $[\Sigma H_2S]_{\mu mol\ L^{-1}}$= -0.008 Eh_{mV} + 3.3). For instance, Eh was minimal in the reservoir (down to 100 mV) and gradually leveled up in the downstream of the dam (up to 400 mV in marine environment).

4.5.2. Redox cycle of mercury in the Sinnamary watershed

Except the LES, HgT_{UNF} distribution remained relatively homogenous (12 ± 2 pmol L^{-1}). It was fairly distributed between dissolved (7 ± 1 pmol L^{-1}) and particulate (5 ± 1 pmol L^{-1}) phases. Maxima of concentrations were usually located in the hypolimnion of the reservoir (Fig. 9). Significant covariation between HgT_{UNF} and HgT_P (r^2 = 70; $[HgT_P]_{pmol\ L^{-1}}$= 0.57 $[HgT_{UNF}]_{pmol\ L^{-1}}$ – 1.35) suggested that particulate load essentially drove mercury distribution into the system. Related to redox, the water HgT_P concentrations exhibited a regular increase from anoxic to suboxic conditions (between 100 and 300 mV) then subsequently declined in oxygenated waters (between 300 and 400 mV). Considering the Hg content of particles, a linear impoverishment with redox elevation was simultaneously recorded (r^2 = 0.72; $[HgT_P]_{pmol\ g^{-1}}$ = -3.8 Eh_{mV} + 1800). We hypothesize that under reducing conditions, in spite of elevated particles Hg content (> 800 pmol g^{-1}), low SPM amounts (< 5 mg L^{-1}) would limit Hg trapping on AVS and/or its precipitation as cinnabar. On the other hand, in oxidic

environments, progressive AVS dissolution would result in reduced SPM amount (< 5 mg L^{-1}) coupled to poor Hg content of particles (HgT_P < 400 pmol g^{-1}). Combination of moderate SPM amounts (above 7 mg L^{-1}) and particle bounded Hg (around 600 pmol g^{-1}) accounted for the observed maximum (around 300 mV of Eh).

The concentrations of DGM exhibited a global trend of diminution with proximity to the ocean (from 0.46 ± 0.27 to bellow 0.05 pmol L^{-1}). Local maxima corresponded to the Sinnamary River (principal water input to the reservoir), the reservoir dam nearest station and the offshore domain (Fig. 9). As a result, DGM was positively related to conductivity (r^2 = 0.91; $[DGM]_{pmol\ L\text{-}1} = 0.013\ Cond_{\mu S\ L\text{-}1} - 0.29$) and negatively to redox (r^2 = 0.78; $[DGM]_{pmol\ L\text{-}1} = -0.001\ Eh_{mV} + 0.51$). Yet, direct geochemical link to both parameters cannot be assessed since they reflect the DGM degassing phenomenon. To the opposite, photochemically driven processes, were apparent through positive evolution between DGM levels and “Secchi depth” (r^2 = 0.63) jointed to negative one with turbidity of water (r^2 = 0.55). This supports previous observations showing relationships between primary production and DGM concentrations in marine and lacustrine waters (Kim and Fitzgerald, 1986; Vandal *et al*., 1991). Regarding Hg speciation, DGM appeared to vary in parallel with HgT_D (r^2 = 0.80; $[DGM]_{pmol\ L\text{-}1} = 0.04\ [HgT_D]_{pmol\ L\text{-}1} + 0.06$) but in mirror with $MMHg_D$ (r^2 = 0.64; $[DGM]_{pmol\ L\text{-}1} = -0.05\ [MMHg_D]_{pmol\ L\text{-}1} + 0.38$). Low DGM levels thus depicted sites of highest $MMHg_D$ concentrations (manly the HTZ and the USE). Since DGM is ultimately formed during the MMHg degradation pathways, the USE not only exhibited sustained methylation mechanisms but may also define an unfavorable milieu for MMHg demethylation.

Except the Sinnamary River and the IS station, out of the direct influence of the reservoir, $MMHg_{UNF}$ distribution exhibited a steady increase with increasing redox (r^2 = 0.88; $[MMHg_{UNF}]_{pmol\ L\text{-}1} = 0.016\ Eh_{mV} + 0.19$). Maximum of $MMHg_P$ concentration was located into the HTZ (30 ± 10 pmol L^{-1}) while that of $MMHg_D$ corresponded to the USE (2.0 ± 0.9

pmol L^{-1}). As observed in the USE, a bulge shape relationship was also reported between ΣH_2S and $MMHg_D$ [or $MMHg_D/HgT_D$ (%)] for the whole Petit-Saut reservoir / Sinnamary Estuary continuum (Fig. 10). Below 1 µmol L^{-1} of ΣH_2S, $MMHg_D$ concentrations varied following the $[MMHg_D]_{pmol\ L\text{-}1}$= 2.0 $[\Sigma H_2S]_{\mu mol\ L\text{-}1}$ + 0.4 (r^2 = 0.79) relationship and $[MMHg_D]_{pmol\ L\text{-}1}$= -2.5 $[\Sigma H_2S]_{\mu mol\ L\text{-}1}$ + 4.9 (r^2 = 0.97) beyond that value. Such patterns were already recorded between sulfate reduction rates and $MMHg_D/HgT_D$ (%) in sediments from the Florida Everglades (USA) by Benoit *et al*. (2003). As formulated by these authors, maxima of MMHg concentrations are generally located at sites of intermediate sulfate reduction rates and moderate ΣH_2S levels (around micromolar). In the present case, maxima of $MMHg_D$ and $MMHg_D/HgT_D$ (%) corresponded to average ΣH_2S and SO_4 concentrations of 0.7 ± 0.5 and 10 ± 3 µmol L^{-1} respectively. Finally, regarding redox influence, a lessening in MMHg content of particles was observed with Eh elevation (r^2 = 0.55; $[MMHg_P]_{pmol\ g\text{-}1}$= -$Eh_{mV}$ + 370). Parallel diminution of logK_d(MMHg) along with ΣH_2S (or FeT_D) concentrations suggested that hypolimnetic formation of AVS (and/or cinnabar) and their partial dissolution into the Sinnamary Estuary would widely control MMHg partitioning into the whole system.

5. SUMMARY AND CONCLUSIONS

The role of the Sinnamary Estuary contrasted with that of a regular pipe convoying dam expelled waters towards the ocean. Indeed, from the Petit-Saut dam to the offshore IS station, mercury undergoes a large panel of geochemical transformations namely reduction/oxidation, methylation/demethylation, trapping and mobilization. Those were extensively driven by redox changes, OM, Fe and S cycles, and water oxygenation.

At the dam end-member of the estuary, discharged waters from the hypolimnion of the reservoir are artificially oxygenated. This results in a brutal "evasion" of DGM and notable

increase of $MMHg_D$ concentrations. To account for $MMHg_D$ behavior, two complementary processes are evoked: (i) an improvement of the SRB methylating activity (ii) an oxidative dissolution of MMHg loaded AVS. Laboratory experiments on the artificial oxygenation of tailrace waters enabled the discrimination between both mechanisms. Indeed, a gradual scavenging of FeT_D, HgT_D HgR_D and $MMHg_D$ species was observed in unfiltered water (presumably on newly formed Fe oxyhydroxides). Yet, in filtered (< 0.45µm) water samples, endogenous formation of $MMHg_D$ widely counterbalances the initial removal mechanism. We thus hypothesized that the recorded $MMHg_D$ increase mainly originates from the partial mobilization of colloidal MMHg due to AVS dissolution.

The USE defines the genuine chemical reactor of the Sinnamary Estuary. Displaying marked Hg speciation and partition shifts, it constitutes a sink for HgT_D. Dissolved phase removal (adsorption and/or (co)precipitation) reflects the successive equilibria between HgT_D and sulfides (monosulfide/AVS and/or pyrite) or HgT_D and iron (Fe oxyhydroxides). Conversely to HgT_D, the USE behaves as a source for $MMHg_D$: USE concentrations of $MMHg_D$ were invariably higher than in dam expelled or tributaries outflowing waters (plus 40 and 110 % on average). Local $MMHg_D$ production (close to 1.0 kg y^{-1}) was mostly conditioned by endogenous Hg methylation processes and partitioning between dissolved and particulate phases. The *in situ* Hg methylation conformed to Benoit's neutral complex hypothesis. Accordingly, balance between water oxygenation which controls SRB activity through production of sulfates and ΣH_2S level that governs Hg bioavailability correspond to sites of maximum $MMHg_D$ concentrations. Besides, acid-base mechanisms, along with Fe cycling, had a significant impact on the MMHg partitioning. For instance, iron driven scavenging of $MMHg_D$ attained 4.9 kg y^{-1} while $MMHg_P$ mobilization was 3.0 kg y^{-1}. It results that at least 30-50 % of the downstream $MMHg_{UNF}$ amount (around 5.5 kg) is endogenically produced. Regarding DGM, the USE virtually transferred 0.2 kg y^{-1} of

elemental Hg to the atmosphere (close to 60 % of the dam DGM outputs). This value however represents a net balance between Hg^{II} reduction (of which 0.3 kg y^{-1} related to Fe cycle) and Hg^{0} oxidation (of which 0.3 kg y^{-1} catalyzed by OM).

Considering Hg, the LES can be divided in three distinct zones that orderly correspond to the reactive (S < 5 ‰), mixing (5 < S < 21 ‰) and dilution (S > 21 ‰) regions of the saline gradient. In the reactive region (S < 5 ‰), weak penetrability of light, rapid turnover of redox sensitive elements and relatively high OM concentrations support the hypothesis of an OM induced DGM oxidation. Besides, high FeT_D concentrations coupled to moderate O_2 levels in presence of ΣH_2S depicted the reactive region as a privileged site for Hg methylation (estimated to 1.2 kg y^{-1}) and its subsequent trapping on Fe oxyhydroxides. In the mixing region (5 < S < 21 ‰), the Amazon plume drives the distributions of the Hg particulate phase (99 % of HgT_{UNF}) while HgR_D and $MMHg_D$ profiles significantly diverged from the saline dilution line. For HgR_D, evoked mechanisms consist in formation of Hg^{II}-organic colloids followed by their flocculation and/or scavenging on newly formed Fe oxyhydroxides. Which concerns $MMHg_D$, increasing water salinity, exposure to light and water oxygenation would limit the net methylation rates and favors the potential complexation of Hg with inorganic ligands. In the dilution (S > 21 ‰) region, HgT_D dominates (67 % of HgT_{UNF}). With distance from the continent, dilution by oceanic waters was apparent through the improvement of the Hg reactive fraction [HgR_{UNF}/HgT_{UNF} (%)] (up to 50 %). Yet, relatively low DGM levels (0.2 ± 0.1 pmol L^{-1}) along with significant methylated percentages (5 % of HgT_{UNF}) suggested that water masses generally remained under the influence of the Amazon plume.

To conclude, the Sinnamary Estuary defines an active chemical reactor with respect to Hg methylation. While respectively 3.0 and 0.5 kg y^{-1} $MMHg_{UNF}$ (50 and 70 % as $MMHg_D$) reach the USE *via* the Petit-Saut dam and river-tributaries, the USE exports *circa* 5.5 kg y^{-1} $MMHg_{UNF}$ (55% as $MMHg_D$) to the LES. In spite of the localized sites of Hg methylation, the

LES mainly acts as a sink for $MMHg_D$. Dilution by oceanic waters, establishment of oxidative conditions, trapping on authigenic particles and their subsequent transfer to sediments lead to the low $MMHg_D$ concentrations observed in oceanic environment.

Acknowledgements: We acknowledge Y. Dominique for his suggestions and technical assistance during *in situ* campaigns and laboratory tasks. We also thank B. Burban, C. Reynouard, P. Cerdan, V. Horeau, R. Aboïkoni, L. Guillemet and R. Vigouroux for their participation and facilitation to sampling and analyses. This work has been financially supported by CNRS (Conseil National de la Recherche Scientifique) and EDF (Electricité de France) grant N° F01381/0.B.

REFERENCES

ALBERTS J. J., SCHINDLER J. E., MILLER R. W. and NUTTER D. E. (1974) Elemental mercury evolution mediated by humic acid. *Science* **184**, 895-897.

ALLARD B. and ARSENIE L. (1991) Abiotic reduction of mercury by humic substances in aquatic system. An important process for the mercury cycle. *Water, Air and Soil Pollution* **56**, 457-464.

AMOUROUX J. M. (2003) Genèse et devenir des mangroves. L'exemple de la Guyane. Cycles de conférences 2002 / 2003-Perspectives: Quel avenir pour l'Homme?

AMYOT M., MIERLE G., LEAN D. and McQUEEN D. J. (1997) Effect of solar radiation on the formation of dissolved gaseous mercury in temperate lakes. *Geochim. Cosmochim. Acta* **61**, 975-987.

AULA, I., BRAUNSCHWEILER, H., LEINO, T., MALIN, I., PORVARI, P., HATANAKA, T., LODENIUS, M. and JURAS, A. (1992) Levels of mercury in the Tucurui reservoir and its surroundings area in Para, Brazil. Poster presented at the "*International Conference on Mercury as a Global Pollutant*", Monterey, USA 31-V, 4-VI.

BAEYENS W. and LEERMAKERS M. (1998) Elemental mercury concentrations and formation rates in the Scheldt estuary and the North Sea. *Marine Chemistry* **60**, 257-266

BECKETT R. and. LE N. P. (1990) The role or organic matter and ionic composition in determining the surface charge of suspended particles in natural waters. *Colloids and Surfaces* **44**, 35-49.

BENOIT J. M., GILMOUR C. C., HEYES A., MASON R. P. and MILLER C. L. (2003) *Geochemical and biological controls over mercury production and degradation in aquatic systems. Biogeochemistry of Environmentally Important Trace Elements* **835**, 262-297.

BENOIT J. M., MASON R. P., GILMOUR C. C. and AIKEN G. R. (2001) Constants for mercury binding by dissolved organic matter isolates from the Florida Everglades. *Geochimica et Cosmochimica Acta* **65**, 4445-4451.

BENOIT J. M., GILMOUR C. C., MASON R. P. and HEYES A. (1999) Sulfide Controls on Mercury Speciation and Bioavailability to Methylating Bacteria in Sediment Pore Waters. *Environ. Sci. Technol.* **33**,. 951-957.

BEUCHER C., WONG W. C. P., RICHARD C., MAILHOT G., BOLTE M. and COSSA D. (2002) Dissolved gaseous mercury formation under UV irradiation of unamended tropical waters from French Guyana. *Science of the Total Environment* **290**, 131-138.

BISINOTI M. C. and JARDIM W. F. (2005) Production of organic mercury from Hg^0: experiments using microcosms. *J. Braz. Chem. Soc.* **14**, 244-248.

BLOOM N. S. and EFFLER S. W. (1990) Seasonal variability in the mercury speciation of Onondaga Lake (New York). *Water, Air, and Soil Pollution* **53**, 25-265.

BLOOM N. S. (1989) Determination of picogram levels of methylmercury by aqueous phase ethylation followed by cryogenic gas chromatography with cold vapour atomic fluorescence detection. *Canadian Journal of Fisheries and Aquatic sciences* **46**, 1131-1140.

BLOOM N. S. and FITZGERALD W. F. (1988) Determination of volatile mercury species at the picogram level by low-temperature gas chromatography with cold-vapour atomic fluorescence detection. *Analytica Chimica Acta* **208**, 151-161.

BOUGHRIET A., OUDDANE B., FISCHER J. C., WARTEL M. and LEMAN G. (1992) Variability of dissolved Mn and Zn in the Seine estuary and chemical speciation of these metals in suspended matter. *Water Research* **26**, 1359-1378.

BOURGOIN L. M., QUEMERAIS B., TURCQ P. M. and SEYLER P. (2003) Transport, distribution and speciation of mercury in the Amazon River at the confluence of black and white waters of the Negro and Solimoes Rivers. *Hydrol. Process.* **17**, 1405-1417.

BOYLE E. V., EDMOND J. M. and SHOLKOVITZ E. R. (1977) The mechanisms of iron removal in estuaries. *Geochimica and Cosmochimica Acta* **41**, 1313-1324.

BRANFIREUN B. A., ROULET N. T., KELLY C. A. and RUDD W. M. (1999) *In situ* sulphate stimulation of mercury methylation in a boreal peatland: toward a link between acid rain and methylmercury contamination in remote environments. *Global Biogeochem. Cycles* **13**, 743-750.

BROUARD D., DOYON J-F. and SCHETAGNE R. (1994) Amplification of mercury concentration in lake whitefish (Coregonus clupeaformis) downstream from the La

Grande 2 reservoir. James Bay, Québec. *Mercury Pollution: Integration and Synthesis, International Conference on Mercury as a Global Pollutant (1992)*, Lewis Publishers, 369–380.

CAI Y., JAFFÉ R. I. and JONES R. D. (1999) Interactions between dissolved organic carbon and mercury species in surface waters of the Florida Everglades. *Applied Geochemistry* **14**, 395-407.

CANAVAN M., CALDWELL C. A., and BLOOM N. S. (2000) Discharge of methylmercury-enriched hypolimnetic water from a stratified reservoir. *The Science of The Total Environment* **260**, 159-170.

CHOE K-Y. and GILL G. A. (2001) Isolation of colloidal monomethyl mercury in natural waters using cross-flow ultrafiltration techniques. *Marine Chemistry* **76**, 305-318.

CHOI S. C., CHASE T. J. and BARTHA R. (1994) Metabolic pathways leading to mercury methylation in Desulfovibrio desulfuricans LS. *Appl. Environ. Microbiol.* **60**, 4072–4077.

COMPEAU G. and BARTHA R. (1985) Sulfate reducing bacteria: principal methylators of Hg in anoxic estuarine sediments. *Appl. Environ. Microbiol*. **50**, 498-502.

COMPEAU G. and BARTHA R. (1984) Methylation and demethylation of mercury under controlled redox, pH and salinity conditions. *Appl. Environ. Microbiol.* **48**, 1203-1207.

COQUERY M., COSSA D. and SANJUAN J. (1997) Speciation and sorption of mercury in two macro-tidal estuaries. *Marine Chemistry* **58**, 213-227.

COSSA D., AVERTY B., BRETAUDEAU J. and SENARD A. S., (2003) Spéciation du mercure dissous dans les eaux marines. *Méthodes d'analyse en milieu marin*, Editions Ifremer 27 pp.; ISBN 2-84433-125-4.

COSSA D., COQUERY M., NAKHLE K. and CLAISSE D. (2002) Dosage du mercure total et du monomethylmercure dans les organismes et les sédiments marins. *Méthodes d'analyse en milieu marin*, Editions Ifremer 27pp.; ISBN 2-84433-105-X.

COSSA D. and GOBEIL C. (2000) Mercury speciation in the lower St. Lawrence estuary. *Canadian Journal of Fisheries and Aquatic Sciences* **57**, 138-147.

COSSA D. and GOBEIL C. (1996) Speciation and mass balance of mercury in the lower Saint Laurent estuary and Saguenay Fjord (Canada). *4th International Conference on Mercury as a Global Pollutant* Book of Abstracts, Hamburg **458**, 4-8.

COSSA D., GOBEIL C. and COURAU P. (1988) Dissolved mercury behavior in the St. Lawrence estuary. Estuar. Cstl. Shelf Sci. 29, 227-230.

DE JUNET A. (2004) Etude qualitative de la matière organique particulaire dans le réservoir de Petit-Saut (Guyane Française) : Composition Isotopique ($\delta^{13}C$), élémentaire (C/N) et pigmentaire. *Master report*, Talence, 41 pp.

DELAUNE R. D., JUGSUJINDA A., DEVAI I. and PATRICK W. H. (2004) Relationship of Sediment Redox Conditions to Methyl Mercury in Surface Sediment of Louisiana Lakes. *Journal of Environmental Science and Health* **39**, 1925-1933.

DUMESTRE J-F., EMILIO C. O., RAMON M. and PEDROS-ALIO C. (2001) Changes in bacterial assemblages in a equatorial river induced by water eutrophication of Petit Saut dam reservoir (French Guiana). *Aquat Microb Ecol* **26**, 209-221.

DZOMBAK D. A. and MOREL F. M. M. (1990) Surface complexation modeling Hydrous ferric oxide: New York John Wiley and Sons, 393 pp.

FURUTANI, A. and RUDD, J.W.M. (1980) Measurement of mercury methylation in lake water and sediment samples. *Appl. Environ. Microbiol*. **40**, 770-776.

GAGNON C., PELLETIER E., MUCCI A. and FITZGERALD W. F. (1996) Diagenetic behavior of methylmercury in organic-rich coastal sediments. *Limnol. Oceanogr.* **41**, 428-434.

GALY-LACAUX C., DELMAS R., KOUADIO G., RICHARD S. and GOSSE P. (1999) Long-term greenhouse gas emissions from hydroelectric reservoir in tropical forest regions. *Global Biochemical Cycle* **13**, 503-517.

GILL G. A. and FITZGERALD W. F. (1985) Mercury sampling of open ocean waters at the picomolar level. *Deep-Sea Research* **32**, 287-297.

GILMOUR C. C., HENRY E. A. and MITCHELL R. (1992) Sulfate Stimulation of Mercury Methylation in Freshwater Sediments. *Environmental Science and Technology* **26**, 2281-2287.

GUENTZEL J. L., POWEL R. T., LANDING W. M. and MASON R. P. (1996) Mercury associated with colloidal material in an estuarine and an open ocean environment. *Marine Chemistry* **55**, 177-188.

GUERIN F. (2004) Emission de gaz à effet de serre (CO_2, CH_4) par les retenues de barrages hydroélectriques en zone tropicale : analyse des processus biogéochimiques en jeu et développement d'un modèle prédictif. Séminaire DGO – UMR EPOC, presentation.

GUIMARAES J. R. D., ROULET M., LUCOTTE M. and MERGLER, D. (2000a) Mercury methylation along a lake-forest transect in the Tapajós river floodplain, Brazilian Amazon: seasonal and vertical variations. *The Science of the Total Environment* **261**, 91-98.

GUIMARAES J. R. D., MEILI M., HYLANDER L. D., SILVA E., ROULET M., MAURO J. B. N. and LEMOS R. A. (2000b) Mercury net methylation in five tropical flood plain regions of Brazil: high in the root zone of floating macrophyte mats but low in surface sediments and flooded soils. *The Science of The Total Environment* **261**, 99-107.

HONEYMAN B. D. and P.H. SANTSCHI P. H. (1989) A brownian-pumping model for oceanic trace metal scavenging: Evidence from Th isotope. *J. Mar. Res*. **47**, 951-992.

HOREAU V., RICHARD S. and CERDAN P. (1998) La qualité de l'eau et son incidence sur la biodiversité. L'exemple de la retenue de Petit Saut (Guyane française). JATBA, *Revue d'Ethnobiologie* **40**, 53-77.

HUYNH F., CHARRON C., BETOULLE J. L., PANECHOU K., GARDEL A., PROST M. T. and LOUBRY D. (1997) Suivi de l'évolution géomorphologieque et botanique de l'estuaire du Sinnamary par télédétection. Rap. Final ORSTOM-EDF, 64 pp.

HYDRECO: Laboratory for biological and chemical monitoring and analysis on the Petit-Saut reservoir. http://hydreco.mediasfrance.org/hydreco/

JACOBS L. A., KLEIN S. M. and HENRY E. A. (1995) Mercury cycling in the water column of a seasonally anoxic urban lake (Onondaga Lake, NY). *Water Air and Soil Pollution* **80**, 1-4.

JENSEN S. and JERNELOV A. (1969) Biological methylation of mercury in aquatic organisms. *Nature* **223**, 753-754.

KIM and FITZGERALD W. F. (1986) Sea-air partitioning of mercury over the equatorial Pacific Ocean. *Science* **231**, 1131-I 133.

KING J. K., SAUNDERS F. M., LEE R. F. and JAHNKE R. A. (1999) Coupling mercury methylation rates to sulfate reduction rates in marine sediments. *Environmental Toxicology and Chemistry* **18**, 1362-1369.

KORTHALS E. T. and WINFREY M. R. (1987) Seasonal and spatial variations in mercury methylation and demethylation in an oligotrophic lake. *Appl. Environ. Microbiol*. **53**, 2397-2404.

LAMBORG C. H., FITZGERALD W. F., SKOOG A. and PIETER T. V. (2004) The abundance and source of mercury-binding organic ligands in Long Island Sound. *Marine Chemistry* **90**, 151-163.

LAURIER F. J. G., COSSA D., GONZALEZ J. L., BEUCHER C. and SARAZIN G. (2002) Mercury Transformations and Exchanges in a High Turbidity Zone Estuary: Implication of the Organic Matter and Amorphous Oxyhydroxides. *Cosmochimica, Geochimica Acta* **18**, 3329-3345.

LEERMAKERS M., GALETTI S., DE GALAN S., BRION N. and BAEYENS W., (2001) Mercury in the Souther North Sea and Sheldt Estuary. *Marine Chemistry* **75**, 229-248.

LIANG L., HORVAT M. and BLOOM N. S. (1994) An improved speciation method for mercury by GC/CVAFS after aqueous phase ethylation and room temperature precollection. *Talanta* **41**, 371-379.

MANTOURA R. F. C., DICKSON A. and RILEY J. P. (1978) The complexation of metals with humic materials in natural waters. *Estuarine and Coastal Marine Science* **6**, 387-408.

MARCHAND C., VERGES E. L., BALTZER F., ALBERIC P., COSSA D. and BAILLIF P. (2005) Heavy metals distribution in mangrove sediments along the mobile coastline of French Guiana. *Marine Chemistry*, **In Press**.

MASON R. P., LAWSON N. M. and SHEU G. R. (2001). Mercury in the Atlantic Ocean: factors controlling air-sea exchange of mercury and its distribution in the upper waters. *Deep-Sea Research* **48**, 2829-2853.

MASON R. P. and SULLIVAN K. A. (1999b) The distribution and speciation of mercury in the South and equatorial Atlantic. *Deep Sea Research Part II* **46**, 937-956.

MASON R. P. and FITZGERALD W. F. (1991) Mercury speciation in open ocean waters. *Water, Air, and Soil Pollution* **56**, 779-789.

MOL J. H., RAMLAL J. S., LIETAR C. and VERLOO M. (2001) Mercury contamination in freshwater, estuarine, and marine fishes in relation to small-scale gold mining in Suriname, South America. *Environmental Research* **86**, 183-197.

MOREL F. M. M., KRAEPIEL A. M. L. and AMYOT M. (1998) The chemical cycle and bioacculumation of mercury. *Annu. Rev. Ecol. Syst.* **29**, 543-566.

MOTA A. M., CRUZ P., VILHENA C. and GONCALVES M.L.S. (2005) Influence of the sediment on lead speciation in the Tagus estuary. *Water Research* **39**, 1451-1460.

MURESAN B., COSSA D., RICHARD S. and DOMINQUE Y. Mercury Cycling in a Tropical Artificial Reservoir: Monomethylmercury Production and Sources. Submitted to *Applied Geochemistry* (Feb. 2006).

MURESAN B., COSSA D., RICHARD S., and BURBANT B. Mercury speciation and exchanges at the air-water interface of a tropical artificial reservoir, French Guiana. To be submitted.

NGUYEN H.L., LEERMAKERS M., KURUNCZI S., BOZO L. and BAEYENS W. (2005) Mercury distribution and speciation in Lake Balaton, Hungary. *Science of The Total Environment* **340**, 231-246.

O'DRISCOLL N. J., SICILIANO S. D., PEAK D., CARIGNAN R. and LEAN D. R. S. (2005) The influence of forestry activity on the structure of dissolved organic matter in lakes: Implications for mercury photoreactions. *Science of the Total Environment* **in press**.

PARKS J. W., LUTZ A. and SUTTON J. A. (1989) Water column methylmercury in the Wabigoon/English River–Lake system: factors controlling concentrations, speciation, and net production.. Can. J. Fish. Aquat. Sci. **46**, 2184-2202.

PERETYAZHKO T., CHARLET L., MURESAN B., KAZIMIROV V. and COSSA D. (2005) Formation of dissolved gaseous mercury in a tropical lake (Petit-Saut reservoir, French Guiana). *Science of The Total Environment*, **In press**.

PERETYAZHKO T. (2002) Formation de Hg^0 dans les milieux aquatiques tropicaux (lacs et sols). Ph.D thesis, University of Grenoble, France, 191 pp.

PONTON D. and VAUCHEL P. (1998) Immediate downstream effects of the Petit-Saut dam on young neotropical fish in a large tributary of the Sinnamary River (French Guiana, South America). *Regulated Rivers: Research & Management* **14**, 227-243.

PORVARI P. (1995) Mercury levels of fish in Tucuruí hydroelectric reservoir and in River Mojú in Amazonia, in the state of Pará, Brazil. *The Science of the Total Environment* **175**, 109-117.

QUEMERAIS B. and COSSA D. (1997) Procedures for sampling and analysis of mercury in natural waters. *Scientific and Technical Report* **ST-31E**, 34 pp.

RAMLAL P. S., KELLY C. A., RUDD J. W. M. and FURUTANI A. (1993) Sites of methylmercury production in remote Canadian Shield lakes. *Can. J. Fish. Aquat. Sci.* **50**, 972-979.

RAVICHADRAN M. (2004) Interactions between mercury and dissolved organic matter—a review. *Chemosphere* **55**, 319-331.

RICHARD S., ARNOUX A., CERDAN P., REYNOUARD C., HOREAU V. and VIGOUROUX R. (2002) Influence of the setting up of a man-made lake on mercury levels in the flesh of fish in a neotropical habitat: the Sinnamary river (French Guiana). *Rev. Ecol.* **8**, 59-76.

RICHARD S., ARNOUX A. and CERDAN P. (1997) Evolution in physico-chemical water quality in the reservoir and downstream following the filling of Petit-Saut dam (French Guiana). *Hydroecol. Appl.* **9** (1/2), 57-83.

RICHARD S. (1996) La mise en eau du barrage de Petit-Saut. Hydrochimie 1 - du fleuve Sinnamary avant la mise en eau, 2 – de le retenue pendant la mise en eau, 3 – du fleuve en aval. *Ph.D thesis*, Univ. of Aix – Marseille I 278 pp.

RODAS D. S., ARIZA J. L. G., GIRALDEZ I., VELASCO A. and MORALES E. (2005) Arsenic speciation in river and estuarine waters from southwest Spain. *Science of The Total Environment* **345**, 207-217.

RODRIGUEZ R. C. M-D., TESSIER E., AMOUROUX D., GUYONEAUD R., DURAN R., CAUMETTE P. and DONARD O. F. X. (2004) Mercury methylation/demethylation and volatilization pathways in estuarine sediment slurries using species-specific enriched stable isotopes. *Marine Chemistry* **90**, 107-123.

ROLFHUS K. R. and FITZGERALD W. F. (2001) The evasion and spatial/temporal distribution of mercury species in Long Island Sound, CT-NY. *Geochimica et Cosmochimica Acta* **65**, 407-418.

ROULET M. and GRIMALDI C. (2001) Le mercure dans les sols d'Amazonie. Origine et comportement du mercure dans les couvertures ferrallitiques du bassin amazonien et des Guyanes. *IRD editions*, Paris 121-166.

ROULET M., LUCOTTE M. and GUIMARAES J. R. D., (2000) Methylmercury in the water, seston and epiphyton of an Amazonian river and its floodplain, Tapajos river, Brazil. *The Science of The Total Environment* **261**, 43-59.

ROULET M., LUCOTTE M., CANUEL R., RHEAULT I., TRAN S. *et al*., (1998a) Distribution and partition of total mercury in waters of the Tapajós River Basin, Brazilian Amazon. *The Science of The Total Environment* **213**, 203-211.

ROULET M., LUCOTTE M., CANUEL R., FARELLA N., COURCELLES M., GUIMARAES J. R. D., MERGLER D. and AMORIM M. (1998b) The geochemistry of mercury in central Amazonian soils developed on the Alter-do-Chao formation of the lower Tapajos River Valley, Para state, Brazil. *The Science of The Total Environment* **223**, 1-24.

RTECS: REGISTRY of TOXIC EFFECTS of CHEMICAL SUBSTANCES. National Institute for Occupation Safety and Health. Washington, D.C. Mercury chloride #: OV9100000.

SCHETAGNE R. and VERDON R. (1999a) Post-impoundment evolution of fish mercury levels at the La Grande complex. Québec, Canada (from 1978 to 1996). *Environmental Science Series* Springer-Verlag, 235-238.

SCHETAGNE R., DOYON J-F. and VERDON R. (1997) Summary report: evolution of fish mercury levels at the La Grande Complex, Québec (1978–1994). Joint report of the Direction principale, Communication et Environnement, Hydro-Québec, and Groupeconseil Genivar Inc., Montréal, Qué.

SEEBERG-ELVERFELDT J., SCHLUTER M., FESEKER T. and KOLLING M. (2005) Rhizon sampling of pore waters near the sediment/water interface of aquatic systems. *Limnology and oceanography*: Methods **3**, 361-371.

SELLERS P., KELLY C. A., RUDD J. W. M. and MACHUTCHON A. (1996) Photodegradation of methylmercury in lakes. *Nature* **380**, 694–697.

SERGIO A. C-S., GUIMARAES J. R. D., MAURO J. B. N., MIRANDA M. R. and AZEVEDO M. F. O. S. (2005) Mercury methylation and bacterial activity associated to tropical phytoplankton. *Science of The Total Environment*, **In Press.**

SHIBU M. P., BALCHAND A. N. and NAMBISAN P. N. K. (1990) Trace metal speciation in a tropical estuary — Significance of environmental factors. *The Science of The Total Environment* **97-98**, 267-287.

SICILIANO S. D., O'DRISCOLL N. J. and LEAN D. R. S. (2002) Microbial reduction and oxidation of mercury in freshwater lakes. *Environ. Sci. Technol.* **36**, 3064-3068.

STEVEN D. M. and BROOKS A. L. (1972) Identification of Amazon River water at Barbados, W. Indies, by salinity and silicate measurements. *Mar. Biol.* **14**, 345-348.

STORDAL M. C., GILL G. A., WEN L. S. and SANTCHI P. H. (1996) Mercury phase speciation in surface water of three Texas estuaries: Importance of colloidal forms. *Limnol. Oceanogr.* **41**, 52-61.

STUMM W., KUMMERT R. and SIGG L. (1980) A ligand exchange model for the adsorption of inorganic and organic ligands at hydrous oxide interfaces. *Croat. Chem. Acta* **53**, 291-312.

TURNER A., MILLWARD G. E. and LEROUX S. M. (2001) Sediment-water partitioning of inorganic mercury in estuaries. *Environ Sci Technol.* **35**, 4648-54.

VANDAL G. M., MASON R. P. and FITZGERALD F. (1991) Cycling of volatile mercury in temperate lakes. *Water Air and Soil Pollution* **56**, 791-803.

VAQUER A., PONS V. and LAUTIER J. (1997) Distribution spatio-temporelle du phytoplancton dans le réservoir de Petit-Saut (Guyane Française). *Hydroécol Appl* **9**,169-193.

VERDON R., BROUARD D., DEMERS C., LALUMIERE R., LAPERLE M. and SCHETAGNE R. (1991) Mercury evolution (1978–1988) in fishes of the La Grande hydroelectric complex, Québec, Canada. *Water Air and Soil Pollution* **56**, 405-417.

WATRAS, C. J., BLOOM N. S., HUDSON R. J. M., GHERINI S., MUNSON R., CLAAS S. A., MORRISON K. A., HURLEY J. P., WIENER J. G., FITZGERALD W. F., MASON R. P., VANDAL G., POWELL D., RADA R., RISLOVE L., WINFREY M., ELDER J., KRABBENHOFT D. P., ANDREN A. W., BABIARZ C., PORCELLA D. B. and HUCKABEE J. W. (1994) Sources and fates of mercury and methylmercury in Wisconsin lakes. *Mercury as a Global Pollutant: Integration and Synthesis*, 153-177.

WEIJDEN C. H., ARNOLDUS M. J. H. L. and MEURS C. J. (1977) Desorption of metals from suspended material in the rhine estuary. *Netherlands Journal of Sea Research* **11**, 130-145.

WEN L.-S., SANTCHI P., GILL G. and PATERNOSTRO C. (1999) Estuarine trace metal distribution in Galveston Bay: importance of colloidal forms in the speciation of the dissolved phase. *Marine Chemistry* **63**, 185–212.

WESTALL J. C. (1987) Adsorption mechanisms in aquatic surface chemistry. *Aquatic surface chemistry: chemical processes at the particle-water interface*, 3-32.

XIAO Z. F., STROMBERG D. and LINDQVIST O. (1995) Influence of humic substances on photolysis of divalent mercury in aqueous solution. *Water Air and Soil Pollution*. **80**, 789-798.

ZAHIR F., RIZWI S. J., HAQ S. K. and KHAN R. H. (2005) Low dose mercury toxicity and human health. *Environmental Toxicology and Pharmacology* **20**, 351-360.

ZHANG H. and LINDBERG S. E. (2001) Sunlight and iron(III)-induced photochemical production of dissolved gaseous mercury in freshwater. *Environ. Sci. Technol.* **35**, 928-935.

TABLE CAPTIONS

Campaign	Period	Season	Sampling site	Type of sample
1999 CRUISE	12/1999	Short wet	USE / LES	Water column
MATOU TOU 1	03-04/2003	Short dry	Tailrace / USE	Water column
MATOU TOU 2	01-02/2004	Short wet	Tailrace / Creeks / USE / LES	Water column / Sediments
MATOU TOU 3	05-06/2004	Long wet	Tailrace / Creeks / USE / LES	Water column / Sediments / Poral waters
MATOU TOU 4	11-12/2004	Long dry	Tailrace / Creeks / USE / LES	Water column / Sediments
MATOU TOU 5	02-03/2005	Short dry	Tailrace / Creeks / USE / LES	Water column

Tab. 1. Summary of the different sampling

	HgT_{UNF} (pmol L^{-1})	HgT_D (pmol L^{-1})	HgT_P (pmol g^{-1})	$MMHg_D$ (pmol L^{-1})	$MMHg_P$ (pmol g^{-1})	DGM (pmol L^{-1})
Sinnamary River	13 ± 2 (6) [10.4 - 15.8]	8 ± 1 (6) [6.0 - 8.9]	1100 ± 400 (6) [490 - 1470]	0.6 ± 0.2 (5) [0.35 - 0.78]	25 ± 15 (5) [17 - 43]	0.40 ± 0.15 (6) [0.24 - 0.67]
Reservoir hypolimnion	13 ± 6 (43) [4.2 - 25]	8 ± 4 (43) [4.0 - 19.4]	1300 ± 250 (37) [100 - 4200]	0.9 ± 0.5 (43) [0.06 - 5.88]	170 ± 60 (43) [15 - 830]	0.29 ± 0.16 (43) [0.07 - 0.74]
Dam tailrace	13 ± 5 (88) [3.8 - 27.9]	8 ± 2 (27) [0.5 - 10.7]	750 ± 650 (27) [30 - 3300]	1.5 ± 0.8 (24) [0.11 - 3.42]	280 ± 100 (24) [27 - 320]	0.3 ± 0.2 (50) [0.06 - 0.95]
USE	11 ± 3 (40) [5.9 - 16.9]	6 ± 2 (40) [2.2 - 10.5]	600 ± 200 (40) [200 - 2500]	2.0 ± 0.9 (40) [0.24 - 4.47]	220 ± 130 (40) [59 - 590]	0.16 ± 0.08 (40) [0.04 - 0.49]
HTZ entrance	19 ± 3 (4) [17.4 - 23.7]	7 ± 2 (4) [3.5 - 7.4]	350 ± 200 (4) [150 - 570]	0.7 ± 0.4 (4) [0.42 - 1.51]	70 ± 40 (4) [37 - 114]	0.08 ± 0.06 (4) [0.05 - 0.13]
Amazon plume	110 ± 90 (6) [15 - 230]	4 ± 2 (7) [1.98 - 6.90]	180 ± 40 (7) [160 - 250]	0.3 ± 0.3 (6) [0.02 - 0.72]	30 ± 20 (6) [8 - 54]	0.05 ± 0.05 (6) [< 0.05 - 0.12]
IS station	3.0 ± 0.8 (2) [2.4 - 3.5]	2.0 ± 0.5 (2) [1.7 - 2.4]	170 ± 100 (2) [100 - 240]	0.09 ± 0.05 (2) [0.05 - 0.12]	12 ± 7 (2) [7 - 17]	0.2 ± 0.1 (2) [0.13 - 0.27]

Tab. 2. Average concentrations (± standard deviations) of total (HgT_{UNF}, HgT_D, HgT_P), monomethylmercury ($MMHg_D$ and $MMHg_P$) and dissolved gaseous (DGM) mercury in main compartments constitutive of the Petit-Saut reservoir / Sinnamary Estuary continuum. Given values correspond to Matoutou 1, 2, 3, 4, 5 and Dec. 1999 campaigns.

Season	HgT_D (pmol L^{-1})			$MMHg_D$ (pmol L^{-1})		
	Tributaries	Dam tailrace	Pass.	Tributaries	Dam tailrace	Pass.
Short wet	3 ± 1 (2)	9 ± 2 (5)	9.2	0.4 ± 0.2 (2)	0.7 ± 0.2 (5)	2.44
Short dry	7 ± 2 (4)	10 ± 2 (5)	10 ± 2 (5)	1.5 ± 0.4 (4)	2.0 ± 0.3 (5)	3.1 ± 0.5 (5)
Long wet	6 ± 3 (3)	6 ± 1 (5)	3.6	0.7 ± 0.1 (3)	1.4 ± 0.2 (5)	2.05
Long dry	8 ± 2 (3)	11 ± 2 (3)	10.2	1.4 ± 0.5 (3)	2.3 ± 0.4 (3)	4.47

Tab. 3. Seasonal variability of dissolved total (HgT_D) and monomethyl ($MMHg_D$) mercury in the principal freshwater inputs to the USE (Creek-tributaries vs Dam tailrace). Effect of the artificial aeration system on HgT_D and $MMHg_D$ levels (Dam tailrace *vs* Pass. station).

FIGURE CAPTIONS

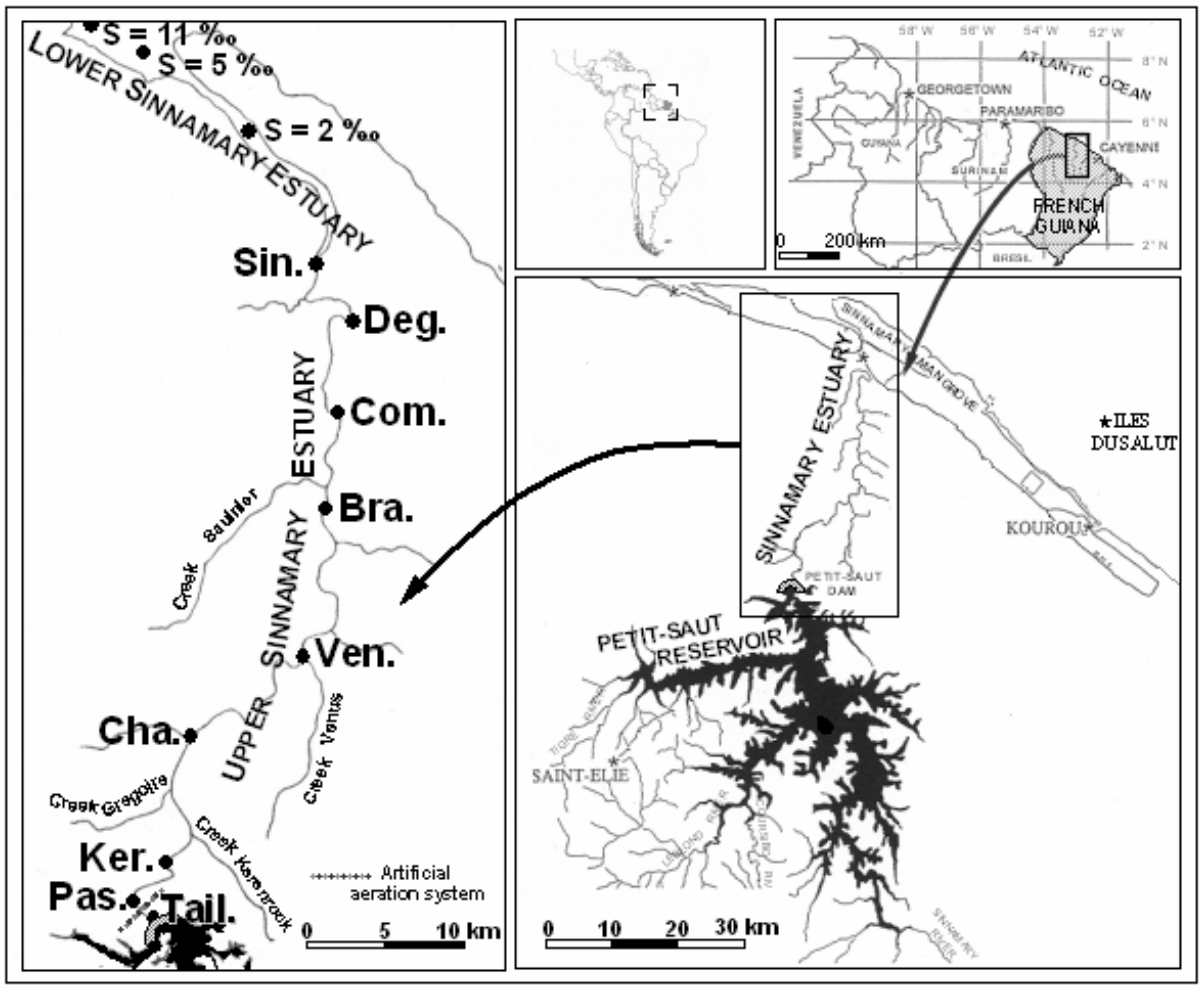

Fig. 1. Study area. Filled circles were sampled during Matoutou 1 (Mar. - Apr./2003), 2 (Jan.-Feb./2004), 3 (May-Jun./2004), 4 (Nov.-Dec./2004) and 5 (Feb.-Mar./2005) campaigns. The USE was invariably sampled at the same eight stations: Pas., Ker., Cha., Ven., Bra., Com., Deg. and Sin. In the LES, the HTZ entrance (S < 5 ‰), the Amazon plume (5 < S < 21 ‰) and the IS station (S > 21 ‰) were individually considered.

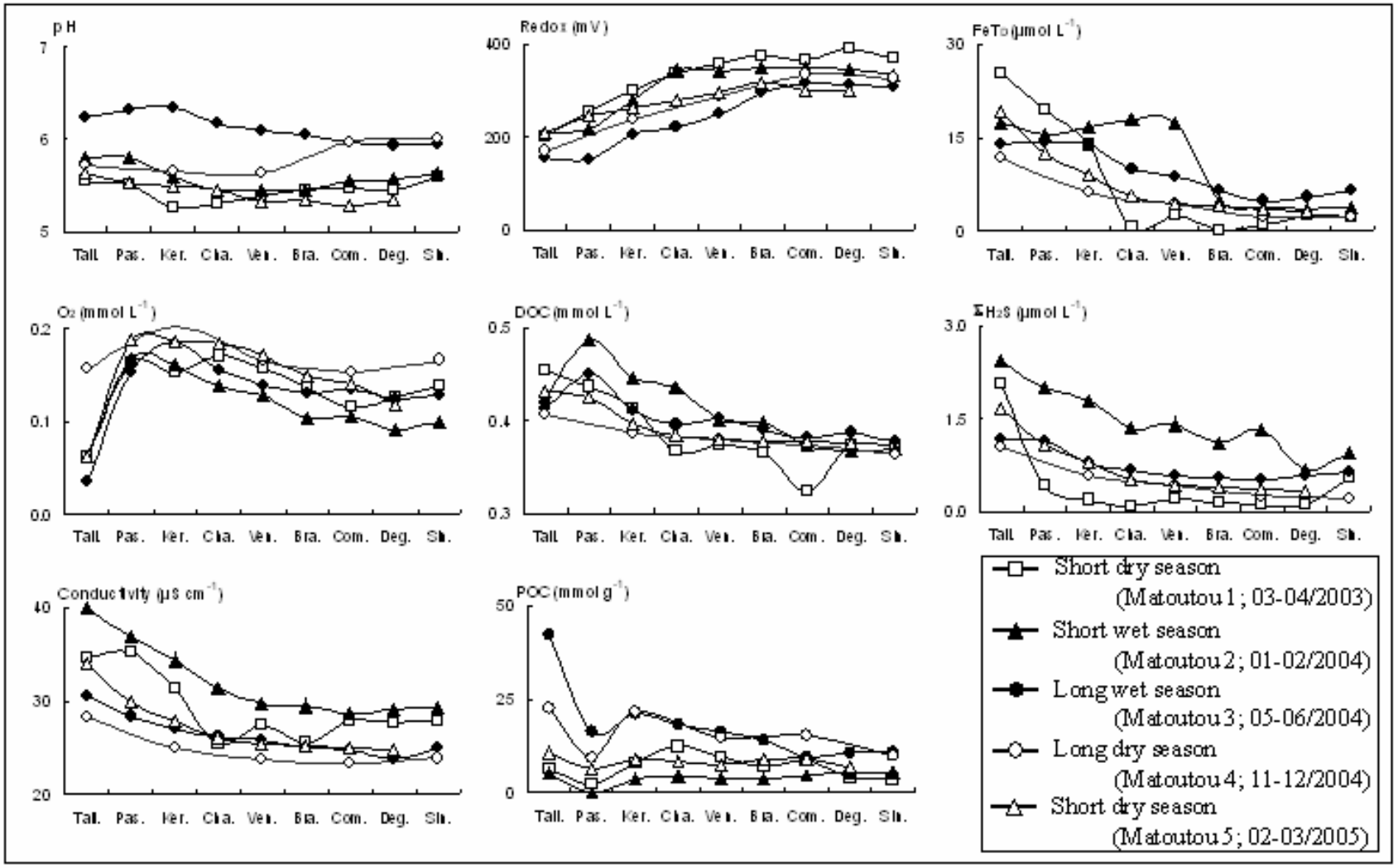

Fig. 2. Transect of physical characteristics and major chemical compounds in the USE. Each graph displays the distribution of a same parameter with regard to Matoutou 1, 2, 3, 4 and 5 campaigns. Dam and LES boundaries were respectively depicted by the Tail. and Sin. stations.

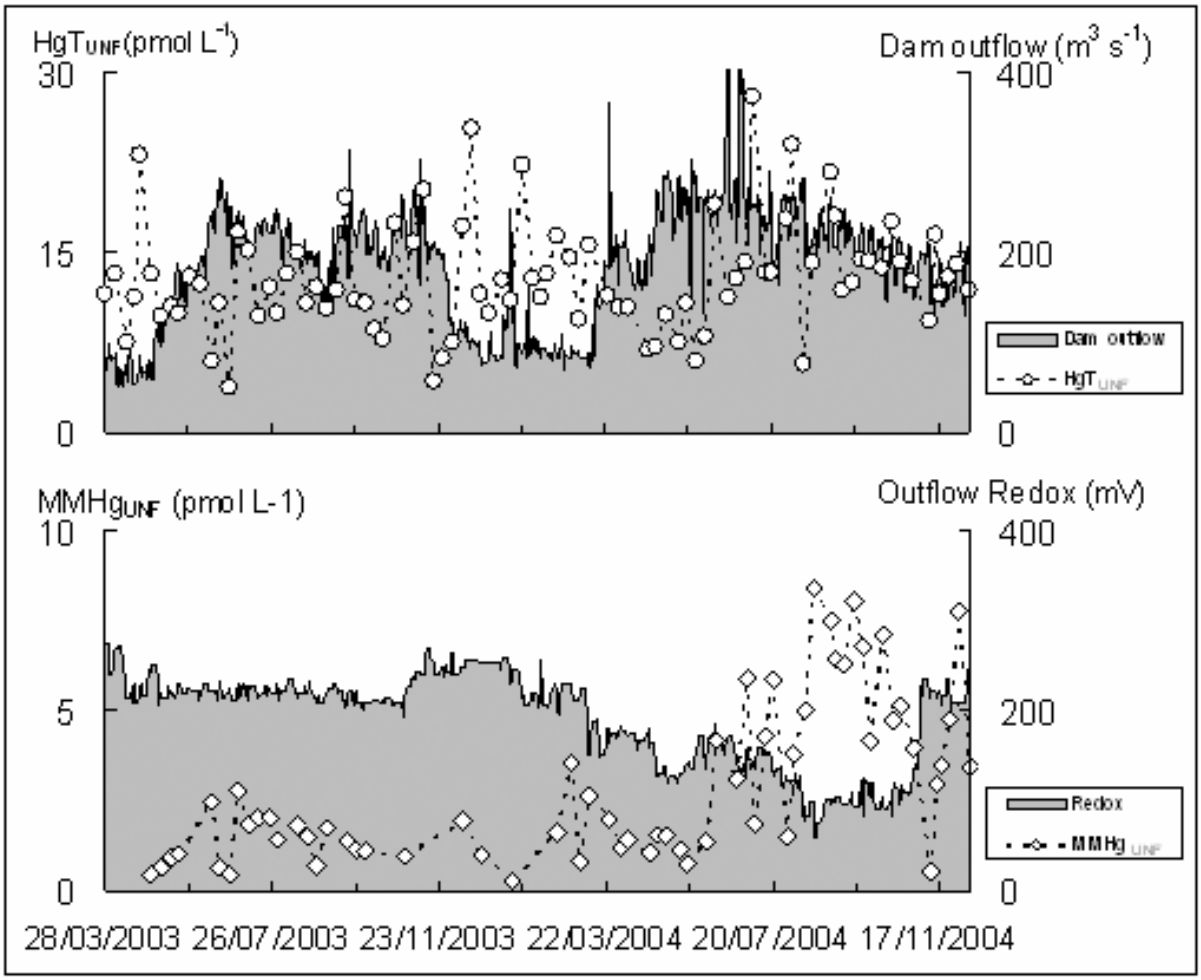

Fig. 3. Monitoring of unfiltered total (HgT_{UNF}) and monomethyl ($MMHg_{UNF}$) mercury in exported waters downstream the dam (Tail. station). Discharge flow and associated redox were daily recorded. Samples for Hg analyses were collected on a weekly basis.

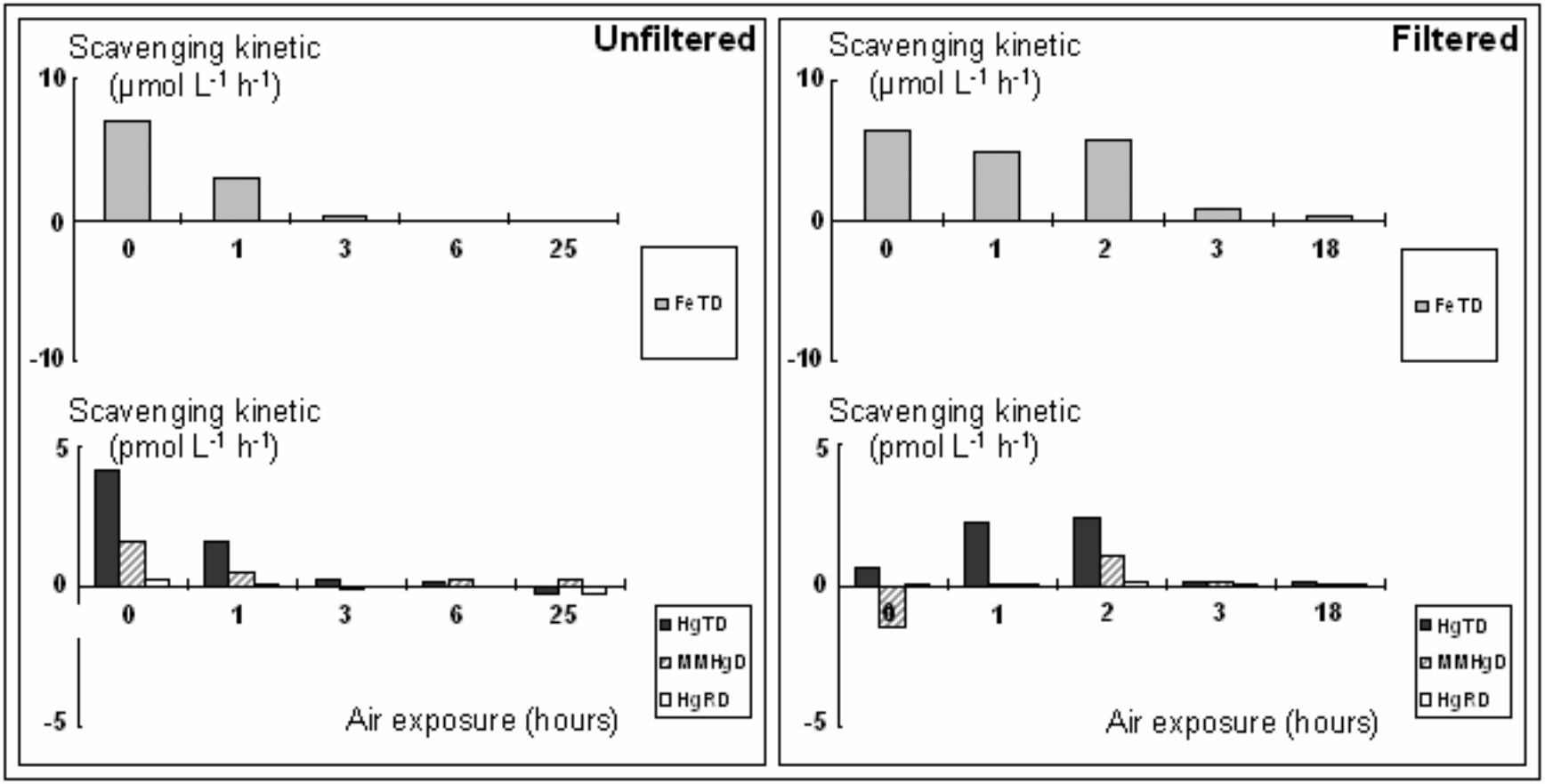

Fig. 4. Monitoring of the scavenging kinetics of FeT_D, HgT_D, HgR_D and $MMHg_D$ in tailrace water from the Petit-Saut dam (Tail. station). Measurements were carried on unfiltered and < 0.45 µm samples.

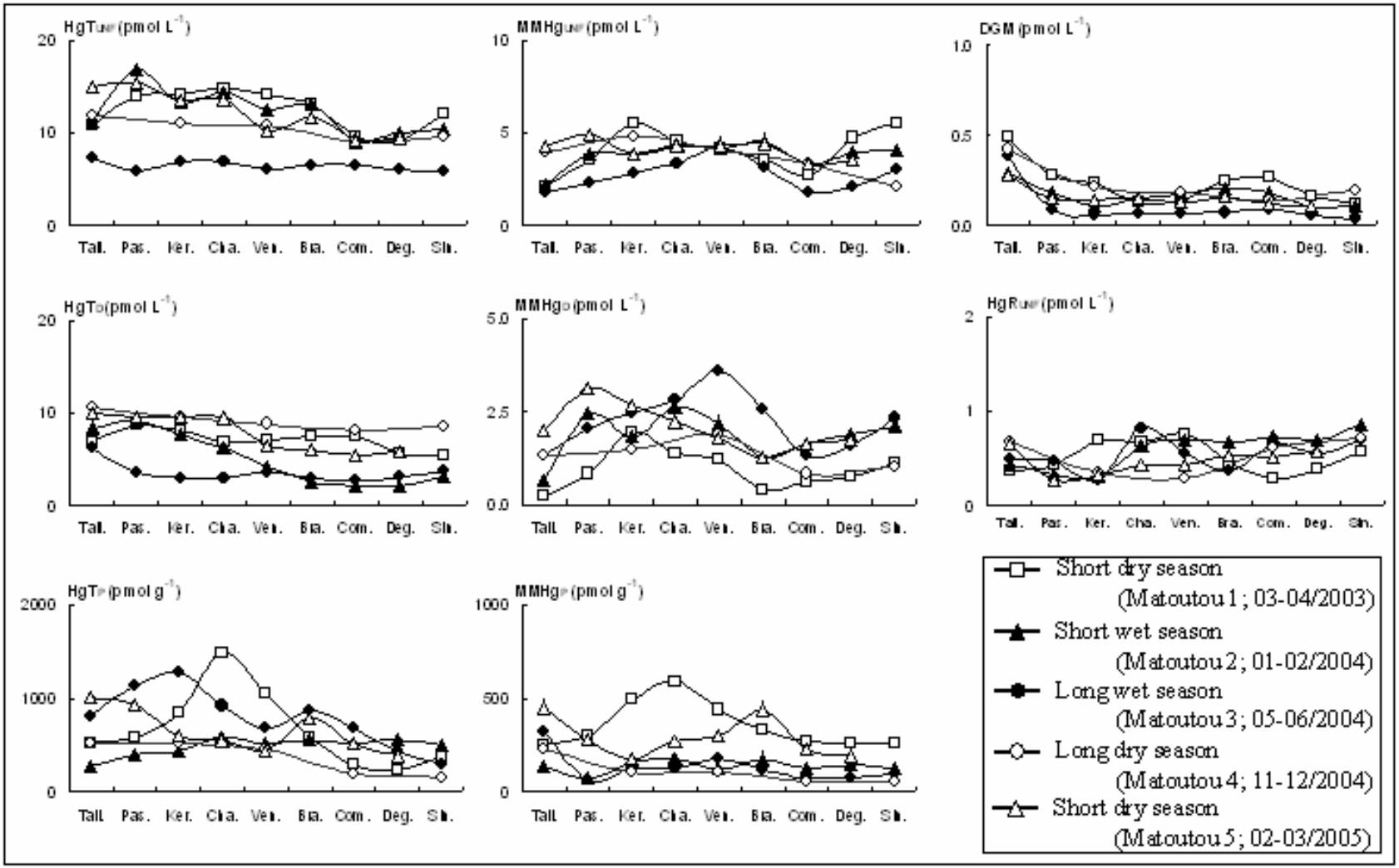

Fig. 5. Transect of main Hg species in the USE. Each graph displays the distribution of a same specie with regard to Matoutou 1, 2, 3, 4 and 5 campaigns. Dam and LES boundaries were respectively depicted by the Tail. and Sin. stations.

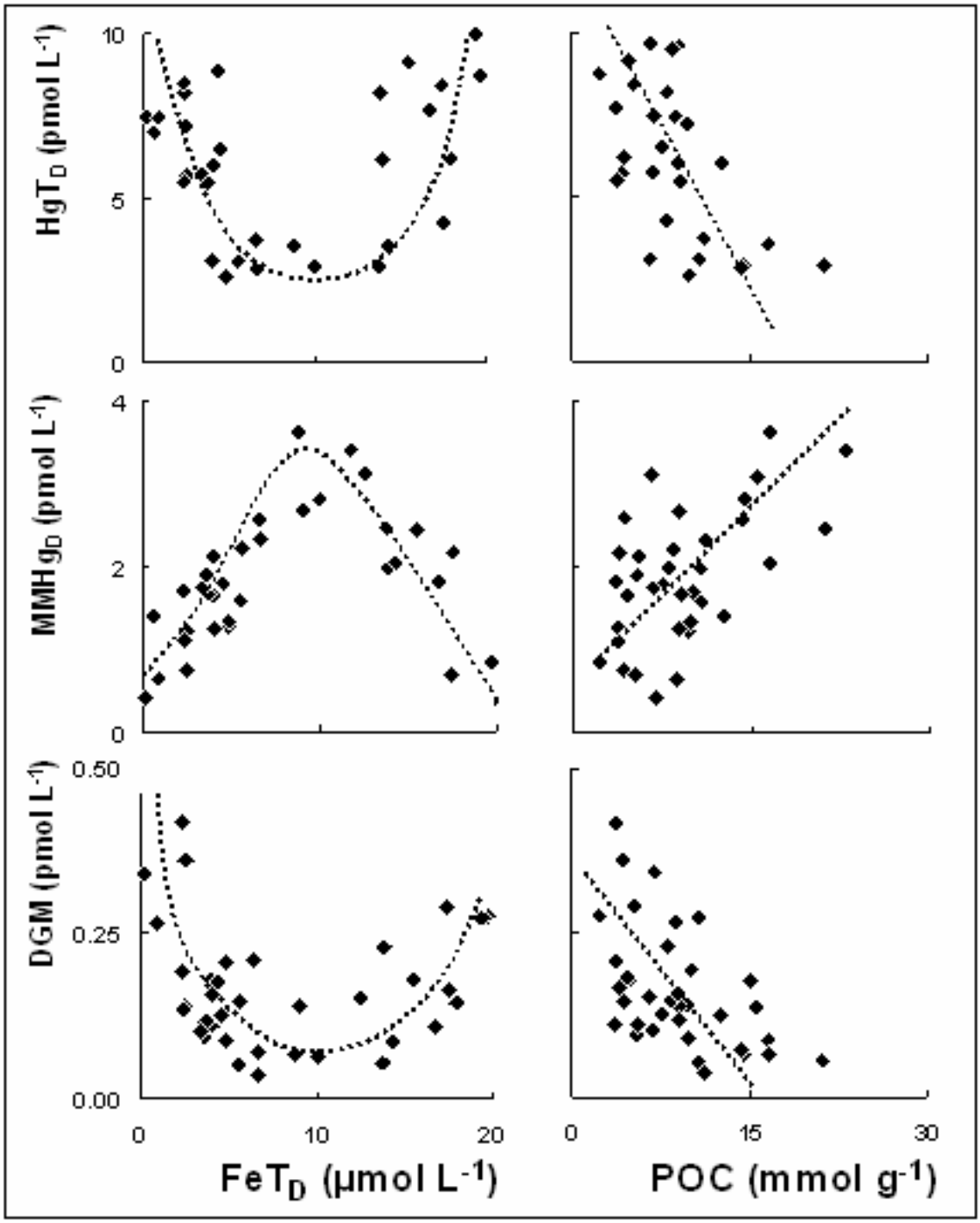

Fig. 6. Dissolved total (HgT_D), monomethyl ($MMHg_D$) and gaseous (DGM) mercury in relation to dissolved total iron (FeT_D) and particulate organic carbon (POC). Figures were plotted using available data from the USE Matoutou 1 to 5 campaigns.

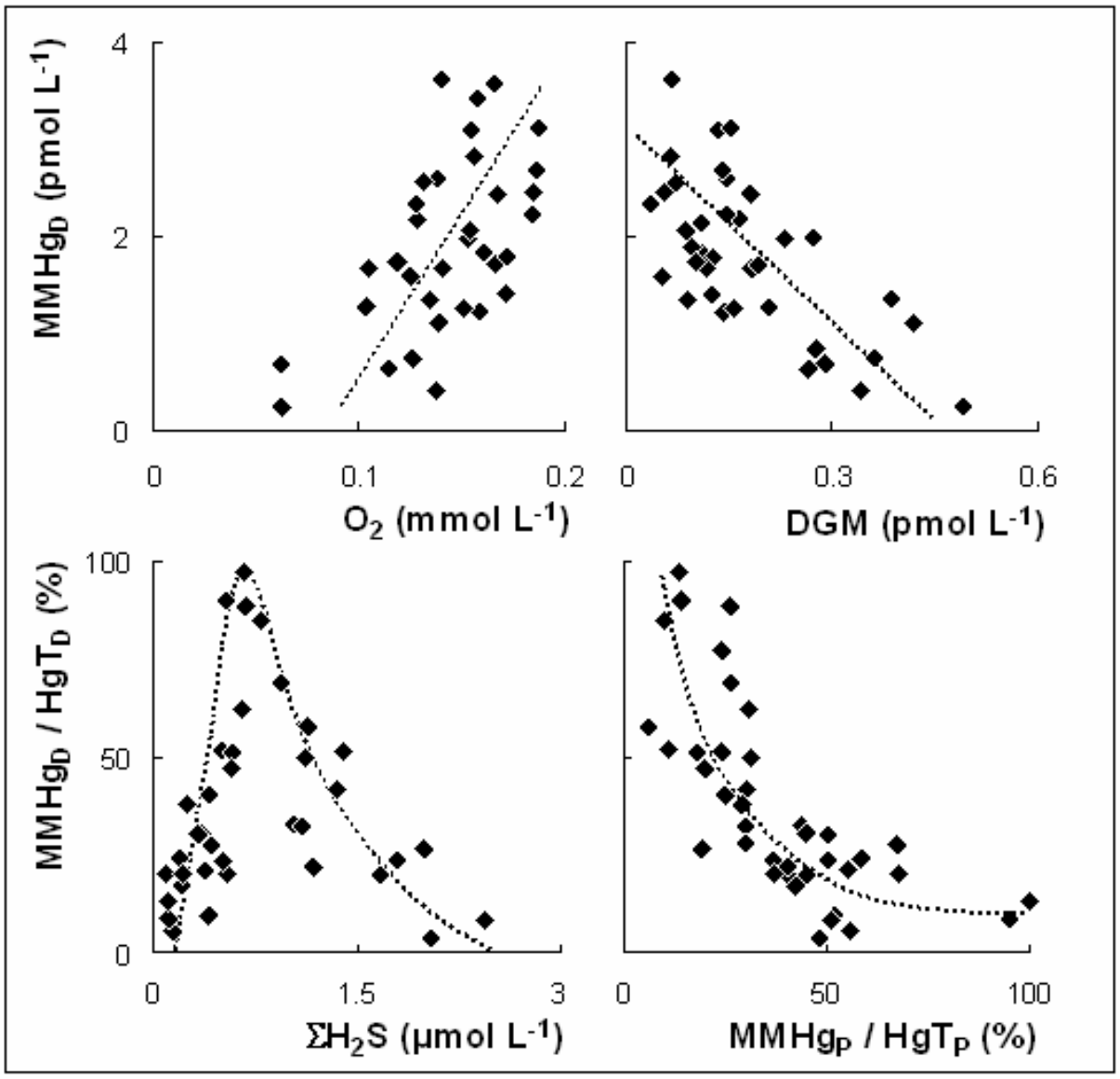

Fig. 7. Upper graphs: dissolved monomethylmercury ($MMHg_D$) as a function of dissolved oxygen (O_2) and dissolved gaseous mercury (DGM). Lower graphs: percentage of dissolved monomethylmercury [$MMHg_D/HgT_D$ (%)] in relation to total sulfides (ΣH_2S) and percentage of particulate monomethylmercury [$MMHg_P/HgT_P$ (%)]. Figures were plotted using available data from the USE Matoutou 1 to 5 campaigns.

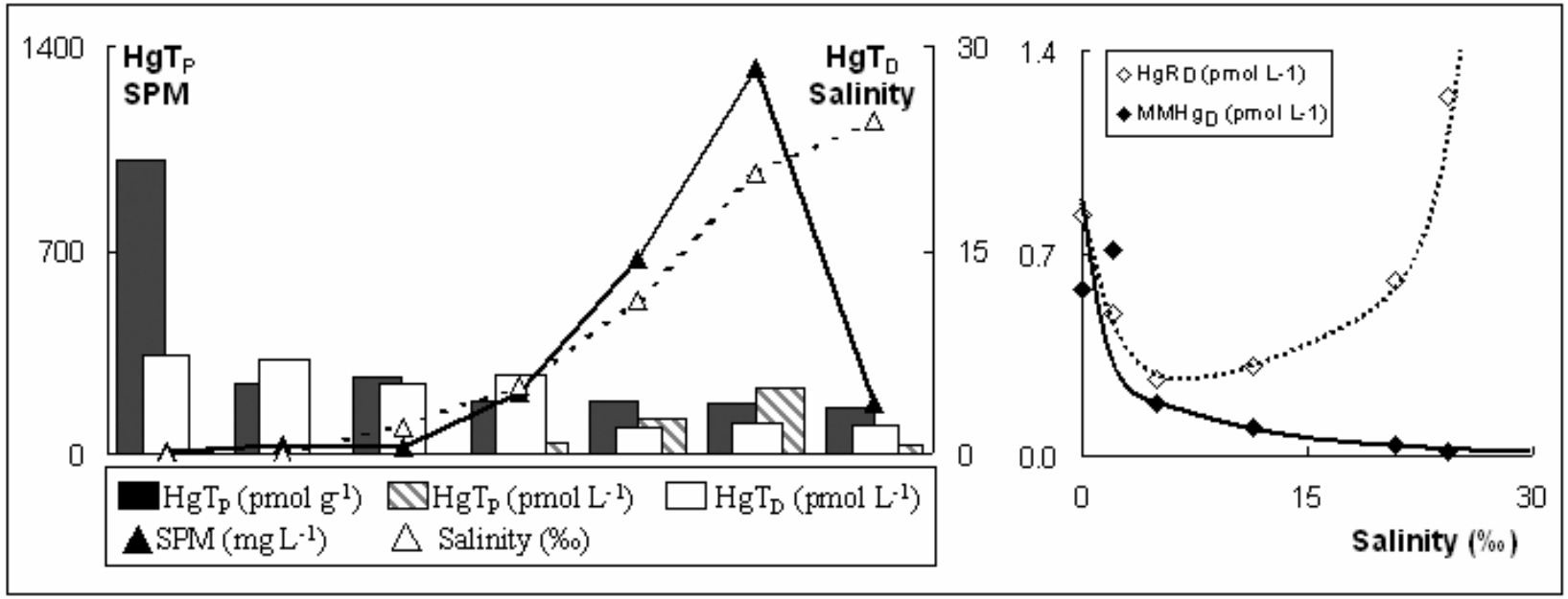

Fig. 8. Transect of total Hg species, suspended particulate matters (SPM) and salinity along the HTZ / Amazon plume continuum (Dec./1999 cruise). Relationships of dissolved reactive (HgR_D) and methylated ($MMHg_D$) mercury to salinity.

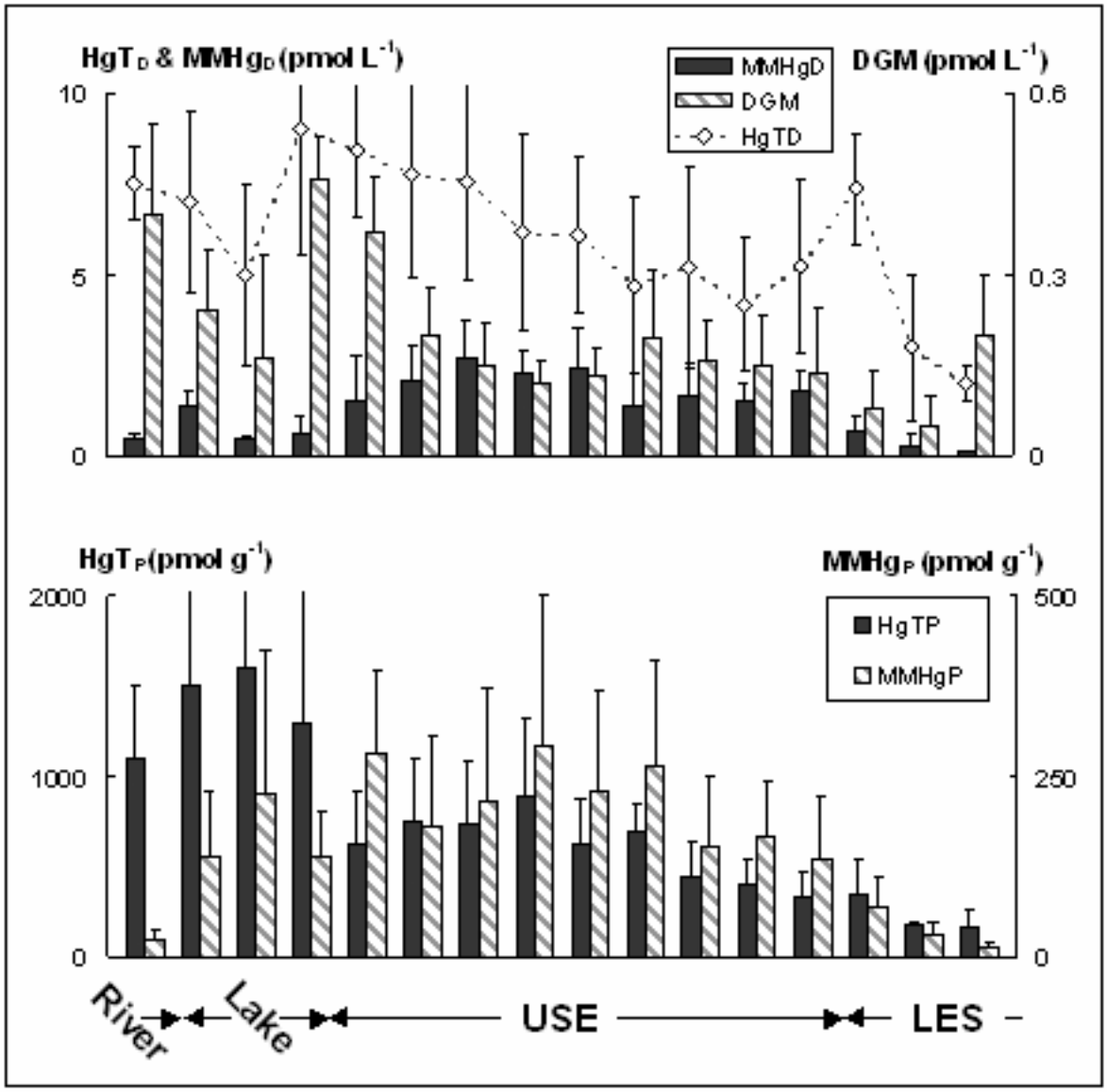

Fig. 9. Transect of main Hg species along the Petit-Saut reservoir / Sinnamary Estuary continuum. Figures were plotted using the average data set from the Matoutou 1, 2, 3, 4 and 5 campaigns. The water column of the reservoir was described using the hypolimnetic concentrations (Muresan *et al.*, under submission).

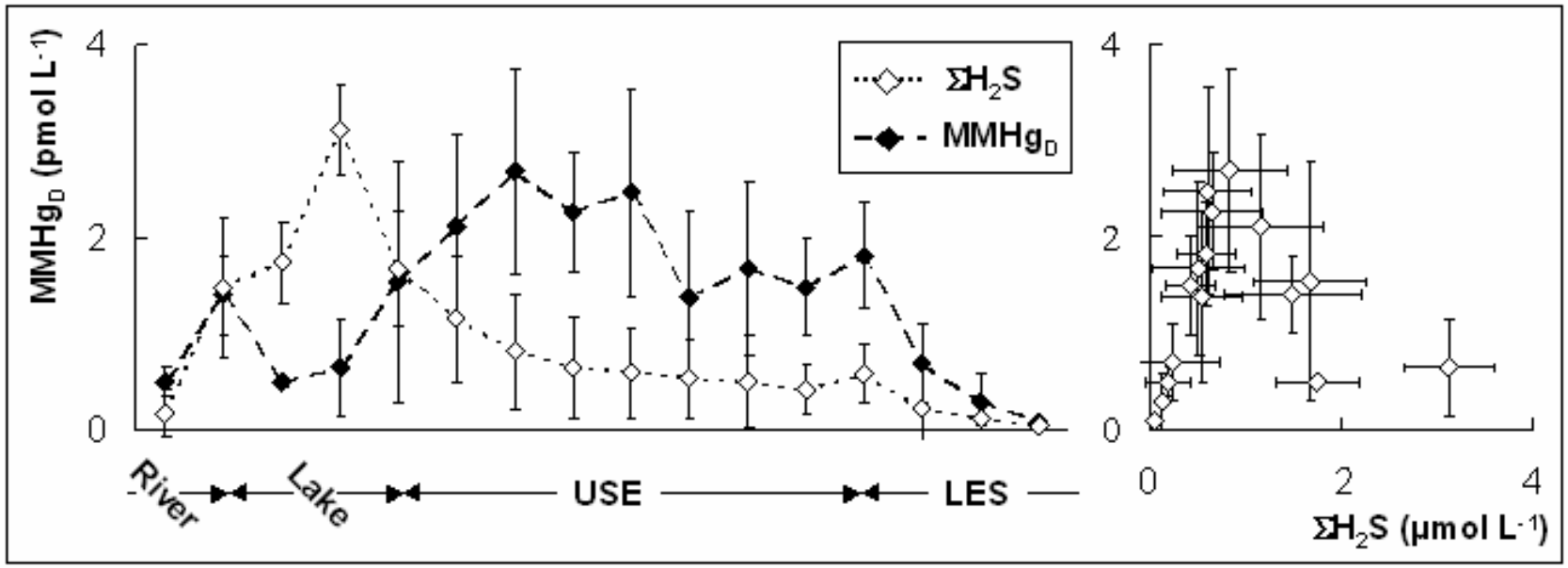

Fig. 10. Distribution and relationship of/between dissolved monomethyl mercury ($MMHg_D$) and sulfides (ΣH_2S) into the Petit-Saut reservoir / Sinnamary Estuary continuum. Figures were plotted using the average data set from the Matoutou 1, 2, 3, 4 and 5 campaigns.

Article IV

Modèle de spéciation du mercure dans les eaux naturelles

RESUME

Afin d'analyser la relation entre spéciation du mercure (Hg) et production de monométhylmercure (MMHg), les complexes du Hg et leur rôle dans la méthylation ont été modélisés au sein du continuum réservoir de Petit-Saut / estuaire du Sinnamary en Guyane Française. Les calculs de spéciation révèlent une distribution opposée des concentrations en complexes minéraux soufrés (eg., HgS^0, $Hg(SH)_2$, $HgS(SH)^-$, HgS_2^{2-}) à l'égard du MMHg. L'analyse en composantes principales indique que la transition entre mercure inorganique et méthylé s'effectue par l'intermédiaire de l'espèce non chargée $HgSO_4$. Ce résultat est compatible avec (i) l'hypothèse selon laquelle l'assimilation du Hg par les bactéries méthylantes a lieu par diffusion passive d'espèces électriquement neutres, et (ii) le fait qu'en milieu sulfurique les sulfates stimulent la production de MMHg. Par ailleurs, en considérant la production *in situ* de MMHg, nous avons émis l'hypothèse que la biodisponibilité de $HgSO_4$ est considérablement accrue aux interfaces rédox [*via* l'oxydation de HgS^0 par $Fe(OH)_3$]. Dans ces régions, la complexation de l'ion libre (Hg^{2+}) oscille entre ligands minéraux et organiques. Finalement, à partir de l'équilibre avec le soufre orthorhombique, la spéciation et la biodisponibilité du Hg ont été modélisées en présence de polysulfures. Les résultats montrent qu'introduire le soufre zéro-valent dans nos calculs limite la méthylation du Hg en substituant des composés chargés à faible $K_{O\text{-}W.}$ [ions HgS_nOH^- et $Hg(S_n)_2^{2-}$] aux espèces neutres plus labiles [$HgSO_4$, $HgClOH$, $HgCl_2$, $Hg(OH)_2$ etc.]. C'est pourquoi, la formation de

complexes Hg-polysulfures constitue d'avantage un puits géochimique qu'une source de Hg biodisponible pour les bactéries méthylantes.

Statut : en cours de soumission à « Ecological Modeling »

Modeling mercury speciation in natural waters

ABSTRACT

To probe the relationship between mercury (Hg) speciation and monomethylmercury (MMHg) production, the distributions of Hg complexes and their significance for methylation were studied in the anthropically perturbed Petit-Saut reservoir / Sinnamary Estuary continuum (French Guiana). Speciation calculations based on the "best available" thermodynamic database indicate that Hg-sulfides species [e.g., HgS^0, $Hg(SH)_2$, $HgS(SH)^-$, HgS_2^{2-}] are reversely related to MMHg concentrations. Principal components analyses also indicate that the passage from inorganic to methylated Hg is achieved through $HgSO_4$ neutral complex. This is consistent with (i) neutral Hg complex theory stating that mercurial uptake by methylating bacteria occurs through passive membrane diffusion and (ii) the fact that, in sulfidic environments, sulfates stimulate the MMHg production. From the *in situ* MMHg production, we hypothesize that $HgSO_4$ bioavailability is excessively enhanced at redox transient margins [presumably *via* $Fe(OH)_3$ induced HgS^0 oxidation]. In these regions, the free ion (Hg^{2+}) complexation shifts between inorganic and organic ligands. Finally, from the equilibrium with orthorhombic sulfur, mercury speciation and bioavailability were studied in presence of polysulfides. The results indicate that introducing zero-valent sulfur in our models contributes to diminish the Hg methylation by substituting low $K_{O-W.}$ ionic compounds [HgS_nOH^- and $Hg(S_n)_2^{2-}$ ions] to neutral and more labile species [$HgSO_4$, $HgClOH$, $HgCl_2$, $Hg(OH)_2$ etc.]. Formation of Hg-polysulfides complexes rather constitutes a sink for methylable Hg species than a source for methylating bacteria.

Keywords: Mercury, Model, Speciation, Iron, Sulfur

1. INTRODUCTION

The study of the metallic geochemistry and its associated mechanisms is becoming more and more mathematical (Boudreau 1997). This trend emerged from the rapid improvement of analytical techniques which granted access to a plethora of numerical data and subsequently conducted to the elaboration of so called integrative models (Levin et al., 1997). When applied to metallic geochemistry, models constitute some idealized mathematical tools that enable to extend the significance of field data beyond its prime value. From the total concentration of a metal, a complexation model shall compute some of its unmeasured or, in the actual state of the art, unmeasurable complexes (Twiss *et al.*, 2000). There remains, however, the question of the reliability of the gained results. The confrontation between several independent models is one way of verifying their common coherence. Another approach consists to analytically determine the modeled species or at least some of their proxies. In the trace metals case (picomolar level) such objective is barely achievable since certain complexes usually occupy less than 1 % of the metal itself. Ultimately, attentive examination of available data from the literature and active criticism regarding the model in/outputs shall provide the field and the limits of the mathematical description.

Metallic complexes are truly dissolved species (i.e., for which a chemical potential can be defined; Stumm and Morgan, 1996) and are expected to be present in any aqueous solution where free metal ions and charged compounds or neutral molecules possessing lone pairs (ligands) co-exist. For instance, metal complexation studies in natural waters are largely focused on association with organic carbon (DOC) and reduced sulfur (ΣH_2S) compounds. It is now generally accepted that complexation changes may considerably alter the speciation, cycling and bioavailability of numerous trace metals of environmental concern (e.g., Cu, Zn, Cd, Hg, Pb). Among those, mercury (Hg) complexation changes (governing partition between dissolved, particulate and gaseous phases along with biological uptake) are particularly

important. Its multiple valence states and chemical associations (with methyl, thiol or sulfide groups) are widely achievable in natural conditions (Baeyens and Leemarkers, 1998; Cossa and Gobeil, 1996; Coquery *et al*., 1997). Besides, Hg cycling involves biologically mediated processes such as reduction/oxidation or methylation/demethylation (e.g., Choi *et al*., 1994; Siciliano 2002). Organomercurial complexes (e.g., monomethylmercury MMHg ones) are species of greatest concern since they have the capacity to collect into organisms (bioaccumulate) and to concentrate up food chains (biomagnify).

Mercury methylation occurs chiefly within redox boundaries where it is thought to be mediated by sulfates reducing bacteria (SRB; Compeau and Bartha, 1985). According to Benoit *et al*. (1999), the availability of Hg for methylation is controlled by the concentration of neutral dissolved Hg complexes rather than the free ion (Hg^{2+}) or total dissolved (HgT_D) concentrations. Since methylation usually prevails in suboxic (sulfates reducing) conditions, the very high formation constants of Hg-S complexes conduced to propose HgS^0 as a pertinent candidate for microbial Hg uptake and ultimately its methylation (Benoit *et al*., 2001a). However, uncertainties of some of the earlier mercury thermodynamic data (Schwarzenbach and Widmer, 1963; Smith and Martell, 1976; Jay *et al*., 1999) and lack of sensitivity or analytical methods for measuring Hg complexes still led to contradictions among studies: the relationship between Hg speciation and its subsequent methylation remains unclear. HgS^0, like any other neutral Hg complex, composes only one of the many species for cellular uptake, but we lack proper evaluation of its relative importance, and we know little about the additional implications of remaining complexes (Golding *et al*., 2001; Page *et al*., 2004). Metal-ion binding modeling had already been demonstrated as a relevant approach for identifying speciation changes of multiple metals occurring simultaneously in natural waters (Taylor *et al*., 2005; Unsworth *et al*., 2006). These models that explicitly combine inorganic solution chemistry and humic ion-binding aid to formulate the concept of

geochemistry of metallic complexes, particularly *via* trace metal complexes concentration profiles that are sensitive indicators of hard-to-detect reactions involving organic matter (OM) and mineral substrata. Hence, when applied to mercurial geochemistry, they should provide critical information on MMHg production in relationship with Hg complexes distributions and measured redox conditions.

In this study, we report the distributions of main Hg complexes and their significance for methylation in the anthropically perturbed Petit-Saut reservoir / Sinnamary Estuary continuum in French Guiana (South America). The scrutinized water-body runs through 250 km of primary forest from the center of French Guiana towards the north where it spills into the Atlantic Ocean (Fig. 1). Its drainage basin spans over 7000 km² of crystalline formation. Between 1989 and 1994, the construction of the hydroelectric dam of Petit-Saut took place. The resulting reservoir (5°04' North, 53°03' West) stretches over 350 km² of uncleared forest and has a maximum depth of 35 m (Huynh *et al*., 1997). Local discharge of elemental Hg to the Petit-Saut reservoir originates principally from the upstream gold-mining area of Saint Elie. The rejected amount of Hg since the last century was (under)estimated to approximately 23 tons (Petot, 1993). In the reservoir, the water-body underwent rapid establishment of an oxygenated epilimnion (down to 5 m depth) and an anoxic hypolimnion (Richard, 1996). The hypolimnion exhibited elevated concentrations of reduced elements (ammonium, sulfides, phosphates, etc.) due to OM degradation and mobilization from the geological substratum (iron, manganese, silica, etc.). The Sinnamary Estuary is a 70 km length macrotidal estuary that develops a high turbidity zone (HTZ) coincidental with the first km of the salt intrusion. Its oceanic end-member consists of the Amazon plume while its freshwater extremity is mainly composed by the hypolimnetic water outflowing from the Petit-Saut reservoir. In order to maintain the dissolved oxygen concentrations compatible with aquatic life, an aeration system was set up in the outflow of the turbines. This system triggered the build up of marked

concentration gradients for several reduced compounds such as dissolved iron and methane. The main characteristic of this system is the high concentrations of OM, Fe, sulfides (ΣH_2S) and MMHg in the hypolimnion of the reservoir and the downstream Sinnamary Estuary (Coquery *et al*., 2003; Muresan *et al*., submitted). Here, we use measured concentrations of total Hg and MMHg in combination with modeled Hg and MMHg complexes concentrations to: (i) determine the Hg and MMHg complexation with inorganic and organic ligands, (ii) probe the role of neutral mercury-sulfide complex, HgS^0, in controlling the Hg methylation (iii) formulate an alternative mechanism linking the Hg complexation to its subsequent methylation. We use the Benoit *et al*. (1999) neutral complex theory in combination with Fe and ΣH_2S data, to support the Hg complexation changes and the modeled mechanisms of Hg methylation.

2. METHODS

2.1. Sample collection

Samples from the Petit-Saut reservoir / Sinnamary Estuary continuum were all but collected during five main campaigns that took place in March-April 2003, January-February 2004, May-June 2004, November-December 2004 and February-March 2005. The sequence between *in situ* campaigns, designated respectively as Matoutou 1, 2, 3, 4 and 5, reflects the major seasons of the guianese climate: the short wet season (from November to February), the short dry season (from February to April), the long wet season (April to July) and the long dry season (from July to November). In the Petit-Saut reservoir, the main sampling station (noted CR for “Center of the Reservoir”) characterizing the average lake waterbody was located in the pre-flood riverbed of the Sinnamary River (4°56.382’N - 53°02.610’W). At the CR site, water-column usually exceeds 20 m depth and displays a sharp and permanent stratification

(Richard *et al*., 1997). During the Matoutou 1 to 3 campaigns, water-column measurements for OM, Fe, SO_4, ΣH_2S and PO_4 were carried out simultaneously to that of Hg. In the Sinnamary Estuary (Fig. 1), water samples were consistently collected starting from the tailrace of the dam (5°03.89'N - 53°02.85'W) downstream to the Amazon plume of particles (5°30.94'N - 53°07.92'W). The location, sampling periods and main geochemical characteristics of every sampled station are provided in detail in Richard (1996) and Muresan *et al*. (submitted). To be consistent with those papers, we choose to call the tidal estuary Upper Sinnamary Estuary (USE) and the saline estuary the Lower Sinnamary Estuary (LES). Finally, to compare with a station remote from the direct LES influence, marine samples were collected during Matoutou 2 and 5 campaigns near the "îles du Salut". Those islands are located *circa* 15 km North, offshore from the city of Kourou (5°16.60'N - 52°35.11'W). Despite the distance with the continent, the corresponding station (noted IS) remained under the influence of the suspended particulate matters (SPM) forming the Amazon plume.

The ultra clean sampling techniques applied for water collection and storage are those presented and discussed in detail by Gill and Fitzgerald (1985), Bloom (1989), Quémerais and Cossa (1997), and Cossa *et al*. (2002 and 2003). In brief, subsurface water samples [20 cm below the air-water interface (AWI)] were collected in acid-cleaned Teflon (FEP) bottles held by hand worn polyethylene gloves. A peristaltic pump and acid-cleaned polypropylene tubing were employed for the deeper water-column. The bottles were rinsed three times, filled, tightly capped and double-bagged, then transported in coolers back to the dam adjacent field laboratory (HYDRECO). Measurements of OM, Fe, SO_4, ΣH_2S, PO_4 and Hg were processed the same day. The sum of all mercury species (HgT) was measured on unfiltered and filtered samples and thus noted respectively HgT_{UNF} and HgT_D. Aliquots were kept to determine MMHg in the unfiltered ($MMHg_{UNF}$), dissolved ($MMHg_D$) and the particulate ($MMHg_P$) phases. The water samples were filtered on LCR and/or Sterivex 0.45 µm membranes; the

LCR membranes are Teflon made while Sterivex membrane consists of hydrophilic PVDF. No significant differences in HgT_D or $MMHg_D$ concentrations were observed between the two materials, upon the condition of discarding the first 20 mL of filtrate. For each sample, filtered amount of water was gravimetrically determined then acidified with 1 % (v/v) Suprapur® HCl. Filters (containing the particulate samples) and corresponding filtered solutions were double bagged and stored at –20 °C in dark conditions until analyzed.

2.2. Analyses

2.2.1. Ancillary parameters – Measurements for major elements were carried out at the HYDRECO field laboratory. In short, total organic and inorganic carbon in the unfiltered (orderly TOC and TIC) and the filtered (orderly DOC and DIC) samples were analyzed by IR spectroscopy after oxidative and/or acidic treatment of the samples. The concentrations of total sulfide (ΣH_2S) and dissolved (<0.45 µm) phosphates (PO_4) and iron (FeT_D) were colorimetrically measured by means of specific photometric test kits (Spectroquant®, Merck). The sulfates (SO_4) content of water was subsequently determined by nephelometry according to Richard *et al*. (1997). Concerning ΣH_2S, 4 ml of water poured from the collection tubing were added to 6 ml of a $ZnCl_2$ trapping solution. Samples were transported to the field laboratory then methylene blue method was applied. For PO_4 determination, a colored chemical complex is formed when adding, in sulfuric conditions, molybdate then ascorbic acid to 10 mL of filtered water sample. Regarding FeT_D, around 2 L of water were collected paying great attention to minimize the headspace of the bottle. After filtration under nitrogen atmosphere, 10 mL of solution were colorimetricaly analyzed. Colored reaction consists in synthesizing an iron red-violet complex as reduced Fe^{II} encounter a triazine derivative in a thioglycolate-buffered medium. To minimize the ΣH_2S oxidation artifacts, SO_4 concentrations were determined in the filtrated water samples initially collected for FeT_D measurements. Sulfate ions react with barium ions to form slightly soluble barium sulfate. The resulting

turbidity is photometrically measured in 10 mL of tested solution within 3-4 hours after collection (turbidimetric method).

2.2.2. Mercury speciation -- All mercury forms in water were detected by cold vapor atomic fluorescence spectrometry (AFS). Total Hg in unfiltered (HgT_{UNF}) and in filtered (HgT_D) samples was determined in compliance with Bloom and Fitzgerald (1988), by the formation of volatile elemental Hg (released by $SnCl_2$ reduction, after 30 minutes of acidic BrCl oxidation, and its preconcentration on a gold column). The detailed procedure is given by Cossa *et al*. (2003). The detection limits, defined as 3.3 times the standard deviation of the blanks, was 0.05 pmol L^{-1} while the reproducibility (the coefficient of variation in percentage of five replicate samples) was lower than 10 %. Monomethylmercury was determined using the method initially proposed by Bloom (1989) and modified by Liang *et al*. (1994) and Leermarkers *et al*. (2001); it was extracted by CH_2Cl_2 from acidified unfiltered ($MMHg_{UNF}$) and filtered ($MMHg_D$) samples and then transferred into 40 mL of deionized water (Milli-Q water) by evaporating the organic solvent. The resulting aqueous solutions were analyzed for MMHg by gas chromatography after ethylation and adsorption/desorption on a Tenax® column. Detection limit was 0.01 pmol L^{-1} for a 100 mL water sample while precision was better than 10 %. The accuracy was tested using the available reference material (IAEA-405) and MMHgCl prepared solutions as internal standards; the recovery was 91 ± 8 %.

2.3. Calculation of filtered methylated and unmethylated Hg speciation

Complexation of Hg in the Petit-Saut reservoir / Sinnamary Estuary continuum was calculated with the “Windermere Humic Aqueous Model” (WHAM 6; Tipping 1994, 1998). In the WHAM 6 approach, humic compounds are represented by hypothetical size-homogenous, rigid, molecules, which carry proton-dissociating groups that can bind metal ions either singly or as bidentate pairs. The interactions are described in terms of intrinsic equilibrium constants and electrostatic terms. Inputs to the WHAM 6 model consisted of the

average pH and total dissolved concentrations of Na, Mg, Al, K, Ca, NH_4, Mn, Fe (Fe^{II} and Fe^{III}), HgT_{UNM}, MMHg, Cl, SO_4, CO_3, PO_4, ΣH_2S, humic (HA) and fulvic (FA) acids measured at each depth (or station). Concentration data for Na, Mg, Fe^{III}, Al, K, Ca, NH_4, Mn and Cl were taken from the HYDRECO 1994 to 2005 chemical monitoring. The HYDRECO field laboratory was set up by "Electricity of France" (EDF), the Petit-Saut dam builder, in order to survey the geochemistry of major elements in the reservoir. HgT_{UNM} stands for unmethylated Hg and was calculated as the difference between HgT_D and $MMHg_D$. The concentrations of HA and FA were estimated from DOC measurements by assuming that dissolved OM contains 50% C (Buffle, 1988) and that all DOC is humic substances with a ratio of [HA] : [FA] of 9 : 1 (Malcolm, 1985; Tipping, 1998; Gallon *et al*., 2004). The existing WHAM 6 thermodynamic database (NIST 2003) was updated with the equilibrium constants given in Table 1 for Hg-polysulfide and sulfide complexes. Additional thermodynamic data for MMHg are presented in Table 2: its intrinsic equilibrium constant (K_{MA}) and associated number of strong binding sites ($\Delta L K_2$) with humic substances were adjusted using the metal-lactic acid ($\log K_{MA} = 2.6$) and metal-NH_3 ($\Delta L K_2 = 3.3$) method suggested by Tipping (1998). Finally, the coherence of the gained results was tested by confronting WHAM 6 to the ECOSAT equilibrium speciation model. The ECOSAT model is a combination of the "non-ideal competitive adsorption" (NICA) isotherm description of binding to heterogeneous material, and the Donnan electrostatic sub-model in which humic substance is assumed to behave as a gel with a homogenous charge and potential distribution (Benedetti *et al*., 1995; Kinniburgh *et al*., 1996; Milne *et al*., 2003). Once its thermodynamic database updated, the ECOSAT results were in the 85 % confidence interval of the WHAM 6 concentrations.

3. RESULTS AND DISCUSSIONS

3.1. Mercury speciation in the dissolved phase

3.1.1. Relationships between HgT_{UNM}, DOC and sulfides

In 10 years of flooding (1995-2005), Hg inputs to the Petit-Saut reservoir were (under)estimated to *circa* 8000 moles (i.e., 1.6 tons Hg, Muresan *et al*., submitted), of which ~ 60 % corresponded to the degradation of the originally immerged OM (vegetation + fauna). Recently (2003-2005), further investigations were carried on the HgT_{UNM} *versus* DOC relationship (Fig. 2). The significant ($p \leq 0.05$) positive correlation ($r^2 = 0.44$; n = 151 and $[HgT_{UNM}]_{pmol\ L\text{-}1} = 30\ [DOC]_{mmol\ L\text{-}1} - 7.6$) indicate that, ten years after the dam impounding completion, DOC keeps on acting as a source and/or mobilizing agent (Ravichandran *et al*., 1998 and 1999) for HgT_{UNM}. This was supported by the fact that, ~ 20 % of the annual Hg inputs (around 100 moles yr^{-1}) still originate from the flooded soil and vegetation (Muresan *et al*., submitted). To discriminate between source and mobilization, we calculated the amount of HgT_{UNM} brought in 1 L solution by 0.41 ± 0.07 mmol of DOC (average concentration in the system). Assuming a homogeneous distribution of Hg between DOC and POC (Particulate Organic Carbon; close to 0.9 nmol g^{-1} HgT_{UNM}), the DOC contribution reaches ~ 87 % of the average HgT_{UNM} water concentration (around 5 ± 3 pmol L^{-1}). Comparatively, the HgT_{UNM} concentrations at equilibrium with cinnabar, $HgS_{(s)}$, [$Ks = 10^{52.1}$; Schwarzenbach and Widmer (1963)] in presence of 1 µmol L^{-1} sulfides and at 5.6 of pH (average values in the system), barely exceeds 1 pmol L^{-1}. Thus, in this particular milieu, the DOC catalyzed HgT_{UNM} mobilization (enhanced production of HgT_{UNM} during the dissolution of cinnabar) seems minor relatively to the DOC intrinsic source.

The nature of Hg bindings to DOC was scrutinized by (i) determining the HgT_{UNM} *versus* ΣH_2S relationship shown in figure 2 and (ii) modeling the main HgT_{UNM} complexes in

the Petit-Saut reservoir. In the first step, we observed a close to linear increase of ΣH_2S with DOC ($r^2 = 0.62$; n = 131), indicating a good relationship (Fig. 2) between the sulfidic and HgT_{UNM} contents of DOC ($r^2 = 0.35$; n = 131 and $[HgT_{UNM}]_{pmol\ L\text{-}1} = 2.3\ [\Sigma H_2S]_{\mu mol\ L\text{-}1} + 2.8$). From the interrelated DOC / ΣH_2S / HgT_{UNM} distributions and the high Hg affinity for sulfide and thiolate ligands (Benoit *et al.*, 1999, 2001b; Lamborg *et al.*, 2003), we presumed that HgT_{UNM}-DOC binding may principally occur though sulfur containing groups. To validate this hypothesis, the WHAM 6 and ECOSAT models were applied to the water-column profiles of HgT_{UNM} from the CR station. The modeled concentrations of relevant HgT_{UNM} complexes (i.e., Hg^{2+}, HgClOH, $HgSO_4$, HgS^0 and HgT_{UNM}-DOC) are given in Table 3 as a function of depth. Computed profiles indicate that in the epilimnion of the reservoir HgT_{UNM}-DOC is the dominant specie (> 99 % of HgT_{UNM}) whereas HgClOH (most abundant inorganic complex) is around 10^{-30} M (around 10^6 HgClOH molecules for the whole lake epilimnion). Once into the reservoir hypolimnion (below 5 m depth), a drastic shift affects the HgT_{UNM} complexation to the benefits of sulfide ligands. Excluding, at this point of the study, the Hg-polysulfide complexes, HgS^0 seems to dominate the speciation of HgT_{UNM} (around 95 % of the total). Concurrently, the HgT_{UNM}-DOC contribution declines to < 4% HgT_{UNM} while HgClOH concentration reaches below 10^{-33} M (close to 10^3 HgClOH molecules for the whole lake hypolimnion). Despite the existence of HgS^0 remains controversial (Zhang and Wang, 2004), modeled data is consistent with Benoit's theory stating that HgS^0 is the dominant neutral dissolved complex in sulfidic environments (Benoit *et al.*, 1999).

In chapter one, we calculated that OM may occupies a large fraction (> 80 %) of the reservoir HgT_{UNM} pool of complexes. In chapter two, we also determined that Hg-S occupy > 95 % of the HgT_{UNM} pool of complexes. To bring together both observations, we presume that sulfur controls the HgT_{UNM} speciation as well in oxygenated (*via* DOC sulfur containing

groups: seemingly thiols) as in sulfidic (*via* the formation of Hg-sulfide species) environments.

3.1.2. Relationships between $MMHg_D$, DOC and sulfides

The MMHg present in the water-column originates both from mobilization of the degrading soil / vegetation and *in situ* methylation processes (Muresan et al., submitted). In a first step, let us consider the role of OM as a source of MMHg to the system. When plotted against DOC, $MMHg_D$ concentrations displayed a decreasing relationship ($r^2 = 0.28$; n = 151 and $[MMHg_D]_{pmol\ L\text{-}1} = -11\ [DOC]_{mmol\ L\text{-}1} + 6.5$) indicating that net $MMHg_D$ production (i.e. methylation minus demethylation) is lowered at high DOC levels (Fig. 2). Superimposed to the positive evolution with HgT_{UNM}, DOC rather defines a scavenging agent for potential MMHg antecessors (e.g., Hg^{2+}, HgClOH, $HgSO_4$, HgS^0 etc.) than a direct source for methylated species. To confirm this assumption, we calculated the amount of MMHg brought in 1 L solution by 0.41 ± 0.07 mmol of DOC (average concentration in the system). Assuming a homogeneous distribution of MMHg between DOC and POC (close to 0.13 nmol g^{-1} MMHg), the DOC contribution reaches < 50 % of the average $MMHg_D$ concentration (around 1.5 ± 0.8 pmol L^{-1}). This value represents a maximum: it does not take into account the MMHg demethylation during OM degradation. Since DOC is not necessary the main source of $MMHg_D$, the endogenous methylation of HgT_{UNM} was investigated through the parallel study of $MMHg_D$ and ΣH_2S concentrations. The bulge shape of the $MMHg_D$ *versus* ΣH_2S relationship suggested an optimum sulfide concentration for mercury methylation (Fig. 2). Sites of low and intermediate ΣH_2S concentrations (< 1 µmol L^{-1}) exhibited analogous variations of both parameters ($r^2 = 0.48$; n = 100 and $[MMHg_D]_{pmol\ L\text{-}1} = 3.3\ [\Sigma H_2S]_{\mu mol\ L\text{-}1} + 0.4$). This is consistent with the hypothesis of neutral Hg-sulfides complexes controlling the bioavailability of inorganic mercury towards SRB (Benoit *et al.*, 2001a, 2003). On the contrary, more sulfidic environments (ΣH_2S > 1 µmol L^{-1}) exhibited inverse variations

between $MMHg_D$ and ΣH_2S concentrations (r^2 = 0.30; n = 56 and $[MMHg_D]_{pmol\ L\text{-}1}$= -0.5 $[\Sigma H_2S]_{\mu mol\ L\text{-}1}$ + 2). This would account for a lessening in Hg bioavailability due to formation of ionic Hg-sulfides complexes or precipitation as cinnabar. Finally, from the Petit-Saut reservoir net production of $MMHg_D$ (around 0.11 % L^{-1} d^{-1} HgT_D; Muresan *et al*., submitted), and residence time of water masses (close to 6 month), the contribution of endogenous methylation mechanisms approaches 60 % (i.e., ~ 1 pmol L-1) of the average $MMHg_D$ water concentration.

Using available data from the literature (Table 2), the intrinsic equilibrium constants of MMHg (K_{MMHg}) and HgT_{UNM} (K_{Hg}) with inorganic ligands were found to correlate positively (Fig. 3). The gained correlation [or LFER for Linear Free-Energy Relationship; Dzombak and Morel, (1990)] suggests that, concerning inorganic ligands (e.g., I^-, Br^-, Cl^-, OH^-, CO_3^{2-}, SO_4^{2-}, HS^-), methylated and unmethylated Hg follow analogous sequences of complexation. Hence, using the K_{MMHg} updated version of WHAM 6 model, the concentration profiles of main $MMHg_D$ complexes (i.e., $MMHg^+$, MMHgCl, $MMHgSO_4^-$, $MMHgS^-$ and MMHg-DOC) were calculated in the water-column of the Petit-Saut reservoir (Table 3). $MMHg_D$ in the epilimnion of the reservoir is essentially composed by MMHg-DOC (> 99 % of the total) whereas MMHgCl (the most abundant inorganic complex) is around 10^{-20} M (around 10^4 MMHgCl molecules per liter). Entering the water-column hypolimnion, the MMHg-DOC contribution to the whole pool of $MMHg_D$ tends to fade out (from > 99 to 80 %) but still prevails. This is in accordance with Choe and Gill (2003) observations: accordingly, only a fraction of OM rather than the bulk controls $MMHg_D$ concentration. Thermodynamic calculations by Zhang and Wang (2004) consistently revealed that in anoxic environments, thiols play a negligible role in the inorganic Hg speciation but can dominate that of MMHg. Unlike HgT_{UNM}, the hypolimnetic contribution of MMHg-sulfide complexes only occupies ~ 19 % of $MMHg_D$ (90 % as $MMHgS^-$) whereas the MMHgCl concentrations reach up to 10^{-16}

M (close to 0.1 ‰ of $MMHg_D$). In a general way, modeled MMHg-halide complexes display higher concentrations than HgT_{UNM} ones (respectively 10^{-16} and 10^{-29} M). Such a shift, also apparent when considering the free ion concentrations ($MMHg^+ \sim 10^{-18}$ *versus* $Hg^{2+} \sim 10^{-39}$ pmol L^{-1}), suggests a lesser affinity of methylated Hg towards sulfur containing groups. This is confirmed by the intrinsic stability ranges of MMHg and Hg with organic (10^{14-18} *versus* 10^{25-34}) and reduced (10^{21} *versus* 10^{40}) sulfur recently reported in the literature (NIST 2003).

3.2. Mercury speciation and methylation

3.2.1. Role of major dissolved species

There are insufficient available data to fully evaluate the natural pool of ligands and their competing effects on Hg methylation, yet proper trends can be reproduced by the model (Han *et al.*, 2006). Relationships between $MMHg_D$ and main dissolved species (ligands and complexes) were therefore scrutinized using modeled and (when accessible) measured concentrations. Considered species, including concentration ranges and associated correlation coefficients with $MMHg_D$ are summarized in Table 4. Let us now consider the individual the role of (i) POC, (ii) DOC and (iii) Fe^{III} and SO_4.

(i) In the particulate, POC was found to be positively correlated with $MMHg_D$ ($r^2 = 0.37$; n = 98 and $[MMHg_D]_{pmol\ L\text{-}1} = 0.12\ [POC]_{mmol\ g\text{-}1} + 0.3$) indicating that organic content from SPM could drive the local distribution of $MMHg_D$. Such a correlation between OM in the solid and $MMHg_D$ levels (or Hg methylation kinetics) was previously reported in estuarine (Choi and Bartha, 1994; Hammerschmidt *et al.*, 2004; Hammerschmidt and Fitzgerald, 2006) and freshwater (Pak and Bartha, 1998) sediments. It is generally accepted that the amount of bacteria at the OM enriched particle surfaces exceed that in the water bulk (Crump *et al.*, 1998). In the present system, substantial SRB populations were measured in biofilms and high SPM regions of the water-column (Jorand pers. com.; Dumestre *et al.*, 1999, 2001) which usually collocated with marked $MMHg_D$ levels (Muresan *et al.*, submitted). Since,

endogenous methylation processes (Section 3.1.2.) prevail on MMHg mobilization from the organic substrata (respectively > 60 and < 40 % of $MMHg_D$ production), POC not only constitutes a privileged substratum for Hg methylation but also defines a major reservoir for newly produced $MMHg_D$.

(ii) In the filtered, high loads of DOC complexes (with the notable exception of Fe^{III} and SO_4 ones) result in low $MMHg_D$ levels (Table 4 and Section 3.1.2.) and elevated HgT_{UNM} concentrations (Section 3.1.1.). Hence, increasing DOC concentrations (as organic complexes, colloids or clusters) would either improve MMHg demethylation and/or inhibit Hg methylation. Since mature DOC molecules are generally too large to cross the cell membrane of bacteria methylation, complexation with dissolved OM generally limits the amount of inorganic mercury available for uptake by methylating bacteria (Winfrey and Rudd, 1990; Gilmour and Henry, 1991; Miskimmin *et al*., 1992; Choi and Bartha, 1994; Barkay *et al*., 1997; Kelly *et al*., 2003). On the other hand, DOC-mediated reduction of MMHg to Hg^0 would reflect the formation of organic free oxidants through the photolysis of DOC complexes (Zhang and Lindberg, 2001) that in turn form the hydroxyl free radical (·OH) capable of breaking the organometallic bond (Sellers *et al*., 1996; Gårdfeldt *et al*., 2001).

(iii) In presence of reduced iron and sulfur, $MMHg_D$ was positively related to Fe^{III} and SO_4 compounds (Table 4). Maxima of total Fe^{III} and SO_4 concentrations (orderly 16 ± 8 and 10 ± 3 µmol L^{-1}) typically corresponded to the redox transient (from 150 to 400 mV) region of the Sinnamary Estuary (Muresan *et al*., submitted). Indeed, elevated and stable Fe^{II} and ΣH_2S concentrations, as for the hypolimnion of the Petit-Saut reservoir, limited the $MMHg_D$ production (Table 4) to most peripheral sites such as oxycline and/or sediment-water interface (Muresan *et al*., under submission). This suggests that pronounced $MMHg_D$ levels (and presumably Hg methylation rates) preferentially occur in the margin between Fe^{III} and SO_4 reducing zones.

From section (i) we concluded that Hg methylation principally occurs at the surface of OM enriched particles. Previous works (e.g., Benoit *et al*., 2001a) showed that a solid-phase is required to stimulate the Hg bioavailability in pure-culture methylation essays. According to section (ii), the ability of DOC to strongly bind mercuric complexes seemingly inhibits the Hg methylation by preventing its transfer to the particulate phase and/or uptake by organisms. At low pH values (locally 5.6 ± 0.2 units), electrostatic repulsions tend to limit the agglomeration and coagulation of organic colloids (Stumm and Morgan, 1996). The DOC would also improve the MMHg demethylation through photolytic formation of hydroxyl free radical. Ultimately, regarding section (iii), Hg methylation preferentially occurs in redox transient domains where Hg speciation shifts between DOC and ΣH_2S complexes.

3.2.2. Role of Hg complexes

As discussed previously, maxima of methylation usually correspond to redox transient domains where DOC competes with ΣH_2S for Hg binding. Modeling Hg complexation in our system, we observed a budge in Hg-inorganic contribution when destabilizing the Hg-sulfide bond; e.g., $HgSO_4$ stepped from 10^{-43} to 10^{-21} M at the hypo / epilimnion interface of the reservoir. In addition, unlike predictions, the whole pool of Hg-sulfide complexes (i.e., HgS^0, $Hg(SH)_2$, $HgS(SH)^-$, HgS_2^{2-}) displayed inverse evolutions with $MMHg_D$ (Table 4). Those observations challenge the general hypothesis stating that HgS^0 is principal neutral dissolved complex affecting microbial uptake and methylation (Benoit *et al*., 1999). Actually, recent studies have demonstrated that several neutral species (such as HgS_5^0 or $HgSO_4$) have a significant impact on the mercury methylation in sulfidic waters (Paquette and Helz, 1997; Jay *et al*., 2000 and 2002; Bloom and Preus, 2003).

Figure 4 shows the scaled Principal Components Analysis (or PCA) for chemical compounds A) and associated mercury complexes B) in the Petit-Saut reservoir / Sinnamary Estuary continuum. The PCA is a classical statistical method that detects structure in the

relationships between variables. Each point of the graphs regroup 18 modeled or measured (in triplicate) concentrations.

Reported data on chemical compounds clearly dissociates $MMHg_D$ from HgT_{UNM}, the principal discriminating factor (F_1 axis) being whether or not redox is variable (Fig. 4.A.). A secondary factor (F_2 axis), namely the oxygen depletion, enables the monitoring of oxidative conditions among sampling stations. Hence, Hg speciation in the water samples from stations displaying low and stable redox (e.g. hypolimnion of the reservoir) is mostly dominated by HgT_{UNM} (around 84 ± 9 % of HgT_D). In those particular conditions, HgT_{UNM} concentrations were significantly related to ΣH_2S, DOC, DIC and to a lesser extent to Fe^{II} and aluminum levels. To the opposite, redox transient stations displayed high $MMHg_D$ concentrations (around 37 ± 4 % of HgT_D) in relationship with Fe^{III}, SO_4, Cl and marginally Hg^{2+} and manganese levels. Thereby, $MMHg_D$ was reversely related to HgT_{UNM} ($r^2 = 0.41$; n = 18 and $[MMHg_D]_{moles\ L\text{-}1} = -0.3\ [HgT_{UNM}]_{moles\ L\text{-}1} + 3\ 10^{-12}$) but exhibited a "X" shape when plotted against Hg^{2+} ($[MMHg_D]$ junction around $7\ 10^{-40}$ M of Hg^{2+}). It is noteworthy that such low $[Hg^{2+}]$ values rather depict the Hg^{2+} aptitude for complexation (presently as MMHg) than actual free ion concentrations. MMHg production in aquatic systems is seldom a simple function of total Hg concentrations (EPRI, 2003) and is influenced by a wide variety of environmental factors (redox, bacterial community, presence of inorganic and organic complexing agents etc.). Reported data yet allow to refine the Hg methylating conditions: (i) reductive waters (presence of reduced Fe and S) of intense OM mineralization (low DOC/DIC ratios) and complexation (e.g., with Al colloids) support high HgT_{UNM} concentrations whereas, (ii) more oxidative (presence of oxidized Fe and S) waters of moderate organic content (intermediate Hg^{2+} levels) enhances $MMHg_D$ concentrations.

To identify the specific influence of Hg complexes on methylation mechanisms, we applied the PCA technique (Fig. 4.B.) to relevant HgT_{UNM} and $MMHg_D$ complexes (with OM,

ΣH_2S, SO_4, and CO_3). Since Hg complexation with Cl and OH ligands (e.g., HgClOH or MMHgCl) barely reflects the redox transient mechanisms (such as OM mineralization and/or sulfate reduction) we chose to neglect its local contribution. Along with their global pool (Fig. 4.A.), HgT_{UNM} and $MMHg_D$ complexes separately distributed on both sides of the F_1 axis (margin between stable and variable redox domains). This suggests that ongoing geochemical processes identically affect the sum of all Hg (or MMHg) species and any individual Hg (or MMHg) complex. Stepping from negative to positive F_1 coordinates (i.e., from the Petit-Saut artificial lake to the Sinnamary Estuary) an uninterrupted sequence of Hg complexes unites HgT_{UNM} to $MMHg_D$. This orderly consists of HgS^0, $HgHCO_3^+$, Hg^{2+}, $HgSO_4$ then $MMHg^+$, $MMHgSO_4^-$, $MMHgCO_3^-$, and $MMHgS^-$. The passage from inorganic to methylated Hg is achieved through $HgSO_4$ neutral complex and MMHg free ion. Specifically, the measured $MMHg_D$ (and modeled $MMHg^+$) concentrations were linearly related to the $HgSO_4$ calculated ones ($r^2 = 0.44$; n = 18 and $[MMHg_D]_{moles\ L\text{-}1} = 6\ 10^{29}\ [HgSO_4]_{moles\ L\text{-}1} + 8\ 10^{-13}$; Fig. 5). This conforms to the neutral Hg complex theory and the fact that, in presence of ΣH_2S, sulfates stimulate MMHg production (Gilmour *et al.*, 1992, Gilmour and Riedel, 1995; Branfireun, 1999). Yet, in contrast with Benoit's formulation (Benoit *et al.*, 1999, 2001a), the measured $MMHg_D$ (and modeled $MMHg^+$) opposes to the calculated HgS^0 ($r^2 = 0.48$; n = 18 and $[MMHg_D]_{moles\ L\text{-}1} = -0.3\ [HgS^0]_{moles\ L\text{-}1} + 3\ 10^{-12}$) concentrations.

3.2.3. $HgSO_4$ and Hg methylation

Because the stability constants for Hg^{2+} complexation with oxidized and reduced sulfur are distant by several orders of magnitude (orderly $10^{2.4}$ and $10^{43.8}$ at I = 0), $HgSO_4$ appears inappropriate for HgT_{UNM} uptake by SRB. Its low concentrations (around 10^{-43} M) and membrane permeability ($P \sim 5.2\ 10^{-4}$ cm s^{-1}), as calculated from the octanol-water partition coefficient ($K_{O\text{-}W.} = 0.98$; SRC logKow program, Meylan and Howard, 1995), hardly support the observed $MMHg_D$ production ($\sim 10^{-21}$ moles $cell^{-1}$ d^{-1}, Dumestre *et al.*, 2001;

Muresan *et al*., submitted). The average cellular uptake rates by passive diffusion for HgS^0 and $HgSO_4$ being 10^{-18} and 10^{-51} moles $cell^{-1}$ d^{-1} respectively (Mason *et al* 1996; Benoit *et al*., 2001a, Jay *et al*., 2002). Interestingly, HgS^0, the dominant neutral complex in solution, was found sufficient to support the $MMHg_D$ production thus confirming its source position for methylable HgT_{UNM} complexes. Besides, modeled $HgSO_4$ concentrations fairly reflected the methylating ability of SRB (Section 3.2.2.) but barely accounted for methylated amounts. We thus concluded that either (i) $HgSO_4$ uptake by passive diffusion can not be fully assumed or (ii) that $HgSO_4$ production is enhanced in redox transient environments (presumably *via* out of equilibrium reduced sulfur Hg complexes oxidation). An attentive study of the HgT_{UNM} complexation at the hypo / epilimnion interface showed that $HgSO_4$ magnifies from 10^{-43} to 10^{-21} M when OM destabilizes the Hg-sulfide bond. Additionally, $HgSO_4$ steps from 10^{-21} to 10^{-16} M when concurrently decreasing ΣH_2S from 10^{-11} to 10^{-12} M (calculated values). Thereby, a 5 % oxidation of HgS^0 to $HgSO_4$ would provide the necessary $HgSO_4$ amount corresponding to the actual $MMHg_D$ production. The out of equilibrium (i.e. biologically catalyzed) mechanisms and intense S cycling (sharp ΣH_2S and SO_4 gradients) associated to MMHg production support those calculations.

The formation of $HgSO_4$ at redox transient boundaries can be formulated using the bacterial leaching of metal sulfides (Schippers and Sand, 1998). These processes are outlined in the following equations:

$$HgS^0 + Fe^{3+} + H^+ = Hg^{2+} + 0.5\ H_2S_n + Fe^{2+} \quad (n > 1) \qquad (1)$$

$$0.5\ H_2S_n + Fe^{3+} = 0.125\ S_8 + Fe^{2+} + H^+ \qquad (2)$$

$$0.125\ S_8 + 1.5\ O_2 + H_2O = SO_4^{2-} + 2H^+ \qquad (3)$$

$$Hg^{2+} + SO_4^{2-} = HgSO_4 \qquad (4)$$

The overall reaction can be written as

$$HgS^0 + 2Fe(OH)_3 + 1.5O_2 + 4H^+ = HgSO_4 + 2Fe^{2+} + 5H_2O \quad (5)$$

Accordingly, $Fe(OH)_3$ oxidizes the HgS^0 of water in presence of DOC. Two sulfates reducers had already been found to grow *via* reduction of iron (Tebo and Obraztsova, 1998), with *D. propionicus* strain 1pr3 specifically being able to grow with ferric oxyhydroxides as an oxidant (Holmes *et al*., 2004). To probe this mechanism we plotted the log ($[HgSO_4]$ / $[HgS^0]$) ratio as a function of log ($[Fe(OH)_3]$ / $[Fe^{2+}]$) ratio. The observed linear relationship {$r^2 = 0.51$; n = 18 and log ($[HgSO_4]$ / $[HgS^0]$) = 0.4 log ($[Fe(OH)_3]$ / $[Fe^{2+}]$) – 29; Fig. 5} suggests that, in sulfidic conditions, the more Fe is present as hydrous oxides, the more $HgSO_4$ is formed from HgS^0. Discrepancy between the actual (0.4) and theoretical (1) slope values seemingly originates from the fact that actual is an integrated view of water column (mostly at equilibrium) whereas theoretical is restricted to the out of the equilibrium redox transient area. From intercept and pH values, the log reaction constant was calculated to ~ 60 ($\Delta_r G^0$ around -340 kJ $mole^{-1}$). As an element of comparison, this roughly corresponds to the standard free energy for abiotic nitrification (of about -350 kJ $mole^{-1}$). The study of slope additionally showed that a five-fold increase in $Fe(OH)_3$ / Fe^{2+} ratio induces a doubling of $HgSO_4$ / HgS^0. Such $Fe(OH)_3$ / Fe^{2+} variations are easily achieved in natural conditions in the vicinity of redox margins (Viollier *et al*., 1997) or cell membranes (Braun, 2001). Actually, it has been demonstrated (Silverman and Lungen, 1959; Ceskova *et al*., 2002; Franzmann *et al*., 2005) that the microbial activity significantly enhances Fe^{II} oxidation kinetics (e.g., *L. ferrooxidans, F. acidiphilum* or *L. ferriphilum* bacteria) thus playing a key role in Hg bioavailability to SRB.

Hg and Fe cycles are subtly connected: (i) in oxic environments, OM induced Fe^{II} formation catalyses the Hg reduction processes (Nriagu, 1994; Zhang and Lindberg, 2001; Peretyazhko, 2002; Peretyazhko *et al*., 2005) while (ii) at redox margins, Fe^{III} was found to enhance the $MMHg_D$ production through HgS^0 oxidation (Fleming *et al*., 2006). Applying the

PCA technique to Fe complexes (Fig. 4.C.), we conjectured that homogenous iron oxidation is achieved through complexation with phosphates (Buffle *et al*., 1989; Davison and De Vitre, 1992; Wolthoorn *et al*., 2004) and proposed the overall sequence in figure 6. Thence, Hg methylation appears as the fragile result of SO_4 reduction (regulating the SRB activity) and Fe^{II} oxidation (providing methylable Hg molecules) mechanisms.

3.3. The (relative) importance of zero-valent sulfur

3.3.1. Hg speciation in presence of polysulfides

Recent works (Paquette and Helz, 1997; Morel *et al*., 1998; Jay *et al*., 2000 and 2002), indicated that precipitated HgS solubility is increased by zero-valent sulfur (S^0). This additional Hg solubility, explained by:

$$Hg^{2+} + 2OH^- + HS^- + (n-1)S^0 = HgS_nOH^- \qquad \log K\,(I = 0) = 77.9 \qquad (6)$$

$$Hg^{2+} + 2OH^- + 2HS^- + 2(n-1)S^0 = Hg(S_n)_2^{2-} \qquad \log K\,(I = 0) = 108.3 \qquad (7)$$

is of environmental interest since Hg-polysulfides (noted HgS_x) may constitute a significant fraction of the whole pool of reduced sulfur Hg complexes. Besides, the presence of lipophilic polysulfide complexes (such as HgS_5^0) could significantly enhance the Hg uptake rate by SRB [$K_{O\text{-}W.}(HgS_5^0)$ = 900-11,000; Jay *et al*., 2000].

To compare HgS_x and $HgSO_4$ roles in Hg methylation, we modeled the dissolved Hg complexation in presence of S^0 for the Petit-Saut reservoir / Sinnamary Estuary continuum. Saturation states of the dissolved phase with respect to rhombic sulfur were calculated with the computer code WHAM 6 and ECOSAT, after modifying their respective thermodynamic database to include the equilibrium constants given in Table 5. The concentration of S^0 in sampled waters was hereafter calculated from measurements of pH, ΣH_2S and reiterative computation of complexable S^0. In accordance with Wang and Tessier (1998), the following mass balances were used for the calculation:

$$\Sigma S(0) = [S^0] + \Sigma(n\text{-}1)[S_n^{2-}] + \Sigma(n\text{-}1)[HS_n^-] + \Sigma(n\text{-}1)[H_2S_n] \quad (8)$$

$$\Sigma H_2S = [H_2S] + [HS^-] + \Sigma[S_n^{2-}] + \Sigma[HS_n^-] + \Sigma[H_2S_n] \quad (9)$$

Measurements of dissolved sulfides (0.1-2 nmol L^{-1}; Cutter and Krahforst, 1988; Knoery and Cutter, 1993; Sukola *et al*., 2005) in surface waters showed that dissolved Hg sulfides species predominate even in aerobic conditions (Dyrssen, 1988; Dyrssen and Wedborg, 1989). Therefore, a 1 nmol L^{-1} ΣH_2S concentration was arbitrary used to model the epilimnetic Hg speciation in presence of polysulfides.

The modeled profiles for ΣH_2S, S^0, HgS^0 and HgS_x in the water-column of the reservoir are given in figure 7. Computed data indicate that, even at nanomolar ΣH_2S levels, mercuric sulfides are the major dissolved species (> 93 % of HgT_{UNM}). In the epilimnion, HgS^0 composes ~ 81 % of HgT_{UNM} whereas HgS_x is around 13 % (mostly as HgS_nOH^-). Regarding Hg complexation by OM, HgT_{UNM}-DOC complexes from surface waters only occupy ~ 6 % of HgT_{UNM}. Gained values support that organically bound Hg (main source of HgT_{UNM} to the system; Section 3.1.1.) is readily mobilized by reduced S ligands once entering the aquatic milieu (e.g., during atmospheric deposition). Further in depth (below 5 m depth), as reaching the anoxic water column hypolimnion, mercuric sulfide contribution steps from 93 to 96 % of HgT_{UNM}. The overall reduced variability masks broad complexation changes: with increasing of ΣH_2S concentrations (from 10^{-9} to 10^{-6} M), ~ 10 % of HgT_{UNM} complexes are transferred from HgS_x to HgS^0. As a result, HgS_nOH^-, the dominant polysulfide complex in solution, represented less than 2 % of hypolimnetic HgT_{UNM} (close to 0.10 ± 0.04 pmol L^{-1}). We speculate that complexation changes may reflect the highest $[HS^-]$ sensitivity to redox variations (correspondingly, $[S^0]$ increased by less than 10 %) and/or kinetic of mercury precipitation as cinnabar (bimolecular reaction of Ks = $10^{52.1}$). Considering Hg complexation by OM (~ 4% of HgT_{UNM}), the formation of HgS_x hardly contributed to remobilize Hg from

its organic shell: HgT_{UNM}-DOC concentrations were found comparable in presence and absence of S^0 (Section 3.1.1.). Actually, modeling the competing effect of HgS_x on Hg complexation, the expected decreases in HgS^0 and HgT_{UNM}-DOC concentrations ($[HgS_x]$ / $[HgS^0] = 10^{24}$ $[S^0]^{3.8}$ with $[HgT_{UNM}\text{-DOC}]$ / $[HgS^0]$ constant) were observed for S^0 concentrations > 0.3 µmol L^{-1} (current values being < 0.2 µmol L^{-1}).

3.3.2. The effect of HgS_x on mercury methylation

According to Jay *et al*. (2002), in natural waters not at equilibrium with cinnabar, Hg-polysulfide complexes would be expected to shift the speciation of mercury from HgS^0 toward charged complexes, thereby decreasing methylation rates. Gained data from our study partially verified this hypothesis: measured $MMHg_D$ concentrations displayed a sharp diminution with increasing of HgS_x levels ($r^2 = 0.63$; n = 18 and $[MMHg_D] = 2.7\ [HgS_x]^{-6.8}$ in pmol L^{-1}; Fig. 5). Yet main shift in mercury speciation barely consisted of HgS^0. Firstly, we plotted the Hg^{2+} concentrations (a proxy of easily complexable [labile] Hg) as a function of $[HgS_x]$ / $[HgS^0]$ ratio. Calculated data {$r^2 = 0.59$; n = 18 and $[Hg^{2+}]_{moles\ L\text{-}1} = -4.4\ 10^{-38}$ ($[HgS_x]$ / $[HgS^0]$) + $2\ 10^{-39}$} show that enhancing the Hg-polysulfide contribution rather deplete the pool of labile HgT_{UNM} complexes (-80 %) than the purely sulfidic one (no significant diminution). This accords with previous authors assuming that at low ΣH_2S concentrations (< 10 µmol L^{-1}), the addition of polysulfides decreases the overall octanol-water partition coefficient ($D_{o.w.}$) of mercury. Sedondly, since substratum for Hg methylation fairly belongs to the labile pool of complexes (Section 3.2.2.), we scrutinized the $MMHg_D$ dependence with $HgSO_4$ specie under the indirect control of Hg-polysulfides. The HgT_{UNM} relative $MMHg_D$ concentrations were found to linearly increased with $[HgSO_4]$ / $[HgS_x]$ ratio {$r^2 = 0.69$; n = 18 and $[MMHg_D]$ / $[HgT_{UNM}] = 2\ 10^{28}$ ($[HgSO_4]$ / $[HgS_x]$) + 0.1}. From both observations we concluded that, in the studied milieu ($\Sigma H_2S \sim 1$ µmol L^{-1} and pH ~ 5.6), the presence of zero-valent sulfur ($S^0 \sim 0.16$ µmol L^{-1}) contributes to diminish the Hg methylation by substituting

low $K_{O\text{-}W.}$ ionic compounds [HgS_nOH^- and $Hg(S_n)_2^{2-}$ ions] to neutral and labile species [$HgSO_4$, HgClOH, $HgCl_2$, $Hg(OH)_2$ etc.].

The comparative behavior of HgS_nOH^- and $Hg(S_n)_2^{2-}$ ions to principal Hg complexes was studied by means of the PCA technique (Fig. 4.D.). As for the purely sulfidic case (Section 3.2.2.; Fig. 4.B.), a continuous chain of inorganic Hg complexes connects HgT_{UNM} to $MMHg_D$: the discriminating factors still being whether or not redox is variable (F_1 axis) and local oxygen depletion (F_2 axis). Accordingly, sulfidic Hg complexes were associated to low oxygen and reduced redox gradients stations whereas methylated Hg species corresponded to more oxygenated and pronounced redox gradients sites. Interestingly, HgS_x and $MMHg_D$ represent chain extremities while Hg^{2+} (a proxy of labile Hg) is the central link. The role of mercury free ion is revealed by plotting Hg^{2+} *versus* ΣH_2S concentrations (Fig. 5). Decreases in [Hg^{2+}] seemingly depict the mobilizing effect of reduced S ligands on labile or OM bounded mercury {$r^2 > 0.9$; $n = 8$ and $[Hg^{2+}]_{moles\ L\text{-}1} = -3\ 10^{-39} \log ([\Sigma H_2S]_{moles\ L\text{-}1}) - 2\ 10^{-38}$}. Due to (i) reduced SRB activity (< 1 µmol L^{-1} ΣH_2S), (ii) formation of ionic Hg-(poly)sulfides complexes and/or mercury precipitation as cinnabar (> 1 µmol L^{-1} ΣH_2S), extreme [ΣH_2S] result in HgT_{UNM} governing the Hg speciation (Section 3.1. and 3.2.). Conversely, recorded peak of Hg^{2+} concentrations would depict the $HgSO_4$ formation during OM catalyzed Fe^{III} reduction (Section 3.2.3). Intermediate [ΣH_2S] (~ 1 µmol L^{-1}), correspond to high $MMHg_D$ / HgT_{UNM} ratios (close to 0.9) due to local production of labile Hg (along with Hg^{2+} ions) capable of undergoing subsequent methylation. It is finally noteworthy that, as shown in Section 3.2.2., $HgSO_4$ precedes the occurrence of methylated Hg complexes indicating that Hg-polysulfides hardly affect the intrinsic mechanisms of mercury methylation (Fig. 6). That is to say that introducing S^0 in our model does not apparently substitute HgS_x to any previously methylation involved HgT_{UNM} complex. Actually, the PCA antagonistic position

of Hg-polysulfides to $MMHg_D$ rather depicts HgS_x as a sink for methylable Hg than an additional direct source for SRB.

4. CONCLUDING REMARKS

This study contributes to our knowledge of sources, transformations and sinks of methylable Hg in sulfidic environments. Using complexation models comprising measured HgT_D and $MMHg_D$ concentrations with well constrained thermodynamic constants, we reconstructed the course of HgT_{UNM} towards methylation. Reported pathway is consistent with (i) neutral Hg complex theory stating that mercurial uptake by methylating bacteria occurs through passive diffusion and (ii) the fact that, in sulfidic environments, sulfates stimulate the MMHg production. The sequence among Hg complexes show that the passage from inorganic to methylated Hg is achieved through $HgSO_4$, whereas Hg-sulfides [e.g., HgS^0, $Hg(SH)_2$, $HgS(SH)^-$, HgS_2^{2-}] are reversely related to MMHg. An important feature of our results is that $HgSO_4$ production and bioavailability is excessively enhanced at redox transient margins [presumably *via* $Fe(OH)_3$ induced HgS^0 oxidation]. In these regions, of rapid Fe and S cycling, the Hg^{2+} complexation shifts between inorganic and organic ligands. Finally, based on equilibrium with orthorhombic sulfur and using PCA technique, it was also possible to determine the relative impact of Hg-polysulfide complexes on Hg methylation. Gained results indicate that introducing zero-valent sulfur in our calculations contributes to diminish the Hg methylation by substituting low $K_{O\text{-}W.}$ ionic compounds [HgS_nOH^- and $Hg(S_n)_2^{2-}$ ions] to neutral and more labile species [$HgSO_4$, $HgClOH$, $HgCl_2$, $Hg(OH)_2$ etc.]. Formation of Hg-polysulfides complexes rather constitutes a sink for methylable Hg species than a source for methylating bacteria.

Geochemistry of labile Hg species, as determined from the application of inorganic-organic complexation models to dissolved water profiles, is still too problematic to remain unstudied. In spite of their low concentrations, the elevated reactivity and/or sensitivity to environmental changes make labile Hg species suitable for redox and biologically mediated reactions. Future *in situ* studies on Hg méthylation should include the measurement of ancillary variables such as Fe oxyhydroxides / sulfides and sulfates, which appear to be involved in regulating the SRB activity and/or providing methylable Hg molecules. Further laboratory determination of the labile Hg species production, including their kinetic features and possible pyritization, also stands as one of the important issues critical to improving our knowledge on the mercury cycling.

Acknowledgments: We whish to thank the INRS-ETE community for sharing its knowledge and particularly A. Tessier, L. Rancourt, C. Gobeil, S. Feyte, R Couture and A. Chappaz for their active support and technical assistance. We also thank B. Burban, C. Reynouard, P. Cerdan, V. Horeau, R. Aboïkoni, L. Guillemet, R. Vigouroux, and Y. Dominique for their participation and facilitation to sampling and analyses. This work has been financially supported by the Quebec-France partnership (# DSUR-QUE-60-107).

REFERENCES

BAEYENS W. and LEERMAKERS M. (1998) Elemental mercury concentrations and formation rates in the Scheldt estuary and the North Sea. *Mar. Chem.* **60**, 257-266

BARKAY T., GILLMAN M. and TURNER R.R., (1997) Effects of dissolved organic carbon and salinity on bioavailability of mercury. *Appl. Environ. Microbiol.* **63**, 4267-4271.

BENEDETTI, M. F., MILNE, C.J. KINNIBURGH, D.G., VAN RIEMSDIJK, W.H. and KOOPAL, L.K. 1995. Metal Ion Binding to Humic Substances: Application of the Non-Ideal Competitive Adsorption Model. Environmental Science & technology, **29**, 446 – 457.

BENOIT J.M., GILMOUR C.C., MASON R.P. and HEYES A. (1999) Sulfide Controls on Mercury Speciation and Bioavailability to Methylating Bacteria in Sediment Pore Waters. *Environ. Sci. Technol.* **33**,. 951-957.

BENOIT J.M., GILMOUR C.C. and MASON R.P. (2001a) The influence of sulfide on solid-phase mercury bioavailability for methylation by pure culture of desulfobulbus propionicus. *Environ. Sci. Technol.* **35**, 127-132.

BENOIT J.M., MASON R.P., GILMOUR C.C. and AIKEN G.R. (2001b) Constants for mercury binding by dissolved organic matter isolates from the Florida Everglades. *Geochimica et Cosmochimica Acta* **65**, 4445-4451.

BENOIT J.M., GILMOUR C.C., HEYES A., MASON R.P. and MILLER C.L. (2003) Geochemical and biological controls over mercury production and degradation in aquatic systems. *Biogeochemistry of Environmentally Important Trace Elements* **835**, 262-297.

BLOOM N.S. (1989) Determination of picogram levels of methylmercury by aqueous phase ethylation followed by cryogenic gas chromatography with cold vapour atomic fluorescence detection. *Canadian Journal of Fisheries and Aquatic sciences* **46**, 1131-1140.

BLOOM N.S. and FITZGERALD W.F. (1988) Determination of volatile mercury species at the picogram level by low-temperature gas chromatography with cold-vapour atomic fluorescence detection. *Analytica Chimica Acta* **208**, 151-161.

BLOOM N.S., PREUS E., KATON J. and HITTNER M. (2003) Selective extractions to assess the biogeochemically relevant fractionation of inorganic mercury in sediment and soils. *Analytica Chimica Acta* **479**, 233-278.

BOUDREAU B.P. (1997) Diagenetic models and their implementations. Modeling transport and reactions in aquatic sediments. Springer, 414 pp; ISBN 3-540-61125-8.

BRANFIREUN B.A., ROULET N.T., KELLY C.A. and RUDD J.W.M. (1999) *In situ* sulphate stimulation of mercury methylation in a boreal peatland: toward a link between acid rain and methylmercury contamination in remote environments. *Global Biogeochemical Cycles* **13**, 743-750.

BRAUN V. (2001) Iron uptake mechanisms and their regulation in pathogenic bacteria. *Int. J. Med. Microbiol.* **291**, 67-79.

BUFFLE J., DE VITRE R.R., PERRET D. and LEPPARD G.G. (1989) Physico-chemical characteristics of a colloidal iron phosphate species formed at the oxic-anoxic interface of an eutrophic lake. *Geochim. Cosmochim. Acta* **53**, 399-408.

BUFFLE J. (1988) Complexation reactions in aquatic systems, Ellis Horwood, 692 pp.

CESKOVA P., MANDL M., HELANOVA S. and KASPAROVSKA J. (2002) Kinetic studies on elemental sulfur oxidation of Acidithiobacillus ferrooxidans: Sulfur limitation and activity of free and adsorbed bacteria. *Biotechnology and Bioengineering* **78**, 24-30.

CHOE K.Y. and GILL G.A. (2003) Distribution of particulate, colloidal, and dissolved mercury in San Francisco Bay estuary. 2. Monomethyl mercury. *Limnol Oceanogr.* **48**, 1547-1556.

CHOI S.C. and BARTHA R. (1994) Environmental factors affecting mercury methylation in estuarine sediments. *Bulletin of Environmental Contamination and Toxicology* **53**, 805-812.

CHOI S.C., CHASE T.J. and BARTHA R. (1994) Metabolic pathways leading to mercury methylation in desulfovibrio desulfuricans LS. *Appl. Environ. Microbiol.* **60**, 4072–4077.

COMPEAU G.C. and BARTHA R. (1985) Sulfate-reducing bacteria: Principal methylators of mercury in anoxic estuarine sediment. *Applied and Environmental Microbiology* **50**, 498-502.

COQUERY M., COSSA D. and SANJUAN J. (1997) Speciation and sorption of mercury in two macro-tidal estuaries. *Marine Chemistry* **58**, 213-227.

COQUERY, M., COSSA, D., AZEMARD, S., PERETYAZHKO, T. AND CHARLET, L., 2003: Methylmercury formation in the anoxic waters of the Petit-Saut reservoir (French Guiana) and its spreading in the adjacent Sinnamary River. Journal de Physique IV, 107, 327-331.

COSSA D., AVERTY B., BRETAUDEAU J. and SENARD A.S., (2003) Spéciation du mercure dissous dans les eaux marines. *Méthodes d'analyse en milieu marin,* Editions Ifremer 27 pp.; ISBN 2-84433-125-4.

COSSA D., COQUERY M., NAKHLE K. and CLAISSE D. (2002) Dosage du mercure total et du monomethylmercure dans les organismes et les sédiments marins. *Méthodes d'analyse en milieu marin,* Editions Ifremer 27pp.; ISBN 2-84433-105-X.

COSSA D. and GOBEIL C. (1996) Speciation and mass balance of mercury in the lower Saint Laurent estuary and Saguenay Fjord (Canada). *4th International Conference on Mercury as a Global Pollutant* Book of Abstracts, Hamburg **458**, 4-8.

CRUMP B.C., BAROSS J.A. and SIMENSTAD C.A. (1998) Dominance of particle-attached bacteria in the Columbia River estuary, USA. *Aquatic Microbial Ecology* **14**, 7-18.

CUTTER G.A. and KRAHFORST C.F. (1988) Sulfide in surface waters of the Western Atlantic Ocean. *Geophys. Res. Lett.* **15**, 1393-1396.

DAVISON W. and DE VITRE R.R. (1992) Iron particles in freshwater. In: BUFFLE J. and LEEUWEN H.P. Editors. *Environmental Particles*, 315-355.

DUMESTRE J.F., EMILIO C.O., RAMON M. and PEDROS-ALIO C. (2001) Changes in bacterial assemblages in a equatorial river induced by water eutrophication of Petit-Saut dam reservoir (French Guiana). *Aquat. Microb. Ecol.* **26**, 209-221.

DUMESTRE J.F., VAQUER A., GOSSE P., RICHARD S. and LABROUE L. (1999) Bacterial ecology of a young equatorial hydroelectric reservoir (Petit-Saut, French Guiana). *Hydrobiologia* **400**, 75-83.

DYRSSEN D. and WEDBORG M. (1989) The state of dissolved trace sulfide in seawater. *Mar. Chem*. **26**, 289.

DYRSSEN D. (1988) Sulfide complexation in surface seawater. *Mar. Chem.* **24**, 143-153.

DZOMBAK D.A. AND MOREL F.M.M. (1990) Surface complexation modeling hydrous ferric oxide. *John Wiley* **New York**, 393 pp.

EPRI -ELECTRIC POWER RESEARCH INSTITUTE- (2003) Implementation of the United States environmental protection agency's methylmercury criterion for fish tissue. Palo Alto, CA 2003. 1005520.

FLEMING E.J., MACK E.E., GREEN P.G. and NELSON D.C. (2006) Mercury methylation from unexpected sources: Molybdate-inhibited freshwater sediments and an iron-reducing bacterium. *Applied and Environmental Microbiology* **72**, 457-464.

FRANZMANN P.D., HADDAD C.M., HAWKES R.B., ROBERTSON W.J. and PLUMB J.J. (2005) Effects of temperature on the rates of iron and sulfur oxidation by selected bioleaching Bacteria and Archaea: Application of the Ratkowsky equation. *Minerals Engineering* **18**, 1304-1314.

GALLON C., TESSIER A., GOBEIL C. and TORRE M.C.A. (2004) Modeling diagenesis of lead in the sediments of a Canadian Shield lake. *Geochim. Cosmochim. Acta* **68**, 3531-3545.

GÅRDFELDT K., SOMMAR J., STRÖMBERG D. and FENG X. (2001) Oxidation of atomic mercury by hydroxyl radicals and photoinduced decomposition of methylmercury in the aqueous phase. *Atmos. Environ.* **35**, 3039-3047.

GILL G.A. and FITZGERALD W.F. (1985) Mercury sampling of open ocean waters at the picomolar level. *Deep-Sea Research* **32**, 287-297.

GILMOUR C.C. and RIEDEL G.S. (1995) Measurement of Hg methylation in sediments using high specific-activity Hg-203 and ambient incubation. *Water Air and Soil Pollution* **80**, 747-756.

GILMOUR C.C., HENRY E.A. and MITCHELL R. (1992) Sulfate stimulation of mercury methylation in freshwater sediments. *Environmental Science & Technology* **26**, 2281-2287.

GILMOUR C.C. and HENRY E.A. (1991) Mercury methylation in aquatic systems affected by acid deposition. *Environmental Pollution* **71**, 131-169.

GOLDING G.R., KELLY C.A., SPARLING R., LOWEWN P.C., RUDD J.W.M. and BARKAY T. (2001) Evidences for facilitated uptake of Hg(II) by vibrio anguillarum and escherchia coli under anaerobic and aerobic conditions. *Limnol. Oceanogr.* **47**, 967-975.

HAMMERSCHMIDT C.R., FITZGERALD W.F., LAMBORG C.H., BALCOM P.H. and VISSCHER P.T. (2004) Biogeochemistry of methylmercury in the sediments of Long Island Sound. *Mar. Chem.* **90**, 31-52.

HAMMERSCHMIDT C.R. and FITZGERALD W.F. (2006) Methylmercury cycling in sediments on the ciontinental shelf of southern New England. *Geochim. Cosmochim. Acta*, In press.

HAN S., GILL G.A., LEHMAN R.D. and CHOE K.Y. (2006) Complexation of mercury by dissolved organic matter in surface waters of Galveston Bay, Texas. *Mar. Chem.* **98**, 156-166.

HOLMES D.E., BOND D.R. and LOVLEY D.R. (2004) Electron transfer by *D. propionicus* to Fe^{III} and graphite electrodes. *Applied and Environmental Microbiology* **70**, 1234-1237.

HUYNH F., CHARRON C., BETOULLE J. L., PANECHOU K., GARDEL A., PROST M. T. and LOUBRY D. (1997) Suivi de l'évolution géomorphologieque et botanique de l'estuaire du Sinnamary par télédétection. *Rap. Final ORSTOM-EDF*, 64 pp.

HYDRECO: Laboratory for biological and chemical monitoring and analysis on the Petit-Saut reservoir. http://hydreco.mediasfrance.org/hydreco/

JAY J.A. (1999) Effect of polysulfides on cinnabar solubility, partitioning, and methylation by Desulfovibrio Desulfuricans. Ph.D. Dissertation. Massachusetts institute of technology, Cambridge.

JAY J.A., MOREL F.M.M. and HEMOND H.F. (2000) Mercury speciation in the presence of polysulfides. *Environ. Sci. Technol.* **34**, 2196-2200.

JAY J.A., MURRAY K.J., GILMOUR C.C., MASON R.P., MOREL F.M.M., ROBERTS A.L. and HEMOND H.F. (2002) Mercury methylation by desulfovibrio desulfuricans ND132 in the presence of polysulfides. *Applied and Environmental Microbiology* **68**, 5741-5745.

KELLY C.A., RUDD J.W.M. and HOLOKA M.H. (2003) Effect of pH on mercury uptake by aquatic bacterium: implications for Hg cycling. *Environ. Sci. Technol.* **37**, 2941-2946.

KINNIBURGH D.G., MILNE C.J., BENEDETTI M.F., PINHEIRO J.P., FILIUS J., KOOPAL L.K. and RIEMSDIJK W.H. (1996) Metal ion binding by humic acid: application of the NICA-Donnan model. *Environ. Sci. Technol*. **30**, 1687-1698.

KNOERY J.R. and CUTTER G.A. (1993) Determination of carbonyl sulfide and hydrogen sulfide species in natural waters using specialized collection procedures and gas chromatography with flame photometric detection. *Anal. Chem.* **65**, 976-982.

LAMBORG C.H., TSENG C.M., FITZGERALD W.F., BALCOM P.H. and HAMMERSCHMIDT C.R. (2003) Determination of the mercury complexation characteristics of dissolved organic matter in natural waters with "reducible Hg" titrations. *Environ. Sci. Technol.* **37**, 3316-3322.

LEERMAKERS M., GALETTI S., DE GALAN S., BRION N. and BAEYENS W. (2001) Mercury in the Souther North Sea and Sheldt Estuary. *Mar. Chem.* **75**, 229-248.

LEVIN S.A., GRENFELL B., HASTINGS A. AND PERELSON A.S. (1997) Mathematical and computational challenges in population and ecosystems science. Science **275**, 334-343

LIANG L., HORVAT M. and BLOOM N.S. (1994) An improved speciation method for mercury by GC/CVAFS after aqueous phase ethylation and room temperature precollection. *Talanta* **41**, 371-379.

MALCOLM R.L. (1985) Geochemistry of stream fulvic and humic substances. In: AIKEN, G.R. *et al*., Humic Substances in Soil, Sediment and Water. Geochemistry, Isolation and Characterisation, Wiley-Interscience, 181-209.

MASON R.P., REINFELDER J.R. and MOREL F.M.M. (1996) Uptake, Toxicity, and Trophic Transfer of Mercury in a Coastal Diatom. *Environ. Sci. Technol.* **30**, 1835-1845.

MEYLAN W.M. and HOWARD P.H. (1995) Atom/fragment contribution method for estimating octanol-water partition coefficients. *J. Pharm. Sci.* **84**, 83-92.

MILNE C.J., KINNIBURGH D.G., RIEMSDIJK W.H. and TIPPING E. (2003) Generic NICA-Donnan for metal-ion binding by humic substances. *Environ. Sci. Technol*. **37**, 958-971.

MISKIMMIN B.M., RUDD J.W.M. and KELLY C.A. (1992) Influence of DOC, pH, and microbial respiration rates on mercury methylation and demethylation in lake water. Can. J. Fish. Aquat. Sci. **49**, 17-22.

MOREL F.M.M., KRAEPIEL A.M.L. and AMYOT M. (1998) The chemical cycle and bioaccumulation of mercury. *Annual Review of Ecology and Systematics* **29**, 543-566.

MURESAN B., COSSA D., RICHARD S. and DOMINQUE Y. Mercury Cycling in a Tropical Artificial Reservoir: Monomethylmercury Production and Sources. Submitted to *Applied Geochemistry* (Feb. 2006).

NIST –National Institute of Standards and Technology- (2003) Critical stability constants of metal complexes database. NIST Standard Reference Database 46, U.S. Dept. Commerce, National Institute of Standard and Technology.

NRIAGU J.O. (1994) Mechanistic steps in the photoreduction of mercury in natural waters. *The science of the total environment* **154**, 1-8.

PAGE B., WANG F., LEMES M. and ZHANG J. (2004) Methylmercury production in natural waters: A comparative study of three different wetland types to determine the bioavailability of mercury. *7th Int. Conference on mercury as a global pollutant* **2**, 1285-1288.

PAK K.R. and BARTHA R. (1998) Mercury methylation and demethylation in anoxic lake sediments and by strictly anaerobic bacteria. *Appl. Environ. Microbiol.* **64**, 1013-1017.

PAQUETTE K. and HELZ G.R. (1997) Inorganic speciation of mercury in sulfidic waters; the importance of zero-valent sulfur. *Environ. Sci. Technol.* **31**, 2148-2153.

PERETYAZHKO T. (2002) Formation de Hg^0 dans les milieux aquatiques tropicaux (Lacs et sols). Ph.D thesis, Univ Grenoble, 161 pp.

PERETYAZHKO T., VAN CAPPELLEN P., MEILE C., COQUERY M., MUSSO M., REGNIER P., CHARLET L. (2005). Biogeochemistry of major redox elements and mercury in a tropical reservoir lake (Petit Saut, French Guiana) *Aquatic Geochemistry* **11**, 33-55.

PETOT J. (1993) Histoire de l'or en Guyane. *L'Harmattan*, Paris, 256 pp.

QUEMERAIS B. and COSSA D. (1997) Procedures for sampling and analysis of mercury in natural waters. *Scientific and Technical Report* ST-31E, 34 pp.

RABENSTEIN D.L. TOURANGEAU M.C. and EVANS C.A. (1976) Proton Magnetic Resonance and Raman Spectroscopic Studies of Methylmercury(II) Complexes of Inorganic Anions. *Can. J. Chem.* **54**, 2517-2525.

RAVICHANDRAN M., AIKEN G.R., RYAN J.N. and REDDY, M.M. (1999) Inhibition of precipitation and aggregation of metacinnabar (mercuric sulfide) by dissolved organic matter isolated from the Florida Everglades. *Environ. Sci. Technol.* **33**, 1418–1423.

RAVICHANDRAN M., AIKEN G.R., REDDY M.M. and RYAN, J.N. (1998) Enhanced dissolution of cinnabar (mercuric sulfide) by dissolved organic matter isolated from the Florida Everglades. *Environ. Sci. Technol.* **32**, 3305–3311.

RICHARD S., ARNOUX A. and CERDAN P. (1997) Evolution in physico-chemical water quality in the reservoir and downstream following the filling of Petit-Saut dam (French Guiana). *Hydroecol. Appl.* **9**, 57-83.

RICHARD S. (1996) La mise en eau du barrage de Petit-Saut. Hydrochimie 1 - du fleuve Sinnamary avant la mise en eau, 2 – de le retenue pendant la mise en eau, 3 – du fleuve en aval. Thèse de Doctorat de l'université Aix – Marseille I (France) 278 pp.

SCHIPPERS A. and SAND W. (1998) Bacterial leaching of metal sulfides proceeds by two indirect mechanisms via thiosulfate or via polysulfides and sulfur. *Applied and Environmental Microbiology* **65**, 319-321.

SCHWARZENBACH G. and SCHELLENBERG M. (1965) Die komplexchemie des methylquecksilber-kations. *Helv. Chim. Acta* **48**, 28-46.

SCHWARZENBACH G. and WIDMER M. (1963) Die Löslichkeit von Metallsulfiden. I. Schwarzes Quecksilbersulfid". *Helvetica Chimica Acta* **46**, 2613–2628.

SCHWARZENBACH G. and FISCHER A. (1960) Die acidität der sulfane und die susammensetzung wässeriger polysulfdlosungen. *Helv. Chim. Acta* **43**, 1365-1390.

SELLERS P., KELLY C.A., RUDD J.W.M. and MACHUTCHON A.R. (1996) Photodegradation of methylmercury in lakes: *Nature* **380**, 694-696.

SICILIANO S.D., O'DRISCOLL N.J. and LEAN D.R.S. (2002) Microbial reduction and oxidation of mercury in freshwater lakes. *Environ. Sci. Technol.* **36**, 3064-3068.

SILVERMAN M.P. and LUNDGREN D.G. (1959) Studies on the chemoautotrophic iron bacterium Ferrobacillus ferrooxidans: II. Manometric studies, *Journal of Bacteriology* **78**, 326-331.

SMITH R.M. and MARTELL A.E. (1976) Critical Stability Constants. **4** Inorganic Complexes. Plenum, New York.

STUMM W. and MORGAN J.J. (1996) Aquatic Chemistry: chemical equilibria and rates in natural waters. 3rd Edition. Wiley-Interscience Publication, John Wiley and Son Inc. ISBN 0-471-51184-6, ISBN 0-471.

SUKOLA K., WANG F. and TESSIER A. (2005) Metal-sulfide species in oxic waters. *Analytica Chimica Acta* **528**, 183-195.

TAYLOR J.H., SMITH E.J., DAVISON W. and SUGIYAMA M. (2005) Resolving and modeling the effects of Fe and Mn redox cycling on trace metal behavior in a seasonally anoxic lake. *Geochimica et Cosmochimica Acta* **69**, 1947-1960.

TEBO B.M. and OBRAZTSOVA A.Y. (1998) Sulfate-reducing bacterium grows with Cr(VI), U(VI), Mn(IV) and Fe(III) as electron acceptors. *FEMS Microbiol. Lett.* **162**, 193-198.

TIPPING E. (1998) Humic ion-binding Model VI: an improved description of the interactions of protons and metal ions with humic substances. *Aqua. Geochem.* **4**, 3-48.

TIPPING E. (1994) WHAM—a chemical equilibrium model and computer code for waters, sediments and soils incorporating a discrete site/electrostatic model of ion binding by humic-substances. *Comp. Geosci.* **20**, 973–1023.

TWISS M.R., ERRECALDE O, FORTIN C, CAMPBELL P.G.C., JUMARIE C, DENIZEAU F, BERKELAAR E., HALE B. and REES K. (2000) Guidelines for studies of metal bioavailability and toxicity why metal speciation should be considered and how! Canadian Network of Toxicology Centres (CNTC) Metal Speciation Theme Team .

UNSWORTH E.R., WARNKEN K.W., ZHANG H., DAVISON W., BLACK F., BUFFLE J., CAO J., CLEVEN R., GALCERAN J., GUNKEL P., KALIS E., KISTLER D., LEEUWEN H.P., MARTIN M., NOËL S., NUR Y., ODZAK N., PUY J., RIEMSDIJK W., SIGG L., TEMMINGHOFF E., WAEBER M.L.T., TOEPPERWIEN S., TOWN R.M., WENG L. and XUE H. (2006) Model predictions of metal speciation in freshwaters compared to measurements by *in situ* techniques. *Environ. Sci. & Technol,* In press.

VIOLLIER E., MICHARD G., JEZEQUEL D., PEPE M. and SARAZIN G. (1997) Geochemical study of a crater lake: Lake Pavin, Puy de Dôme, France. Constraints afforded by the particulate matter distribution in the element cycling within the lake. *Chemical Geology* **142**, 225-241.

WANG F. and TESSIER A. (1998) Voltametric determination of elemental sulfur in pore waters. *Limnol. Oceanogr.* **43**, 1353-1361.

WINFREY M.R. and RUDD J.W.M. (1990) Environmental factors affecting the formation of methylmercury in low pH lakes: a review. *Environ. Toxicol. Chem.* **9**, 853-869.

WOLTHOORN A, TEMMINGHOFF E.J.M., WENG L. and RIEMSDIJK W.H. (2004) Colloid formation in groundwater: effect of phosphate, manganese, silicate and dissolved organic matter on the dynamic heterogeneous oxidation of ferrous iron. *Applied Geochemistry* **19**, 611-622.

ZHANG H. and LINDBERG S.E. (2001) Sunlight and iron(III)-induced photochemical production of dissolved gaseous mercury in freshwater. *Environ. Sci. Technol.* **35**, 928-935.

ZHANG J. and WANG F. (2004) Thiols in wetland interstitial waters and their role in mercury and methylmercury speciation. *Limnol. Oceanogr.* **49**, 2276-2286.

Tables captions

Reaction	log*K*	Reference
$Hg^{2+} + 2HS^- = Hg(SH)_2$	**40.4**	Benoit *et al.*, 1999
$Hg^{2+} + OH^- + HS^- = HgS^0$	**43.8**	Benoit *et al.*, 1999
$Hg^{2+} + OH^- + 2HS^- = HgS(SH)^-$	**48.6**	Benoit *et al.*, 1999
$Hg^{2+} + 2OH^- + 2HS^- = HgS_2^{2-}$	**53.6**	Benoit *et al.*, 1999
$Hg^{2+} + 2OH^- + HS^- + 4S^0 = HgS_5OH^-$	**77.9**	Jay *et al.*, 2000
$Hg^{2+} + 2OH^- + 2HS^- + 8S^0 = Hg(S_5)_2^{2-}$	**108.3**	Jay *et al.*, 2000

Tab. 1. Equilibrium constants (T = 25 °C, I = 0) and corresponding reactions for HgT_{UNM} sulfide complexes used in this study.

Reaction	log*K*	Reference
$MMHg^+ + SO_4^{2-} = MMHgSO_4^-$	**0.9**	Rabenstein et al., 1976
$MMHg^+ + Cl^- = MMHgCl$	**5.5**	Schwarzenbach *et al.*, 1965
$MMHg^+ + CO_3^{2-} = MMHgCO_3^-$	**5.7**	Rabenstein et al., 1976
$MMHg^+ + Br^- = MMHgBr$	**6.6**	Schwarzenbach *et al.*, 1965
$MMHg^+ + I^- = MMHgI$	**8.6**	Schwarzenbach *et al.*, 1965
$MMHg^+ + OH^- = MMHgOH$	**9.5**	NIST 2003
$2MMHg^+ + OH^- = MMHg_2OH^+$	**11.9**	NIST 2003
$MMHg^+ + OH^- + HS^- = MMHgS^-$	**21.0**	NIST 2003
$2MMHg^+ + OH^- + HS^- = MMHg_2S$	**37.5**	NIST 2003
$3MMHg^+ + OH^- + HS^- = MMHg_3S^+$	**44.5**	NIST 2003

Tab. 2. Equilibrium constants (T = 25 °C, I = 0) and corresponding reactions for MMHg complexes used in this study.

Depth (m)	Hg^{2+} (10^{-40} M)	HgClOH (10^{-34} M)	$HgSO_4$ (10^{-43} M)	HgS^0 (% of HgT_{UNM})	HgT_{UNM}-DOC (% of HgT_{UNM})
0.1	8600	76000	4800	< 1	> 99
5	12	11	9	93.4	6.4
10	2	3	2	95.0	3.9
15	4	5	4	95.2	3.7
20	11	9	10	95.9	3.4
25	15	11	13	96.3	3.1
30	10	6	12	96.2	3.1
	$MMHg^+$ (10^{-19} M)	MMHgCl (10^{-17} M)	$MMHgSO_4^-$ (10^{-23} M)	$MMHgS^-$ (% of $MMHg_D$)	MMHg-DOC (% of $MMHg_D$)
0.1	$2\ 10^{-3}$	$1\ 10^{-3}$	$5\ 10^{-4}$	< 1	> 99
5	37	18	10	14.9	81.3
10	7	4	2	18.1	81.1
15	6	3	2	16.8	82.5
20	8	4	3	13.3	86.0
25	16	8	5	18.3	79.8
30	58	27	27	19.6	73.0

Tab. 3. Water-column distributions of Hg and MMHg free ions, labile (with OH^-, Cl^- and SO_4^{2-}) and strong (with reduced S and DOC) complexes. Reported values were calculated with the WHAM 6 and ECOSAT speciation codes supposing a well oxygenated epilimnion (epilimnetic ΣH_2S negligible) and in absence of polysulfides.

Specie	Correlation coefficient	Concentration (M)
DOC	**-0.52**	$4.5 \pm 0.6\ (10^{-4})$
Fe^{II}	**-0.42**	$3.9 \pm 3.2\ (10^{-5})$
Fe^{III}	**0.66**	$8.0 \pm 7.3\ (10^{-6})$
SO_4	**0.65**	$6.9 \pm 3.4\ (10^{-6})$
H^+	**-0.75**	$2.8 \pm 0.6\ (10^{-6})$
ΣH_2S (< 10^{-6} M)	**0.69**	$1.2 \pm 0.7\ (10^{-6})$
(> 10^{-6} M)	**-0.55**	
HgT_{UNM}	**-0.64**	$4.7 \pm 1.7\ (10^{-12})$
HgS^0	**-0.69**	$4.5 \pm 1.6\ (10^{-12})$
HgT_{UNM}-DOC	**-0.45**	$2.0 \pm 0.7\ (10^{-13})$
HgS_x	**-0.53**	$1.4 \pm 0.9\ (10^{-13})$
Hg^{2+}	**0.02**	$6.3 \pm 3.9\ (10^{-40})$
$HgSO_4$	**0.66**	$9.4 \pm 6.6\ (10^{-43})$
MMHg-DOC	**0.50**	$7.4 \pm 3.4\ (10^{-13})$
$MMHgS^-$	**0.84**	$4.7 \pm 3.9\ (10^{-13})$
$MMHg^+$	**0.76**	$4.3 \pm 3.5\ (10^{-18})$
$MMHgSO_4^-$	**0.68**	$3.2 \pm 2.5\ (10^{-22})$

Tab. 4. Correlation coefficients with respect to $MMHg_D$ [significant ($p = 0.05$) at $r > 0.40$] and associated concentrations for chemical species relevant to Hg methylation.

Reaction	log*K*	Reference
$H_2S = HS^- + H^+$	**-7.0**	NIST 2003
$1/8\ S_{8,rhom} = S^0$	**-6.8**	Boulègue 1978b
$HS^- + 2S^0 = HS_3^-$	**8.8**	Schwarzenbach and Fischer, 1960
$HS^- + 3S^0 = HS_4^-$	**17.2**	Schwarzenbach and Fischer, 1960
$HS^- + 4S^0 = HS_5^-$	**23.4**	Schwarzenbach and Fischer, 1960
$HS^- + 5S^0 = HS_6^-$	**27.3**	Schwarzenbach and Fischer, 1960
$H^+ + HS^- + 2S^0 = H_2S_3$	**13.2**	Schwarzenbach and Fischer, 1960
$H^+ + HS^- + 3S^0 = H_2S_4$	**21.2**	Schwarzenbach and Fischer, 1960
$H^+ + HS^- + 4S^0 = H_2S_5$	**27.1**	Schwarzenbach and Fischer, 1960
$H^+ + HS^- + 5S^0 = H_2S_6$	**32.8**	Schwarzenbach and Fischer, 1960
$OH^- + HS^- + 2S^0 = S_3^{2-}$	**14.9**	Cloke 1963a
$OH^- + HS^- + 3S^0 = S_4^{2-}$	**24.5**	Cloke 1963a
$OH^- + HS^- + 4S^0 = S_5^{2-}$	**31.3**	Cloke 1963a
$OH^- + HS^- + 5S^0 = S_6^{2-}$	**37.8**	Cloke 1963a

Tab. 5. Equilibrium constants (T = 25 °C, I = 0) relevant to the sulfides and polysulfides system.

Figure captions

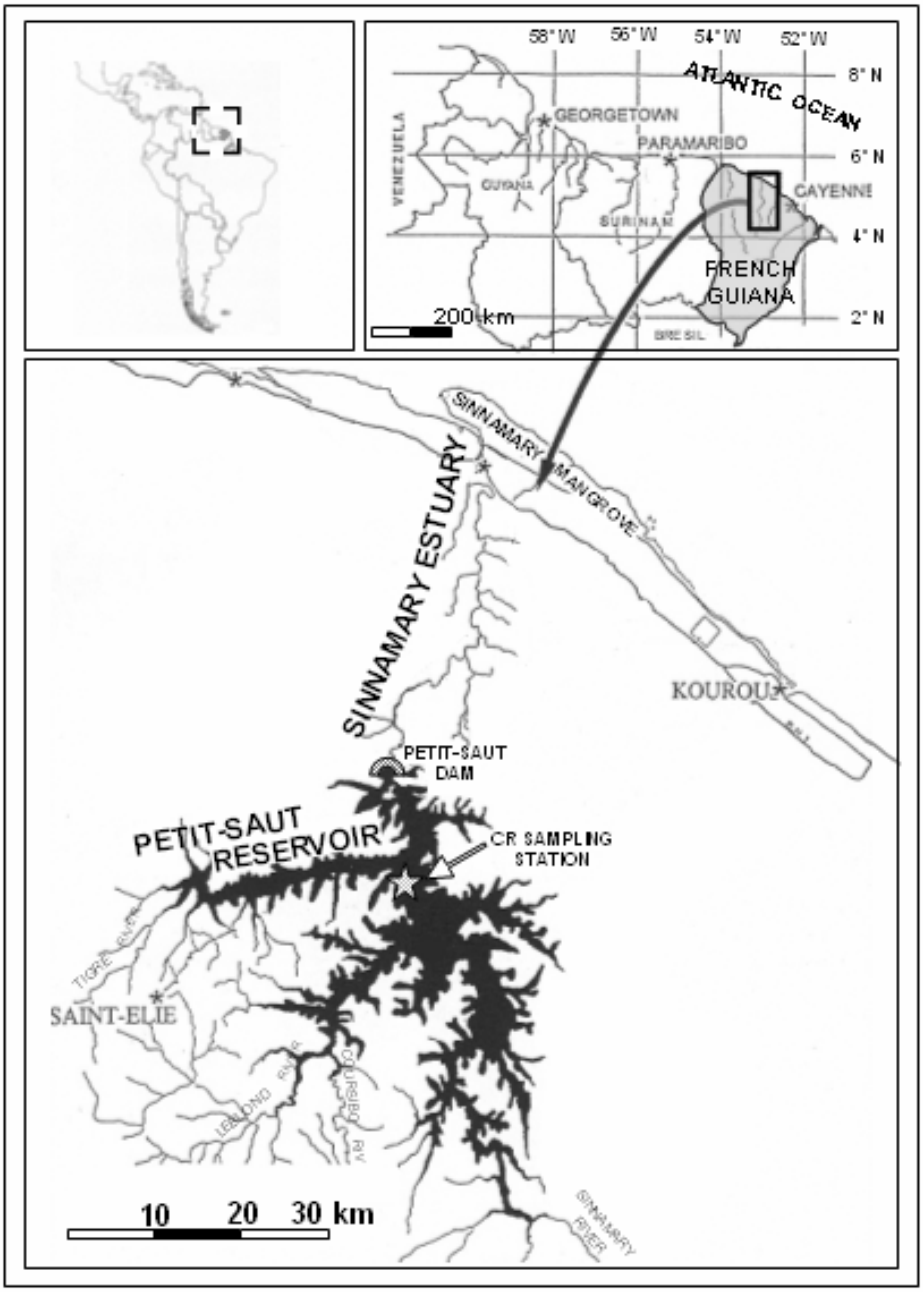

Fig. 1. Location map of the Petit-Saut reservoir / Sinnamary Estuary continuum. Detailed map of the areas where (and dates when) sampling occurred including associated geochemical descriptions is given in Muresan *et al*. (under submission).

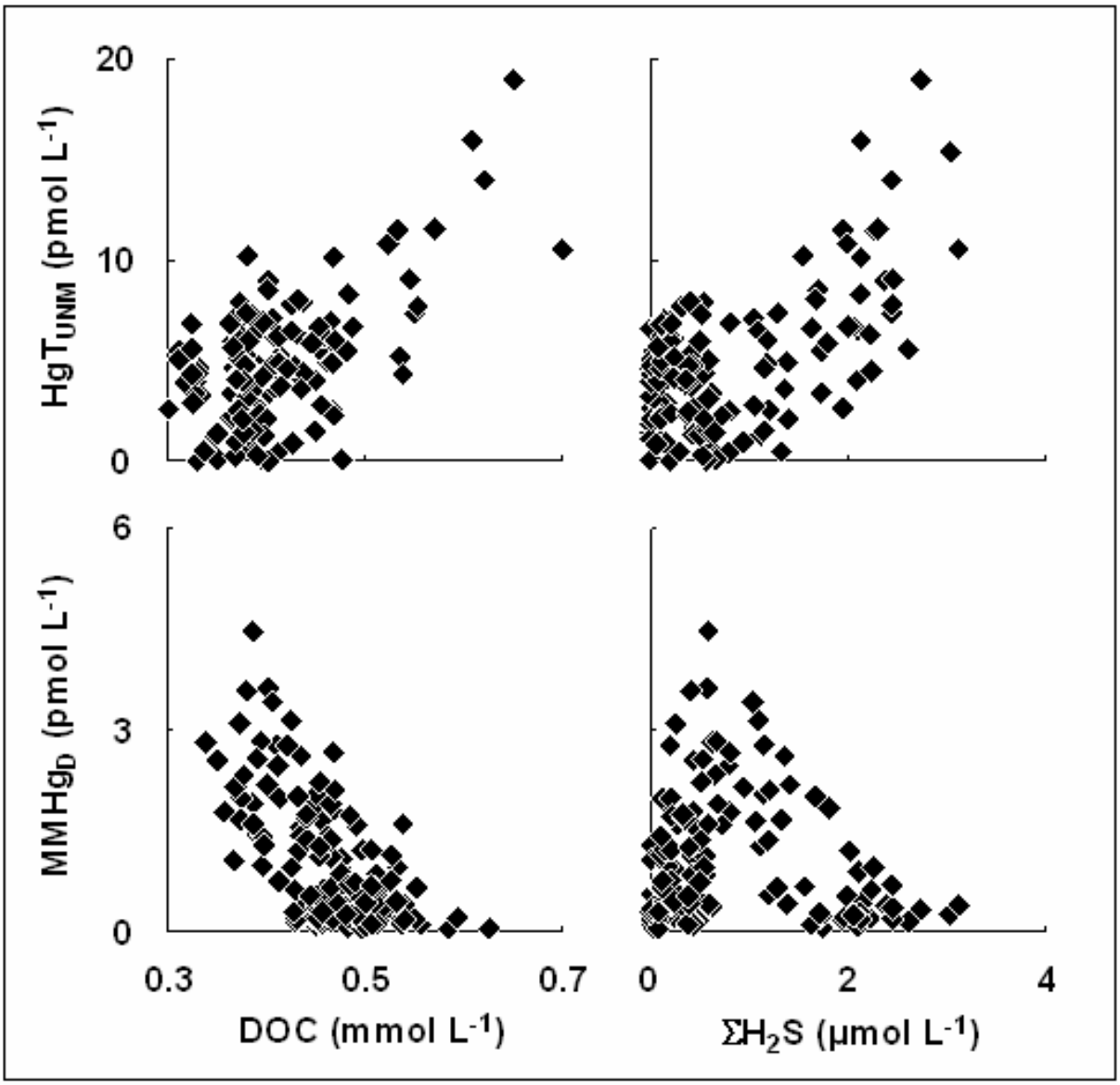

Fig. 2. Distributions of dissolved unmethylated (HgT_{UNM}) and methylated ($MMHg_D$) mercury concentrations in relationship with organic (DOC) and sulfidic (ΣH_2S) content of water.

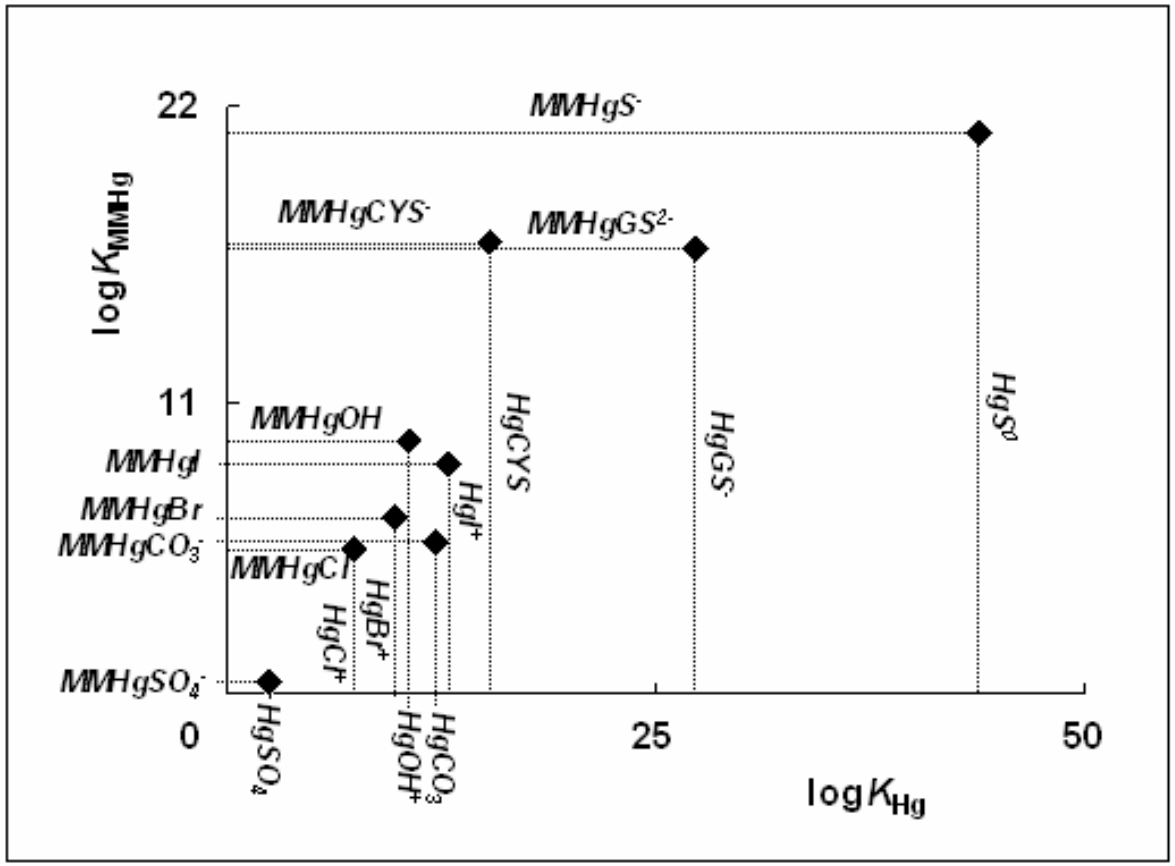

Fig. 3. Correlation between the intrinsic equilibrium constants of MMHg (K_{MMHg}) and HgT_{UNM} (K_{Hg}) with inorganic and organic ligands (T = 25 °C, I = 0). Thermodynamic constants originate from Table 2 and Zhang et al. (2004) article.

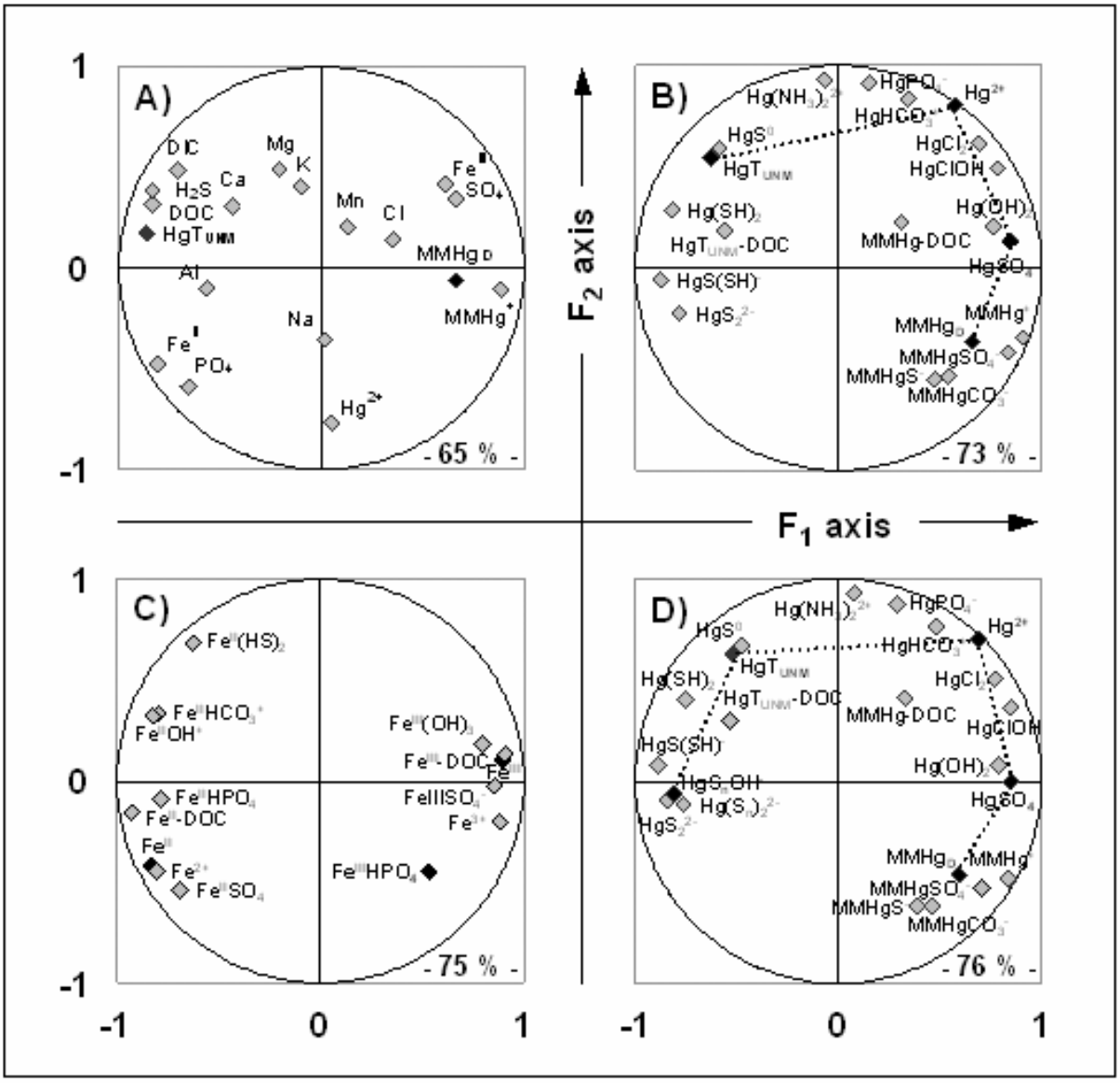

Fig. 4. Principal component analysis (or PCA) of A) the dissolved chemical compounds, B) associated HgT_{UNM}, $MMHg_D$ and C) Fe complexes. The PCA of HgT_{UNM} and $MMHg_D$ complexes in presence of polysulfides is shown in Fig. 4.D.. For ease comparison, relevant species are marked by black diamonds. Broken lines indicate the scrutinized pathway for Hg methylation.

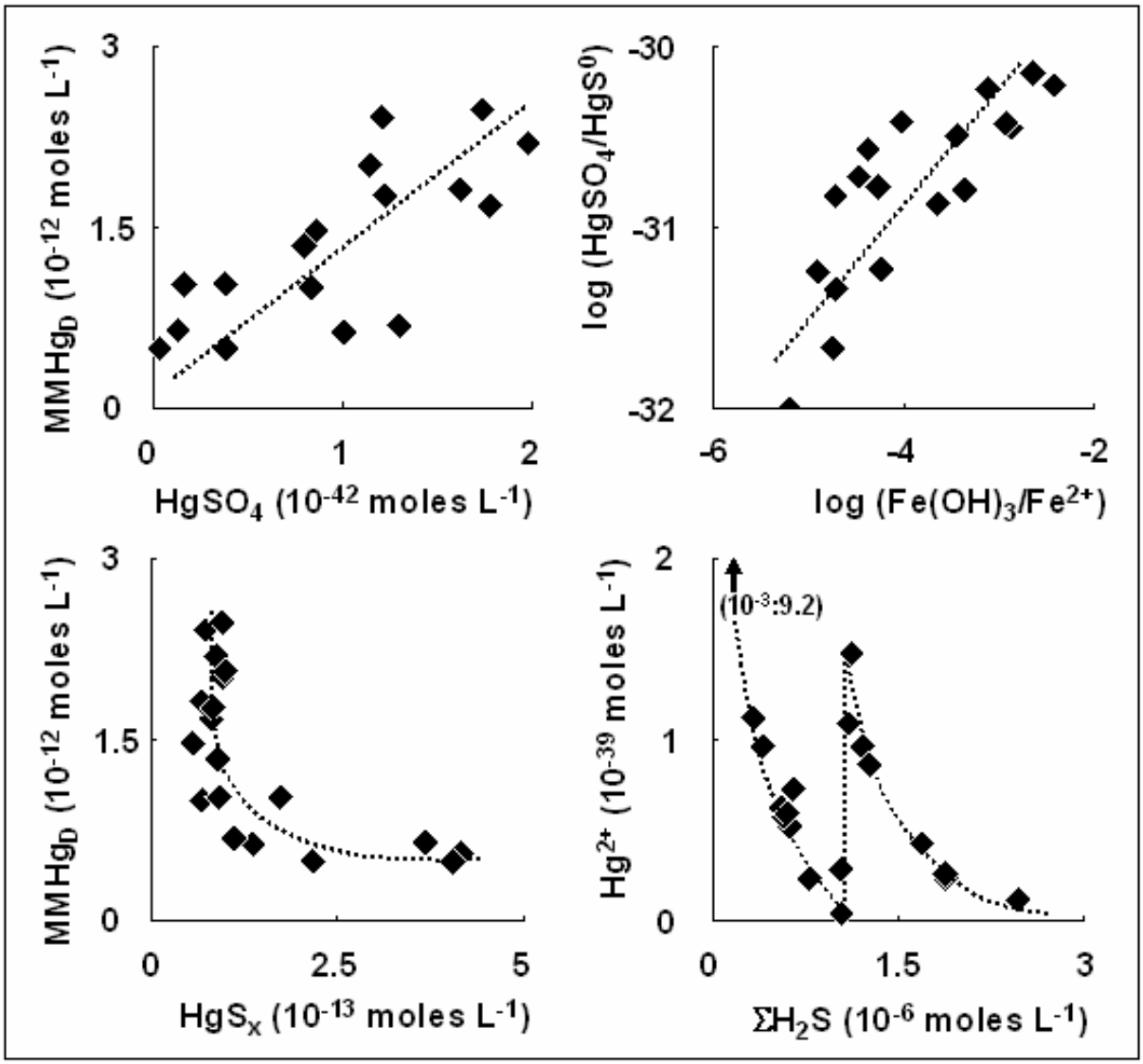

Fig. 5. Left column: relationships between $MMHg_D$ and $HgSO_4$ or HgS_x concentrations. Right column: relationships between $[Fe(OH)_3]$ / $[Fe^{2+}]$ and $[HgSO_4]$ / $[HgS^0]$ ratios and, ΣH_2S and Hg^{2+} concentrations. Each point of the graphs regroup 2 modeled (WHAM 6 and ECOSAT) or 8 measured concentrations.

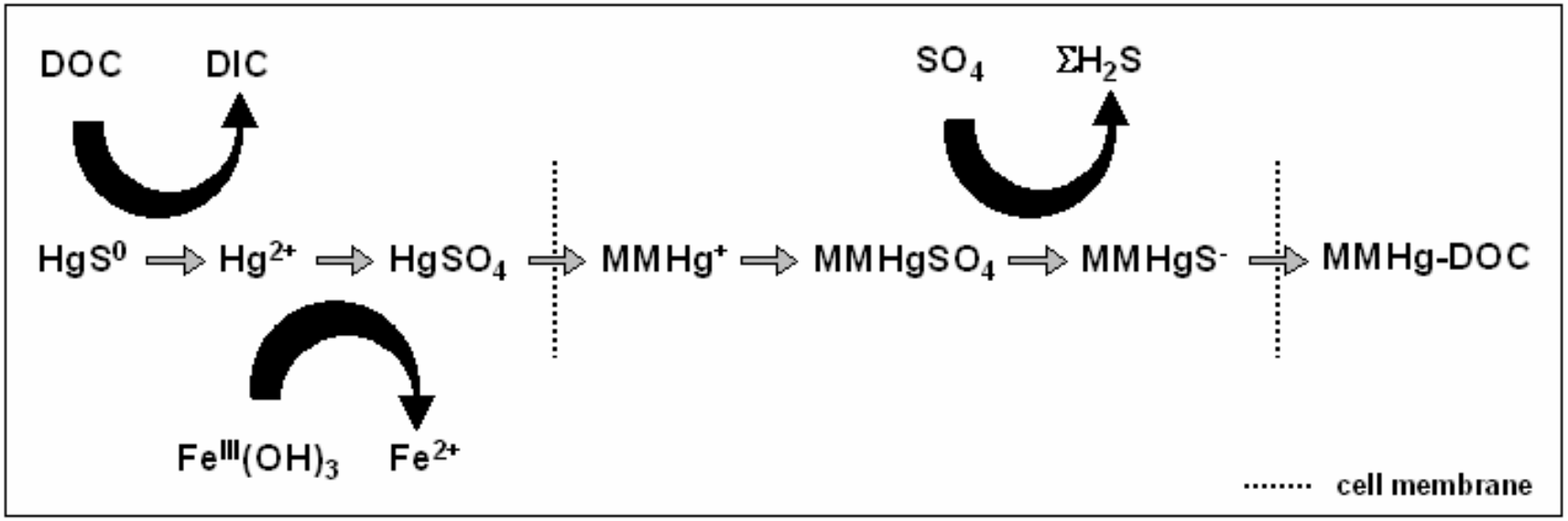

Fig. 6. Geochemical and biological controls over HgT_{UNM} complexation in relationship with $MMHg_D$ production.

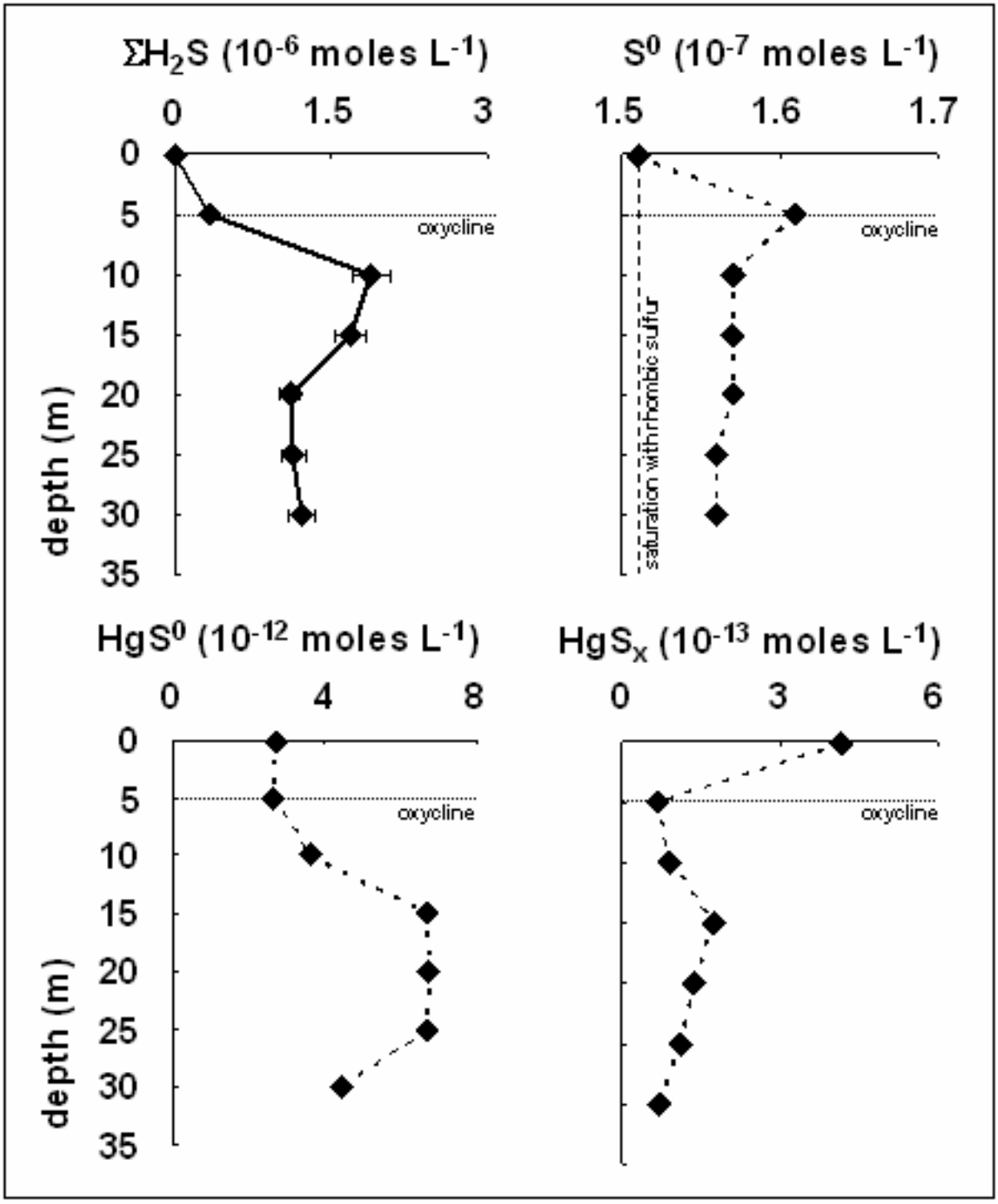

Fig. 7. Profiles of ΣH_2S, S^0, HgS^0 and HgS_x in the water-column of the Petit-Saut reservoir (station CR). Measured (in triplicate) and calculated profiles correspond to straight and broken ones. The horizontal dashed lines depict the water-column oxycline whereas the vertical dashed line indicates the S^0 saturation with orthorhombic sulfur (Table 5).

4. CONCLUSION GENERALE

4.1. Rappel des objectifs

Le programme « Mercure en Guyane » vise à identifier les stocks de Hg présents en Guyane, les transformations qu'il subit, les flux de ce métal sous diverses formes, et finalement son mode d'accumulation le long des chaînes trophiques qui conduisent à la bioamplification du MMHg chez les espèces prédatrices puis à l'intoxication des amérindiens, suite à une forte consommation de poissons. La présente étude s'inscrit dans cette problématique ; son objectif principal est de déterminer le rôle de la retenue de Petit-Saut dans le cycle local du mercure, en particulier vis-à-vis des processus endogènes de réduction et de méthylation. Au terme de ce travail, les réponses attendues doivent permettre de fournir une base scientifique pour l'élaboration et l'application de futures politiques d'aménagement, notamment celle concernant l'impact de la construction de barrages en milieu tropical.

Objectifs : Les recherches développées dans le cadre de cette thèse se proposent d'apporter des éléments de réponse aux questions suivantes :

- La retenue de Petit-Saut est-elle une source ou un puits de mercure pour l'atmosphère ?
- Quel est le cycle du mercure dans la retenue ? Quelle en est la part anthropique et naturelle ?
- Quel devenir pour le mercure issu de la retenue en contrebas du barrage?
- Quelles sont les conditions chimiques et les formes du mercure propices à la methylation ?

Ces problématiques constituent le cœur du travail réalisé. Elles ont été discutées, chacune à leur tour, dans un article leur étant directement consacré. Ces articles constituent par conséquent le corps du présent document. L'objectif final de ce dernier étant (nous l'espérons) d'enrichir la compréhension du lecteur sur le cycle biogéochimique du mercure dans l'écosphère tropicale : dans l'atmosphère, l'hydrosphère, la géosphère et la biosphère.

4.2. Rappel des résultats principaux

Les données recueillies au cours des missions MATOUTOU 1 à 5 (2003-2005) sur le site de la retenue de Petit-Saut, analysées au centre IFREMER de Nantes puis modélisées à l'INRS-ETE au Québec sont réunies sous forme de 4 articles dans ce document. Elles se résument à :

ARTICLE I : Le Hg atmosphérique au niveau de la retenue est majoritairement d'origine océanique. Les concentrations moyennes dans l'air et la pluie sont respectivement de 12 ± 2 pmol m^{-3} et 16 ± 12 pmol L^{-1}. A la surface de la retenue, le mercure dissous gazeux (DGM) atteint 350 ± 200 fmol L^{-1}. Le flux atmosphérique entrant représente 14 moles a^{-1} (60 nmol m^{-2} a^{-1}) dont ~ 75 % sous forme de précipitations. Le flux atmosphérique sortant représente 23 moles a^{-1} dont ~ 90 % (90 nmol m^{-2} a^{-1}) par évasion à l'interface air / eau. Des variations significatives sont relevées à l'échelle des différentes saisons et de l'alternance jour-nuit.

ARTICLE II : Dans l'épilimnion de la retenue de Petit-Saut, Hg total (HgT) et MMHg représentent 4 ± 2 et 0,3 ± 0,2 pmol L^{-1} sous forme dissoute et 200 ± 150 et 80 ± 70 pmol g^{-1} sous forme particulaire. Dans l'hypolimnion, HgT et MMHg représentent 8 ± 4 et 0,9 ± 0,5 pmol L^{-1} dans le dissous et 1300 ± 950 et 170 ± 90 pmol g^{-1} dans la fraction particulaire. La distribution bimodale du MMHg dans la colonne d'eau désigne la chemocline et l'interface benthique en tant que sites privilégiés de méthylation. Le flux cumulé de mercure vers la retenue de Petit-Saut est en grande partie d'origine naturelle (> 95 % des apports). En amont de la retenue, les principaux affluents contribuent à importer chaque année 76 moles de HgT_{UNF} dont 4,7 moles sous forme de $MMHg_{UNF}$. Les indices « UNF » et « D » désignent les échantillons non filtrés et la fraction dissoute. Le barrage exporte chaque année 78 moles de HgT_{UNF} dont 13,5 moles sous forme de $MMHg_{UNF}$. Selon un bilan de masse, la production *in situ* de $MMHg_{UNF}$ (i.e. $MMHg_D$) atteint 8,1 (7,3) moles a^{-1} soit un taux de méthylation de 0,06 (0,08) % j^{-1}.

ARTICLE III : L'estuaire du Sinnamary est un environnement dynamique qui présente des gradients rédox prononcés et où la matière organique est rapidement recyclée. En amont de la zone d'intrusion saline (ou USE), HgT et MMHg représentent 6 ± 2 et 2,0 ± 0,9 pmol L^{-1} dans le dissous et 600 ± 200 et 220 ± 130 pmol g^{-1} dans le particulaire. Le mercure subit un large spectre de

transformations biogéochimiques couplant changements de phase et de spéciation en relation avec les cycles de la matière organique, du fer et du soufre. Arrivant en zone saline (ou LES), les particules charriées par le fleuve Sinnamary se mélangent à la matière en suspensions (180 ± 40 pmol g^{-1}) formant le panache de l'Amazone. Le $MMHg_D$ présente alors un comportement non conservatif illustré à l'aide d'un modèle de complexation. L'estuaire du Sinnamary réunit des conditions propices à la méthylation mises en exergue par le fait que l'USE exporte 60 % de $MMHg_{UNF}$ en plus qu'il en importe : 27 contre 17 moles a^{-1}.

ARTICLE IV : L'étude des complexes du mercure dans le continuum réservoir de Petit-Saut / estuaire du Sinnamary montre que l'espèce $HgSO_4$ joue un rôle charnière entre Hg non méthylé (HgT_{UNM}) et MMHg. En s'appuyant sur l'analyse des distributions et les données déjà présentes dans la littérature, nous avons émis l'hypothèse que le complexe $HgSO_4$ est préférentiellement formé dans les zones à fort gradient rédox. Finalement, l'introduction du soufre zéro-valent dans nos modèles de spéciation s'accompagne d'une diminution des niveaux mesurés de MMHg.

4.3. Synthèse des résultats principaux

Vers un modèle général ?

Depuis l'atmosphère en passant par la retenue, l'estuaire du Sinnamary et jusqu'à l'océan atlantique, la construction du barrage de Petit-Saut perturbe profondément le cycle naturel du mercure à l'échelle locale.

Le mercure atmosphérique accède directement à la retenue *via* les précipitations. Cette source représente 11 ± 7 moles a^{-1} de HgT_{UNF} (près de 75 % du dépôt total) dont 0,7 moles a^{-1} sous forme de $MMHg_{UNF}$. L'intense rayonnement solaire et une végétation éparse favorisent les mécanismes de photoréduction dans les eaux de surface de la retenue et par conséquent le recyclage du mercure aquatique vers l'atmosphère. L'évasion atteint 23 ± 10 moles a^{-1}. La variabilité saisonnière est marquée : en saisons humides les dépôts dominent (150 *vs* 130 pmol m^{-2} j^{-1}) tandis qu'en saisons sèches il s'agit de l'évasion (400 *vs* 100 pmol m^{-2} j^{-1}). En moyenne, les flux annuels de Hg entrants et sortants à l'interface air / eau de la retenue (respectivement 60 et 90 nmol m^{-2} a^{-1}) sont comparable à ceux de l'océan Atlantique (respectivement 40 et 110 nmol m^{-2} a^{-1}).

Depuis 1995 (date de mise en eau du barrage), les entrées

cumulées de Hg dans la retenue de Petit-Saut sont estimées à environ 8000 moles. Celles-ci sont en grande partie (> 95 %) d'origine « naturelle » : dégradation des sols et de la végétation immergée. De nos jours, la retenue importe principalement le mercure *via* ses affluents : soit 76 moles a^{-1} de HgT_{UNF} dont 4,7 moles a^{-1} en tant que $MMHg_{UNF}$. Les sources historiques (sols + végétation ennoyée) ne représentent plus que ~ 20 % des apports *via* les affluents. Bien qu'apparente, la signature de la zone minière de St.-Elie demeure cantonnée (sauf événements pluviaux majeurs) en amont des cours d'eau orpaillés (Courcibo et Leblond). Une fois dans de la retenue, le mercure subit toute une chaîne complexe de transformations couplant changements de substrat et de spéciation. A terme, le Hg est transféré vers l'atmosphère, les sédiments, le biota ainsi qu'en contrebas du barrage. On estime que ce dernier exporte 78 moles a^{-1} de HgT_{UNF} dont 13,5 moles a^{-1} de $MMHg_{UNF}$.

A partir du bilan de masse en MMHg et de la distribution verticale des espèces de Hg, nous avons conclu que la retenue constitue un site privilégié de méthylation. La production *in situ* de MMHg a lieu dans des sites particuliers que sont la chemocline et l'interface benthique. A l'aide d'outils de modélisation, nous avons montré que ces sites, couplant conditions rédox transitoires et intense recyclage de la MO, Fe et S, favorisent la formation d'espèces inorganiques méthylables de mercure. La production *in situ* de $MMHg_{UNF}$ (ou de $MMHg_D$) atteint pour l'ensemble de la retenue 8,1 (7,3) moles a^{-1} soit un taux de méthylation de 0,06 (0,08) % j^{-1}. Cette valeur met en évidence le rôle de réacteur chimique joué par la retenue de Petit-Saut : altération de la spéciation du mercure au profit des composés méthylés.

L'estuaire du Sinnamary représente plus qu'un simple tuyau convoyant l'eau exportée par la retenue vers l'océan Atlantique. Il définit le véritable réacteur chimique du système regroupant (parmi d'autres) des processus de partition et de méthylation (10 moles a^{-1}) du mercure. Ces processus résultent avant tout de l'oxygénation incomplète persistante des masses d'eau anoxiques exportées par la retenue. L'expression de gradients rédox prononcés couplée à un intense recyclage de la MO, Fe et S, y favorisent la production d'espèces inorganiques méthylables de Hg ainsi que l'activité des bactéries sulfatoréductrices (agents reconnus de la méthylation). Par ailleurs, l'existence d'une source permanente de $MMHg_{UNF}$ en amont (17 moles a^{-1} au niveau des oxygénateurs) contribue à maintenir les concentrations de l'estuaire à un niveau élevé tout au long de l'année.

L'estuaire du Sinnamary est une source significative de Hg pour le milieu côtier : 62 moles a^{-1} de HgT_{UNF} dont 27 moles a^{-1} de $MMHg_{UNF}$. Le cycle côtier du mercure est perturbé par les apports constants et en grande partie méthylés de l'estuaire : la zone saline de l'estuaire joue un rôle de dilution et de réacteur chimique pour le mercure fluviatile. Au sein de cette région, nous avons mis en évidence : (i) un comportement non conservatif du Hg de la phase dissoute, (ii) un appauvrissement global en mercure des particules suite au mélange avec le panache de l'Amazone et (iii) une dilution progressive des concentrations par les masses d'eau océaniques. Le piégeage du Hg réactif sous forme colloïdale dans la région de turbidité et sa floculation sont des phénomènes majeurs. Plus au large, la diminution rapide des concentrations de $MMHg_D$ suggère un ralentissement des mécanismes de méthylation (oxygénation accrue des eaux, diminution des niveaux de MO) et/ou l'activation des mécanismes de déméthylation (formation de chlorocomplexes, photodégradation du MMHg formé).

Au final, le continuum retenue de Petit-Saut / estuaire du Sinnamary définit un pôle de transformation du Hg associant un substrat abondant (mais aux sources variées) à des sites actifs de méthylation (aux interfaces rédox).

4.4. Perspectives

Au fur et à mesure du traitement des résultats, de nouvelles questions se sont posées. Certaines d'entre elles (une grande partie en fait !) n'ont pas obtenu de réponse dans le cadre de ce travail. Les causes en sont le manque de temps, de moyens financiers ainsi que l'inadéquation de nos compétences et accessoirement celle des techniques d'investigation. Cette section présente ces « questions qui restent à résoudre » et donne quelques pistes de recherche pour approfondir la compréhension du cycle du mercure dans les lacs artificiels tropicaux.

- Quelle sera l'évolution des échanges de Hg à l'interface air / eau à l'échelle du temps de vie du barrage ?
- Quelle est la part de Hg anthropique dans le dépôt de Hg atmosphérique au niveau de la retenue ?
- Quelles sont les souches de bactéries impliquées dans les processus d'oxydation / réduction aphotiques ? Quels en sont les mécanismes ?

- Quelle sera l'évolution des niveaux de MMHg dans la retenue à l'échelle du temps de vie du barrage ?
- Comment les niveaux de MMHg dans la retenue de Petit-Saut affecteront-ils ceux de l'estuaire du Sinnamary ?
- Quelles sont les souches de bactéries impliquées dans les processus de méthylation / déméthylation ? Quels en sont les mécanismes ?
- Quelle part est occupée par les processus de méthylation abiotiques ?
- Quel rôle jouent les biofilms (fixés sur les sols, les troncs d'arbres immergés, la matière en suspension etc.) dans la méthylation du Hg ?
- Quelles sont les transformations du Hg dans les sédiments anoxiques de la retenue ?
- Existe-t-il une distinction fondamentale entre le cycle du Hg à la chemocline et à l'interface benthique ?
- Quel est le devenir du mercure dans l'océan Atlantique hauturier ?

Par ailleurs, au cours de cette thèse, quelques éléments de remédiation quant à l'état du système sont venus compléter les questions sur le devenir du cycle local du mercure. Ils intègrent le fait que la décontamination des milieux aquatiques dépend de la compétition entre réactions de méthylation et de réduction de ce métal. En effet, la méthylation contribue à l'imprégnation des chaînes alimentaires tandis que la réduction favorise le recyclage du Hg vers l'atmosphère.

(i) En surface de la retenue, l'approfondissement progressif de la photocline avantage les processus de photoréduction du Hg divalent et de photodégradation du MMHg.

(ii) Plus en profondeur, au voisinage de l'oxycline, l'export du Hg^0 néoformé, une baisse de l'acidité ainsi qu'une oxydation (réduction) accrue du Fe (S) par rapport au S (Fe) bénéficierait à la réduction du Hg.

Autrement,

(iii) Le substrat initialement immergé pourrait de nos jours s'avérer un support privilégié de fixation du Hg de la colonne d'eau mais également de méthylation au niveau des biofilms.

(iv) L’accroissement de l’activité de l’opéron *mer* au sein des bactéries résistantes au mercure permettrait de réduire ce dernier et dans certains cas de déméthyler le MMHg.

A ce jour, les travaux visant à étudier le cycle du mercure dans les milieux aquatiques tropicaux sont l’apanage des grandes puissances économiques (Etats-Unis d’Amérique, Australie, Union Européenne, Brésil, Chine, Japon, etc.). Or les régions tropicales regroupent des pays qui ne peuvent s’offrir les moyens de cette recherche (Guinée, Soudan, Tchad, Laos, Vietnam, Bengladesh etc.). Une simple constatation : sur 50 articles majeurs concernant le cycle du Hg en milieu tropical, seulement 7 proviennent des pays tropicaux en voie de développement (Elsevier publications). Il ne faut cependant pas généraliser : l’ambassade de France a financé en 2003 l’achat d’un analyseur de Hg au Vietnam et plusieurs thèses pour des géochimistes… Ce déséquilibre profond contribue à une connaissance fragmentée des conséquences de la pollution par le Hg et de sa méthylation. En effet, si la problématique du mercure est un enjeu global, il est dommage qu’il n’en soit pas de même pour son étude. La question est de savoir si nous voulons transmettre aux régions concernées la compétence d’analyse des métaux trace plutôt que de financer des projets ponctuels et provisoires ?

BIBLIOGRAPHIE

AMORIM M.I., MERGLER D., BAHIA M.O., DUBEAU H., MIRANDA D., LEBEL J., BURBANO R.R. et LUCOTTE M. (2000) Cytogenetic damage related to low levels of methylmercury contamination in the Brazilian Amazon. *An. Acad. Bras. Cienc*. **72**, 497-507.

AMOUROUX D., WASSERMAN J.C., TESSIER E. et DONARD O.F.X. (1999) Elemental mercury in the atmosphere of a tropical Amazonian Forest (French Guiana). *Environ. Sci. Technol.* **33**, 3044-3048.

BOUDOU A., BRACHET R.M., COQUERY M., DURRIEUX G. et COSSA D. (2005). Synergic effect of goldmining and gamming on mercury contamination in fish. *Environ. Sci. Technol.* **39**, 2448-2454.

CARMOUZE J.P., LUCOTTE M. et BOUDOU A. (2001) Le mercure en Amazonie Rôle de l'homme et de l'environnement, risques sanitaires. *Ird (éditions)* **ISBN : 2709914670**, 494 pp

COMITE FRANÇAIS des BARRAGES et RESERVOIRS (2005) Base bibliographique sur le barrage de Petit-Saut. Quelques chiffres. www.barrages-cfbr.org

CHARLET L. et BOUDOU A. (2002). Cet or qui file un mauvais mercure. *La Recherche* **359**, 52-59.

CENTRAL INTELLIGENCE AGENCY (2005) United States government profiles of countries and non-self-governing territories around the world.
http://www.cia.gov/cia/publications/factbook/

COQUERY M., COSSA D., AZEMARD S., PERETYAZHKO T. et CHARLET L. (2003) Methylmercury formation in the anoxic waters of the Petit-Saut reservoir (French Guiana) and its spreading in the adjacent Sinnamary River. *Journal de Physique IV* **107**, 327-331.

CORDIER S., GRASMICK C., PASSELAIGUE P.M., MANDEREAU L., WEBER J-P. et JOUAN M. (1997) Imprégnation de la population guyanaise par le mercure : niveaux et sources d'exposition. *BEH* **14**, 59-61.

CORDIER S. et GRASMICK C. (1994) Etude de l'imprégnation par le mercure dans la population guyanaise. *Rapport Réseau*

National de Santé Publique/ Direction Générale de la Santé. 28 pp.

DELANNON T.C. (2000) L'Or en Guyane : éclats et artifices. *La Documentation française* 157 pp.

DOLBEC J., MERGLER D., PASSOS C.-J.S., MORAIS S.S. et LEBEL J. (2000) Methylmercury exposure affects motor performance of a riverine population of the Tapajós River, Brazilian Amazon. *Int Arch Occup Environ Health* **73**, 195-203.

ELSEVIER PUBLICATIONS (2006) Electronic collection of science, technology and medicine full text and bibliographic information. http://www.sciencedirect.com/

ENVIRONNEMENT CANADA (2005) Le mercure dans l'environnement http://www.ec.gc.ca/MERCURY/

EVANS R.D. (1986) Sources of mercury contamination in the sediments of small headwater lakes in southcentral Ontario, Canada. Arch. Environ. *Contam. Toxicol.* **15**, 505-512.

FRÉRY N., BRACHET R.M., MAILLOT E., DEHEEGER M., MERONA B. et BOUDOU A. (2001) Gold-mining activities and mercury contamination of native amerindian communities in French Guiana: Key role of fish in dietary uptake. *Environmental Health Perspectives* **109**, 449-456.

FRERY N., MAILLOT E. et DEHEEGER M. (1999) Exposition au mercure de la population amérindienne Wayana de Guyane. *Institut de veille sanitaire*, 83 pp.

GRANDJEAN P., WHITE R.F., NIELSEN A., CLEARY D. et ESANTOS E.C.O. (1999) Methylmercury neurotoxicity in amazonian children downstream from goldmining. *Environmental Health Perspectives* **107**, 587-591.

GUEDRON S., GRIMALDI C., CHAUVEL C., SPADINI L. et GRIMALDI M. (2006) Weathering *versus* atmospheric contributions to mercury contents in French Guiana soils. *Applied Geochemistry*, sous presse.

HOREAU V., RICHARD S. et CERCAN P. (1998) La qualité de l'eau et son incidence sur la biodiversité. L'exemple de la retenue de Petit Saut (Guyane Française). JATBA, *Revue d'Ethnobiologie* **40**, 53-77.

HUYNH F., CHARRON C., BETOULLE J.L., PANECHOU K., GARDEL A., PROST M.T. et LOUBRY D. (1997) Suivi de l'évolution géomorphologique et botanique de l'estuaire du Sinnamary

par télédétection. *Final report ORSTOM-EDF*, 64pp.

HYDRO-QUEBEC (2005) Suivi de la teneur de mercure dans les réservoirs. http://www.hydroquebec.com/

JOHNSON M.G. (1987) Trace element loadings to sediments of fourteen Ontario lakes and correlations with concentrations in fish. *Can. J. Fish. Aquat. Sci.* **44**, 3-13.

LACERDA L.D. (1997b). Evolution of mercury contamination in Brazil. *Water Air Soil Pollut.* **97**, 247-255.

LACERDA L.D. (1997a) Global emissions of Hg from gold and silver mining. *Water. Air Soil Pollut.* **97**, 209-221.

LEBEL J., MERGLER D., BRANCHES F.J.P., LUCOTTE M., AMORIM M., LARRIBE F. ET DOLBEC J. (1998) Neurotoxic effects of low level methylmercury contamination in the Amazon Basin. *Environmental Research* **89**, 20-32.

LEBEL J., MERGLER D., LUCOTTE M., AMORIM M., DOLBEC J., MIRANDA D., ARANTÈS G., RHEAULT I. et PICHET P. (1996) Evidence of early nervous system dysfunction in Amazonian population exposed to low levels of monomethylmercury. *Neurotoxicology* **17**, 157-168.

MAMERE N.M., BILLARD M. et COCHET Y. (2004) Proposition de résolution N° 1503 tendant à la création d'une commission d'enquête sur l'orpaillage en Guyane. *Assemblée Nationale.*

MASON R.P., FITZGERALD W.F. et MOREL F.M.M. (1994) The biogeochemical cycling of elemental mercury: Anthropogenic influences. *Geochimica et Cosmochimica Acta* **58**, 3191-3198.

MERCURE en GUYANE (2001) Rapport finaux 1^{ERE} et 2EME. Région de Saint Elie et retenue de Petit Saut. / Région du Haut Maroni et lieux de référence ECEREX et MATECHO. *CNRS*. http://www.cnrs.fr/Cnrspresse/n390/html/n390a03.htm

MERGLER D. (2006) Ecosystem Approach to Mercury and Health in the Amazon Basin. *International Conference on Rivers and Civilization*. Wisconsin USA, **Abstract**.

MINING, MINERALS, SUSTAINABLE DEVELOPMENT. (2002) International Institute for Environment and Development, *MMSD* http://www.iied.org/mmsd/finalreport/index.html

NRIAGU J.O. (1989) A global assessment of natural sources of atmospheric trace metals. *Nature* **338**, 47-49.

ORGANISATION MONDIALE de la SANTE (1983) Mesure des modifications de l'état nutritionnel. *Genève.* 104 pp.

PORVARI P. (1995) Mercury levels of fish in Tucuruı´ hydroelectric reservoir and in river Moju´ in Amazonia, in the state of Para, Brazil. *Sci. Total Environ.* **175**, 109-117.

RASMUSSEN P.E., VILLARD D.J., GARDNER H.D., FORTESCUE J.A.C., SCHIFF S.L. et SHILTS W.W. (1998b) Mercury in lake sediments of the precambrian shield near Huntsville, Ontario, Canada. *Environ. Geol.* **33**, 170-182.

RICHARD S., ARNOUX A. et CERDAN P. (1997) Evolution in physico-chemical water quality in the reservoir and downstream following the filling of Petit-Saut dam (French Guiana). *Hydroecol. Appl.* **9**, 57-83.

ROULET M. et GRIMALDI C. (2001) Le mercure dans les sols d'Amazonie. Origine et comportement du mercure dans les couvertures ferrallitiques du bassin amazonien et des Guyanes. *Editions IRD*, 121-166.

ROULET M., LUCOTTE M., FARELLA N., SERIQUE G., COELHO H., PASSOS C.J.S., SILVA E.J., ANDRADE P.S., MERGLER D. et GUIMARAES J.R.D. (1999) Effects of recent human colonization on the presence of mercury in amazonian ecosystem. *Water, Air and Soil Pollution* **112**, 297-313.

SISSAKIAN C. (1997) Présentation générale de l'aménagement hydroélectrique de Petit-Saut (Guyane Française) et du programme de suivi écologique lié à sa mise en eau. *Hydroécol. Appl*. **9**, 1-21.

UNITED NATIONS ENVIRONMENTAL PROGRAM (2002) The Global Mercury Assessment report. 306 pp. http://www.unep.org/

UNITED NATIONS INDUSTRIAL DEVELOPMENT ORGANIZATION (2005) Meeting on the "Global Partnership for Mercury Management in Artisanal and Small-Scale Gold Mining". http://www.unido.org/

WORLD COMMISSION et DAMS (2000) Dams and development, a new frame work for decision-making. *Earthscan Publications* VA, 356 pp.

ANNEXES

Le peuple français
proclame solennellement
son attachement aux Droits
de l'Homme et aux principes de la
souveraineté nationale tels qu'ils ont été
définis par la Déclaration de 1789,
confirmée et complétée par
le préambule de la Constitution
de 1946, ainsi qu'aux droits
et devoirs définis dans la Charte
de l'environnement
de 2004.

Charte de l'environnement

la constitutionnalisation du développement durable

« Le peuple français,

« Considérant,

« Que les ressources et les équilibres naturels ont conditionné l'émergence de l'humanité ;

« Que l'avenir et l'existence même de l'humanité sont indissociables de son milieu naturel ;

« Que l'environnement est le patrimoine commun des êtres humains ;

« Que l'homme exerce une influence croissante sur les conditions de la vie et sur sa propre évolution ;

« Que la diversité biologique, l'épanouissement de la personne et le progrès des sociétés humaines sont affectés par certains modes de consommation ou de production et par l'exploitation excessive des ressources naturelles ;

« Que la préservation de l'environnement doit être recherchée au même titre que les autres intérêts fondamentaux de la Nation ;

« Qu'afin d'assurer un développement durable, les choix destinés à répondre aux besoins du présent ne doivent pas compromettre la capacité des générations futures et des autres peuples à satisfaire leurs propres besoins ;

« proclame :

Article 1
Chacun a le droit de vivre dans un environnement équilibré et respectueux de la santé.

Article 2
Toute personne a le devoir de prendre part à la préservation et à l'amélioration de l'environnement.

Article 3
Toute personne doit, dans les conditions définies par la loi, prévenir les atteintes qu'elle est susceptible de porter à l'environnement ou, à défaut, en limiter les conséquences.

Article 4
Toute personne doit contribuer à la réparation des dommages qu'elle cause à l'environnement, dans les conditions définies par la loi.

Article 5
Lorsque la réalisation d'un dommage, bien qu'incertaine en l'état des connaissances scientifiques, pourrait affecter de manière grave et irréversible l'environnement, les autorités publiques veillent, par application du principe de précaution et dans leurs domaines d'attributions, à la mise en œuvre de procédures d'évaluation des risques et à l'adoption de mesures provisoires et proportionnées afin de parer à la réalisation du dommage.

Article 6
Les politiques publiques doivent promouvoir un développement durable. À cet effet, elles concilient la protection et la mise en valeur de l'environnement, le développement économique et le progrès social.

Article 7
Toute personne a le droit, dans les conditions et les limites définies par la loi, d'accéder aux informations relatives à l'environnement détenues par les autorités publiques et de participer à l'élaboration des décisions publiques ayant une incidence sur l'environnement.

Article 8
L'éducation et la formation à l'environnement doivent contribuer à l'exercice des droits et devoirs définis par la présente Charte.

Article 9
La recherche et l'innovation doivent apporter leur concours à la préservation et à la mise en valeur de l'environnement.

Article 10
La présente Charte inspire l'action européenne et internationale de la France. »

LE CYCLE DU MERCURE

(Selon Environnement Canada)

Jusqu'au milieu des années 1960, on a pensé que le mercure était relativement stable et inactif dans l'environnement. On sait maintenant que son cycle global est compliqué : il passe d'un milieu naturel à l'autre (vivant et inanimé), il est transporté à grande distance, et il subit des transformations chimiques (figure ci-après). Là où il n'existe pas de source directe de pollution par le mercure, la plus grande partie des apports provient de la pluie, de la neige et d'autres formes de précipitations tels que les aérosols. Une fois déposé sur le sol ou dans l'eau, une partie de ce mercure est transformée chimiquement et devient volatile. Il peut dés lors s'évaporer et retourner dans l'air pour être transporté sur de longues distances et se redéposer. Les océans et les lacs reçoivent en outre du mercure apporté par les cours d'eau. Les eaux souterraines et de ruissellement entraînent aussi d'importantes quantités de mercure dans les lacs, en particulier dans les milieux humides.

Dans la colonne d’eau, le mercure peut être transformé en deux espèces organiques majeures : le monométhylmercure et le diméthylmercure. Le premier de ces deux composés est le plus préoccupant pour l'environnement. Il subit une bioamplification le long des chaînes alimentaires jusqu'à atteindre des concentrations qui sont toxiques pour le poisson et la faune. Le second s'évapore dans l'air ou se transforme en monométhylmercure, surtout dans les systèmes marins. La quantité totale de monométhylmercure qui est produite dépend de nombreux facteurs qu'on ne comprend pas encore entièrement. La quantité de mercure inorganique présente dans l'environnement est un facteur important : elle est le substrat indispensable à la formation de méthylmercure. La plus grande partie du monométhylmercure se forme dans la couche supérieure des sédiments au fond des lacs. Certains types de bactéries peuvent à la fois former et décomposer du monométhylmercure, mais cela peut aussi se faire sans leur aide. Les conditions des lacs, comme une faible profondeur, un faible pH (l'acidité), une température assez élevée et une faible salinité, comptent parmi les facteurs qui favorisent la production de monométhylmercure. La quantité de matière organique dans l’eau et les sédiments, comme les plantes et les animaux décomposés, est très importante parce qu'elle est une source d'alimentation pour les bactéries. Les réservoirs d'eau sont particulièrement préoccupants car ils instaurent des conditions favorables pour la méthylation. C'est pourquoi la concentration de

monométhylmercure mesurée dans les poissons de réservoir est relativement élevée pendant une période pouvant aller jusqu'à 30 ans après la construction d'un barrage.

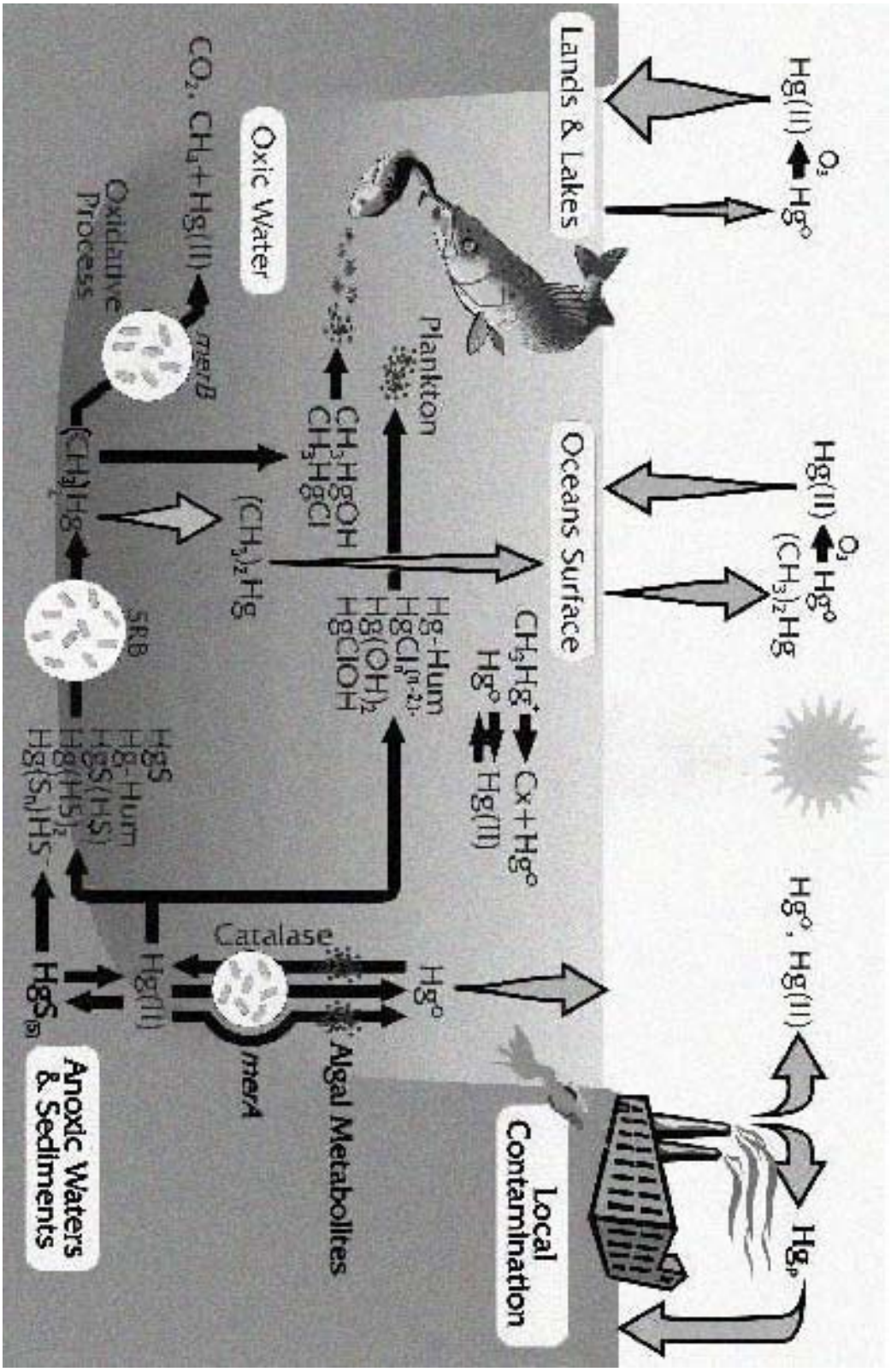

CYCLE BIOGEOCHIMIQUE DU MERCURE. Le mercure présente un forte aptitude à se bioaccumuler au sein des espèces vivantes et à se bioamplifier le long des chaînes trophiques. Cette propriété est déterminée par les transformations et les transferts qu'il subit. Les flèche noires correspondent aux transformations, celle grises aux transferts.

L'IMPREGNATION PAR LE MERCURE DE LA POPULATION DE SINNAMARY

(Selon l'Institut de Veille Sanitaire)

La retenue d'eau du barrage de Sinnamary est un milieu anoxique et riche en matière organique donc propice à la méthylation du mercure. On observe une bioamplification du méthylmercure chez les poissons. La consommation de poissons par la population de Sinamary étant essentiellement basée sur la pêche locale, il s'est avéré nécessaire de réaliser une enquête afin d'en étudier l'impact sanitaire. En novembre 2001, une enquête transversale a été réalisée avec comme objectif principal d'évaluer l'imprégnation mercurielle des personnes résidant en aval du barrage et de valider les estimations issues de l'enquête réalisée en 1994 par le RNSP. A cet égard, une mèche de cheveux a été prélevée afin de doser le mercure. Les résultats montrent que peu de personnes ont une concentration mercurielle supérieure à 10 µg g^{-1} de cheveux, la valeur seuil recommandée par l'OMS. Ces dépassements concernent 5% de la population enquêtée, 6% des adultes, 2% des enfants et aucune femmes en âge de procréer. Les résultats objectivent une relation entre la concentration de mercure et la consommation de poissons. En particulier, la consommation de poissons de fleuve est très liée à une concentration de mercure élevée. L'analyse des facteurs de variation de l'imprégnation mercurielle montre en outre qu'un mode de vie traditionnel, basé sur une consommation des produits de la pêche et de la chasse en forêt est significativement associé à une concentration élevée de mercure dans le cheveu.

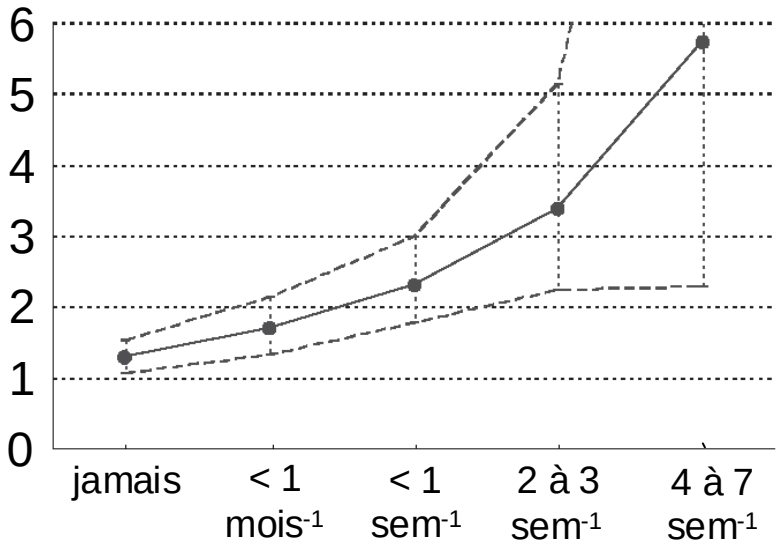

Moyennes géométriques des concentrations de Hg dans les cheveux (µg g^{-1}) par fréquence de consommation de poisson de fleuve et leurs intervalles de confiance.

Série : "Les méthodes d'analyses en milieu marin"

Spéciation du mercure dissous dans les eaux marines : Dosages du mercure total, gazeux, réactif, mono et diméthylmercure

Daniel Cossa

Bernard Averty

Jane Bretaudeau

Anne Sophie Sénard

Institut Français de Recherche pour l'Exploitation durable de la Mer (IFREMER), BP 21105, F.44311 Nantes cedex 03

Juin 2003 (CossaHg-Eau5.doc)

SOMMAIRE

AVANT PROPOS

Ce document fait partie d'une série de fascicules intitulée "Les méthodes d'analyses en milieu marin". Cette série s'adresse bien sûr d'abord aux analystes, mais elle sera probablement utile aux gestionnaires de l'environnement ainsi qu'aux étudiants intéressés par les spécificités analytiques du milieu marin. Ces méthodes sont employées à l'Ifremer dans les programmes de recherche comme ceux de surveillance de la qualité du milieu. Elles sont validées par la pratique de nombreux laboratoires spécialisés dans l'étude des matrices marines. La plupart d'entre-elles ont fait l'objet d'exercices d'intercomparaisons internationales, en particulier dans le cadre du CIEM (Conseil international d'exploration de la mer), de l'AIEA (Agence internationale de l'énergie atomique), ou du BCR (Bureau des références de la Commission européenne). Certaines de ces méthodes constituent les méthodes de référence du Réseau National d'Observation de la Qualité du milieu marin (RNO) du Ministère de l'Aménagement du territoire et de l'Environnement géré et réalisé par l'Ifremer.

RESUME

Dans ce fascicule sont décrites les méthodes et protocoles de prélèvement et d'analyse permettant le dosage du mercure gazeux dissous (HgGD) incluant le mercure élémentaire (Hg^0) et le diméthylmercure (DMHg), du mercure "réactif" (HgR ou "facilement réductible" qui est essentiellement constitué par diverses formes inorganiques du mercure), du monométhylmercure (MMHg) et du mercure total (HgT) dissous dans les eaux marines. Ces techniques permettent le dosage de traces avec des limites de détection se situant entre 4 à 60 pg L^{-1} suivant les espèces chimiques et les volumes d'eau utilisés. Du fait de l'ajustement possible du volume d'échantillon analysé, la gamme des concentrations mesurables au dessus de la limite de détection mesurable est de plusieurs ordres de grandeur. Les répétabilités des différents dosages se situent entre 5 et 15 % dépendant du volume d'échantillon et des niveaux de concentration.

ABSTRACT

Sampling and analytical techniques for mercury speciation in sea water are described. They allow the determination of elemental mercury (Hg^0), dimethylmercury (DMHg), reactive mercury (HgR or "easily reducible mercury" which consists of mainly inorganic mercury species), monomethylmercury (MMHg) and total mercury (HgT) dissolved in sea water. These techniques allow the detection of trace amounts, between 4 and 60 pg L^{-1}, depending on the chemical species and the sampled volume. The ranges of measurable concentrations are of several orders of magnitude and reproducibilities vary between 6 and 15 % according to the species and concentration levels.

INTRODUCTION

Le mercure est un élément métallique parmi les plus toxiques qui atteint le milieu marin de sources naturelles et anthropiques. La connaissance de sa répartition et de ses transferts dans les différents réservoirs marins, de même que la surveillance des niveaux de contamination ne peuvent être atteints que par l'obtention de données fiables. Nous décrivons ici les techniques et protocoles de prélèvement et d'analyse éprouvés permettant le dosage du mercure gazeux incluant le mercure élémentaire (Hg^0) et le diméthylmercure (DMHg), du mercure "réactif" (HgR ou "facilement réductible" qui est constitué essentiellement des formes inorganiques du mercure), du monométhylmercure (MMHg) et du mercure total (HgT) dissous dans les eaux marines.

A partir de l'expérience réunie lors du développement des techniques analytiques pour la détermination des métaux en trace dans les eaux naturelles, des études systématiques sur les sources de contamination par le mercure et leur contrôle ont été effectuées (ex. Bloom et Crecelius, 1983; Fitzgerald *et al.*, 1983; Gill et Fitzgerald, 1985). Ces études s'accordent sur les préalables à l'obtention de résultats fiables sur les concentrations naturelles en eau de mer. Il faut notamment:

- prélever et conserver l'eau "proprement" dans des récipients appropriés. L'utilisation de matériaux en téflon spécialement nettoyé pour le prélèvement et le stockage des échantillons est nécessaire ;
- choisir des protocoles analytiques compatibles avec le dosage des contaminants à l'état de traces c'est-à-dire en sélectionnant ceux qui requièrent un minimum de manipulations et les plus faibles quantités de réactifs chimiques ;
- travailler dans un environnement "propre" incluant l'utilisation d'une "salle blanche" ou au moins d'une hotte à flux laminaire ;
- disposer d'une méthode de détection analytique suffisamment sensible pour mesurer quelques picogrammes (pg) de mercure.

La combinaison de techniques ultra-propres de prélèvement, de stockage et de traitement des échantillons avec une méthode de détection très sensible, la spectrométrie de fluorescence atomique (SFA) a permis d'acquérir la conviction que les teneurs naturelles en mercure total dissous dans la plupart des eaux marines non contaminées se situent pour la plupart entre 0,1 et 2 ng L^{-1}. En absence de matériau de référence certifié, cette conviction provient de la convergence entre la bonne précision des mesures et la capacité d'interprétation des résultats.

Le principe du dosage du mercure utilisé dans ces protocoles repose sur la volatilité du mercure élémentaire (Hg^0) à la température ambiante. Le mercure vapeur est quantifié par SFA, où le nuage de vapeur de mercure est soumis à l'excitation d'un faisceau lumineux de longueur d'onde 254 nm et la fluorescence émise est mesurée à la même longueur d'onde. La détermination du mercure gazeux dissous (HgGD) ne requiert pas de traitement préalable de l'échantillon (l'échantillon est dégazé sous flux d'argon), alors que celle du HgR nécessite une réduction préalable du Hg^{II} en Hg^0 par le $SnCl_2$ et celle du HgT une dissociation des organomercuriels au BrCl avant la réduction (Bloom et Crecelius, 1983). La méthode de dosage des formes méthylées (MMHg et DMHg) utilise la chromatographie cryogénique (Bloom, 1989). Dans le cas précis du MMHg il s'agit de l'optimisation de la technique combinant l'hydruration et la chromatographie cryogénique (Tseng *et al.*, 1998). Quelle que soit l'espèce chimique mesurée la détection est réalisée par SFA. La SFA est à la base de la norme française AFNOR T90-113-2 et de la méthode EPA 1631 ayant cours aux Etats-Unis d'Amérique pour mesurer du mercure total dans l'eau.

1. PRELEVEMENT, FILTRATION ET CONSERVATION DES ECHANTILLONS

Plusieurs documents ont énoncé les principes et décrit les pratiques du travail sur les traces. La contribution pionnière du Conseil National des Recherches du Canada dans le domaine est exposée dans un article de synthèse dans lequel Sturgeon et Berman (1987) décrivent l'état de l'art pour l'échantillonnage et le stockage des eaux en vue du dosage des métaux-traces. Ils passent en revue les matériaux utilisables et leur nettoyage, les échantillonneurs, les méthodes de prélèvement et leur évaluation, la filtration, la préconcentration, la préservation et le stockage. Les « salles blanches », ou laboratoires propres, ont été décrites dans divers articles (ex.: Boutron, 1990). L'échantillonnage et les méthodes analytiques sont détaillées dans plusieurs autres (ex.: Kramer, 1994 ; Nolting et Jong, 1994). Les techniques de contrôle de la qualité dans ce domaine spécifique sont présentées entre autres par Taylor (1987) et Keith (1991). Il est important de souligner à ce stade que ces derniers auteurs insistent particulièrement sur la prise en compte, dans le processus de contrôle de la qualité, des étapes de prélèvement et de traitement préalable des échantillons, souvent négligées par le passé. De façon plus exhaustive, Howard et Statham (1993) donnent la philosophie qui soutient la mise au point des analyses de traces. Les premières précautions sont le contrôle de la qualité de l'air et des matériaux utilisés, et la protection de l'échantillon de l'influence de l'opérateur. Dans ce qui suit nous nous bornerons à décrire les protocoles choisis pour leur adaptation aux eaux marines.

L'échantillonnage s'effectue soit directement dans la bouteille de stockage en téflon FEP ou PFA pour les eaux de surface (opérateur ayant soin de revêtir des gants en polyéthylène), soit avec une pompe pneumatique en téflon de type PFD-1 (ASTI) à laquelle sont branchés des tubes en téflon pour les eaux de subsurface et jusqu'à une centaine de mètres de profondeur. Pour les eaux profondes on utilise des bouteilles de type Go-Flo (General Oceanic) enduites intérieurement d'un revêtement téflon. Ces techniques ne diffèrent pas de celles décrites par Chiffoleau *et al.* (2003) pour d'autres métaux traces et auxquelles on pourra se référer pour plus de détail. La différence essentielle réside dans le matériau de stockage des échantillons d'eau de mer. Dans le cas du dosage du mercure, on utilise exclusivement un flaconnage en téflon PFA ou FEP, plus facilement nettoyable que le PTFE en raison d'un état de surface qui favorise moins d'adsorption.

Les dosages du HgGD et DMHg s'effectuent sur des échantillons non filtrés, ceux du HgR et HgT dissous après filtration des échantillons sur des filtres en téflon hydrophilisés de type LCR de 0,5 µm de porosité et de 45 mm de diamètre (Millipore). Le dispositif et la méthode de filtration sont similaires à ceux décrits pour les autres éléments traces (Chiffoleau *et al.*, 2003). Immédiatement après leur prélèvement les échantillons sont maintenus à l'abri de la lumière et au froid.

Les dosages de HgGD, DMHg, et HgR doivent être faits dans les heures qui suivent le prélèvement à pH naturel. Les échantillons destinés aux dosages du MMHg sont acidifiés à pH 2 par ajout d'HCl (type Suprapur, Merck) et conservés à l'obscurité à +4°C jusqu'au moment de l'analyse qui doit intervenir le plus rapidement possible. Les échantillons destinés au dosage du HgT sont acidifiés à l'HCl (type Suprapur, Merck) à pH inférieur à 2 (0,5 %, v/v). A l'abri de la lumière et au froid ces échantillons peuvent se conserver plusieurs semaines à condition de visser hermétiquement les bouchons des flacons pour éviter les échanges gazeux. Cette opération est effectuée au moyen d'une pince multiprise en matière plastique. Les flacons téflon sont conservés dans un double emballage de sacs en polyéthylène.

2. NETTOYAGE DU FLACONNAGE ET AUTRE MATERIEL

Tout matériel de prélèvement utilisé sur le terrain ou en laboratoire est conditionné, manipulé et stocké de manière à éviter toute contamination. Le lavage en bacs en polyéthylène réservés à cet usage se fait en environnement propre. La manipulation requiert l'usage systématique de gants en polyéthylène. Le stockage hors poussières est réalisé dans un double emballage en sacs en polyéthylène.

Pour le nettoyage du matériel neuf on procède de la manière suivante :

1. Laver au détergent ou à l'alcool éthylique ou méthanol.
2. Rincer à l'eau du robinet puis à l'eau déionisée, type Milli-Q (Millipore).
3. Immerger dans un bac contenant HNO_3 50 % (v/v) type ACS pendant 5 jours.
4. Rincer à l'eau du robinet puis à l'eau déionisée.
5. Immerger dans un bac contenant HCl 10 % (v/v) type ACS pendant 5 jours.
6. Rincer à l'eau déionisée.
7. S'il s'agit de flacons, les remplir d'eau déionisée et y ajouter HCl concentré purifié type Seastar ou Suprapur (Merck) pour obtenir une solution à 0,5 % (v/v).
8. Fermer les flacons en utilisant une pince multiprise et les mettre dans deux sacs en polyéthylène.

Les flacons peuvent être conservés tels quels jusqu'à l'emploi. Les flacons destinés à recevoir des échantillons pour le dosage du HgT doivent recevoir avec l'ajout d'HCl en phase 5, 0,1 % (v/v) de la solution de BrCl. Les autres matériaux en matière plastique sont séchés et gardés dans un double emballage de sacs en polyéthylène. Pour les matériaux usagés on saute les étapes 2, 3 et 4.

3. REACTIFS

Les solutions sont préparées et conservées dans des flacons en téflon FEP de 125 mL lavés selon la technique précédemment décrite. Les manipulations sont effectuées sous hotte à flux laminaire de classe 100 (norme US). Pour éviter toute contamination par l'air ambiant pendant le stockage, les bouchons sont vissés à l'aide d'une pince type multiprise et les flacons enveloppés dans deux sacs en polyéthylène. Dans le cas de la solution de BrCl, toutes les étapes sont réalisées sous une hotte chimique aspirante en faisant attention aux vapeurs de brome très nocives qui peuvent se former.

3.1. Solution de BrCl

Dissoudre 1,1 g de $KBrO_3$ puis 1,5 g de KBr dans 20 mL d'eau déionisée. Ajouter 80 mL de HCl concentré purifié de type Seastar. La solution peut être stockée à +4°C pendant plusieurs jours. Les cristaux de $KBrO_3$ et KBr sont purifiés au préalable au four à 250 °C pendant au moins 12 heures.

3.2. Solution d'NH_2OH, HCl

Dissoudre 30 g de chlorhydrate d'hydroxylamine dans 70 mL d'eau déionisée. La solution est purgée par de l'azote purifié sans mercure pendant quelques heures après addition de 100 µL de la solution de $SnCl_2$. Le stockage ne peut excéder 2 semaines à +4°C.

3.3. Solution de $SnCl_2$

Dissoudre 20 g de $SnCl_2$, $2H_2O$ dans 12,5 mL d'HCl concentré purifié de type Seastar. Chauffer au bain-marie jusqu'à dissolution sans dépasser 60°C. Après refroidissement, compléter à 100 mL avec de l'eau Milli-Q. La solution est purifiée par barbotage à l'azote pendant quelques heures. La solution ainsi préparée se conserve environ 15 jours à +4°C.

3.4. Solution d'$NaBH_4$

Dissoudre 1 g de $NaBH_4$ dans 100 mL d'eau Milli-Q. La solution doit être renouvelée toute les 4 heures. Avant utilisation faire barboter de l'argon ultrapur sans mercure pendant 10 minutes. La solution est maintenue au bain de glace et à l'abri de la lumière pendant l'utilisation.

3.5. Solutions standard de mercure inorganique

Les dilutions sont effectuées dans des fioles jaugées en téflon PFA (Savillex) de 100 mL. Les solutions sont stockées dans des flacons téflon FEP de 125 mL à +4°C à l'abri de la lumière.

3.5.1 Solution diluante

Toutes les solutions de mercure inorganique sont préparées en utilisant une solution diluante qui permet une stabilisation du mercure. Cette solution, qui constitue en outre le zéro de la gamme d'étalonnage, contient 10 mL d'HNO_3 concentré (type Seastar ou Suprapur, Merck) et 2 mL de $K_2Cr_2O_7$ 10 % (p/v) et une quantité d'eau déionisée (type Milli-Q, Millipore) suffisante pour 1 litre.

3.5.2. Solution mère

On dilue une solution certifiée à 10 g L^{-1} (type NIST-3133) au dixième avec la solution diluante pour obtenir une solution mère à 1 g L^{-1}. Cette solution se garde un an.

3.5.3. Solution de travail

A partir de la solution mère on prépare par trois dilutions successives au centième une solution de travail à 1 ng L^{-1}. Cette solution se conserve pendant 3 semaines.

3.6. Solution standard de MMHg

Les dilutions sont effectuées dans des fioles jaugées en téflon PFA (Savillex) de 100 mL. Le solutions sont stockées dans des flacons téflon FEP de 125 mL à +4°C à l'abri de la lumière.

3.6.1. Solution mère

Dans une fiole jaugée de 100 mL en téflon PFA (Savillex), dissoudre 0,1252 g de chlorure de méthylmercure dans de l'isopropanol. Cette solution se conserve pendant 3 mois.

3.6.2. Solution de travail

La solution à 1 g L^{-1} est diluée dans une solution aqueuse de HCl à 0,5 % afin d'obtenir une solution à 0,2 ng mL^{-1}. Cette solution se conserve quelques semaines. Afin d'évaluer la variation de la concentration en MMHg de cette solution, il est recommandé de mesurer la concentration en mercure total et mercure inorganique (mercure "réactif"); la différence (MMHg = HgT-HgR) entre ces deux dosages permet de tester la conservation de la solution.

4. DETECTEURS ET PIEGES

Les détecteurs de fluorescence atomique utilisés avec succès proviennent de trois fabricants : (1) Tekran, modèle 2500, (2) PSAnalytical, modèle Merlin et (3) Spectra-France, modèle MLD-500. Les autres détecteurs disponibles sur le marché n'ont pas été testés.

La purification des gaz et la pré-concentration du mercure avant mesure sont effectuées sur des pièges de sable doré (Figure 1). Le mercure en phase gazeuse, présent dans le gaz, est amalgamé sur une mince pellicule d'or qui recouvre des grains de sable garnissant un tube en quartz. Le sable utilisé est un sable dit "de Fontainebleau" purifié au préalable par lavage à l'acide nitrique, rinçage à l'eau déionisée et calcination à 600 °C. Le sable est ensuite recouvert d'une fine couche d'or au moyen d'un métalliseur ou évaporateur cathodique du type de ceux utilisés en microscopie électronique (ex.: Hammer II, Technics).

Le piégeage des vapeurs acides est réalisé sur des cartouches de chaux sodée du type de celle illustrée sur la figure 2. Ce piège est conditionné par chauffage à 120 °C. Il permet aussi la fixation d'une partie de la vapeur d'eau présente dans le gaz vecteur.

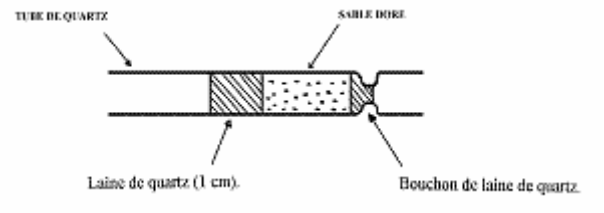

Figure 1. Piège de sable doré

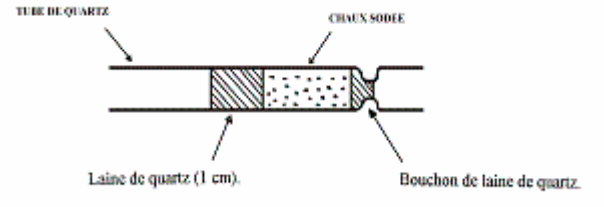

Figure 2. Piège de chaux sodée

5. DOSAGE DU MERCURE GAZEUX, REACTIF ET TOTAL DISSOUS

5.1. Principe

Le mercure gazeux dissous (HgGD) comprend le mercure élémentaire (Hg^0) et le diméthylmercure dissous ($Hg(CH_3)_2^0$). Cette dernière molécule est instable aux pH inférieurs à 7,5 et à la lumière, on la trouve cependant en quantité significative sous les thermoclines océaniques (Mason et Fitzgerald, 1990 ; Cossa *et al.*, 1997). Le mercure « réactif » (HgR) comprend essentiellement les espèces chimiques minérales et les éventuels complexes organiques labiles au pH de la réduction, c'est-à-dire autour de 2. Le mercure total dissous (HgT) est constitué de l'ensemble des espèces chimiques oxydables par BrCl, ce qui inclut les espèces inorganiques et organiques, en particulier les composés alkylés, dont le monométhylmercure. Toutes ces espèces chimiques doivent être réduites en mercure élémentaire volatil (Hg^0), préconcentrées par amalgamation sur piège de sable doré (Fig. 1) puis analysés par SFA.

La chaîne analytique et le dispositif sont décrits sur la figure 3. Pour mesurer le HgGD, l'échantillon d'eau de mer est mis à barboter sous un courant d'argon purifié dans un récipient

en téflon FEP. Le mercure gazeux est récupéré sur un piège de sable doré, lequel est ensuite chauffé à 550°C pour décomposer l'amalgame et libérer la vapeur de mercure dans un SFA. Cette méthode a été initialement décrite par Bloom et Crecelius (1983). La mesure du HgR est basée sur le même principe. Cependant, il est nécessaire de réduire le Hg^{II} en Hg^0 par la solution de $SnCl_2$ avant l'étape de barbotage à l'argon. Pour le dosage du HgT, se rajoute en préalable la transformation en Hg^{II} aisément réductible toutes les formes organiques en particulier les composés alkylés. La rupture de la liaison Hg-C ou Hg-S est réalisée par l'action du BrCl ; une solution de chlorhydrate d'hydroxylamine est utilisée ensuite pour neutraliser l'excès de BrCl, avant de procéder à la réduction au $SnCl_2$.

5.2. Système analytique

L'analyse se fait impérativement sous une hotte à flux laminaire de Classe 100, équipée d'un filtre à charbon actif. Le système analytique est décrit sur la figure 3. Il comprend une ligne constituée de tube téflon (PFA) où l'argon traverse successivement :

- un dispositif de purification du gaz vecteur comprenant un piège de sable doré et un filtre téflon (Vacu-Gard L3749, Whatman),
- un débitmètre (type Aalborg ou Platon),
- une électro-vanne 4-voies (type NResearch) qui permet d'inclure ou non la cellule de dégazage (flacon laveur type Savillex en téflon PFA) dans le circuit d'argon,
- un piège de chaux sodée (Figure 2),
- un piège doré (Figure 1), équipé d'un ruban de chauffage Ni-Cr (1,5 Ω sous 24 volts, la fréquence de sa mise sous tension étant programmable sur l'automate),
- une électro-vanne 3-voies (type NResearch) permettant d'orienter le courant d'argon soit vers le détecteur de SFA, soit à l'air libre,
- un détecteur par fluorescence atomique et un système d'acquisition de données sur un PC (ou un enregisteur).

La partie de la ligne entre la vanne 4 voies et le piège doré peut être maintenue en permanence à 65 °C par un fil chauffant afin d'éviter la possible condensation de vapeur de mercure sur les tubulures, le septum ou le piège de chaux sodée. Les électrovannes et le chauffage sont commandé par un boîtier automatique (type CREA-Automatisme).

5.3. Procédure analytique

5.3.1. HgGD

Introduire un volume suffisant, habituellement de 300 à 600 mL, d'échantillon d'eau de mer non filtré dans la cellule de dégazage. Au sortir de la bonbonne sous une pression de 1,8 bar et après purification au travers d'un piège de sable doré et d'un filtre en téflon (PTFE), l'argon traverse successivement un débitmètre muni d'une vanne derégulation, l'échantillon dans la cellule de dégazage, puis le piège de vapeur d'acide (piège de chaux sodée, Fig. 2) et le piège d'amalgamation (piège de sable doré, Fig. 1). L'échantillon est purgé de son mercure volatil sous un flux d'argon 250 mL min^{-1} suivant le niveau de concentration de HgGD attendu. Le piège doré est ensuite chauffé à 550 °C pendant 1 min et le signal de fluorescence enregistré sous un flux d'argon de 150 mL min^{-1}. Deux minutes séparent deux dosages successifs pour permettre le refroidissement du piège doré. La concentration en mercure élémentaire (Hg^0) est calculée par différence entre HgGD et DMHg.

5.3.2. HgR

Dans la cellule de dégazage, ajouter 0,5 mL de la solution de $SnCl_2$ à 50 ou 100 mL de l'échantillon. Faire barboter l'argon à un débit de 250 mL min^{-1} pendant 6 à 12 minutes (la cellule de dégazage pour la mesure du HgR et du HgT est distincte de celle du HgGD, de façon à ne pas avoir de trace chlorure stanneux pouvant réduire le Hg^{II} lors de la mesure du HgGD). Chauffer le piège de pré-concentration à 550 °C pendant 1 min sous flux d'argon de 150 mL min^{-1}.

5.3.3. HgT

Dans un flacon téflon (PFA) de 125 mL, ajouter 0,2 mL de la solution de BrCl à 100 mL de filtrat d'eau de mer. On vérifie que la coloration persiste pendant l'heure que dure la réaction. La quantité de BrCl à ajouter doit être ajustée si la coloration disparaît. Après une heure, ajouter 0,5 mL de la solution d'hydroxylamine nécessaire à la disparition de la coloration jaune traduisant la neutralisation de l'excès de BrCl. Verser de 50 à 100 mL de l'échantillon ainsi traité dans le flacon de dégazage. Y ajouter 0,5 mL de la solution de $SnCl_2$ et procéder comme précédemment.

5.3.4. Blancs

Le blanc est défini comme la quantité de mercure contenue dans les réactifs (ainsi qu'un bruit de fond permanent qu'il s'agit de minimiser selon la procédure décrite à la section 5.4.4) ; il ne doit pas dépasser 10 pg. La valeur du blanc est obtenue à l'issu d'un cycle analytique effectué immédiatement après passage d'un échantillon. Ainsi l'échantillon déjà dégazé reçoit 0,5 mL de la solution de $SnCl_2$, dans le cas du dosage d'HgR, et 0,2 mL de BrCl, 0,5 mL de $SnCl_2$ et de NH_2OH, HCl dans le cas du dosage d'HgT. Pour HgGD un barbotage d'argon seul suffit.

5.3.5. Étalonnage

Il se fait à partir de la hauteur (ou l'aire) de pic par comparaison avec la hauteur (ou l'aire) de pic d'un standard d'environ 200 pg de mercure. Le standard peut être soit une solution aqueuse de 1 ng L^{-1} utilisée selon la procédure normale soit du mercure gazeux. Dans ce dernier cas, on injecte au travers du septum (Figure 3) 0,01 à 0,02 mL d'air saturé en mercure. La connaissance de la température permet de calculer la quantité de mercure injectée. Par exemple, 0,01 mL de vapeur saturée à 20°C contient 132 pg de mercure élémentaire.

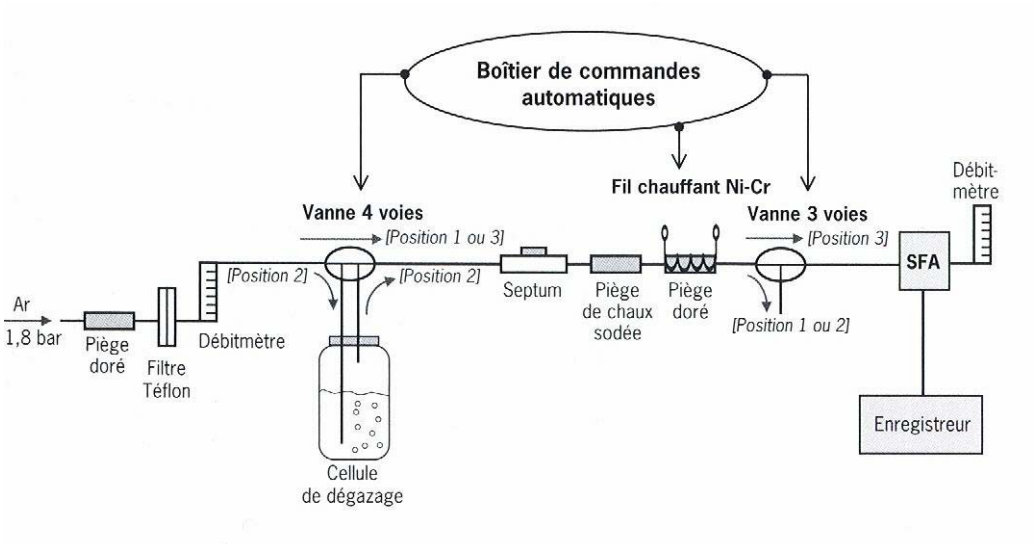

Figure 3. Schéma du montage analytique du dosage du mercure gazeux, "réactif" et total dissous dans l'eau de mer

5.4. Séquences analytiques

L'appareillage semi-automatique utilisé à l'Ifremer est piloté par un boîtier de commandes (Figure 3) développé expressément par la société CREA-Automatisme (crea.automatisme@wanadoo.fr). Avant de procéder à des analyses, il convient de stabiliser le détecteur pendant une heure environ.

5.4.1. Phase 1 : *Balayage du piège doré* (durée 5 sec)

Introduire un volume adéquat d'échantillon selon les espèces chimiques à doser dans la cellule de dégazage. L'argon circule pendant quelques secondes dans le circuit les vannes 3 et 4 voies en position 1 (voir figure 3).

5.4.2. Phase 2 : *Dégazage* (durée 6 à 60 min)

La vanne 4 voies bascule permettant le barbotage de l'argon dans la cellule (position 2 selon la figure 3). S'agissant des dosages du HgR ou du HgT on aura introduit préalablement 0,5 mL de la solution de $SnCl_2$. Selon le volume de l'échantillon on programmera une durée de barbotage de 6 min (pour 50 mL) à 60 min (pour 600 mL).

5.4.3. Phase 3 : *Balayage du piège doré* (durée 10 sec)

Durant cette séquence, on assèche le piège doré avant chauffage, la vanne 4 voies revenant en position 1.

5.4.4. Phase 4 *: Mesure* (durée 1 min)

Il s'agit de la phase de chauffage du piège et de libération de la vapeur de mercure de son amalgame sur l'or. La vanne 3 voies bascule en position 3 (figure 3), permettant au flux d'argon d'atteindre le détecteur de fluorescence ; le piège est alors chauffé par la résistance Ni-Cr à 550 °C. Le pic d'émission correspondant au passage de la vapeur de Hg^0 survient environ 30 sec après le début du chauffage et redescend à la ligne de base après une minute.

5.4.5. Phase 5 : *Refroidissement du piège* (durée 2 min.)

Le piège se refroidit avec les vannes en position 1 pendant 2 minutes. En fin de phase, le système est prêt pour une nouvelle analyse.

5.5. Contrôle de qualité

Les critères d'évaluation des performances de la méthode sont empruntés à Taylor (1987).

5.5.1. Justesse

Du fait de l'absence d'une eau marine de référence pour la détermination du mercure dissous, la justesse de la méthode n'est pas établie avec certitude. La participation à des exercices d'intercomparaison indique un niveau de fiabilité. Lors du dernier exercice organisé avec les universités du Connecticut (Groton, USA) et du Maryland (Solomon, USA) ainsi qu'avec Frontier Geosciences (Seattle, USA) et le Centre Saint-Laurent (Montréal, Canada), la valeur de consensus était de $1,0 \pm 0,08$ ng L^{-1} (Quémerais *et al.*, 1998) et la moyenne de nos mesures était de $0,8 \pm 0,1$ ng L^{-1}.

5.5.2. Précision

La répétabilité de la méthode exprimée par le coefficient de variation (défini comme le rapport de l'écart-type à la moyenne) varie avec les concentrations moyennes. Elle varie de 5 % pour une concentration voisine de 1 ng L^{-1} à 15 % pour des valeurs voisines de 0,1 ng L^{-1}. Ces valeurs ont été obtenues pour des prises d'essai de 50 mL et pour 6 replicats.

5.5.3. Limite de détection

La limite de détection est définie comme 3,29 fois l'écart-type des blancs ; le facteur multiplicatif de 3,29 tient compte des erreurs de types I et II (Taylor, 1987). La limite de détection calculée journellement varie de 0,02 à 0,06 ng L^{-1} pour un échantillon de 100 mL.

5.5.4. Rythme analytique

La séquence analytique permet environ 6 dosages à l'heure. Cependant, en raison des faibles teneurs rencontrées (le plus souvent inférieures à 1 ng L^{-1}) un soin particulier doit être accordé à obtenir des blancs le plus bas possible. Ceci nécessite de nombreux cycles analytiques consécutifs sur un même "blanc". Ce processus "nettoie" progressivement la ligne analytique. Ces conditions particulières de dosage de traces rendent difficile, compte tenu aussi de la nécessité d'étalonnages fréquents (tous les 5 échantillons environ), de réaliser plus 25 analyses par jour.

5.5.5. Domaine d'application

Du fait de l'ajustement possible du volume d'échantillon analysé, la gamme des concentrations mesurables au dessus de la limite de détection mesurable est très étendue. Dans le cas de la détermination du mercure total dissous, pour les eaux très concentrées en matière organique dissoute on peut être amené à augmenter la quantité de solution de BrCl (le maintien de la coloration jaune est un critère d'une quantité suffisante de BrCl) à ajouter à l'échantillon. De plus, un temps de réaction du BrCl supérieur à une heure peut s'avérer nécessaire dans certains cas.

6. DOSAGE DU METHYLMERCURE DISSOUS

6.1. Principe

Le dosage du diméthylmercure, espèce volatile, consiste en un simple barbotage de l'échantillon par un courant d'hélium et un piégeage des espèces volatiles sur une colonne chromatographique dans l'azote liquide. La colonne est ensuite réchauffée, et les composés volatils (Hg° et DMHg°) libérés sont quantifiés en SFA (ex., Bloom, 1989). Différentes méthodes de dosage du monométhylmercure (MMHg) dans les eaux ont été passées en revue par Horvat (1996). Celles dont la sensibilité et l'obtention de blancs suffisamment bas permettent une application au dosage du MMHg dans les eaux marine font appel à la formation de composés alkylés ou d'hydrures (ex., Bloom, 1989; Tseng *et al.*, 1998). Dans le premier groupe les méthodes basées sur l'éthylation, utilisées pour la détermination du MMHg dans les matrices biologiques et les sédiments (ex., Cossa *et al.*, 2002), présentent l'inconvénient d'une interférence avec les chlorures et donc de nécessiter une extraction préalable. C'est pourquoi la méthode par hydruration présentée ici a été choisie. Elle permet d'atteindre des seuils de détection très faibles (< 5pg L^{-1}), mais n'est applicable qu'à des eaux de mer à faible teneurs en matière organique dissoute. Dans le cas d'eau riches en matière organique on adapte la méthode d'éthylation après extraction par solvant organique, telle que décrite dans un précédent fascicule (Cossa *et al.*, 2002).

Les hydrures volatils de métaux sont connus pour être formés par addition de tétrahydroborure de sodium ($NaBH_4$). Cette volatilité est utilisée comme technique de pré-concentration et de séparation.

Les réactions mises en œuvre sont les suivantes :

$$MeHg^+ + NaBH_4 + 3\ H_2O \rightarrow MeHgH + 3\ H_2 + H_3BO_3 + Na^+$$

$$Hg^{2+} + 2\ NaBH_4 \rightarrow Hg° + B_2H_6 + 2\ Na^+ + H_2$$

En 1998, Tseng *et al.* ont proposé un protocole permettant une récupération quantitative des hydrures formés. La méthode de dosage de méthylmercure proposée se compose de différentes étapes : (1) la formation d'hydrures volatils avec $NaBH_4$, (2) leur préconcentration par cryogénie (-196°C), (3) leur séparation par chromatographie gazeuse, et (4) leur détection par spectrométrie d'absorption atomique (SAA), ou fluorescence atomique (SFA) ou encore par spectrométrie de masse après ionisation par plasma d'argon (ICPMS). Nous avons choisi la SFA pour sa sensibilité et son faible coût. Ainsi les hydrures formés sont concentrés puis séparés par chromatographie cryogénique avant d'être atomisés (800°C) et entraînés sous forme de vapeur par un courant d'hélium jusqu'à un détecteur.

Les modifications apportées à la méthode de Tseng *et al.* sont minimes, mais ont permis une amélioration du seuil de détection d'un facteur 20. Il s'agit de la réduction et stabilisation du blanc par l'utilisation d'une quantité minimale de réactifs et d'un détecteur de SFA très sensible (détection absolue de 0,1 à 0,3 pg de Hg).

Le schéma conceptuel du dosage et le dispositif analytique sont décrits respectivement sur les figures 4 et 5.

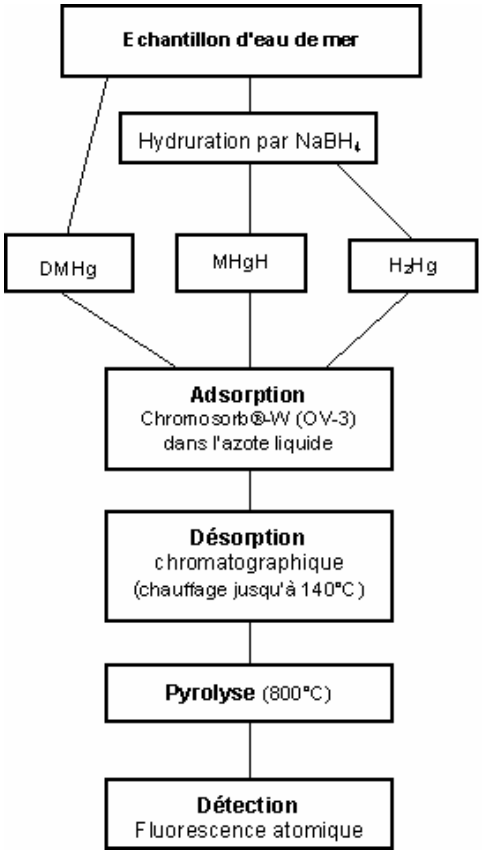

Figure 4. Diagramme analytique de dosage du méthylmercure dans l'eau de mer

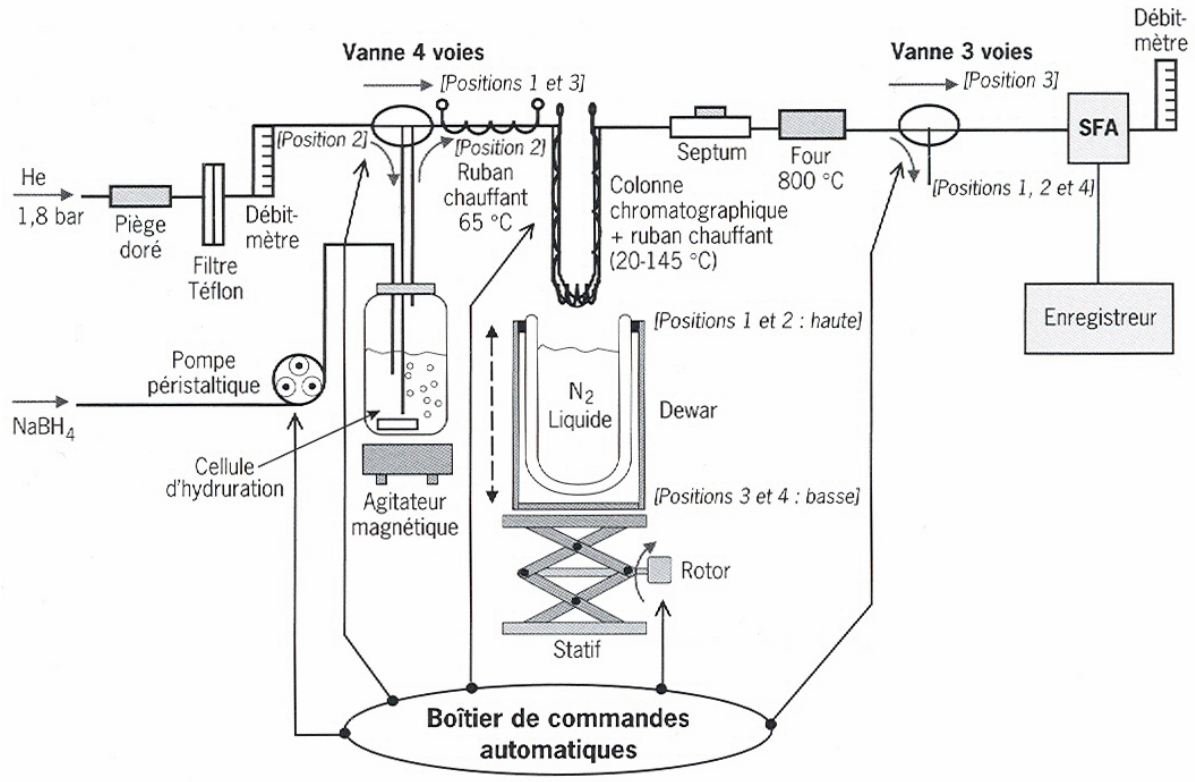

Figure 5. Schéma du montage analytique du dosage du méthylmercure dans l'eau de mer

6.2. Système analytique

Le système analytique est décrit sur la figure 5. Il comprend une ligne d'hélium constituée de tube téflon (PFA) qui traverse successivement :

- un dispositif de purification du gaz vecteur comprenant un piège de sable doré et un filtre téflon (Vacu-Gard L3749, Whatman),
- un débitmètre (type Aalborg ou Platon),
- une électro-vanne 4-voies qui permet d'orienter l'argon soit vers une cellule d'hydruration en verre borosilicaté de 250 mL, décontaminé à 450°C, puis silanisé (5% DMDCS dans le toluène), soit directement vers la colonne chromatographique constituée d'un tube en U en verre borosilicaté silanisé (∅ext. 6 mm et ∅int. 4 mm) et remplie de Chromosorb WAW-DMCS (60/80 mesh imprégné de 15% d'OV-3); une résistance de 20 Ω en Ni-Cr, alimentée sous 24 volts, enroulée autour de la colonne permet d'atteindre 145 °C (la fréquence de sa mise sous tension étant programmable sur l'automate),
- un porte septum,
- un four à pyrolyse à une température de 800°C constitué de laine de quartz dans un tube en quartz de 10 cm de long et 0,8 cm de diamètre intérieur.
- une électro-vanne 3-voies permettant l'isolation du SFA,
- un détecteur par fluorescence atomique et un système d'acquisition de données sur un PC (ou un enregistreur).
- un débitmètre en sortie de SFA permettant la régulation du débit d'hélium à 35 et 30 mL^{-1} pour des températures respectives de la colonne chromatographique de 30 et 145 °C.

Une pompe péristaltique (type Ismatec) permet l'introduction de la solution de borohydrure de sodium. Un boîtier d'automatisme commande les vannes, la pompe péristaltique, le moteur du statif et le chauffage de la résistance.

Tous les tuyaux sont en téflon (PFA) ainsi que les raccords (PTFE). Les connections entre les différentes parties du circuit doivent être aussi courtes que possible pour éviter les volumes morts. Le raccord entre la sortie de la colonne et l'entrée du dernier four est enveloppé dans une résistance chauffante à 65°C afin d'éviter les condensations de mercure élémentaire sur des "points froids" (Figure 5).

6.3. Procédure analytique

L'échantillon aqueux est placé dans la cellule d'hydruration (Figure 5). L'hélium qui sert de gaz vecteur est, à la sortie de la bonbonne, sous 1,8 bar et est purifié grâce à un piège de sable doré qui amalgame les traces de Hg présentes dans le gaz et à un filtre téflon. La vanne 4 voies permet au flux d'hélium soit de traverser directement la colonne chromatographique immergée dans l'azote liquide, soit de barboter à travers l'échantillon (débit 1000 mL min^{-1}) où est introduit la solution de $NaBH_4$ à l'aide d'une pompe péristaltique sous un débit de 0,35 mL min^{-1}, pendant 5 minutes. Le taux d'hydruration est identique à pH naturel ou à pH 2. Le choix du pH est fonction du type de conservation de l'échantillon. Si l'analyse peut se faire rapidement après le prélèvement, il est préférable de travailler à pH naturel. Les hydrures formés sont entraînés par l'hélium et piégés sur la colonne dans un bain d'azote liquide. Après avoir purgé le circuit par un courant d'hélium pour chasser le dihydrogène qui a pu se former lors de l'ajout de $NaBH_4$, la colonne est sortie de son bain d'azote et réchauffée progressivement jusqu'à atteindre 145 °C. Les hydrures sont exclus de la colonne à une

température inférieure à 30 °C, la vapeur d'eau piégée est expulsée à une température nettement supérieure ; une vanne 3 voies évacue à l'air libre le flux d'hélium afin que la vapeur d'eau n'atteigne pas le détecteur de fluorescence. Le débit d'hélium pendant la chromatographie passe de 35 mL min^{-1} lorsque la colonne est froide jusqu' 30 mL min^{-1} lorsque la température atteint 140°C.

L'identification des pics est réalisée d'après leur temps de rétention. Dans les conditions décrites ci-dessus, les temps de rétention respectifs du mercure inorganique et du monométhylmercure sont de 1 min 50 s et 3 min après le début du chauffage de la colonne (Figure 6).

Une courbe d'étalonnage est tracée chaque jour à partir d'ajouts de MMHg dans 200 mL d'eau Milli-Q. On a pu vérifier la linéarité de la courbe jusqu'à 500 pg L^{-1}, ainsi que l'identité des facteurs de réponse respectifs des eaux douces et des eaux de mer. L'estimation du rendement d'hydruration peut être réalisée en comparant l'aire du pic obtenue par ajout d'une quantité connue de MMHg en solution à l'aire de pic obtenue par injection d'une quantité équivalente de mercure gazeux (Hg^0) au niveau du septum (Figure 5).

Les blancs doivent être vérifiés régulièrement ; ils sont souvent négligeables. Les blancs déterminés à partir du dosage du MMHg dans 200 mL d'eau Milli-Q donnent des valeurs de l'ordre du picogramme de MMHg par litre. Ces traces proviennent en partie de l'eau Milli-Q, en partie de la solution de $NaBH_4$ (on détermine cette proportion en doublant la quantité de réactif utilisée). Lors du calcul des concentrations la partie du blanc due à l'eau Milli-Q n'est pas déduite des mesures.

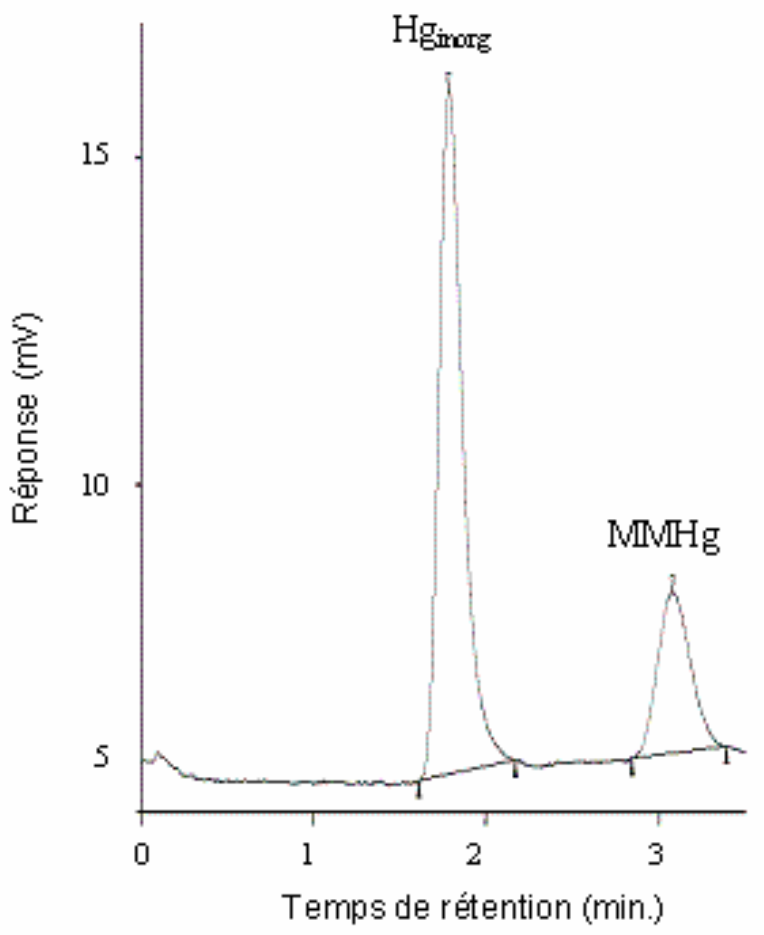

Figure 6. Chromatogramme typique pour une quantité de MMHg de 20 pg.

6.4. Séquences analytiques

L'arrivée d'hélium est maintenue ouverte en permanence. L'appareillage semi-automatique utilisé à l'Ifremer est piloté par un boîtier de commandes (Figure 5) développé expressément par la société CREA-Automatisme (crea.automatisme@wanadoo.fr). Avant de procéder à des analyses, il convient de stabiliser le détecteur pendant une heure environ.

6.4.1. Phase 1 : *Refroidissement de la colonne* (durée 1 min)

La colonne est plongée dans l'azote liquide. La vanne 4 voies dirige l'hélium directement vers la colonne (Position 1, figure 5) à raison de 1000 mL min^{-1} tandis qu'en sortie de four les effluents sont rejetés dans l'atmosphère grâce à la vanne 3 voies. Pendant ce temps, 200 mL d'échantillon sont introduits dans la cellule d'hydruration qui est ensuite mise en circuit.

6.4.2. Phase 2 : *Formation d'hydrures* (durée 5 min)

La solution de $NaBH_4$ à 1% est introduite dans l'échantillon avec un débit de 0,35 mL min^{-1} pendant 5 min sous agitation magnétique. En même temps, grâce au basculement de la vanne 4 voies (Position 2, figure 5), l'hélium purge l'échantillon, entraînant ainsi les hydrures formés vers la colonne en tête de laquelle ils sont piégés.

6.4.3. Phase 3 : *Complément d'extraction des hydrures* de l'échantillon (durée 2 min)

Durant cette séquence, les vannes restant dans la Position 2 (Figure 5), on parachève la purge des hydrures sous flux d'hélium sans ajout de $NaBH_4$.

6.4.4. Phase 4 : *Elution et acquisition des données* (durée 3 min 30 s)

Il s'agit de la phase d'élution des composés du mercure. Le support du vase Dewar s'abaisse provocant la sortie de la colonne de l'azote liquide. Simultanément, le gaz vecteur est orienté directement vers la colonne chromatographique grâce à la vanne 4 voies (Position 3, figure 5), shuntant ainsi la cellule d'hydruration, et en aval, grâce à la vanne 3 voies, vers le détecteur SFA (Position 3, figure 5). Le débit d'hélium passe à 35 mL min^{-1} grâce au débitmètre placé en sortie du SFA. Après 2 minutes à température ambiante la colonne est chauffée progressivement jusqu'à 30°C. L'acquisition des données a lieu pendant cette phase.

6.4.5. Phase 5 : *Séchage de la colonne* (durée 6 min.)

Pendant le dégazage, l'hélium a entraîné de la vapeur d'eau qui s'est trouvée piègée sur la colonne. On élimine cette eau en portant le chauffage de la colonne à son maximum (environ 145 °C), et on évacue la vapeur formée dans l'atmosphère (vanne 3 voies en position 4, figure 5). En fin de phase, le système est prêt pour une nouvelle analyse .

6.5. Contrôle de qualité des dosages

Les critères d'évaluation des performances de la méthode sont empruntés à Taylor (1987).

6.5.1. Justesse

La justesse de la méthode n'a pu être établie en raison de l'absence d'une eau de mer de référence certifiée en MMHg.

6.5.2. Précision

La répétabilité de la méthode exprimée par le coefficient de variation (défini comme le rapport de l'écart-type à la moyenne pour 6 analyses du même échantillon) varie de 15 % pour un échantillon de concentration proche de la limite de détection à 6 % pour un échantillon de 100 pg L^{-1} ou plus.

6.5.3. Limite de détection

La limite de détection est définie comme 3,3 fois l'écart-type de la concentration d'un échantillon dont la teneur est proche de zéro (dans la pratique du présent dosage il s'agit des blancs) ; le facteur multiplicatif de 3,3 tient compte des erreurs de types I et II (Taylor, 1987). La limite de détection calculée journellement varie de 1 à 4 pg L^{-1}.

6.5.4. Rythme analytique

En tenant compte des blancs et de l'étalonnage, on peut analyser quotidiennement une quinzaine d'échantillons.

6.5.5. Domaine de validité

La linéarité de la réponse a été vérifiée de la limite de détection à 500 pg L^{-1} pour des eaux de mer à faible teneur en matière organique dissoute (c'est-à-dire inférieure à environ 2 mg L^{-1}). Dans le cas d'eau riches en matière organique on doit procéder à une extraction préalable du MMHg à pH 2 par un volume de dichlorométhane équivalent à celui de l'échantillon aqueux. On procède à une extraction en retour par évaporation du solvant en présence de 50 mL d'eau Milli-Q. Sur cette phase aqueuse extraite on procède à un dosage du MMHg par éthylation selon la procédure décrite dans un précédent fascicule (Cossa *et al.*, 2002). En raison de l'étape d'extraction la variabilité des blancs plus élevée et la limite de détection n'est que de 10 pg L^{-1} dans le meilleur cas.

BIBLIOGRAPHIE

Bloom, N.S. 1989. Determination of picogram levels of methylmercury by aqueous phase ethylation, followed by cryogenic gas chromatography with atomic fluorescence detection. *Can. J. Fish. Aquat. Sci.*, ***46*** : 1131-1140.

Bloom, N.S. et E.A. Crecelius. 1983. Determination of mercury in seawater at sub-nanogram per liter levels. *Mar. Chem.*, ***14*** : 49-59.

Boutron, C.F. 1990. A clean laboratory for ultralow concentration heavy metal analysis. *Fresenius J. Anal. Chem.*, ***337*** : 482-491

Chiffoleau, J.F., D. Auger et E. Chartier. 2003. *Dosage de certains métaux traces (Cd, Co, CU, Fe, Ni, Pb, Zn) dissous dans l'eau de mer par absorption atomique après extraction liquide-lliquide.* Méthodes d'analyse en milieu marin. Co-édition Ifremer et Ministère de l'Ecologie et du Développement Durable. 39 pp. ISBN 2-84433-104-1.

Cossa, D., J.M. Martin, K. Takayanagi et J. Sanjuan. 1997. The Distribution and Cycling of Mercury in the Western Mediterranean. *Deep Sea Res.*, ***44*** : 721-740.

Cossa, D, M. Coquery, K. Nakhlé et D. Claisse. 2002. *Dosage du mercure total et du monométhylmercure dans les organismes et les sédiments marins.* Méthodes d'analyse en milieu marin. Co-édition Ifremer et Ministère de l'Ecologie et du Développement Durable. 26 pp. ISBN 2-84433-105-X

Fitzgerald, W.F., G.A. Gill et A.D. Hewitt. 1983. *Air/sea exchange of mercury*. In: C.S. Wong, E. Boyle, K.W. Bruland, J.M. Burton et E.D. Goldberg (éd.), Trace metals in sea water. Édition Plenum Press, New York, pp. 297-316.

Gill, G.A. et W.F. Fitzgerald. 1985. Mercury sampling of open ocean waters at the picomolar level. *Deep Sea Res.*, ***32*** : 287-297.

Horvat, M. 1996. *Mercury analysis and speciation in environmental samples.* p. 1-31. *In*: Regional and Global Cycles of Mercury: Sources, Fluxes, and Mass Balances. W. Baeyens, R. Ebinghaus and O. Vasiliev éditeurs. Kluwer Academic Publishers, Dordrecht, The Netherlands.

Howard, A.G. et P.J. Statham. 1993. *Trace inorganic analysis: philosophy and practice.* Édition John Wiley & Sons Ltd, Chichester, 182 p.

Keith, L.H. 1991. *Environmental Sampling and Analysis: A Practical Guide*. Lewis Publishers, Boca Raton.

Kramer, K.J.M. 1994. Inorganic contaminants in the water column: sampling and sampling strategy. *Intern. J. Environ. Anal. Chem., 57* : 179-188.

Mason, R.P. et W.F. Fitzgerald. 1990. Alkylmercury species in the equatorial Pacific. *Nature, Lond., **347*** : 457-459.

Nolting, R.F. et J.T.M. Jong. 1994. Sampling and analytical methods for the determination of trace metals in surface seawater. *Intern. J. Environ. Anal. Chem., 57* : 189-196.

Quémerais, B. D. Cossa, B. Rondeau, T.T. Pham et B. Fortin. 1998. Mercury distribution in relation to iron and manganese in the waters of the St. Lawrence River. *Sci. Total Environ., **213*** : 193-201.

Sturgeon, R. et S. Berman. 1987. Sampling and storage of natural water for trace metals. In: *Critical reviews in analytical chemistry.* Vol. 18(3). Édition CRC Press, pp. 209-244.

Taylor, J. K. 1987. *Quality Assurance of Chemical Measurements.* Lewis Publishers, New York, USA.

Tseng, C.M., A. de Diego, H. Pinaly, D. Amouroux et O.F.X. Donard. 1998. Cryofocusing coupled to atomic absorption spectrometry for rapid and simple mercury speciation in environmental matrices. *J. Anal. Atom. Spectro., **13*** : 755-764.

Série : "Les méthodes d'analyses en milieu marin"

Dosage du mercure et du monométhylmercure dans les organismes et les sédiments marins

Daniel Cossa[1]**,**

Marina Coquery[2]**,**

Khaled Nakhlé[1] **et**

Didier Claisse[1]

1. Institut Français de Recherche pour l'Exploitation durable de la Mer (IFREMER), BP 21105, F.44311 Nantes cedex 03

2. Institut National de l'Environnement Industriel et des Risques (INERIS), BP 2, F.60550 Verneuil-en-Halattte

Mars 2002 (CossaHg3.doc)

SOMMAIRE

AVANT PROPOS

Ce document fait partie d'une série de fascicules intitulée "Les méthodes d'analyses en milieu marin". Cette série s'adresse bien sûr d'abord aux analystes, mais elle sera probablement utile aux gestionnaires de l'environnement ainsi qu'aux étudiants intéressés par les spécificités analytiques du milieu marin. Ces méthodes sont employées à l'Ifremer dans les programmes de recherche comme ceux de surveillance de la qualité du milieu. Elles sont validées par la pratique de nombreux laboratoires spécialisés dans l'étude des matrices marines. La plupart d'entre-elles ont fait l'objet d'exercices d'intercomparaisons internationales, en particulier dans le cadre du CIEM (Conseil international d'exploration de la mer), de l'AIEA (Agence internationale de l'énergie atomique), ou du BCR (Bureau des références de la Commission européenne). Certaines de ces méthodes constituent les méthodes de référence du Réseau National d'Observation de la Qualité du milieu marin (RNO) du Ministère de l'Aménagement du territoire et de l'Environnement géré et réalisé par l'Ifremer.

RESUME

Ce fascicule est consacré à la description des méthodes de prélèvement des organismes et sédiments marins, de préparation des échantillons et du dosage du mercure total (toutes espèces chimiques confondues) utilisées dans le cadre du Réseau National d'Observation de la Qualité du milieu marin (RNO) depuis 1997 et du dosage du monométhylmercure dans les organismes et les sédiments marins. Le mercure total est dosé par spectrophotométrie d'absorption atomique après minéralisation par voie sèche et pré-concentration par amalgamation sur un piège doré. Cette méthode semi-automatique qui permet le dosage du mercure total présent dans des échantillons solides avec un rythme analytique élevé, présente aussi l'avantage de bonnes sensibilité et un blanc extrêmement bas. Pour une prise d'essai d'environ 20 milligrammes (poids sec) la limite de détection et la reproductibilité sont respectivement de 0,007 $ng.mg^{-1}$ (poids sec) et meilleure que 7 %. La méthode de dosage du monométhylmercure fait appel à son isolation par éthylation et chromatographie, puis son dosage par spectrofluorimétrie atomique. L'éthylation permet un dosage spécifique du monométhylmercure et la détection par fluorescence atomique permet d'atteindre une grande sensibilité. Pour une prise d'essai de quelques dizaines de milligrammes la limite de détection est de 0,004 $ng.mg^{-1}$ (poids sec) et la reproductibilité de 10 %. Les justesses de ces méthodes analytiques sont évaluées systématiquement au moyen d'échantillons de référence certifiés.

ABSTRACT

The sampling, the preparation and the determination of total mercury (the whole chemical mercury species together) and monomethylmercury in biota and sediments are described. These procedures are used for the French Mussel Watch Program (Réseau National d'Observation) since 1997. The total mercury determination procedure consists of the following automatic sequences: a dry ashing of the sample, the elemental mercury amalgamation on a gold trap, and an atomic absorption spectrophotometric measurement. The method is rapid, sensitive, and reproducible with a very low blank. With a 20 milligram sample the detection limit and the reproducibility are 0.007 $ng.mg^{-1}$ (dry weight) and 7 % respectively. The monomethylmercury determination method consists of an ethylation and a chromatography step for the isolation of the molecule and an atomic fluorescence measurement for its quantification. For a 20 milligrams sample (dry weight), the detection limit and the reproducibility are 0.004 $ng.mg^{-1}$ (dry weight) and 10 % respectively. The accuracy of the techniques is assessed on a regular basis using a certified reference material.

INTRODUCTION

Le mercure est un élément métallique parmi les plus toxiques qui atteint le milieu marin de source naturelle et anthropique. La connaissance de sa répartition et de son cycle dans les différents réservoirs marins, de même que la surveillance des niveaux de contamination sont des objectifs qui ne peuvent être atteints que par l'obtention de données fiables découlant de procédures de prélèvement et d'analyse éprouvées. Nous décrivons ici les techniques et protocoles analytiques établis internationalement pour le dosage du mercure total dans les organismes et les sédiments marins, et du méthylmercure dans les organismes. Ces techniques sont appliquées en France par l'Ifremer dans le Réseau National d'Observation de la qualité du milieu marin (RNO).

1. LE PRELEVEMENT

Nous distinguerons dans ce chapitre les prélèvements d'organismes marins des prélèvements de sédiments qui n'obéissent pas à la même stratégie d'échantillonnage.

Les variations des concentrations en contaminants observées dans les organismes vivants résultent de la juxtaposition des variations des niveaux de contamination du milieu marin et des variations d'accumulation des contaminants par les organismes liées à des processus physiologiques saisonniers. Dans les sédiments déposés, bien que les variations saisonnières des flux de matière sur les fonds puissent affecter les concentrations en contaminant, les échelles temporelles impliquées dans les changements observés sont plus longues du fait du lissage des concentrations par la bioperturbation des sédiments superficiels. Aussi le suivi dans le monde vivant se fait sur une base saisonnière alors que le suivi dans les sédiments se fait sur une base pluriannuelle.

1.2. Echantillons d'organismes marins

1.1.1. Dates et fréquences

Les teneurs en contaminants des organismes marins varient en fonction des organes considérés. Dans un objectif de suivi des concentrations dans le milieu, il conviendra donc de faire les dosages toujours sur la même fraction : dosage dans la chair totale pour des organismes de petites tailles comme les mollusques ou dosage dans un organe ou tissu particulier pour organismes de plus grande taille comme les poissons (muscle ou foie par exemple). Au cours de l'année, les teneurs en contaminants chimiques des organismes marins varient, en fonction des ressources alimentaires ou de l'activité de reproduction. Le choix de la période d'échantillonnage est donc un facteur-clé. Les lignes directrices de la surveillance internationale recommandent un échantillonnage annuel des organismes marins pendant la période de repos sexuel (Ospar, 1999). Le RNO a adopté un prélèvement trimestriel régulier, qui permet d'appréhender les variations saisonnières.

1.1.2. Choix des organismes

La surveillance de la contamination chimique des organismes marins s'appuie de préférence sur des espèces sédentaires de manière à ce que les niveaux de contamination observés soient représentatifs d'une zone géographique précise. C'est ainsi que les moules et les huîtres ont été choisies dans le cadre du RNO. L'aptitude à la bioaccumulation des contaminants chimiques par les mollusques variant au cours de leur cycle de vie avec une phase plus stable entre 2 et 3 ans, les individus prélevés constituent un lot homogène d'organismes dans leur 3ème année. Exceptionnellement, on devra se contenter d'animaux d'âge légèrement différents de cet optimum. On conservera les mêmes caractéristiques pendant toute la durée du programme de surveillance. Quoiqu'il en soit, les mollusques doivent être adultes et non sénescents (Cossa, 1989). Sur le littoral français métropolitain, l'expérience montre que des moules de taille comprise entre 45 et 55 mm (et en aucun cas hors de la fourchette extrême de 35 à 65 mm) correspondent à la classe d'âge recherchée. En cas d'utilisation d'huîtres, celles-ci devront être dans leur troisième année.

L'échantillonnage de poissons, comme celui des mollusques, est pratiqué au même endroit d'une année sur l'autre. Cependant par chalutage la zone couverte est souvent de plusieurs centaines de mètres carrés, alors que, pour les mollusques, elle est beaucoup plus restreinte. Chez les poissons, les dosages de contaminants réalisés sur plusieurs individus de taille différentes permettent de préciser la gamme de variation des concentrations rencontrées chez une même espèce (Cossa *et al.*, 1992). Les instructions du programme international de surveillance de la Convention d'Oslo et Paris, dites lignes directrices d'OSPAR, recommandent des choix d'espèce et l'échantillonnage "stratifié" de 5 classes de taille minimum, composées de 5 individus au moins par classe de taille (Ospar, 1999).

1.1.3. Conditionnement et préparation des échantillons

Toutes les précautions doivent être prises pour éviter la contamination des échantillons sur le lieu de prélèvement et pendant le transport au laboratoire d'analyse. Il convient notamment d'éviter les contacts avec des éléments métalliques susceptibles d'apporter une contamination supplémentaire.

Mollusques bivalves :

Un échantillon est composé d'un nombre d'individus suffisant pour produire un résultat intégrant les variations individuelles. Les lignes directrices de la surveillance internationale (Ospar, 1999) recommandent des échantillons de 50 moules (± 10 %) ou 10 huîtres (± 10 %).

Collecte : Les mollusques sont détachés de leur support un à un, en prenant soin de ne pas endommager le pied lors du sectionnement du byssus. Ils sont rincés extérieurement à l'eau de mer sur les lieux du prélèvement puis placés dans un sachet en polyéthylène et transportés jusqu'au lieu d'épuration en évitant les écarts thermiques importants. Les animaux doivent en effet rester vivants et capables d'avoir une activité normale de filtration pendant la phase d'épuration subséquente.

Epuration : Les coquillages sont épurés de manière à les débarrasser des particules non assimilées (particules présentes dans le système digestif et pseudo-fécès) afin que l'analyse ne porte que sur les teneurs en mercure des tissus des coquillages. La durée de l'épuration est de 24 h d'immersion dans un bac contenant de l'eau de mer décantée, issue de la région de prélèvement. Cette eau n'est, en effet, pas susceptible de modifier de façon perceptible les teneurs en contaminant des coquillages. On utilise des bacs d'environ 30 L en plastique incolore, les pigments pouvant constituer une source de contamination. Ces bacs, nettoyés (cf.

§ 1.4.2), sont pourvus d'un portoir perforé permettant d'isoler les coquillages du fond du bac où se déposent les digestions. Il est recommandé de ne pas utiliser de système de bullage pouvant introduire des contaminants dans l'eau.

Décoquillage : A l'issue de l'épuration, les mollusques sont décoquillés avec un scalpel en acier inoxydable, en évitant d'endommager le mollusque avec la lame pour limiter la perte de liquide intratissulaire. La chair est mise à égoutter sur un entonnoir de Buchner en verre pendant 30 minutes. Toutes les précautions sont prises pour éviter la contamination de l'échantillon pendant cette phase (matériel nettoyé cf. §1.4., travail sous hotte à flux laminaire si possible, port de gants en polyéthylène non poudrés). Pendant la phase d'égouttage, la chair des mollusques est protégée des contaminations par le milieu ambiant par une feuille d'aluminium qui recouvre l'entonnoir (on peut aussi travailler sous hotte à flux laminaire équipée d'un filtre dit absolu de 0,2 µm). La chair égouttée est ensuite broyée et homogénéisée au broyeur en verre et acier inox type Virtis® avant d'être placée dans un pilulier préalablement taré, puis congelée en attendant la lyophilisation.

On relève, pour chaque échantillon, le poids humide des tissus mous, de manière à pouvoir déterminer la teneur en matière sèche après la lyophilisation, et la taille et le poids moyens des coquilles des mollusques qui entrent dans l'échantillon afin de déterminer un indice de condition moyen du lot analysé (le rapport masse des tissus mous / masse des coquille par exemple). On calculera enfin le poids moyen des coquilles du lot analysé.

Poissons :

Les poissons sont emballés individuellement dans des sacs hermétiques en polyéthylène de taille adéquate et conservés au froid, éventuellement congelés si le traitement des échantillons doit être différé de plus de quelques heures. On identifie les échantillons et on note la taille et le poids de chaque individu. Chaque poisson prélevé est disséqué sous hotte à flux laminaire équipée d'un filtre dit absolu (0,2µm). La dissection est faite sur une plaque de polyéthylène, à l'aide de scalpels en acier inoxydable et de pinces en polyéthylène. Pour les poissons plats, le poisson est placé face ventrale contre la plaque. A l'aide de pinces et du scalpel, la peau est détachée des muscles dorsaux, en prenant soin de ne pas mettre la face extérieure de la peau en contact avec le muscle mis à nu. Le muscle est ensuite prélevé, dans une zone éloignée des viscères pour éviter le risque de contamination par migration de liquides biologiques d'un organe à l'autre. L'échantillon est placé dans un pilulier en verre et congelé en attendant la lyophilisation (cf. §1.3).

1.2. Echantillons de sédiments

1.2.1. Stratégie d'échantillonnage

Dans les sédiments, deux stratégies d'échantillonnage sont possibles : prélèvement de carottes de sédiments pour étudier les variations temporelles des niveaux de contamination ou bien prélèvement de l'horizon superficiel.

Pour les carottes, en fonction des taux de sédimentations de la zone, la période étudiée sera plus ou moins longue. Dans les conditions rencontrées le plus souvent sur le littoral français, une carotte de 40 cm permet une analyse temporelle sur plus de 100 ans de dépôt. La fréquence d'échantillonnage de l'horizon superficiel comme des carottes dépend étroitement des vitesses de sédimentation et de l'intensité de la bioperturbation. Un échantillonnage décennal est souvent suffisant par le RNO en France métropolitaine.

L'évaluation des évolutions des niveaux de contamination dans le temps sur un site se fait par prélèvement de carottes de plusieurs dizaines de centimètres de hauteur, chaque horizon présentant une image du niveau de contamination du milieu lors du dépôt de cet horizon lissée par la bioperturbation. Pour l'analyse spatiale des niveaux de contamination des sédiments superficiels, l'échantillon est prélevé dans le centimètre supérieur en chaque point. Le choix des sites de prélèvement est tributaire de la présence de sédiments fins (vases et limons) qui, par nature, peuvent piéger efficacement les contaminants chimiques.

1.2.2. Prélèvement et conditionnement de l'échantillon

Les prélèvements de sédiments peuvent se faire directement à l'aide d'une spatule en polyéthylène ou polypropylène sur l'estran découvert à basse mer ou nécessiter des moyens nautiques pour les zones plus au large : prélèvement à la benne Ekman à manche sous trois mètres d'eau maximum, voire mise en œuvre de moyens lourds (portique, grue) pour l'utilisation d'une benne Shipeck ou d'un carottier-boîte Reineck (équipé de boîtes en acier inoxydable). Pour le prélèvement de sédiment en vue de l'échantillonnage de différents horizons, on utilise de préférence un carottier-boîte type Reineck qui permet un prélèvement de plusieurs dizaines de centimètres de hauteur en respectant la stratification du sédiment et l'interface benthique.

Pour chaque horizon du sédiment à échantillonner, une fraction est prélevée à l'aide d'une spatule en polyéthylène (ou polypropylène), de préférence dans la partie centrale du prélèvement qui n'a pas été en contact avec la boîte métallique du carottier qui pourrait être source de contamination. La stratégie présentée ici s'applique à des mesures dans le sédiment total, en éliminant cependant les plus grosses particules (coquilles, graviers, etc.) dès l'échantillonnage. L'échantillon prélevé est placé dans un pilulier en polystyrène cristal, emballé individuellement dans un sac en polyéthylène et congelé en attendant la lyophilisation.

Le port des gants en polyéthylène ou vinyl non poudrés est indispensable lors des manipulations des échantillons. Après chaque prélèvement, les spatules sont rincées à l'eau Milli-Q® et stockées dans un sachet en polyéthylène.

Afin d'être pleinement exploitables, les résultats des analyses de contaminants métalliques doivent être accompagnés d'un certain nombre de paramètres : granulométrie (au moins évaluation de la proportion de particules de taille inférieure à 63µm), teneur en eau, en aluminium, en manganèse, en fer, en lithium, en carbone organique total, en carbonates.

Le dosage de l'aluminium, du manganèse, du fer, et du lithium peut se faire sur le même échantillon que celui qui a été prélevé pour l'analyse du mercure. En revanche, des échantillons complémentaires doivent être collectés, respectivement, pour l'analyse granulométrique (environ 50 g) et pour l'évaluation de la teneur en eau (20 g suffisent). Les piluliers contenant ces échantillons sont conservés au frais mais non congelés. Les piluliers utilisés pour l'évaluation de la teneur en eau ont été préalablement tarés (précision au mg). Le dosage du carbone organique nécessite certaines précautions comme celles requises pour le dosage des contaminants organiques : l'échantillon est prélevé à la spatule en acier inoxydable, stocké dans un pilulier en verre et congelé jusqu'à l'analyse. Le dosage des carbonates ne nécessite pas de précautions particulières et peut être fait sur le même échantillon que celui qui sert au dosage du carbone organique.

1.3. Lyophilisation des échantillons

Pour les organismes marins comme pour les sédiments, les analyses sont réalisées sur des échantillons secs et les résultats sont exprimés par rapport au poids sec. La lyophilisation est le meilleur moyen d'obtenir rapidement des échantillons rigoureusement secs, et dès lors faciles à conserver à moindre coût. Cette méthode de séchage offre de bonnes garanties de conservation de l'échantillon à condition de prendre les précautions nécessaires pour éviter toute contamination dans l'appareil et de stocker les échantillons lyophilisés à l'abri de l'humidité.

Les conditions de lyophilisation (durée notamment) dépendent de l'appareil. La présence d'un système de chauffage des échantillons qui facilite l'évaporation de l'eau permet d'accélérer le processus. Il faut s'assurer alors que les échantillons ne sont pas portés à une température supérieure à 14°C. Après lyophilisation complète, les piluliers sont rapidement refermés pour éviter contamination et reprise d'humidité. Ils se conservent alors dans un endroit sec, à température ambiante et à l'abri de la lumière.

1.4. Traitement et entretien du matériel et du flaconnage

1.4.1. Matériel de prélèvement

Tout matériel de prélèvement utilisé sur le terrain ou en laboratoire doit être maintenu en bon état de fonctionnement et de propreté et ne doit pas présenter de trace de corrosion. Il doit être manipulé et stocké avec les précautions nécessaires pour éviter la contamination : éviter le contact des mains sur le matériel de prélèvement, protéger le matériel contre les poussières et les graisses entre deux utilisations (emballage dans des sacs en polyéthylène). En cours d'utilisation et entre chaque échantillon, le gros matériel, tel le carottier, est rincé à l'eau de mer prélevée directement sur le site. Le petit matériel (entonnoirs, couteaux, spatules, scalpels, etc.) est rincé à l'eau du robinet puis à l'eau MilliQ®.

A la fin de chaque campagne, le matériel de prélèvement est rincé à l'eau du robinet. Le matériel de petites dimensions (benne Ekman, boîte de carottier, etc.), après rinçage à l'eau du robinet et séchage à l'air libre, est stocké individuellement dans un sac en polyéthylène jusqu'à sa prochaine utilisation.

1.4.2. Matériel pour la préparation des échantillons

Bacs pour l'épuration des coquillages : traitement des bacs neufs

Ce traitement a pour but d'éliminer les agents chimiques de fabrication et de démoulage. Il est fait une fois pour toutes sous réserve d'une utilisation exclusive des bacs pour l'épuration des coquillages en eau claire. L'opération se compose successivement de :

- lavage au détergent pur (sans phosphates) avec une éponge douce ne rayant pas la surface ;
- rinçage à l'eau du robinet ;
- trempage dans une solution d'acide nitrique diluée (HNO_3 dilué à 2%) pendant 4 jours. Les bacs et leurs portoirs ajourés, sont remplis jusqu'au bord de la solution acide et recouverts de leur couvercle.
- rinçage à l'eau MilliQ®. Egouttage, sans essuyer.

- stockage des bacs fermés, avec les portoirs à l'intérieur.
- Les bidons en polyéthylène servant au transport de l'eau d'épuration sont traités de la même façon avant la première utilisation.

Entretien courant

Les bacs et jerricans sont réservés à l'épuration des coquillages. Avant chaque utilisation les jerricans doivent être rincés une fois avec un peu d'eau de mer avant remplissage.

A la fin de la phase d'épuration, les bacs sont vidés, rincés sommairement si nécessaire avec un peu d'eau de mer. Ils doivent être égouttés rapidement et stockés fermés et ne doivent jamais être lavés avec un détergent ou tout autre produit. L'eau de mer utilisée pour l'épuration suffit à en assurer la propreté, sans risque de contamination.

1.4.3. Flaconnage

Flaconnage pour les échantillons d'organismes marins

Les piluliers en verre sont pourvus de couvercle en plastique. Les couvercles sont rincés à l'eau du robinet puis à l'eau Milli-Q®. Ils sont alors séchés à l'étuve dans des sachets plastiques ouverts puis stockés secs dans les sachets fermés en attendant que les piluliers soient disponibles. Les piluliers neufs sont d'abord lavés avec un détergent pur (sans phosphates), abondamment rincés à l'eau du robinet puis à l'eau MilliQ®. Ils sont alors passés au four pendant 8 heures à 450°C. Après refroidissement (sans les sortir du four), ils sont rebouchés avec les couvercles plastiques et stockés jusqu'à utilisation.

Flaconnage pour les échantillons de sédiments

Les piluliers et leur couvercle sont en plastique (polystyrène crystal). Les couvercles sont de préférence en plastique blanc pour éviter les risques de contamination par les pigments des plastiques. Ils subissent avant usage :

- un lavage avec un détergent pur (sans phosphates);
- un traitement acide par immersion dans une solution d'acide nitrique diluée (HNO_3 de qualité "pour analyse" dilué à 10%), 5 jours à température ambiante ou 3 jours à 40°C.
- un rinçage abondant à l'eau MilliQ®.

Les piluliers secs sont conservés en sacs en polyéthylène jusqu'à utilisation.

2. DOSAGE DU MERCURE TOTAL

La méthode décrite ici est utilisée pour le dosage du mercure total dans les huîtres, les moules et les sédiments analysés dans le cadre du Réseau National d'Observation de la qualité du milieu marin (RNO) depuis 1997. Elle remplace la méthode Sanjuan et Cossa (1993) qui a été utilisée à partir d'octobre 1992 et qui consistait en l'automatisation de la méthode utilisée précédemment (Thibaud, 1986). Il s'agit d'une méthode semi-automatique qui permet le dosage du mercure total présent dans des échantillons solides de tissus d'organismes ou de sédiment avec un rythme analytique élevé. Pour une prise d'essai de 20 milligrammes environ la limite de détection et la reproductibilité sont respectivement de 0,007 $ng.mg^{-1}$ (poids sec), et meilleure que 7 %. La justesse est évaluée systématiquement au moyen d'échantillons de référence certifiés.

2.1. Principe

Après calcination, on procède à la volatilisation du mercure présent dans un échantillon solide. Le mercure élémentaire formé est entraîné sous forme de vapeur par un courant d'oxygène et amalgamé sur un piège de sable doré. Après chauffage du piège pour dissocier l'amalgame or-mercure formé, la vapeur de mercure est envoyée dans la cellule d'un spectrophotométre d'absorption atomique où elle est quantifiée. L'appareil utilisé est construit par la firme ALTEC sous le nom de AMA-254®. Cette technique présente l'avantage d'une grande rapidité, de bonnes sensibilité et reproductibilité et un blanc extrêmement bas puisque aucun réactif chimique n'est utilisé pour la minéralisation.

2.2. Matériel et instrumentation

L'appareil utilisé est conçu pour la mesure directe du mercure dans un échantillon solide ou liquide de petit volume sans aucun traitement chimique préalable. Il est piloté par un micro-ordinateur équipé d'un logiciel dédié. L'appareil, un spectrophotomètre d'absorption atomique, est présenté sur la figure 1 et sa description sur la figure 2.

Figure 1. Analyseur de vapeur froide de mercure AMA-254® (Altec)

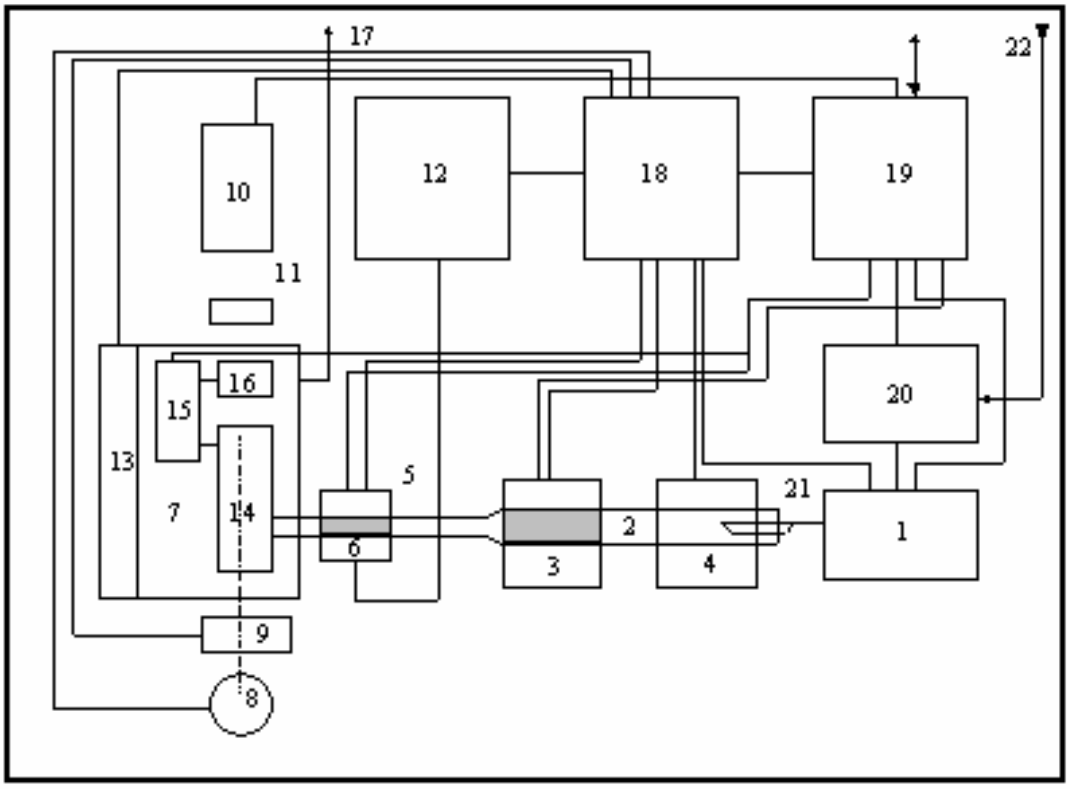

Figure 2. Schéma de fonctionnement de l'analyseur AMA-254®

1: Système d'introduction automatique de l'échantillon
2: Tube catalytique
3: Four catalytique (900 °C)
4: Four de décomposition (750 °C)
5: Amalgameur (piège de sable doré)
6: Four du piège doré
7: Support des cellules optiques
8: Lampe au mercure
9: Obturateur
10: Photomultiplicateur
11: Filtre interférentiel
12: Source électrique
13: Chauffage des cellules optiques
14: Grande cellule optique
15: Cuve de transfert
16: Petite cellule optique
17: Evacuation des gaz
18: Source électrique
19: Electronique et interface-PC
20: Régulateur du débit d'oxygène
21: Nacelle porte échantillon
22: Entrée d'oxygène

2.3. Réactifs

2.3.1. Eau déionisée

L'eau déionisée utilisée est obtenue à partir d'un système Milli-Q®. Cette eau contient moins de 0,5 ng de mercure par litre.

2.3.2. Solution diluante

Toutes les solutions de mercure sont préparées en utilisant une solution diluante qui permet une stabilisation du mercure. Cette solution, qui constitue en outre le zéro de la gamme d'étalonnage, contient 10 ml d'HNO_3 concentré (Merck, SupraPur) et 4 ml de $K_2Cr_2O_7$ à 10 % (p/v) et une quantité d'eau déionisée suffisante pour 1 litre.

2.3.3. Solution mère de mercure à 1 g.l^{-1}

A une solution concentrée (Merck) contenant 1,000 ± 0,002 g de mercure on ajoute une quantité suffisante de solution diluante pour un litre. Dans un flacon en Téflon (FEP) fermé hermétiquement à la pince multiprise, cette solution se conserve plus d'un an à l'abri de la lumière.

2.3.4. Solution de travail

A partir de la solution mère on prépare, par dilutions successives au moyen de la solution diluante, une solution de travail (ST) de concentration 0,5 mg.l^{-1}. La gamme étalon comporte six (6) points :

- 1er point : 2,5 ng Hg, c'est à dire 5 µl de la ST
- 2ème point : 5,0 ng Hg, c'est-à-dire 10 µl de la ST
- 3ème point : 7,5 ng Hg, c'est-à-dire 15 µl de la ST
- 4ème point : 10,0 ng Hg, c'est-à-dire 20 µl de la ST
- 5ème point : 12,5 ng Hg, c'est-à-dire 25 µl de la ST
- 6ème point : 15,0 ng Hg, c'est-à-dire 30 µl de la ST.

De manière générale la partie linéaire de la courbe d'étalonnage correspond à des absorbances inférieures à 0,3 correspondant le plus souvent à des quantités de mercure inférieures à 12,5 ng. Toutefois, pour des absorbances plus élevées le mode de calcul de la concentration corrige ce manque de linéarité. La stabilité de calibration du détecteur AMA-254® est grande. La gamme d'étalonnage est valide pour des semaines voire plus. Il est toutefois nécessaire de procéder à une vérification de la pente de la courbe d'étalonnage en vérifiant seulement un ou deux points de la gamme et d'utiliser des matériaux de référence certifiés lors de chaque série de mesures.

2.4. Procédure

Environ 10 à 30 mg d'échantillon lyophilisé sont pesés exactement (± 0,05 mg) dans une cuvette en nickel spécialement conçue à cet effet (21, figure 2). La masse nominale en mg est fournie au logiciel qui pilote l'appareil et effectue les calculs. La cuvette a été préalablement chauffée à 600°C pour nettoyage. Déposée sur son portoir, cette cuvette (21) est introduite automatiquement dans le four de l'appareil (4) par un système automatique (1), lors de la mise en marche de la séquence analytique. L'appareil procède ensuite automatiquement. Dans le four (4), l'échantillon est porté progressivement à 550 °C. Les produits de décomposition, incluant le mercure, sont entraînés par un flux d'oxygène au travers d'un tube « catalytique » (2) contenant un produit solide de composition inconnue de l'utilisateur (brevet). Les oxydes de soufre et d'azote y sont piégés. Le mercure sous forme élémentaire (Hg°) s'en échappe pour atteindre le piège doré (5) sur lequel il s'amalgame. Les autres gaz entraînés par le flux d'oxygène sont expulsés de l'appareil après passage sur une cartouche de charbon activé (17). Le piège et la cellule de mesure sont maintenus à 120 °C pour éviter une éventuelle condensation du mercure ou de la vapeur d'eau (6 et 13). Le mercure amalgamé est ensuite libéré par brusque chauffage du piège doré (5 et 6) jusqu'à 550 °C ; la vapeur de Hg° ainsi libérée est entraînée par le flux d'oxygène vers les cellules d'absorption atomique (14-16) pour y être quantifiée à une longueur d'onde de 254 nm (10).

Il est absolument nécessaire que tout le matériel métallique utilisé durant les analyses (cuvettes en nickel, pinces permettant la saisie des cuvettes, etc.) soit calciné à 550 °C immédiatement avant usage afin de minimiser les sources de contamination.

2.5. Calcul des concentrations

Au cours des analyses l'ordinateur calcule les quantités de mercure présent dans l'échantillon à partir des absorbances en se rapportant à la courbe d'étalonnage. Les résultats sont rapportés en absorbance, en quantité (ng) et en concentration de mercure par unité de masse d'échantillon ($mg.kg^{-1}$). Bien que le logiciel procède à une correction de linéarité, on s'efforce de choisir les masses d'échantillons permettant de travailler dans la zone de linéarité. L'absorbance du blanc (réponse de l'appareil avec une cuvette de Ni vide) est retranchée automatiquement.

2.6. Contrôle de qualité des dosages

Les critères d'évaluation des performances de la méthode sont empruntés à Taylor (1987). Les valeurs utilisées pour les calculs des performances ci-dessous ont été obtenues entre novembre 2000 et avril 2001.

2.6.1. Justesse

La justesse de la méthode a été établie à partir d'échantillons de référence certifiés de tissu d'organismes ou de sédiments marins produits par le Conseil National de Recherches-Canada (DORM-1 et DORM-2, MESS-2) et l'Agence Internationale de l'Energie Atomique (IAEA-

142). Le DORM est un muscle de poisson, le MESS un sédiment marin et l'IAEA-142 un tissu de moule. Les résultats sont consignés dans le tableau 1.

Tableau 1. Moyennes et intervalles de confiance à 95 % pour les valeurs trouvées et les valeurs certifiées ($mg.kg^{-1}$p.s.) ; n = 6.

	MESS-2	**IAEA-142**	**DORM-1**	**DORM-2**
Valeur certifiée	0,092 ± 0,009	0,126 ± 0,016	0,798 ± 0,074	4,36 ± 0,26
Valeur trouvée	0,089 ± 0,001	0,120 ± 0,006	0,854 ± 0,013	4,41 ± 0,04

2.6.2. Précision

La répétabilité de la méthode exprimée par le coefficient de variation (défini comme le rapport de l'écart-type à la moyenne) varie avec les concentrations moyennes. Elle est de 1 % pour un échantillon concentré (4,36 $mg.kg^{-1}$), le matériau de référence certifié DORM-2 et de 7 % pour un échantillon de plus faible concentration (0,126 $mg.kg^{-1}$), le matériau de référence certifié IAEA-142. Ces valeurs ont été obtenues pour des prise d'essai d'environ 20 mg (poids sec) et pour 6 replicats.

2.6.3. Limite de détection

La limite de détection est définie comme 3,29 fois l'écart-type de la concentration d'un échantillon dont la teneur est proche de zéro (dans la pratique du présent dosage il s'agit des blancs) ; le facteur multiplicatif de 3,29 tient compte des erreurs de types I et II (Taylor, 1987). La limite de détection calculée journellement varie de 0,004 à 0,015 $mg.kg^{-1}$ (pour un échantillon de 20 mg en poids sec). Elle est en moyenne de 0,007 $mg.kg^{-1}$.

2.6.4. Rythme analytique

Compte tenu de l'absence de minéralisation des échantillons et du processus d'assurance de qualité, on évalue à 60 le nombre quotidien d'analyses, incluant les échantillons, les blancs et les échantillons de référence certifiés.

3. DOSAGE DU METHYLMERCURE DANS LES ORGANISMES ET LES SEDIMENTS MARINS

3.1. Principe (Figure 3)

Après solubilisation de l'échantillon en milieu alcalin (organismes) ou acide (sédiments), on procède à l'éthylation du monométhylmercure (MMHg) en solution par du tétraéthylborate de sodium ($NaBEt_4$). L'éthylméthylmercure (MHgEt) formé, ainsi que le diéthylmercure formé par éthylation du mercure inorganique ($(Et)_2Hg$), étant volatils, sont alors entraînés par un courant d'azote et piégés sur un support adsorbant (Tenax®). Les dérivés volatils du mercure sont ensuite désorbés du Tenax® par chauffage, puis séparés par chromatographie en phase gazeuse, pyrolysés et enfin détectés par fluorescence atomique.

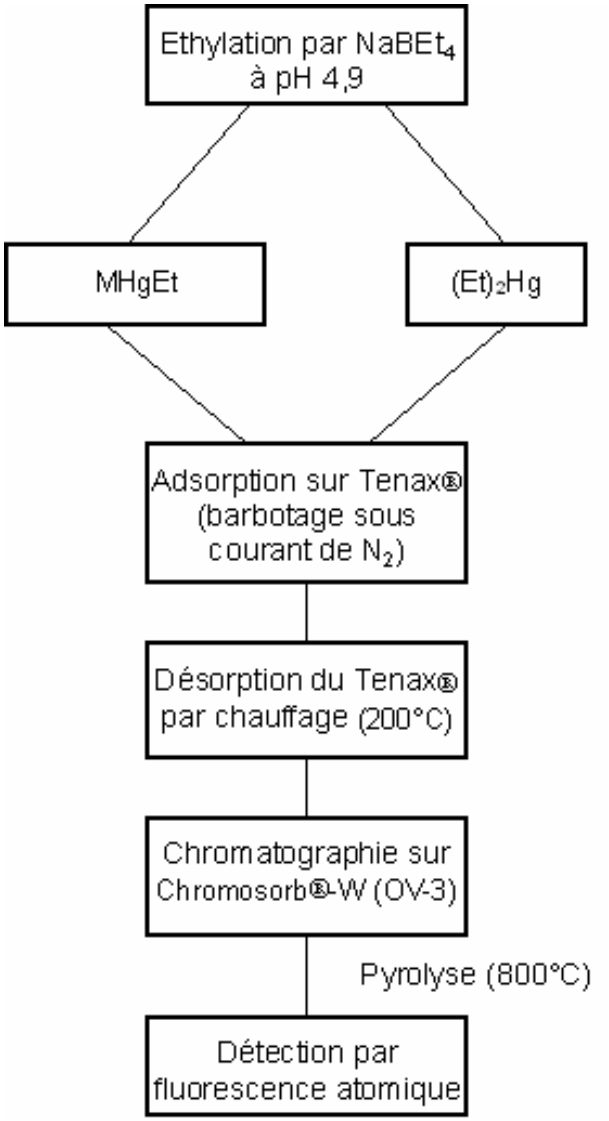

Figure 3. Schéma des séquences analytiques pour le dosage du méthylmercure (MMHg)

3.2. Préparation des solutions

3.2.1. Solution standard de monométhylmercure (MMHg)

Solution mère de concentration 1 g.l^{-1} en MMHg

Cette solution est préparée par dissolution de 0,1252 g de chlorure de méthylmercure dans de l'isopropanol, le tout étant porté à un volume final de 100 ml.

Solution de travail de concentration 1 µg.l^{-1} en MMHg

La solution à 1 g.l^{-1} est diluée successivement au 1/100ème dans une solution aqueuse de HCl à 0,5 % afin d'obtenir une solution à 1 ng.ml^{-1}. Cette solution doit être conservée au réfrigérateur. Afin d'évaluer la variation de la concentration en MMHg de ce standard, il est recommandé de mesurer la concentration en mercure total et mercure inorganique tous les mois ; la différence entre ces deux dosages constitue la concentration en MMHg.

2.3.2. Solution tampon acétate de sodium/acide acétique

Pour que la réaction d'éthylation se déroule dans les meilleures conditions, le pH du milieu doit être de 4,9. On ajuste donc le pH par une solution tampon d'acétate de sodium 2M que l'on prépare de la manière suivante: dans un flacon en téflon de 250 ml, on pèse 41 g de $Na_2C_2H_3O_2$ (Suprapur®, Merck) puis 31,8 g d'acide acétique glacial (pour analyse®, Merck) ; on complète à 250 ml avec de l'eau MilliQ®. Cette solution, stockée à l'abri de la lumière et à +4°C, peut être gardée plusieurs mois.

3.2.4. Potasse méthanolique à 25%

On pèse dans un flacon en téflon d'un litre 250 g d'hydroxyde de potassium (pour analyse, Merck) et on complète à 1 litre avec du méthanol (Atrasol®). La dissolution est très exothermique, il est donc recommandé d'utiliser un bain de glace. Cette solution peut être conservée plusieurs mois si elle est maintenue dans l'obscurité.

3.2.5. Solution de tétraéthylborate de sodium ($NaBEt_4$) à 1 %

Le $NaBEt_4$ solide s'oxyde très facilement au contact de l'air, il est de plus inflammable. Sa mise en solution doit donc être rapide et se faire sous atmosphère d'azote. Cette opération est menée dans une boîte à gants.

On prépare d'abord, une solution de KOH à 2 % (2 g dans 100 ml d'eau MilliQ®), qui servira de solution diluante. Ensuite, sous boîte à gants, on fait barboter de l'azote dans la solution. Ensuite on dissout un gramme de $NaBEt_4$ (Strem Chemicals) dans un flacon dans 100 ml de solution diluante. On transvase rapidement cette solution dans des flacons en téflon de 10 ou 30 ml sans les remplir, puis on les ferme hermétiquement. Ils sont conservés au congélateur (-18 °C) jusqu'à utilisation. Un flacon neuf sera utilisé pour chaque série d'analyse.

3.3. Extraction du MMHg

3.3.1. Sédiments

La méthode d'extraction du MMHg est inspirée de celle de Baeyens *et al.* (1999) modifiée par Leemakers *et al.* (2001). Dans des tubes à centrifuger Oak-Ridge en téflon de 37 mL (PFA à bouchon à vis en PVDF), peser exactement une prise d'essai (échantillon lyophilisé) d'environ 200 mg. Ajouter 8 mL de HNO_3 4M (Suprapur®, Merck). Fermer les tubes et les agiter. Laisser reposer 3 heures. On extrait ensuite deux fois par 5 mL de CH_2Cl_2 (Suprasolv®, Merck) pendant 2 heures sous agitation. Séparer les phases dans une petite ampoule en téflon (PFA) et recueillir le solvant surnageant dans une bouteille en téflon de 125 mL. Cet extrait peut se conserver 4 jours à +4 °C à l'abris de la lumière. Ajouter 60 mL d'eau MIlliQ® et évaporer le solvant au bain marie à 70°C. La solution aqueuse est enfin purgée à l'azote (purifiée sans mercure) afin de se débarrasser de toutes traces de CH_2Cl_2. La solution aqueuse ne se conserve pas et doit être éthylée le jour même.

3.3.2. Organismes

Dans des tubes à centrifuger Oak-Ridge en téflon de 37 mL (PFA à bouchon à vis en PVDF), peser exactement une prise d'essai (échantillon lyophilisé) d'environ 200 mg. Ajouter 10 mL de la solution de potasse alcoolique à 25 %. Fermer les tubes et les agiter. Laisser reposer 12 heures. Les tubes fermés hermétiquement sont chauffés ensuite à 75 °C pendant 3 heures. Laisser les refroidir puis ajuster les volumes au trait de jauge (37 mL) avec du méthanol. Pour les échantillons présentant des concentrations de MMHg très faibles nécessitant l'éthylation de plus de 60 µL (voir section 3.4.2), on procèdera à une extraction de la solution de potasse alcoolique par CH_2Cl_2 avec une procédure semblable à celle utilisée pour les sédiments. La conservation d'extrait organique est de 4 jours à +4 °C à l'abris de la lumière.

3.4. Ethylation et détection des dérivés alkylés du mercure

L'éthylation du mercure et du méthylmercure permet de les isoler de leur matrice par entraînement gazeux, en raison de la volatilité des composés formés, avant de les séparer par chromatographie. Ils sont ensuite détectés par fluorescence atomique. Cette méthode est adaptée des travaux de Liang *et al.* (1994).

3.4.1. Description du système réactionnel

Le système d'éthylation est représenté sur la figure 4. Le circuit comprend des éléments en téflon et verre borosilicaté et en quartz. Le matériel en verre présentant des sites de fixation pour le mercure est préalablement silanisé (5 % DMDCS dans le toluène: Sylon CT, Supelco).

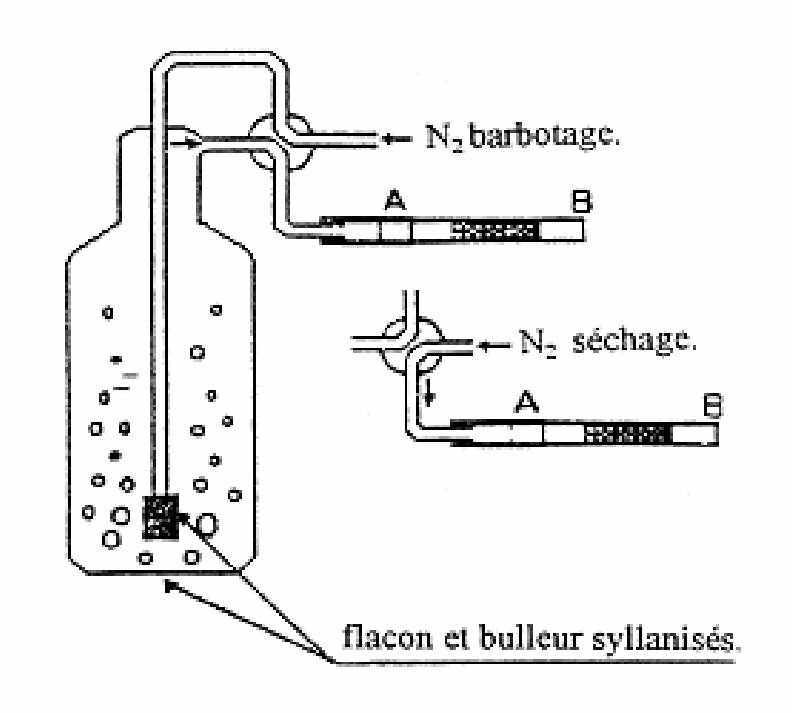

Figure 4. Système d'éthylation

Pour préparer un piège de Tenax®, introduire d'abord un tampon de laine de quartz silanisée dans une colonne de quartz silanisée et tasser légèrement au moyen d'un petit tube en Téflon. Y introduire environ 100 mg de Tenax® à l'aide d'un petit entonnoir. Finir en maintenant le tout par un autre morceau de laine de quartz (Figure 5).

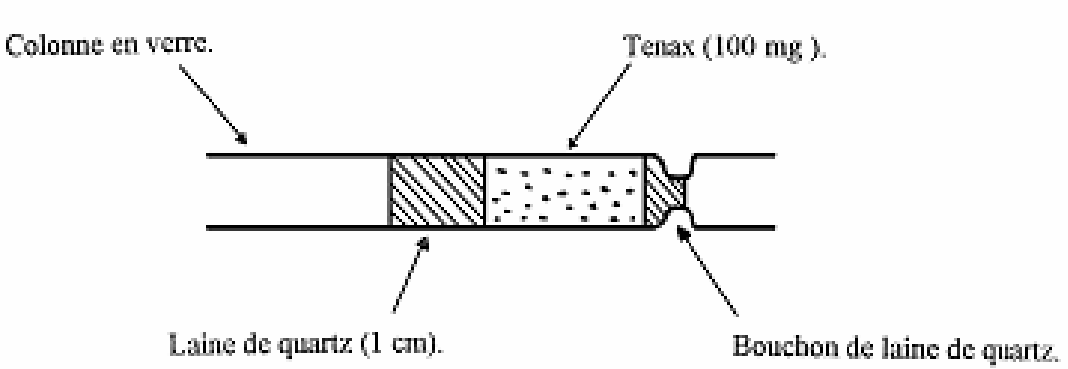

Figure 5. Piège de Tenax® pour l'adsorption des composés éthylés volatils

3.4.2. Protocole expérimental

Avant de procéder à des analyses il convient lors de la mise en route de procéder à une décontamination de l'appareillage.

Mise en route du système chromatographique *(Figure 6)*

On chauffe le four à 800°C et on ouvre l'arrivée d'argon, dont le débit doit rester à 35 mL min^{-1}. On laisse le circuit se stabiliser pendant 30 minutes. Le piège de Tenax® est alors chauffé à 200 °C jusqu'à ce que le chromatogramme obtenu soit plat.

Ethylation et adsorption sur le Tenax®

Mettre 150 ml d'eau MilliQ® dans le flacon de barbotage en verre silanisé (Figure 4) et y faire barboter le gaz (azote C, 300 ml min^{-1}) pendant environ trois minutes, puis y fixer la cartouche de Tenax®. Cette procédure permet de minimiser la valeur des blancs. Ajouter ensuite dans l'ordre, 300µl de solution tampon (pH 4,9), puis 20 à 60 µl de l'échantillon solubilisé dans la potasse alcoolique ou quelques millilitres de l'extrait évaporé, enfin 150 µl de la solution de $NaBEt_4$. Refermer alors le flacon de barbotage et homogénéiser en l'agitant doucement. Recouvrir le flacon de papier aluminium afin d'éviter les réactions photochimiques. Laisser réagir pendant 15 minutes. Faire barboter ensuite 10 minutes l'azote (azote C, 300 ml min^{-1}) pour piéger les espèces éthylées volatiles sur le piège de Tenax®. Enfin, court-circuiter le barboteur au moyen de la vanne 4 voies (Figure 4) et débarrasser le Tenax® des traces d'humidité sous courant d'azote pendant 5 minutes. Les dérivés éthylés sont adsorbés à la tête du piège de Tenax® (Figure 7). On vérifie chaque jour que la stabilité de la réponse à une prise d'essai d'un matériau de référence certifié pour le MMHg. De plus, pour vérifier la stabilité du détecteur et le rendement d'éthylation; un étalon est analysé plusieurs fois au cours d'une même journée de travail. Les blancs sont évalués dans les mêmes conditions que l'échantillon en omettant bien sûr l'ajout de l'aliquote d'échantillon ; ils sont généralement négligeables.

Dans le cas d'échantillons biologiques solubilisés dans la potasse alcoolique, on vérifie systématiquement l'absence d'effet de matrice en analysant des volumes différents d'échantillon. La solution de $NaBEt_4$ et la solution tampon sont conservées à + 4°C entre chaque utilisation.

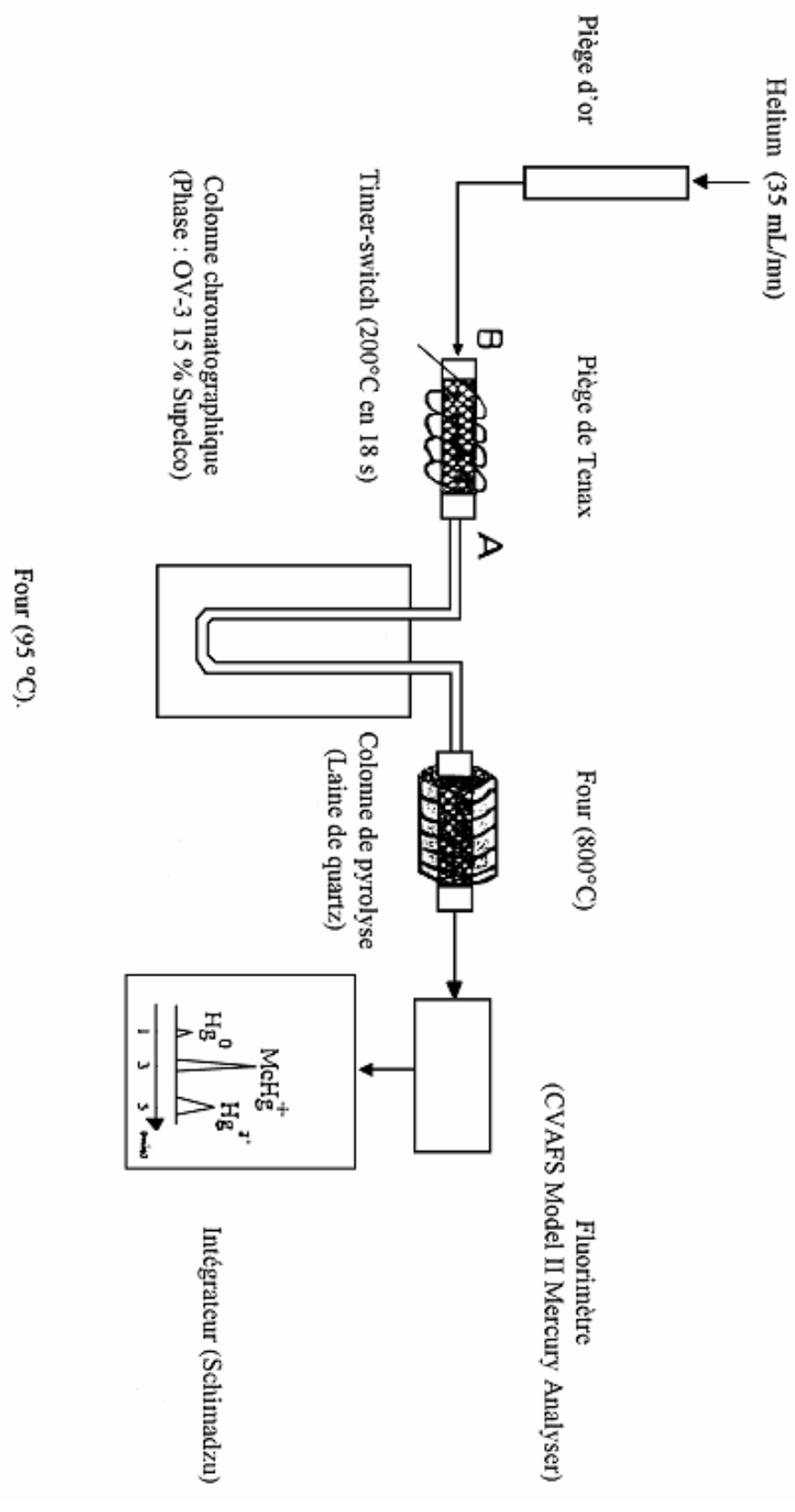

Figure 6. Montage chromatographique.

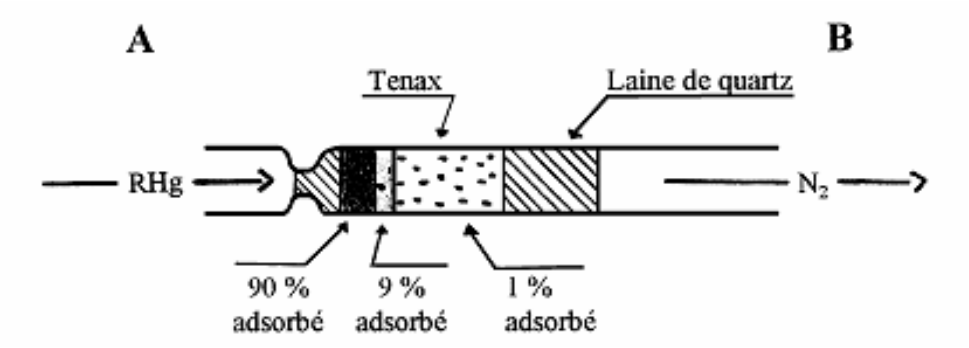

Figure 7. Adsorption des organomercuriels volatils sur la cartouche de Tenax® ; RHg : MHgEt, $(Et)_2Hg$, et autres composés alkylés volatils

Chromatographie

La chaîne analytique est décrite sur la figure 6. Le débit d'argon est de35 ml min^{-1}. Le piège de Tenax® est maintenu dans le circuit chromatographique en position inverse de celle de l'adsorption ("backflush") (Figure 8).

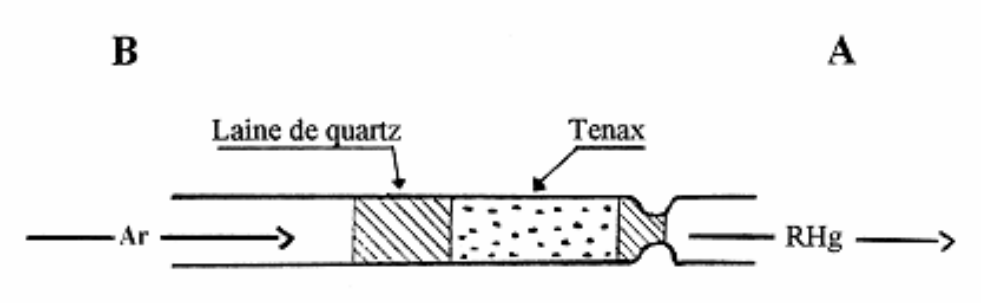

Figure 8. Désorption des organomercuriels volatils de la cartouche de Tenax® ; RHg : MHgEt, $(Et)_2Hg$, et autres composés alkylés volatils

Remarque : 1- Il est important de faire attention à la manière dont on introduit le piège de Tenax® dans le système analytique. En effet, pour éviter tous problèmes de différences de pression, l'embout d'arrivée d'argon doit être en premier connecté à l'extrémité B du piège puis l'autre extrémité peut être assemblée. Pour ôter le piège du système analytique, on doit procéder de manière inverse, en déconnectant d'abord l'extrémité A du piège.

Une fois la cartouche de Tenax® installée sur la ligne chromatographique, on procède à son chauffage rapide grâce à un fil chauffant de Ni-Cr. La température de 200°C est atteinte en moins de 18 secondes. La colonne chromatographique (Chromosorb-W® avec une phase de 15% OV-3, Supelco), maintenue à 95°C, permet la séparation des différents composés du mercure, qui, après passage à travers le four à pyrolyse à 800 °C, sont quantifiés sous forme de mercure élémentaire dans un spectrophotomètre dit à vapeur froide (CVAFS) (Figure 6).

3.5. Calcul des concentrations

On calcule la masse de MMHg en évaluant l'aire de pic donnée par un intégrateur enregistreur.

La masse de méthylmercure ($\mathbf{m_{PE}}$) en pg dans la prise d'essai correspond à :

$$\mathbf{m_{PE}} = \frac{\mathbf{A_{MES}} \times \mathbf{m_{STD}}}{\mathbf{A_{STD}}}$$

avec :

$\mathbf{m_{PE}}$: masse de MMHg dans la prise d'essai (pg),

$\mathbf{A_{MES}}$: aire mesurée pour l'échantillon analysé,

$\mathbf{m_{STD}}$: masse de MMHg contenue dans la prise d'essai de standard de MMHg,

$\mathbf{A_{STD}}$: aire mesurée pour la prise d'essai du standard de MMHg,

On détermine le rendement d'éthylation (ρ), en comparant l'aire ou la hauteur mesurée pour un standard en MMHg (concentration exactement connue) et celle obtenue pour une injection de deux (2) µL de vapeur saturée de mercure on a alors :

La concentration de méthylmercure dans l'échantillon analysé (pg g^{-1}) est alors *:*

$$\mathbf{M_{ECH}} = \left(\frac{\mathbf{m_{PE}} \times \mathbf{Vol_{MES}}}{\mathbf{Vol_{PE}} \times \mathbf{m_{ECH}}} \right) / \rho$$

avec :

$\mathbf{M_{ECH}}$: masse de MMHg dans l'échantillon analysé (pg g^{-1}),

$\mathbf{m_{PE}}$: masse de MMHg dans la prise d'essai (pg),

$\mathbf{Vol_{MES}}$: volume de l'échantillon (environ 37 mL),

$\mathbf{Vol_{PE}}$: volume de la prise d'essai de l'échantillon analysé (µL),

$\mathbf{m_{ECH}}$: masse d'échantillon pesée en mg,

ρ : rendement d'éthylation.

3.6. Contrôle de qualité des dosages

3.6.1. Justesse

On utilise un échantillon certifié de chair de moule (AIEA 142) comme échantillon représentatif des mollusques et l'IAEA-405 ou l'IAEA-356 pour les sédiments. L'échantillon est solubilisé et éventuellement extrait (cf. § 3.3) le jour 1 est utilisé jusqu'au jour 5 pour contrôler la justesse des résultats. Chaque jour et sur chaque poste d'éthylation, on réalise systématiquement au moins une mesure du rendement d'éthylation.

Lors des dosages effectués au cours d'une année (38 pour l'année 1998-99) les concentrations obtenues sur le dosage du MMHg dans le matériel certifié AIEA-142 ont varié de 31 à 57 $ng.g^{-1}$ (poids sec) avec une moyenne de 43 ng g^{-1} (poids sec), la valeur certifiée de MMHg étant de 43 à 51 $ng.g^{-1}$ (poids sec).

3.6.2. Précision

La précision définie comme le coefficient de variation de 5 replicats de l'AIEA-142 était pour la même année 1998-99, de 17 %, et la reproductibilité dans la même journée de 10 %.

3.6.3. Limite de détection

La limite de détection définie comme trois fois l'écart-type sur une valeur faible varie au cours du temps entre 2 et 4 ng g^{-1} (poids sec).

3.6.4. Rythmes analytiques

S'il l'on dispose de deux flacons d'éthylation travaillant en parallèle, le rythme analytique peut être d'une dizaine d'échantillons par jour. Cela tient compte des blancs, des échantillons de référence certifiés et des standards.

3.6.5. Domaine de validité

La linéarité de la réponse a été étudiée pour différentes prises d'essai d'un solubilisat d'échantillon standard certifié. La linéarité existe sur plusieurs ordres de grandeur. La reproductibilité est maximale pour des prises d'essai correspondant à des quantités de MMHg d'environ un nanogramme.

BIBLIOGRAPHIE

Baeyens, W., Leermakers, Molina, R., Holsbeek, L. et Joiris, C.R. 1999. Investigation of headspace and solvent extraction methods for the determination of dimethyl- and monomethylmercury in environmental matrices. *Chemosphere*, 39, 1107-1117.

Claisse D. 1999. *Historique et bilan général de la surveillance du RNO dans les organismes marins*. In: RNO 25 ans de surveillance du milieu marin. Actes du colloque. Ifremer Nantes 27 – 28 octrobre 1999 pp 56-62.

Cossa, D. 1989. A review of the use of *Mytilus* spp. as quantitative indicators of cadmium and mercury contamination in coastal waters. *Oceanol. Acta*, 12, 417-432.

Cossa, D., Auger, D., Averty, B., Luçon, M., Masselin, P. et Noel, J. 1992. Flounder (*Platichthys flesus)* Muscle as an Indicator of Metal and Organochlorine Contamination of French Atlantic Coastal Waters. *Ambio*, 21, 176-181.

Leermakers, M., Galetti, S., de Galan, S. Brion, N. et Baeyens, W. 2001. Mercury in the Southern North Sea and Scheldt Estuary. *Mar. Chem*., 75, 229-248.

Liang, L., Horvat, M. et Bloom, N.S. 1994. An improved speciation method for mercury by GC/CVAFS after aqueous phase ethylation and room temperature precollection. *Talanta*, 41, 371-379.

Nakhlé K. 1999. *Le flet comme bioindicateur quantitatif de la contamination de l'estuaire de la seine par le cadmium et le mercure*. Rapport de DEA. Ifremer Univ. Paris VII : 33p.

Ospar. 1999. Lignes directrices JAMP de la surveillance continue des contaminants dans le milieu vivant. Commission Ospar, *Lignes directrices de la surveillance N° 1999-2*. Londres, UK, 54 pages.

Sanjuan, J. et Cossa, D. 1993. *Dosage automatique du mercure total dans les organismes marins par fluorescence atomique*. Rapport Ifremer, *R. INT. DEL / 93.12 / NANTES*. Nantes, France.

Taylor, J. K. 1987. *Quality Assurance of Chemical Measurements.* Lewis Publishers, New York, USA.

Thibaud, Y. 1986. *La minéralisation des tissus biologiques en vue de la détermination du mercure*. Rapport Ifremer, *DERO 86-15 MR*, Nantes, France.

Biofilm composition and mercury availability as key complementary factors for mercury accumulation in fish *(Curimata cyprinoides)* from a disturbed Amazonian freshwater system

Soumis à *Environmental Toxicology and Chemistry*

Yannick Dominique[†§], Régine Maury-Brachet[†], Bogdan Muresan[‡], Régis Vigouroux[§], Sandrine Richard[§], Daniel Cossa[‡], André Mariotti[‖] and Alain Boudou[† *]

† LEESA, UMR CNRS 5805, University of Bordeaux 1, Place Dr Peyneau, 33120 Arcachon, France

‡ IFREMER, Département Polluants Chimiques, BP 21105, 44311 Nantes, France

§ HYDRECO, Laboratoire Environnement, 97388 Kourou, Guyane, France

‖BioMCo, UMR 7618, University Paris VI-CNRS-INRA, EGER, 78850 Thiverval-Grignon, France.

* corresponding author

Tel.: +33-556-22-39-21

Fax : +33-556-54-93-83

E-mail address: a.boudou@epoc.u-bordeaux1.fr

Abstract

A comparative study of mercury accumulation levels in the benthivorous/omnivorous fish species *Curimata cyprinoides* shows very marked differences between concentrations measured in individuals collected from the superficial layers of the Petit-Saut hydroelectric reservoir and downstream in the Sinnamary river (French Guiana, Amazonian Basin): in the dorsal skeletal muscle, mercury concentrations were ten times higher in fish from the downstream zone. Stomach contents and carbon/nitrogen stable isotope ratios showed that biofilms and the associated invertebrate communities represented important food sources at the two sites. $\delta^{13}C$ measurements indicate that biofilms in the flooded forest zone of the reservoir consist of endogenous primary producers; downstream, they are based on exogenous organic matter and micro-organisms, mainly from the anoxic layers of the reservoir. HgT and MeHg concentrations in the biofilms and associated invertebrates were much higher at the downstream site as compared to the reservoir. Our results clearly show the importance of MeHg export from the anoxic layers of this tropical reservoir. We conclude that differences between biofilm composition and MeHg concentrations in the food ingested could explain the marked differences observed between mercury levels in fish.

Keywords: Mercury, fish, Amazonian hydroelectric reservoir, biofilms

Introduction

Numerous field studies have shown the key role of artificial reservoirs in the biogeochemical cycling of mercury, leading to the production of monomethylmercury (MeHg), the organic form of the metal able to biomagnify along the aquatic foodwebs [1-4]. There are marked differences between reservoirs, in relation to (i) the mercury sources (atmosphere, drainage basin, or direct anthropogenic discharges) and (ii) the ecological characteristics of the hydrosystems, including climatic conditions. These differences affect mercury methylation rates and biomagnification patterns along the aquatic foodwebs, within the reservoirs and/or downstream.

In the Amazonian Basin, several dams have been built in Brazil, Surinam, French Guiana, and are often affected by goldmining activities, with point source inputs of elemental mercury (Hg^0) from mining sites using the amalgamation technique for gold extraction, and the release into the water of eroded soil particles naturally enriched with mercury [5, 6]. In French Guiana, the Petit-Saut hydroelectric reservoir, in the Sinnamary basin, is an ideal area for assessing the impact of goldmining and reservoir construction on mercury contamination of freshwater systems [7-9]. It was filled in 1994, flooding 360 km^2 of equatorial rain forest, and leading to anoxia in most of the water column. Ten years after flooding, the oxicline was located around 6 m below the surface, with a maximal depth of 35 m. This reservoir covers former goldmining sites that were very active at the end of the 19^{th} century and receives large contributions from present mining sites. The deep anoxic water column represents a large proportion of the water, which feeds the turbines of the hydroelectric plant and the Sinnamary River below the dam.

We present here a comparative study of mercury bioaccumulation levels in *Curimata cyprinoides*, a fish species abundant in the oxic layer of the reservoir and downstream, in the Sinnamary River. The results show a very marked difference between the two sites: Hg

concentrations in the skeletal muscle were ten times higher in fish collected from the downstream zone. Marked differences were also observed in gills, liver and kidneys concentrations. We explain these differences using a multidisciplinary approach, which enables us to determine the mercury chemical forms in the water and to investigate the trophic exposure conditions of the two fish populations, given that fish get most of their mercury from food [10-12]. Metal transfers from ingested food were analyzed using stomach content and stable carbon and nitrogen isotope ratio determinations, to define comparatively the diet pathways for the two populations and to measure the trophic sources of mercury (Hgtotal and MeHg).

Material and Methods

Study area

This field study was based on two sampling sites. The first site was located within the Petit-Saut hydroelectric reservoir, 20 km upstream of the dam, in a flooded forest zone (Reservoir site). The water depth varied between 12 and 20 m, at about 300 m from the lake bank. The primary forest was not cut before flooding in 1994; the submerged trees were still intact and represented an important support to biofilm development within the oxic and anoxic layers of the reservoir. The second site was on the Sinnamary river, between 0.5 and 5 km downstream of the dam (Downstream site). The river depth was less than 3 m, with an average width of 30 m.

Water and biological samples were collected in March 2003. The main physico-chemical characteristics of the water in the oxic layers of the reservoir (0-6 m) and downstream in the Sinnamary River, based on monthly measurements during the period March 2002/March 2003, are shown in Table 1.

Water sampling and mercury species determinations

Water samples were collected in Teflon (FEP) bottles using a peristaltic pump (Masterflex) and a polyethylene tubing or using a Teflon-coated Niskin bottle (General Oceanic). Arm-length polyethylene gloves were worn during the operations; further details of the sampling procedure are given elsewhere [13]. Teflon and plastic ware were washed and stored according to ultra-clean procedures. Filtrations were performed within 4 hours after the sampling through hydrophilized teflon membranes (LCR, Millipore; 0.45 µm pore size). Filtered water samples for total dissolved mercury (HgT_D) and monomethylmercury ($MeHg_D$) determinations were stored in Teflon bottles (FEP), acidified with concentrated HCl (0.5% v/v, Merck Suprapur) at 4°C. Filters for particulate mercury (HgT_P) determination were stored at -18°C before analyses.

All mercury species were detected by cold vapor atomic fluorescence spectrometry (AFS) as Hg^0 using a Brooks Rand model II or Tekran model 2500 detector. The AFS detectors were calibrated using saturated mercury vapour. HgT_D concentrations were determined after mercury compounds decomposition by bromine oxidation similar to the EPA 1631 method [14]. Then, divalent Hg was reduced as Hg^0 with $SnCl_2$ (0.1 ml of an acidic 50% (w/v) solution was added to 100 ml of sample). The sample was then sparged from the sample with Hg-free argon and Hg^0 amalgamated on a golden sand trap. By heating the gold trap the mercury vapor was transferred and quantified into the AFS. HgT_P was measured similarly after nitric acid mineralization (90°C; 3 h) in Teflon (PFA) reactors. Accuracy for HgT_D has been checked using 0RMS solution from National Research Council of Canada as a certified reference material (CRM). Determined values were in good agreement with certified values (10.3 ± 1 $ng.l^{-1}$ *versus* 12.6 ± 1.1 $ng.l^{-1}$. Dissolved MeHg was extracted using dichloromethane, followed by aqueous phase ethylation ($NaBEt_4$) according to [15] and [16]. This method has been shown exempt from organic matter interference and widely used in

natural waters. In the absence of any reference material for MeHg in natural waters, the method accuracy has been checked using the standard addition technique with a MeHg solution in isopropanol; the recovery was better than 80%. The CRM IAEA-405 was used for MeHg in solid, with values within the confidence limits of the sample (5.67 ± 0.9 $ng.g^{-1}$ *versus* 5.49 ± $ng.g^{-1}$). Method precisions (relative standard deviation evaluated by replicate determinations) averaged 15 % for HgTD, HgTP and MeHgD.

Biota sampling and mercury determinations

Adult fish were collected using nets (25 m x 2 m; 10 to 70 mm mesh size). An initial sorting was carried out on the boat in order to select individuals with a body length between 10 and 20 cm. Fish were individually weighed (total body weight, ± 0.5 g, wet wt) and measured (standard length, from nose to caudal fin basis: ± 0.5 cm) in order to select two homogeneous batches from each sampling site. Nevertheless, the age of the fish could differ between the two sites if, for example, food resources and energy expenditures led to different growth rates. It is difficult to determine the age of tropical fish using traditional techniques based on scales or otolites, because temperature variations between seasons are minimal. Using opercula bones, it was possible to identify the growth marks and to determine if there were significant differences between the two fish samples, without determining the exact age of the individuals. Age determination will necessitate a detailed study based on fish collected on a monthly basis in order to define the links between the numerous growth marks on the opercula bones and the impact of seasonal rhythms [17]. The numbers of main growth marks were estimated on ten fish from each site by three independent readers.

The sex of the fish was determined by visual examination of gonads. Liver, kidneys and gill arches were collected whole and a small muscle sample (2-4 g, wet wt) was taken from the dorsal lateral part of the body. Preliminary studies based on Hg measurements on several muscle samples taken from different parts of the fish body indicated homogeneity of metal

distribution in this tissue (data not shown) and therefore the muscle fragment collected was representative of the whole skeletal muscle compartment. Organ samples were frozen and shipped from Cayenne to Arcachon, France, under dry ice, with final storage in the laboratory at –20°C.

Biofilms were collected using vertical artificial substrates (glass slides: 26 x 6 cm) immersed at different depths in the oxic layer of the reservoir (0.5, 2 and 5 m) and downstream on the Sinnamary River, close to the bank at a depth of -2 m. After a colonization period of 6 months (October 2002 to March 2003), biofilms were removed by scrapping and transferred to Teflon bottles, dried (72 h at 40°C) and analysed in order to determine HgT and MeHg concentrations.

Benthic invertebrates were collected using artificial substrates. Five traps were immersed for 15 days at each site, close by the artificial substrates for biofilm collection. Using this procedure representative samples of all the benthic invertebrate communities could be obtained. After 15 days of immersion, traps were removed and put into individual clean plastic bags. Once in the laboratory, each trap was placed at the top of a column composed of three different mesh filters (1000, 500 and 100 µm) and washed abundantly three times with water collected from the two sampling sites. Previous studies have shown that with this procedure 95 % of invertebrates present in the substrate can be collected (data not shown). Next, each filter was placed under a stereomicroscope and each invertebrate present on the filter was manually removed and identified, before being pooled with individuals of the same taxon (family or genus level) in Teflon vials at - 20°C.

Total Hg concentrations in biofilms, invertebrates and fish organs were determined by flameless atomic absorption spectrometry. Analyses were carried out automatically after thermal decomposition at 750 °C under an oxygen flow (AMA 254).

MeHg concentrations were determined in biological samples after extraction with KOH-methanol (v/v) solution, for 12 hours in the dark at room temperature, then 3 hours at 75 °C. The pH of this solution was then adjusted to 4.9 with 2 M sodium acetate before ethylation with sodium tetraethylborate. Volatile Hg species were purged with mercury-free nitrogen and collected on Tenax. All mercury species were separated by isothermal gas chromatography (60 °C) prior to pyrolysis (900 °C) and detected using cold vapor atomic fluorescence spectrometry (CVAFS, Tekran 2500) [15]. The validity of the analytical methods was checked during each series of measurements against three standard biological reference materials (TORT2, DOLT2 and DOLT3 from the National Research Council of Canada, for total Hg and IAEA 142 for MeHg); values were consistently within the certified ranges (data not shown).

Method precision of total Hg and MeHg determinations, estimated from five replicates of fish muscle samples, was 5 and 9%, respectively. Mercury concentrations in biota were expressed on a dry weight basis (dry wt: 72 h at 60°C).

Fish diet determination

Fish diets for the two *C. cyprinoides* populations were defined from analysis of stomach contents and determination of stable nitrogen and carbon isotope ratios ($\delta^{15}N$ and $\delta^{13}C$) on skeletal muscles.

After dissection, stomach contents from a minimum of 10 fish per site were analysed under a stereomicroscope, using Dollfuss tanks, in order to make a semi-quantitative inventory of the different elements: sediment particles; terrestrial and aquatic vegetal materials; zooplankton; benthic invertebrates; other aquatic or terrestrial insects [18].

For stable isotope determinations, skeletal muscle samples (100 mg, wet wt) were treated with a methanol-chloroform (1/2) solution, to be defatted. This treatment is important for soft

tissues because lipids are poorer in ^{13}C than proteins and the amount of muscular lipids may directly influence $\delta^{13}C$ measurement. Moreover, muscular lipid ratios present inter- and intra-specific fluctuations [19]. After lipid removal, samples were dried (60°C for 48 h) and ground to a fine powder with a pestle and mortar. Samples were analysed for $^{13}C/^{12}C$ and $^{15}N/^{14}N$, total carbon and nitrogen with an Elemental Analyser coupled with an Isotope Ratio Mass Spectrometer (EA-IRMS). Samples were introduced in tin capsules and combusted in a flow of oxygen and helium to reduce all carbon and nitrogen forms to pure CO_2 and N_2 respectively; the pure gases were then separated on a GC column (3m PoropakQ) before being introduced in the "IsoPrime" mass spectrometer. Isotope ratios were reported in parts per thousand (‰) relative to standards (PeeDee Belemnite for carbon and atmospheric N for nitrogen), and defined in delta notation as:

$$\delta^{13}C \text{ or } \delta^{15}N = (Rsample/Rstandard - 1) \times 10^3$$

where $R = {}^{13}C/{}^{12}C$ or $^{15}N/^{14}N$. Biota tend to have less ^{13}C than standard and have negative $\delta^{13}C$ values; conversely, most biota have more ^{15}N relative to air and have positive $\delta^{15}N$ signatures [20].

Statistical data treatment

All the results are expressed as means ± standard errors. To study the site effect on biometric parameters, $\delta^{13}C/\delta^{15}N$ determinations and Hg concentrations in fish organs, we performed variance (ANOVA) and covariance (ANCOVA) analyses after checking assumptions (normality and homoscedasticity of the error term). If the assumption was met, the parametric Student t test was applied. If the assumption was not met, the non parametric Mann-Whitney U test was used. In each test, $p<0.05$ was considered significant. All statistical investigations were performed using *STATISCA* version 6.1 software.

Results and Discussion

Total mercury and methylmercury concentrations in fish

Two fish sample sets consisting of 25 and 41 adults were collected from the Reservoir and Downstream stations, respectively. No significant differences were observed between standard length and body weight ($p<0.05$ – Student t test) (Table 2). The sex ratio was similar for the two sample sets (76 and 70% of females). The mean numbers of growth marks on the opercula bones were not statistically different ($p<0.05$ - Mann-Whitney U test), indicating similar mean life span for the two fish samples.

Mean HgT concentrations in dorsal skeletal muscle were ten times higher in fish sampled from downstream : 3.40 ± 0.24 µg g^{-1} compared to 0.32 ± 0.05 µg g^{-1} (dry wt) in the reservoir (Figure 1). In the other organs, similar differences were also observed with ratios of 2.6 for the liver, 6.3 for the gills and 9.8 for the kidneys. No significant differences were observed between males and females ($p<0.05$ - Mann-Whitney U test).

In fish from the reservoir, similar MeHg fractions of HgT were observed in the skeletal muscle, gills and kidneys, close to 80 %. In the liver, only 33 ± 3 % of the metal was in the methylated form (Figure 2). These results are in agreement with numerous data obtained from freshwater or marine fish species. The Hg demethylation which occurs in liver cells, leads to a low MeHg/HgT ratio and inorganic Hg elimination *via* the bile, sometimes with re-absorption through the gut wall [21, 22]. In fish collected from downstream, the MeHg fraction was close to 100% in the skeletal muscle, gills and kidneys, and was 46 ± 14 % in the liver (Figure 2).

Mercury availability

In contrast to Finland and some Canadian hydroelectric systems [4, 23, 24], where fish Hg contamination downstream is less than or equivalent to rates in the reservoir, and in

agreement with data obtained on La Grande 2 Reservoir in North Québec [2], our results on *C. cyprinoides* show very marked differences in Hg accumulation levels in favour of individuals living in the downstream zone.

Mercury accumulation in fish results from the actions and interactions of a large set of abiotic, biotic and contamination factors [10, 12, 21]. Numerous field or experimental studies indicate the predominance of the trophic exposure route: estimations consider that the food uptake for MeHg represents more than 85 % of the total uptake [12, 21, 25]. In combination with exposure conditions, the structural and functional characteristics of the fish, which control uptake mechanisms, storage processes at organ and cell levels and depuration efficiency, also play a key role.

HgT and MeHg concentrations measured in unfiltered and filtered water samples collected within the oxic layer in the reservoir (0-6 m) and downstream on the Sinnamary River are shown in Table 3. For all the different parameters, significantly higher levels were observed downstream. In the dissolved fraction, the ratios between the mean concentrations "Downstream/Reservoir" are 4.9 for HgT and 8.8 for MeHg. These data are in agreement with early results obtained in 1999 and 2001 at the same sites [13]. The anoxic layers of the Petit-Saut hydroelectric reservoir show high dissolved MeHg concentrations up to 0.6 ng L^{-1} (about 30 % of the dissolved HgT concentration), while quite low levels were measured in the oxic superficial layers (0.06 ± 0.03 ng L^{-1}). These anoxic zones are associated to the development of anaerobic bacteria, especially sulfate-reducing bacteria (SRB), considered as the main methylating agents in aquatic systems [26-28]. The four turbines of the hydroelectric power-station which supply the Sinnamary river downstream from the dam are fed with waters from the anoxic layers of the reservoir. This requires the construction of artificial falls to maintain a dissolved oxygen concentration over 2 mg.L^{-1} [29]. Thus the hydroelectric reservoir contributes to a considerable exportation of MeHg downstream. Our measurements show that

approximately 70 % of MeHg is exported in particulate form (> 0.45 µm - Table 3), associated with living microorganisms and detrital organic matter with various minerals.

Differences between Hg concentrations measured in the two fish samples collected in the reservoir and downstream, notably in the skeletal muscle, are in agreement and similar to those observed for MeHg in the dissolved fraction of the water. But, in the present case, two main arguments tend to confirm the weak importance of the direct route of exposure for *C. cyprinoides*. First, several other fish species living in the reservoir and downstream present similar Hg concentrations in the muscle, and this despite the large differences between HgT/MeHg levels in the water. For example, no significant difference was observed between Hg concentrations measured in the omnivorous species *Triportheus rotundatus* of similar body weight and length: [HgT] = 1.8 ± 0.1 and 1.6 ± 0.1 $\mu g.g^{-1}$ (dry wt) from fish collected in the reservoir and the Sinnamary River downstream, respectively. Secondly, our results on the mercury organotropism in *C. cyprinoides* exhibit a distribution, which is typical of a MeHg exposure to the trophic route. In agreement with experimental studies based on a strict control of MeHg uptake from artificially contaminated prey [10, 30, 31], quite low Hg concentrations were determined in gills, which correspond to the main uptake interface for pollutants during exposure *via* the surrounding water. On the other hand, concentrations measured in the skeletal muscle are close to those determined in kidneys (Reservoir and Downstream sites) and liver (Downstream site).

Curimata cyprinoides feeding characteristics

C. cyprinoides from French Guiana is considered to be a benthivorous/omnivorous species, feeding on biofilms (submerged tree trunks, rocks, sediment surface) and associated small benthic invertebrates [18]. Detritivory and omnivory are particularly common foraging modes for tropical freshwater fish, which can be described as opportunist feeders [32]. The environmental changes induced by the construction of the hydroelectric reservoir have led to

severe ecological disturbances, including changes in the alimentary behaviour of *C. cyprinoides* living in the areas upstream and downstream from the dam. No marked differences were observed between the stomach content of the two fish groups. Organic detritus and sand particles represented more than 90% of stomach contents, with small amount of invertebrate carapace debris, in agreement with the detritivorous regime of this species. The origins of organic components in a detritical matrix in the stomach are difficult to identify. Thus, the detritivory and omnivory foraging modes are particularly difficult to define using conventional diet analyses. $\delta^{13}C$ and $\delta^{15}N$ reflect the isotopic composition of ingested food during the fish life, the skeletal muscle being a long-term isotopic food signature integrator [33]. Enrichment in ^{13}C along the food chains is generally small (1‰ between two trophic levels) or not significant. This relative stability in ^{13}C ratio enables us to differentiate between sources of organic carbon: allochthonous versus autochthonous or pelagic versus benthic [34, 35]. In contrast, during nitrogen incorporation, ^{15}N enrichment occurs resulting in a progressive enrichment in $\delta^{15}N$ values of approximately 3-5‰ for each trophic transfer along a food chain [34, 36]. The simultaneous use of C and N isotopes is a useful strategy to reveal feeding links among consumers [34].

Significant differences were observed between C and N isotopes in fish muscles from the two sites ($p<0.05$ - Mann-Whitney U test; Table 4), with a marked decrease for the $\delta^{13}C$ (7.9 ‰) and $\delta^{15}N$ (2.6 ‰) in favour of fish collected downstream. This suggest two different carbon sources at the bottom of the *C. cyprinoides* foodwebs in the reservoir and downstream. The primary producers in the superficial layers of the reservoir are represented by pelagic bacterio-phytoplankton and periphyton communities in the biofilms on the tree trunks of the flooded forest, which represent an important colonization surface since the dam impoundment in 1994: the estimated tree trunk surface in the whole flooded forest area is closed to 3.10^9 m^2. $\delta^{13}C$ determinations on bacterio-phytoplankton samples indicate an average value of -32.5 ±

0.4 ‰ [37], significantly lower than that measured for *C. cyprinoides* from this reservoir site (-28.2 ± 0.8 ‰). On the other hand, $\delta^{13}C$ determinations on biofilms indicate an average value of -27.4 ± 0.9 ‰, very close to the fish muscle value. Downstream , $\delta^{13}C$ in *C. cyprinoides* muscle (-36.1 ± 0.3 ‰) was also similar to the carbon isotope ratio measured on biofilms collected from rocks in the Sinnamary River (-36.3 ± 1.6 ‰), whereas $\delta^{13}C$ in the pelagic organic matter was significantly higher (-33.2 ± 0.4 ‰) [42]. Pigment analysis (Junet and Abril, unpubl.) and microscopic observations, show that biofilms collected on the tree trunks in the reservoir are principally made of *Chlorophyceae*, exhibiting a $\delta^{13}C$ around -28 ‰ [37], associated with *Cyanophyceae* and small invertebrate species. Downstream from the dam, lower $\delta^{13}C$ could be assigned to methanotrophic bacteria from the reservoir and characterized by a very low $\delta^{13}C$, between -40 and -70 ‰ [37, 38]. This effect may be magnified by the presence of chironomid larvae living in biofilms from the downstream zone: their tubes have been shown to act as microsites of intense methanogen methanotroph activity [39]. *Chlorobiacae* are also present, with a $\delta^{13}C$ of around -15 ‰ [37, 40]. Thus the $\delta^{13}C$ characteristics of the biofilms strongly suggest that they represent an essential part of organic carbon input to *C. cyprinoides.* In the superficial layers of the flooded forest zone of the reservoir biofilms consist of endogenous primary producers; downstream in the Sinnamary River, they are based on exogenous organic matter and micro-organisms, mainly from the anoxic layers of the reservoir.

There was a 2.6 ‰ difference of $\delta^{15}N$ in fish muscle from the two sites, suggesting that they differ by one trophic level within their respective foodwebs. $\delta^{15}N$ of biofilms, like $\delta^{13}C$ results, were also different between the two sites: -0.7 ± 0.4 ‰ in the reservoir and -3.1 ± 0.1 ‰ in the downstream zone [37]. These differences could be attributed to biofilm taxonomic composition. In the superficial oxic layers of the reservoir, with low dissolved nitrogen concentrations (< 1 $\mu molN.L^{-1}$), *Cyanophyceae* are able to incorporate an important

part of atmospheric nitrogen, which contributes to negative values of $\delta^{15}N$. Downstream, the organic fraction in the biofilms is mainly based on highly recycled dead organic matter from the microbial loop located near the reservoir oxicline, and also on the living micro-organisms that make up this microbial loop, responsible for important recycling processes in biofilms from the downstream zone. Moreover, artificial falls just below the dam are able to increase atmospheric nitrogen dissolution in the water, leading to a decrease in $\delta^{15}N$ values in micro-organisms.

The marked differences observed between $\delta^{15}N$ in biofilms and fish from the two sampling zones, close to 12 ‰, could be explained by the presence of several intermediary trophic levels [41, 42]. Stomach content analysis reveals the presence of small invertebrate exoskeletons or carapaces, which represent between 5 and 10% of the stomach content. In the reservoir, benthic invertebrate communities associated with biofilms are well developed and composed of different grazer-filter taxa (*Leptophlebiidae* and *Trichoptera* larvae, *Concostracea*), small *Chironomidae* and carnivorous *Odonate* larvae. Due to limiting physical and chemical parameters, the living invertebrate fauna downstream in the river is represented only by small *Chironomidae* larvae, with dead pelagic and benthic invertebrates from the reservoir; no endemic zooplanktonic species are present in the downstream zone up to the Sinnamary estuary. Recent studies on chironomid larvae in German lakes have shown high intraspecific variability for $\delta^{15}N$ values, which can exhibit a range equivalent to five trophic levels [43].

HgT and MeHg means in biofilms were significantly higher in samples collected downstream (Table 5). MeHg concentrations in biofilms which represent 27% and 40% of HgT in the Reservoir and downstream, respectively, were two times higher downstream. In the benthic invertebrates collected, the MeHg concentrations were 2.5 higher downstream and MeHg represented 68 and 88% of HgT in the Reservoir and downstream, respectively.

Differences between MeHg concentrations determined in the food ingested from the two sites are large and could alone explain the differences observed between mercury levels in the fish organs. According to the structural and functional properties of the digestive barrier of fish, it is well known that mercury trophic transfers from ingested food are mainly based on MeHg uptake, with an absorption rate generally higher than 85% [10]. The MeHg transfers between prey and predators are cumulative, with a high storage capacity in the skeletal muscle compartment [10, 12]. Moreover, downstream, the water flow dictates greater swimming activity, whereas physical efforts are more reduced in the Reservoir. For this reason, energy requirements are probably greater downstream ; they necessitate an increase in the quantity of food ingested, all the more so because the organic carbon content in biofilms is lower in the downstream zone (40% against 17% on average – [37]) : fish living in the Sinnamary River would need to ingest more food than those living in the reservoir, increasing the differences between the trophic exposure to MeHg.

Curimatidae, and more especially *C. cyprinoides*, are widely distributed in French Guiana and also in the whole Amazonian basin. Our study clearly shows that this detritivorous/benthivorous species could be an excellent model to investigate the fundamental links between mercury contamination of freshwater systems and anthropogenic impacts, such as artificial reservoir construction, *via* metal trophic transfers from biofilms and benthic invertebrate communities. It could be used in close complementarity with a piscivorous fish species – *Hoplias aimara* or *H. malabaricus* -, as an indicator of methylmercury biomagnification along the foodwebs in the Amazonian basin [44].

Acknowledgments **–** We would like to thank the following: Prof. F.J. Meunier (Museum national d'histoire naturelle, Paris) for assisting in the determination of growth marks on fish opercula; Dr D. Gerdeaux (INRA, Station d'Hydrobiologie lacustre, Thonon, France) for advice on our results on stable isotopes in fish muscle samples; Dr G. Abril and his PhD student A. de Junet (UMR CNRS EPOC, University of Bordeaux 1) for unpublished data on stable isotopes which they generously made available to us. This work was supported by the French National Scientific Research Center (CNRS/PEVS, "Mercury in French Guiana" research programme), the European Union (E.C. Feder funds), the French Ministry of Research (FNS), the French Ministry of the Environment (DIREN Guyane), the Guiana Region and Electricity of France (EDF). We are grateful to authorities in French Guiana for assistance during organization and follow-up of the missions.

References

1. Jackson TA. 1991. Biological and environmental control of mercury accumulation by fish in lakes and reservoirs of Northern Manitoba. *Canada. Can. J. Fish. Aquat. Sci.* **48**: 2449-2470
2. Verdon R, Brouard D, Demers C, Lalumière R, Laperle M, Schetagne R. 1991. Mercury evolution (1978-1988) in fishes of the La Grande hydroelectric complex, Québec, Canada. *Water, Air, Soil Pollut.* **56**: 405-417
3. Porvari P. 1995. Mercury levels of fish in Tucuruí hydroelectric reservoir and in River Mojú in Amazonia, in stata of Pará, Brazil. *Sci. Tot. Environ.* **175**: 109-117.
4. Lucotte M, Schetagne R, Thérien N, Langlois C, Tremblay A. 1999. *Mercury in the biogeochemical cycle: natural environment and hydroelectric reservoirs of northern Québec.* Springer, Berlin, Germany.
5. Lacerda LD, Salomons W. 1998. *Mercury from gold and silver mining: a chemical time bomb?* Springer, Berlin, Germany.
6. Roulet M, Lucotte M, Farella N, Serique G, Coelho H, Sousa Passos C J, Jesus da Silva E, Scavone de Andrade P, Mergler D, Guimaraes JRD, Amorim M. 1999. Effects of recent human colonization on the presence of mercury in Amazonian ecosystems. *Water Air Soil Pollut.* **112**: 297-313.
7. Richard S, Arnoux A, Cerdan P, Reynouard C, Horeau V. 2000. Mercury levels of soils, sediments and fish in French Guiana, South America. *Water, Air, Soil Pollut.* **124**: 221-244.
8. Coquery M, Cossa D, Peretyazhko T, Azemard S, Charlet L. 2003. Methylmercury formation in the anoxic waters of Petit-Saut reservoir (French Guiana) and its spreading in adjacent Sinnamary River. *J. Phys.* **107**: 327-331.

9. Boudou A, Maury-Brachet R, Coquery M, Durrieu G, Cossa D. 2005. Synergic effect of goldmining and damming on mercury contamination in fish. *Environ. Sci. Technol.* **39**: 2448-2454.

10. Boudou A, Ribeyre F. 1997. Mercury in the food web: accumulation and transfer mechanisms. In Sigel A, Sigel H, eds, *Metal ions in biological systems - Mercury and its effects on environment and biology.* Dekker M, New-York, U.S.A., pp 289-320.

11. Morel FMM, Kraepiel AML, Amyot M. 1998. The chemical cycle and bioacculumation of mercury. *Annu. Rev. Ecol. Syst.* **29**: 543-566.

12. Wiener JG, Krabbenhoft DP, Heinz GH, Scheuhammer AM. 2002. Ecotoxicology of mercury. In: Hoffman J, Rattner BA, Burton GA, Cairns J, eds, *Handbook of Ecotoxicology.* CRC Press, New-York, U.S.A., pp 409-463.

13. Coquery M, Cossa D. 1995. Mercury speciation in the surface waters of the North sea. *Neth. J. Sea. Res.* **34**: 245-257.

14. E.P.A (U.S. Environmental Protection Agency). 1999. Method 1631, Revision B: Mercury by oxidation, purge and trap, and cold vapor atomic fluorescence spectrometry.

15. Bloom NS. 1989. Determination of picogram levels of methylmercury by aqueous phase ethylation, followed by cryogenic gas chromatography with cold vapour atomic fluorescence detection. *Can. J. Fish. Aquat. Sci.* **46**: 1131-1140.

16. Horvat M, Liang L, Bloom NS. 1993. Comparison of distillation with other current isolation methods for the determination of methylmercury compound in low levels environmental samples. *Anal. Chim. Acta* **282**: 153-168.

17. Meunier JF, Rojas-Beltran R, Boujard T, Lecomte F. 1994. Rythmes saisonniers de la croissance chez quelques Téléosteens de Guyane française. *Rev. Hydrobiol. Trop.* **27**: 423-440.

18. Merona de B, Vigouroux R, Horeau V. 2003. Changes in food resources and their utilization by fish assemblages in large tropical reservoir in South America (Petit-Saut Dam, French Guiana). *Acta Oecologia* **24**: 147-156.

19. Niro de MJ, Epstein S. 1978. Influence of diet on the distribution of carbon isotopes in animals. *Geochim. Cosmochim. Acta* **42**: 495-506.

20. Jepsen DB, Winemiller KO. 2002. Structure of tropical river food webs revealed by stable isotope ratios. *Oikos* **96**: 46-55.

21. Jackson TA. 1998. Mercury in aquatic ecosystems. In Langston WJ, Bebianno MJ, eds, *Metal Metabolism in Aquatic Environments*. Chapman & Hall, London, U.K., pp 77-158.

22. Loumbourdis NS, Danscher G. 2004. Autometallographic tracing of mercury in frog liver. *Environ. Pollut.* **129**: 299-304.

23. Bodaly RA, St Louis VL, Paterson MJ, Fudge RJP, Hall BD, Rosenberg DM, Rudd J WM. 1997. Bioaccumulation of mercury in the aquatic food chain in newly flooded areas. In Sigel A, Sigel H, eds, *Metal ions in biological systems - Mercury and its effects on environment and biology*. Dekker M, New-York, U.S.A., pp 259-287.

24. Porvari P. 1998. Development of fish mercury concentrations in Finish reservoirs from 1979 to 1994. *Sci. Tot. Environ.* **213**: 279-290.

25. Hall BD, Bodaly RA, Fudge RJP, Rudd JWM, Rosenberg DM. 1997. Food as the dominant pathway of methylmercury uptake by fish. *Water, Air, Soil Pollut.* **100**: 13-24.

26. Gilmour CC, Henry E, Mitchell R. 1992. Sulfate stimulation of mercury methylation in freshwater sediments. *Environ. Sci. Technol.* **26**: 2281-2287.

27. Rudd JWM. 1995. Sources of methylmercury to freshwater ecosystems: a review. *Water, Air, and Soil Pollut.* **80**: 697-713.

28. King JK, Kostka JE, Frisher ME, Saunders FM, Jahnke RA. 2001. A quantitative relationships that's demonstrates mercury methylation rates in marine sediments are based on the community composition and activity of sulfate-reducing bacteria. *Environ. Sci. Technol.* **35**: 2491-2496.

29. Richard S, Arnoux A, Cerdan P. 1997. Evolution in physico-chemical water quality in the reservoir and downstream following the filling of Petit-Saut Dam (French Guiana). *Hydroecol. Appl.* **9**: 57-83.

30. Simon O, Boudou A. 2001. Direct and trophic contamination of the herbivorous carp *Ctenopharyngodon idella* by inorganic mercury and methylmercury. *Ecotoxicol. Environ. Saf.* **50**: 48-59.

31. Gonzalez P, Dominique Y, Massabuau JC, Boudou A, Bourdineaud JP. 2005. Comparative effects of dietary methylmercury on gene expression in liver, skeletal muscle, and brain of the zebrafish (*Danio rerio*). *Environ. Sci. Technol.* **39**: 3972-3980.

32. Planquette P, Keith P, Le Bail PY, 1996. Atlas des poissons d'eau douce de Guyane (tome 1). Collection du Patrimoine Naturel, MNHN (Paris).

33. Heisslein RH, Hallard KA, Ramlal P. 1993. Replacement of sulfur, carbon, and nitrogen in tissue of growing broad whitefish (*Coregonus nasus*) in response to a change in diet traced by $\delta^{34}S$, $\delta^{13}C$, and $\delta^{15}N$. *Can. J. Fish. Aquat. Sci.* **50**: 2071-2076.

34. Peterson BJ. 1999. Stables isotopes as tracers of inorganic matter input and transfert in benthic food webs: a review. *Acta Oecologia* **20**: 479-487.

35. Hobson KA, Fisk A. 2002. A stable isotope ($\delta^{13}C$, $\delta^{15}N$) model for the North Sea Water food web: implications for evaluating trophodynamics and the flow of energy and contaminants. *Deep Sea Res.* **49**: 5131-5150.

36. Cabana G, Rasmussen JB. 1994. Modelling food chain structure and contaminant bioaccumulation using stable nitrogen isotopes. *Nature* **372**: 255-257.

37. Junet de A. 2004. Etude qualitative de la matière organique particulaire dans le réservoir de Petit-Saut (Guyane Française): composition isotopique ($\delta^{13}C$), élémentaire (C/N) et pigmentaire. Master II report, Univ. of Bordeaux 1, France.

38. Boschker HTS, Middelburg JJ. 2002. Stable isotopes and biomarkers in microbial ecology. *FEMS Microbiol. Ecol.* **40**: 85-95.

39. Kajan R, Frenzel P. 1999. The effect of chironomid larvae on production, oxidation and fluxes of methane in a flooded rice soil. *FEMS Microbiol.* **28**: 121-129.

40. Schouten S, Rupstra W, Kok M, Hopmans E, Summons R, Volkan J, Sinninghe Damste J. 2001. Molecular organic tracers of biogeochemical process in a saline meromictic lake (Ace Lake). *Geochim. Cosmochim. Acta* **65**: 1629-1640.

41. Mc Cutchan Jr. JH, Lewis Jr. M, Kendall C, McGrath C. 2003. Variation in trophic shift for stable isotope ratios of carbon, nitrogen, and sulfur. *Oikos* **102**: 378-390.

42. Haubert D, Langel R, Scheu S, Ruess L. 2005. Effects of food quality, starvation and life stage on stable isotope fractionation in Collembola. *Pedobiol.* **49**: 229-237.

43. Grey J, Kelly A, Jones RI. 2004. High intraspecific variability in carbon and nitrogen stable isotope ratios of lake chironomid larvae. *Limnol. Oceanogr*. **49**: 239-244.

44. Durrieu G, Maury-Brachet R, Boudou A. 2005. Golmining and mercury contamination of the piscivorous fish *Hoplias aimara* in French Guiana (Amazon basin). *Ecotox. Environ. Saf.* **60**: 315-323.

Table captions

Sampling Sites	Temp. (°C)	pH	Cond. ($\mu s.cm^{-1}$)	Oxygen ($mg.L^{-1}$)	Oxygen (%)	Turbidity (NTU)	Redox (mV)
Reservoir	29.6 (28-31.9)	5.9 (4.9-6.7)	21.0 (18-30)	4.6 (0-7.6)	60 (0-99)	3.1 (1.7-8.5)	379 (310-441)
Downstream	27.4 (26.8-28.3)	5.5 (4.8-5.9)	28.6 (24-34)	5.7 (4.4-6.6)	73 (70-82)	3.9 (3.4-4.5)	281 (243-321)

Table 1: Physico-chemical characteristics of the water based on monthly measurements during the one year period (March 2002 to March 2003), in the superficial layers (0-6 m) of the Petit-Saut hydroelectric reservoir (Reservoir site) and downstream in the Sinnamary River (Downstream site). Means and minimum-maximum values in brackets.

Sampling Sites	Number of fishes	Sex ratio (% of females)	Body weight (g, wet wt)	Standard length (cm)	Opercula growth marks
Reservoir	25	76	155 ± 45	16.8 ± 1.5	4.8 ± 0.3
Downstream	41	70	136 ± 22	16.5 ± 0.9	5.0 ± 0.5

Table 2: Biometric characteristics, sex ratio and number of growth marks on the opercula bones of the two fish samples collected from the superficial layers (0-6m) of the Petit-Saut hydroelectric reservoir (Reservoir site) and downstream in the Sinnamary River (Downstream site). Means ± standard errors.

Samplin Sites	HgT unfiltered ($ng\ L^{-1}$)	HgT dissolved ($ng\ L^{-1}$)	HgT particulate ($ng\ g^{-1}$, dry wt)	MeHg unfiltered ($ng\ L^{-1}$)	MeHg dissolved ($ng\ L^{-1}$)	MeHg particulate ($ng\ g^{-1}$, dry wt)
Reservoir	0.52 ± 0.07	0.33 ± 0.03	37.2 ± 6.4	0.12 ± 0.02	0.06 ± 0.03	16.1 ± 5.7
Downstream	2.27 ± 1.10	1.62 ± 0.48	66.8 ± 8.9	1.57 ± 0.26	0.53 ± 0.11	64.5 ± 13.3

Table 3: Total mercury (HgT) and methylmercury (MeHg) concentrations in the water from the two sampling sites: the superficial layers (0-6 m) in the Petit-Saut hydroelectric reservoir (Reservoir site) and downstream in the Sinnamary River (Downstream site). Means ± standard errors (n=3).

HgT = inorganic Hg (Hg^0 + Hg^{II}) + organic Hg (including MeHg).

Sampling Sites	Organisms	$\delta^{13}C$ (‰)	$\delta^{15}N$ (‰)
Reservoir	Biofilm	-27.4 ± 0.9	-0.7 ± 0.4
	Fish	-28.2 ± 0.8	11.2 ± 0.4
Downstream	Biofilm	-36.3 ± 1.6	-3.1 ± 0.1
	Fish	-36.1 ± 0.3	8.6 ± 0.3

Table 4 : Carbon and nitrogen stable isotope ratios ($\delta^{13}C$ and $\delta^{15}N$) in biofilms (n = 3) and in the skeletal muscle of *Curimata cyprinoides* (n = 8), from the two sampling sites: the superficial layer (0-6 m) in the Petit-Saut hydroelectric reservoir (Reservoir site) and downstream in the Sinnamary River (Downstream site). Means ± standard errors.

Sampling Sites	Biofilms		Benthic invertebrates	
	HgT (ng g^{-1} dry wt)	MeHg (ng g^{-1} dry wt)	HgT (ng g^{-1} dry wt)	MeHg (ng g^{-1} dry wt)
Reservoir	116 ± 10 (n=10)	32 ± 10 (n=4)	283 (182-391)	192 (124-228)
Downstream	161 ± 14 (n=10)	64 ± 8 (n=4)	574 ± 128 (n=10)	503 ± 342 (n=3)

Table 5: Total mercury (HgT) and methylmercury (MeHg) concentrations measured in biofilms (6 months' colonization on artificial substrates) and in benthic invertebrates collected from the two sites: oxic superficial layers in the flooded forest area in the Petit-Saut hydroelectric reservoir (Reservoir site) and on the Sinnamary River (Downstream site).

Means ± standard errors for Hg determinations in biofilms; means with min-max values for Hg determinations in benthic invertebrate samples of the Reservoir site (5 taxa: *Chironomidae*, *Concostracae*, *Corixidae*, *Leptophlebiidae* and *Trichoptera* larvae) – means ± standard errors for Hg determinations in benthic invertebrate samples from the Downstream site (*Chironomidae* larvae only).

Figure captions

Figure 1: Mean total mercury concentrations in the skeletal dorsal muscle, liver, gills and kidneys of *Curimata cyprinoides* collected from the Petit-Saut hydroelectric reservoir (Reservoir site, n=25) and downstream in the Sinnamary River (Downstream site, n=41).

Bars represent standard errors.

***** : significantly different with $p<0.05$ (Mann-Whitney U test).

Figure 2: Mean percentages of methylmercury (MeHg) with regard to total mercury concentrations (HgT) in the skeletal dorsal muscle, liver, gills and kidneys of *Curimata cyprinoides* collected from the Petit-Saut hydroelectric reservoir (Reservoir site, n=25) and downstream in the Sinnamary River (Downstream site, n=41).

Bars represent standard errors.

***** : significantly different with $p<0.05$ (Mann-Whitney U test).

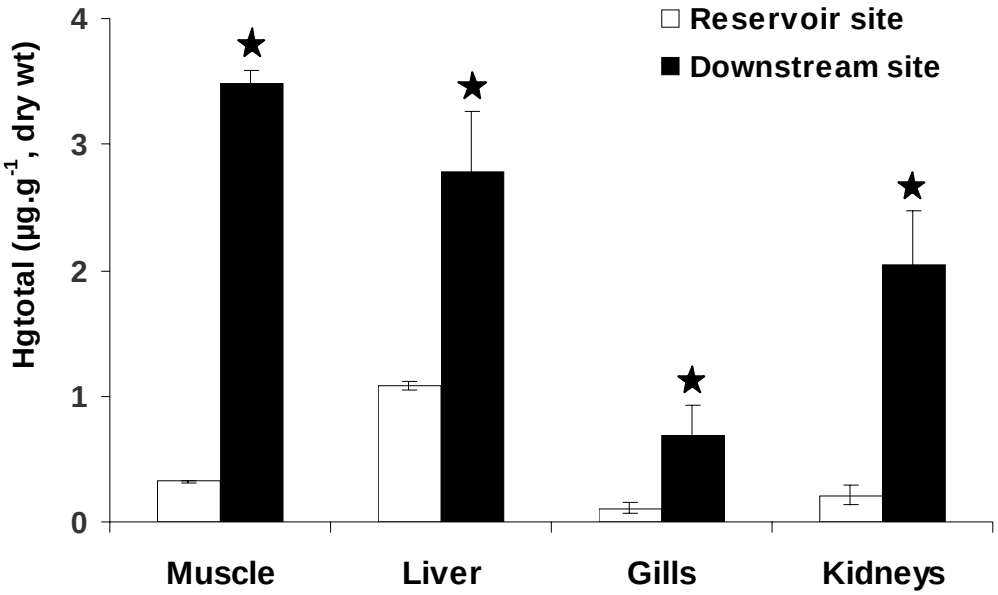
Reservoir site
Downstream site
Hgtotal (µg.g-1, dry wt)
4
3
2
1
0
Muscle
Liver
Gills
Kidneys

Fig. 1

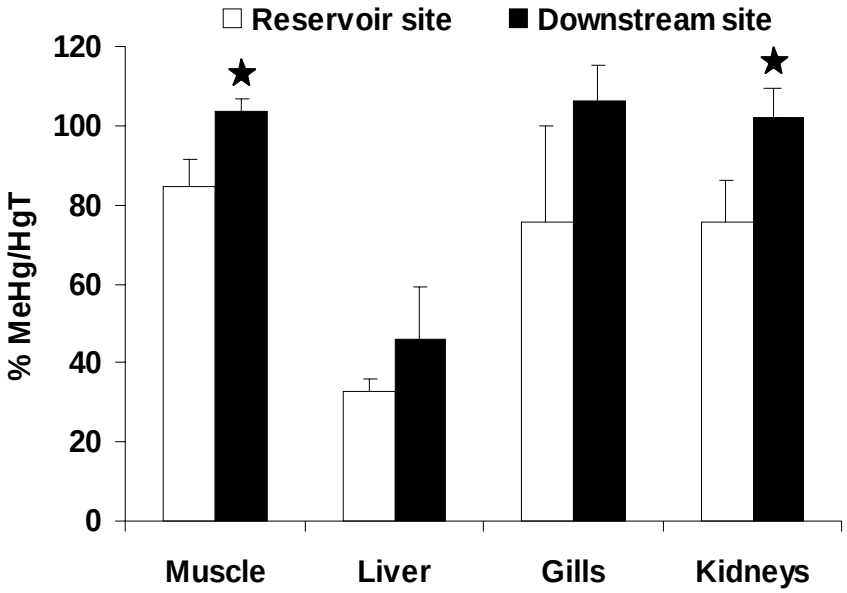
Reservoir site
Downstream site
% MeHg/HgT
120
100
80
60
40
20
0
Muscle
Liver
Gills
Kidneys

Fig. 2

Available online at www.sciencedirect.com
SCIENCE DIRECT®
Science of the Total Environment xx (2005) xxx–xxx
Science of the Total Environment
An International Journal for Scientific Research into the Environment and its Relationship with Humankind
www.elsevier.com/locate/scitotenv

Formation of dissolved gaseous mercury in a tropical lake (Petit-Saut reservoir, French Guiana)

T. Peretyazhko [a,*], L. Charlet [a], B. Muresan [b], V. Kazimirov [c], D. Cossa [b]

[a] *Observatory of Earth and Planetary Sciences (OSUG), University of Grenoble-1, F.38041 Grenoble, France*
[b] *Institut Français de Recherche pour l'Exploitation de la Mer, BP 21105, F.44311 Nantes, Cedex 3, France*
[c] *Chemical Department of Kiev Taras Shevchenko University, Kiev, Ukraine*

Received 7 October 2004; accepted 16 June 2005

Abstract

Formation of dissolved gaseous mercury (DGM) and its volatilization from aquatic systems can be considered as a natural attenuation process, which limits the methylation of mercury (Hg) and Hg accumulation in fish. Although gold-mining activity and erosion of tropical soils lead to increased Hg concentration in aquatic systems, little is known about DGM production and distribution in tropical aqueous systems. Our work explores the vertical distribution and principal sources of DGM in a meromictic Amazonian reservoir. Dissolved gaseous mercury measurements carried out in Petit-Saut reservoir (French Guiana, South America) revealed DGM increase in the surface waters and at the bottom layers of the reservoir during the dry season. As in arctic and temperate lakes, high DGM concentrations in surface waters were attributed to sunlight-mediated photochemical processes. Dissolved gaseous mercury concentrations in the anaerobic hypolimnion were larger than in temperate or arctic lakes. In order to elucidate Hg(II) reduction pathways in the bottom layer of tropical reservoir, laboratory Hg(II) reduction experiments were performed with anoxic aqueous suspensions of surface sediments either untreated or treated by γ-ray and NaN_3. Our results indicated that DGM production at the bottom layer of Petit-Saut reservoir was biologically mediated. Dissolved gaseous mercury formation rates in the surface sediment suspensions were of the same order of magnitude as formation rates in freshwater lakes reported in literature.

Keywords: Dissolved gaseous mercury; DGM; Petit-Saut reservoir; Reduction

1. Introduction

In natural waters, mercury is distributed among several chemical forms including dissolved gaseous mercury [DGM], a number of inorganic divalent mercury(II) species and organic mercury, chiefly methylmercury [CH_3Hg^+] (Morel et al., 1998). Dissolved

* Corresponding author. Current address. Ecosystem Science Division, Hilgard Hall 246, University of California, Berkeley, CA 94720-3110, USA. Tel: +1 510 643 9951; fax: +1 510 643 2940.
E-mail address: tperetya@nature.berkeley.edu (T. Peretyazhko).

0048-9697/$ - see front matter © 2005 Elsevier B.V. All rights reserved.
doi:10.1016/j.scitotenv.2005.06.016

gaseous mercury is composed primarily of elemental mercury [Hg(0)] (Vandal et al., 1991; Zhang and Lindberg, 2001; Tseng et al., 2004) which plays an important role in the environmental mercury cycle. It represents nearly 95% of the atmospheric mercury, while DGM account for only 10% to 50% of the total dissolved mercury in aquatic systems (Kim and Fitzgerald, 1986; Vandal et al., 1991; Fitzgerald and Mason, 1994). The formation of DGM can favor the removal of mercury from the natural system, as it can escape to the atmosphere. The volatilization of mercury reduces the Hg burden in surface waters and soils (e.g., Peretyazhko, 2002) and can be considered a natural attenuation process, which limits the methylmercury production and accumulation in fish (Nriagu, 1994). In tropical environments, gold-mining activity (Pfeiffer and Lacerda, 1988) and erosion of tropical soils (Roulet et al., 1999) lead to increase in mercury concentration, including methylmercury, in aquatic systems (Peretyazhko et al., 2005). However, little is known about DGM production and distribution in tropical aqueous systems. Thus, identification of mechanisms of DGM formation is important in study of Hg cycling in tropical ecosystems.

The processes involved in the production of DGM in natural waters are still subject of debate. In general, two types of reduction are considered: biotic and abiotic processes. Various abiotic photochemical reactions are responsible for DGM production in surface waters of temperate, arctic or tropical lakes (Amyot et al., 1997b,c; Beucher et al., 2002; Tseng et al., 2004). They may include direct photolysis, photoreduction involving inorganic particles [e.g., Fe(III) and Mn(IV) (hydr)oxides] or organic matter (Nriagu, 1994; Amyot et al., 1997b; Zhang and Lindberg, 2001). Biotic reduction by phytoplankton and microbial communities may also play a significant part as demonstrated under laboratory and field conditions (Barkay et al., 1989; Mason et al., 1995). In anoxic waters mercury can be reduced by microorganisms (Baldi, 1997; Morel et al., 1998), Fe(II) in presence of mineral particles (Charlet et al., 2002) or organic matter (Allard and Arsenie, 1991). Little information is available on in situ Hg(II) reduction in anoxic waters.

The objectives of our work were to study vertical distribution and principal sources of DGM in a tropical lake. Dissolved gaseous mercury measurements carried out in Petit-Saut reservoir, French Guiana, South America, demonstrated that DGM production was more intensive in the anoxic bottom layer during the dry season. Laboratory experiments with surface sediments were designed to elucidate Hg(II) reduction pathways (i.e., biotic vs. abiotic) and to determine reduction rates in anoxic conditions.

2. Materials and methods

2.1. Study site

Reservoir Petit-Saut is located on the Sinnamary River, French Guiana, South America. The construction of the dam took place from 1989 to 1995. The reservoir covers 80 km of the Sinnamary River course, flooding 360 km^2 of uncleared tropical rainforest with at the most 35 m of water. At the times of sampling in 1999, dead tree trunks were still emergent from the water. The total water volume stored is 3.5 10^9 m^3, the mean annual river inflow is 260 m^3 s^{-1} and the average residence time of water in the reservoir is about 5 months (Galy-Lacaux et al., 1997).

Water samples were taken at two sites (Fig. 1): Roche Genipa (N4°56′474″, W53°02′468″) and Saint Eugene (N4°51′250″, W53°04′155″). Roche Genipa site is situated in the deepest, central part of the reservoir (up to 35 m depth), along the former Sinnamary River bed, while Saint Eugene is in a lateral branch of the lake, where the depth of the lake column is only 18 to 20 m depending on the season. At the time of sampling the depths of the water column were 27 and 18 m at Roche Genipa and Saint Eugene sites, respectively.

Sampling was performed in December (end of dry season) 1999. For laboratory experiments on DGM production surface sediments and near-bottom water were collected at Roche Genipa sampling site in October 2000 (dry season).

Vertical distributions of temperature, pH and dissolved oxygen measured at Roche Genipa and Saint Eugene sampling sites are summarized in Fig. 2. Vertical profiles of temperature show a 3–5 m thick, well-mixed epilimnion overlying a thermocline, which extends down to 16 m at Roche Genipa sampling site, below and down to 27 m depth the temperature is constant (Fig. 2a). At Saint Eugene sampling site temperature drops gradually from

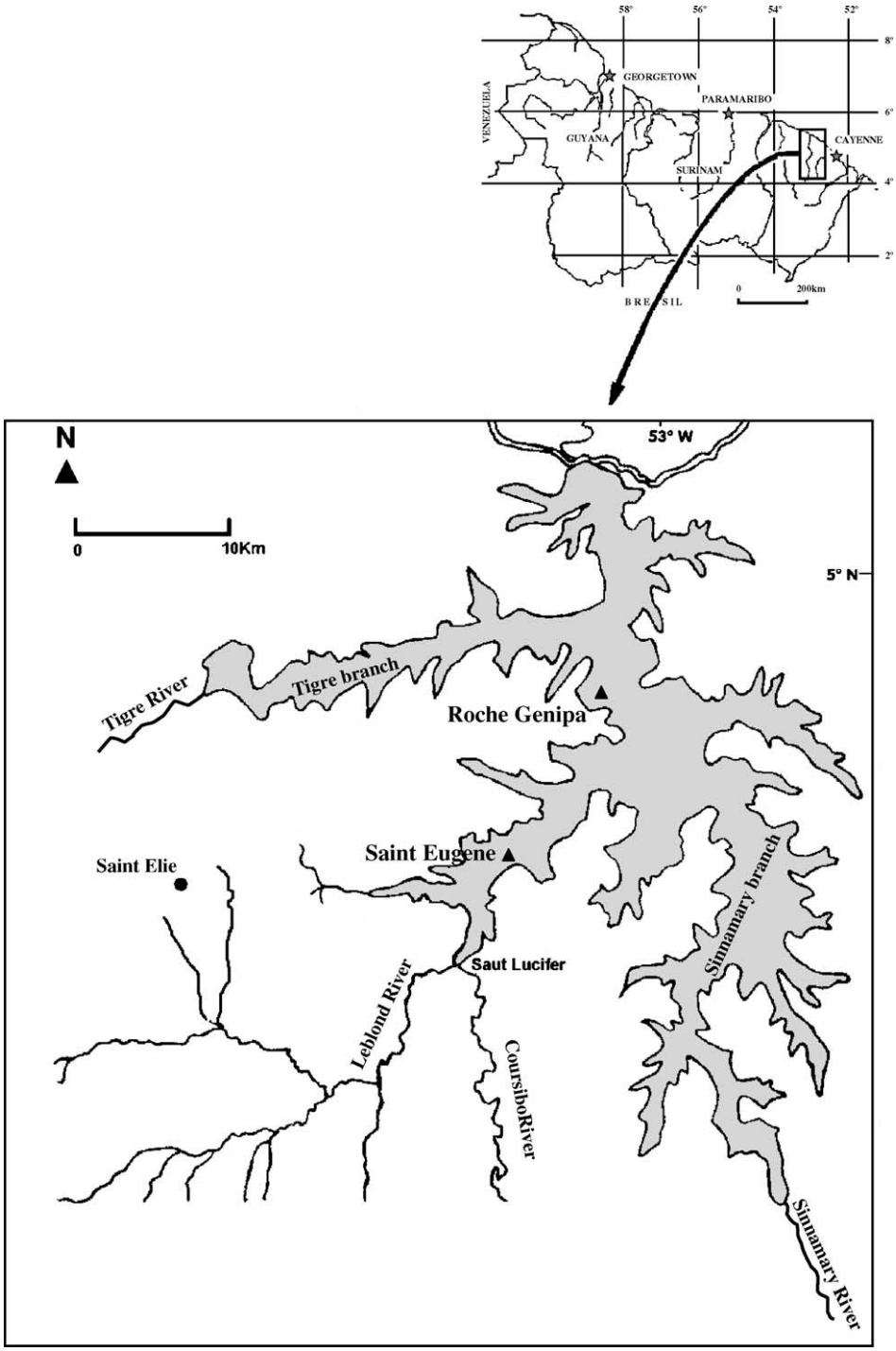

Fig. 1. Petit-Saut reservoir, French Guiana. The map shows the sampling sites, Roche Genipa and Saint Eugene, as well as the locations of the gold mining operation of Saint Elie. The dam is located at the northernmost end of the lake.

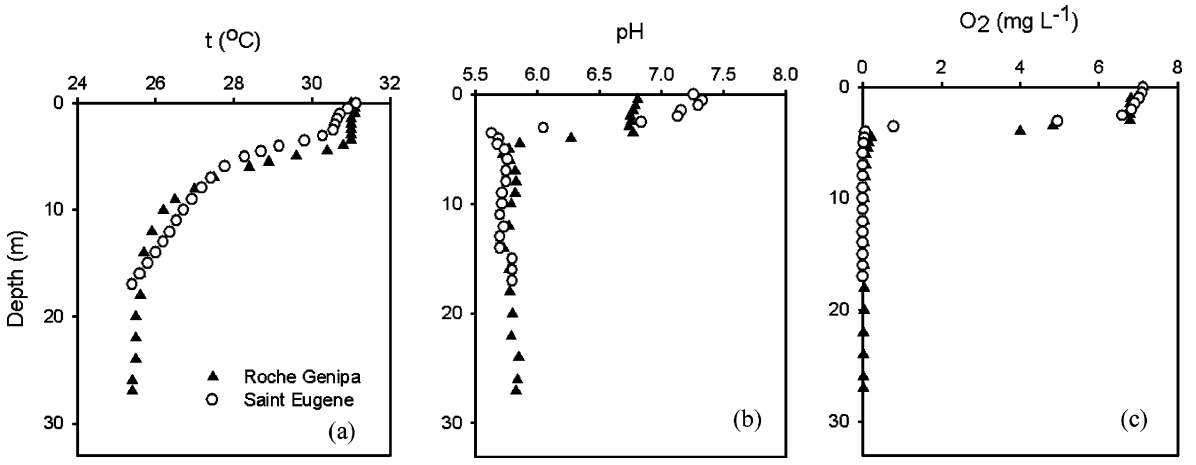

Fig. 2. Vertical profiles of (a) temperature, (b) pH and (c) dissolved O_2 at Roche Genipa and Saint Eugene sampling sites measured during the dry season.

~31 °C (4 m) to 25.5 °C (18 m, Fig. 2a). The surface waters are fully oxygenated: the epilimnion is saturated with respect to O_2 (~7 mg L^{-1}) at both sites. Below the epilimnion, the O_2 concentration decreases sharply to below detection limit over depth intervals of about 1.5 to 2 m at Roche Genipa site and 3.5 m at Saint Eugene site. The drop in O_2 is accompanied by a decrease of pH (Fig. 2b), due to the release of protons by oxygen reduction coupled to the oxidation of organic compounds and inorganic reduced species (van Cappellen and Wang, 1996).

Possible localized sources of mercury to the Petit-Saut reservoir include the flooded soils, the upstream Saint Elie gold-mining area (Fig. 1) as well as the impounded former mining site "Adieu Vat", located near the Roche Genipa sampling site (Charlet and Boudou, 2002; Charlet and Peretyashko, 2003). Mercury concentrations measured during the dry season (December 1999) in Petit-Saut reservoir are summarized in Table 1. More details on mercury biogeochemistry in the tropical lake can be found in Coquery et al. (2003) and Peretyazhko et al. (2005). In this paper we present DGM measurements in water columns performed in December 1999 (end of dry season). Unfortunately, we were not able to measure DGM vertical distributions during wet season as the detector was working unstable due to tropical humid conditions.

2.2. Sampling and analysis

Bulk water samples were collected using an ultra-clean Teflon pumping system, including an all-Teflon diaphragm pump and Teflon tubing. Non-filtered water samples for DGM analysis were transferred into 500-mL Teflon (FEP) bottles, sealed in double polyethylene bags and stored at 4 °C in the dark. All Teflon and plastic ware was washed and stored following ultra-clean procedures (Coquery and Cossa, 1995). Surface sediments were collected with the Eckman dredge and stored in plastic bags, transported and kept at +4 °C until the use in experiments on DGM production. The experiments were performed within one month after sampling.

Table 1
Mercury concentrations in Petit-Saut reservoir measured in December 1999 (end of dry season)

	HgT dissolved[a] (pmol L^{-1})	HgT particulate[a] (pmol L^{-1})	Hg reactive[b] (pmol L^{-1})	CH_3Hg^+ dissolved[a] (pmol L^{-1})
Petit-Saut reservoir (surface waters)	3–19	1–14	0.5–0.9	0.11 ± 0.05
Roche Genipa (>10 m)	18 ± 2	1.1 ± 0.5	1.6 ± 0.2	2.8 ± 0.7

[a] Coquery et al., 2003; [b] Peretyazhko et al., 2005.

Dissolved gaseous mercury was analyzed in the field (along the shore) using cold vapor atomic fluorescence spectroscopy (CVAFS) within 4–5 h after sampling in the field laboratory. A ~250 mL filtered water sample (a precise volume was determined after DGM measurements) was purged for 20 min with ultra pure Ar at 250 mL min^{-1} and DGM concentration was determined after gold amalgamation. Blank was 70 fmol L^{-1} and detection limit [defined as three times the standard deviation of the blank] was 50 fmol L^{-1}. The values of blank and of successive blank measurements were reproducible (variability of the blanks was less than 5%) which let us conclude that sampling time and Ar flow rate were appropriate to remove all DGM from solution.

The saturation index (S.I.) for DGM in the lake relative to equilibrium with Hg(0) in the atmosphere (DGM is mainly Hg(0), Vandal et al., 1991; Zhang and Lindberg, 2001; Tseng et al., 2004) was determined by the following equation

$$\text{S.I.} = \frac{C_w \times H}{C_g} \times 100 \quad (1)$$

where C_w and C_g are concentrations of Hg(0) in the lake water (mol L^{-1}) and air (mol L^{-1}), respectively, and H is the dimensionless Henry's law constant for Hg(0), $Hg(0)_g/Hg(0)_{aq}$, corrected to ambient temperature (Samemasa, 1975). The atmosphere average Hg(0) concentration was about 7.5 pmol m^{-3} (Amouroux et al., 1999).

2.3. Laboratory study of DGM production in aqueous suspensions of surface sediments

2.3.1. Chemicals

All chemicals were of analytical grade and were used without further purification. Polyethylene gloves were worn for Hg(II) solution preparation and during the reduction experiments. A 5 mmol L^{-1} Hg(II) stock solution was prepared from $HgCl_2$ (J.T. Baker) in 10% (v/v) ultrapure HNO_3 (Suprapur, Merck) in 250-mL Teflon (FEP) bottle. The bottle was sealed in double polyethylene bags and stored in a refrigerator. The stock solution could be kept for several months. A fresh 2.5 μmol L^{-1} initial Hg(II) solution was prepared from the stock solution (5 mmol L^{-1}) in 4% (v/v) ultrapure HNO_3 before each experiment. A 10% NaN_3 solution was prepared from NaN_3 (Fisher). A 0.1 mol L^{-1} reagent grade MOPS buffer solution (3-(*N*-morpholino) propanesulfonic acid, Fisher) was titrated to pH 7 with 1 mol L^{-1} NaOH. A pH electrode (VWR, Symphony electrode) was calibrated using pH 4 and 7 buffers (Fisher). All solutions were prepared with high purity 18 MΩ cm^{-1} water (Milli-Q, Millipore). Argon gas (ultra high purity grade) was used to deoxygenate sediment suspensions and in DGM measurements. The sediment suspensions were kept in a glove box (Coy Laboratory Products Inc., Model A) containing a mixed gas atmosphere (85%N_2, 15% CO_2, 5% H_2). Black Teflon bottles (250 mL, FEP) previously acid washed according to Coquery and Cossa (1995) procedure, were used in order to avoid light penetration and possible Hg(II) photoreduction (Amyot et al., 1994; Amyot et al., 1997c).

2.3.2. Reduction experiments

Ten grams of undried surface sediments (2.7 g air-dry basis) were added in a black Teflon bottle to 150 mL water sampled at Roche Genipa site. The pH value was adjusted to 6 by addition of 0.1 M MOPS solution. This pH value was chosen as it is close to the pH measured in the bottom waters of the tropical reservoir (Fig. 2b). The final solid concentration was 18 g L^{-1}. Argon gas was passed overnight through the suspension to eliminate traces of dissolved oxygen. The suspensions were kept for a week in a glove box at 23–25 °C to allow development of anoxic conditions.

Some sediment samples (and necessary solutions) were exposed to γ-ray irradiation (25 kGy) for 24 h in order to sterilize the samples. Suspensions were then prepared according to the same procedure as described above. A solution of NaN_3 was added to each suspension in order to stop any residual bacterial activity (1% final concentration, A. Leverman, pers. communication). The NaN_3 solution was analyzed for total dissolved mercury content, which was about 5.5 ± 0.9 pmol L^{-1}.

After the week incubation time in the glove box, the suspension pH value was between 5.8 and 6. Our preliminary experiments demonstrated that pH did not change after addition of the acidified Hg(II) solution and remained constant until the end of the reduction experiments due to the presence of MOPS buffer. Without MOPS pH decreased by 3 to 4 pH units

when Hg(II) solution was added. Each Teflon bottle with sediment suspension was then connected to an acid washed Teflon bubbler to purge all aqueous DGM out of solution. Several blanks were then determined by passing a mercury-free Ar gas through sediment suspension for 20 min at a flow rate of 250 mL min^{-1}. The DGM concentration was never larger than 110 fmol L^{-1}. The experiment was initiated with the addition of aliquots of 2.5 μmol L^{-1} Hg(II) or 5 mmol L^{-1} Hg(II) solution to the suspension ($t=0$ min) to obtain initial Hg(II) concentrations of 2.5, 4.4 or 250 nmol L^{-1}. It should be noted, when picomolar concentration levels of Hg(II). were added, no DGM production was observed (i.e., DGM was below the detection limit). This is likely due to Hg(II) adsorption to sediment particles at these low concentration levels. Dissolved gaseous mercury produced was measured by CVAFS method with Tekran 2500 detector. Production of DGM was measured regularly during the first three–four hours. Our preliminary experiments demonstrated that the most intensive DGM production occurred in the first hours of the reaction, after what, the DGM produced steadily decreased with time. At selected times DGM purged out of the Teflon bottle, was trapped on the gold trap, released by heating the gold trap to 500 °C during one minute and finally detected by CVAFS. Preliminary experiments on DGM production were performed with water samples collected from the anoxic layer of the lake. We detected an increase in DGM production up to 6.4 pmol L^{-1} during 4-h anaerobic incubation in dark conditions (Fig. 3). Therefore, the results on DGM production in sediment suspensions at each time point were corrected by subtracting the DGM concentration produced in water samples from the DGM concentrations measured in sediment suspensions.

3. Results and discussion

3.1. DGM distribution in Petit-Saut reservoir

By the end of dry season (December 1999), DGM concentrations were 200 and 270 fmol L^{-1} near the water/air interface at Roche Genipa and Saint Eugene sampling sites, respectively (Fig. 4, Table 2). During the wet season, average surface DGM concentration reached 979 ± 50 fmol L^{-1} (S.I. 2937%, June 1998) as demonstrated by Amouroux et al. (1999). We compared DGM distribution in the stratified Petit-Saut tropical reservoir with those reported for temperate and arctic lakes (Table 2). In general, in lakes under temperate and arctic climate DGM maximum

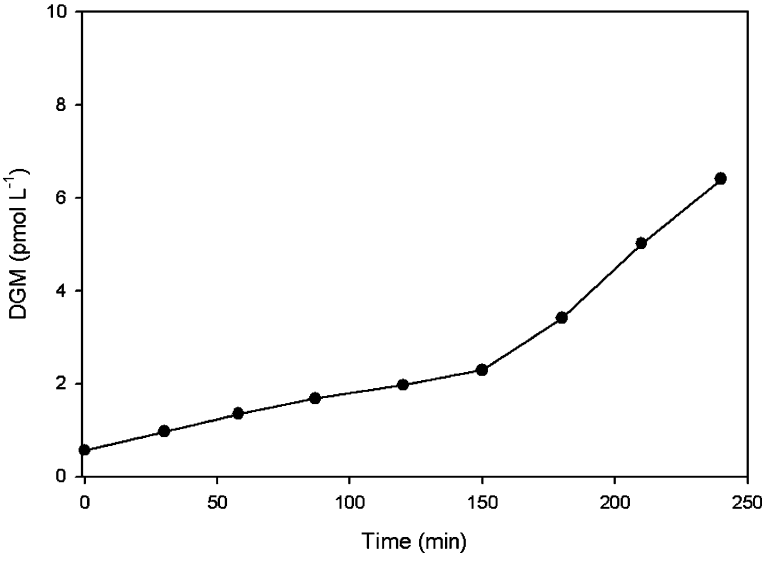

Fig. 3. Cumulated DGM production in an aqueous sample from the anoxic layer of Petit-Saut reservoir. Anoxic water sample was kept in dark, Ar gas was used to purge DGM produced.

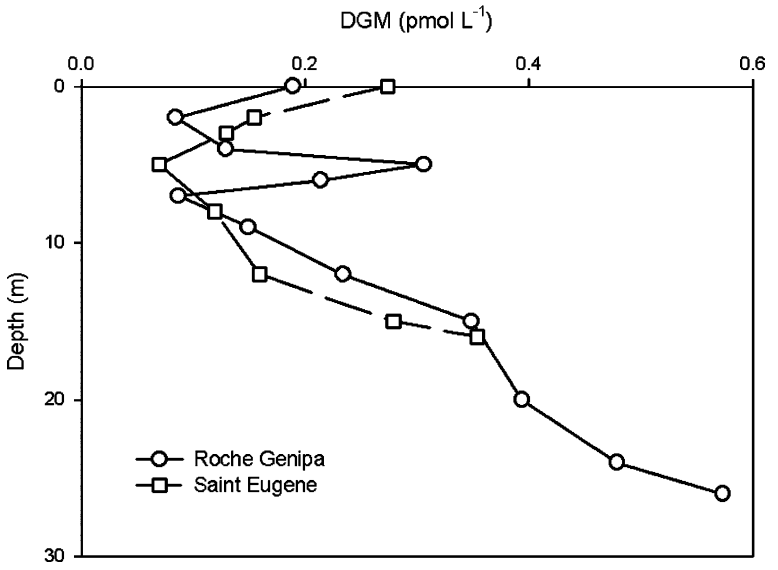

Fig. 4. Vertical profiles of dissolved gaseous mercury (DGM) measured during the dry season.

concentrations were detected in surface waters [Table 2, (Amyot et al., 1997c; Tseng et al., 2004)]. Saturation index in the Petit Saut surface waters were of the same order of magnitude as in temperate and arctic lake waters suggesting similar mechanisms of DGM production. In surface waters, DGM production has been shown to be due to sunlight-mediated photochemical processes (Amyot et al., 1994; Nriagu, 1994; Mason et al., 1995; Xiao et al., 1995; Amyot et al., 1997c; Zhang and Lindberg, 2001; Tseng et al., 2004). Laboratory studies with surface waters collected form the Petit-Saut reservoir further demonstrated that DGM was produced by photoreduction processes (Beucher et al., 2002). The Hg(II) reduction was related to the availability of organic matter, presented at relatively high concentrations (8–10 mg L^{-1}, Peretyazhko et al., 2005), and, consequently, to mercury complexation by DOC.

A DGM concentration peak of 310 fmol L^{-1} at the oxycline was observed at the Roche Genipa site in December (Fig. 2c, 4). This peak might be due to an increased bacterial activity at the oxic/anoxic interface (Amyot et al., 1997c). In fact a maximum of bacteria concentration level was found exactly in this layer in Petit-Saut reservoir in dry season (Dumestre et al., 1997).

Vertical DGM concentration profiles had maximum concentrations of 570 and 350 fmol L^{-1} in the bottom layer at Roche Genipa and Saint Eugene sampling sites, respectively (Fig. 4). In the water column DGM concentrations decreased continuously upwards down to 90 and 70 fmol L^{-1} below the oxycline, i.e., at 7 m (Roche Genipa site) and 5 m (Saint Eugene site), respectively. Vertical profiles of S.I. demonstrated that the waters were all supersaturated with respect to DGM, for both sites at all depths in dry season. Moreover, S.I. was higher in the anoxic bottom layer than in the surface waters (Table 2). In some temperate lakes, DGM levels increased with depth and the presence of high DGM concentrations at the bottom layer might be attributed to both inflow of Hg-enriched waters from nearby contamination sources (Lake Ontario, Amyot et al., 2000) and biological or nonphotochemical abiotic Hg(II) reduction (Lake Ontario, Lake Erie, Lake 658, Amyot et al., 1997c; Amyot et al., 2000; Poulain et al., 2004). Development of the anaerobic conditions might be an important factor in DGM production. As shown by Poulain et al. (2004), DGM concentrations negatively correlated with O_2 level at the sediment–water interface and increased when O_2 dropped below 0.01 mg L^{-1}. In the tropical reservoir dissolved mercury concentration in the inflow rivers was lower than in hypolimnion (Coquery et al., 2003). During the dry season, the O_2 concentration was below detection limit below 2 m at Roche Genipa site and 3.5 m at

Table 2
Levels of DGM concentration and saturation indices (S.I.) in arctic, temperate and tropical lakes

	DGM (fmol L^{-1})[a]	S.I. (%)[b]	t (°C)
Arctic lakes			
Alaskan lakes[f]	ep[c]: 100–230	300–800	12–15
	met[d]: 40–150	180–500	5–15
	hyp[e]: ≈70	≈250	4–5
Canadian lakes[g]	ep: 290–160	115–187	1–3
Temperate lakes			
Palette Lake, USA[h]	ep: 120	360	2
	met: 120	360	2.8
	hyp: 150	460	3
Palette Lake, USA[h]	ep: 260–350	930–1180	19.5
	met: 60	140	6
	hyp: 75	170	6
Lake Ontario[j]	ep: 360–370	1430	22
	met: 480	1340–1880	10–22
	hyp: 480	1270	8–10
Lake Ontario[j]	ep: ≈650	2250	17.4
	met: ≈990	2770–3420	10–17.4
	hyp: 1280	3590	10
Lake Erie (Canada)[k]	ep: 180–200	515–573	21
	met: 296–330	690–870	10–22
	hyp: 100–120	210–250	10
Forested lakes (Canada)[k]	ep: 270–360		22
	met: 100–200		10–22
	hyp: 19–75		10
Boreal Lake 658[l]	ep: 400–1500		20–25
	met: 0–1300		5–25
	bl[m]: 0–300		5–10
Tropical lake			
Petit-Saut reservoir[n]	ep: 190–270	664–915	31
	met: 70–310	430–876	25.5–31
	hyp: 260–400	1143–1742	25.4
	bl: 350–570	1522–2453	25.4

[a] DGM: dissolved gaseous mercury; [b] S.I.: saturation index; [c] ep: epilimnion; [d] met: metalimnion; [e] hyp: hypolimnion; [f] Tseng et al., 2004; [g] Amyot et al., 1997b; [h] Vandal et al., 1991; [j] Amyot et al., 2000; [k] Amyot et al., 1997c; [l] Poulain et al., 2004; [m] bl: bottom layer; [n] measured in December 1999 (dry season).

Saint Eugene site (Fig. 2c). Thus, we suggested that DGM was produced in situ, i.e., in anoxic hypolimnion. This production was more intensive in the anoxic bottom layer, where sediments appeared to be a major source of DGM in Petit-Saut reservoir (Table 2). Dissolved gaseous mercury concentrations found at the bottom layer were larger than in temperate or arctic lakes, except Lake Ontario (Amyot et al., 2000, Table 2). However, in Lake Ontario, together with in situ production, large DGM concentrations are due to inflow of Hg-enriched waters from nearby contamination sources. We suggest that besides anoxic conditions, temperature difference between arctic, temperate and tropical lakes, i.e., a difference in reaction kinetics, might also be responsible for the intensive DGM production in the bottom layer of the stratified tropical lake. Thus, average temperature in temperate or arctic lake hypolimnion was 2 to 10 °C whereas it was ~25 °C in Petit-Saut lake hypolimnion (Table 2). It was shown that higher temperature enhances methylation processes due to its effect on microbial activity (Ullrich et al., 2001). We suggest that at the same time DGM production also becomes an important process limiting the methylmercury production. Other factors, however, like differences in mineralogy, organic matter content and microorganism population may also affect DGM production. Measurements of DGM and physico-chemical parameters in other tropical freshwater systems should be carried out in order to determine principal parameters controlling DGM production.

3.2. DGM production at water/surface sediments interface

The mechanisms of DGM production occurring at the bottom layer of Petit-Saut reservoir were studied in laboratory with water collected from bottom layer and surface sediments.

By the end of experiment 3.2%, 0.67% and 0.52% of the initially added Hg(II) (250, 4.4 and 2.5 nmol L^{-1}, respectively) were transformed to DGM in the aqueous suspensions of surface sediments (Fig. 5). These results demonstrated that the amount of DGM produced depended on the initial spiked Hg(II) concentration and decreased with decrease of Hg(II) input. Our data could be fitted satisfactory well by both first- and second-order kinetics indicating the complex nature of the process. The same phenomenon has been observed by Zhang and Lindberg (2001) in the Fe(III)-enhanced photochemical Hg(II) reduction. Since no information was available on the nature and concentration of the reductant, a pseudo-first-order kinetics was assumed. The values of first-order rate constants and values of half-time were summarized in Table 3. Dissolved gaseous mercury formation rates in surface sediment suspensions were of the same order of magnitude as

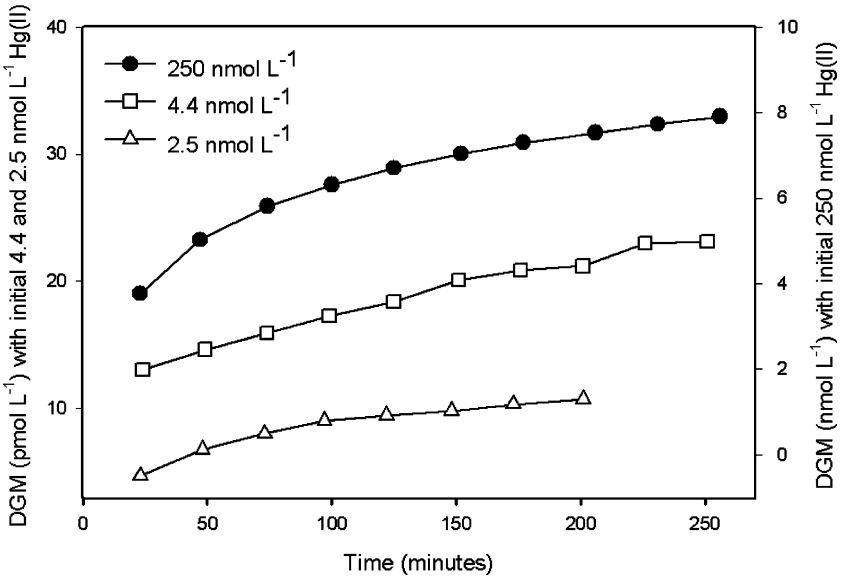

Fig. 5. Cumulated DGM production in aqueous suspension of untreated surface sediment with three initial Hg(II) concentrations.

rate constants observed for freshwater lake samples (Vandal et al., 1995; Mason et al., 1995). Mass balance calculations and laboratory reduction experiments with various microorganisms demonstrated the rates of DGM formation in the range between $3 \cdot 10^{-6}$ and $18 \cdot 10^{-5}$ min^{-1} (Table 4).

Production of gaseous mercury in suspensions, pretreated by gamma-rays irradiation and NaN_3, was only observed for the highest Hg(II) concentration (Fig. 6), i.e., for a 250 nmol L^{-1}. The total DGM produced never exceeded 20 pmol L^{-1} after a 2.5 h reaction time, a value 400 times lower than the DGM concentration recorded after reaction with untreated sediment. The observed rate constant for a sterilized sample is two orders of magnitude lower ($1 \cdot 10^{-7}$ min^{-1}) than for the corresponding non-sterilized sample.

The contrast between experiments run with sterilized sediments and raw sediments indicates that the Hg(II) reduction in the dark in anoxic surface sediment suspensions is a biologically mediated phenomenon. According to the laboratory results we can conclude that at the bottom layer of the tropical stratified reservoir Petit-Saut, the DGM formation mechanism is a biotically induced mechanism. It should be noted that Hg(II) concentrations used in the reduction experiment were larger than levels of Hg(II) concentrations in Petit-Saut reservoir (Table 1) since we were not able to detect DGM production when picomolar concentrations of Hg(II) were added.

Table 3
Observed first-order rate constants, k_{obs}, and half-time of DGM production in aqueous suspensions of surface sediments

$Hg(II)_{initial}$ (nmol L^{-1})	k_{obs} (R^2)[c] (min^{-1})	$t_{1/2}$ (days)
250[a]	$6 \cdot 10^{-5}$ (0.89)	8
250[b]	$1 \cdot 10^{-7}$ (0.86)	4814
4.4[b]	$1 \cdot 10^{-5}$ (0.98)	48
2.5[b]	$1 \cdot 10^{-5}$ (0.89)	48

[a] Untreated surface sediment suspension; [b] surface sediment suspension treated by γ-ray and NaN_3 (1%); [c] observed first-order rate constants obtained from linear regression of $\ln([Hg(II)]_{initial} - [DGM]_t)$ vs. time; R^2 is the coefficient of determination.

Table 4
Observed first-order rate constants reported for various aquatic environments

	k_{obs} (min^{-1})
Pallette Lake, USA[a]	
Epilimnion (1–3m)	$6 \cdot 10^{-6}$–$17.4 \cdot 10^{-5}$
Metalimnion (9m)	$2.7 \cdot 10^{-5}$–$4 \cdot 10^{-5}$
Heat sterilized	$7.2 \cdot 10^{-6}$–$1.2 \cdot 10^{-5}$
Marine microorganisms[b]	$2.8 \cdot 10^{-6}$–$6.7 \cdot 10^{-5}$
Upper Mystic Lake, USA[b]	
surface waters	$4.9 \cdot 10^{-6}$–$3.7 \cdot 10^{-5}$

[a] Vandal et al., 1995; [b] Mason et al., 1995.

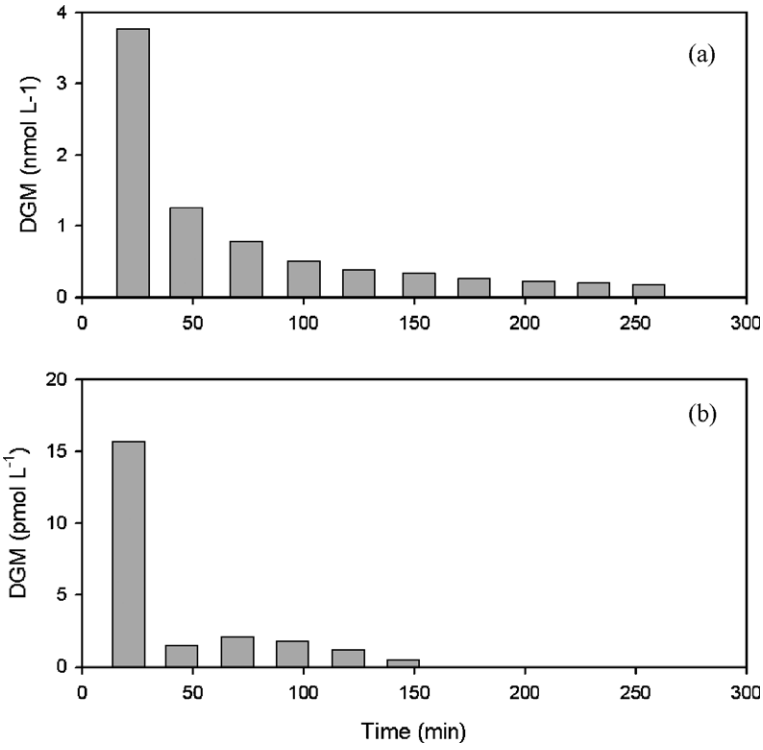

Fig. 6. Dissolved gaseous mercury concentration in surface sediment suspensions initially spiked with 250 nmol L^{-1} Hg(II) (a) untreated and (b) γ-ray and NaN_3 treated.

However, the Hg(II) concentration added was below the minimum inhibitory concentration (MIC, the greatest concentration at which bacteria can grow), which ranges from 0.005 to 0.1 mmol L^{-1} (Hassen et al., 1998). Addition of the amounts of Hg(II) from 0.1 to 9 nmol L^{-1} can lead to an increase in the amount of mercury-resistant bacteria able to reduce Hg(II) during incubation (Baldi, 1997). Bacterial Hg(II) reduction is mediated by a mercuric reductase encoded by the mercury resistant (merA) operon. Studies of Poulain et al. (2004) showed that merA transcripts were not detected in hypolimnion and anoxic bottom-water samples of Lake 658 suggesting the unknown mechanisms of microbial Hg(II) reduction.

The reduction rate constants are rather low, so the DGM produced represents only a small portion of the initial Hg(II). In our experimental conditions only 0.5% to 3.2% of the mercury added are reduced within 4 h. Although, this rate may appear to be low, it must be considered with respect to the water residence time. The lake average residence time is about 5 months and little sedimentation occurs in the lake (Galy-Lacaux et al., 1997). Then the aqueous Hg(II) residence time is of the same order as water residence time. The characteristic time for Hg(II) reduction in aqueous suspension of nonsterilized sediments does not exceed 96 days (three months, Table 3). Therefore, dissolved mercury which comes in contact with the sediment (Table 1) might be reduced by the sediment before it leaves the reservoir dam, however, adsorption to sediments particles or methylation may compete with Hg(II) reduction.

4. Conclusions

Vertical distributions of DGM were studied in a permanently stratified tropical reservoir. We found the DGM increase in the surface waters and at the bottom layer of the reservoir during the dry season. Similar to arctic and temperate lakes, high DGM concentrations in surface waters were attributed to sunlight-mediated photochemical processes (Beucher et al., 2002). Development of the anaerobic conditions in the bottom

layer of the reservoir might be an important factor for DGM production. DGM concentrations found at the bottom layer was larger than in temperate or arctic lakes. This can be explained by a temperature difference in bottom waters between lakes of different climate zones, i.e., by a difference in reaction kinetics. The average temperature in temperate or arctic lake hypolimnion was between 2 and 10 °C whereas it was ~25 °C in the tropical lake studied. However, these observations are related only to the end of dry season. In order to examine a seasonal DGM variation, a detailed annual study of DGM distributions is still required. Laboratory experiments with surface sediments indicated that DGM production at the bottom layer of Petit-Saut reservoir was biologically mediated. Dissolved gaseous mercury formation rates in surface sediment suspensions were of the same order of magnitude as formation rates in freshwater lakes reported in literature ($6 \cdot 10^{-5}$–$1 \cdot 10^{-5}$ min^{-1}, Table 4). In spite of relatively low reduction rate constants, the reaction time of reduction (three months) is low comparing to aqueous Hg(II) residence time (five months). Consequently, dissolved mercury, which comes in contact with the sediment, could be biotically reduced before to leave the reservoir dam. Thus, production of DGM might decrease Hg burden in the tropical reservoir and, consequently, limits the methylmercury production. However, further investigation of the fate of DGM produced at the bottom layer of a tropical reservoir is necessary. We need to examine if DGM produced is volatilized to the atmosphere or undergoes chemical transformations (i.e., oxidation, Amyot et al., 1997a; Lalonde et al., 2001).

Acknowledgements

This study was financially supported by the program “Mercury in French Guiana” of the CNRS-MATE-FEDER. T.P. acknowledges a fellowship of the French Ministry for Foreign Affairs.

References

Allard B, Arsenie I. Abiotic reduction of mercury by humic substances in aquatic system—an important process for the mercury cycle. Water Air Soil Pollut 1991;56:457–63.

Amouroux D, Wasserman JC, Tessier E, Donard OFX. Elemental mercury in the atmosphere of a tropical Amazonian forest (French Guiana). Environ Sci Technol 1999;33:3044–8.

Amyot M, Mierle G, Lean DRS, Mcqueen DJ. Sunlight-induced formation of dissolved gaseous mercury in lake waters. Environ Sci Technol 1994;28:2366–71.

Amyot M, Gill GA, Morel FMM. Production and loss of dissolved gaseous mercury in coastal seawater. Environ Sci Technol 1997a;31:3606–11.

Amyot M, Lean D, Mierle G. Photochemical formation of volatile mercury in high Arctic lakes. Environ Toxicol Chem 1997b; 16:2054–63.

Amyot M, Mierle G, Lean D, McQueen DJ. Effect of solar radiation on the formation of dissolved gaseous mercury in temperate lakes. Geochim Cosmochim Acta 1997c;61:975–87.

Amyot M, Lean DRS, Poissant L, Doyon MR. Distribution and transformation of elemental mercury in the St Lawrence River and Lake Ontario. Can J Fish Aquat Sci 2000;57: 155–63.

Baldi F. Microbial transformation of mercury species and their importance in the biogeochemical cycle of mercury. In: Sigel H, Sigel H, editors. Metal Ions in Biological Systems; 1997. p. 213–57.

Barkay T, Liebert C, Gillman M. Environmental significance of the potential for Mer(Tn21)-mediated reduction of Hg 2+ to Hg 0 in natural waters. Appl Environ Microbiol 1989;55: 1196–202.

Beucher C, Wong-Wah-Chung P, Richard C, Mailhot G, Bolte M, Cossa D. Dissolved gaseous mercury formation under UV irradiation of unamended tropical waters from French Guyana. Sci Total Environ 2002;290:131–8.

Charlet L, Boudou A. Cet or qui file un mauvais mercure. La Recherche 2002;359:52–9.

Charlet L, Peretyashko T. Storm recharge of a stratified tropical dam reservoir: the Petit-Saut dam reservoir, French Guyana, South America. Revue de Géographie Alpine 2003;91:93–9.

Charlet L, Bosbach D, Peretyashko T. Natural attenuation of TCE, As, Hg linked to the heterogeneous oxidation of Fe(II): an AFM study. Chem Geol 2002;190:303–19.

Coquery M, Cossa D. Mercury speciation in surface waters of the North Sea. J Sea Res 1995;34:245–57.

Coquery M, Cossa D, Azemard S, Peretyazhko T, Charlet L. Methylmercury formation in the anoxic waters of the Petit-Saut reservoir (French Guiana) and its spreading in the adjacent Sinnamary river. J Physique IV 2003;107:327–31.

Dumestre JF, Labroue L, Galy-Lacaux C, Reynouard C, Richard S. Biomasses et activites bacteriennes dans la retenue et a l‘aval du barrage de Petit-Saut (Guyane): influence sur les emissions de methane et la consommation d’oxygene. Hydroecol Appl 1997; 9:139–67.

Fitzgerald WF, Mason R. The global mercury cycle: oceanic and anthropogenic aspects. In: Baeyens W, editor. Global and regional mercury cycles: sources fluxes and mass; 1994. p. 85–108.

Galy-Lacaux C, Delmas R, Jambert C, Dumestre J-F, Labroue L, Richard S, et al. Gaseous emissions and oxygen consumption in hydroelectric dams: a case study in French Guyana. Glob Biogeochem Cycles 1997;11:471–83.

Hassen A, Saidi N, Cherif M, Boudabous A. Resistance of environmental bacteria to heavy metals. Bioresour Technol 1998;64:7–15.

Kim JP, Fitzgerald WF. Sea–air partitioning of mercury in the equatorial Pacific Ocean. Science 1986;231:1131–3.

Lalonde JD, Amyot M, Kraepiel AML, Morel FMM. Photooxidation of Hg(0) in artificial and natural waters. Environ Sci Technol 2001;35:1367–72.

Mason RP, Morel FMM, Hemond HF. The role of microorganisms in elemental mercury formation in natural waters. Water Air Soil Pollut 1995;80:775–87.

Morel FMM, Kraepiel AML, Amyot M. The chemical cycle and bioaccumulation of mercury. Annu Rev Ecol Syst 1998;29: 543–66.

Nriagu JO. Mechanistic steps in the photoreduction of mercury in natural waters. Sci Total Environ 1994;154:1–8.

Peretyazhko, T. Formation de Hg(0) dans des milieux anoxiques tropicaux. Thesis. Universite Joseph Fourrier, Grenoble, 2002.

Peretyazhko T, Van Cappellen P, Meile C, Coquery M, Musso M, Regnier P, et al. Biogeochemistry of major redox elements and mercury in a tropical reservoir lake (Petit Saut French Guiana). Aquat Geochem 2005;11:33–55.

Pfeiffer WC, Lacerda LD. Mercury inputs into the Amazon region. Brazil Environ Technol Lett 1988;9:325–30.

Poulain AJ, Amyot M, Findlay D, Telor S, Barkay T, Hintelmann H. Biological and photochemical production of dissolved gaseous mercury in a boreal lake. Limnol Oceanogr 2004;49:2265–75.

Roulet M, Lucotte M, Farella N, Serique G, Coelho H, Passos CJS, et al. Effects of recent human colonization on the presence of mercury in Amazonian ecosystems. Water Air Soil Pollut 1999;112:297–313.

Samemasa I. The solubility of elemental mercury vapor in water. Bull Chem Soc Japan 1975;48:1795–8.

Tseng CM, Lamborg C, Fitzgerald WF, Engstrom DR. Cycling of dissolved elemental mercury in Arctic Alaskan lakes. Geochim Cosmochim Acta 2004;68:1173–84.

Ullrich SM, Tanton TW, Abdrashitova SA. Mercury in the aquatic environment: a review of factors affecting methylation. Crit Rev Environ Sci Technol 2001;33:241–93.

van Cappellen P, Wang Y. Cycling of iron and manganese in surface sediments: a general theory for the coupled transport and reaction of carbon, oxygen, nitrogen, sulfur, iron and manganese. Am J Sci 1996;296:197–243.

Vandal GM, Mason RP, Fitzgerald WF. Cycling of volatile mercury in temperate lakes. Water Air Soil Pollut 1991;56:791–803.

Vandal GM, Fitzgerald WF, Rolfhus KR, Lamborg CH. Modeling the elemental mercury cycle in Pallette Lake, Wisconsin, USA. Water Air Soil Pollut 1995;80:529–38.

Xiao Z, Stromberg D, Lindqvist O. Influence of humic substances on photolysis of divalent mercury in aqueous solution. Water Air Soil Pollut 1995:789–98.

Zhang H, Lindberg SE. Sunlight and iron(III)-induced photochemical production of dissolved gaseous mercury in freshwater. Environ Sci Technol 2001;35:928–35.

Je mange quand j’ai faim
Je dors quand j’ai sommeil
Le sot rit de moi
Le sage me reconnaît

Tsan le Paresseux